DEVELOPMENTS IN PETROLEUM SCIENCE 32

fluid mechanics for petroleum engineers

ELEMÉR BOBOK

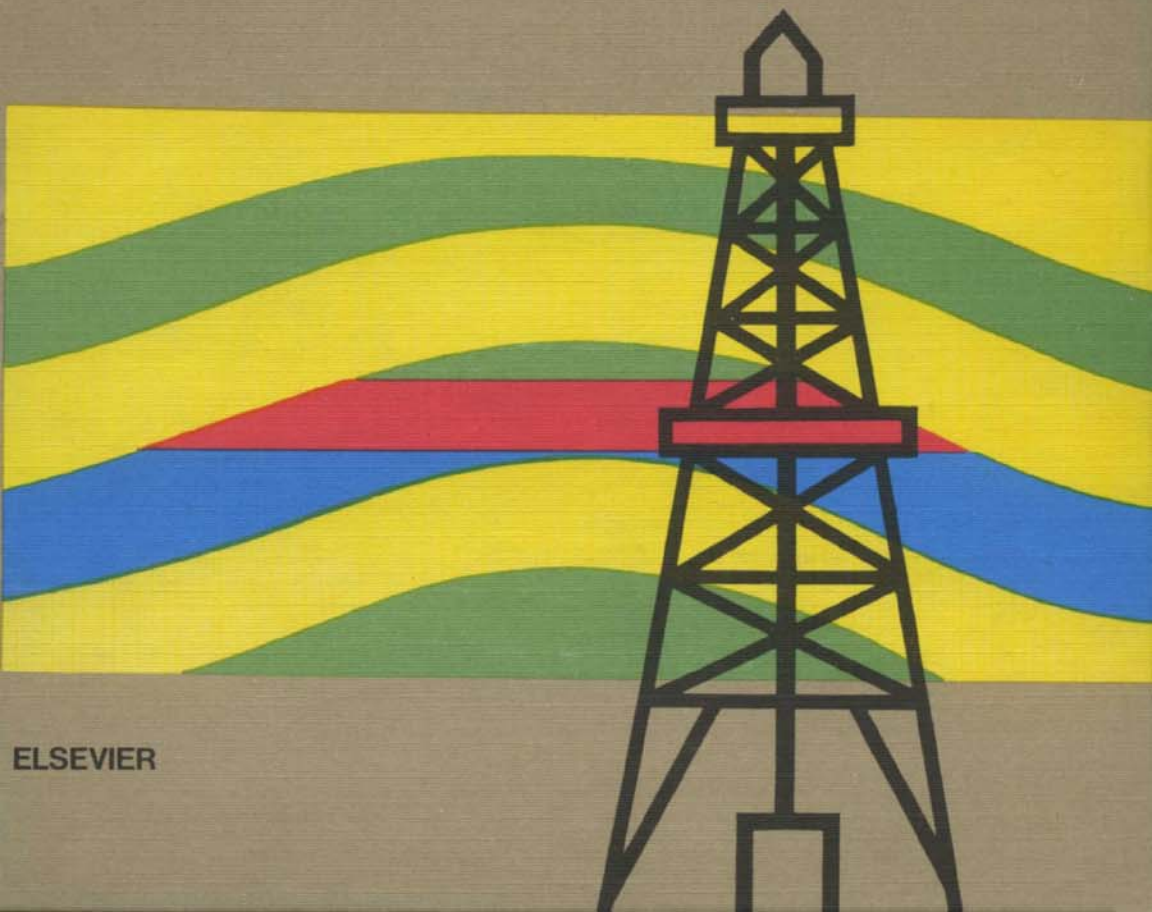

ELSEVIER

Developments in Petroleum Science, 32

FLUID MECHANICS FOR PETROLEUM ENGINEERS

This page intentionally left blank

Developments in Petroleum Science, 32

FLUID MECHANICS FOR PETROLEUM ENGINEERS

by

ELEMÉR BOBOK Ph. D.

Mechanical Engineer
Associate Professor

Petroleum Engineering Department
University of Miskolc, Hungary

ELSEVIER

Amsterdam—London—New York—Tokyo 1993

This book is an enlarged and revised version of the original
Hungarian ÁRAMLÁSTAN BÁNYAMÉRNÖKÖKNEK, Műszaki Könyvkiadó, Budapest

Translated by the author

Joint edition published by
Elsevier Science Publishers B. V., Amsterdam, The Netherlands
and
Akadémiai Kiadó, Budapest, Hungary

Exclusive sales rights in

the East European countries, Democratic People's Republic of Korea, Republic of Cuba,
Socialist Republic of Vietnam, People's Republic of Mongolia
and the successor states of the Soviet Union and Yugoslavia
Akadémiai Kiadó, P. O. Box 245, H-1519
Budapest, Hungary

all remaining areas

Elsevier Science Publishers
Sara Burgerhartstraat 25,
P. O. Box 211, 1000 AE Amsterdam, The Netherlands

Library of Congress Cataloging-in-Publication Data

Bobok, Elemér, 1938—
[Áramlástan bányamérnököknek. English]
Fluid mechanics for petroleum engineers/by Elemér Bobok;
[translated by the author].
p. cm. — (Developments in petroleum science; 32)
Enl. & rev. ed. of: Áramlástan bányamérnököknek.
Includes bibliographical references (p.) and index.
ISBN 0-444-98668-5
1. Petroleum pipelines—Fluid dynamics. I. Title. II. Series.
TN879.5.B57 1992
665.5—dc20

92-21858
CIP

Printed in Hungary

DEVELOPMENTS IN PETROLEUM SCIENCE

Advisory Editor: G. V. Chilingarian

1 A. G. COLLINS
GEOCHEMISTRY OF OILFIELD WATERS

2 W. H. FERTL
ABNORMAL FORMATION PRESSURES

3 A. P. SZILAS
PRODUCTION AND TRANSPORT OF OIL AND GAS

4 C. E. B. CONYBEARE
GEOMORPHOLOGY OF OIL AND GAS FIELDS IN SANDSTONE BODIES

5 T. F. YEN and G. V. CHILINGARIAN (Editors)
OIL SHALE

6 D. W. PEACEMAN
FUNDAMENTALS OF NUMERICAL RESERVOIR SIMULATION

7 G. V. CHILINGARIAN and T. F. YEN (Editors)
BITUMENS, ASPHALTS AND TAR SANDS

8 L. P. DAKE
FUNDAMENTALS OF RESERVOIR ENGINEERING

9 K. MAGARA
COMPACTION AND FLUID MIGRATION

10 M. T. SILVA and E. A. ROBINSON
DECONVOLUTION OF GEOPHYSICAL TIME SERIES IN THE EXPLORATION FOR OIL AND NATURAL GAS

11 G. V. CHILINGARIAN and P. VORABUTR
DRILLING AND DRILLING FLUIDS

12 T. D. VAN GOLF-RACHT
FUNDAMENTALS OF FRACTURED RESERVOIR ENGINEERING

13 J. FAYERS (Editor)
ENHANCED OIL RECOVERY

14 G. MOZES (Editor)
PARAFFIN PRODUCTS

15 O. SERRA
FUNDAMENTALS OF WELL-LOG INTERPRETATION
A. The Acquisition of Logging Data
B. The Interpretation of Logging Data

16 R. E. CHAPMAN
PETROLEUM GEOLOGY

17 E. C. DONALDSON, G. V. CHILINGARIAN and T. F. YEN
ENHANCED OIL RECOVERY
A. Fundamentals and Aspects
B. Processes and Operations

18 A. P. SZILAS
PRODUCTION AND TRANSPORT OF OIL AND GAS
A. Flow Mechanics and Production
B. Gathering and Transportation

19 G. V. CHILINGARIAN (Editor)
SURFACE OPERATIONS IN PETROLEUM SCIENCE, I AND II

20 A. J. DIKKERS
GEOLOGY IN PETROLEUM PRODUCTION

21 W. F. RAMIREZ
APPLICATION OF OPTIMAL CONTROL THEORY TO ENHANCED OIL RECOVERY

22 E. C. DONALDSON, G.V. CHILINGARIAN and T. F. YEN (Editors)
MICROBIAL ENHANCED OIL RECOVERY

23 J. HAGOORT
FUNDAMENTALS OF GAS RESERVOIR ENGINEERING

24 W. LITTMANN
POLYMER FLOODING

25 N. K. BAIBAKOV, W. J. CIESLEWICZ and A. R. GARUSHEV
THERMAL METHODS OF PETROLEUM PRODUCTION

26 D. MADER
HYDRAULIC PROPPANT FRACTURING AND GRAVEL PACKING

27 G. DA PRAT
WELL TEST ANALYSIS FOR FRACTURED RESERVOIR EVALUATION

28 E. B. NELSON (Editor)
WELL CEMENTING

29 R. W. ZIMMERMAN
COMPRESSIBILITY OF SANDSTONES

30 G. V. CHILINGAR, S. J. MAZZULLO and H. R. RIEKE (Editors)
CARBONATE RESERVOIR CHARACTERIZATION

31 E. C. DONALDSON (Editor)
MICROBIAL ENHANCEMENT OF OIL RECOVERY — RECENT ADVANCES

32 E. BOBOK
FLUID MECHANICS FOR PETROLEUM ENGINEERS

PREFACE

Fluid mechanics forms an essential part of the knowledge of petroleum engineers. Its applications can be found in almost every area of petroleum engineering including drilling, well completing, production technology, transportation and refining. The design methods and everyday practice of these special fields apply their own application-oriented hydraulics. These independently developed branches of applied fluid mechanics are often not very well integrated. There seems to be a need to treat these individual sections together within the general framework of continuum mechanics. In addition, the elegance and logical structure of this theory may influence the way of thinking of petroleum engineers.

The main purpose of this book to provide the petroleum engineer with a systematic analytical approach to the solution of fluid flow problems. Certain general laws relating to the conservation or balance of mass, momentum, energy and entropy form the starting point. These basic principles which are in integral form are found to be equivalent to differential field equations in regions where flow variables are continuous. These conservation and balance equations, however, form an indeterminate system, insufficient to yield specific solutions unless further equations are supplied. Within the embracing concept of conservation laws and balance equations it is necessary to define ideal materials by certain further conditions called constitutive relations. The balance equations and the constitutive relations together with the boundary conditions can lead to a mathematical model of a phenomenon and to the solution of a particular problem. The solution thus obtained may be verified by experimental investigations. This is the underlying approach followed in the book, which is organized into ten chapters.

In Chapter 1 the properties of the fluid are dealt with. The principles of kinematics are treated in Chapter 2. Chapter 3 reviews the balance equations of mass, momentum, angular momentum, kinetic, internal and total energy and entropy. All equations are introduced in both integral and differential form, using Gibbs's tensor notation.

Chapter 4 deals with the flow of inviscid fluids. The effect of viscosity is insignificant for the flow of low viscosity fluids for short distances. Most problems of gas dynamics may be solved with sufficient accuracy by neglecting viscous effects.

The exciting phenomena of shock waves are treated in Chapter 5. Relationships for shock conditions are derived from discontinuous balance equations.

Laminar flow of Newtonian fluids is dealt with in Chapter 6. An important, brief treatment of turbulent flow can be found in Chapter 7. The most frequent one-dimensional applications of the two former chapters are discussed in Chapter 8 together with a wide range of useful empirical data.

Chapter 9 deals with the pipe flow of different types of non-Newtonian fluids.

The flow of multiphase mixtures is treated in Chapter 10, and includes liquid—gas, liquid—liquid and liquid—solid mixtures flowing in both horizontal and vertical pipes.

This book represents the outcome of the author's 25-year-experience as an engineer, teacher, researcher and consultant in the field of fluid mechanics. This material was partly designed for a two-semester graduate course in fluid mechanics at the Department of Petroleum Engineering of Miskolc University. Some other parts were prepared for post-graduate courses.

Finally, the author wishes to express his gratitude to his friends and colleagues, especially Prof. H. C. J. Varga, for their invaluable suggestions and discussions.

E. Bobok

CONTENTS

CHAPTER 1

FLOW PROPERTIES OF FLUIDS

1.1 The fluid state

It is an everyday experience that all matter exists in either the fluid or the solid state. This also invariably applies under the physical circumstances of hydrocarbon production and technology. The different molecular structure of fluids and solids manifests itself in different macroscopic properties. From the point of view of this book only those properties are of interest, which relate to the motion of fluids, or the conditions affecting this motion. In the fluid state molecules have great mobility; translation, rotation and vibration are all allowed. In contrast to this, a solid is characterized by a restricted molecular mobility, only vibration and rotation about a fixed average position is possible. Fluids and solids behave differently under the action of external forces. A solid has tensile strength, while a fluid has none (except for viscoelastic materials). Fluids have no shape of their own, they always fill their container, adopting its shape. A fluid resists compressive forces only if it is kept in a container. Solids can withstand shearing stress up to their elastic limit, whereas fluids subjected to shearing stresses deform immediately and for as long as the stress is applied. The force of friction between two solids depends on the pressure which compresses the two surfaces; fluid friction is independent of the applied pressure. Between solids frictional forces can exist at rest, whereas in fluids shear stresses vanish in the hydrostatic state. Fluids are isotropic materials, in contrast to most solids. These differences in mechanical behavior help to define what is a fluid.

A fluid is considered to be an isotropic material which deforms continuously under the influence of an applied external force. The characteristic form of fluid motion is that of flow, which is represented mathematically by a continuous transformation of three-dimensional Euclidean space into itself. Any fluid, no matter how viscous, will flow even under the slightest tangential stress. Tangential stresses between adjacent fluid particles are proportional to the rate of deformation and disappear when the flow ceases; remnant stresses cannot exist in fluids.

A fluid may be either a liquid or a gas. Liquids are relative incompressible, whereas gases are highly compressible. Liquids have a constant density and volume (slightly dependent on temperature), gases tend to expand infinitely. A liquid can have a free surface at which the pressure is constant and equal to the gas or vapor pressure over it.

The molecules of gases are spaced far away from each other, and have a high translation energy. The kinetic energy of this molecular translation is much greater than the energy of attraction between the molecules. The average distance between the molecules of a liquid is much smaller; the translation kinetic energy being less than the energy of attraction between the molecules. The distribution of the translation energy among the molecules of a liquid follows Maxwell's distribution law. Certain molecules therefore may have enough kinetic energy to overcome the attraction of adjacent molecules. These molecules can thus escape from the liquid and form a vapor. Liquids, consequently, exert a vapor pressure which is the pressure attained by the vapor when left in contact with its liquid until equilibrium is achieved at constant temperature. The vapor pressure is a function of temperature.

The main difference between a gas and a vapor is that a gas cannot be liquified by compression alone. For a vapor this is obviously possible.

An essential difference between liquids and gases lies in their compressibility. Since liquids can only be compressed very slightly, even at very high pressures, they can be considered to be incompressible. Thus pressure becomes a simple mechanical variable and is no longer a thermodynamic variable. In this case mechanical and thermal processes may be considered separately. In contrast to the cases for a liquid, the density of a gas is strongly affected by changes in pressure and temperature. Since pressure now is a variable of the thermal state, mechanical and thermal processes must be considered simultaneously.

1.2 The continuum model of fluids

Like any other material a fluid is discrete at the microscopic level. The dimensions typically involved in engineering problems are however, much greater than molecular distances. A mathematical description of fluid flow consequently requires that the actual molecular structure be replaced by a hypothetical continuous medium, called the *continuum*. This continuum continuously occupies a three-dimensional space, and can be infinitely subdivided while still preserving its original properties. In the continuum model the actual material is replaced by continuous functions of physical quantities. The actual physical processes are represented by the evolution of these continuous functions in space and time. This spatial- and time-evolution can be expressed by means of partial differential equations. The value of such a function at a certain point is obtained as an average value in the infinitesimal volume dV surrounding the point. The essential mathematical simplification of the continuum model is that this average value is, in the limiting case, assigned to the point itself.

This infinitesimal fluid element of volume dV must contain a sufficient number of molecules to allow a statistical interpretation of the continuum. When the molecular dimensions are very small compared with any characteristic dimension

of the flow system, the average values obtained in this fluid element may be considered as variables at a given point. This infinitesimal fluid element is called a fluid particle. This notion of a fluid particle is not to be confused with any particle of the molecular theory.

To illustrate the limiting process by which the local continuum properties can be defined, consider a small volume ΔV surrounding a point P, the mass of fluid in ΔV is now Δm. The ratio

$$\varrho = \frac{\Delta m}{\Delta V}$$

will asymptotically approach a certain limiting value, as ΔV becomes smaller. When ΔV has decreased to a certain value $\Delta V'$ striking random fluctuations begin to appear since the number of molecules is too low to produce a statistically valid result. Thus the density is defined as

$$\varrho = \lim_{\Delta V \to \Delta V'} \frac{\Delta m}{\Delta V} = \frac{\mathrm{d}m}{\mathrm{d}V}. \tag{1.1}$$

The limiting process is carried out only to $\Delta V'$ instead of to zero. This approximation can never be valid when the characteristic dimensions of the fluid system are but slightly larger than the molecular distances. The latter is the case when a fluid flows through very narrow capillaries, or in the rarefied atmosphere of high-altitude flights.

1.3 Variables of state

If any material system is left alone for a sufficient length of time, it will achieve a state of equilibrium. In this equilibrium state all macroscopically measurable quantities are independent of time. Variables that depend only on the state of the system are called variables of state. The pressure p and the density ϱ are obviously variables of the mechanical state of the system. The thermal state of the system can also be characterized by the pressure and density, but it is an experimental observation that the density of the system is not solely a function of its pressure; a third variable of state, the temperature T, must be considered. The relation between the variables of state can be expressed by the equation of state

$$p = p(\varrho, T). \tag{1.2}$$

In the equation of state, the density is often replaced by its reciprocal called the specific volume

$$\vartheta = \frac{1}{\varrho}. \tag{1.3}$$

In general it is not possible to express the equation of state in a simple analytic form. It can only be tabulated or plotted against the variables of state. It is obvious

that an equation such as

$$p = p(\vartheta, T) \tag{1.4}$$

can be represented by a surface in the coordinate system ϑ, T, p. This surface of state consists of piecewise continuous surface parts, as shown in *Fig. 1.1*. It is customary to plot this relation as projected onto any one of the three planes $p-\vartheta$, $p-T$, or $\vartheta-T$. In such a projection the third variable of state is treated as a parameter. The most common diagram of state is that of water as shown in *Fig. 1.2*. Thus we obtain isothermal curves (isotherms) in the p, ϑ plane, the isobars in the ϑ, T plane and the isochores in the p, T plane. The shape of the surface of state is characteristic of a particular material.

Three partial derivatives of the equation of state determine three important properties of a material.

The coefficient of thermal expansion is defined by the expression

$$\alpha = \frac{1}{\vartheta}\left(\frac{\partial \vartheta}{\partial T}\right)_p, \tag{1.5}$$

or, expressed in terms of the density:

$$\alpha = -\frac{1}{\varrho}\left(\frac{\partial \varrho}{\partial T}\right)_p. \tag{1.6}$$

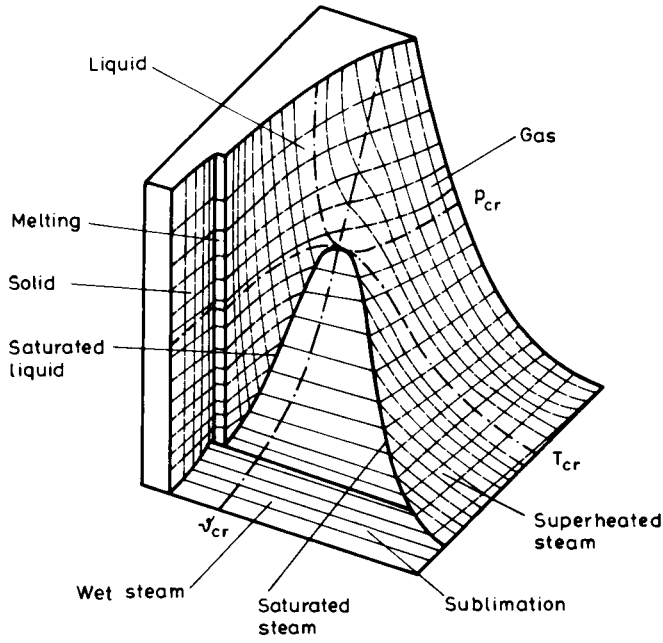

Fig. 1.1. Surface of thermal state

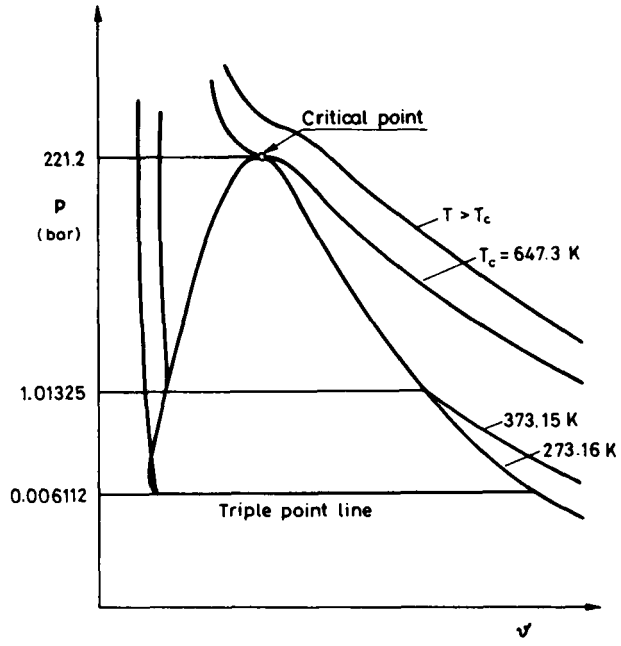

Fig. 1.2. State diagram of water

The isothermal compressibility is defined by the derivative

$$\beta = -\frac{1}{\vartheta}\left(\frac{\partial \vartheta}{\partial p}\right)_T, \tag{1.7}$$

or, in terms of the density:

$$\beta = \frac{1}{\varrho}\left(\frac{\partial \varrho}{\partial p}\right)_T. \tag{1.8}$$

The isochoric pressure coefficient is obtained as

$$\pi = \frac{1}{p}\left(\frac{\partial p}{\partial T}\right)_\varrho. \tag{1.9}$$

Since α, β and π are interrelated through the variables of state, Eqs (1.5)—(1.9) can also be considered as expressions of the equation of state. The latter can then be written as

$$\pi = \frac{\alpha}{\beta p}. \tag{1.10}$$

In certain regions of the surface of state, the equations of state can be determined experimentally. Such a degenerated equation of state is the condition of incompres-

sibility

$$\varrho = \text{const}. \tag{1.11}$$

The condition of incompressibility does not exclude the density varying with the temperature. Since many flows may be considered to be isothermal, the condition of incompressibility merely signifies a constant density at a given temperature while a flow problem is being solved. Usually a reference density ϱ_0 is given (generally at 15 °C), from which the density at an arbitrary temperature can be obtained as

$$\varrho_T = \varrho_0[1 + \alpha(T - T_0)]. \tag{1.12}$$

At constant temperature the variation in the density as a function of pressure can be expressed as

$$\varrho = \varrho_0[1 + \beta(p - p_0)]. \tag{1.13}$$

For gases at low pressures and remote from the two-phase boundary the equation of state of an ideal gas,

$$\frac{p}{\varrho} = RT, \tag{1.14}$$

provides reasonable accuracy for engineering calculations. In this equations R is the gas constant with dimensions [J/kg °C].

More suitable to calculations in the field of petroleum engineering, where greater pressures are involved, is the modified equation of state:

$$\frac{p}{\varrho} = ZRT, \tag{1.15}$$

where Z is the dimensionless compressibility factor. This can be obtained from a diagram, where Z is plotted against the reduced pressure at constant values of reduced temperature. The compressibility factor chart of Viswanath and Su is shown in *Fig. 1.3*.

When the energy relations, i.e. the exchange of work and heat between a system and its surroundings are considered it seems to be necessary to define two further variables of state the internal energy ε, and the enthalpy i. For a simple system ε and i are functions of any two of p, ϑ and T. Thus the so-called caloric equation of state can be written

$$\varepsilon = \varepsilon(\vartheta, T), \tag{1.16}$$

$$i = i(\vartheta\, T). \tag{1.17}$$

A specific material can be characterized by its equations of state. These equations cannot be deduced from thermodynamic principles; they are obtained experimentally. For incompressible fluids and for perfect gases the caloric equations of

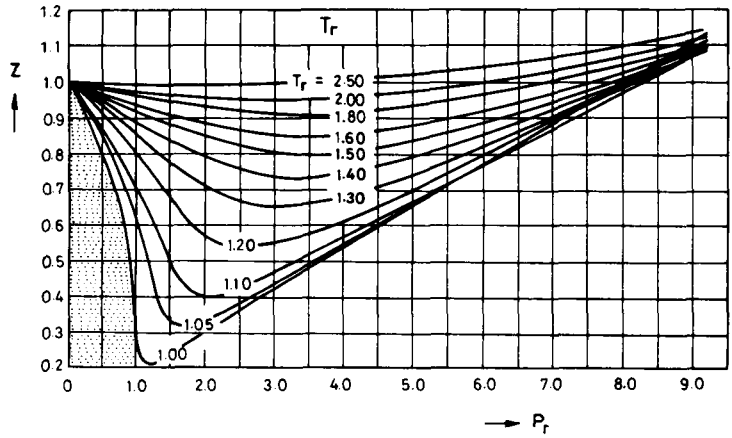

Fig. 1.3. Compressibility factor of pure gases

state are obtained in very simple form

$$\varepsilon = c_v T, \tag{1.18}$$

$$i = c_p T, \tag{1.19}$$

where c_v and c_p are the heat capacities at constant volume (or density) and at constant pressure. The relations between c_v and c_p are obtained in the form

$$c_p - c_v = R, \tag{1.20}$$

and

$$\frac{c_p}{c_v} = \kappa. \tag{1.21}$$

Both c_v, c_p, R and $\varkappa$ are important material constants. They are tabulated in *Table 1.1.*

Variables of state can be classified as either intensive or extensive variables.

Intensive variables are related to the points of a system, thus they are point functions. Velocity, pressure and temperature are typical intensive variables. Intensive variables can relate to a finite region only if their distributions are uniform. In this case both the values of a variable relating to the whole region, and that relating to a part of it must be the same.

Extensive variables are related to a finite region of a system, thus they are set functions. The mass of the system is such an extensive variable, and so are the volume, momentum, energy, entropy, etc. Set functions are additive, for example the momentum of a certain body is equal to the sum of the momentums of its parts. Specific quantities such as density or specific enthalpy would seem to be intensive variables since their values vary from point to point in the manner of point functions. There is, however, an essential difference between such specific quan-

Table 1.1.

	c_p [J/kg °C]	c_v [J/kg °C]	R [J/kg °C]	κ	ϱ(1 bar) [kg/m^3]
Air	1005	718	287	1.40	1.2763
Butane	1663	520	143	1.11	2.668
Carbon dioxide	825	636	189	1.31	1.977
Ethane	1666	1389	277	1.22	1.356
Ethylene	1465	1168	297	1.24	1.2605
Hydrogen	14235	10113	4122	1.41	0.0899
Methane	2177	1658	519	1.30	0.7168
Nitrogen	1043	746	297	1.40	1.2505
Oxygen	913	653	260	1.40	1.429
Propane	1550	1361	189	1.14	2.019
Superheated steam	1860	1398	462	1.33	0.7936

tities and real intensive variables. The specific quantities may be integrated over a region thus producing an extensive variable; for a real intensive variable such an integration has no physical meaning.

Intensive and extensive variables play different roles in physical processes. The state of a material system can be determined by as many extensive variables as there are types of interaction between the system and its surroundings. An interaction of certain type may induce either equilibrium or a process of change. A characteristic pair of intensive and extensive variables are associated with any interaction. The characteristic intensive variable is that one which is uniformly distributed at equilibrium. For instance, experimental observations show that thermal equilibrium can exist only if the temperature has a uniform distribution throughout the whole system. A homogeneous velocity distribution is associated with the condition of mechanical equilibrium. A system with a uniformly distributed velocity U is at rest in a coordinate system moving with the velocity U. Thus temperature and velocity have particular significance as the characteristic variables of thermal and mechanical interaction.

If the distribution of the characteristic intensive variable is not homogeneous, the equilibrium condition is terminated and certain processes are induced accompanied by changes in the extensive variables. These changes are directed so as to neutralize the inhomogeneity. Fluxes of extensive quantities may be convective, i.e. transferred by macroscopic motion, or conductive, i.e. transferred by molecular motion only. Conductive fluxes can be expressed by the product of a conductivity coefficient and the gradient of the characteristic intensive variable. These conductivity coefficients are important material properties.

1.4 Conductivity coefficients

In petroleum engineering the material systems considered may be in mechanical and thermal interaction with their surroundings. In the case of mechanical interaction the stress is the conductive flux of momentum. This conductive momentum flux for one-dimensional motion is expressed as

$$\tau = \mu \frac{dv_x}{dy}, \tag{1.22}$$

where τ is the momentum conductively transferred across a unit area per unit time, dv_x/dy is the velocity gradient, and μ is a coefficient of proportionality the dynamic viscosity coefficient, usually called just the viscosity. The viscosity coefficient μ is a characteristic property of fluids. Its value for a particular fluid may be a function of temperature, pressure and the shear rate.

In the simplest case the viscosity coefficient is a function of the temperature only. For isothermal fluids the viscosity is then constant. If the viscosity is independent of the shear rate the fluid is called Newtonian. The viscosity of all Newtonian liquids decreases with increasing temperature at constant pressure. The viscosity of gases increases with temperature at constant pressure.

The viscosity of pure liquids depends strongly on the temperature, but is relative insensitive to pressure variations. At extremely high pressures ($p \sim 1000$ bar) the viscosity of a liquid increases remarkably with pressure. The viscosity of gases at low pressures may be calculated based on kinetic theory. Above 8–10 bars the effect

Table 1.2.

	ϱ [kg/m³]	α [1/°C]	β [m²/N]	c^* [J/kg °C]	k [W/m °C]	μ [Pas]	ν [m²/s]
		$\times 10^{-5}$	$\times 10^{-6}$			$\times 10^{-4}$	$\times 10^{-6}$
Ammonia	610	122	114	473	0.494	2.20	0.378
Benzol	879	106	98	1738	0.154	6.51	0.796
Brine	1050	17	48.5	4175	0.602	11.03	1.076
Ethyl alcohol	794	109	101	2430	0.215	6.15	1.65
Fuel oil	930	106	96	1860	0.141	48.17	51.8
Gasoline	721	114	118	2177	0.140	4.09	0.59
Glycerine	1255	50	108	2428	0.285	1.4800	680
Kerosene	800	97	55	1910	0.135	2200	2.75
Mercury	13546	18.1	4	139	9.304	15.54	0.1147
Methyl alcohol	792	119	104	2470	0.212	5.84	0.735
Engine oil	911	102	82	2240	0.160	846	94
Water	1000	18	49.6	4183	0.598	10.046	1.00

* c = heat capacity.

of pressure becomes significant. In many hydrodynamic equations it is common to use the quotient of the viscosity divided by the density. This is the so-called kinematic viscosity,

$$\nu = \frac{\mu}{\varrho}, \tag{1.23}$$

with the dimensions [m^2/s]. Both the dynamic and kinematic viscosities of some common fluids are tabulated in *Table 1.2.*

In the case of thermal interaction between a system and its surroundings the conductive flux of the internal energy for the one-dimensional case is given by

$$q = -k \frac{dT}{dx}, \tag{1.24}$$

where q is the rate of flow of internal energy across a unit area per unit time, dT/dx the temperature gradient, and k is the thermal conductivity coefficient. Its dimensions are [W/m °C]. The thermal conductivity coefficient depends on the temperature, and for gases to a certain degree on the pressure.

CHAPTER 2

KINEMATICS

Preliminary remarks

The mathematical notation used in this book is that of the familiar Gibbsian vector and tensor analysis. Most of the used vector operations are standard, but in a few cases may appear unusual. For this reason it is convenient to define all operations in terms of vector components.

Scalar quantities are denoted by italic letters.

Except in a few special situations italic letters with an arrow are used to denote vectors, in a fixed rectangular coordinate system the scalar components can be written as

$$\vec{a} = a_x \vec{i} + a_y \vec{j} + a_z \vec{k} .$$

The scalar (dot, or inner) product of two vectors is denoted by

$$\vec{a}\vec{b} = a_x b_x + a_y b_y + a_z b_z .$$

The vector (or cross) product of two vectors is written as

$$\vec{a} \times \vec{b} = \begin{vmatrix} \vec{i} & \vec{j} & \vec{k} \\ a_x & a_y & a_z \\ b_x & b_y & b_z \end{vmatrix} = (a_y b_z - a_z b_y)\vec{i} + (a_z b_x - a_x b_z)\vec{j} + (a_x b_y - a_y b_x)\vec{k} .$$

The dyadic (or outer) product of two vectors obtains a second-order tensor (dyad):

$$\vec{a} \circ \vec{b} = \begin{bmatrix} a_x b_x & a_x b_y & a_x b_z \\ a_y b_x & a_y b_y & a_y b_z \\ a_z b_x & a_z b_y & a_z b_z \end{bmatrix} .$$

The symbols grad Φ, div $\vec{a}$, curl $\vec{a}$, Grad $\vec{a}$ and Div A will be used in their familiar senses, thus

$$\text{grad } \Phi = \nabla\Phi = \frac{\partial \Phi}{x}\vec{i} + \frac{\partial \Phi}{y}\vec{j} + \frac{\partial \Phi}{z}\vec{k}$$

$$\text{div } \vec{a} = \nabla\vec{a} = \frac{\partial a_x}{\partial x} + \frac{\partial a_y}{\partial y} + \frac{\partial a_z}{\partial z}$$

$$\operatorname{curl} \vec{a} = \nabla x \vec{a} = \left(\frac{\partial a_z}{\partial y} - \frac{\partial a_y}{\partial z}\right)\vec{i} + \left(\frac{\partial a_x}{\partial z} - \frac{\partial a_z}{\partial x}\right)\vec{j} + \left(\frac{\partial a_y}{\partial x} - \frac{\partial a_x}{\partial y}\right)\vec{k}$$

$$\operatorname{Grad} \vec{a} = \vec{a} \circ \nabla = \begin{bmatrix} \frac{\partial a_x}{\partial x} & \frac{\partial a_x}{\partial y} & \frac{\partial a_x}{\partial z} \\ \frac{\partial a_y}{\partial x} & \frac{\partial a_y}{\partial y} & \frac{\partial a_y}{\partial z} \\ \frac{\partial a_z}{\partial x} & \frac{\partial a_z}{\partial y} & \frac{\partial a_z}{\partial z} \end{bmatrix}.$$

Second-order tensors are denoted uppercase bold face letters. The components of a tensor **A** will be denoted as

$$\mathbf{A} = \begin{bmatrix} A_{xx} & A_{xy} & A_{xz} \\ A_{yx} & A_{yy} & A_{yz} \\ A_{zx} & A_{zy} & A_{zz} \end{bmatrix}.$$

The divergence of a tensor is denoted by

$$\operatorname{Div} \mathbf{A} = \mathbf{A}\nabla = \left(\frac{\partial A_{xx}}{\partial x} + \frac{\partial A_{xy}}{\partial y} + \frac{\partial A_{xz}}{\partial z}\right)\vec{i} + \left(\frac{\partial A_{yx}}{\partial x} + \frac{\partial A_{yy}}{\partial y} + \frac{\partial A_{yz}}{\partial z}\right)\vec{j} +$$

$$+ \left(\frac{\partial A_{zx}}{\partial x} + \frac{\partial A_{zy}}{\partial y} + \frac{\partial A_{zz}}{\partial z}\right)\vec{k}.$$

The scalar product of two tensors can be written as

$$\mathbf{A} : \mathbf{B} = A_{xx}B_{xx} + A_{xy}B_{xy} + A_{xz}B_{xz} + A_{yx}B_{yx} + A_{yy}B_{yy} +$$

$$+ A_{yz}B_{yz} + A_{zx}B_{zx} + A_{zy}B_{zy} + A_{zz}B_{zz}.$$

These notations, and others like them are frequently used in fluid mechanics.

2.1 Eulerian and Lagrangian description of fluid motion

Fluid flow is the characteristic form of motion of fluid continua, an intuitive mechanical concept based on direct experimental observations. Mathematically it means the continuous transformation of three-dimensional Euclidean space into itself. This transformation is an infinite set of one-parameter families of deformations with respect to the real parameter t: time. The initial instant $t=0$ can be totally arbitrary, and the values of the parameter t can range continuously across the interval

$$-\infty < t < \infty.$$

The continuity of time is given by the axiom of continuity: the motion has continuous partial time derivatives of as many orders as needed. For most mechanical investigations, partial derivatives of the first and second order are sufficient.

In continuum mechanics two types of descriptions of motion are possible. These are called the material, or Lagrangian, and the spatial, or Eulerian, descriptions.

The material or Lagrangian description

The material description is an immediate extension of the method of point-mass mechanics. Fluid particles are considered to represent individual point masses and the paths of these particles are traced in the fluid flow in order to formulate the orthogonal coordinate system, which is shown in *Fig. 2.1.* Naturally it could also be curvilinear, but for now a rectangular Cartesian coordinate system is chosen. Let the particle under consideration be at the point P given by the position vector $\vec{R}(X, Y, Z)$ at the time $t=0$. At time t, this particle will occupy the position P^*, given by the position vector $\vec{r}(x, y, z)$. In this case the vector

$$\vec{r}=x\vec{i}+y\vec{j}+z\vec{k}$$

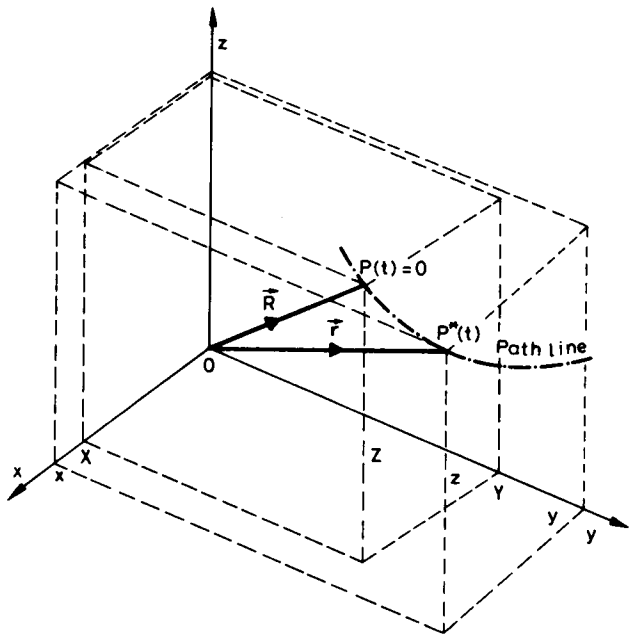

Fig. 2.1. Path line of a fluid particle

is determined as a function of both the vector

$$\vec{R} = X\vec{i} + Y\vec{j} + Z\vec{k}$$

and of the time t, and the flow is represented by the transformation

$$\vec{r} = \vec{r}(\vec{R}, t), \tag{2.1}$$

of which the scalar components are:

$$x = x(\vec{R}, t) = x(X, Y, Z, t),$$
$$y = y(\vec{R}, t) = y(X, Y, Z, t),$$
$$z = z(\vec{R}, t) = z(X, Y, Z, t).$$

If $\vec{R}$ is kept fixed, while t is varied, Eq. (2.1) determines the path of the particle P, as shown in *Fig. 2.1*. If the time t is kept fixed, Eq. (2.1) determines the transformation of the region initially occupied by the fluid into its position at time t. Let us assume that the initially distinct points remain distinct during their entire motion. This means that any closed surface moving together with the fluid continuum separates the fluid on both sides of it completely and permanently. This is shown in *Fig. 2.2*. Both of these methods can be used in the visual observation of the flow. An example for the first method would be a photograph taken with backlighting with a long exposure time, as shown in *Fig. 2.3*. Here very fine aluminium powder was added to the flow, thus making it possible to observe the flow path of the particles. *Figure 2.4* demonstrates the second method and shows

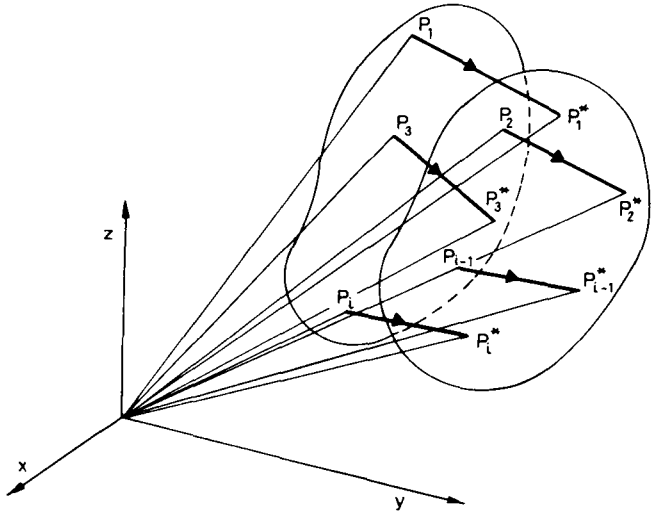

Fig. 2.2. Deformation of a flowing material volume

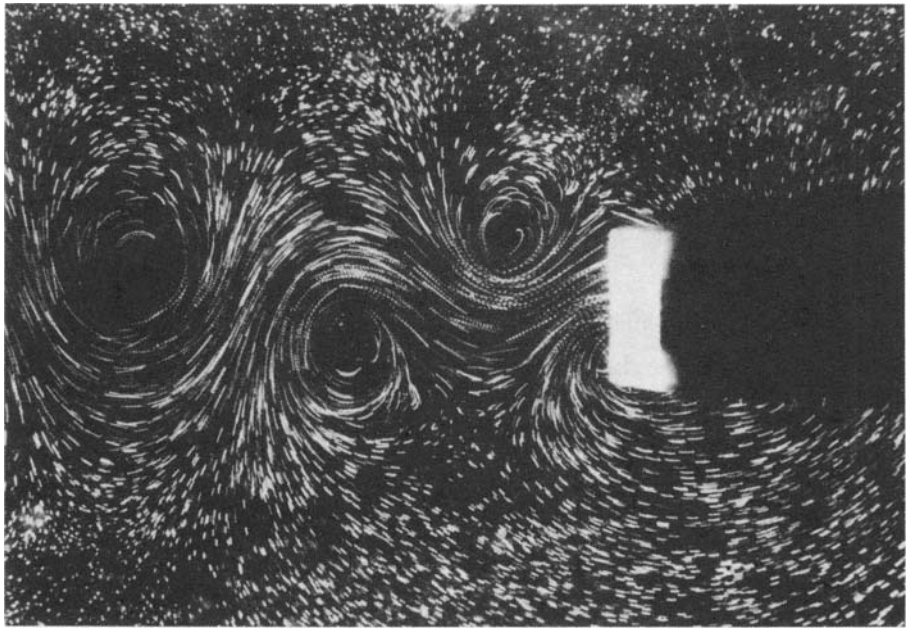

Fig. 2.3. Path lines behind an obstacle

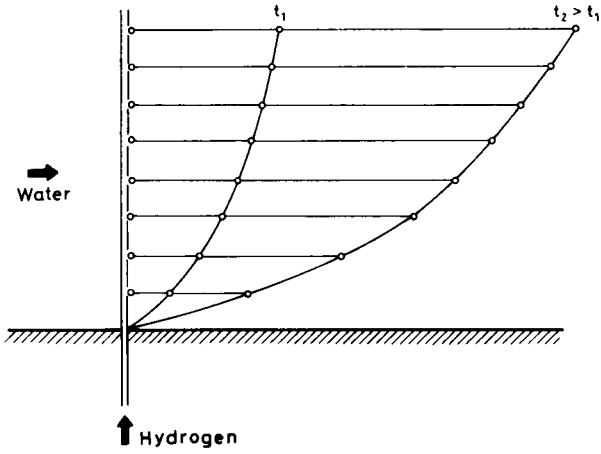

Fig. 2.4. Deformation of a series of small hydrogen bubbles flowing with water

the deformation of a line of small-sized hydrogen bubbles flowing with water at two different instants in time. The inverse of the transformation can be defined as

$$\vec{R} = \vec{R}(\vec{r}, t) .$$

To characterize the motion of a particle defined by the initial coordinates X, Y, Z, we obtain expressions of the form familiar from point-mass kinematics.

The velocity $\vec{v}$ of the particle is defined as

$$\vec{v} = \frac{\mathrm{d}\vec{r}}{\mathrm{d}t} = \frac{\mathrm{d}}{\mathrm{d}t}(\vec{r}(\vec{R}, t)) . \tag{2.2}$$

Its components in the directions of the coordinate axes are:

$$v_x = \frac{\mathrm{d}x}{\mathrm{d}t} = \frac{\partial}{\partial t}(x(\vec{R}, t)) ,$$

$$v_y = \frac{\mathrm{d}y}{\mathrm{d}t} = \frac{\partial}{\partial t}(y(\vec{R}, t)) ,$$

$$v_z = \frac{\mathrm{d}z}{\mathrm{d}t} = \frac{\partial}{\partial t}(z(\vec{R}, t)) .$$

It is obvious that $\vec{v}$ is a function of certain material variables which relate to the chosen individual fluid particle. These time derivatives expressed in terms of Lagrangian variables are called material, or substantial derivatives.

The Eulerian or spatial description

D'Alembert and Euler were the pioneers of the spatial description of flow. Instead of the observation of individual fluid particles in the flow, they introduced the concept of the velocity field to describe the state of motion at any given point during the course of time. The velocity field is a function of position and time, and gives the velocity of a particle at a position $\vec{r}$ at a time t. The velocity and other flow variables are not related to a given particle of fixed identity, but to a given point in space, which happens to be there. Studying the evolution of such a function in space and time is much more informative, than the hopeless effort of tracing the path of an infinite number of individual particles.

The material, or Eulerian description replaces the flow variables which relate to the particles of the continuum, with the continuous distribution functions of these quantities. The density or the pressure is given by the scalar functions

$$\varrho = \varrho(\vec{r}, t) ,$$

$$p = p(\vec{r}, t) ,$$

while the velocity or the acceleration is obtained from the vectorial functions

$$\vec{v} = \vec{v}(\vec{r}, t),$$

$$\vec{a} = \vec{a}(\vec{r}, t).$$

Classical field theory is a sufficient mathematical formalism to express Euler's conception: the motion can be directly described by means of partial differential equations relating the quantities ϱ, p, $\vec{v}$, $\vec{a}$, etc.

By means of Eq. (2.1) and its inverse, any quantity which is the function of the spatial variables $\vec{r}$, t is also a function of the material variables $\vec{R}$, t and conversely. If we wish to replace the material variables by spatial ones we must solve Eq. (2.1) for the unknowns X, Y, Z expressing them in terms of x, y, z. Substituting these into Eq. (2.2) we obtain the velocity in Eulerian form.

To replace the Eulerian description of flow by the Lagrangian one, it is necessary to take the time integrals of the scalar components of Eq. (2.3):

$$x = \int v_x(x, y, z, t)\,\mathrm{d}t = f_x(x, y, z, t) + K_x,$$

$$y = \int v_y(x, y, z, t)\,\mathrm{d}t = f_y(x, y, z, t) + K_y,$$

$$z = \int v_z(x, y, z, t)\,\mathrm{d}t = f_z(x, y, z, t) + K_z,$$

in which K_x, K_y, K_z are constants of integration.

Solving this system of equations for the coordinates x, y, z, we obtain:

$$x = \varphi_x(K_x, K_y, K_z, t),$$

$$y = \varphi_y(K_x, K_y, K_z, t),$$

$$z = \varphi_z(K_x, K_y, K_z, t).$$

If the constants of the integration are regarded to be Lagrangian variables, these equations determine the motion of the fluid particle initially situated at the point $X = K_x$, $Y = K_y$, $Z = K_z$.

This integration procedure is not easily carried out because of mathematical difficulties. A particularly interesting example of the integration was demonstrated by Maxwell.

2.2 The velocity field

In contrast to the Lagrangian description, the Eulerian treatment does not trace individual particles in the flow. It rather describes what happens at every fixed point in the flow space as a function of time. At any instant of time there are, at every point of the fluid flow, velocity vectors with a definitive length and direction. This set of velocity vectors forms the velocity field. The point function of four variables (x, y, z, t) which determines the velocity distribution in space and time

can be expressed as

$$\vec{v} = \vec{v}(\vec{r}, t) . \tag{2.3}$$

Its scalar components are:

$$v_x = v_x(x, y, z, t) ,$$

$$v_y = v_y(x, y, z, t) ,$$

$$v_z = v_z(x, y, z, t) .$$

Each scalar component of the vector point function of the velocity field is a scalar point function of four variables.

Consider the vectors $\vec{v}$ to be bound vectors fixed to the position vector $\vec{r}$.

Streamlines then are instantaneous curves in the velocity vectors. The concept of streamlines is sufficient for a complete understanding of the flow and for the interpretation of visual observations. The absolute value of the velocity can be characterized by the density of streamlines: the number of streamlines intersecting a unit surface perpendicular to them is proportional to the magnitude of the velocity. Velocity vectors are the tangent vector to the streamlines at all ordinary points. *Figure 2.5* shows the flow pattern developed around a flat plate in a uniform flow. The term "flow pattern" refers to the set of streamlines in the observed region. In the vicinity of the two edges of the plate the streamlines are more densely packed, reflecting the greater velocity values.

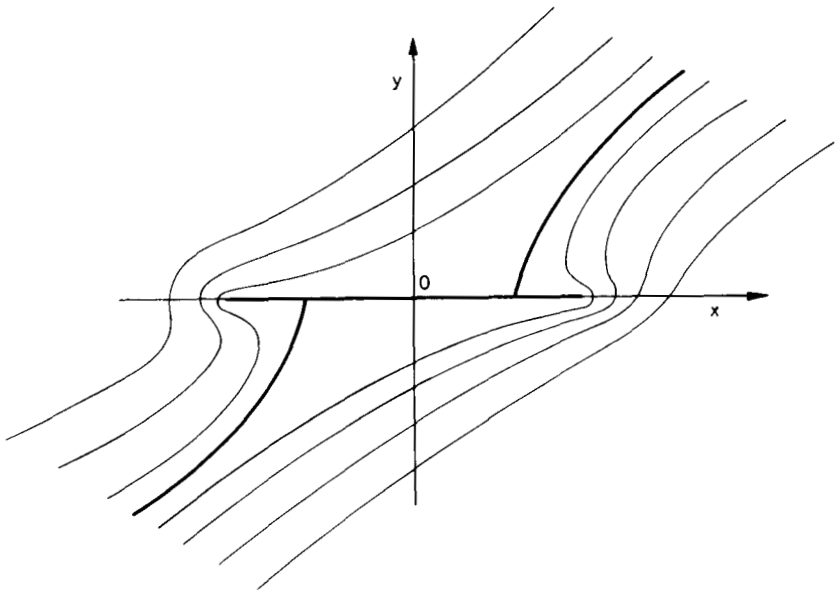

Fig. 2.5. Streamlines around a flat plate placed in parallel flow

The differential equation defining a streamline can be written as

$$\vec{v} \times \mathrm{d}\vec{r}_s = 0 . \tag{2.4}$$

Since the element of arc length along a streamline is parallel to the velocity, their vector product must be zero. The components of this vector product can be determined from the following determinant:

$$\vec{v} \times \mathrm{d}\vec{r}_s = \begin{vmatrix} \vec{i} & \vec{j} & \vec{k} \\ v_x & v_y & v_z \\ \mathrm{d}x & \mathrm{d}y & \mathrm{d}z \end{vmatrix} = 0 .$$

The result is

$$(v_y \mathrm{d}z - v_z \mathrm{d}y)\,\vec{i} + (v_z \mathrm{d}x - v_x \mathrm{d}z)\,\vec{j} + (v_x \mathrm{d}y - v_y \mathrm{d}x)\,\vec{k} = 0 ,$$

or in another form:

$$\frac{\mathrm{d}x}{v_x} = \frac{\mathrm{d}y}{v_y} = \frac{\mathrm{d}z}{v_z} . \tag{2.5}$$

When integrating this equation the time t is taken as a parameter, thus such an integration yields a "snapshot". The shape of streamlines generally changes with time.

Path lines

A path line is the trajectory of a fluid particle of fixed identity. The description of the paths of individual fluid particles is a characteristic example of the Lagrangian method. This problem is inherently different from that of the determination of streamlines. To determine path lines based on the velocity field we must solve the differential equation

$$\frac{\mathrm{d}\vec{r}}{\mathrm{d}t} = \vec{v}(\vec{r}, t) . \tag{2.6}$$

We may take $\vec{r}(0) = \vec{R}$ as a boundary condition. Thus we obtain the system of scalar differential equations:

$$\frac{\mathrm{d}x}{v_x(x, y, z, t)} = \frac{\mathrm{d}y}{v_y(x, y, z, t)} = \frac{\mathrm{d}z}{v_z(x, y, z, t)} = \mathrm{d}t . \tag{2.7}$$

In this system of equations the coordinates x, y, z are unknown functions of the time t, if the values X, Y, Z corresponding to $t = 0$ are fixed. A comparison of Eqs (2.5) and (2.7) shows the essential difference between them; thus streamlines and path lines do not in general coincide. There is an exception: the case of steady flow. Then the parameter t is eliminated, and the shape of the streamlines and path lines is the same and unchanged with time.

Stream surface, stream tube

Consider an arbitrary curve L in the velocity field. The set of streamlines passing through this curve L form a stream surface *(Fig. 2.6)*. The velocity vector is perpendicular to the surface normal vector at every point of the stream surface. This can be formulated as

$$\vec{v}\,\mathrm{d}\vec{A}=0\,. \tag{2.8}$$

Since the velocity vector has no normal component on the stream surface, there is no flux across it. Thus a solid boundary of a rigid or a deformable body can be

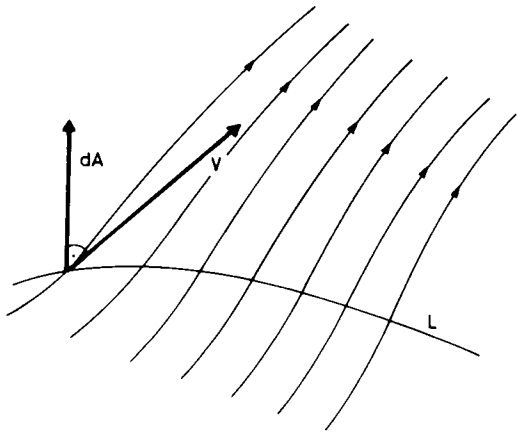

Fig. 2.6. Stream surface

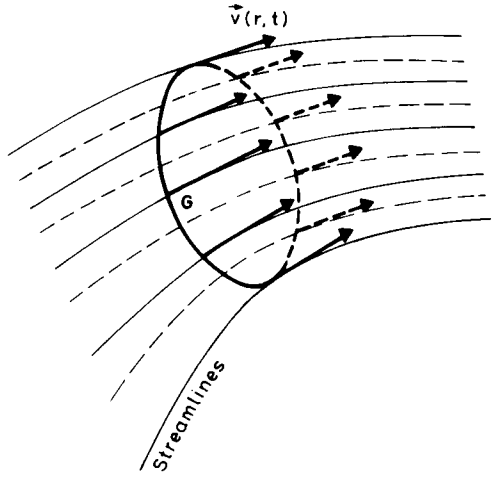

Fig. 2.7. Stream tube

replaced by a stream surface. This boundary surface may be stationary e.g. a wall, or may be moving, e.g. a bubble in a water flow.

Consider now a closed curve (G) in the velocity field $\vec{v}(\vec{r}, t)$. The streamlines passing through this closed curve form a stream tube. Since the surface of the stream tube is a stream surface, it is impervious to the fluid. This is shown in *Fig. 2.7.* The impervious walls of the tubes can be replaced by stream tubes. Thus the boundary condition can be expressed by the equation

$$\vec{v}\,\mathrm{d}\vec{A}=0\,.$$

Planar flow

If the flow is the same in all planes parallel to a fixed xy plane and the velocity has no z-component, the motion is called planar flow:

$$\vec{v}=v_x(x, y, t)\,\vec{i}+v_y(x, y, t)\,\vec{j}\,.$$

The stream surfaces of the planar flow are planes parallel to each other with congruent flow patterns. The investigation of planar flow can be carried out using simpler mathematical methods than required for three-dimensional flows. Thus three-dimensional flows are often approximated by a set of planar flows.

Important properties of the velocity field are obtained from its divergence and curl. If the divergence of the velocity field vanishes

$$\operatorname{div}\vec{v}=0\,, \tag{2.9}$$

the vector field $\vec{v}(\vec{r}, t)$ is solenoidal. In a solenoidal velocity field a streamline does not originate from a point nor does it terminate at a point. As shown in *Fig. 2.8,* streamlines of solenoidal velocity fields can extend from infinity to infinity (a), or can close onto themselves (b), or end on the boundary surface of the fluid (c). If the divergence of the velocity field does not vanish, there must be a source (or sources) of the velocity field. Such a source may be located at discrete points. At such a point, a number of streamlines originate, depending on the strength of the source (d). Sources may be continuously distributed along a line, on a surface or even throughout a region. This latter condition pertains to compressible fluid flows. The curl of the velocity field is obtained as

$$\operatorname{curl}\vec{v}=\nabla\times v=\begin{vmatrix}\vec{i} & \vec{j} & \vec{k}\\ \dfrac{\partial}{\partial x} & \dfrac{\partial}{\partial y} & \dfrac{\partial}{\partial z}\\ v_x & v_y & v_z\end{vmatrix}=$$

$$=\left(\frac{\partial v_z}{\partial y}-\frac{\partial v_y}{\partial z}\right)\vec{i}+\left(\frac{\partial v_x}{\partial z}-\frac{\partial v_z}{\partial x}\right)\vec{j}+\left(\frac{\partial v_y}{\partial x}-\frac{\partial v_x}{\partial y}\right)\vec{k}\,.$$

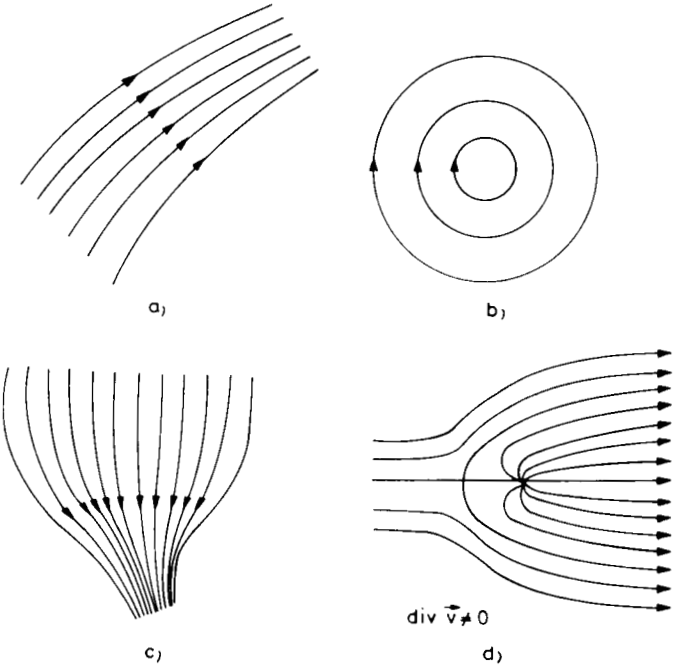

Fig. 2.8. Solenoidal velocity fields (*a*, *b*, *c*) and velocity field around a singular point (*d*)

The curl of the velocity field is itself a vector field:

$$\vec{\Omega} = \text{curl}\, \vec{v}\,. \tag{2.10}$$

If the vector field of $\vec{\Omega}$ does not vanish, the motion of the fluid particle is the so-called vortex motion. The axial vector $\vec{\Omega}$ is called the vorticity vector; its direction is the axis of spin, and its magnitude Ω is the strength of vorticity which is proportional to the angular velocity.

If the curl of the velocity field vanishes, i.e.

$$\text{curl}\, \vec{v} = 0\,,$$

the flow is irrotational. For irrotational flows a velocity potential Φ exists of which the velocity components can be determined.

2.3 The acceleration field

The acceleration is the rate of change of the velocity experienced by a moving particle. It can be expressed as the time derivative of the velocity:

$$\vec{a} = \frac{\mathrm{d}\vec{v}}{\mathrm{d}t}\,. \tag{2.11}$$

Acceleration vectors form an acceleration field, which can be determined from the velocity field directly by using Eq. (2.11). The vector differential of the velocity field is:

$$\mathrm{d}\vec{v} = \mathrm{d}v_x\vec{i} + \mathrm{d}v_y\vec{j} + \mathrm{d}v_z\vec{k}\,.$$

Since the velocity components are scalar point functions of four variables, their differentials are:

$$\mathrm{d}v_x = \frac{\partial v_x}{\partial t}\mathrm{d}t + \frac{\partial v_x}{\partial x}\mathrm{d}x + \frac{\partial v_y}{\partial y}\mathrm{d}y + \frac{\partial v_z}{\partial z}\mathrm{d}z\,,$$

$$\mathrm{d}v_y = \frac{\partial v_y}{\partial t}\mathrm{d}t + \frac{\partial v_y}{\partial x}\mathrm{d}x + \frac{\partial v_y}{\partial y}\mathrm{d}y + \frac{\partial v_z}{\partial z}\mathrm{d}z\,,$$

$$\mathrm{d}v_z = \frac{\partial v_z}{\partial t}\mathrm{d}t + \frac{\partial v_z}{\partial x}\mathrm{d}x + \frac{\partial v_z}{\partial y}\mathrm{d}y + \frac{\partial v_z}{\partial z}\mathrm{d}z\,.$$

Substituting into Eq. (2.11) and taking into account Eq. (2.2), we obtain the equations:

$$a_x = \frac{\partial v_x}{\partial t} + v_x\frac{\partial v_x}{\partial x} + v_y\frac{\partial v_x}{\partial y} + v_z\frac{\partial v_z}{\partial z}\,,$$

$$a_y = \frac{\partial v_y}{\partial t} + v_x\frac{\partial v_y}{\partial x} + v_y\frac{\partial v_y}{\partial y} + v_z\frac{\partial v_y}{\partial z}\,,$$

$$a_z = \frac{\partial v_z}{\partial t} + v_x\frac{\partial v_z}{\partial x} + v_y\frac{\partial v_z}{\partial y} + v_z\frac{\partial v_z}{\partial z}\,.$$

This can be written in a more simple form as

$$\vec{a} = \frac{\partial \vec{v}}{\partial t} + (\vec{v}\nabla)\,\vec{v}\,. \tag{2.12}$$

The second term of Eq. (2.12) can be expressed as a dyadic product:

$$\vec{a} = \frac{\partial \vec{v}}{\partial t} + (\vec{v} \circ \nabla)\,\vec{v}\,. \tag{2.13}$$

This dyadic or outer product of the two vectors $\vec{v}$ and ∇ determines a tensor of second order

$$\mathbf{D} = \vec{v} \circ \nabla = \begin{vmatrix} \frac{\partial v_x}{\partial x} & \frac{\partial v_x}{\partial y} & \frac{\partial v_x}{\partial z} \\ \frac{\partial v_y}{\partial x} & \frac{\partial v_y}{\partial y} & \frac{\partial v_y}{\partial z} \\ \frac{\partial v_z}{\partial x} & \frac{\partial v_z}{\partial y} & \frac{\partial v_z}{\partial z} \end{vmatrix}$$

which is called the tensor derivative or the gradient tensor of the velocity field. Thus we may use the following notation:

$$\vec{a} = \frac{\partial \vec{v}}{\partial t} + \mathbf{D}\vec{v} = \frac{\partial \vec{v}}{\partial t} + (\text{Grad}\,\vec{v})\,\vec{v}\,. \tag{2.14}$$

It is obvious that the acceleration is the material derivative of the velocity field. In each of the above expressions for the acceleration field, a local and a convective component may be separated.

The first term $\partial\vec{v}/\partial t$ is the local acceleration. It represents the change in the velocity field apparent to an observer fixed in the spatial coordinate system. If the local acceleration component vanishes, i.e.

$$\frac{\partial \vec{v}}{\partial t} = 0\,,$$

the flow is steady.

The second term is the convective acceleration. It represents the acceleration which, in a steady motion coinciding with $\vec{v}$ at time $t=0$, is necessary to direct the particles along their appointed paths at the required velocity. Thus convective acceleration occurs because the fluid particles move in an inhomogeneous velocity field.

It is obvious, that though during steady flow the local acceleration vanishes, the convective acceleration is not necessarily zero, and thus the material acceleration is also not zero. The convective acceleration vanishes if the velocity field is homogeneous in the direction of the motion. Such a case is that of one-dimensional flow of an incompressible fluid in a pipe of constant cross-section.

A very interesting problem is represented by a sudden change in the velocity field, for example the flow induced by the motion of the piston of a reciprocating pump. Then only instantaneous local acceleration occurs; the convective component develops at a later stage, when the local acceleration generates inhomogeneities in the velocity field.

An important parameter was introduced by Szebehely, to measure the unsteadiness of a flow. It illustrates the relative importance of the local and convective accelerations:

$$\alpha = \frac{\left|\dfrac{\partial \vec{v}}{\partial t}\right|}{|(\vec{v}V)\,\vec{v}|}\,. \tag{2.15}$$

For a steady motion without acceleration (steady flow of an incompressible fluid in a pipe or duct of constant cross-section). Szebehely's number is an indeterminate expression of the type 0/0. If the flow is steady, but the velocity field is inhomogeneous (for example in a diffuser), $\alpha = 0$. For a transient flow in a pipe of constant cross-section (for example in the case of waterhammer), $\alpha = \infty$.

2.4 Motion of an infinitesimal fluid particle

Imagine an infinitesimal rectangular fluid particle of fixed identity in a flowing fluid. Its sides dx, dy and dz are parallel to the coordinate axes. Let one of its corners at a given instant be the arbitrarily chosen point P, determined by its position vector $\vec{r}$. We shall investigate the velocity field at the same instant in the infinitesimal neighborhood of point P. Let the position vector of the opposite corner P' of this rectangular particle be $\vec{r}+d\vec{r}$. The velocity at point P is $\vec{v}$, while at point P' it is $\vec{v}+d\vec{v}$. Then a Taylor-series expansion yields for the velocity at the neighboring point P':

$$\vec{v}+d\vec{v}=\vec{v}+\mathbf{D}\,d\vec{r}\,,$$

where $\mathbf{D}$ is the derivative tensor of the velocity field

$$\mathbf{D}=\mathrm{Grad}\,\vec{v}=\vec{v}\circ\nabla\,.$$

As for any second-order tensor, the derivative tensor can be divided to a symmetric and a skew-symmetric part:

$$\mathbf{S}=\frac{1}{2}(\vec{v}\circ\nabla+\nabla\circ\vec{v})\,, \tag{2.16}$$

$$\mathbf{\Omega}=\frac{1}{2}(\vec{v}\circ\nabla-\nabla\circ\vec{v})\,. \tag{2.17}$$

Thus the infinitesimal change in velocity can be written as:

$$d\vec{v}=\frac{1}{2}(\vec{v}\circ\nabla+\nabla\circ\vec{v})\,d\vec{r}+\frac{1}{2}(\vec{v}\circ\nabla-\nabla\circ\vec{v})\,d\vec{r}\,. \tag{2.18}$$

The skew-symmetric part can be decomposed further and expressed by its vector invariant:

$$\frac{1}{2}(\vec{v}\circ\nabla-\nabla\circ\vec{v})\,d\vec{r}=\frac{1}{2}[(d\vec{r}\nabla)\,\vec{v}-(d\vec{r}\,\vec{v})]=$$

$$=\frac{1}{2}[(\nabla\times\vec{v})\times d\vec{r}]=\frac{1}{2}\,\mathrm{curl}\,\vec{v}\times d\vec{r}\,. \tag{2.19}$$

As is well-known the angular velocity of a rotating rigid body is given by

$$\vec{\omega}=\frac{1}{2}\,\mathrm{curl}\,\vec{v}\,. \tag{2.20}$$

Thus the skew-symmetric part of Grad $\vec{v}$ can be related to the curl of fluid particles. For this reason $\mathbf{\Omega}$ is called the vorticity tensor of the flow.

Its matrix can be written easily based on its binary form:

$$\mathbf{\Omega}=\begin{bmatrix} 0 & \frac{1}{2}\left(\frac{\partial v_x}{\partial y}-\frac{\partial v_y}{\partial x}\right) & \frac{1}{2}\left(\frac{\partial v_x}{\partial z}-\frac{\partial v_z}{\partial x}\right) \\ \frac{1}{2}\left(\frac{\partial v_y}{\partial x}-\frac{\partial v_x}{\partial y}\right) & 0 & \frac{1}{2}\left(\frac{\partial v_y}{\partial z}-\frac{\partial v_z}{\partial y}\right) \\ \frac{1}{2}\left(\frac{\partial v_z}{\partial x}-\frac{\partial v_x}{\partial z}\right) & \frac{1}{2}\left(\frac{\partial v_z}{\partial y}-\frac{\partial v_y}{\partial z}\right) & 0 \end{bmatrix}. \tag{2.21}$$

The relationship between the vorticity tensor and the curl of the velocity field is expressed by the equation

$$\mathbf{\Omega}\,\mathrm{d}\vec{r}=\operatorname{curl}\vec{v}\times\mathrm{d}\vec{r}\,. \tag{2.22}$$

It is clear, that the skew-symmetric vorticity tensor transforms the vector $\mathrm{d}\vec{r}$ to a vector perpendicular to itself.

The symmetric part of the derivative tensor of the velocity field cannot be related to either a translation, or a rigid-body like rotation. Thus this can be thought of as a quantity, which expresses the difference between the flow of the fluid and the motion of a rigid body. This type of motion is the deformation, which can be both dilation and deformation of shape.

Cauchy was the first to recognize that fluid flow can be decomposed into the sum of three components:

1. A pure uniform translation with velocity $\vec{v}$;
2. An average rigid body-like angular rotation with angular velocity $\vec{w}$;
3. A deformation, with velocity $\vec{v}_{\mathrm{def}}=\mathbf{S}\,\mathrm{d}\vec{r}$.

Let us now consider in more detail the velocity of deformation. It is the product of the symmetric tensor $\mathbf{S}$ and the vector element of distance $\mathrm{d}\vec{r}$. The linear transformation between $\vec{v}_{\mathrm{def}}$ and $\mathrm{d}\vec{v}$ is expressed by the tensor $\mathbf{S}$. For this reason $\mathbf{S}$ is called the deformation tensor or the rate of strain tensor. Its matrix can be written as:

$$\mathbf{S}=\begin{bmatrix} \frac{\partial v_x}{\partial x} & \frac{1}{2}\left(\frac{\partial v_x}{\partial y}+\frac{\partial v_y}{\partial x}\right) & \frac{1}{2}\left(\frac{\partial v_x}{\partial z}+\frac{\partial v_z}{\partial x}\right) \\ \frac{1}{2}\left(\frac{\partial v_y}{\partial x}+\frac{\partial v_x}{\partial y}\right) & \frac{\partial v_y}{\partial y} & \frac{1}{2}\left(\frac{\partial v_y}{\partial z}+\frac{\partial v_z}{\partial y}\right) \\ \frac{1}{2}\left(\frac{\partial v_z}{\partial x}+\frac{\partial v_x}{\partial z}\right) & \frac{1}{2}\left(\frac{\partial v_z}{\partial y}\,\frac{\partial v_y}{\partial z}\right) & \frac{\partial v_z}{\partial z} \end{bmatrix}. \tag{2.23}$$

Since the tensor is symmetric it contains six independent quantities. Its principal diagonal represents the three linear strain rates. Their sum is the first scalar invariant of the deformation tensor. It can be seen that this is the divergence of the

velocity field which is a measure of the rate of change of dilation

$$\Theta = \operatorname{div} \vec{v} . \tag{2.24}$$

The three other symmetric element pairs express the rate of change of the distortion; in other words the rate of shear deformation. They have special importance for the construction of constitutive equations.

Truesdell has pointed out, that angular velocity is not the most comprehensive measure of the vorticity of any motion. He proposed to introduce a dimensionless parameter, the Truesdell number

$$\mathrm{T} = \sqrt{\frac{\boldsymbol{\Omega} : \boldsymbol{\Omega}}{\mathbf{S} : \mathbf{S}}} = \frac{\Omega}{\sqrt{2\mathbf{S} : \mathbf{S}}} . \tag{2.25}$$

For irrotational flows $\boldsymbol{\Omega} = 0$, but $\mathbf{S} \neq 0$. In this case $\mathrm{T} = 0$.

For a rotating rigid body $\mathbf{S} = 0$, $\boldsymbol{\Omega} \neq 0$, thus $\mathrm{T} = 0$.

For the pure translation of a rigid body $\mathrm{T} = 0/0$, an indeterminate expression. In general all fluid flows can be characterized by a Truesdell number within the range $0 \leqq \mathrm{T} < \infty$.

2.5 Rotational motion, vorticity field

As was shown, the total motion of a fluid particle may be considered to represent the sum of three components: a translation, an angular rotation and a deformation. The vector, which is equal to twice the angular velocity of the particle, is called the vorticity vector after Helmholtz. The vorticity vector is the curl of the velocity field

$$\vec{\Omega} = \operatorname{curl} \vec{v} = \nabla \times v . \tag{2.26}$$

The angular rotation vector may be considered a derivative of the velocity field, forming a vector field itself. The vorticity field

$$\vec{\Omega} = \vec{\Omega}(\vec{r}, t) ,$$

can be represented by vortex lines, which are tangential to the vorticity vectors at all points.

The vortex lines can be determined from the equation

$$\vec{\Omega} \times \mathrm{d}\vec{r} = 0 , \tag{2.27}$$

or

$$\operatorname{curl} \vec{v} \times \mathrm{d}\vec{r} = 0 ,$$

where $\mathrm{d}\vec{r}$ is the vectorial element of arc length. Since $\vec{\Omega}$ and $\mathrm{d}\vec{r}$ are parallel, their vector product is necessarily zero. The instantaneous axes of rotation of fluid particles are tangential vortex lines. Since the axes of rotation change with time, the shape of the vortex lines will also change.

A vortex tube may be defined as the surface swept out by the vortex lines passing through a given closed curve. The intensity of the vortex tube is determined by the flux of the vorticity vector at any cross-section.

A well-known identity of vector analysis is

$$\operatorname{div}(\operatorname{curl}\vec{v})=0\,, \tag{2.28}$$

or

$$\nabla(\nabla\times\vec{v})=0\,.$$

Consider a vortex tube as shown in *Fig. 2.9*. Let the volume V be an arbitrary finite region of the vortex tube. It readily follows that

$$\int_V \operatorname{div}\operatorname{curl}\vec{v}\,\mathrm{d}V=0\,.$$

Using Gauss's divergence theorem

$$\int_V \operatorname{div}\operatorname{curl}\vec{v}\,\mathrm{d}V=\int_{(A)}\operatorname{curl}\vec{v}\,\mathrm{d}\vec{A}\,. \tag{2.29}$$

The total closed surface (A) which bounds the volume V, consists of the vortex tube cross-sections A_1 and A_2, plus the vortex tube wall A_3. Since surface A_3 is a vortex surface curl $\vec{v}$ and $\mathrm{d}\vec{A}$ are mutually perpendicular, and, thus their scalar product vanishes. Since the normals to the surfaces at A_1 and A_2 are opposite, the sign of the surface integrals over A_1 and A_2 will be opposite,

$$\int_{A_2}\operatorname{curl}\vec{v}\,\mathrm{d}\vec{A}-\int_{A_1}\operatorname{curl}\vec{v}\,\mathrm{d}\vec{A}=0\,. \tag{2.30}$$

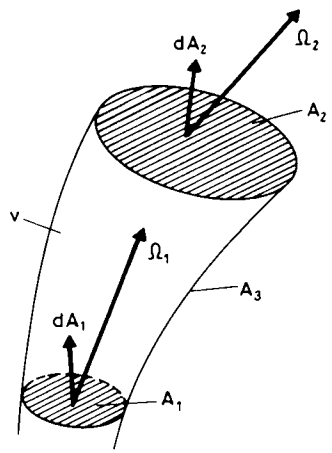

Fig. 2.9. Vortex tube

This equation expresses the second Helmholtz theorem: the intensity of a vortex tube remains constant as the tube moves with the fluid.

For an infinitesimal vortex tube this statement is especially significant. In this case

$$\operatorname{curl} \vec{v}_1 \mathrm{d}\vec{A}_1 = \operatorname{curl} \vec{v}_2 \mathrm{d}\vec{A}_2 , \tag{2.31}$$

or

$$\vec{\Omega}_1 \mathrm{d}\vec{A}_1 = \Omega_2 \mathrm{d}\vec{A}_2 . \tag{2.32}$$

A direct consequence of the above is that the narrower the vortex tube, the greater the angular velocity of the particles in it.

The identity div curl $\vec{v} = 0$ expresses the fact that the vorticity field is solenoidal. If this is the case, then the vortex lines or the vortex tube are either closed curves, or else extend to the boundary of the flowing fluid.

We wish to emphasize, that Helmholtz's theorem is valid only for an instantaneous state of the flow. The change with time can be determined using the methods of dynamics.

The strength of a vortex tube cannot be measured directly at a particular point, as is possible for the vorticity vector. In contrast, velocity measurements can be carried out relative easily, while the relationship between the strength of the vortex tube and the velocity distribution is readily determined. The circulation is one of the most important concepts of fluid mechanics which is suitable to express the above relationship.

The circulation around any closed curve in the fluid is defined by the integral

$$\Gamma = \int_{(G)} \vec{v} \mathrm{d}\vec{r} . \tag{2.33}$$

In Cartesian coordinates

$$\Gamma = \int_{(G)} (v_x \mathrm{d}x + v_y \mathrm{d}y + v_z \mathrm{d}z) . \tag{2.34}$$

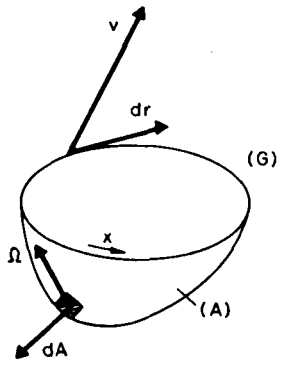

Fig. 2.10. Circulation along a closed curve

For a closed curve (G) Stokes's theorem gives

$$\Gamma = \int_{(G)} \vec{v} \mathrm{d}\vec{r} = \int_{A} \operatorname{curl} \vec{v} \mathrm{d}\vec{A} = \int_{A} \vec{\Omega} \mathrm{d}\vec{A} . \tag{2.35}$$

Thus the circulation along a closed curve (G) is the vorticity discharge through any surface A bounded by (G) (see *Fig. 2.10*). Note, that the convex side of the surface is positive, the outward surface normal on this side is chosen to be positive. The positive direction around (G) is taken as the direction of rotation of a right-handed screw. In a plane this means a counterclockwise direction.

Irrotational flow, velocity potential

A very important special case of fluid flow is that of irrotational flow, where

$$\operatorname{curl} \vec{v} = 0 . \tag{2.36}$$

Consider the well-known identity of vector analysis

$$\operatorname{curl} \operatorname{grad} \Phi = 0 , \tag{2.37}$$

or

$$\nabla \times \nabla \Phi = 0 .$$

It is obvious, that the irrotational velocity field can be expressed as the gradient of a scalar point function

$$\vec{v} = \operatorname{grad} \Phi . \tag{2.38}$$

The function $\Phi(\vec{r}, t)$ is termed the velocity potential. It can be shown to be given by

$$\Phi - \Phi_0 = \int_{S} \operatorname{grad} \Phi \, \mathrm{d}\vec{r} = \int_{S} \vec{v} \mathrm{d}\vec{r} , \tag{2.39}$$

where Φ_0 is an appropriate additive constant. The surfaces

$$\Phi(\vec{r}, t) = \text{const.},$$

are called level surfaces of the field or equipotential surfaces. Velocity vectors are perpendicular to equipotential surfaces.

2.6 Relationships between the acceleration- and the vorticity fields

Important relationships can be obtained for the fluid flow by examining some of the obvious identities relating to the acceleration, vorticity, dilatation and shape deformation. As is well-known, acceleration can be written as:

$$\vec{a} = \frac{\mathrm{d}\vec{v}}{\mathrm{d}t} = \frac{\partial v}{\mathrm{d}t} + (\vec{v}\nabla)\,\vec{v} . \tag{2.40}$$

The convective term may be further subdivided using the identity

$$(\vec{v}\nabla)\,\vec{v} = \operatorname{curl}\vec{v}\times\vec{v} + \operatorname{grad}\frac{v^2}{2}. \tag{2.41}$$

After substitution the divergence of the acceleration may be expressed as:

$$\operatorname{div}\vec{a} = \operatorname{div}\left(\frac{\partial\vec{v}}{\partial t}\right) + \operatorname{div}(\operatorname{curl}\vec{v}\times\vec{v}) + \operatorname{div}\operatorname{grad}\left(\frac{v^2}{2}\right). \tag{2.42}$$

Since the operations $\frac{\partial\ldots}{\partial t}$ and div are independent, the order of these operations may be reversed, i.e.

$$\operatorname{div}\vec{a} = \frac{\partial}{\partial t}(\operatorname{div}\vec{v}) + \operatorname{div}(\operatorname{curl}\vec{v}\times\vec{v}) + \Delta\frac{v^2}{2}. \tag{2.43}$$

A well-known identity of vector analysis is

$$\operatorname{div}(\operatorname{curl}\vec{v}\times\vec{v}) = \vec{v}\operatorname{curl}\operatorname{curl}\vec{v} - \operatorname{curl}\vec{v}\operatorname{curl}\vec{v}. \tag{2.44}$$

Substituting this into Eq. (2.43) we obtain

$$\operatorname{div}\vec{a} = \frac{\partial(\operatorname{div}\vec{v})}{\partial t}\vec{v}\operatorname{curl}\operatorname{curl}\vec{v} - \operatorname{curl}\vec{v}\operatorname{curl}\vec{v} + \Delta\frac{v^2}{2}. \tag{2.45}$$

Another form may be obtained by starting from the equation:

$$\vec{a} = \frac{\partial\vec{v}}{\partial t} + (\operatorname{Grad}\vec{v})\,\vec{v} = \frac{\partial\vec{v}}{\partial t} + (\vec{v}\circ\nabla)\,\vec{v}. \tag{2.46}$$

By taking the divergence of the above expression we get

$$\operatorname{div}\vec{a} = \frac{\partial(\operatorname{div}\vec{v})}{\partial t} + \mathbf{S}:\mathbf{S} - \boldsymbol{\Omega}:\boldsymbol{\Omega}, \tag{2.47}$$

where $\mathbf{S}:\mathbf{S}$ and $\boldsymbol{\Omega}:\boldsymbol{\Omega}$ denote scalar or inner product of tensors.

This is clearly a relationship between the acceleration on the one side and the dilatation, the deformation and the vorticity on the other. This equation can be written in terms of the Truesdell number as

$$\operatorname{div}\vec{a} = \frac{\mathrm{d}}{\mathrm{d}t}(\operatorname{div}\vec{v}) + (1 - T^2)\,\mathbf{S}:\mathbf{S}. \tag{2.48}$$

These kinematical relationships will assume an important role in the dynamics of flow.

2.7 The transport theorem: the material derivative of a volume integral over a volume of flowing fluid

In general terms flow variables which describe the motion of the continuum are functions only of position and time. The governing laws of mechanics on the other hand relate to a material system, a region of the flowing fluid with a fixed identity. Extensive variables of the system can be expressed as volume integrals of some point functions over a flowing fluid volume. The rate of change of such a quantity is the material derivative of the integral over a volume changing with time.

If the control volume of the integration is fixed in space, the order of differentiation and integration can be inverted. Let $\Psi(\vec{r}, t)$ be any continuously differentiable scalar or vector point function in the region $V(\vec{r})$. Thus we have

$$\frac{\partial}{\partial t}\int_V \Psi \mathrm{d}V = \int_V \frac{\partial \Psi}{\partial t}\mathrm{d}V. \tag{2.49}$$

For a material volume the order of differentiation and integration cannot be inverted in this manner.

Let $V(\vec{r}, t)$ denote an arbitrarily chosen volume which is moving with the flowing fluid. It is constituted of the same identifiable particles. Thus $V(\vec{r}, t)$ is obtained as

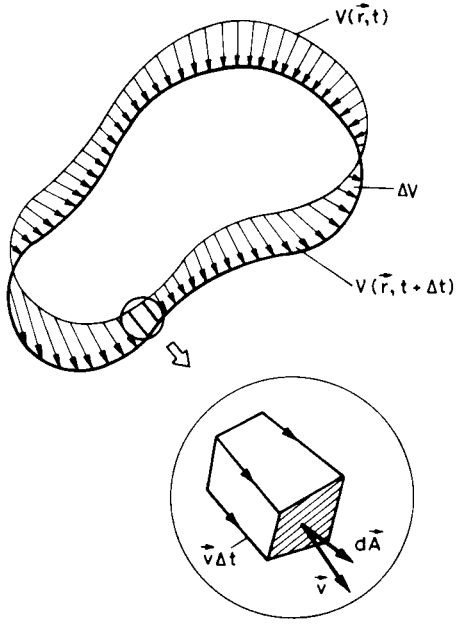

Fig. 2.11. Material volume in the flowing fluid

successive configurations of these particles. It is assumed that any point function $\Psi(\vec{r}, t)$ is continuous, differentiable and single-valued throughout the finite region $V(\vec{r}, t)$, bounded by the closed surface (A). In *Fig. 2.11* we have shown a volume at times t and $t+\Delta t$ as it moves and deforms in space. The volume and point function are shown at two consecutive instants separated by the interval Δt. $V(\vec{r}, t)$ and $\Psi(\vec{r}, t)$, are interdependent with $V(\vec{r}, t+\Delta t)$ and $\Psi(\vec{r}, t+\Delta t)$. Thus the following volume integrals are obtained:

$$\int_{V(\vec{r}, t)} \Psi(\vec{r}, t)\,\mathrm{d}V, \qquad \text{and} \qquad \int_{V(\vec{r}, t+\Delta t)} \Psi(\vec{r}, t+\Delta t)\,\mathrm{d}V.$$

These represent discrete instantaneous values. The time derivative we seek is given by:

$$\frac{\mathrm{d}}{\mathrm{d}t}\int_V \Psi \mathrm{d}V = \lim_{\Delta t \to 0} \frac{1}{\Delta t}\left[\int_{V(\vec{r}, t+\Delta t)} \Psi(\vec{r}, t+\Delta t)\,\mathrm{d}V - \int_{V(\vec{r}, t)} \Psi(\vec{r}, t)\,\mathrm{d}V\right]. \quad (2.50)$$

This can be written as:

$$\frac{\mathrm{d}}{\mathrm{d}t}\int_V \Psi \mathrm{d}V = \lim_{\Delta t \to 0} \frac{1}{\Delta t}\left[\int_{V(\vec{r}, t+\Delta t)} \Psi(\vec{r}, t+\Delta t)\,\mathrm{d}V - \right.$$

$$\left. - \int_{V(\vec{r}, t+\Delta t)} \Psi(\vec{r}, t)\,\mathrm{d}V + \int_{V(\vec{r}, t+\Delta t)} \Psi(\vec{r}, t)\,\mathrm{d}V - \int_{V(\vec{r}, t)} \Psi(\vec{r}, t)\,\mathrm{d}V\right].$$

It is clear, that the limits of integration of the first and second term in the right-hand side are the same. Since the limits of integration are independent of Δt, the limit can be taken inside the integral sign. It is also evident that $\Psi(\vec{r}, t+\Delta t)$ and $\Psi(\vec{r}, t)$ are evaluated at the same points in space so that the integrand is the partial derivative w.r.t. time of Ψ:

$$\int_{V(\vec{r}, t+\Delta t)} \lim_{\Delta t \to 0} \frac{\Psi_{(\vec{r}, t+\Delta t)} - \Psi_{(\vec{r}, t)}}{\Delta t}\,\mathrm{d}V = \int_V \frac{\partial \Psi}{\partial t}\,\mathrm{d}V.$$

Since the integrands of the third and fourth terms are the same, we may replace the two separate integrals by the integral over the difference of the two volumes:

$$\int_{V(\vec{r}, t+\Delta t)} \Psi(\vec{r}, t)\,\mathrm{d}V - \int_{V(\vec{r}, t)} \Psi(\vec{r}, t)\,\mathrm{d}V = \int_V \Psi(\vec{r}, t)\,\mathrm{d}V.$$

During the time interval Δt, the moving volume sweeps out and leaves behind the volume difference designated by ΔV in *Fig. 2.11*. The differential volume element of this region can obviously be expressed in terms of the velocity, the time

interval and the infinitesimal surface element:

$$\mathrm{d}V = \vec{V}\Delta t \cdot \mathrm{d}A\,.$$

This relationship allows us to express the volume integral as a surface integral. Since we can cancel Δt in the numerator and the denominator of the integrand, the latter will be independent of Δt. Thus the boundary limit of the integral remains the same:

$$\lim_{\Delta t \to 0} \frac{1}{\Delta t} \int_{\Delta V} \Psi \mathrm{d}V = \lim_{\Delta t \to 0} \frac{1}{\Delta t} \int_{(A)} \Psi \Delta t \cdot \vec{v} \mathrm{d}\vec{A} = \int_{(A)} \Psi \vec{v} \mathrm{d}\vec{A}\,.$$

Thus the rate of change of the total function integrated over a material volume $V(t)$ equals the rate of change of the total function Ψ integrated over the fixed volume V, which is an instantaneous configuration of $V(t)$, plus the flux $\Psi\vec{v}$ across the bounding surface. This is known as the transport theorem, originally stated by Euler:

$$\frac{\mathrm{d}}{\mathrm{d}t} \int_V \Psi \mathrm{d}V = \int_V \frac{\partial \Psi}{\partial t} \mathrm{d}V + \int_{(A)} \Psi \vec{v} \mathrm{d}\vec{A}\,. \tag{2.51}$$

This equation expresses for a given point function Ψ, a time derivative of an integral taken over a material volume, whose bounding surface moves with the velocity of the flow $\vec{v}$.

We can easily imagine a volume $V(t)$ bounded by the surface (A) moving with an arbitrary velocity $\vec{u}$. This velocity differs from the velocity $\vec{v}$ of the flowing particles of the fluid. It may be the speed of sound or even the propagation velocity of a shock surface. The integration over the volume will be material with respect to the velocity $\vec{U}$. Thus the material derivative of the integral which relates to the velocity $\vec{U}$ is:

$$\frac{\mathrm{d}_u}{\mathrm{d}t} \int_V \Psi \mathrm{d}V = \int_V \frac{\partial \Psi}{\partial t} \mathrm{d}V + \int_{(A)} \Psi \vec{U} \mathrm{d}\vec{A}\,. \tag{2.52}$$

In this way we can express material derivatives for each phase of a multicomponent system in terms of the velocities of the different phases. This is necessary in order to write balance equations for multicomponent media.

CHAPTER 3

BALANCE EQUATIONS

3.1 The principle of conservation of mass

The principle of conservation of mass states that the mass of a body is constant during its motion. This can be stated in the rate form as the rate of change with time of the mass of a body being zero. It is obvious that for a material system the above statement can be expressed mathematically.

Consider the volume $V(\vec{r}, t)$ flowing with the fluid. It is constituted of the same particles of fixed identity. The volume $V(\vec{r}, t)$ and its bounding surface $A(\vec{r}, t)$ vary in time representing successive configurations of the same fluid particles. This is illustrated in *Fig. 3.1.*

Let an infinitesimal volume element be located at a point P, characterized by the position vector $\vec{r}$, within the flowing volume under consideration. The scalar density point function $\varrho(\vec{r}, t)$ may be considered constant within this infinitesimal volume, thus the mass element is $\varrho \mathrm{d}V$. Since mass is an extensive variable, the total mass of the volume $V(\vec{r}, t)$ is the sum of the infinitesimal mass elements, thus it is the volume integral of the density over the volume $V(\vec{r}, t)$. The principle of conservation of mass can be expressed as the material derivative of this volume integral:

$$\frac{\mathrm{d}}{\mathrm{d}t} \int_{V_i} \varrho \mathrm{d}V = 0 . \tag{3.1}$$

Applying Euler's transport theorem this expression becomes:

$$\int_V \frac{\partial \varrho}{\partial t} \mathrm{d}V + \int_{(A)} \varrho \vec{v} \mathrm{d}\vec{A} = 0 . \tag{3.2}$$

Therefore, the sum of rate of change of mass within the fixed volume V, which is an instantaneous configuration of $V(t)$, and the mass flux $\varrho \vec{v}$ across the bounding surface of V is zero. The first term represents the local rate of change of mass within the fixed volume V. The surface integral represents the mass which crosses the bounding surface A. This convective mass flux equals the local rate of change of mass.

A conductive mass flux may also occur, primarily as the result of a concentration gradient. This is the so-called ordinary diffusion. The conductive mass flux $\vec{j}$ is

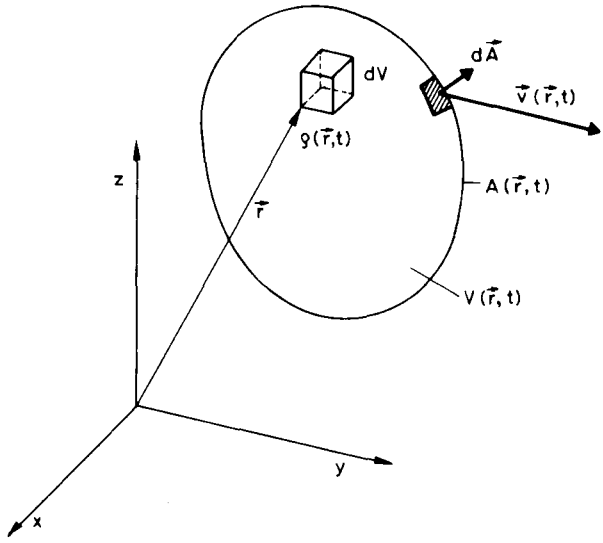

Fig. 3.1. Material volume of the flowing fluid

given by Fick's law

$$\vec{j} = -D \operatorname{grad} \varrho\,, \tag{3.3}$$

where D is the so-called diffusivity. This is one of the characteristic physical properties of the fluid, with dimensions [m²/s].

Within the volume V under consideration there may also be mass sources or sinks; for instance, the rate of mass produced within V by chemical reactions. (Note that conductive mass flux, sources and sinks relate only to some species of mass.) If this is the case the mass balance equation becomes

$$\int_V \frac{\partial \varrho_i}{\partial t}\,\mathrm{d}V + \int_{(A)} (\varrho_i \vec{v}_i - D_i \operatorname{grad} \varrho_i)\,\mathrm{d}\vec{A} = \int_V \xi_i \mathrm{d}V; \qquad i = 1, 2, \ldots n, \tag{3.4}$$

where ξ is the strength of the sources or sinks per unit volume. Either of these equations represents the mass balance equation for the i-th species. When all n equations are added together one obtains

$$\int_V \frac{\partial \varrho}{\partial t}\,\mathrm{d}V + \int_{(A)} \varrho \vec{v}\,\mathrm{d}\vec{A} = 0\,. \tag{3.5}$$

Since the total mass of the body is always constant, it is necessary for the conductive fluxes (the sum of the sources and the sinks), to vanished.

The conservation of mass equation may be rewritten in differential form. The term representing the surface integral may be transformed into a volume integral

by means of Gauss's divergence theorem:

$$\int_V \left[\frac{\partial \varrho}{\partial t} + \operatorname{div}(\varrho \vec{v})\right] \mathrm{d}V = 0 . \tag{3.6}$$

Since the limit of integration is arbitrary and ϱ and $\vec{v}$ are continuous functions with continuous derivatives, the integrand must be zero. Removing the integral signs we obtain the well-known continuity equation; the differential equation form of the law of conservation of mass:

$$\frac{\partial \varrho}{\partial t} + \operatorname{div}(\varrho \vec{v}) = 0 . \tag{3.7}$$

This equation can be expanded both for Cartesian, and cylindrical coordinates:

$$\frac{\partial \varrho}{\partial t} + \frac{\partial}{\partial x}(\varrho v_x) + \frac{\partial}{\partial y}(\varrho v_y) + \frac{\partial}{\partial z}(\varrho v_z) = 0 , \tag{3.8}$$

$$\frac{\partial \varrho}{\partial t} + \frac{1}{r}\frac{\partial}{\partial r}(r\varrho v_r) + \frac{1}{r}\frac{\partial}{\partial \varphi}(\varrho v_\varphi) + \frac{\partial}{\partial z}(\varrho v_z) = 0 . \tag{3.9}$$

The continuity equation may be transformed into

$$\frac{\partial \varrho}{\partial t} + \vec{v} \operatorname{grad} \varrho + \varrho \operatorname{div} \vec{v} = 0 . \tag{3.10}$$

It is clear that the first and second terms represent the local and the convective terms of the material derivative of the density field. Thus we obtain

$$\frac{\partial \varrho}{\partial t} + \varrho \operatorname{div} \vec{v} = 0 . \tag{3.11}$$

For a fluid of constant density, this equation reduces to

$$\operatorname{div} \vec{v} = 0 , \tag{3.12}$$

whether the flow is steady or not, i.e. whether or not the flow is locally time-dependent.

The principle of conservation of mass may be formulated in either integral or differential form. Both forms express the same physical principle. When applying the integral form it is important to remember that the enclosing surface A must be closed: it encloses a finite volume V of the space through which the fluid flows. Some parts of the boundary surface may consist of real material boundaries, such as pipe walls. Since solid walls are impervious the normal component of the velocity at the wall must be zero, i.e. here $\vec{v}\,\mathrm{d}\vec{A} = 0$. Thus a solid wall is always a stream surface. Sometimes the control volume V includes an immersed body which interrupts the continuity of the fluid as shown in *Fig. 3.2*. In this case the control volume is a multiply connected continuous region, and thus the continuity equa-

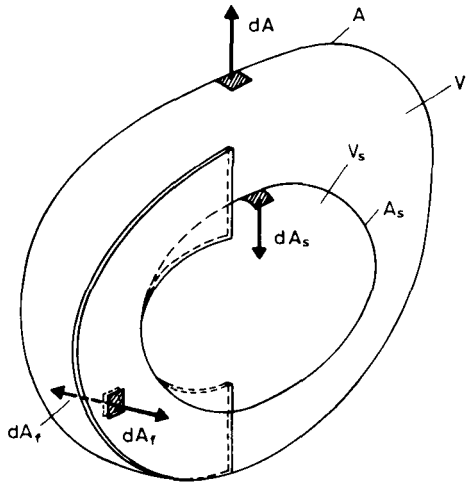

Fig. 3.2. Multiple connected material volume

tion cannot be written in the form of Eq. (3.2). The discontinuity within the fluid mass must be excluded by introducing an additional control surface (A_2) around its boundary, while it is also necessary to introduce a cut (A_3), which makes the volume V into a single connected region bounded by a single closed surface ($A+A_2+A_3$). In this manner formulas written in integral form may be rendered applicable to flows involving discontinuities. In general the integral form of a balance equation describes the relationship between certain quantities within a finite volume and across its bounding surface.

Differential balance equations on the other hand express the relationships for the derivatives of these quantities at a given point of the fluid. Most of the problems treated in this book make use of differential equations, but there are many cases in which application of the integral form is the more suitable.

3.2 The balance of momentum

Newton's second law of motion is perhaps the most important statement in the field of dynamics. As is well-known this states that the rate of change of the momentum of a body equals the sum of the external forces acting on it. To apply this law to a flowing material fluid system consider the volume V, bounded by the simple closed surface (A), made up of the identical particles of fixed identity. The momentum of an infinitesimal volume element of the fluid is $\varrho\vec{v}\,\mathrm{d}V$. Since the momentum is an extensive flow variable, the total momentum of the mass of fluid under consideration is the integral of the infinitesimal momentum over the material

volume V. The rate of change of momentum is obviously expressed by the material derivative of this volume integral.

The external forces acting on the fluid are of two types; body forces and surface forces. Body forces arise either from action at a distance such as the gravitational force or electromagnetic forces, or they occur by reason of the choice of an accelerating frame of reference, e.g. the centrifugal force or the Coriolis force. Such a body force is proportional to the mass, and may be represented by the vector $\vec{g}$ per unit mass. Summed over the volume it is the volume integral of $\varrho\vec{g}\,\mathrm{d}V$.

The surface forces are due to whatever medium is adjacent to the bounding surface (A), for example the solid wall of a pipeline or the adjacent fluid mass around a jet. The intensity of the surface forces acting on a unit surface is represented by the stress vector $\vec{t}$, thus the force acting on an infinitesimal surface area $\mathrm{d}\vec{A}$ is equal to $\vec{t}\,\mathrm{d}A$. The total surface force acting on the fluid inside (A) is the surface integral of $\vec{t}\,\mathrm{d}A$.

The mathematical terms the aboves becomes

$$\frac{\mathrm{d}}{\mathrm{d}t}\int_V \varrho\vec{v}\,\mathrm{d}V = \int_V \varrho\vec{g}\,\mathrm{d}V + \int_{(A)} \vec{t}\,\mathrm{d}A\,. \tag{3.13}$$

There is a further essential difference between body forces and surface forces. While $\vec{g}$ is a single-valued vector point function, the stress vector $\vec{t}$ can adopt infinitely many vectorial values at a given point for each orientation of the unit normal vector of the surface element $\mathrm{d}A$. The field of the stress vectors $\vec{t}$ is not a regular vector field. The stress vector is not a vector point function. It is a function of both the position vector $\vec{r}$ and the direction of the unit normal vector $\vec{n}$, thus

$$\vec{t} = \vec{t}(\vec{r}, t, \vec{n})\,. \tag{3.14}$$

In spite of this we shall express surface forces in the form of a point function. This is made possible by introducing the concept of the stress tensor.

Cauchy's theorem allows us to express the stress vector for a fixed value of $\vec{r}$ as $\vec{n}$ varies. Cauchy's theorem can be stated as follows: If the stress vectors acting across three mutually perpendicular planes at a given point are known, then all stress vectors at that point can be determined. They are given by the equation

$$\vec{t} = \mathbf{T}(\vec{r}, t)\cdot\vec{n}\,, \tag{3.15}$$

as linear functions of a Cartesian tensor of second order. This second-order tensor is independent of the unit normal vector of the surface. It is a tensor point function which determines the state of stress of the fluid. $\mathbf{T}$ is called the stress tensor. Equation (3.15) can be written in matrix form as

$$\begin{bmatrix} t_x \\ t_y \\ t_z \end{bmatrix} = \begin{bmatrix} T_{xx} & T_{xy} & T_{xz} \\ T_{yx} & T_{yy} & T_{yz} \\ T_{zx} & T_{zy} & T_{zz} \end{bmatrix} \begin{bmatrix} n_x \\ n_y \\ n_z \end{bmatrix}. \tag{3.16}$$

Examining this matrix equation it can be easily recognized how the matrix of the stress tensor maps the normal vector $\hat{n}$ into the stress vector $\vec{t}$. In this sense the stress tensor completely determines the state of stress. Knowing the components of the matrix the stress vector can be obtained for any arbitrary surface if its (unit) normal vector $\hat{n}$ is known. The components of the stress vector in the Cartesian reference frame are given by:

$$\vec{t}=(T_{xx}n_x+T_{xy}n_y+T_{xz}n_z)\,\vec{i}+(T_{yx}n_x+T_{yy}n_y+T_{yz}n_z)\,\vec{j}+ \\ +(T_{zx}n_x+T_{zy}n_y+T_{zz}n_z)\,\vec{k}\,. \tag{3.17}$$

As is shown in *Fig. 3.3* the first letter in the index of a stress tensor element designates the reference axes which is perpendicular to the plane in which the stress occurs. The second letter designates the direction of this component. The normal components T_{xx}, T_{yy}, and T_{zz} are the normal stresses the others, T_{xy}, $T_{xz}\ldots$, etc., are the shear stresses.

Applying Euler's transport theorem and replacing the stress vector by the stress tensor, the balance of momentum equation can be written as

$$\int_V \frac{\partial(\varrho\vec{v})}{\partial t}\,\mathrm{d}V+\int_{(A)}\varrho\vec{v}(\vec{v}\,\mathrm{d}\vec{A})=\int_V \varrho\vec{g}\,\mathrm{d}V+\int_{(A)}\mathbf{T}\,\mathrm{d}\vec{A}\,. \tag{3.18}$$

The first term on the left-hand side of the equation expresses the rate of change of momentum within the fixed volume V. The second term represents the convec-

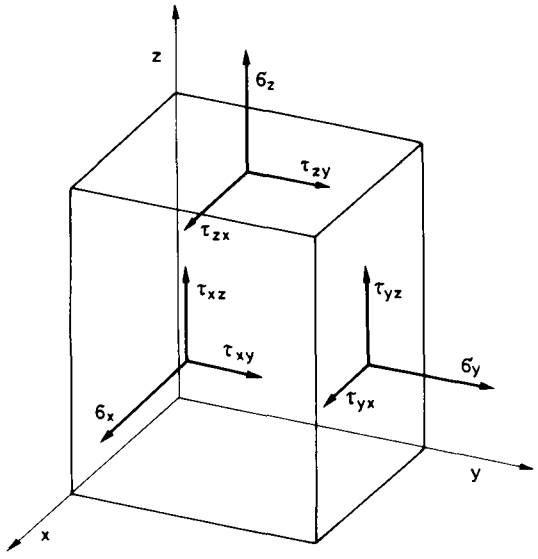

Fig. 3.3. Stress components on an infinitesimal fluid element

tive momentum flux which crosses the bounding surface of the fluid mass. On the right-hand side the first term represents the resultant body force while the second one represents the resultant of the surface forces acting on the bounding surface.

The balance of momentum equation may be rewritten in differential form. Its surface integrals may be transformed into volume integrals by means of the divergence theorem. We first apply this to the identity which relates to the convective momentum flux:

$$\int_{(A)} \varrho \vec{v}(\vec{v}\, \mathrm{d}\vec{A}) = \int_{(A)} \varrho(\vec{v} \circ \vec{v})\, \mathrm{d}\vec{A}\,. \tag{3.19}$$

Thus we obtain

$$\int_{V} \left[\frac{\partial(\varrho \vec{v})}{\partial t} + \mathrm{Div}\,(\varrho \vec{v} \circ \vec{v})\right] \mathrm{d}V = \int_{V} (\varrho \vec{g} + \mathrm{Div}\,\mathbf{T})\, \mathrm{d}V\,. \tag{3.20}$$

Since the limits of integration are arbitrary and the integrands are continuous functions with continuous derivatives, the integral signs may be removed, yielding the differential equation

$$\frac{\partial(\varrho \vec{v})}{\partial t} + \mathrm{Div}\,(\varrho \vec{v} \circ \vec{v}) = \varrho \vec{g} + \mathrm{Div}\,\mathbf{T}\,. \tag{3.21}$$

The total rate of change of the momentum within the unit volume equals the external forces acting on it. The local and the convective derivatives of the momentum can be clearly recognized on the left-hand side. Of interest is the second term on the right-hand side of the equation, which represents the resultant of the surface forces acting on a unit volume of the flowing fluid. This resultant surface force is a vector point function which depends only on the position vector and time. It is independent of either the chosen coordinate system or the shape of the unit volume. Div $\mathbf{T}$ forms a vector field in contrast to the stress vector $\vec{t}$ which is also a function of the unit normal vector. The divergence of the stress tensor field expresses the inhomogeneity of the state of stress of the flowing fluid.

Let us examine a further physical property of the stress tensor. The momentum equation may be written as

$$\frac{\partial(\varrho \vec{v})}{\partial t} + \mathrm{Div}\,(\varrho \vec{v} \circ \vec{v} - \mathbf{T}) = \varrho \vec{g}\,. \tag{3.22}$$

The terms representing the local and the convective momentum flux are easily recognized. In this form the physical meaning of the stress tensor is very obvious: the stress tensor $\mathbf{T}$ represents the conductive flux of the momentum. This conductive momentum flux is transported by virtue of molecular motion, i.e. the continual random interchange of molecules between adjacent fluid elements produces a transfer of momentum. This phenomenon can be descripted by the laws of probability and the methods of statistics. From probability distributions it is possible to determine averages or mean values for such parameters as velocity, pressure, etc.

These mean values can then be related to the macroscopically measurable quantities. Molecular motion disperses the momentum. This tendency of equalization occurs macroscopically as a deterministic process. This is the reason why it is possible to give a phenomenological description of the conductive momentum flux in a continuum.

The idea of a momentum flux without accompanying macroscopic motion may be unfamiliar. Let us consider an example of this from the field of petroleum engineering. Imagine a pump connected to a pipeline. The pipeline-filling fluid is at rest. Starting the pump, the pressure increases, and the fluid flow accelerates quickly. Even if the velocity of the flowing fluid is about 1 m/s, the acceleration and the increase in pressure rising propagate as a wave throughout the pipeline with the speed of sound, some 1000 m/s. As the fluid mass starts to flow faster the momentum is transferred by convection, at the velocity of the flow. In this example the propagation of the pressure increase and the acceleration is carried out by means of conductive momentum transfer.

Cauchy's equation of motion

Equation (3.22) is valid for any fluid, and indeed for any continuous medium, regardless of whether mass is conserved or not. Taking into account the principle of conservation of mass, the equation of motion (Eq. 3.21) can be written in a simpler form. Expanding the derivatives of the products on the left-hand side we obtain:

$$\varrho \frac{\partial \vec{v}}{\partial t} + \vec{v} \frac{\partial \varrho}{\partial t} + \vec{v} V(\varrho \vec{v}) + \varrho (\vec{v} V) \vec{v} = \varrho \vec{g} + \operatorname{Div} \mathbf{T} . \tag{3.23}$$

The second and the third terms on the left-hand side vanish on account of the continuity equation. Dividing by the density, a very simple and elegant equation is obtained:

$$\frac{\mathrm{d}\vec{v}}{\mathrm{d}t} = \vec{g} + \frac{1}{\varrho} \operatorname{Div} \mathbf{T} . \tag{3.24}$$

This is Cauchy's equation of motion which expresses the balance of momentum for a unit fluid mass. The scalar components of Cauchy's equation in Cartesian coordinates can be easily written as

$$\begin{aligned}
\frac{\partial v_x}{\partial t} + v_x \frac{\partial v_x}{\partial x} + v_y \frac{\partial v_x}{\partial y} + v_z \frac{\partial v_x}{\partial z} &= g_x + \frac{1}{\varrho} \left(\frac{\partial \sigma_x}{\partial x} + \frac{\partial \tau_{xy}}{\partial y} + \frac{\partial \tau_{xz}}{\partial z} \right), \\
\frac{\partial v_y}{\partial t} + v_x \frac{\partial v_y}{\partial x} + v_y \frac{\partial v_y}{\partial y} + v_z \frac{\partial v_y}{\partial z} &= g_y + \frac{1}{\varrho} \left(\frac{\partial \tau_{yx}}{\partial x} + \frac{\partial \sigma_y}{\partial y} + \frac{\partial \tau_{yz}}{\partial z} \right), \\
\frac{\partial v_z}{\partial t} + v_x \frac{\partial v_z}{\partial x} + v_y \frac{\partial v_z}{\partial y} + v_z \frac{\partial v_z}{\partial z} &= g_z + \frac{1}{\varrho} \left(\frac{\partial \tau_{zx}}{\partial x} + \frac{\partial \tau_{zy}}{\partial y} + \frac{\partial \sigma_z}{\partial z} \right).
\end{aligned} \tag{3.25}$$

In cylindrical coordinates:

$$\frac{\partial v_r}{\partial t}+v_r\frac{\partial v_r}{\partial r}+\frac{v_\varphi}{r}\frac{\partial v_r}{\partial \varphi}-\frac{v_\varphi^2}{r}+v_z\frac{\partial v_r}{\partial z}=$$

$$=g_r+\frac{1}{\varrho}\left(\frac{1}{r}\frac{\partial}{\partial r}(r\sigma_r)+\frac{1}{r}\frac{\partial \tau_{\varphi r}}{\partial \varphi}-\frac{\tau_{\varphi\varphi}}{r}+\frac{\partial \tau_{zr}}{\partial z}\right), \tag{3.26}$$

$$\frac{\partial v_\varphi}{\partial t}+v_r\frac{\partial v_\varphi}{\partial r}+\frac{v_\varphi}{r}\frac{\partial v_\varphi}{\partial \varphi}+\frac{v_r v_\varphi}{r}+v_z\frac{\partial v_\varphi}{\partial z}=$$

$$=g_\varphi+\frac{1}{\varrho}\left(\frac{1}{r^2}\frac{\partial}{\partial r}(r^2\tau_{r\varphi})+\frac{1}{r}\frac{\partial \sigma_\varphi}{\partial \varphi}+\frac{\partial \tau_{z\varphi}}{\partial z}\right), \tag{3.27}$$

$$\frac{\partial v_z}{\partial t}+v_r\frac{\partial v_z}{\partial r}+\frac{v_\varphi}{r}\cdot\frac{\partial v_z}{\partial \varphi}+v_z\frac{\partial v_z}{\partial z}=$$

$$=g_z+\frac{1}{\varrho}\left(\frac{1}{r}\frac{\partial(r\tau_{rz})}{\partial r}+\frac{1}{r}\frac{\partial \tau_{\varphi z}}{\partial \varphi}+\frac{\partial \sigma_z}{\partial z}\right) \tag{3.27a}$$

This system of partial differential equations is the so-called stress equation of motion. There are many types of fluids with many different types of stress tensor. Thus we have equations of motion for inviscid fluids (Euler's equation), for linearly viscous fluids (Navier—Stokes equation) and further types of equations for the great variety of non-Newtonian fluids.

Invoking the principle of the conservation of mass does not place any restriction on the general applicability of Cauchy's equation to a homogeneous one-phase flow. In multicomponent systems mass transfer may be important, thus the equation of motion for any phase must be used in the form of Eq. (3.22).

3.3 The balance of angular momentum

The principle of conservation of angular momentum belongs to the axioms of mechanics. In spite of its general validity it has been largely neglected in textbooks written for petroleum engineers. The treatment of the equation for the balance of angular momentum is usually restricted to the verification of the theorem of symmetry of the stress tensor. Nevertheless the balance of angular momentum equation is of great value in solving flow problems where torques are more significant than forces, e.g. in turbomachinery as it is shown in Csanády's excellent book.

The principle of conservation of angular momentum states that the rate of change of angular momentum of a material volume of fluid V equals the resultant torque exerted by any external forces on this volume of fluid. In order to discuss this statement in more detail, consider an arbitrary material volume V bounded by the closed surface (A), which is moving with the fluid. Let $\vec{r}$ denote the position vector of an arbitrary point within the volume. At this point the infinitesimal mass

element $\varrho\,\mathrm{d}V$ has an angular momentum, relative to the origin of the coordinate system, of $\vec{r}\times\varrho\vec{v}\,\mathrm{d}V$; the torque due the body forces is $\vec{r}\times\varrho\vec{g}\,\mathrm{d}V$, and the torque due the surface forces is $\vec{r}\times\mathbf{T}\,\mathrm{d}\vec{A}$. Taking the substantial derivative of the volume integral of the angular momentum over the material volume V, and integrating the torques over V and (A) we get the equation

$$\frac{\mathrm{d}}{\mathrm{d}t}\int_V \vec{r}\times\varrho\vec{v}\,\mathrm{d}V=\int_V \vec{r}\times\varrho\vec{g}\,\mathrm{d}V+\int_{(A)}\vec{r}\times\mathbf{T}\,\mathrm{d}\vec{A}\,. \tag{3.28}$$

Its left-hand side may be transformed as follows:

$$\frac{\mathrm{d}}{\mathrm{d}t}\int_V \vec{r}\times\varrho\vec{v}\,\mathrm{d}V=\int_V\left[\frac{\mathrm{d}}{\mathrm{d}t}(\vec{r}\times\varrho\vec{v})+(\vec{r}\times\varrho\vec{v})\,\mathrm{div}\,\vec{v}\right]\mathrm{d}V=$$

$$=\int_V\frac{\partial\vec{r}}{\partial t}\times\varrho\vec{v}+\vec{r}\times\varrho\frac{\partial\vec{v}}{\partial t}+(\vec{r}\times\vec{v})\left(\frac{\partial\varrho}{\partial t}+\varrho\,\mathrm{div}\,\vec{v}\right)\mathrm{d}V. \tag{3.29}$$

The first term on the right-hand side represents the cross product of parallel vectors (since $\vec{v}=\mathrm{d}\vec{r}/\mathrm{d}t$), and thus vanishes. It is easy to recognize the continuity equation in the third and fourth terms on the right-hand side and thus their sum must also be zero. By this means

$$\frac{\mathrm{d}}{\mathrm{d}t}\int_V \vec{r}\times\varrho\vec{v}\,\mathrm{d}V=\int_V\vec{r}\times\varrho\frac{\partial\vec{v}}{\partial t}\mathrm{d}V. \tag{3.30}$$

Applying the divergence theorem the surface integral can be written as

$$\int_{(A)}\vec{r}\times\mathbf{T}\,\mathrm{d}\vec{A}=\int_V(\vec{r}\otimes\mathbf{T})V\mathrm{d}V\,. \tag{3.31}$$

This volume integral contains a relative rare operation within the brackets: the tensorial product of a vector and a second-order tensor. The quantity $(\vec{r}\times\mathbf{T})$ is a tensor of second-order, its divergence is naturally a vector. To construct the matrix of the tensor $(\vec{r}\times\mathbf{T})$ we may determine its columns, multiplying $(\vec{r}\times\mathbf{T})$ by the unit vectors $\vec{i}$, $\vec{j}$, and $\vec{k}$:

$$\begin{aligned}(\vec{r}\times\mathbf{T})\,\vec{i}&=\vec{r}\times\mathbf{T}\vec{i},\\(\vec{r}\times\mathbf{T})\,\vec{j}&=\vec{r}\times\mathbf{T}\vec{j},\\(\vec{r}\times\mathbf{T})\,\vec{k}&=\vec{r}\times\mathbf{T}\vec{k}\,.\end{aligned} \tag{3.32}$$

Let us complete the products in detail:

$$\mathbf{T}\vec{i}=\begin{bmatrix}\sigma_x & \tau_{xy} & \tau_{xz}\\ \tau_{yx} & \sigma_y & \tau_{yz}\\ \tau_{zx} & \tau_{zy} & \sigma_z\end{bmatrix}\begin{bmatrix}1\\0\\0\end{bmatrix}=\sigma_x\vec{i}+\tau_{yx}\vec{j}+\tau_{zx}\vec{k}\,. \tag{3.33}$$

Similarly we get:

$$\mathbf{T}\vec{j}=\tau_{xy}\vec{i}+\sigma_y\vec{j}+\tau_{zy}\vec{k}\,, \tag{3.34}$$

and,

$$\mathbf{T}\vec{k}=\tau_{xz}\vec{i}+\tau_{yz}\vec{j}+\sigma_z\vec{k}\,. \tag{3.35}$$

After this we may determine the cross products of $\vec{r}\times\mathbf{T}\vec{i}$, $\vec{r}\times\mathbf{T}\vec{j}$ and $\vec{r}\times\mathbf{T}\vec{k}$ as follows:

$$\vec{r}\times\mathbf{T}\vec{i}=\begin{bmatrix}\vec{i} & \vec{j} & \vec{k}\\ x & y & z\\ \sigma_x & \tau_{yx} & \tau_{zx}\end{bmatrix}=(y\tau_{zx}-z\tau_{yx})\vec{i}+(z\sigma_x-x\tau_{zx})\vec{j}+(x\tau_{yx}-y\sigma_x)\vec{k}\,. \tag{3.36}$$

In the same way we obtain

$$\vec{r}\times\mathbf{T}\vec{j}=(y\tau_{zy}-z\sigma_y)\vec{i}+(z\tau_{xy}-x\tau_{zy})\vec{j}+(x\sigma_y-y\tau_{xy})\vec{k}\,, \tag{3.37}$$

and,

$$\vec{r}\times\mathbf{T}\vec{k}=(y\sigma_z-z\tau_{yz})\vec{i}+(z\tau_{xz}-x\sigma_z)\vec{j}+(x\tau_{yz}-y\tau_{xz})\vec{k}\,. \tag{3.38}$$

Thus the matrix of the tensor $(\vec{r}\otimes\mathbf{T})$ can be written as

$$(\vec{r}\otimes\mathbf{T})=\begin{bmatrix} y\tau_{zx}-z\tau_{yx} & y\tau_{zy}-z\sigma_y & y\sigma_z-z\tau_{yz}\\ z\sigma_x-x\tau_{zx} & z\tau_{xy}-x\tau_{zy} & z\tau_{xz}-x\sigma_z\\ x\tau_{yx}-y\sigma_x & x\sigma_y-y\tau_{xy} & x\tau_{yz}-y\tau_{xz}\end{bmatrix}. \tag{3.39}$$

The divergence of this tensor is:

$$\begin{aligned}(\vec{r}\otimes\mathbf{T})\nabla=&\left[\frac{\partial}{\partial x}(y\tau_{zx}-z\tau_{yx})+\frac{\partial}{\partial y}(y\tau_{zy}-z\sigma_y)+\frac{\partial}{\partial z}(y\sigma_z-z\tau_{yz})\vec{i}+\right.\\ &+\frac{\partial}{\partial x}(z\sigma_x-x\tau_{zx})+\frac{\partial}{\partial y}(z\tau_{xy}-x\tau_{zy})+\left.\frac{\partial}{\partial z}(z\tau_{xz}-x\sigma_z)\right]\vec{j}+\\ &+\left[\frac{\partial}{\partial x}(x\tau_{yx}-y\sigma_x)+\frac{\partial}{\partial y}(x\sigma_y-y\tau_{xy})+\frac{\partial}{\partial z}(x\tau_{yz}-y\tau_{xz})\right]\vec{k}\,.\end{aligned} \tag{3.40}$$

Completing the calculations we get:

$$\begin{aligned}(\vec{r}\otimes\mathbf{T})\nabla=\mathrm{Div}\,(\vec{r}\otimes\mathbf{T})=&\left(y\frac{\partial\tau_{zx}}{\partial x}-z\frac{\partial\tau_{yx}}{\partial x}+\tau_{zy}+y\frac{\partial\tau_{zy}}{\partial y}-z\frac{\partial\sigma_y}{\partial y}+y\frac{\partial\sigma_z}{\partial z}-\right.\\ &\left.-\tau_{yz}-z\frac{\partial\tau_{yz}}{\partial z}\right)\vec{i}+\left(z\frac{\partial\sigma_x}{\partial x}-\tau_{zx}-x\frac{\partial\tau_{zx}}{\partial z}+z\frac{\partial\tau_{zy}}{\partial y}-x\frac{\partial\tau_{zy}}{\partial y}+\right.\\ &\left.+\tau_{xz}+z\frac{\partial\tau_{xz}}{\partial z}-x\frac{\partial\sigma_z}{\partial z}\right)\vec{j}+\left(\tau_{yz}+x\frac{\partial\tau_{yx}}{\partial x}-y\frac{\partial\sigma_x}{\partial x}+x\frac{\partial\sigma_y}{\partial y}-\right.\\ &\left.-\tau_{xy}-y\frac{\partial\tau_{xy}}{\partial y}+x\frac{\partial\tau_{yz}}{\partial z}-y\frac{\partial\tau_{xz}}{\partial z}\right)\vec{k}\,.\end{aligned} \tag{3.41}$$

This expression is rather cumbersome in the above scalar form. The tensor form is more concise:

$$\mathrm{Div}\,(\vec{r}\otimes\mathbf{T}) = \vec{r}\times\mathrm{Div}\,\mathbf{T} + (\mathbf{T}\otimes\nabla)\vec{r}\,. \tag{3.42}$$

The first term of the right-hand side expresses the torque of the resultant of the surface forces acting on a unit volume of the fluid; the second term is an operation of the type where the tensorial operator $(\mathbf{T}\otimes\nabla)$ acts on the position vector $\vec{r}$, to produce an axial vector:

$$(\mathbf{T}\otimes\nabla)\vec{r} = (\tau_{zy}-\tau_{yz})\vec{i} + (\tau_{xz}-\tau_{zx})\vec{j} + (\tau_{yx}-\tau_{xy})\vec{k}\,. \tag{3.43}$$

Substituting into the angular momentum equation we obtain:

$$\int_V \vec{r}\times\left(\varrho\frac{\partial\vec{v}}{\partial t} - \varrho\vec{g} - \mathrm{Div}\,\mathbf{T}\right)\mathrm{d}V = \int_V (\mathbf{T}\otimes\nabla)\vec{r}\,\mathrm{d}V. \tag{3.44}$$

The sum within the brackets on the left-hand side can be recognized as representing the momentum equation which in this form equals zero. Thus the integrand on the right-hand side must also equal zero. This condition is satisfied when

$$\begin{aligned} \tau_{zy} &= \tau_{yz}\,, \\ \tau_{xz} &= \tau_{zx}\,, \\ \tau_{yx} &= \tau_{xy}\,. \end{aligned} \tag{3.45}$$

This means that the stress tensor is symmetric if the flowing fluid satisfies the continuity equation, the momentum equation and the angular momentum equation. The postulate of the symmetry of the stress tensor is equivalent to the determination of three scalar functions from three scalar eqations. If the stress tensor is symmetric the momentum equation and the angular momentum equation are not idependent, one of them may be chosen to solve a flow problem, the other is replaced by the postulate of symmetry.

3.4 The balance of kinetic energy

Let E_k denote the kinetic energy of a material volume:

$$E_k = \int_V \varrho\frac{v^2}{2}\,\mathrm{d}V. \tag{3.46}$$

Although the kinetic energy is an extensive variable it is not a quantity which is conserved. Thus the balance equation of kinetic energy does not express a conser-

vation law. It is not an axiom of mechanics and can be derived from the continuity and the momentum equations.

Using the transport theorem the rate of change of E_k can be written as:

$$\frac{\mathrm{d}}{\mathrm{d}t}\int_V \varrho\frac{v^2}{2}\,\mathrm{d}V=\int_V \frac{\mathrm{d}}{\mathrm{d}t}\left(\varrho\frac{v^2}{2}\right)\mathrm{d}V+\int_V \varrho\frac{v^2}{2}\operatorname{div}\vec{v}\,\mathrm{d}V. \tag{3.47}$$

The integrands of the right-hand side of the equation are readily obtained. Multiplying Cauchy's equation of motion by $\vec{v}$:

$$\varrho\vec{v}\frac{\mathrm{d}\vec{v}}{\mathrm{d}t}=\varrho\vec{g}\vec{v}+\vec{v}\operatorname{Div}\mathbf{T}. \tag{3.48}$$

By similarly multiplying the continuity equation by $\frac{v^2}{2}$:

$$\frac{v^2}{2}\cdot\frac{\mathrm{d}\varrho}{\mathrm{d}t}+\frac{v^2}{2}\varrho\operatorname{div}\vec{v}=0. \tag{3.49}$$

Adding the two equations we get

$$\varrho\vec{v}\frac{\mathrm{d}\vec{v}}{\mathrm{d}t}+\frac{v^2}{2}\frac{\mathrm{d}\varrho}{\mathrm{d}t}+\varrho\frac{v^2}{2}\operatorname{div}\vec{v}=\varrho\vec{g}\vec{v}+\vec{v}\operatorname{Div}\mathbf{T}. \tag{3.50}$$

From the chain rule it follows that:

$$\vec{v}\frac{\mathrm{d}\vec{v}}{\mathrm{d}t}=\frac{\mathrm{d}}{\mathrm{d}t}\left(\frac{v^2}{2}\right). \tag{3.51}$$

It is similarly obvious that

$$\varrho\frac{\mathrm{d}}{\mathrm{d}t}\left(\frac{v^2}{2}\right)+\frac{v^2}{2}\frac{\mathrm{d}\varrho}{\mathrm{d}t}=\frac{\mathrm{d}}{\mathrm{d}t}\left(\varrho\frac{v^2}{2}\right). \tag{3.52}$$

Thus Eq. (3.50) can be written as

$$\frac{\mathrm{d}}{\mathrm{d}t}\left(\varrho\frac{v^2}{2}\right)+\varrho\frac{v^2}{2}\operatorname{div}\vec{v}=\varrho\vec{g}\vec{v}+\vec{v}\operatorname{Div}\mathbf{T}. \tag{3.53}$$

Applying the identity

$$\operatorname{div}(\mathbf{T}\vec{v})=\vec{v}\operatorname{Div}\mathbf{T}+\mathbf{T}:\vec{v}\circ\nabla. \tag{3.54}$$

the following expression is obtained:

$$\frac{\mathrm{d}}{\mathrm{d}t}\left(\varrho\frac{v^2}{2}\right)+\varrho\frac{v^2}{2}\operatorname{div}\vec{v}=\varrho\vec{g}\vec{v}+\operatorname{div}(\mathbf{T}\vec{v})-\mathbf{T}:\vec{v}\circ\nabla. \tag{3.55}$$

This equation can be integrated over an arbitrary volume V to give

$$\int_V \frac{\mathrm{d}}{\mathrm{d}t}\left(\varrho \frac{v^2}{2}\right)\mathrm{d}V + \int_V \varrho \frac{v^2}{2}\operatorname{div}\vec{v}\,\mathrm{d}V = \int_V \varrho\vec{g}\vec{v}\,\mathrm{d}V + \\ + \int_V \operatorname{div}(\mathbf{T}\vec{v})\,\mathrm{d}V - \int_V \mathbf{T}:\vec{v}\circ\nabla\mathrm{d}V. \tag{3.56}$$

Applying the transport theorem to the left-hand side and the divergence theorem to the second integral on the right-hand side of the equation we get

$$\frac{\mathrm{d}}{\mathrm{d}t}\int_V \varrho\frac{v^2}{2}\mathrm{d}V = \int_V \varrho\vec{g}\vec{v}\,\mathrm{d}V + \int_{(A)} \vec{v}\mathbf{T}\,\mathrm{d}\vec{A} - \int_V \mathbf{T}:\vec{v}\circ\nabla\mathrm{d}V. \tag{3.57}$$

This equation states that the rate of change in kinetic energy of a moving material volume is equal to the rate at which work is being done on the volume by the body forces and the surface forces, diminished by a "dissipation" term involving the interaction of stress and deformation. This latter term must represent the rate at which work is being done in changing the volume and shape of the fluid body. A certain proportion of this power may be recoverable, but the rest must be accounted for as heat.

The local and the convective rate of change of the kinetic energy may also be separated applying the transport theorem

$$\int_V \frac{\partial}{\partial t}\left(\varrho\frac{v^2}{2}\right)\mathrm{d}V + \int_{(A)} \varrho\frac{v^2}{2}\vec{v}\,\mathrm{d}\vec{A} + \int_V \mathbf{T}:\vec{v}\circ\nabla\mathrm{d}V = \\ = \int_V \varrho\vec{g}\vec{v}\,\mathrm{d}V + \int_{(A)} \vec{v}\mathbf{T}\,\mathrm{d}A\,. \tag{3.58}$$

In this equation the first term on the left-hand side represents the rate of change of kinetic energy within the fixed volume V. The next term represents the convective kinetic energy flux which crosses the bounding surface of this volume. The third term represents the loss of kinetic energy. This rate of work is transformed into internal energy; this transformation of work into heat is irreversible.

The balance of kinetic energy equation can be also written in differential form. The material derivative of the specific kinetic energy may be separated into the local and the convective parts

$$\frac{\mathrm{d}}{\mathrm{d}t}\left(\varrho\frac{v^2}{2}\right) = \frac{\partial}{\partial t}\left(\varrho\frac{v^2}{2}\right) + \vec{v}\operatorname{grad}\left(\varrho\frac{v^2}{2}\right). \tag{3.59}$$

It should also be remembered that

$$\vec{v}\operatorname{grad}\left(\varrho\frac{v^2}{2}\right) + \frac{v^2}{2}\operatorname{div}\vec{v} = \operatorname{div}\left(\varrho\frac{v^2}{2}\vec{v}\right). \tag{3.60}$$

Substituting these into Eq. (3.55) we obtain

$$\frac{\partial}{\partial t}\left(\varrho\frac{v^2}{2}\right)+\operatorname{div}\left(\varrho\frac{v^2}{2}\vec{v}-\vec{v}\mathbf{T}\right)=\varrho\vec{g}\vec{v}-\mathbf{T}:\vec{v}\circ\nabla. \tag{3.61}$$

It is clear that the first term represents the local rate of change of the specific kinetic energy within a fixed unit volume. The divergence term includes the convective and the conductive kinetic energy fluxes. The terms on the right-hand side represent the sources and sinks of the kinetic energy. The power of the external forces gv refers to a source, the kinetic energy loss $\mathbf{T}:\vec{v}\circ\nabla$ reflects a sink.

Note that the balance of kinetic energy equation is a scalar equation in spite of the vector and tensor variables in it. In Cartesian coordinates we can write:

$$\begin{aligned}
&\frac{\partial}{\partial t}\left(\varrho\frac{v^2}{2}\right)+\frac{\partial}{\partial x}\left(\varrho\frac{v^2}{2}v_x-\sigma_x v_x-\tau_{xy}v_y-\tau_{xz}v_v\right)+\\
&+\frac{\partial}{\partial y}\left(\varrho\frac{v^2}{2}v_y-\tau_{yx}v_x-\sigma_y v_y-\tau_{yz}v_z\right)+\\
&+\frac{\partial}{\partial z}\left(\varrho\frac{v^2}{2}v_z-\tau_{zx}v_x-\tau_{zy}v_y-\sigma_z v_z\right)=\varrho(g_x v_x+g_y v_y+g_z v_z)-\\
&-\left(\sigma_x\frac{\partial v_x}{\partial x}+\tau_{xy}\frac{\partial v_x}{\partial y}+\tau_{xz}\frac{\partial v_x}{\partial z}+\tau_{yx}\frac{\partial v_y}{\partial x}+\sigma_y\frac{\partial v_y}{\partial y}+\right.\\
&\left.+\tau_{yz}\frac{\partial v_y}{\partial z}+\tau_{zx}\frac{\partial v_z}{\partial x}+\tau_{zy}\frac{\partial v_z}{\partial y}+\sigma_z\frac{\partial v_z}{\partial z}\right).
\end{aligned} \tag{3.62}$$

An important special case is that where the body forces form a conservative field, in which

$$\vec{g}=-\operatorname{grad}U. \tag{3.63}$$

The conservative field is steady, i.e.

$$\frac{\partial U}{\partial t}=0, \tag{3.64}$$

thus the material derivative of the potential is simply

$$\frac{\partial U}{\partial t}=\vec{v}\operatorname{grad}U. \tag{3.65}$$

The scalar function $U(\vec{r})$ is the potential energy of a unit fluid mass. It is an extensive variable, thus the total of the potential energy of a fluid mass within a volume V is

$$\mathcal{U}=\int_V \varrho U\,\mathrm{d}V. \tag{3.66}$$

It is easy to see that

$$\frac{\mathrm{d}}{\mathrm{d}t}\int_V \varrho U\,\mathrm{d}V = \int_V \varrho\frac{\mathrm{d}U}{\mathrm{d}t}\mathrm{d}V + \int_V \left(U\frac{\mathrm{d}\varrho}{\mathrm{d}t} + U\varrho\,\mathrm{div}\,\vec{v}\right)\mathrm{d}V. \tag{3.67}$$

Thus the rate of work done by external body forces may be expressed as the potential energy flux per unit time,

$$\int_V \varrho\vec{g}\vec{v}\,\mathrm{d}V = \frac{\mathrm{d}}{\mathrm{d}t}\int_V \varrho U\,\mathrm{d}V. \tag{3.68}$$

Substituting into Eq. (3.58) we obtain the balance of kinetic energy equation in a conservative field:

$$\frac{\mathrm{d}}{\mathrm{d}t}\int_V \left(\frac{v^2}{2}+U\right)\varrho\,\mathrm{d}V + \int_V \mathbf{T}:v\circ\nabla\mathrm{d}V = \int_{(A)} \vec{v}\mathbf{T}\,\mathrm{d}\vec{A}\,. \tag{3.69}$$

It can be seen that the rate of change of the sum of the kinetic and potential energy and the rate of conversion into internal energy equals the rate of work done by surface forces when the fluid flows in a potential field.

This is the general form of the balance of kinetic energy equation. Its special forms can be derived in accordance with how the stress tensor differs for certain type of fluids. These will be treated in detail in the sections dealing with the dynamics of perfect fluids. Newtonian fluids, and different types of non-Newtonian fluids.

3.5 The principle of conservation of energy

Any material system is characterized by its energy content. Energy occupies a position of distinction amongst the other extensive variables. Whatever interaction occurs between a material system and its surroundings, the transfer of energy invariably accompanies the transport of other extensive variables. Certain interactions are accompanied the transport of a certain type of energy. Kinetic energy increases or decreases due to mechanical interactions; a change in internal energy accompanies thermal interactions.

But the fundamental axiom is the principle of conservation of energy which applies to closed systems only. The energy content of an open system may change depending on the action of its surroundings. Consider a system in mechanical and thermal interaction with its surroundings. In this case the change in the total energy is the change in the sum of the kinetic and the internal energy:

$$\frac{\mathrm{d}E}{\mathrm{d}t} = \frac{\mathrm{d}}{\mathrm{d}t}\int_V \left(\frac{v^2}{2}+\varepsilon\right)\varrho\,\mathrm{d}V \tag{3.70}$$

where ε is the specific internal energy.

The action of the surroundings may take the form of mechanical work and/or heat.

The application of the principle of conservation of energy to this open system leads to the equation

$$\frac{\mathrm{d}}{\mathrm{d}t}\int_V \left(\frac{v^2}{2}+\varepsilon\right)\varrho\,\mathrm{d}V = \int_V \varrho\vec{g}\vec{v}\,\mathrm{d}V + \int_{(A)} \vec{v}\mathbf{T}\,\mathrm{d}\vec{A} - \int_{(A)} \vec{q}\,\mathrm{d}\vec{A}\,. \tag{3.71}$$

The rate of change of the kinetic and internal energy within the material volume equals the sum of the rate of work done by external body forces, the rate of work done by surface forces, and the rate at which heat is conducted into the volume of fluid. The heat flux vector $\vec{q}$ has the dimensions $[\mathrm{W/m^2}]$.

Applying the transport theorem the material derivative can be replaced by a local and a convective part:

$$\int_V \frac{\partial}{\partial t}\left(\frac{v^2}{2}+\varepsilon\right)\varrho\,\mathrm{d}V + \int_{(A)} \left(\frac{v^2}{2}+\varepsilon\right)\varrho\vec{v}\,\mathrm{d}\vec{A} = \int_V \varrho\vec{g}\vec{v}\,\mathrm{d}V + \\ + \int_{(A)} \vec{v}\mathbf{T}\,\mathrm{d}\vec{A} - \int_{(A)} \vec{q}\,\mathrm{d}\vec{A}\,. \tag{3.72}$$

In this equation V and (A) do not represent a moving volume and surface; rather they are instantaneous configurations fixed in space. Thus the first term gives the local rate of change of the kinetic and internal energy in the fixed volume V. The second term expresses the convective fluxes of the kinetic and internal energy due to the bulk flow across the fixed boundary surface (A).

By using the divergence theorem the surface integrals can be replaced by volume integrals. Since the volume V is arbitrarily chosen, the equations are also valid for the integrands. In this way we obtain the energy equation in differential form. The material form of the equation can be written:

$$\varrho\frac{\mathrm{d}}{\mathrm{d}t}\left(\frac{v^2}{2}+\varepsilon\right) = \varrho\vec{g}\vec{v} + \operatorname{div}(\vec{v}\mathbf{T}) - \operatorname{div}\vec{q}\,. \tag{3.73}$$

The local (spatial) form is obtained as

$$\frac{\partial}{\partial t}\left[\left(\frac{v^2}{2}+\varepsilon\right)\varrho\right] + \operatorname{div}\left[\left(\frac{v^2}{2}+\varepsilon\right)\varrho\vec{v} - \vec{v}\mathbf{T} + \vec{q}\right] = \varrho\vec{g}\vec{v}. \tag{3.74}$$

Subtracting the kinetic energy equation from the total energy equation, we get the equation for the balance of the internal energy:

$$\frac{\partial}{\partial t}(\varrho\varepsilon) + \operatorname{div}(\varrho\varepsilon\vec{v} + \vec{q}) = \mathbf{T} : \vec{v} \circ \nabla. \tag{3.75}$$

In integral form this can also be written as

$$\int_V \frac{\partial}{\partial t}(\varrho\varepsilon)\,\mathrm{d}V + \int_{(A)} (\varrho\varepsilon\vec{v} + \vec{q})\,\mathrm{d}\vec{A} = \int_V \mathbf{T} : \vec{v} \circ \nabla \mathrm{d}V. \tag{3.76}$$

It is easy to recognize the terms representing local and convective flux of the internal energy. There is also a term representing a flux of a non-mechanical power: the heat flux. The term on the right-hand side of the equation represents a source of internal energy. This is the mechanical contribution of its increase. While $-\mathbf{T} : \vec{v} \circ \nabla$ represents a loss of mechanical energy, it produces internal energy within the volume V. If the flow is at rest $\vec{v} = 0$, thus the balance of internal energy equation becomes

$$\frac{\partial}{\partial t}(\varrho\varepsilon) + \operatorname{div} \vec{q} = 0\,. \tag{3.77}$$

Substituting

$$\varepsilon = cT, \tag{3.78}$$

and

$$\vec{q} = -k \operatorname{grad} T, \tag{3.79}$$

the well-known differential equation for the conduction of heat is obtained

$$\frac{\partial}{\partial t}(\varrho c T) = \operatorname{div}(k \operatorname{grad} T)\,. \tag{3.80}$$

Assuming that the density, the heat capacity and the coefficient of thermal conductivity are constant, we get

$$\frac{\partial T}{\partial t} = \frac{k}{\varrho c}\left(\frac{\partial^2 T}{\partial x^2} + \frac{\partial^2 T}{\partial y^2} + \frac{\partial^2 T}{\partial z^2}\right). \tag{3.81}$$

For the steady state this can be written in the simple form

$$\frac{\partial^2 T}{\partial x^2} + \frac{\partial^2 T}{\partial y^2} + \frac{\partial^2 T}{\partial z^2} = 0\,. \tag{3.82}$$

3.6 The balance of entropy

The entropy is a thermodynamic variable of state; an extensive quantity. It cannot be experienced directly; as a derived variable entropy represents a measure of the irreversibility of a change of state.

Irreversible changes of state necessarily involve currents in the system. The increase in entropy during an irreversible process must be related to these currents.

Entropy is not a quantity which is conserved. There is no axiom to determine the rate of change of entropy during an irreversible process. Thus we can only derive

the balance of entropy equation by starting from the internal energy equation.

$$\varrho \frac{\mathrm{d}\varepsilon}{\mathrm{d}t} + \operatorname{div} \vec{q} = \mathbf{T} : \vec{v} \circ \nabla. \tag{3.83}$$

Separating the dissipative part of the stress tensor we get

$$\mathbf{T} = -p\mathbf{I} + \mathbf{V}, \tag{3.84}$$

where p is the pressure, $\mathbf{I}$ is the unit tensor, $\mathbf{V}$ is the viscous stress tensor. Since $\mathbf{V}$ is symmetric, the product of $\mathbf{V}$ and the antisymmetric part of $\vec{v} \circ \nabla$ must vanish. Thus

$$\varrho \frac{\mathrm{d}\varepsilon}{\mathrm{d}t} + \operatorname{div} \vec{q} = -p \operatorname{div} \vec{v} + \mathbf{V} : \mathbf{S}, \tag{3.85}$$

where $\mathbf{S}$ is the rate of deformation tensor. The first law of thermodynamics can be written as

$$\mathrm{d}\varepsilon = T\mathrm{d}s - p\mathrm{d}\left(\frac{1}{\varrho}\right). \tag{3.86}$$

Dividing by $\mathrm{d}t$ we get

$$\frac{\mathrm{d}\varepsilon}{\mathrm{d}t} = T\frac{\mathrm{d}s}{\mathrm{d}t} - p\frac{\mathrm{d}}{\mathrm{d}t}\left(\frac{1}{\varrho}\right). \tag{3.87}$$

Substituting this into the internal energy equation, and since

$$p \operatorname{div} \vec{v} = \varrho p \frac{\mathrm{d}}{\mathrm{d}t}\left(\frac{1}{\varrho}\right), \tag{3.88}$$

we obtain

$$\varrho T \frac{\mathrm{d}s}{\mathrm{d}t} = \mathbf{V} : \mathbf{S} - \operatorname{div} \vec{q}. \tag{3.89}$$

Dividing by the temperature we have

$$\frac{\mathrm{d}s}{\mathrm{d}t} = \frac{\mathbf{V} : \mathbf{S}}{T} - \frac{\operatorname{div} q}{T}. \tag{3.90}$$

Using the identity

$$\operatorname{div}\left(\frac{\vec{q}}{T}\right) = \frac{1}{T}\operatorname{div} \vec{q} - \frac{\vec{q} \operatorname{grad} T}{T^2}, \tag{3.91}$$

the local form of the balance of entropy equation can be written as

$$\frac{\partial(\varrho s)}{\partial t} + \operatorname{div}\left(\varrho s\vec{v} + \frac{\vec{q}}{T}\right) = \frac{\mathbf{V} : \mathbf{S}}{T} - \frac{\vec{q} \operatorname{grad} T}{T^2}. \tag{3.92}$$

It is easy to recognize on the left-hand side the terms representing the local rate of change of the entropy, its convective flux $\varrho s\vec{v}$, and its conductive flux $\vec{q}/T$. On

the right-hand side of the equation terms representing the entropy sources are found. The inclusion of the coductive flux term in the entropy equation shows that entropy is always exchanged simultaneously with the internal energy.

Considering the source terms, it is obvious that the absolute temperature is always positive, while the dissipating mechanical power is also positive, i.e.

$$T>0; \qquad \mathbf{V}:\mathbf{S}>0\,.$$

Since

$$\vec{q}=-k\,\mathrm{grad}\,T\,,$$

the right-hand side of the equation, i.e. the source of entropy, can only be positive, thus

$$\frac{\mathbf{V}:\mathbf{S}}{T}+k\left(\frac{\mathrm{grad}\,T}{T}\right)^2\geqq 0\,. \tag{3.93}$$

The internal energy flux always produces an increase in entropy, therefore a certain fraction of the total energy content is lost. This is in accordance with the second law of thermodynamics.

3.7 Mechanical equilibrium of fluids

If the velocity field is equal to zero throughout the entire field, i.e.

$$\vec{v}\equiv 0\,.$$

the fluid body is in mechanical equilibrium.

Substituting this into the balance of momentum equation a simple expression is obtained,

$$0=\int_V \varrho\vec{g}\,\mathrm{d}V+\int_{(A)}\mathbf{T}\,\mathrm{d}\vec{A}\,. \tag{3.94}$$

The concept of fluidity entails that tangential stresses cannot exist at rest. Thus the stress tensor can be obtained as

$$\mathbf{T}=-p\mathbf{I}\,. \tag{3.95}$$

It may then be shown from equilibrium considerations that the normal stress at any point has the same value in all directions. This state of stress is called hydrostatic, and can be written in matrix form as

$$\mathbf{T}=\begin{bmatrix} -p & 0 & 0 \\ 0 & -p & 0 \\ 0 & 0 & -p \end{bmatrix}, \tag{3.96}$$

where p is the hydrostatic pressure which at a given point is uniform in all directions.

As is well known, the stress tensor has one set of orthogonal axes — the three principal axes — for which the shear stresses vanish, and along which only the principal normal stresses σ_1, σ_2 and σ_3 exist. Note that these three principal stresses are generally not identical; only the hydrostatic normal stresses are the same in all directions.

For a compressible fluid the pressure is a well-defined thermodynamic variable of state which satisfies the relation

$$T\,\mathrm{d}s=\mathrm{d}\varepsilon+p\,\mathrm{d}\left(\frac{1}{\varrho}\right). \tag{3.97}$$

It should be noticed that this equation defines fluid pressure as a thermodynamic variable. Therefore, in general,

$$p=p(\varrho, S)\,.$$

For an incompressible fluid a simpler relation is introduced

$$T\,\mathrm{d}s=\mathrm{d}\varepsilon; \qquad \varrho=\text{const.}$$

Consequently pressure does not enter into the thermodynamical treatment of an incompressible fluid, it is an entirely different type of variable.

For an incompressible fluid the pressure is not a thermodynamic variable. It is merely a scalar variable, satisfying the momentum equation:

$$0=\int_V \varrho\vec{g}\,\mathrm{d}V-\int_{(A)} p\,\mathrm{d}\vec{A}\,. \tag{3.98}$$

Applying the divergence theorem the surface integral is changed into a volume integral

$$\int_V (\varrho\vec{g}-\operatorname{grad} p)\,\mathrm{d}V=0\,.$$

Since the volume V can be arbitrarily chosen, and the infinitesimal volume $\mathrm{d}V$ is not equal to zero, the integrand must be equal to zero, i.e.

$$\varrho\vec{g}-\operatorname{grad} p=0\,. \tag{3.99}$$

This is the law of hydrostatics; its scalar component in rectangular coordinates is written as,

$$\varrho g_x=\frac{\partial p}{\partial x},$$

$$\varrho g_y=\frac{\partial p}{\partial y},$$

$$\varrho g_z=\frac{\partial p}{\partial z}\,.$$

After substituting $\vec{v} \equiv 0$, the continuity equation becomes

$$\frac{\partial \varrho}{\partial t} = 0 .$$

This equality expresses the condition that the density field must remain steady for the equilibrium state to be maintained.

The internal energy balance at rest can be written as

$$\varrho \frac{\partial \varepsilon}{\partial t} = -\operatorname{div} \vec{q} . \tag{3.100}$$

This determines the temperature distribution at rest.

To determine the shape of a free fluid surface the curl of Eq. (3.99) is first taken. Since

$$\operatorname{curl} \operatorname{grad} p \equiv 0 ,$$

we obtain

$$\varrho \operatorname{curl} \vec{g} + \operatorname{grad} \varrho \times \vec{g} = 0 . \tag{3.101}$$

Multiplying this equation by $\vec{g}$, the second term vanishes. The only term which remains is

$$\vec{g} \operatorname{curl} \vec{g} = 0 . \tag{3.102}$$

Expressing this in rectangular coordinates we get

$$g_x \left(\frac{\partial g_z}{\partial y} - \frac{\partial g_y}{\partial z} \right) + g_y \left(\frac{\partial g_x}{\partial z} - \frac{\partial g_z}{\partial x} \right) + g_z \left(\frac{\partial g_y}{\partial x} - \frac{\partial g_x}{\partial y} \right) = 0 . \tag{3.103}$$

This equation places a restriction on the body forces. Mechanical equilibrium can exist only if the body force field satisfies the above equation. It is clear that this condition can be satisfied by all conservative body forces, i.e. those which can be derived from a scalar potential such as

$$\vec{g} = -\operatorname{grad} U .$$

Since

$$\operatorname{curl} \operatorname{grad} U \equiv 0 ,$$

Eq. (3.102) is satisfied.

In this case the first term of Eq. (3.101) vanishes. The second term can thus be written

$$\operatorname{grad} \varrho \times \operatorname{grad} U = 0 . \tag{3.104}$$

Therefore, the potential surfaces of the body force coincide with the surfaces of constant density. It can be seen, that these surfaces are perpendicular to the resultant of the body forces. This is why the free surface of a liquid in a gravity field is horizontal.

For a conservative body force the hydrostatic equation can be written as

$$\varrho \operatorname{grad} U = \operatorname{grad} p . \tag{3.105}$$

Therefore, the equipotential surfaces coincide with the isobaric surfaces.

The pressure distribution for a gas at rest is easily determined, since pressure and density are directly related variables

$$p=p(\varrho), \qquad \varrho=\varrho(p).$$

A fluid in which density and pressure are directly related is called barotropic. In this case the pressure force acting on a unit mass of gas has a potential $\mathscr{P}$, thus

$$\frac{1}{\varrho}\operatorname{grad} p=\operatorname{grad}\int_{p_0}^{p}\frac{\mathrm{d}p}{\varrho}=\operatorname{grad}\mathscr{P}. \tag{3.106}$$

For a barotropic fluid in a conservative body force field the hydrostatic equation is given by

$$\operatorname{grad}(U+\mathscr{P})=0, \tag{3.107}$$

or in another form

$$U+\mathscr{P}=\text{const.} \tag{3.108}$$

For the atmosphere in the gravity force field, assuming a uniform temperature distribution, the gravity potential is given by

$$U=g(z-z_0),$$

where z is the vertical coordinate, z_0 is its value on the ground surface.

The barotropic potential for the isothermic case can be expressed as

$$\mathscr{P}=\int_{p_0}^{p}\frac{\mathrm{d}p}{\varrho}=\frac{p_0}{\varrho_0}\int_{p_0}^{p}\frac{\mathrm{d}p}{p}=\frac{p_0}{\varrho_0}\ln\frac{p}{p_0}.$$

The equilibrium equation is obtained as

$$g(z-z_0)+\frac{p_0}{\varrho_0}\ln\frac{p}{p_0}=\text{const.}$$

The boundary condition $z=z_0$; $p=p_0$ shows the constant, to be zero. Thus the pressure distribution along z is

$$p(z)=p_0\exp\frac{\varrho_0 g}{p_0}(z-z_0), \tag{3.109}$$

where z_0 is any reference height and p_0 and ϱ_0 are the corresponding pressure and the density.

The pressure distribution for an isentropic or a polytropic fluid can be similarly derived.

For an incompressible fluid the hydrostatic equation is obtained in terms of the gravity field as

$$-\varrho\operatorname{grad} U=\operatorname{grad} p,$$

or

$$p+\varrho U=\text{const.}$$

The pressure distribution is given by

$$p-\varrho g z=\text{const.}$$

Since at the free surface $z=0$ and $p=p_0$, and introducing a depth-coordinate $h=-z$, we get

$$p=p_0+\varrho g h\,. \tag{3.110}$$

This is the most frequently used equation in hydrostatics.

CHAPTER 4

PERFECT FLUID FLOW

4.1 The perfect fluid

The fundamental property which distinguishes a fluid from other continuous media is that it cannot be in equilibrium in the presence of tangential stresses. If any infinitesimal tangential stress acts in the fluid the mechanical equilibrium comes to an end, and some form of fluid flow begins to develop. Thus, in a moving fluid mass tangential forces occur as well as normal forces. But in most engineering problems the tangential forces are relatively small, and may thus be neglected. The most simple description of fluid flow is developed on the hypothesis of purely normal pressure, and this assumption is automatically implied when speaking of a perfect or inviscid fluid. A perfect fluid at rest or in motion is in a hydrostatic state of stress which satisfies the equation

$$\vec{t} = -p\vec{n} \,. \tag{4.1}$$

In other words: at any point within a flowing perfect fluid the pressure is the same in all directions; it forms a scalar field. The pressure is positive when the stress vector $\vec{t}$ tends to compress the fluid. The pressure is independent of the surface normal vector n, i.e.

$$p = p(\vec{r}, t) \,.$$

The hypothetic model of the perfect fluid is particularly applicable to fluids which have a low viscosity, such as water, gasoline and the common gases.

Solving the majority of fluid flow problems involves the determination of the velocity and pressure distributions as functions of the coordinates and time. This problem can be considerably simplified by assuming that the viscosity of the fluid is zero. Typical cases for which this assumption is valid are flow through orifices, the discharge from large tanks, the flow around aerofoils, etc. In such problems the flow of the main fluid mass has the greater importance. Viscous effects are significant only in the flow immediately adjacent to the solid boundaries; moving away from the walls the shear stresses decrease rapidly.

That region of the flow where fluid friction is important is known as the boundary layer. The main flow, outside of the boundary layer can be described by the equations derived for perfect fluids.

4.2 Euler's equation

The equation of motion for a perfect fluid is obtained by substitution the stress tensor

$$\mathbf{T} = -p\mathbf{I}\,, \tag{4.2}$$

into Cauchy's equation of motion:

$$\frac{\partial \vec{v}}{\partial t} = \vec{g} + \frac{1}{\varrho}\,\mathrm{Div}\,(-p\mathbf{I})\,. \tag{4.3}$$

After expanding the terms representing the local and convective components of the acceleration, and taking into account the identity

$$\mathrm{Div}\,(-p\mathbf{I}) = -\,\mathrm{grad}\,p\,,$$

the result is:

$$\frac{\partial \vec{v}}{\partial t} + (\vec{v}\nabla)\,\vec{v} = \vec{g} - \frac{1}{\varrho}\,\mathrm{grad}\,p\,. \tag{4.4}$$

This equation of motion is the so-called Euler equation. Its physical meaning is obvious: the acceleration equals the sum of body force and the pressure force acting on a unit mass of flowing fluid. Its components in Cartesian coordinates are:

$$\begin{aligned}
&\frac{\partial v_x}{\partial t} + v_x\frac{\partial v_x}{\partial x} + v_y\frac{\partial v_x}{\partial y} + v_z\frac{\partial v_x}{\partial z} = g_x - \frac{1}{\varrho}\,\frac{\partial p}{\partial x}\,,\\
&\frac{\partial v_y}{\partial t} + v_x\frac{\partial v_y}{\partial x} + v_y\frac{\partial v_y}{\partial y} + v_z\frac{\partial v_y}{\partial z} = g_y - \frac{1}{\varrho}\,\frac{\partial p}{\partial y}\,,\\
&\frac{\partial v_z}{\partial t} + v_x\frac{\partial v_z}{\partial x} + v_y\frac{\partial v_z}{\partial y} + v_z\frac{\partial v_z}{\partial z} = g_z - \frac{1}{\varrho}\,\frac{\partial p}{\partial z}\,.
\end{aligned} \tag{4.5}$$

Euler's equation can be also written in cylindrical coordinates:

$$\begin{aligned}
&\frac{\partial v_r}{\partial t} + v_r\frac{\partial v_r}{\partial r} + \frac{v_\varphi}{r}\,\frac{\partial v_r}{\partial \varphi} - \frac{v_\varphi^2}{r} + v_z\frac{\partial v_r}{\partial r} = g_r - \frac{1}{\varrho r}\,\frac{\partial}{\partial r}(rp)\,,\\
&\frac{\partial v}{\partial t} + v_r\frac{\partial v_\varphi}{\partial r} + \frac{v_\varphi}{r}\,\frac{\partial v_\varphi}{\partial \varphi} + \frac{v_r v_\varphi}{r} + v_z\frac{\partial v_\varphi}{\partial z} = g_\varphi - \frac{1}{\varrho r}\,\frac{\partial p}{\partial \varphi}\,,\\
&\frac{\partial v_z}{\partial t} + v_r\frac{\partial v_z}{\partial r} + \frac{v_\varphi}{r}\,\frac{\partial v_z}{\partial \varphi} + v_z\frac{\partial v_z}{\partial z} = g_z - \frac{1}{\varrho}\,\frac{\partial p}{\partial z}\,.
\end{aligned} \tag{4.6}$$

Following Lamb Euler's equation can be further modified. The convective component of the acceleration may be expanded by applying the identity:

$$(\vec{v}\nabla)\,\vec{v} = \mathrm{grad}\,\frac{v^2}{2} + \mathrm{curl}\,\vec{v}\times\vec{v}\,.$$

Substituting this into the equation of motion, yields

$$\frac{\partial \vec{v}}{\partial t} + \operatorname{curl} \vec{v} \times \vec{v} + \operatorname{grad} \frac{v^2}{2} = \vec{g} - \frac{1}{\varrho} \operatorname{grad} p \,. \tag{4.7}$$

This form of Euler's equation is particularly useful in recognizing whether a flow is rotational or not. If it is not, the substitution of curl $\vec{v} = 0$ leads to a simpler expression,

$$\frac{\partial \vec{v}}{\partial t} + \operatorname{grad} \frac{v^2}{2} = \vec{g} - \frac{1}{\varrho} \operatorname{grad} p \,. \tag{4.8}$$

In most instances the external body force $\vec{g}$ is conservative, and has a potential U; gravitational and centrifugal fields are examples of such conservative fields. In such a field each fluid particle has a potential energy which is a function of its position in the field. The force exerted on a unit fluid mass is the negative of the gradient of the potential,

$$\vec{g} = -\operatorname{grad} U \,.$$

The pressure force acting on the unit mass may also be conservative, having a potential $\mathscr{P}$. This assumption is valid when the pressure and density are directly related, i.e.

$$p = p(\varrho); \qquad \varrho = \varrho(p) \,.$$

A flow in which the density and the pressure are directly related is called barotropic. The barotropic nature of the flow may arise from certain conditions (e.g. a gas in isentropic motion) or it may be an inherent property of the fluid itself (e.g. an incompressible fluid). The potential of the pressure force acting on a unit mass of barotropic fluid is

$$\mathscr{P} = \int_{p_0}^{p} \frac{\mathrm{d}p}{\varrho} \,.$$

It is easy to see that

$$-\frac{1}{\varrho} \operatorname{grad} p = -\operatorname{grad} \int_{p_0}^{p} \frac{\mathrm{d}p}{\varrho} = -\operatorname{grad} \mathscr{P} \,.$$

Substituting the potentials U and $\mathscr{P}$ into Eq. (4.4) we obtain the simple formula

$$\frac{\partial \vec{v}}{\partial t} + (\vec{v}\nabla)\,\vec{v} = -\operatorname{grad}(U + \mathscr{P}) \,, \tag{4.9}$$

which shows that the acceleration may be obtained from a potential when the body forces are conservative and the flow is barotropic. This is the fundamental property which uniquely characterizes barotropic motion. Expanding the convective ac-

celeration term we obtain the equation

$$\frac{\partial \vec{v}}{\partial t} + \operatorname{curl} \vec{v} \times \vec{v} = -\operatorname{grad}\left(U + \mathscr{P} + \frac{v^2}{2}\right). \tag{4.10}$$

The sum within the brackets on the right-hand side represents the mechanical energy content of a unit mass of the flowing fluid. Alongside the potentials U and $\mathscr{P}$ it is easy to recognize the kinetic energy term $\frac{v^2}{2}$. Thus the mechanical energy can be defined as:

$$E = U + \mathscr{P} + \frac{v^2}{2}. \tag{4.11}$$

By means of Eq. (4.11) Euler's equation can be written as

$$\frac{\partial \vec{v}}{\partial t} + \operatorname{curl} \vec{v} \times \vec{v} = -\operatorname{grad} E. \tag{4.12}$$

Note, that on the left-hand side of this equation there are only purely kinematic quantities, obtained as the gradient of the mechanical energy. Thus it is immaterial what type of energy contributes to the sum of Eq. (4.11); there is no difference between a pump running against a 200 m difference in water level or a 20 bar back-pressure.

Euler's equation can also be expressed in terms of intrinsic derivatives. The intrinsic form of Euler's equation can be obtained by introducing a natural coordinate system, in which one coordinate is along the streamline and the other two are normal to it. In this coordinate system $\vec{s}$ is measured along a streamline in the direction of the velocity vector, $\vec{n}$ is measured normal to it toward the concave side of the streamline, $\vec{b}$ is normal to both $\vec{s}$ and $\vec{n}$. The unit vectors $\vec{e}_s$, $\vec{e}_n$ and $\vec{e}_b$ are respectively the tangent, the normal and the binormal vectors to the congruence of the streamlines, satisfying the expression

$$\vec{e}_s \times \vec{e}_n = \vec{e}_b.$$

If we consider only steady flow then the streamlines and path lines are the same curves. In this system the velocity vector can be written as

$$\vec{v} = v\vec{e}_s + 0\vec{e}_n + 0\vec{e}_b.$$

The unit vector $\vec{e}_s$ depends only on s. Since

$$\frac{\partial \vec{v}}{\partial t} = 0,$$

the acceleration can be expressed as

$$(\vec{v}V)\,\vec{v} = v(\vec{e}_s V)\,v\vec{e}_s = \vec{v}\,\frac{\partial v}{\partial s}\,\vec{e}_s + v^2\,\frac{\partial \vec{e}_s}{\partial s}.$$

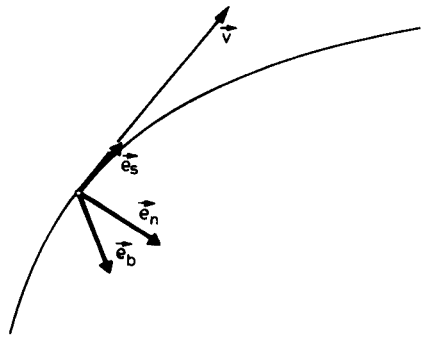

Fig. 4.1. Intrinsic coordinate system

Referring to *Fig. 4.1* it is obvious, that

$$\frac{\partial \vec{e}_s}{\partial t} = \frac{\mathrm{d}\vec{e}_s}{\mathrm{d}s} = \frac{|\vec{e}_s|\,\mathrm{d}\vartheta\,\vec{e}_n}{R\,\mathrm{d}\vartheta} = \frac{1}{R}\vec{e}_n .$$

Substituting this into Euler's equation we have

$$v\frac{\partial v}{\partial s}\vec{e}_s + \frac{v^2}{R}\vec{e}_n = \vec{g} - \frac{1}{\varrho}\operatorname{grad} p , \tag{4.13}$$

where R is the radius of curvature of the streamline. Multiplying this equation by the unit vectors $\vec{e}_s$, $\vec{e}_n$ and $\vec{e}_b$, three scalar equations are obtained for the components in the tangential, normal and binormal directions:

$$v\frac{\partial v}{\partial s} = g_s - \frac{1}{\varrho}\frac{\partial p}{\partial s}, \tag{4.14a}$$

$$\frac{v^2}{R} = g_n - \frac{1}{\varrho}\frac{\partial p}{\partial n}, \tag{4.14b}$$

$$0 = g_b - \frac{1}{\varrho}\frac{\partial p}{\partial b}. \tag{4.14c}$$

For barotropic flow in a gravity field

$$v\frac{\partial v}{\partial s} = -\frac{\partial}{\partial s}(gz + \mathscr{P}), \tag{4.15a}$$

$$\frac{v^2}{R} = -\frac{\partial}{\partial n}(gz + \mathscr{P}), \tag{4.15b}$$

$$0 = -\frac{\partial}{\partial b}(gz + \mathscr{P}). \tag{4.15c}$$

If the fluid is incompressible, i.e. $\mathscr{P} = \frac{p}{\varrho}$

$$v\frac{\partial v}{\partial s} = -\frac{\partial}{\partial s}\left(gz + \frac{p}{\varrho}\right), \tag{4.16a}$$

$$\frac{v^2}{R} = -\frac{\partial}{\partial n}\left(gz + \frac{p}{\varrho}\right), \tag{4.16b}$$

$$0 = -\frac{\partial}{\partial b}\left(gz + \frac{p}{\varrho}\right). \tag{4.16c}$$

The first equation in each of the above three sets of equations is a common one-dimensional form of the momentum equation. In the binormal direction a hydrostatic equation is obtained. The most important result follows from the equation for the normal component, viz. that the radius of curvature of the streamlines depends on the change in the potential energy and the pressure. Thus R cannot decrease arbitrarily, it must satisfy Eq. (4.16b). When a flow rounds a corner, the streamlines cannot entirely follow the sudden turning of the wall. The radius of curvature of the streamline cannot be infinitely small, from Eq. (4.16c) it follows that its decrease must be in accordance with the equation

$$R = -\frac{v^2}{\frac{\partial}{\partial n}\left(gz + \frac{p}{\varrho}\right)}. \tag{4.17}$$

Thus a streamline which rounds a corner or a sharp edge separates from the wall becoming a so-called free streamline. The pressure along a free streamline is

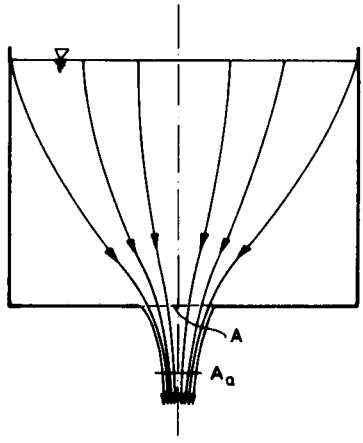

Fig. 4.2. Separation of free streamlines

constant. If gravitational effects are neglected, the velocity is also constant along it. Between the wall and the free streamline a stagnant region is formed inside which there is a constant pressure.

As *Fig. 4.2* shows, an outflowing jet experiences a contraction, the so-called "vena contracta" effect, as a result of the separation of the free streamline. The actual cross-section of the flowing fluid A_a is smaller than the cross-section A of the opening. The coefficient of contraction C_c is defined as the ratio of the minimum jet area, or vena contracta area, to the area of the opening:

$$C_c = \frac{A_a}{A}. \tag{4.18}$$

The vena contracta effect occurs at orifice meters, pipe inlets, turbomachines and in many other engineering applications.

The velocity field of a barotropic flow

The velocity field of a barotropic flow cannot be arbitrary, but must be in agreement with Eq. (4.12). Taking the curl on both sides of the equation it is clear that

$$\operatorname{curl}\left(\frac{\partial \vec{v}}{\partial t} + \vec{\Omega} \times \vec{v}\right) = 0. \tag{4.19}$$

Since the partial derivative w.r.t. time and the curl are independent operations their order can be interchanged:

$$\frac{\partial \vec{\Omega}}{\partial t} + \operatorname{curl}(\vec{\Omega} \times \vec{v}) = 0. \tag{4.20}$$

Expanding the double cross product we obtain

$$\operatorname{curl}(\vec{\Omega} \times \vec{v}) = (\vec{v}\nabla)\vec{\Omega} - (\vec{\Omega}\nabla)\vec{v} + \vec{\Omega} \operatorname{div} \vec{v} - \vec{v} \operatorname{div} \vec{\Omega}.$$

Since

$$\operatorname{div} \vec{\Omega} = \nabla(\nabla \times \vec{v}) = 0,$$

it is obvious, that

$$\frac{\partial \vec{\Omega}}{\partial t} + (\vec{v}\nabla)\vec{\Omega} = (\vec{\Omega}\nabla)\vec{v} - \vec{\Omega} \operatorname{div} \vec{v}. \tag{4.21}$$

On the left-hand side terms reflecting the local and the convective rate of change of the vorticity can be recognized. Thus

$$\frac{\mathrm{d}\vec{\Omega}}{\mathrm{d}t} = (\vec{\Omega}\nabla)\vec{v} - \vec{\Omega} \operatorname{div} \vec{v}. \tag{4.22}$$

If a velocity field satisfies Euler's equation, it must also satisfy Eq. (4.22).

Euler's equation is particularly simple for irrotational barotropic flow. In this case

$$\operatorname{curl} \vec{v} = 0 ,$$

thus a velocity potential exists, which may be defined as

$$\vec{v} = \operatorname{grad} \Phi . \tag{4.23}$$

After substitution, and interchanging the order of the $\frac{\partial}{\partial t}$ and grad operators we have

$$\operatorname{grad}\left(\frac{\partial \Phi}{\partial t} + \frac{v^2}{2} + U + \mathscr{P}\right) = 0 . \tag{4.24}$$

For steady flow this is reduced to

$$\operatorname{grad}\left(\frac{v^2}{2} + U + \mathscr{P}\right) = 0 . \tag{4.25}$$

If the fluid is incompressible, this can be written as

$$\operatorname{grad}\left(\frac{v^2}{2} + \frac{p}{\varrho} + U\right) = 0 . \tag{4.26}$$

Taking the line integrals of Eqs (4.24)—(4.25) leads to the integration of total differentials. Thus we obtain the oldest equation of hydrodynamics, the well-known Bernoulli equation.

4.3 The Bernoulli equation

The Bernoulli equation is the first line integral of the equation of motion. The equation can take various forms, depending on the particular kinematical or dynamical assumptions relating to the motion. The equation

$$\frac{\partial \vec{v}}{\partial t} + \operatorname{curl} \vec{v} \times \vec{v} = -\operatorname{grad}\left(U + \mathscr{P} + \frac{v^2}{2}\right)$$

is suitable as a starting point for the present discussion. If the flow is steady

$$\frac{\partial \vec{v}}{\partial t} = 0 .$$

Integrating along streamlines or vortex lines, the integral of the curl $\vec{v} \times \vec{v}$ term vanishes. The scalar product $(\operatorname{curl} \vec{v} \times \vec{v})\, \mathrm{d}\vec{r}$ is zero when $\mathrm{d}\vec{r}$ is parallel to $\vec{v}$ or curl $\vec{v}$.

Integration over the section 1–2 of the streamline yields

$$\int_1^2 \mathrm{d}\vec{r} \operatorname{grad} E = \int_1^2 \mathrm{d}E = E_2 - E_1 = 0 . \tag{4.27}$$

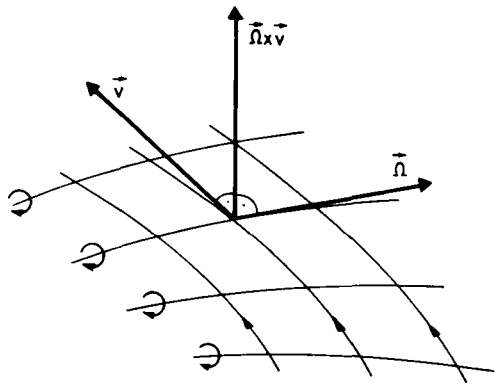

Fig. 4.3. Equipotential surfaces of mechanical energy

The physical meaning of this result is particularly important; it is the well-known Bernoulli theorem. The total mechanical energy content of a unit mass of fluid is constant along any streamline or vortex line of a steady barotropic flow,

$$E = U + \mathscr{P} + \frac{v^2}{2} = \text{const.} \tag{4.28}$$

The value of the mechanical energy E along different streamlines will, in general, vary. It is obvious, that the streamlines which fit the same vortex line are characterized by the same constant energy, thus the so-called iso-energetic surfaces can be generated.

This statement may be derived from the Euler-equation of steady flow. Since

$$\text{curl}\,\vec{v}\times\vec{v} = -\text{grad}\,E\,, \tag{4.29}$$

it is obvious, that the vector field curl $\vec{v}\times\vec{v}$ is conservative since its curl vanishes

$$\text{curl}\,(\vec{\Omega}\times\vec{v}) = -\text{curl grad}\,E = 0\,. \tag{4.30}$$

It can be seen, that the scalar function E is the potential of the velocity field $\vec{\Omega}\times\vec{v}$. The equipotential surfaces of E are perpendicular to the vector $\vec{\Omega}\times\vec{v}$. Thus the coincident stream surfaces and vortex surfaces of a steady barotropic flow are the equipotential surfaces of the mechanical energy as is shown in *Fig. 4.3*.

If in addition to the preceeding, the flow is irrotational, the Bernoulli equation is valid along any curve, or between any two points in the flowing fluid.

Bernoulli's equation has a simpler form for incompressible fluids:

$$E = \frac{v^2}{2} + \frac{p}{\varrho} + U = \text{const.} \tag{4.31}$$

In the most common practical case the field of the external force is the gravitational field. If we consider a mass of fluid under the influence of gravity, and select some

arbitrary horizontal plane at which the potential energy of the fluid is zero, then the potential energy of the fluid varies directly with the distance above the arbitrary plane. If h is the distance above the chosen plane, the potential energy of a unit mass of fluid is

$$U=gh\,.$$

Dividing Eq. (4.31) by the gravitational constant g, we obtain the Bernoulli equation of the dimension of length,

$$\frac{v^2}{2g}+\frac{p}{\varrho g}+h=\text{const.} \tag{4.32}$$

This well-known form is particularly suitable for the graphical representation of the distribution of specific energies along a streamline.

It is a well-known fact that the density of gases is relatively small. Thus the gravitational force is negligibly small compared to the intertial and pressure forces. This is the reason why the gravitational potential can be omitted:

$$\frac{v^2}{2}+\int_{p_0}^{p}\frac{\mathrm{d}p}{\varrho}=\text{const.} \tag{4.33}$$

The barotropic potential $\mathscr{P}$ can be determined from the relationship between the density and the pressure.

If the flow is isothermal

$$\frac{p}{\varrho}=\frac{p_0}{\varrho_0}\,. \tag{4.34}$$

Substituting to Eq. (4.33), and after integration we have:

$$\frac{v^2}{2}+\frac{p_0}{\varrho_0}\ln\frac{p}{p_0}=\text{const.} \tag{4.35}$$

When an inviscid ideal gas flows through an adiabatic system the flow is isentropic. The relationship between the pressure and the density for the isentropic case is

$$\frac{p}{\varrho^{\kappa}}=\frac{p_0}{\varrho_0^{\kappa}}\,. \tag{4.36}$$

After substitution into Eq. (4.33), integration leads to the result

$$\frac{v^2}{2}+\frac{\kappa}{\kappa-1}\frac{p_0}{\varrho_0}\left[\left(\frac{p}{p_0}\right)^{\frac{\kappa-1}{\kappa}}-1\right]=\text{const.} \tag{4.37}$$

Since

$$\left(\frac{p}{p_0}\right)^{\frac{\kappa-1}{\kappa}}=\frac{T}{T_0}\,, \tag{4.38}$$

substituting into Eq. (4.37), and applying the equation of state for an ideal gas, we obtain

$$\frac{v^2}{2} + \frac{\kappa}{\kappa - 1} R(T - T_0) = \text{const.} \tag{4.39}$$

It is evident, that the second term of the equation represents the difference in the specific enthalpies. As it is well known, the heat capacity of a gas at constant pressure is given by

$$c_p = \frac{\kappa}{\kappa - 1} R . \tag{4.40}$$

The specific enthalpy can be written as

$$i = c_p T . \tag{4.41}$$

Thus the isentropic Bernoulli equation becomes

$$\frac{v^2}{2} + i = \text{const.} \tag{4.42}$$

Another form is obtained by replacing RT by p/ϱ in Eq. (4.39), viz.

$$\frac{v^2}{2} + \frac{\kappa}{\kappa - 1} \frac{p}{\varrho} = \text{const.} \tag{4.43}$$

These equations all relate to an arbitrary point in the flowing gas. To evaluate the constant on the right-hand side of the equation, a reference point or a reference state must be chosen. This reference point may be that where the gas is at rest. Thus any gas flow may be considered to be a flow coming from an infinite reservoir. The conditions in this reservoir are denoted by the subscript 0.

The flow variables of this fictitious reservoir are identical to those at any point of the system at which the velocity is zero. Thus these variables are called reservoir or stagnation variables. For example the constant of Eq. (4.42) is the stagnation enthalpy. The stagnation pressure, density, temperature, etc. are defined in a similar manner.

Such a stagnation point occurs at the nose of an immersed body, where the flowing fluid is brought to rest and the kinetic energy of the fluid is thus converted into enthalpy. This stagnation enthalpy is equal to the enthalpy in the reservoir irrespective of the location of the stagnation point. (Note, that this statement is valid only for isentropic flow.)

The stagnation pressure can be measured by a Pitot tube. This measuring device consists of three main parts as shown in *Fig. 4.4*. The head is placed in the flow with its nose directed in the opposite direction to the velocity. At the nose the fluid is brought to rest, and a stagnation point occurs. This point is connected to a pressure-measuring device; commonly an U-tube manometer. Thus the manometer measures the stagnation pressure.

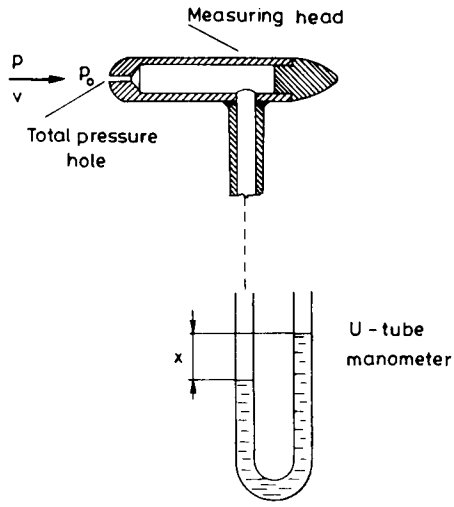

Fig. 4.4. Pitot tube

The development of the stagnation point is an isentropic process. The stagnation enthalpy is equal to the reservoir enthalpy. Thus the temperature read by a stationary thermometer is equal to the temperature read in the reservoir. For a thermometer to measure the temperature of the flowing gas it would be necessary for it to move at the same velocity as the gas. This would be an impractical measuring technique, thus the temperature of the flowing gas is determined indirectly, applying a kinetic energy correction

$$T = T_0 - \frac{v^2}{2c_p}. \tag{4.44}$$

For supersonic flows the Pitot tube is unsuitable for determining stagnation parameters.

4.4 Simple applications of the Bernoulli equation

There is a rather large range of problems in fluid mechanics to which the perfect fluid model can be successfully applied, yielding solutions adequate for the petroleum engineer. One such problem is that of velocity measurements based on the measurement of the dynamic pressure. The most simple device for this is the Pitot tube.

As shown in *Fig. 4.4*, the opening of the right-angled bend is directed upstream so that a stagnation point occurs at this opening. In front of the opening the fluid is at rest; its stagnation pressure is p_0. The Bernoulli equation can be written

for the streamline leading to the stagnation point. Far from the Pitot tube the flow is undisturbed, its velocity is v and the static pressure is p. Thus

$$\frac{v^2}{2}+\frac{p}{\varrho}=\frac{p_0}{\varrho}. \tag{4.45}$$

The static pressure can be measured using a piezometer opening. The difference between the stagnation and the static pressure is obtained by connecting both points to the opposite ends of a differential manometer. The hydrostatic equation for the U-tube is

$$p+\varrho gh+\varrho_m gx=p_0+\varrho g(h+x).$$

Thus

$$p_0-p=xg(\varrho_m-\varrho), \tag{4.46}$$

where ϱ_m is the density of the manometer liquid. Substituting this into Eq. (4.45), the velocity is

$$v=\sqrt{2gx\frac{\varrho_m-\varrho}{\varrho}}. \tag{4.47}$$

A more sophisticated way of performing this measurement is that of using the so-called Prandtl tube, which is a combined Pitot and static tube, as depicted in *Fig. 4.5.*

To measure the stagnation pressure accurately is not difficult. Any opening at the nose of the device can provide an accurate stagnation pressure by simply directing the nose against the flow. On the other hand it is frequently difficult to measure accurately the static pressure p, or the difference p_0-p. The velocity and the pressure distribution along the wall of the tube may be obtained either from potential theory or experimentally. The holes for measuring the static pressure are placed in a position where the pressure is the same as in the undisturbed flow. A differential gauge across the stagnation pressure and the static pressure connections gives the pressure difference p_0-p. The Bernoulli equation between the

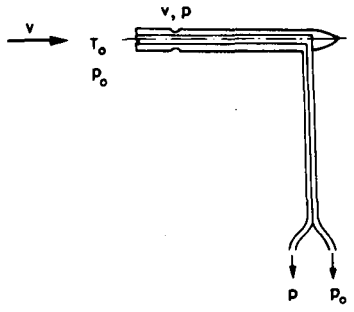

Fig. 4.5. Prandtl tube

stagnation point and the static pressure hole may be written as

$$\frac{p_0}{\varrho} = \frac{p}{\varrho} + \frac{v^2}{2}. \tag{4.48}$$

The velocity can thus be obtained as

$$v = \sqrt{\frac{2}{\varrho}(p_0 - p)}, \tag{4.49}$$

if the dynamic pressure is known. It is obvious that the smaller the device, the more accurately the measured velocity approaches the local value at a given point.

The above relations apply only to an incompressible flow. For compressible flows, the subsonic and the supersonic cases must be treated separately. In this book relations are presented only for subsonic flow. The Bernoulli equation for an isentropic process is

$$\frac{v^2}{2} + \frac{\kappa}{\kappa - 1}\frac{p}{\varrho} = \frac{\kappa}{\kappa - 1}\frac{p_0}{\varrho_0}. \tag{4.50}$$

Applying

$$\frac{p}{\varrho^\kappa} = \frac{p_0}{\varrho_0^\kappa}$$

the velocity is obtained as

$$v = \sqrt{\frac{2\kappa}{\kappa - 1}\frac{p_0}{\varrho_0}\left[1 - \left(\frac{p}{p_0}\right)^{\frac{\kappa-1}{\kappa}}\right]}. \tag{4.51}$$

Note, that ϱ_0 can be calculated if the stagnation pressure and temperature are known. Since

$$\frac{p_0}{\varrho_0} = RT_0,$$

the velocity can be computed from the equation

$$v = \sqrt{\frac{2\kappa}{\kappa - 1}RT_0\left[1 - \left(\frac{p}{p_0}\right)^{\frac{\kappa-1}{\kappa}}\right]}. \tag{4.52}$$

This equation shows that the Prandtl tube is not suitable for measuring subsonic velocities without modification. The stagnation pressure and the static pressure need to be each measured separately, instead of only their difference $p_0 - p$. In addition, it is necessary to measure the stagnation temperature, thus a thermocouple must be inserted at the nose of the Prandtl tube. The heat capacities c_p and c_v of the pure gas, or the multicomponent gas mixture must be known, to obtain

$$R = c_p - c_v,$$

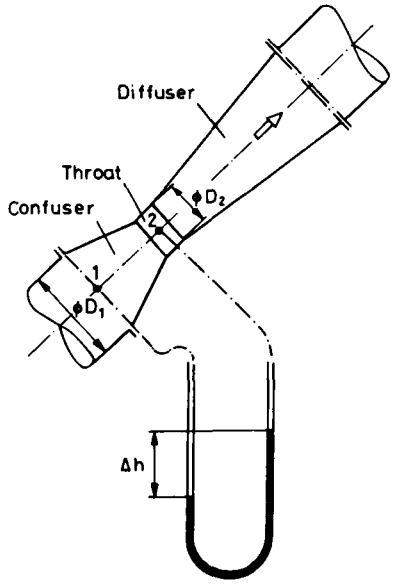

Fig. 4.6. Venturi meter

and

$$\kappa = \frac{c_p}{c_v}.$$

Sometimes the Prandtl tube is used to determine the flow rate in a pipe or a channel. This instrument is especially suitable for irregularly-shaped cross-sections. In this case, one may subdivide the cross-section into arbitrary regions. It is convenient to use regions of equal shape and size (e.g. squares). Velocities may be determined for every areal element of such a grid. After numerical integration the flow rate is obtained.

For the direct measurement of the flow rate through a pipe, the Venturi meter is a simple and accurate instrument. As shown in *Fig. 4.6* the Venturi tube includes a converging section (the confuser), a throat, where the cross-sectional area is smallest, and a diffuser. When a fluid flows through the converging section its velocity increases, while the static pressure decreases. The pressure difference reaches a maximum between the inlet (1) and the throat (2). The pressure difference $(p_1 - p_2)$ can be measured by means of a differential U-tube gage. This static pressure difference is directly related to the flow rate Q. For the sake of generality, consider a Venturi meter fitted to an inclined pipe section. Using the notation shown in *Fig. 4.6*, assume an incompressible fluid flowing steadily. In this case the Bernoulli equation can be written as

$$\frac{v_1^2}{2} + \frac{p_1}{\varrho} + g z_1 = \frac{v_2^2}{2} + \frac{p_2}{\varrho} + g z_2 . \tag{4.53}$$

The continuity equation, assuming a uniform velocity distribution at the inlet and at the throat, is:

$$Q = \frac{D_1^2 \pi}{4} v_1 = \frac{D_2^2 \pi}{4} v_2 .$$

Thus the velocity at the throat can be expressed as

$$v_2 = \sqrt{\frac{2\left[\frac{p_1 - p_2}{\varrho} + g(z_1 - z_2)\right]}{1 - \left(\frac{D_2}{D_1}\right)^4}} . \tag{4.54}$$

Applying the law of hydrostatics to the U-tube manometer we obtain

$$p_1 - p_2 = \varrho g(z_2 - z_1) + (\varrho_m - \varrho)\, g\, \Delta h , \tag{4.55}$$

where ϱ_m is the density of the manometer liquid. Usually $\varrho_m > \varrho$. Substituting into the previous equation v_2 is obtained:

$$v_2 = \sqrt{\frac{2g\,\Delta h \frac{\varrho_m - \varrho}{\varrho}}{1 - \left(\frac{D_2^2}{D_1}\right)^4}} . \tag{4.56}$$

The flow rate can be expressed by

$$Q = \frac{D_2^2 \pi}{4} \sqrt{\frac{2g\left(\frac{\varrho_m}{\varrho} - 1\right)\Delta h}{1 - \left(\frac{D_2}{D_1}\right)^4}} . \tag{4.57}$$

The flow rate obtained for these conditions is an ideal flow rate. The difference between the ideal and the actual flow rate is due to the fluid friction, the non-uniform velocity distribution, and some contraction of the flow at the throat. The actual flow rate can be expressed as

$$Q_a = \alpha \frac{D_2^2 \pi}{4} \sqrt{\frac{2g\left(\frac{\varrho_m}{\varrho} - 1\right)\Delta h}{1 - \left(\frac{D_2}{D_1}\right)^4}} , \tag{4.58}$$

in which α is a dimensionless discharge coefficient. For accurate measurements the discharge coefficient can be determined by calibrating the Venturi meter, with a weighing, during the measuring time interval. The error usually is smaller than 1%.

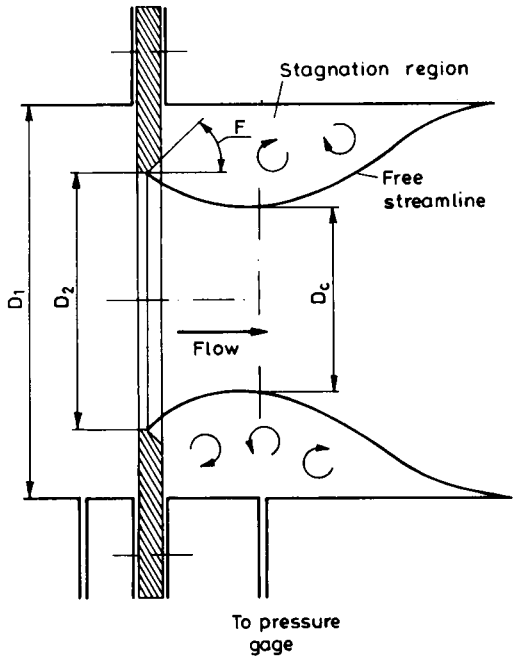

Fig. 4.7. Orifice meter

The most frequently used device for measuring flow rates is the well-known orifice meter. As shown in *Fig. 4.7*, this is a thin, flat circular plate with a concentric hole in it, which is clamped between two flanges at any joint in a pipeline. The sharp-edged hole of the orifice plate has a calibrated diameter D_2. From the sharp edge of the opening free streamlines separate, forming an axisymmetric stream surface, which represents the boundary between the contracting stream tube and the stagnation region of constant pressure. The static pressure connections are made taking into the vena contracta effect. The upstream tap is commonly located at a distance D_1 upstream of the orifice plate, while the downstream tap is placed at the minimum-pressure position, which is assumed to be at the vena contracta. The Bernoulli equation between cross-sections 1 and C can be written as

$$\frac{p_1}{\varrho} + \frac{c_1^2}{2} = \frac{p_c}{\varrho} + \frac{c_c^2}{2}. \tag{4.59}$$

The continuity equation is

$$A_c c_c = C_c A_2 c_c = A_1 c_1 , \tag{4.60}$$

where C_c is the so-called contraction coefficient.

The pressure difference $p_1 - p_c$ can be expressed as

$$p_1 - p_c = x(\varrho_m - \varrho)\, g\,. \tag{4.61}$$

The upstream velocity c_1 is obtained as

$$c_1 = \sqrt{\frac{2x(\varrho_m - \varrho)g}{\varrho\left(\frac{D_1^4}{C_c^2 D_2^4} - 1\right)}}\,. \tag{4.62}$$

Thus the flow rate can be correlated with the manometer level difference x:

$$Q = \frac{D_1^2 \pi}{4} \sqrt{\frac{2x(\varrho_m - \varrho)g}{\varrho\left(\frac{D_1^4}{C_2^2 D_2^4} - 1\right)}}\,. \tag{4.63}$$

For flange taps the pressure holes are placed immediately before and behind the orifice plate. Since the pressure is uniform in the stagnation region, this tap arrangement causes only a negligible error.

When liquid discharges from a tank through an opening near its bottom, the flow may be regarded as steady, if the free surface area in the tank A_1 is large compared with the area of the opening A_2. From the continuity equation we get

$$v_1 = \frac{A_2}{A_1} v_2\,.$$

Since $A_2 \ll A_1$, it is obvious that $v_1^2 \ll v_2^2$, thus the kinetic energy term $\frac{v_1^2}{2g}$ in the Bernoulli equation is negligible. Consider a streamline from the free surface to the opening, as shown in *Fig. 4.8*. Using this notation the Bernoulli equation is

$$\frac{p_1}{\varrho g} + z_1 + \frac{v_1^2}{2g} = \frac{p_2}{\varrho g} + z_2 + \frac{v_2^2}{2g}\,. \tag{4.64}$$

Since the pressure of both the free surface and the outflowing fluid is equal to

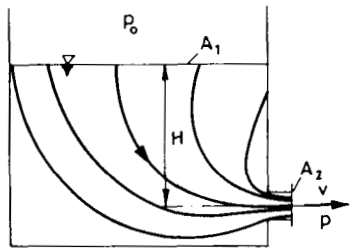

Fig. 4.8. Outflow from a closed container

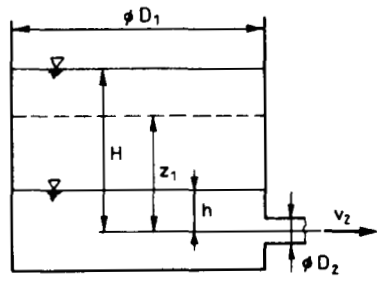

Fig. 4.9. Cylindrical tank with outflow opening

the atmospheric pressure, we have

$$\frac{v_2^2}{2g} = z_1 - z_2 ,$$

from which we obtain

$$v_2 = \sqrt{2gH} . \tag{4.65}$$

This result is known as Torricelli's law.

The determination of the time interval required for draining a tank is another related problem. Consider an open cylindrical tank, as shown in *Fig. 4.9*. Using the notation of the figure, assume that the discharge velocity may be calculated using Torricelli's law. This is an approximation, but it is well known, that this discharge process is not steady. In this case:

$$v_2 = \sqrt{2gz_1} .$$

The continuity equation is

$$\frac{D_1^2\pi}{4} v_1 = \frac{D_2^2\pi}{4} v_2 .$$

The velocity at which the free surface subsides is

$$v_1 = -\frac{\mathrm{d}z_1}{\mathrm{d}t} .$$

Combining these equations we have

$$-\frac{\mathrm{d}z_1}{\mathrm{d}t} = \left(\frac{D_2}{D_1}\right)^2 \sqrt{2gz_1} .$$

Separating the variables, we can integrate between the relevant integration limits: if $t=0$, $z_1 = H$; if $t=T$, $z_1 = h$. The final result is

$$T = \sqrt{\frac{2}{g}} \left(\frac{D_1}{D_2}\right)^2 \left(\sqrt{H} - \sqrt{h}\right) . \tag{4.66}$$

This also is an ideal value, because of contraction of outflowing fluid.

4.5 The Cauchy—Lagrange integral of Euler's equation

The Euler equation can also be integrated for unsteady flow, provided that the flow is irrotational and barotropic. For irrotational flow

$$\vec{v} = \text{grad } \Phi ; \tag{4.67}$$

thus Euler's equation is obtained as

$$\frac{\partial}{\partial t}(\text{grad } \Phi) + \text{grad}\left(\frac{v^2}{2} + \mathscr{P} + U\right) = 0 . \tag{4.68}$$

Since

$$\frac{\partial}{\partial t}(\text{grad } \Phi) = \text{grad } \frac{\partial \Phi}{\partial t} , \tag{4.69}$$

we can write

$$\text{grad}\left(\frac{\partial \Phi}{\partial t} + \frac{v^2}{2} + \mathscr{P} + U\right) = 0 . \tag{4.70}$$

Taking the line integral of Eq. (4.70) it is obvious, that the integrand is a total differential:

$$\int_1^2 \text{grad}\left(\frac{\Phi}{t} + \frac{v^2}{2} + \mathscr{P} + U\right) \mathrm{d}\vec{r} = \int_1^2 \mathrm{d}\left(\frac{\partial \Phi}{\partial t} + \frac{v^2}{2} + \mathscr{P} + U\right) = 0 .$$

Its integration yields the Bernoulli equation for unsteady flow

$$\frac{\partial \Phi}{\partial t} + \frac{v^2}{2} + \mathscr{P} + U = C(t) . \tag{4.71}$$

The constant of integration may be chosen as an arbitrary function of time determined by the boundary conditions. But since Φ may be changed by any arbitrary function of time without in any way affecting the flow, the constant $C(t)$ can be absorbed in $\partial\Phi/\partial t$, and the Bernoulli equation is obtained in the form

$$\frac{\partial \Phi}{\partial t} + \frac{v^2}{2} + \mathscr{P} + U = k . \tag{4.72}$$

Here k is a constant for the entire flow which may be chosen as one prefers. This form of the Bernoulli equation is frequently called the Cauchy—Lagrange integral of the Euler equation. It can be seen, that the energy level of field of flow is not steady. The specific mechanical energy can be expressed as

$$E_m = \frac{v^2}{2} + \mathscr{P} + U = k - \frac{\partial \Phi}{\partial t} . \tag{4.73}$$

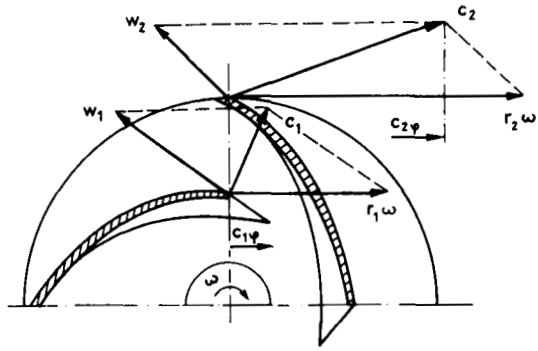

Fig. 4.10. Centrifugal impeller with velocity triangles

This equation was considered by Wislicenus to be the basic equation describing the performance of turbomachines. It is obvious that energy transfer in a perfect fluid can be possible for an unsteady flow only. As an example, the energy addition due to the impeller of a centrifugal pump can be calculated from Eq. (4.73).

Consider *Fig. 4.10*, in which a centrifugal impeller is depicted together with the velocities at the inlet and outlet. The peripheral velocity component c_φ of the irrotational flow can be expressed in terms of the velocity potential Φ as

$$c_\varphi = \frac{1}{r}\frac{\partial \Phi}{\partial \varphi}. \tag{4.74}$$

Applying the chain rule, we can also write as

$$\frac{\partial \Phi}{\partial t} = \frac{\partial \Phi}{\partial(\varphi - \omega t)}\frac{\partial(\varphi - \omega t)}{\partial t} = -\omega \frac{\partial \Phi}{\partial(\varphi - \omega t)}, \tag{4.75}$$

where ωt is the periodicity of the transient flow.

Since this unsteady flow is periodic

$$\frac{\partial \Phi}{\partial(\varphi - \omega t)} = \frac{\partial \Phi}{\partial \varphi}. \tag{4.76}$$

Combining these expressions, the time derivative of the velocity potential Φ can be expressed in terms of the velocity component c_φ as

$$\frac{\partial \Phi}{\partial t} = -\omega r c_\varphi, \tag{4.77}$$

where ω is the angular velocity of the impeller. The energy increase between the outlet and inlet is obtained as

$$\Delta E = -\left(\frac{\partial \Phi}{\partial t}\right)_2 - \left(-\frac{\partial \Phi}{\partial t}\right)_1 = -\omega(r_2 c_{2\varphi} - r_1 c_{1\varphi}). \tag{4.78}$$

This can be expressed in terms of the circulation as

$$\Delta E = \frac{\omega \Gamma}{2\pi}. \tag{4.79}$$

For rotational unsteady flow Euler's equation can be integrated along a streamline or along a vortex line. In these cases

$$(\operatorname{curl} \vec{v} \times \vec{v})\, \mathrm{d}\vec{r} = 0,$$

and thus we can write

$$\int_1^2 \frac{\partial \vec{v}}{\partial t}\, \mathrm{d}\vec{r} + \left[\frac{v^2}{2} + \mathscr{P} + U\right]_1^2 = 0. \tag{4.80}$$

This equation seems to be analogous to the Bernoulli equation for irrotational, unsteady flow. An essential difference between them is that while the irrotational unsteady Bernoulli equation is valid for the whole field of flow, the rotational form may only be written along a streamline or along a vortex line.

An important feature of irrotational flow is that three velocity components can be determined knowing only one scalar function, the velocity potential Φ. Since

$$\vec{v} = \operatorname{grad} \Phi,$$

the Bernoulli equation can be written

$$\frac{\partial \Phi}{\partial t} + \frac{1}{2}\left[\left(\frac{\partial \Phi}{\partial x}\right)^2 + \left(\frac{\partial \Phi}{\partial y}\right)^2 + \left(\frac{\partial \Phi}{\partial z}\right)^2\right] + \mathscr{P} + U = k. \tag{4.81}$$

The continuity equation can obtained in the form

$$\frac{\partial \varrho}{\partial t} + \operatorname{div}(\varrho \operatorname{grad} \Phi) = 0, \tag{4.82}$$

or

$$\frac{\partial \varrho}{\partial t} + \varrho \Delta \Phi + \operatorname{grad} \Phi \operatorname{grad} \varrho = 0. \tag{4.83}$$

For an incompressible fluid

$$\frac{\partial \varrho}{\partial t} = 0; \qquad \operatorname{grad} \varrho = 0,$$

thus we obtain the Laplace equation for the velocity potential:

$$\Delta \Phi = \frac{\partial^2 \Phi}{\partial x^2} + \frac{\partial^2 \Phi}{\partial y^2} + \frac{\partial^2 \Phi}{\partial z^2} = 0. \tag{4.84}$$

If the Laplace equation is satisfied by Φ in a volume V at the boundary (A) of which Φ is known, so that on (A)

$$\Phi = \Phi_A(x, y, z),$$

the problem is called the Dirichlet problem.

Another case is that where, instead of Φ, its normal derivative is given at the boundary. Then

$$\frac{\partial \Phi}{\partial n} = \frac{\partial \Phi_A}{\partial n}(x, y, z)$$

on (A).

This problem is the so-called Neumann problem. The solution of the Dirichlet and the Neumann problems is unique. For two-dimensional flows in particular, complex variable functions can be successfully supplied.

4.6 Kelvin's vortex theorem

As it is known, circulation around any closed curve in the fluid is defined by the integral

$$\Gamma = \int_{(G)} \vec{v}\, \mathrm{d}\vec{r}\,. \tag{4.85}$$

Consider now a closed material curve G moving with the fluid. A material curve consists of identical fluid particles, changing its shape and position with time. Thus the circulation around this moving circuit must change. The rate of change of the circulation around this material curve G may be calculated as

$$\frac{\mathrm{d}\Gamma}{\mathrm{d}t} = \frac{\mathrm{d}}{\mathrm{d}t} \int_{(G)} \vec{v}\, \mathrm{d}\vec{r}\,. \tag{4.86}$$

It is obvious that

$$\frac{\mathrm{d}}{\mathrm{d}t} \int_{(G)} \vec{v}\, \mathrm{d}\vec{r} = \int_{(G)} \frac{\mathrm{d}\vec{v}}{\mathrm{d}t}\, \mathrm{d}\vec{r} + \int_{(G)} \vec{v}\, \frac{\mathrm{d}}{\mathrm{d}t}(\mathrm{d}\vec{r})\,. \tag{4.87}$$

As is shown in *Fig. 4.11:*

$$\frac{\mathrm{d}}{\mathrm{d}t}(\mathrm{d}\vec{r}) = \mathrm{d}\vec{v}\,.$$

For conservative body forces and for barotropic flow

$$\frac{\mathrm{d}\vec{v}}{\mathrm{d}t} = -\mathrm{grad}\,(U + \mathscr{P}), \tag{4.88}$$

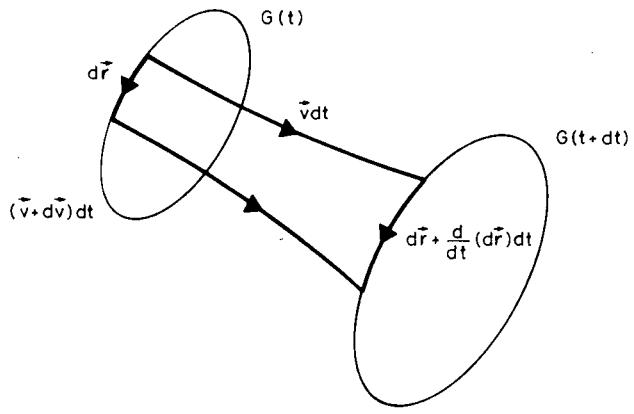

Fig. 4.11. Circulation along a closed material curve in the flowing fluid

while on the other hand

$$\vec{v}\,d\vec{v}=d\left(\frac{v^2}{2}\right).$$

After substitution

$$\frac{d\Gamma}{dt}=-\int_{(G)} d\vec{r}\,\mathrm{grad}\,(U+\mathscr{P})+\int_{(G)} d\left(\frac{v^2}{2}\right). \tag{4.89}$$

Both integrands on the right-hand side are total differentials, thus these integrals over a closed curve must vanish, i.e.

$$\frac{d\Gamma}{dt}=0. \tag{4.90}$$

An important consequence of Kelvin's theorem is that if an inviscid barotropic fluid is initially at rest, or if the circulation around any circuit in at a plane cutting in the upstream all the streamlines is zero, the subsequent motion downstream from this plane must be irrotational.

4.7 The law of conservation of energy for perfect fluid flow

It was previously shown, that the Bernoulli equation expresses the conservation of mechanical energy for the flow of a perfect fluid, provided that the body forces are conservative, and the flow irrotational and barotropic. This equation is valid for a unit mass of fluid at any point in the entire field of flow.

In the subsequent section we shall consider an arbitrary finite volume of flowing fluid in order to determine the rate of change of its kinetic and internal energy.

Substituting

$$\mathbf{T} = -p\mathbf{I}$$

into the general balance of kinetic energy equation (Eq. 3.70) leads to the following expression:

$$\frac{\mathrm{d}}{\mathrm{d}t}\int_V \varrho\frac{v^2}{2}\,\mathrm{d}V = \int_V \varrho\vec{g}\vec{v}\,\mathrm{d}V + \int_V p\,\mathrm{div}\,\vec{v}\,\mathrm{d}V - \int_{(A)} p\vec{v}\,\mathrm{d}A\,. \tag{4.91}$$

If the body forces are conservative

$$\vec{g} = -\mathrm{grad}\,U\,.$$

If the flow is barotropic the pressure forces acting on a unit mass of fluid also have a potential given by

$$\mathscr{P} = \int_{p_0}^{p}\frac{\mathrm{d}p}{\varrho}\,.$$

Since the field of body forces is steady

$$\frac{\partial U}{\partial t} = 0\,,$$

and thus for the material derivative we have

$$\frac{\mathrm{d}U}{\mathrm{d}t} = \vec{v}\,\mathrm{grad}\,U\,.$$

After substitution, and applying the divergence theorem to the surface integral on the right-hand side, Eq. (4.91) becomes

$$\frac{\mathrm{d}}{\mathrm{d}t}\int_V \varrho\left(\frac{v^2}{2}+U\right)\mathrm{d}V = \int_V [p\,\mathrm{div}\,\vec{v} - \mathrm{div}\,(p\vec{v})]\,\mathrm{d}V\,. \tag{4.92}$$

It is obvious, that

$$p\,\mathrm{div}\,\vec{v} - \mathrm{div}\,(p\vec{v}) = p\,\mathrm{div}\,\vec{v} - p\,\mathrm{div}\,\vec{v} - \vec{v}\,\mathrm{grad}\,p\,. \tag{4.93}$$

Taking into account that

$$\frac{\mathrm{d}\mathscr{P}}{\mathrm{d}t} = \frac{\partial\mathscr{P}}{\partial t} + \vec{v}\,\mathrm{grad}\,\mathscr{P}\,, \tag{4.94}$$

and

$$\frac{1}{\varrho}\,\mathrm{grad}\,p = \mathrm{grad}\,\mathscr{P}\,, \tag{4.95}$$

we obtain

$$\varrho \vec{v} \operatorname{grad} \mathscr{P} = \varrho \left(\frac{\mathrm{d}\mathscr{P}}{\mathrm{d}t} - \frac{\partial \mathscr{P}}{\partial t} \right). \tag{4.96}$$

After substitution, Eq. (4.92) becomes

$$\frac{\mathrm{d}}{\mathrm{d}t} \int_V \varrho \left(\frac{v^2}{2} + U + \mathscr{P} \right) \mathrm{d}V = \int_V \varrho \frac{\partial \mathscr{P}}{\partial t} \mathrm{d}V . \tag{4.97}$$

This may be written in differential form as

$$\frac{\mathrm{d}}{\mathrm{d}t} \left(\frac{\dot{v}^2}{2} + U + \mathscr{P} \right) = \frac{\partial \mathscr{P}}{\partial t} . \tag{4.98}$$

The terms representing the local and the convective rate of change of the mechanical energy may be split, i.e.

$$\frac{\partial}{\partial t} \left(\frac{v^2}{2} + U + \mathscr{P} \right) + \vec{v} \operatorname{grad} \left(\frac{v^2}{2} + U + \mathscr{P} \right) = \frac{\partial \mathscr{P}}{\partial t} . \tag{4.99}$$

If the flow is steady

$$\vec{v} \operatorname{grad} \left(\frac{v^2}{2} + U + \mathscr{P} \right) = 0 . \tag{4.100}$$

There are two special situations in which this equation is fulfilled:

$\vec{v} = 0$, represents the hydrostatic case

$\frac{v^2}{2} + U + \mathscr{P} = \text{const}$, represents a steady, irrotational flow with a conservative body force.

Generally the velocity vector and the gradient vector of the mechanical energy must be orthogonal, thus their scalar product vanishes. This general equation (4.100) shows that for a steady flow the velocity vector is tangential to the constant surfaces of the mechanical energy.

The law of conservation of energy for the flow of a perfect fluid can be written as

$$\frac{\mathrm{d}}{\mathrm{d}t} \int_V \varrho \left(\frac{v^2}{2} + \varepsilon \right) \mathrm{d}V = \int_V \varrho \vec{g} \vec{v} \, \mathrm{d}V - \int_{(A)} \vec{v} p \, \mathrm{d}\vec{A} - \int_{(A)} q \, \mathrm{d}\vec{A} . \tag{4.101}$$

Subtracting the kinetic energy equation from the above we obtain the equation for the balance of the internal energy

$$\frac{\mathrm{d}}{\mathrm{d}t} \int_V \varrho \varepsilon \, \mathrm{d}V = - \int_V p \operatorname{div} \vec{v} \, \mathrm{d}V - \int_{(A)} \dot{q} \, \mathrm{d}\vec{A} . \tag{4.102}$$

The left-hand side of this equation may be transformed applying the transport theorem

$$\frac{\mathrm{d}}{\mathrm{d}t}\int_V \varrho\varepsilon\,\mathrm{d}V=\int_V\left[\frac{\mathrm{d}(\varrho\varepsilon)}{\mathrm{d}t}+\varrho\varepsilon\,\mathrm{div}\,\vec{v}\right]\mathrm{d}V=$$

$$=\int_V\left(\varrho\frac{\mathrm{d}\varepsilon}{\mathrm{d}t}+\varepsilon\frac{\mathrm{d}\varrho}{\mathrm{d}t}+\varepsilon\varrho\,\mathrm{div}\,\vec{v}\right)\mathrm{d}V. \tag{4.103}$$

The second and third terms vanish due to the continuity equation. The surface integral on the right-hand side of Eq. (4.102) can be transformed into a volume integral by applying the divergence theorem. Thus we get

$$\int_V \varrho\frac{\mathrm{d}\varepsilon}{\mathrm{d}t}\mathrm{d}V=-\int_V p\,\mathrm{div}\,\vec{v}\,\mathrm{d}V-\int_V \mathrm{div}\,\vec{q}\,\mathrm{d}V. \tag{4.104}$$

Now we can easily write this equation in differential form:

$$\varrho\frac{\mathrm{d}\varepsilon}{\mathrm{d}t}=-p\,\mathrm{div}\,\vec{v}-\mathrm{div}\,\vec{q}\,. \tag{4.105}$$

Using the continuity equation the divergence of the velocity can be expressed as

$$\mathrm{div}\,\vec{v}=-\frac{1}{\varrho}\frac{\mathrm{d}\varrho}{\mathrm{d}t}=\varrho\left(-\frac{1}{\varrho^2}\right)\frac{\mathrm{d}\varrho}{\mathrm{d}t}=\varrho\frac{\mathrm{d}}{\mathrm{d}t}\left(\frac{1}{\varrho}\right). \tag{4.106}$$

Substituting into the balance of internal energy equation it is obvious that

$$p\,\mathrm{div}\,\vec{v}=\varrho p\frac{\mathrm{d}}{\mathrm{d}t}\left(\frac{1}{\varrho}\right)=\varrho p\frac{\mathrm{d}\vartheta}{\mathrm{d}t}, \tag{4.107}$$

and therefore it represents the rate of the work done by the pressure per unit volume of the perfect fluid. ϑ is the specific volume of the fluid. The equation

$$\varrho\frac{\mathrm{d}\varepsilon}{\mathrm{d}t}+\varrho p\frac{\mathrm{d}\vartheta}{\mathrm{d}t}=-\mathrm{div}\,\vec{q}\,, \tag{4.108}$$

obtained from Eqs (4.105) and (4.107), is simply the well-known first law of thermodynamics for a system in equilibrium. The fact that this equation is obtained as a rate expression does not contradict the idea of equilibrium. It simply states, that the system (now a fluid particle of unit volume) passes only through equilibrium states.

For adiabatic systems (i.e. with boundaries which are perfectly insulated w.r.t. a heat flux), the heat flow vector $\vec{q}$ vanishes, thus we get

$$\varrho\frac{\mathrm{d}\varepsilon}{\mathrm{d}t}+\varrho p\frac{\mathrm{d}\vartheta}{\mathrm{d}t}=0. \tag{4.109}$$

If the perfect fluid is an ideal gas

$$\varepsilon = c_v T;$$

after substitution, the following equation is obtained

$$c_v \frac{\mathrm{d}T}{\mathrm{d}t} + p \frac{\mathrm{d}\vartheta}{\mathrm{d}t} = 0. \tag{4.110}$$

Using Eqs (4.106) and (4.107) this becomes

$$c_v \frac{\mathrm{d}T}{\mathrm{d}t} = \frac{p}{\varrho^2} \frac{\mathrm{d}\varrho}{\mathrm{d}t}.$$

Consider the well-known thermodynamical relationships

$$\frac{p}{\varrho} = RT,$$

$$\kappa = \frac{c_p}{c_v},$$

$$c_p - c_v = R.$$

Substituting we have

$$\frac{R}{\kappa - 1} \frac{\mathrm{d}T}{\mathrm{d}t} = RT \frac{1}{\varrho} \frac{\mathrm{d}\varrho}{\mathrm{d}t}, \tag{4.111}$$

and after a little manipulation the following equation can be written:

$$\frac{1}{\kappa - 1} \frac{\mathrm{d}}{\mathrm{d}t} (\ln T) = \frac{\mathrm{d}}{\mathrm{d}t} (\ln \varrho). \tag{4.112}$$

This may be expressed as

$$\frac{\mathrm{d}}{\mathrm{d}t} \left[\ln \left(\frac{T}{\varrho^{\kappa - 1}} \right) \right] = 0. \tag{4.113}$$

It is obvious, that in this case

$$\frac{\mathrm{d}}{\mathrm{d}t} \left(\frac{T}{\varrho^{\kappa - 1}} \right) = 0, \tag{4.114}$$

or in another form

$$\frac{\mathrm{d}}{\mathrm{d}t} \left(\frac{p}{\varrho^{\kappa}} \right) = 0. \tag{4.115}$$

Separating the local and convective rate of change we have:

$$\frac{\partial}{\partial t} \left(\frac{p}{\varrho^{\kappa}} \right) + \tilde{v} \operatorname{grad} \left(\frac{p}{\varrho^{\kappa}} \right) = 0. \tag{4.116}$$

For steady flow

$$\vec{v}\,\mathrm{grad}\left(\frac{p}{\varrho^{\kappa}}\right)=0\,, \tag{4.117}$$

therefore, along the streamlines

$$\frac{p}{\varrho^{\kappa}}=\mathrm{const.} \tag{4.118}$$

The physical meaning of this is, that the flow of a perfect fluid in an adiabatic system must be isentropic.

4.8 The Vázsonyi—Crocco equation

Now we shall determine the relationships between the kinematic and thermal variables for an ideal perfect gas flow. We restrict our considerations to the case of steady flow only. Euler's equation for steady rotational flow is

$$\vec{\Omega}\times\vec{v}+\mathrm{grad}\,\frac{v^2}{2}=-\frac{1}{\varrho}\,\mathrm{grad}\,p\,. \tag{4.119}$$

The specific enthalpy of the gas is defined by the equation

$$i=\varepsilon+\frac{p}{\varrho}\,. \tag{4.120}$$

Differentiating this equation we get

$$\mathrm{grad}\,i=\mathrm{grad}\,\varepsilon+p\,\mathrm{grad}\left(\frac{1}{\varrho}\right)+\frac{1}{\varrho}\,\mathrm{grad}\,p\,. \tag{4.121}$$

The first law of thermodynamics can be expressed in terms of the entropy S as

$$T\,\mathrm{d}S=\mathrm{d}\varepsilon+p\,\mathrm{d}\left(\frac{1}{\varrho}\right). \tag{4.122}$$

Since the flow is steady, the local rates of change in the total differentials vanish, thus

$$\vec{v}T\,\mathrm{grad}\,S=\vec{v}\,\mathrm{grad}\,\varepsilon+\vec{v}p\,\mathrm{grad}\left(\frac{1}{\varrho}\right). \tag{4.123}$$

Since the velocity is not zero in the flow we may divide by $\vec{v}$, thus

$$T\,\mathrm{grad}\,S=\mathrm{grad}\,\varepsilon+p\,\mathrm{grad}\left(\frac{1}{\varrho}\right). \tag{4.124}$$

Substituting into Eq. (4.121) we get

$$\mathrm{grad}\,i=T\,\mathrm{grad}\,S+\frac{1}{\varrho}\,\mathrm{grad}\,p\,. \tag{4.125}$$

Rearranging this to express the pressure force acting on a unit mass of gas, and substituting into Euler's equation, the Vázsonyi—Crocco equation is obtained:

$$\vec{\Omega} \times \vec{v} = T \operatorname{grad} S - \operatorname{grad}\left(\frac{v^2}{2} + i\right). \tag{4.126}$$

For steady adiabatic flow

$$i + \frac{v^2}{2} = i_0, \tag{4.127}$$

where i_0 is the so-called stagnation enthalpy.

The Vázsonyi—Crocco equation differs from Euler's equation in the term T grad S. It is obvious, that the equation

$$\vec{\Omega} \times \vec{v} = -\operatorname{grad}\left(\frac{v^2}{2} + i\right) \tag{4.128}$$

is valid for isentropic flow. Multiplying the Vázsonyi—Crocco equation by the velocity, the left-hand side of the equation vanishes. Similarly the $\vec{v}$ grad S term must be zero since the entropy is constant along a streamline. Thus we have

$$\vec{v} \operatorname{grad}\left(\frac{v^2}{2} + i\right) = \vec{v} \operatorname{grad} i_0 = 0; \tag{4.129}$$

therefore, the sum of the kinetic energy and the enthalpy is constant along a streamline. An important consequence of the Vázsonyi—Crocco equation is that a steady planar or axisymmetric gas flow must be irrotational, if the entropy and the stagnation enthalpy is constant.

The rate of the vorticity can be expressed in terms of the thermal variables T and S. The flow need not to be barotropic. Taking the curl of the acceleration field:

$$\operatorname{curl} \vec{a} = \frac{\mathrm{d}\vec{\Omega}}{\mathrm{d}t} - \vec{\Omega} \operatorname{div} \vec{v} - (\vec{\Omega} V)\, \vec{v}, \tag{4.130}$$

substituting the divergence of the velocity

$$\operatorname{div} \vec{v} = -\frac{1}{\varrho} \frac{\mathrm{d}\varrho}{\mathrm{d}t},$$

and dividing by the density we obtain

$$\frac{1}{\varrho} \operatorname{curl} \vec{a} = \frac{1}{\varrho} \frac{\mathrm{d}\vec{\Omega}}{\mathrm{d}t} + \vec{\Omega} \frac{\mathrm{d}}{\mathrm{d}t}\left(\frac{1}{\varrho}\right) - \frac{1}{\varrho} (\vec{\Omega} V)\, \vec{v}.$$

Remembering that

$$\frac{\mathrm{d}}{\mathrm{d}t}\left(\frac{\vec{\Omega}}{\varrho}\right) = \frac{1}{\varrho} \frac{\mathrm{d}\vec{\Omega}}{\mathrm{d}t} + \vec{\Omega} \frac{\mathrm{d}}{\mathrm{d}t}\left(\frac{1}{\varrho}\right),$$

and substituting, the so-called Beltrami equation is obtained:

$$\frac{\mathrm{d}}{\mathrm{d}t}\left(\frac{\vec{\Omega}}{\varrho}\right)=\frac{1}{\varrho}\operatorname{curl}\vec{a}+(\vec{v}\circ\nabla)\frac{\vec{\Omega}}{\varrho}. \tag{4.131}$$

For barotropic flow

$$\vec{a}=-\operatorname{grad}\left(\frac{v^2}{2}+U+\mathscr{P}\right), \tag{4.132}$$

therefore,

$$\operatorname{curl}\vec{a}=0. \tag{4.133}$$

Thus, in this case the Beltrami equation becomes

$$\frac{\mathrm{d}}{\mathrm{d}t}\left(\frac{\vec{\Omega}}{\varrho}\right)=(\vec{v}\circ\nabla)\frac{\vec{\Omega}}{\varrho}. \tag{4.134}$$

In general

$$\operatorname{curl}\vec{a}=-\operatorname{curl}\left(\frac{1}{\varrho}\operatorname{grad}p\right)=\operatorname{curl}(T\operatorname{grad}S-\operatorname{grad}i), \tag{4.135}$$

therefore

$$\operatorname{curl}\vec{a}=\operatorname{grad}T\times\operatorname{grad}S. \tag{4.136}$$

Substituting this result into the Vázsonyi equation

$$\frac{\mathrm{d}}{\mathrm{d}t}\left(\frac{\vec{\Omega}}{\varrho}\right)=\frac{1}{\varrho}\operatorname{grad}T\times\operatorname{grad}S+(\vec{v}\circ\nabla)\frac{\vec{\Omega}}{\varrho}. \tag{4.137}$$

The term $\frac{1}{\varrho}\operatorname{grad}T\times\operatorname{grad}S$ shows, that if the entropy field is not constant, vortex diffusion occurs in the flow, irrespective of the Helmholtz vortex theorem.

For a steady flow with a uniform stagnation enthalpy the Vázsonyi—Crocco equation can be written as

$$\vec{\Omega}\times\vec{v}=T\operatorname{grad}S. \tag{4.138}$$

Rearranging to express grad S and substituting into the expression grad $T\times$ grad S we obtain

$$\operatorname{grad}T\times\operatorname{grad}S=\frac{1}{T}[\operatorname{grad}T\times(\vec{\Omega}\times\vec{v})]=T(\vec{\Omega}\times\vec{v})\times\operatorname{grad}\frac{1}{T}.$$

Thus,

$$\operatorname{grad}T\times\operatorname{grad}S=T\left[\vec{v}\left(\vec{\Omega}\operatorname{grad}\frac{1}{T}\right)-\vec{\Omega}\frac{\mathrm{d}}{\mathrm{d}t}\left(\frac{1}{T}\right)\right]. \tag{4.139}$$

Therefore the Vázsonyi vortex equation can be written in a simpler form:

$$\frac{\mathrm{d}}{\mathrm{d}t}\left(\frac{\vec{\Omega}}{\varrho T}\right)=\left(\frac{\vec{v}}{T}\circ\nabla\right)\frac{\vec{\Omega}}{\varrho}. \tag{4.140}$$

The consequence of Vázsonyi's equation is that along any streamline of a plane flow

$$\frac{\Omega}{\varrho T} = \text{const.} \tag{4.141}$$

The Vázsonyi—Crocco equation is especially applicable to non-barotropic flows — e.g. explosion shocks — in engineering practice.

4.9 Small perturbations at the speed of sound

In a great number of engineering problems one is interested in the perturbation of a given flow. The motion of the perturbations relative to the fluid is called the wave motion, and the velocity of propagation the wave velocity. In the preceding sections the equations required to treat this phenomenon have already been introduced. A description of such a system requires the use of the continuity equation,

$$\frac{\mathrm{d}\varrho}{\mathrm{d}t} + \varrho \operatorname{div} \vec{v} = 0 ;$$

the momentum equation, neglecting body forces,

$$\frac{\mathrm{d}\vec{v}}{\mathrm{d}t} + \frac{1}{\varrho} \operatorname{grad} p = 0 ;$$

the energy equation, assuming an adiabatic system,

$$\varrho c_v \frac{\mathrm{d}T}{\mathrm{d}t} + p \operatorname{div} \vec{v} = 0 ;$$

and, finally, the equation of state, for an ideal gas

$$\frac{p}{\varrho} = RT .$$

It is known, that during thermal processes of gases the condition

$$\left(\frac{\partial p}{\partial \varrho}\right)_s > 0$$

is always valid. If the pressure rises, the density must increase. Thus a new variable of state may be defined by the equation

$$a = \sqrt{\left(\frac{\partial p}{\partial \varrho}\right)_{s=\text{const}}} , \tag{4.142}$$

and a modified barotropic potential can be introduced:

$$\tilde{\mathcal{P}} = \int \frac{\mathrm{d}p}{a\varrho}. \tag{4.143}$$

Substituting these new variables, the continuity and momentum equation can be expressed as

$$\frac{\mathrm{d}\tilde{\mathcal{P}}}{\mathrm{d}t} + a \operatorname{div} \vec{v} = 0, \tag{4.144}$$

$$\frac{\mathrm{d}\vec{v}}{\mathrm{d}t} + a \operatorname{grad} \tilde{\mathcal{P}} = 0. \tag{4.145}$$

This pair of conjugate equations can be used to describe the propagation of small disturbances in a steady gas flow or at rest.

Assume that the amplitude of the pressure wave is very small relative to the equilibrium pressure. All flow variables are considered to represent small perturbations relative to the steady state. It is an empirical fact that the quantity a, which has the dimensions of a velocity, is much greater than the flow velocity $\vec{v}$.

After expanding the material derivatives of Eqs (4.144) and (4.145) we obtain the equations

$$\frac{\partial \tilde{\mathcal{P}}}{\partial t} \vec{v} \operatorname{grad} \tilde{\mathcal{P}} + a \operatorname{div} \vec{v} = 0, \tag{4.146}$$

and

$$\frac{\partial \vec{v}}{\partial t} + (\vec{v}\nabla)\vec{v} + a \operatorname{grad} \tilde{\mathcal{P}} = 0. \tag{4.147}$$

Neglecting the terms $(\vec{v}\nabla)\,\vec{v}$ and $\vec{v}$ grad $\tilde{\mathcal{P}}$ the following equations are obtained:

$$\frac{\partial \tilde{\mathcal{P}}}{\partial t} + a \operatorname{div} \vec{v} = 0, \tag{4.148}$$

$$\frac{\partial \vec{v}}{\partial t} + a \operatorname{grad} \tilde{\mathcal{P}} = 0. \tag{4.149}$$

Upon differentiating w.r.t. time:

$$\frac{\partial^2 \tilde{\mathcal{P}}}{\partial t^2} + a \operatorname{div} \frac{\partial \vec{v}}{\partial t} = 0, \tag{4.150}$$

$$\frac{\partial^2 \vec{v}}{\partial t^2} + a \operatorname{grad} \frac{\partial \tilde{\mathcal{P}}}{\partial t} = 0. \tag{4.151}$$

Substituting $\frac{\partial \vec{v}}{\partial t}$ and $\frac{\partial \tilde{\mathscr{P}}}{\partial t}$ from the preceding equations, we obtain

$$\frac{\partial^2 \tilde{\mathscr{P}}}{\partial t^2} + a^2 \nabla \tilde{\mathscr{P}} = 0\,, \tag{4.152}$$

$$\frac{\partial^2 \vec{v}}{\partial t^2} + a^2 \nabla \vec{v} = 0\,. \tag{4.153}$$

These equations for $\tilde{\mathscr{P}}$ and $\vec{v}$ have the well-known form of the wave equation. It is thus evident that pressure — and velocity — perturbations propagate wavelike in a compressible fluid. The quantity a is called the speed of sound since it is the velocity at which a perturbation propagates through the fluid. [Note, that all perturbations (pressure-, velocity- or density-waves) propagate at the same velocity.] The speed of sound is a variable of the thermal state, its particular formula varies according to the type of thermal process. For the isentropic case

$$a = \sqrt{\kappa \frac{p}{\varrho}} = \sqrt{\kappa R T}, \tag{4.154}$$

while the isothermal speed of sound is

$$a = \sqrt{\frac{p}{\varrho}} = \sqrt{RT}, \tag{4.155}$$

and for a polytropic change of state

$$a = \sqrt{n \frac{p}{\varrho}} = \sqrt{nRT}. \tag{4.156}$$

($n =$ polytropic heat capacity ratio.)

It is obvious that wave propagation cannot take place in incompressible fluids. If a real liquid is considered to be compressible the wave equations are valid in the same form. The only difference lies in the equation of state. Thus for a compressible liquid the speed of sound is obtained as

$$a = \sqrt{\frac{B}{\varrho}}, \tag{4.157}$$

i.e. a function of the bulk modulus of elasticity B. The speed of sound in this case is almost always nearly constant, except when the minimum pressure falls below the vapor pressure of the liquid. The modified barotropic potential is

$$\tilde{\mathscr{P}} = \frac{p}{a\varrho}. \tag{4.158}$$

Thus it is possible to recognize a rather strict analogy between the propagation of sound waves in gases and elastic waves in liquids. On the basis of this analogy it becomes possible to calculate wave propagation and waterhammer in both crude oil and natural gas pipelines.

4.10 Dynamical similarity of ideal gas flows

The non-linear nature of Euler's equation may cause serious mathematical difficulties when solving a problem on the flow of ideal gas. Numerical methods may occasionally be applicable, but sometimes experimental investigation is the only way to determine the distribution of the flow variables. In this case it is very important to know whether the results measured with a particular experimental setup are applicable to another, similar, situation. In general it is assumed that the flow boundaries are geometrically similar for the two processes to be compared. This geometrical similarity is a necessary but not a sufficient condition for the complete similarity of the two flows investigated. It is obvious that an aerofoil of a compressor blade should have the same profile as its counterpart tested in a wind tunnel.

The idea of dynamical similarity is originally due to Stokes. Dynamical similarity implies identical solutions of the differential equations for the two cases. The equations must therefore, be identical; the only difference may be a constant multiplier. Dynamical similarity requires that the flow variables of the two cases should be related by the equations

$$\tilde{r}' = \alpha_r \tilde{r} \qquad t' = \alpha_t t \qquad \tilde{v}' = \alpha_v \tilde{v} \qquad \varrho' = \alpha_\varrho \varrho \qquad p' = \alpha_p p \,.$$

The scale factors α must be constant for the whole flow field. The first equation expresses the geometrical similarity. For the two flows the following continuity equations are obtained:

$$\frac{\mathrm{d}\varrho'}{\mathrm{d}t'} + \varrho' \operatorname{div}' \tilde{v}' = 0 \,, \tag{4.159}$$

and

$$\frac{\mathrm{d}\varrho}{\mathrm{d}t} + \varrho \operatorname{div} \tilde{v} = 0 \,. \tag{4.160}$$

Analogously, the Euler equations are

$$\frac{\mathrm{d}\tilde{v}'}{\mathrm{d}t'} + \frac{1}{\varrho} \operatorname{grad}' p' = 0 \,, \tag{4.161}$$

and

$$\frac{\mathrm{d}\tilde{v}}{\mathrm{d}t} + \frac{1}{\varrho} \operatorname{grad} p = 0 \,. \tag{4.162}$$

Substituting into the continuity equations, we find

$$\frac{\alpha_\varrho}{\alpha t}\frac{\mathrm{d}\varrho}{\mathrm{d}t}+\frac{\alpha_\varrho \alpha_v}{\alpha_r}\varrho \operatorname{div}\vec{v}=0\,. \tag{4.163}$$

Since α_ϱ/α_t and $\alpha_\varrho\ \alpha_v/\alpha_r$ must be the same constants, we have

$$\alpha_t=\frac{\alpha_r}{\alpha_v}\,. \tag{4.164}$$

This requirement applies to unsteady flow only. For steady flows the continuity equations are always identical. Equation (4.164) shows that the scale factors for length, velocity and time are not independent. While two of the three scale factors may be chosen at random, the third one is then fixed. In Euler's equation the scale factors for the length and the velocity are chosen while the scale factor for the time is obtained from Eq. (4.164). Thus we get

$$\frac{\alpha_v^2}{\alpha_r}\frac{\mathrm{d}\vec{v}}{\mathrm{d}t}+\frac{\alpha_p}{\alpha_\varrho \alpha_r}\frac{1}{\varrho}\operatorname{grad} p=0\,. \tag{4.165}$$

From Eqs (4.162) and (4.165) we readily obtain

$$\alpha_v^2=\frac{\alpha_p}{\alpha_\varrho}\,. \tag{4.166}$$

Therefore,

$$\frac{\varrho_1 v_1^2}{p_1}=\frac{\varrho_2 v_2^2}{p_2}\,. \tag{4.167}$$

After a little manipulation we have

$$\frac{v_1^2}{\kappa\dfrac{p_1}{\varrho_1}}=\frac{v_2^2}{\kappa\dfrac{p_2}{\varrho_2}}\,. \tag{4.168}$$

It is easy to recognize in the denominator the square of the isentropic speed of sound. Taking the square root of both side of the equation, we obtain

$$\frac{v_1}{a_1}=\frac{v_2}{a_2}\,. \tag{4.169}$$

It now follows from this equation, that in order for two ideal gas flows to be dynamically similar the so-called Mach number

$$M=\frac{v}{a} \tag{4.170}$$

must be the same at the corresponding points of each flow. The Mach number is the most important parameter in compressible flow theory.

It also follows that, if R or κ is the same, the equation of state is automatically the same in the two cases. For isothermal flow this condition is always satisfied, but for isentropic flow slight differences may occur. If the flow is polytropic the difference can be larger and it is necessary to carry out a more detailed analysis.

4.11 Critical flow variables

For compressible flows two regions of different behavior can be recognized depending on the Mach number. If the flow velocity is smaller than the local speed of sound, i.e.

$$v<a\,,$$

the Mach number is smaller than unity

$$M<1\,,$$

and the flow region is called *subsonic.*

If the velocity of the flowing gas is greater than the local speed of sound, the inequalities

$$v>a,$$

and

$$M>1$$

define the *supersonic* flow region.

The limiting condition separating the two flow regions is that of the so-called *critical* flow, for which

$$v=a, \quad \text{and} \quad M=1\,,$$

i.e. the velocity of the gas flow is equal to the local speed of sound.

To determine the critical flow variables consider a flow system as shown in *Fig. 4.12.* There is an infinitely large reservoir connected to a channel of variable

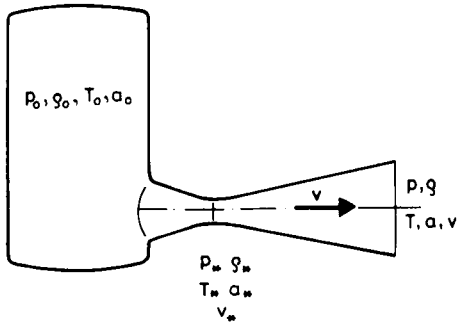

Fig. 4.12. Flow channel with variable cross section

cross-section. The variables of state in the reservoir are denoted by the subscript 0. It is obvious that the velocity in the infinitely large reservoir must be zero. The Bernoulli equation for this isentropic flow can be written as

$$\frac{v^2}{2}+\frac{\kappa}{\kappa-1}\frac{p}{\varrho}=\frac{\kappa}{\kappa-1}\frac{p_0}{\varrho_0}. \tag{4.171}$$

By introducing the definition of the speed of sound into Eq. (4.171), we obtain

$$\frac{v^2}{2}+\frac{a^2}{\kappa-1}=\frac{a_0^2}{\kappa-1}, \tag{4.172}$$

where a_0 is the speed of sound corresponding to the conditions in the reservoir. In the critical state

$$v=v_*=a_*. \tag{4.173}$$

Substituting into Eq. (4.172) we obtain

$$\frac{a_*^2}{2}+\frac{a_*^2}{\kappa-1}=\frac{a_0^2}{\kappa-1}, \tag{4.174}$$

which yields the critical speed of sound as

$$a_*=a_0\sqrt{\frac{2}{\kappa+1}}. \tag{4.175}$$

It is obvious that the critical flow velocity has the same value

$$v_*=a_0\sqrt{\frac{2}{\kappa+1}}. \tag{4.176}$$

The critical speed of sound can be expressed as

$$a_*^2=\kappa RT_*, \tag{4.177}$$

while the speed of sound in the reservoir is

$$a_0^2=\kappa RT_0. \tag{4.178}$$

Comparing these two equations we have

$$T_*=T_0\frac{2}{\kappa+1}. \tag{4.179}$$

Applying the Clapeyron equation to the isentropic processes the critical pressure can be determined as

$$p_*=p_0\left(\frac{2}{\kappa+1}\right)^{\frac{\kappa}{\kappa-1}}. \tag{4.180}$$

Table 4.1. Critical flow variables for ideal gases

	a_*/a_0	T_*/T_0	p_*/p_0	ϱ_*/ϱ_0
Argon	0.865	0.749	0.486	0.650
Helium	0.867	0.752	0.488	0.649
Carbon monoxide	0.913	0.833	0.528	0.634
Air	0.913	0.834	0.529	0.635
Oxygen	0.913	0.834	0.529	0.635
Nitrogen	0.913	0.834	0.529	0.635
Hydrogen	0.911	0.830	0.525	0.633
Ammonia	0.930	0.865	0.543	0.627
Carbon dioxide	0.933	0.870	0.546	0.628
Superheated vapor	0.927	0.859	0.542	0.631
Methane	0.932	0.868	0.545	0.628
Ethane	0.9492	0.9009	0.5606	0.6223
Propane	0.9667	0.9346	0.5765	0.6169
Butane	0.9736	0.9479	0.5828	0.6148

Since

$$\frac{p}{\varrho^\kappa} = \frac{p_0}{\varrho_0^\kappa} = \frac{p_*}{\varrho_*^\kappa},$$

the density of the critical gas flow is

$$\varrho_* = \varrho_0 \left(\frac{2}{\kappa+1}\right)^{\frac{1}{\kappa-1}}. \tag{4.181}$$

The critical flow variables for a number of ideal gases, are listed in *Table 4.1.*

The flow variables can be expressed in terms of the Mach number. Let the isentropic Bernoulli equation

$$\frac{v^2}{2} + \frac{a^2}{\kappa-1} = \frac{a_0^2}{\kappa-1}$$

be multiplied by the factor $(\kappa-1)/a^2$, then

$$\frac{\kappa-1}{2}\frac{v^2}{a^2} + 1 = \frac{a_0^2}{a^2}. \tag{4.182}$$

The following relations are obtained immediately

$$\frac{a_0}{a} = \sqrt{1 + \frac{\kappa-1}{2} M^2}, \tag{4.183}$$

$$\frac{T_0}{T} = 1 + \frac{\kappa-1}{2} M^2, \tag{4.184}$$

$$\frac{p_0}{p} = \left(1 + \frac{\kappa - 1}{2} M^2\right)^{\frac{\kappa}{\kappa - 1}}, \tag{4.185}$$

$$\frac{\varrho_0}{\varrho} = \left(1 + \frac{\kappa - 1}{2} M^2\right)^{\frac{1}{\kappa - 1}}. \tag{4.186}$$

If the flow is isentropic, the reservoir variables a_0, T_0, p_0 and ϱ_0 are constant throughout the flow.

4.12 Variation in area for isentropic flow

In many engineering devices used in the natural gas industry, the flow of a gas may be either accelerated or decelerated. Different kinds of orifices and nozzles are used to control the performance of natural-gas producing wells. Nozzles are used in gas turbines to convert internal energy into kinetic energy. For an incompressible flow the relation between the area and the velocity is obvious: an increase in area leads to a decrease in the velocity, and vice versa. It will be shown that for a compressible flow the variation in the area of the flow channel by itself does not determine the nature of the velocity change. The effects of compressibility are most readily illustrated by considering a steady isentropic flow in a channel of variable cross-sectional area. The flow is considered to be one-dimensional: all flow parameters are taken to be constant across a cross-section perpendicular to the flow. The continuity equation in this case is

$$\varrho v A = \text{const},$$

where A is the cross-sectional area of the flow.

Taking the logarithm, and after differentiation, we have

$$\frac{\mathrm{d}\varrho}{\varrho} + \frac{\mathrm{d}v}{v} + \frac{\mathrm{d}A}{A} = 0. \tag{4.187}$$

Euler's equation may be written as

$$v \frac{\mathrm{d}v}{\mathrm{d}x} = -\frac{1}{\varrho} \frac{\mathrm{d}p}{\mathrm{d}x}. \tag{4.188}$$

After some manipulation we obtain

$$v\,\mathrm{d}v = -\frac{1}{\varrho} \frac{\mathrm{d}p}{\mathrm{d}\varrho} \mathrm{d}\varrho = -a^2 \frac{\mathrm{d}\varrho}{\varrho} \tag{4.189}$$

or,

$$\frac{\mathrm{d}\varrho}{\varrho} = -\frac{v\,\mathrm{d}v}{a^2}. \tag{4.190}$$

After substituting into the continuity equation we have

$$-\frac{v\,\mathrm{d}v}{a^2}+\frac{\mathrm{d}v}{v}=\frac{\mathrm{d}A}{A}. \tag{4.191}$$

Introducing the Mach number, this gives

$$(M^2-1)\frac{\mathrm{d}v}{v}=\frac{\mathrm{d}A}{A}. \tag{4.192}$$

This area-velocity relation illustrates some very important effects of the Mach number.

The value of $M=0$ relates to an incompressible fluid, for which $a=\infty$, and for which a decrease in area produces a directly proportional increase in velocity. The equation

$$-\frac{\mathrm{d}v}{v}=\frac{\mathrm{d}A}{A} \tag{4.193}$$

clearly expresses this relation.

For values of M between 0 and 1 the flow is subsonic. In this region

$$M^2-1<0,$$

thus the relation is qualitatively the same as for an incompressible fluid. A decrease in area results in a velocity increase, but the rise in the velocity is relatively greater compared to that of the incompressible flow, since $M^2-1<0$.

For compressible flows, surprising results occur in the supersonic region, where $M>1$. In this case

$$M^2-1>0,$$

thus the sign of both sides of Eq. (4.192) is the same. In contrast to the case of incompressible or subsonic flow, an increase in area will now cause an increase in the velocity. This is best understood by considering Eq. (4.190), which can be expressed in terms of the Mach number as

$$\frac{\mathrm{d}\varrho}{\varrho}=-M^2\frac{\mathrm{d}v}{v}. \tag{4.194}$$

It is obvious, that for $M>1$ the decrease in the density is faster than the increase in the velocity. Since the mass of the flow must remain constant, the velocity must increase as the area increases in order to maintain the continuity law.

At the sonic speed of flow, $M=1$. Examining Eq. (4.192) it is clear that the condition $M=1$ can be realized only at the throat of the channel in accordance with the condition $\mathrm{d}A=0$. The inverse of this statement does not hold, the Mach number is not necessarily 1 at the location where the area reaches a minimum. For subsonic flows $\mathrm{d}A=0$ corresponds to $\mathrm{d}v=0$, which means a maximum velocity. If the flow is supersonic a velocity minimum occurs at the throat.

In accordance with the above, an outflowing jet of gas can never have a velocity which is greater than the critical speed of sound. Consider a large reservoir with an outflow opening. If the ambient pressure p_a is greater than the critical value, i.e.

$$p_a > p_* = p_0 \left(\frac{2}{\kappa+1} \right)^{\frac{\kappa}{\kappa-1}},$$

the outflow velocity may be calculated from the Bernoulli equation in the form

$$\frac{v^2}{2} + \frac{\kappa}{\kappa-1} \frac{p}{\varrho} = \frac{\kappa}{\kappa-1} \frac{p_0}{\varrho_0}.$$

The result is

$$v = \sqrt{\frac{2\kappa}{\kappa-1} \frac{p_a}{\varrho_a} \left[1 - \left(\frac{p_0}{p_a} \right)^{\frac{\kappa-1}{\kappa}} \right]}. \tag{4.195}$$

This velocity must be always smaller than the critical speed of sound.

If the ambient pressure is smaller than the critical value

$$p_a < p_*,$$

the condition at the outflow opening approaches the critical state ($M=1$). When the critical velocity is reached, the mass flow has reached a maximum, and any further increase in the reservoir pressure p_0 cannot increase the outflow velocity or the mass flow. The outflowing gas has a greater pressure and density (e.g. p_*, and ϱ_*) than the ambient pressure and density. This jet at the critical pressure will expand in area until the ambient pressure is reached, crossing a shock surface with a finite pressure jump while the entropy increases.

Finally, we determine the relation between the variation of the cross-sectional area of the channel and the Mach number. The flow is assumed to be steady and isentropic, thus the Bernoulli equation can be written as

$$\frac{v^2}{2} + \frac{\kappa}{\kappa-1} \frac{p}{\varrho} = \text{const.}$$

Substituting the speed of sound into this, we obtain

$$\frac{v^2}{2} + \frac{a^2}{\kappa-1} = \text{const.}$$

Differentiating this equation we get

$$v\,\mathrm{d}v + \frac{2}{\kappa-1} a\,\mathrm{d}a = 0. \tag{4.196}$$

Taking the logarithm of the expression of the Mach number, after differentation, leads to the equation

$$\frac{dM}{M} = \frac{dv}{v} - \frac{da}{a}. \tag{4.197}$$

Eliminating $\frac{da}{a}$ from both equations we obtain, after some manipulation:

$$\frac{dM}{M} = \left(\frac{\kappa-1}{2}M^2+1\right)\frac{dv}{v}. \tag{4.198}$$

Expressing dv/v as

$$\frac{dv}{v} = \frac{dA}{A}\,\frac{1}{M^2-1}, \tag{4.199}$$

and substituting, we get

$$\frac{M^2-1}{\frac{\kappa-1}{2}M^2+1}\,\frac{dM}{M} = \frac{dA}{A}. \tag{4.200}$$

Integrating this expression, the desired relation is found to be

$$\frac{M_1}{M}\left[\frac{\left(\frac{\kappa-1}{2}\right)M^2+1}{\left(\frac{\kappa-1}{2}\right)M_1^2+1}\right]^{\frac{\kappa+1}{2(\kappa-1)}} = \frac{A}{A_1}, \tag{4.201}$$

where A_1 is an arbitrary cross-sectional area and M_1 is the Mach number at A_1.

Let this arbitrary cross section be the throat of the nozzle, where $M_1 = M_* = 1$. Thus

$$\frac{A}{A_*} = \frac{1}{M}\left[\frac{2}{\kappa+1}+\left(\frac{\kappa-1}{\kappa+1}\right)M^2\right]^{\frac{\kappa+1}{2(\kappa-1)}}. \tag{4.202}$$

This relationship is shown in *Fig. 4.13* for a flow of air ($\kappa = 1.4$). It can be seen in a quantitative representation that supersonic flow can only be realized with a convergent–divergent nozzle.

The relation between the cross-sectional area and any other flow variable may be determined once the relation between the Mach number and the cross-sectional area is known. Thus we can calculate the distribution of the pressure, the temperature, and the density as:

$$p = p_*\left[\frac{2}{\kappa+1}\left(1+\left(\frac{\kappa-1}{2}\right)M^2\right)\right]^{-\frac{\kappa}{\kappa+1}}, \tag{4.203}$$

$$T=T_*\left[\frac{2}{\kappa+1}\left(1+\left(\frac{\kappa-1}{2}\right)M^2\right)\right]^{-1}, \tag{4.204}$$

$$\varrho=\varrho_*\left[\frac{2}{\kappa+1}\left(1+\left(\frac{\kappa-1}{2}\right)M^2\right)\right]^{-\frac{1}{\kappa+1}}. \tag{4.205}$$

Knowing the pressure distribution along a given nozzle has a special importance. The relation between the nozzle area ratio A_*/A and the pressure ratio p/p_0 can be expressed using Eqs (4.202) and (4.203) as

$$\frac{A_*}{A}=\left(\frac{p}{p_0}\right)^{\frac{1}{\kappa}}\sqrt{\frac{1-\left(\frac{p}{p_0}\right)^{\frac{\kappa-1}{\kappa}}}{\frac{\kappa-1}{\kappa}\left(\frac{2}{\kappa+1}\right)^{\frac{\kappa+1}{\kappa-1}}}}. \tag{4.206}$$

This expression is plotted in *Fig. 4.14*, where it can be seen that the curve is double valued. The upper section is the subsonic branch, the lower one corresponds to supersonic flow.

If the flow is subsonic throughout the outlet, the critical area A_* is less than the cross-section of the throat, and the point on the curve corresponding to the flow cannot reach point B. It reaches only to point C and then turns back along the same curve. If critical flow occurs at the throat, $A_*/A=1$. The point corresponding to the flow has moved to B and it will then continue to move along the supersonic curve up to some point E, determined by the exit area of the nozzle ($A_*/A_E<1$).

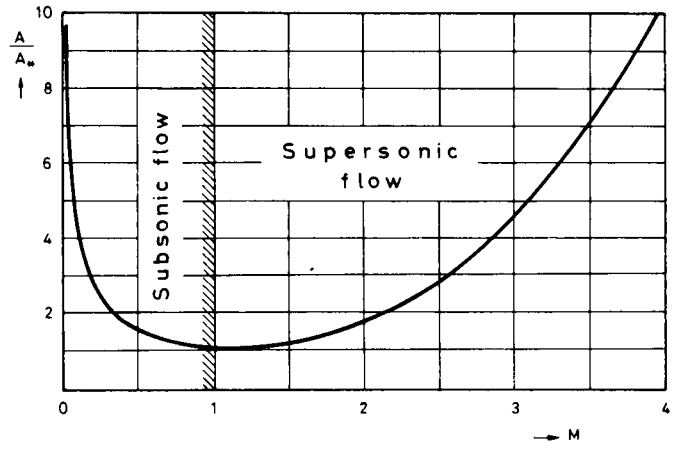

Fig. 4.13. Cross-section distribution of a supersonic nozzle

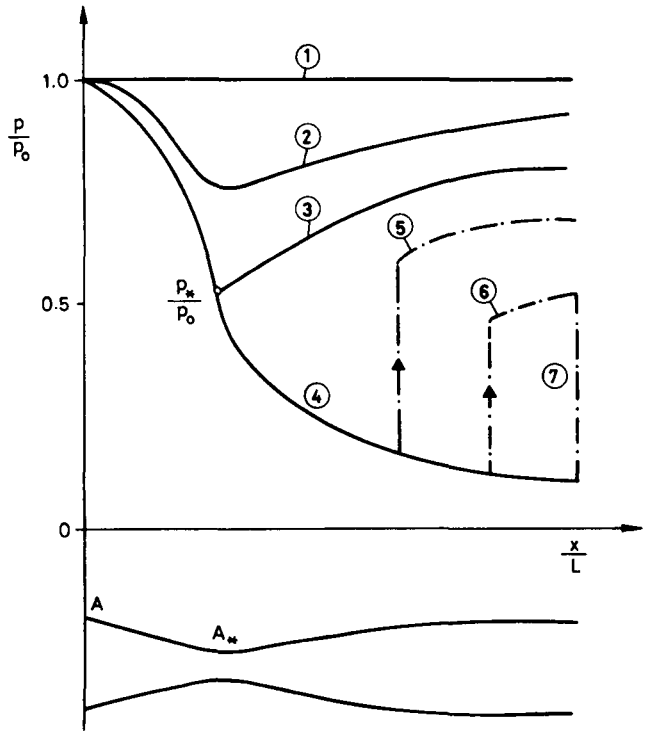

Fig. 4.14. Typical pressure distributions of a supersonic nozzle

Some typical pressure distributions are shown in *Fig. 4.14*. If the exit pressure of the nozzle is equal to the stagnation pressure there will be no flow (curve 1). If the exit pressure is slightly smaller than the reservoir pressure, the convergent-divergent nozzle performs like a conventional Venturi tube; the flow is subsonic thorough (curve 2). If the exit pressure is reduced further, the critical velocity and pressure are reached at the throat, as curve 3 shows. In this case the velocity reaches the critical sonic velocity at the throat but cannot be supersonic thorough the diffuser. The minimum pressure which can occur in the nozzle is represented by the end of curve 4. For the exit pressures that lie between p_3 and p_4 there are no isentropic solutions. This implies that at intermediate exit pressures some type of non-isentropic process must occur somewhere along the flow. For an inviscid flow the only possibility is the occurrence of shock waves in the supersonic region. The pressure jump which accompanies such a shock is represented by curve 5. After the shock the supersonic flow reverts to subsonic flow, resulting in the exit pressure p_5. As the exit pressure decreases, the shock moves downstream as represented by curve 6. At some exit pressures, such as p_7, the shock occurs outside the

nozzle. With a further decrease of the exit pressure the flow through the nozzle is no longer affected, only the character of the shock waves in the outflowing jet will change.

4.13 High velocity gas flow in pipes with friction

The following discussion deals with the case of a relative high velocity gas flow through a perfectly insulated adiabatic pipe. The pipe has a constant, but not necessarily circular cross-section. The term, „relative high velocity gas flow" will be used in the sense of a compressible flow with a velocity greater than 50 m/s. The flow may be either subsonic or supersonic.

The flow system is adiabatic, but the flow is not isentropic because of the friction. Since the velocity is relatively high, the flow must be turbulent (see Chapter 7). The only important consequence of this for the present investigation is that the velocity at any cross-section of the pipe is considered to be constant. The flow is steady, thus the heat capacity of the gas is constant.

It is important to remember that for compressible fluids, pressure is not simply the mechanical normal stress, but a well defined thermodynamic variable. Therefore, the drop in pressure is caused not only by the friction of the fluid, but also by the change in the thermal state.

It is known that thermodynamic processes affecting gases can be represented by means of relatively simple diagrams, in which complicated functions may be represented by simple, smooth curves. For a non-isentropic process the entropy–enthalpy diagram (the so-called Mollier diagram) is a convenient graphical representation. In this diagram the actual physical processes proceed in the direction of increasing entropy. For any gas flow in an adiabatic system the energy equation is of the form

$$\frac{v^2}{2} + i = i_0 ,$$

where the ordinate i can be considered to represent a distorted factor comprising the velocity, the temperature, the speed of sound and the Mach number.

Taking those flows for which mass-flux the density ϱv is constant, the so-called Fanno lines are obtained in the $S-i$ diagram. Therefore, along a Fanno line

$$\mathrm{d}(\varrho v) = 0 . \tag{4.207}$$

This may be expressed as

$$\mathrm{d}(\varrho v) = \left[\left(\frac{\partial \varrho}{\partial p}\right)_s \mathrm{d}p + \left(\frac{\partial \varrho}{\partial s}\right)_p \mathrm{d}s\right] v + \varrho \, \mathrm{d}v = 0 . \tag{4.208}$$

Since

$$T \, \mathrm{d}S = \mathrm{d}i - \frac{\mathrm{d}p}{\varrho} , \tag{4.209}$$

while from the energy equation

$$\mathrm{d}i = -v\,\mathrm{d}v\,, \tag{4.210}$$

and using the equation for speed of sound

$$a^2 = \frac{\mathrm{d}p}{\mathrm{d}\varrho}\,,$$

Eq. (4.208) may be rewritten as:

$$\mathrm{d}(\varrho v) = \left(1 - \frac{v^2}{a^2}\right)\varrho\,\mathrm{d}v - \left[\frac{\varrho T}{a^2} - \left(\frac{\partial \varrho}{\partial S}\right)\right] v\,\mathrm{d}s = 0\,. \tag{4.211}$$

The term in the square bracket is always positive. It is obvious that $\varrho T/a^2$ is positive, while the $-(\partial\varrho/\partial S)$ term must be also positive since at constant pressure the entropy must always increase with decreasing density. Since for the critical flow ($v=a$) condition the first term must be zero, while the second term is not, only $\mathrm{d}s=0$ satisfies the equation. Thus the Fanno flow at sonic velocities must be isentropic. It is obvious that the entropy of the gas flowing through the pipe can only increase, thus

$$\frac{\mathrm{d}s}{\mathrm{d}l} > 0\,.$$

Examining the equality

$$\varrho\left(1 - \frac{v^2}{a^2}\right)\frac{\mathrm{d}v}{\mathrm{d}l} = \left[\frac{\varrho T}{a^2} - \left(\frac{\partial \varrho}{\partial s}\right)\right] v\,\frac{\mathrm{d}s}{\mathrm{d}l} \tag{4.212}$$

it is seen that if

$$v < a, \qquad \frac{\mathrm{d}v}{\mathrm{d}l} > 0\,,$$

while on the other hand if

$$v > a, \qquad \frac{\mathrm{d}v}{\mathrm{d}l} < 0\,.$$

Therefore, a subsonic flow through a duct of constant cross-sectional area will accelerate in the direction of the flow, until the critical velocity is approached. The entropy has a maximum at $v=a$, thus the subsonic Fanno flow never exceeds the speed of sound. If the ambient pressure is suitably low, a subsonic Fanno flow can reach the speed of sound at the outlet end of the pipe.

A Fanno flow can only be supersonic if it already arrives at the inlet cross-section of the pipe as a supersonic flow. Since the supersonic velocity is greater than the velocity of propagation of any disturbances through the flowing gas, the flow at the inlet is independent of the conditions which prevailed before it reached the inlet. The entropy can increase only to a certain extent, therefore the point representing the gas on the Mollier diagram can proceed only along a Fanno line corresponding to the given mass-flux density, with v approaching the value gaining the maximum

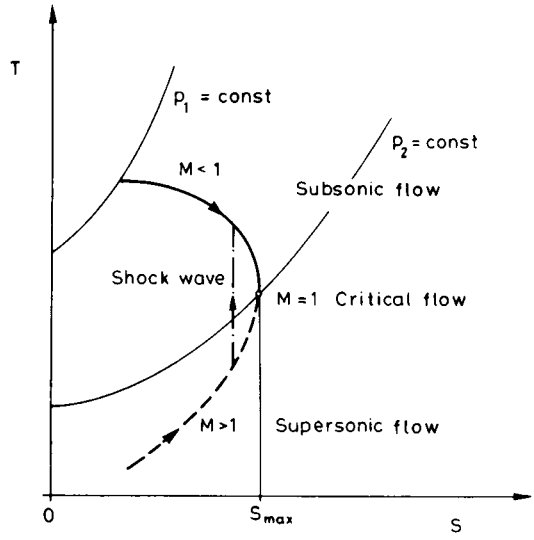

Fig. 4.15. Shock waves in supersonic flow

possible entropy, i.e. the critical velocity, at the outlet. Thus the velocity decreases throughout the pipe in the flow direction.

For a supersonic Fanno flow the entropy maximum occurs at the distance l_{cr} from the inlet. If the length of the pipe l is smaller than l_{cr}, the flow is decelerating, though still supersonic, throughout the pipe. If $l = l_{cr}$ the flow decelerates to the critical velocity at the outlet end. For pipes longer than l_{cr} the flow decelerates, but it cannot reach the critical velocity before the end of the pipe. There is, however, an additional entropy increase caused by the jump in pressure by which the supersonic flow suddenly becomes subsonic. This subsonic flow will the accelerate and reach the critical velocity at the outlet end of the pipe. This is illustrated in *Fig. 4.15*. The pressure jump is a shock wave which is an adverse phenomenon in the pipe flow. For this reason certain velocity ranges have to be excluded in pipe flow.

To avoid that the entropy maximum is reached before the end of the pipe, we shall determine the critical length l_{cr} depending on the Mach number.

Let us begin with the balance equation of kinetic energy, applying for an infinitesimal length $\mathrm{d}l$ of the pipe. It can be written in differential form as

$$v\,\mathrm{d}v + \frac{\mathrm{d}p}{\varrho} + \frac{\lambda\,\mathrm{d}l}{D}\,\frac{v^2}{2} = 0\,. \tag{4.213}$$

The third term expresses the mechanical energy loss, in which D is the diameter of the pipe, λ is a dimensionless friction factor. Friction factor calculations will be detailed in Chapter 8. For a non-circular channel the diameter may be replaced by

the hydraulic radius. The velocity and the friction factor are not constant throughout the flow: a subsonic flow will accelerate, while a supersonic flow will decelerate; for this reason it is necessary to use the kinetic energy equation in a differential form. By dividing Eq. (4.213) by the pressure p we get

$$\frac{\varrho}{p} v\,\mathrm{d}v + \frac{\mathrm{d}p}{p} + \frac{\varrho}{p}\frac{v^2}{2}\frac{\lambda\,\mathrm{d}l}{D} = 0. \tag{4.214}$$

The ratio ϱ/p can be expressed by the speed of sound

$$\frac{\varrho}{p} = \frac{\kappa}{a^2}. \tag{4.215}$$

By substituting Eq. (4.215) into Eq. (4.214) we obtain

$$\frac{\lambda\,\mathrm{d}l}{D} = \frac{2a^2}{\kappa v^2}\left[\frac{\kappa}{a^2} v\,\mathrm{d}v - \frac{\mathrm{d}p}{p}\right]. \tag{4.216}$$

In order to get a relationship between $\lambda\,\mathrm{d}l/D$ and the Mach number, we shall express the variables p, v and a by M. The equation of state can be written as

$$\frac{\mathrm{d}p}{p} = \frac{\mathrm{d}\varrho}{\varrho} + \frac{\mathrm{d}T}{T}. \tag{4.217}$$

The continuity equation for a duct of constant cross-sectional area is

$$\frac{\mathrm{d}v}{v} + \frac{\mathrm{d}\varrho}{\varrho} = 0. \tag{4.218}$$

By combining Eqs (4.217) and (4.218) we obtain

$$\frac{\mathrm{d}p}{p} = \frac{\mathrm{d}T}{T} - \frac{\mathrm{d}v}{v}. \tag{4.219}$$

The speed of sound for isentropic flow can be expressed as

$$\frac{2\,\mathrm{d}a}{a} = \frac{\mathrm{d}T}{T}. \tag{4.220}$$

By substituting Eq. (4.220) into Eq. (4.219) we have

$$\frac{\mathrm{d}p}{p} = \frac{2\,\mathrm{d}a}{a} - \frac{\mathrm{d}v}{v}. \tag{4.221}$$

Considering, that

$$M = \frac{v}{a},$$

Eq. (4.216) after substitution can be written as

$$\frac{\lambda\,\mathrm{d}l}{D} = \frac{2}{\kappa M^2}\left[(1-\kappa M^2)\frac{\mathrm{d}v}{v} - \frac{2\,\mathrm{d}a}{a}\right]. \tag{4.222}$$

It is easy to recognize, that

$$\frac{\mathrm{d}M}{M} = \frac{\mathrm{d}v}{v} - \frac{\mathrm{d}a}{a}. \tag{4.223}$$

By differentiation of

$$\frac{v^2}{2} + \frac{a^2}{\kappa - 1} = \text{const},$$

the following relationship is obtained:

$$v\,\mathrm{d}v + \frac{2a\,\mathrm{d}a}{\kappa - 1} = 0.$$

After some modification we get

$$\frac{\mathrm{d}a}{a} = -\frac{\kappa - 1}{2}\frac{v\,\mathrm{d}v}{a^2}. \tag{4.224}$$

The substitution of Eq. (4.224) into (4.223) leads to the expression

$$\frac{\mathrm{d}M}{M} = \frac{\mathrm{d}v}{v}\left(1 + \frac{\kappa - 1}{2}M^2\right). \tag{4.225}$$

Now we obtain easily, that

$$\frac{\mathrm{d}v}{v} = \frac{1}{\frac{\kappa - 1}{2}M^2 + 1}\frac{\mathrm{d}M}{M} \tag{4.226}$$

and

$$\frac{\mathrm{d}a}{a} = -\frac{\frac{\kappa - 1}{2}M^2\frac{\mathrm{d}M}{M}}{\frac{\kappa - 1}{2}M^2 + 1}. \tag{4.227}$$

These expressions will be substituted into Eq. (4.222), thus we get

$$\frac{\lambda\,\mathrm{d}l}{D} = \frac{2}{\kappa M^3}\frac{1 - M^2}{1 + \frac{\kappa - 1}{2}M^2}\mathrm{d}M. \tag{4.228}$$

Another convenient expression is

$$\frac{\mathrm{d}M}{\mathrm{d}l} = \frac{\lambda}{D}\frac{\kappa M^3}{2}\frac{\frac{\kappa - 1}{2}M^2 + 1}{1 - M^2}. \tag{4.229}$$

Integrating this differential equation, the distribution of the Mach number along the length of the pipe can be determined. This is equivalent to the velocity distribution throughout the pipe.

The critical length l_{cr}, at which the entropy maximum occurs can be determined by integrating the expression

$$l_{cr} = \frac{20}{\kappa\lambda} \int_{M}^{1} \frac{(1-M^2)\,\mathrm{d}M}{M^3\left(\frac{\kappa-1}{2}M^2+1\right)}. \tag{4.230}$$

This expression can be easily integrated by expanding it into partial fractions. The result is

$$l_{cr} = \frac{D}{\kappa\lambda}\left(\frac{1-M^2}{M^2} + \frac{\kappa+1}{2}\ln\frac{M^2\frac{\kappa-1}{2}+1}{\frac{\kappa-1}{2}M^2+1}\right). \tag{4.231}$$

By integrating Eq. (4.229) the relation between the length and Mach number is obtained. Knowing the Mach number at any point along the pipe, the flow variables can be determined. In engineering practice it is more convenient to calculate the lengths of the pipe which correspond to arbitrarily chosen values of the Mach number. Assuming, that the reservoir variables p_0, ϱ_0, T_0 and a_0 are known, we obtain the flow variables for any point as

$$a = \frac{a_0}{\sqrt{1+\frac{\kappa-1}{2}M^2}}, \tag{4.232}$$

$$v = a_0 \frac{M}{\sqrt{1+\frac{\kappa-1}{2}M^2}}, \tag{4.233}$$

$$p = p_0\left[1+\frac{\kappa-1}{2}M^2\right]^{\frac{\kappa}{1-\kappa}}, \tag{4.234}$$

$$\varrho = \varrho_0\left[1+\frac{\kappa-1}{2}M^2\right]^{\frac{1}{1-\kappa}}, \tag{4.235}$$

$$T = T_0 \frac{1}{1+\frac{\kappa-1}{2}M^2}. \tag{4.236}$$

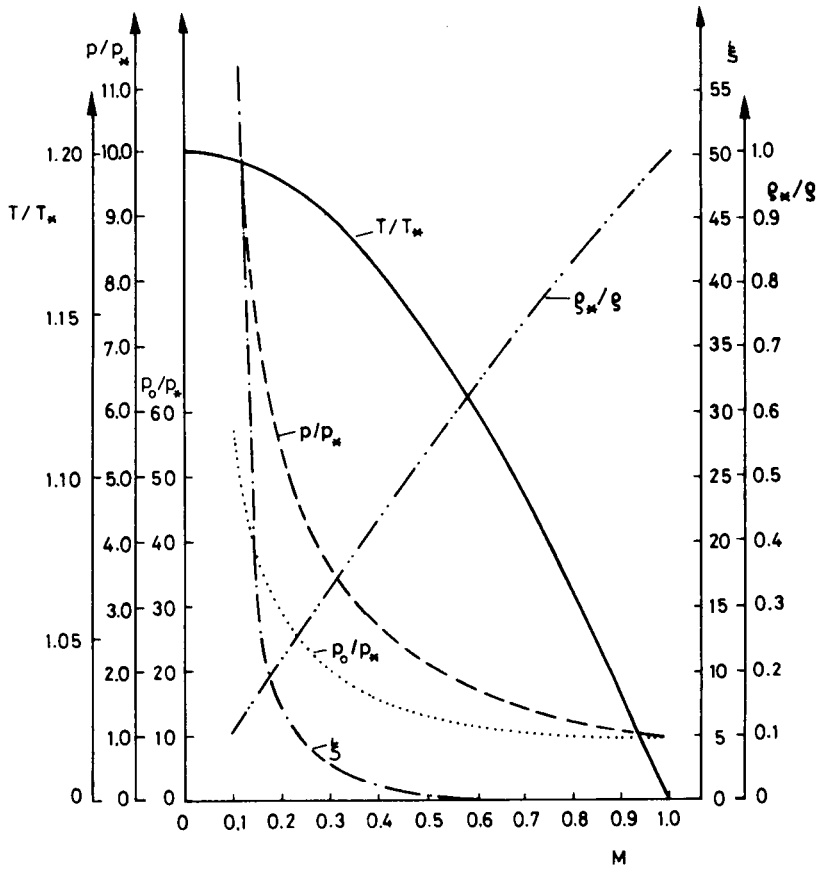

Fig. 4.16. Flow variables of supersonic flow with friction

The calculated values are shown graphically in *Fig. 4.16.*

For non-isentropic flow there is another important feature: the stagnation pressure decreases in the direction of the flow. It is known, that for an infinitesimal change in entropy

$$\mathrm{d}S = c_v \frac{\mathrm{d}T}{T} - (c_p - c_v) \frac{\mathrm{d}p}{p}. \tag{4.237}$$

Since the stagnation temperature is independent of the irreversibility ($\mathrm{d}T = 0$), the entropy increase in the direction of the flow is obtained as

$$S_2 - S_1 = -(c_p - c_v) \ln \frac{p_{02}}{p_{01}}. \tag{4.238}$$

The drop in the stagnation pressure can be determined from:

$$\ln \frac{p_{01}}{p_{02}} = \frac{S_2 - S_1}{c_p - c_v} = \frac{\kappa}{2} \int_1^2 \frac{\lambda M^2}{D} \mathrm{d}l . \tag{4.239}$$

This rather simplified theoretical treatment of friction effects in pipes may be satisfactory for subsonic flows. For supersonic and especially transonic flows, a more sophisticated treatment is necessary.

CHAPTER 5

SHOCK WAVES IN COMPRESSIBLE FLOW

5.1 Shock surfaces

It is a rather common phenomenon that abrupt changes occur at the bounding surface of a fluid mass. This happens for example when starting a pump or a compressor, or while opening or closing a valve. The abrupt change in the variables of flow at the boundary disturbs the equilibrium or the previously established flow pattern of the fluid. This disturbance propagates throughout the entire fluid mass. The need for understanding such phenomena arises in a wide variety of engineering problems, for example gas outbursts, waterhammer in pipelines, and the noise of turbomachines or nozzles. The same basic physical principles underlie all of these wave phenomena. Thus it is necessary to introduce a treatment of these phenomena in which will combine the scientific and practical aspects of shock wave phenomena.

Weak and strong singularities

Disturbances which propagate wavelike in a continuum represent singularities of the set of functions of the flow and the variables of state of the medium. These singularities can be distinguished both from the point of view of their mathematical formalism and their physical meaning.

A weak singularity is a surface across which the flow variables themselves are continuous, but certain derivatives of these variables are discontinous between the two sides of the surface. Sound waves are small disturbances with infinitesimal or very small amplitudes in a compressible medium. They form weak singular surfaces.

A surface is termed a strong singularity with respect to any variable of flow or state if across it both the continuous set function and its derivative undergo a finite discontinuity. A shock surface in a compressible medium is an example of such a strong singularity. A strong disturbance in a compressible medium propagates with a considerable amplitude. Under certain circumstances shock surfaces develop from these waves of considerable amplitude. The mechanism of generating shock waves may be illustrated in the following. The amplitudes of the velocity, pressure and density-disturbances are negligibly small relative to their values at equilibrium. Thus the speed of sound may be considered to remain constant over a wave period. Let us expand the well-known equation for the speed of sound into a Taylor series

in terms of the value ϱ_0 in the undisturbed fluid. Thus we have

$$a^2 = \frac{\mathrm{d}p}{\mathrm{d}\varrho} = \left(\frac{\mathrm{d}p}{\mathrm{d}\varrho}\right)_0 + \left(\frac{\mathrm{d}^2 p}{\mathrm{d}\varrho^2}\right)_0 (\varrho - \varrho_0) + \ldots$$

For a small-amplitude disturbance, when

$$\varrho - \varrho_0 \ll \varrho_0 ,$$

only the first term of the Taylor series needs to be considered. This term depends only on the equilibrium variables, and is thus independent of the size of the perturbation. Each point of the wave surface propagates with the same velocity, thus the shape of the wave remains the same.

Consider now a perturbation which has a finite amplitude. The speed of propagation is no longer constant, it depends on the amplitude since the difference $\varrho - \varrho_0$ can no longer be neglected in comparison to ϱ_0. The subsequent phases of the distortion of a sinusoidal wave as it propagates are shown in *Fig. 5.1.* It is obvious that in the region of compression where $\varrho - \varrho_0 > 0$, the wave velocity is higher than in the region of expansion, where $\varrho - \varrho_0 < 0$. Thus the periods of expansion became longer, while the shape of the originally sinusoidal wave distorts

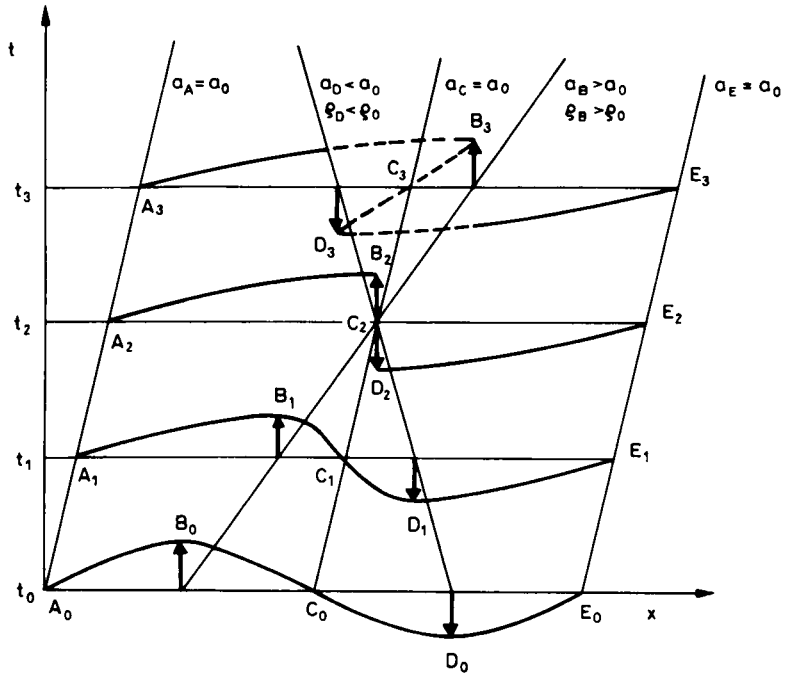

Fig. 5.1. Development of a shock wave

more and more during the course of propagation. It can be seen that the *characteristic lines* are inclined more during the compressional period and they would eventually cross leading to the situation at the instant t_2. The regions of compression are steepening while the regions of expansion are flattening. The situation at $t=t_3$ is obviously impossible since three different values of the density cannot simultaneously occur at a given point such as x_3. Actually, before this happens, or even before the situation $t=t_2$ arises, the gradients of the velocity and the temperature during the period of compression become so great that the conductive transport of momentum and the transfer of heat are no longer negligible. These produce a diffusive action which counteracts the steepening tendency. The two opposing effects achieve a balance; the compressive stage of the wave reaches a steady state, propagating without further distortion. It is then a shock wave.

The thickness of the shock-wave front is very small; approximately equal to the free path of the molecules of the gas. In this thin region, the gradients of the flow variables are extremely large. It may be a suitable approximation to consider this very thin layer of large variations to be a singular surface which contains the discontinuities of the flow variables: velocity, density, and pressure.

The classical differential equations of continuum mechanics are no longer valid for a flow in which shock waves occur. The flow region is not a single connected continuum because of the presence of the shock surfaces. The flow variables and their derivatives suffer a jump (discontinuity) on this surface. The classical differential equations apply only to individual continuous regions which are characterized by continuous functions with continuous derivatives. Thus the equations for the conservation of mass and the balance of momentum and energy must be modified to take into account the discontinuous conditions. Before proceeding with a detailed analysis of this procedure we must revise some basic concepts of differential geometry and kinematics. Consider an arbitrarily chosen material volume V as it is shown in *Fig. 5.2*. The regular surface S divides this volume into two regions V^+ and V^-. Let $\Phi(\vec{r})$ be a function which is continuous and differentiable in both regions though not at the surface S. From the regions V^+ and V^- the function $\Phi(\vec{r})$ approaches the two different limiting values Φ^+ and Φ^- at the surface S. Following Christoffel the jump in Φ while crossing the surface S at the point $\vec{r}_0$ is denoted by the symbol

$$\llbracket \Phi \rrbracket = \Phi^+ - \Phi^- . \tag{5.1}$$

Since the function Φ at the surface S is not continuous, the surface S is considered to be a singular surface with respect to Φ. The quantity $\llbracket \Phi \rrbracket$, the so-called jump function is a function of its position on S. When the jump function is applied to a second-order tensor, the jump of this tensor may be divided into a transverse and a longitudinal component. For vectors such a jump is given by the identity:

$$\llbracket \vec{f} \rrbracket = \vec{n} \operatorname{div} \vec{f} - \vec{n} \times \operatorname{curl} \vec{u} . \tag{5.2}$$

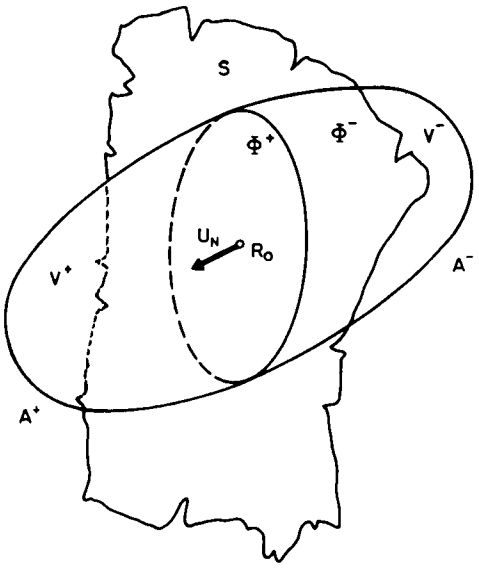

Fig. 5.2. Material volume consisting of a singular surface

The theoretical basis of all geometrical and kinematic theorems referring to singular surfaces is Hadamard's lemma which states the following: If Φ is continuous and differentiable in an interior region V^+ with a smooth boundary S, Φ and $\partial_k \Phi$ approach the finite limits Φ^+ and $\partial_k \Phi^+$ as S is approached along paths interior to V^+. (k is the kth partial derivative of Φ.) Let $\vec{S} = \vec{S}(\lambda)$ be a smooth curve on S, and let the limit Φ^+ be differentiable along this curve. Then:

$$\frac{\mathrm{d}\Phi^+}{\mathrm{d}\lambda} = \partial_k \Phi \cdot \frac{\mathrm{d}S^k}{\mathrm{d}\lambda}. \tag{5.3}$$

(k as subscript and superscript means covariant and contravariant derivatives.)

This means, that the total differential can be determined from the boundary limit of one side of the singular surface only. The function Φ need not be defined on the other side of S. If it is, and if the limits Φ^- and $\partial_k \Phi^-$ also exist and are smooth, a similar result holds for them but $\mathrm{d}\Phi^-/\mathrm{d}\lambda$ is unrelated to $\mathrm{d}\Phi^+/\mathrm{d}\lambda$. Applying Hadamard's lemma to singular surfaces, the superficial and geometrical conditions of compatibility can be derived.

If the lemma (5.3) is applied to the boundary limit on each side of the singular surface S, and the expression for the $(-)$ side is subtracted from that for the $(+)$ side, we obtain the equation:

$$\frac{\mathrm{d}}{\mathrm{d}\lambda}[\Phi] = [\partial_k \Phi] \frac{\mathrm{d}S^k}{\mathrm{d}\lambda} = \left[\partial_k \Phi \cdot \frac{\mathrm{d}S^k}{\mathrm{d}\lambda}\right]. \tag{5.4}$$

Thus the tangential derivative of the jump function $\llbracket \Phi \rrbracket$ is equal to the jump of the tangential derivative of the function Φ on the surface S.

Since the values of Φ in the regions V^+ and V^- are independent of one another, the limiting values of the normal derivatives of Φ on both sides of the singular surface need not be related in any way:

$$\left\llbracket \frac{d\Phi}{dn} \right\rrbracket = \text{arbitrary value}. \tag{5.5}$$

The consequence of expressions (5.4) and (5.5) is that any jump function is spread out smoothly over the surface S; there is no abrupt change from one part of S to another. On week singular surfaces the definitive parameters of the flow are continuous; jumps can occur only in their derivatives. In this case the jump in the derivative of any continuous scalar or vector field can be expressed by the unit normal vector of the singular surface and a proportionality factor, which may be either a scalar or a vector function. Weingarten's theorems state this in the following form:

$$\llbracket \operatorname{grad} a \rrbracket = \vec{n}\alpha, \tag{5.6}$$

$$\llbracket \operatorname{div} \vec{b} \rrbracket = \vec{n}\vec{\beta}, \tag{5.7}$$

$$\llbracket \operatorname{curl} \vec{b} \rrbracket = \vec{n} \times \vec{\beta}, \tag{5.8}$$

$$\llbracket \operatorname{Grad} \vec{b} \rrbracket = \vec{n} \circ \vec{\beta}, \tag{5.9}$$

where a and $\vec{b}$ are arbitrary functions.

These equations embody the theorem, that the longitudinal and transverse jumps of the gradient of a continuous vector are equal to the jumps of its divergence and curl respectively:

$$\vec{\beta} = \vec{n} \llbracket \operatorname{div} \vec{b} \rrbracket - \vec{n} \times \llbracket \operatorname{curl} \vec{b} \rrbracket. \tag{5.10}$$

It follows from the above, that the only possible jump in the gradient in a continuous irrotational field must be normal, while for a continuous solenoidal field it is transverse.

5.2 Kinematics of motion of singular surfaces: the speed of displacement

To determine the speed of displacement of a moving singular surface consider a surface as shown in *Fig. 5.3*. Let the points on this surface be given by the expression:

$$\vec{r} = \vec{r}(\vec{R}_p, t).$$

Here the point $\vec{R}_p$ is not to be thought of as a material particle of any motion, even though it is useful to visualization the moving singular surface as a

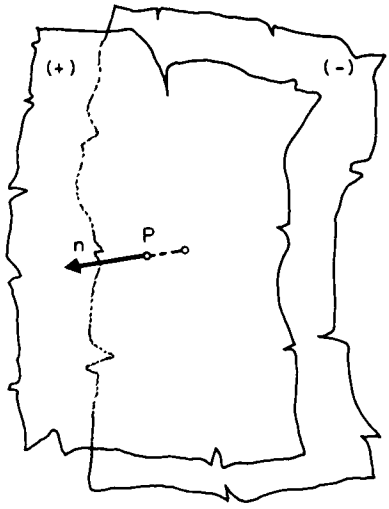

Fig. 5.3. Displacement speed of a singular surface

configuration of identifiable particles changing with time. We should also be careful not to confuse the "particle" of a continuum with the particles of corpuscular theories. Our "particle" is a portion of matter enclosed within an infinitesimal volume element.

The velocity of the surface point P is defined by the equation

$$\vec{u} = \left.\frac{\partial \vec{r}}{\partial t}\right|_{\vec{R}_p = \text{const}}. \tag{5.11}$$

Eliminating the parameter $\vec{R}_p$, the equation

$$f(\vec{r}, t) = 0 \tag{5.12}$$

defines the surface. Thus, if

$$f(\vec{r}, t) < 0,$$

this refers to a domain V^- behind (relative to the direction of displacement) of the moving surface. The expression

$$f(\vec{r}, t) > 0$$

refers to the domain V^+ in front of the moving surface. It is a convertion, that the unit normal vector is taken to be oriented in this direction, as shown in *Fig. 5.3*. The total derivative w.r.t. time of expression (5.12) is:

$$\frac{\mathrm{d}f}{\mathrm{d}t} = \frac{\partial f}{\partial t} + \vec{u}\,\mathrm{grad}\, f. \tag{5.13}$$

Let $\vec{n}$ be the unit normal vector of the surface:

$$\vec{n} = \frac{\operatorname{grad} f}{|\operatorname{grad} f|}, \tag{5.14}$$

thus the normal component of the velocity of the moving surface is

$$U_N = \vec{u}\,\vec{n} = \vec{u}\,\frac{\operatorname{grad} f}{|\operatorname{grad} f|}. \tag{5.15}$$

Using Eqs (5.12) and (5.13) we get

$$U_N = \frac{-\dfrac{\partial f}{\partial t}}{\left(\dfrac{\partial f}{\partial x}\right)^2 + \left(\dfrac{\partial f}{\partial y}\right)^2 + \left(\dfrac{\partial f}{\partial z}\right)^2}. \tag{5.16}$$

Thus all possible velocities u of the moving surface have the same normal component of U_N, which is called the speed of displacement of the surface. The speed of displacement depends only on the shape and position of the surface, it is independent of our choice of parameter in the expression $\vec{r} = \vec{r}(\vec{R}_p, t)$, and is obtained within a fixed coordinate system.

Speed of propagation

The motion of the singular surface is not the same as the motion of the particles which constitute the surface at any particular instance. The moving discontinuity changes continuously while sweeping across the fluid mass.

Consider *Fig. 5.4*. The speed of displacement at the point P characterizes the motion of the singular surface in the fixed coordinate system. The velocity of the

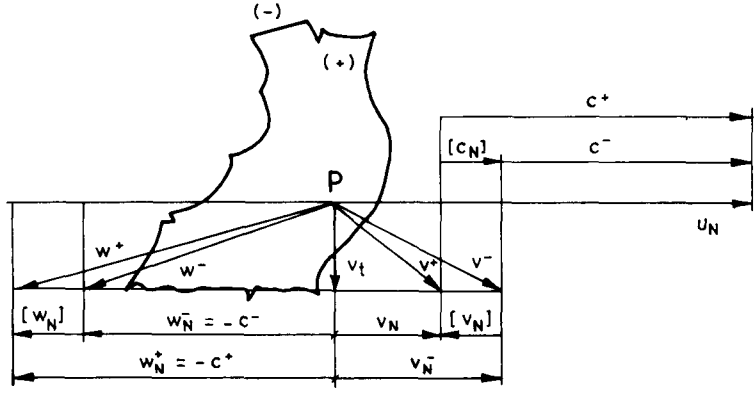

Fig. 5.4. Propagation speed of a singular surface

flow $\vec{v}$ is different on both sides of the surface: it is $\vec{v}^+$ in front of the surface, and $\vec{v}^-$ behind it. The speed of propagation of the singular surface is obtained in a coordinate system relative to the particles which are situated on it at a particular instant, thus

$$c = U_N - \vec{v}\vec{n}\,. \tag{5.17}$$

Because of the jump in the velocity $\vec{v}$, the speed of propagation also has a jump at the singular surface, and there is a finite difference in it between the two sides of the surface, thus:

$$[c] = c^+ - c^-\,.$$

Since the speed of displacement is unchanged across the surface, the jump in the speed of propagation is the negative of the jump in the normal velocity component of the material

$$[c] = -[v_N]\,. \tag{5.18}$$

The relative velocity of the flow is obatined in a coordinate system relative to the singular surface. Its normal component is the negative of the speed of propagation

$$w_N = -c\,. \tag{5.19}$$

The jump in the relative velocity is obviously equal to the jump in $\vec{v}$:

$$[\vec{w}] = [\vec{v}]\,. \tag{5.20}$$

The speed of propagation of a weak singular surface is the same on both sides of the surface, since the velocity v does not change across the surface. Because of this essential difference the speed of propagation of a weak singular surface is designated by a. Singular surfaces can propagate in a continuum at rest. In this case the speed of propagation and the speed of displacement are obviously the same.

Jump in the time derivative of a continuous function

The jump in the derivative of a continuous function across a weak singular surface is determined by the normal unit vector of the surface and a proportionality factor characteristic of the function. This follows directly from Weingarten's theorem. It is possible to determine the jump of the time derivative as follows:

Let the function $f(\vec{r},t)=0$ represent a weak singular surface.

We take $f(\vec{r},t)>0$ to mean the region in front of the singular surface (relative to the direction of propagation of the surface), while $f(\vec{r},t)<0$ refers to the region behind it. The unit normal vector of the singular surface is

$$\vec{n} = \frac{\operatorname{grad} f}{|\operatorname{grad} f|}\,. \tag{5.21}$$

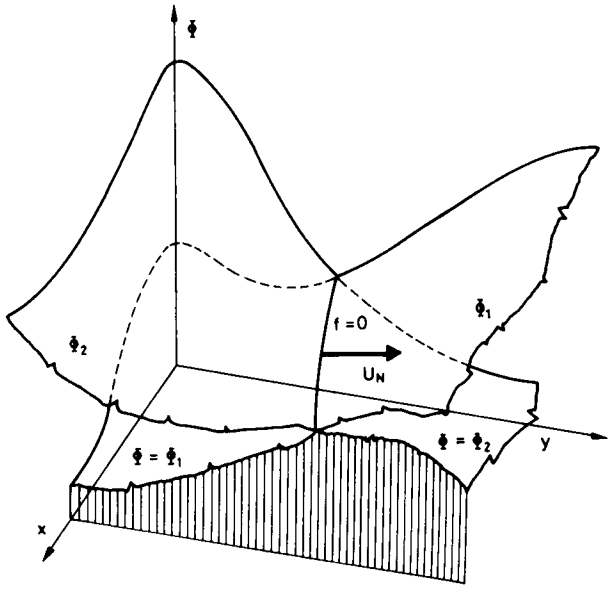

Fig. 5.5. Weak singular surface

The speed of displacement of the surface is

$$U_N = \frac{\dfrac{\partial f}{\partial t}}{|\operatorname{grad} f|}. \tag{5.22}$$

Let us suppose, that any set function Φ is continuous across the weak singular surface, but at least one component of its gradient has lost its continuity across the surface $f(\vec{r},t)=0$. Consider now *Fig. 5.5*. Though it is only a sketch of a two-dimensional case, it may aid in visualizing the problem. Let $\Phi_1(\vec{r},t)$ and $\Phi_2(\vec{r},t)$ be continuous and regular set functions, even at the singular surface. In front of the surface

$$\Phi \equiv \Phi_2, \qquad \text{if} \qquad f(\vec{r},\, t)>0\,,$$

and behind it

$$\Phi \equiv \Phi_1, \qquad \text{if} \qquad f(\vec{r},\, t)<0\,,$$

while on the singular surface itself

$$\Phi \equiv \Phi_1 \equiv \Phi_2 \qquad \text{if} \qquad f(\vec{r},\, t)=0\,.$$

Since the value of Φ is identical on both sides of the surface, the jump must be zero:

$$[\![\Phi]\!] = \Phi_2 - \Phi_1 = 0\,. \tag{5.23}$$

It follows, that the differential of Φ must be zero:

$$\mathrm{d}\llbracket\Phi\rrbracket = \llbracket\mathrm{d}\Phi\rrbracket = \left\llbracket \frac{\partial\Phi}{\partial t}\mathrm{d}t + \frac{\partial\Phi}{\partial x}\mathrm{d}x + \frac{\partial\Phi}{\partial y}\mathrm{d}y + \frac{\partial\Phi}{\partial z}\mathrm{d}z \right\rrbracket = 0,$$

as is the differential of the equation of the surface:

$$\mathrm{d}f = \frac{\partial f}{\partial t}\mathrm{d}t + \frac{\partial f}{\partial x}\mathrm{d}x + \frac{\partial f}{\partial y}\mathrm{d}y + \frac{\partial f}{\partial z}\mathrm{d}z = 0.$$

It is obvious, that these two equations cannot be linearly independent, their corresponding terms may differ only by a proportionality factor, i.e.

$$\left\llbracket \frac{\partial\Phi}{\partial t} \right\rrbracket = \alpha \frac{\partial f}{\partial t}; \quad \left\llbracket \frac{\partial\Phi}{\partial x} \right\rrbracket = \alpha \frac{\partial f}{\partial x}; \quad \text{etc.}$$

After dividing by $|\operatorname{grad} f|$, we have

$$\llbracket \operatorname{grad}\Phi \rrbracket = \vec{n}\alpha, \tag{5.24}$$

or

$$\left\llbracket \frac{\partial\Phi}{\partial t} \right\rrbracket = -\alpha U_N. \tag{5.25}$$

Thus the jump in the local derivative of any set function is the product of the speed of displacement and a proportionality factor. Since the speed of propagation is the difference between the speed of displacement and the normal component of the material velocity, while further

$$\frac{\partial\Phi}{\partial t} = \frac{\partial\Phi}{\partial t} + \vec{v} \operatorname{grad}\Phi,$$

the jump in the total derivative w.r.t. time of any set function at a weak singular surface is

$$\left\llbracket \frac{\partial\Phi}{\partial t} \right\rrbracket = -\alpha U_N + \alpha\vec{v}\vec{n} = \alpha a. \tag{5.26}$$

Therefore, the jump in the material derivative of Φ is the product of the speed of propagation, and a proportionality factor having the same tensorial rank as Φ.

5.3 Weak singular surfaces in compressible flow

Chapter 4 in this book has been concerned with continuous motion of perfect fluids; acoustic waves are propagating surfaces in the flow region, such that the flow variables themselves are continuous, but certain derivatives of these variables are discontinuous there. Such surfaces are called weak singular surfaces. The nature of weak singular surfaces and their propagation in a general three-dimensional compressible flow can be investigated especially easily in ideal gas flows. In

absence of singular surfaces the basic equations i.e. the continuity-, momentum-, and energy equation together with the equation of state can be written in the well-known form

$$\frac{\mathrm{d}\varrho}{\mathrm{d}t} + \varrho \operatorname{div} \vec{v} = 0 , \tag{5.27}$$

$$\frac{\mathrm{d}\vec{v}}{\mathrm{d}t} = -\operatorname{grad} p , \tag{5.28}$$

$$\varrho c_v \frac{\mathrm{d}T}{\mathrm{d}t} = p \operatorname{div} \vec{v} , \tag{5.29}$$

$$\frac{p}{\varrho} = RT. \tag{5.30}$$

At the weak singular surface the derivatives of the flow variables are discontinuous. Thus derivatives in the Eqs (5.27) to (5.29) can be replaced by their jump functions. Thus the continuity equation is

$$\left[\left[\frac{\mathrm{d}\varrho}{\mathrm{d}t}\right]\right] + \varrho \left[\left[\operatorname{div} \vec{v}\right]\right] = 0 . \tag{5.31}$$

The equation of motion can be written as

$$\left[\left[\frac{\mathrm{d}\vec{v}}{\mathrm{d}t}\right]\right] = - \left[\left[\operatorname{grad} p\right]\right] . \tag{5.32}$$

The energy equation at the singular surface, after some manipulation using Eqs (4.72) and (4.76) is obtained as

$$\varrho \left[\left[\frac{\mathrm{d}p}{\mathrm{d}t}\right]\right] = \kappa p \left[\left[\frac{\mathrm{d}\varrho}{\mathrm{d}t}\right]\right] . \tag{5.33}$$

The jump in the derivatives can be easily expressed using Weingarten's theorems:

$$\begin{aligned} \left[\left[\operatorname{grad} p\right]\right] &= \alpha \vec{n} , & \left[\left[\frac{\mathrm{d}p}{\mathrm{d}t}\right]\right] &= -\alpha a , \\ \left[\left[\operatorname{grad} \varrho\right]\right] &= \vec{n}\beta , & \left[\left[\frac{\mathrm{d}\varrho}{\mathrm{d}t}\right]\right] &= -\beta a , \\ \left[\left[\operatorname{div} \vec{v}\right]\right] &= \gamma \vec{n} , & \left[\left[\frac{\mathrm{d}\vec{v}}{\mathrm{d}t}\right]\right] &= -\vec{\gamma} a . \end{aligned} \tag{5.34}$$

Substituting into Eqs (5.31) to (5.33), the following expressions are obtained:

$$\begin{aligned} -\beta a + \varrho \vec{\gamma} \vec{n} &= 0 , \\ -\varrho \vec{\gamma} a + \alpha \vec{n} &= 0 , \\ -\varrho \alpha a + \kappa \beta a p &= 0 . \end{aligned} \tag{5.35}$$

Multiplying the first equation by a, the second by $\hat{n}$ and adding, we get

$$-\beta a^2+\alpha=0\,. \tag{5.36}$$

Substituting the expression for α from Eq. (5.36) into Eq. (5.35) the result is

$$-\varrho\beta a^3+\kappa p\beta a=0\,,$$

which can also be written as

$$a(\kappa p-\varrho a^2)=0\,.$$

Its solutions are

$$a_1=0\,, \tag{5.37}$$

and

$$a_2=\sqrt{\kappa\frac{p}{\varrho}}\,. \tag{5.38}$$

For an incompressible perfect fluid, since $\varrho=$constant,

$$\text{-[grad } \varrho\text{]-}=0$$

is obtained, from which it follows that

$$\alpha=0\,,\qquad \beta=0\,,\qquad \hat{\gamma}=0\,.$$

Naturally the speed of propagation of the singular surface is also zero, i.e.

$$a=0\,.$$

The first solution $a_1=0$ shows that weak singular surfaces in incompressible fluids are made up of the same particles as the rest of the fluid: in other words these surfaces are material. Such a material singular surface is a vortex sheet.

The second solution is known from elementary physics: it is the formula for the speed of sound. This second type of weak singular surface is a sound wave which carries the discontinuity in the pressure gradient.

The speed of sound is a thermal-state variable, since it is a function of the pressure and the density. Thus it changes from point to point on the singular surface and should more accurately be called the local speed of sound. This deduction of the sound velocity is relatively simple, mathematically rigorous, and valid for any arbitrary motion of a perfect fluid.

5.4 Discontinuous balance equations at a shock surface

A strong disturbance of a medium at rest, or of a low-speed gas flow, propagates through the medium as a wave carrying a jump discontinuity of pressure, density, velocity, temperature, etc. This phenomenon is called a shock wave. Under certain conditions shock surfaces can also be observed to occur in high speed gas flows.

In the previous sections of this chapter such surfaces were, from the theoretical point of view, considered to be strong singular surfaces. The propagation and behaviour of such shock surfaces will now be investigated. The tool used in this investigation is the theory of discontinuous balance equations.

Consider a material volume V within which there occurs a singular surface S with respect to a set function $\Phi(\vec{r},t)$. We assume that the singular surface S divides the volume V into two regions V^+ and V^-, in each of which Φ is continuously differentiable, though not on the surface S. The singular surface is assumed to be smooth and to be moving with a speed of displacement U_N. The material boundary surface (A) is also divided by S into two parts A^+ and A^- as shown in *Fig. 5.2*. We define the velocities u^+ and u^- as follows:

$$\hat{u}^+ \equiv \begin{cases} \dfrac{\partial \vec{r}}{\partial t} = \vec{v} & \text{on the surface } A^+ \\ U_N \vec{n} & \text{on the surface } S, \end{cases} \tag{5.39}$$

$$\hat{u}^- \equiv \begin{cases} \dfrac{\partial \vec{r}}{\partial t} = \vec{v} & \text{on the surface } A^- \\ U_N \vec{n} & \text{on the surface } S. \end{cases} \tag{5.40}$$

Since the singular surface S is the common boundary surface of regions V^+ and V^- we can write the following equation:

$$\frac{\mathrm{d}}{\mathrm{d}t} \int_V \Phi \, \mathrm{d}V = \frac{\mathrm{d}^+}{\mathrm{d}t} \int_{V^+} \Phi \, \mathrm{d}V + \frac{\mathrm{d}^-}{\mathrm{d}t} \int_{V^-} \Phi \, \mathrm{d}V. \tag{5.41}$$

In this expression $\mathrm{d}^+/\mathrm{d}t$ indicates that we are to take the time derivative of the volume integral over that region which at that instant coincides with volume V^+ and is material with respect to the velocity field U^+. The derivative $\mathrm{d}^-/\mathrm{d}t$ is similarly defined. Since Φ and U are continuously differentiable in the regions V^+ and V^-, and approach continuous limits on the singular surface S, the usual transport theorem may be applied. Thus we obtain:

$$\frac{\mathrm{d}^+}{\mathrm{d}t} \int_{V^+} \Phi \, \mathrm{d}V = \int_{V^+} \frac{\partial \Phi}{\partial t} \mathrm{d}V + \int_{A^+} \Phi \, \vec{v} \, \mathrm{d}\vec{A} - \int_S \Phi^+ U_N \mathrm{d}A, \tag{5.42}$$

$$\frac{\mathrm{d}^-}{\mathrm{d}t} \int_{V^-} \Phi \, \mathrm{d}V = \int_{V^-} \frac{\partial \Phi}{\partial t} \mathrm{d}V + \int_{A^-} \Phi \, \vec{v} \, \mathrm{d}\vec{A} + \int_S \Phi^- U_N \mathrm{d}A. \tag{5.43}$$

Substituting into Eq. (5.41) we obtain the material derivative of the volume integral of Φ over a volume which contains the singular surface S.

This derivative contains the usual local and convective terms, as well as an additional term corresponding to the convective change produced by the jump

moving with a speed U_N across the surface S, i.e.

$$\frac{\mathrm{d}}{\mathrm{d}t}\int_V \Phi\,\mathrm{d}V=\int_V \frac{\partial\Phi}{\partial t}\mathrm{d}V+\int_{(A)}\Phi\,\vec{v}\,\mathrm{d}\vec{A}-\int_S [\![\Phi]\!]U_N\,\mathrm{d}A\,. \tag{5.44}$$

Let it be assumed that the function Φ represents the specific value of any extensive variable of state for a unit mass of material. This general balance equation is valid for any arbitrary material volume, whether or not it contains a singular surface. Then, using Eq. (5.44) to express the left-hand side of Eq. (5.41), we obtain

$$\int_V \frac{\partial(\varrho\Phi)}{\partial t}\mathrm{d}V+\int_{(A)}\varrho\Phi\,\vec{v}\,\mathrm{d}\vec{A}-\int_S [\![\Phi]\!]U_N\,\mathrm{d}A=\int_{(A)} j_N\,\mathrm{d}A+\int_V \varrho q\,\mathrm{d}V\,, \tag{5.45}$$

where j_N is the normal component of the conductive flux of Φ.

Let V be a sufficiently small material volume containing the singular surface S. Let the quantities $\varrho\Phi$ and $\varrho\vec{q}$ be bounded, while on both side of the singular surface $\varrho\Phi$, $\vec{v}$ and j_N approach boundary limits which are continuous functions of position. Let the surface (A) approach infinitesimally close to S so, that the regions V^+ and V^- vanish while the surface S remains finite in the limit. The volume integrals of Eq. (5.45) then vanishes in the limit, and the expression takes the following form:

$$\int_S \left(-[\![\varrho\Phi v_N]\!]-[\![\varrho\Phi]\!]U_N+[\![j_N]\!]\right)\mathrm{d}A=0\,. \tag{5.46}$$

Here v_N is the normal component of the material velocity, j_N is the normal component of the influx of Φ. Since the surface S is finite (bounded) the integrand must vanish, i.e.

$$-[\![\varrho\Phi v_N]\!]-[\![\varrho\Phi U_N]\!]+[\![j_N]\!]=0\,. \tag{5.47}$$

After some manipulation this equation can be written in a simpler form.

We now consider two rules: 1) the sum of two jump functions is equal to the jump of the sum of the particular variables; 2) the continuous multiplier of a jump function may be written both inside and outside the bracket. Thus we obtain the equation

$$[\![\varrho\Phi(v_N-U_N)]\!]+[\![j_N]\!]=0\,. \tag{5.48}$$

This can be expressed in terms of the speed of propagation of the strong singular surface:

$$-[\![\varrho\Phi c]\!]+[\![j_N]\!]=0\,. \tag{5.49}$$

This equation represents Kotchine's theorem: at a singular surface the general balance equation implies the equality of the jumps of the convective and conductive fluxes. The convective flux is defined by the relative velocity $-c$ in the coordinate system relative to the singular surface.

5.5 Balance equations at a shock surface

Conservation of mass equation

Equation (5.49) represents the most general form of the balance equation for a strong singular surface. This can be used to obtain balance equations for different extensive variables, depending on which flow variable has a discontinuity on the surface. In the balance equation for mass (i.e. conservation of mass) the density ϱ is the integrand as was shown in Chapter 3. Thus the function Φ in Eq. (5.49) must be identical to the unit value. Since the conductive mass flux (diffusion) may be disregarded, $j_N = 0$. Therefore, the mass balance equation for a unit area of the shock surface is

$$\dashv[\varrho c]\vdash = 0\,, \tag{5.50}$$

or, in another form

$$\varrho^+ c^+ - \varrho^- c^- = 0\,. \tag{5.51}$$

The physical meaning of the above equation can be easily illustrated. The shock surface propagates across the gas mass as a shock wave with speed c. In the coordinate system relative to the shock surface the relative velocity of the gas particles is obviously $-c$. Since the speed of displacement U_N undergoes no jump at the shock surface, while the normal velocity v_N does, the speed of propagation also undergoes a jump across the shock surface. In front of the shock surface the speed of propagation is c^+, behind it it is c^-. In the relative coordinate system moving with the shock surface the relative velocity of the gas arriving at the singular surface is $-c^+$, the velocity of the departing gas flow is $-c^-$. Thus the equation

$$\varrho^+ c^+ = \varrho^- c^-$$

expresses the equality of the relative mass fluxes across the shock surface. Thus the mass of the flowing gas remains unchanged across a shock surface.

Balance of momentum

The discontinuous balance of momentum equation can be obtained analogously from Eqs (5.26) and (5.49). In this case $\Phi \equiv \vec{v}$, and $j_N \equiv p\vec{n}$, using which we obtain the equation

$$\dashv[\varrho c \vec{v}]\vdash = \dashv[p\vec{n}]\vdash\,. \tag{5.52}$$

Thus the jump in the momentum of an ideal gas across a shock wave is equal to the jump in the pressure. Since the mass flux is continuous across the shock surface it may be taken out of the bracket. After this the balance of momentum equation can be split into a normal and a tangential scalar equation:

$$\varrho c \dashv[v_N]\vdash = \dashv[p]\vdash\,, \tag{5.53}$$

$$\varrho c \dashv[v_t]\vdash = 0\,. \tag{5.54}$$

The first equation shows, that the shock wave carries a jump in the normal component of the velocity. This velocity jump is proportional of the jump in pressure since

$$v_N^+ - v_N^- = \frac{p^+ - p^-}{\varrho c}. \tag{5.55}$$

Since the mass flux ϱc is constant we may substitute both $\varrho^+ c^+$ and $\varrho^- c^-$, the result is the same.

The jump in the normal component can be expressed as:

$$\llbracket v_N \rrbracket = \llbracket u_N - c \rrbracket . \tag{5.56}$$

Since the displacement speed u_N is constant across the shock surface

$$\llbracket v_N \rrbracket = - \llbracket c \rrbracket ; \tag{5.57}$$

thus the jump in the normal component of the velocity is the negative of the jump in the propagation speed. Using this relationship the balance of momentum equation can also be written in terms of the speed of propagation:

$$\llbracket \varrho c^2 + p \rrbracket = 0 . \tag{5.58}$$

This expresses that the jump in the sum of the convective and conductive momentum flux is zero in terms of a relative coordinate system which moves along with the shock wave. In other words: the sum of the conductive and convective momentum flux is constant across the shock surface:

$$\varrho^+ c^{+2} + p^+ = \varrho^- c^{-2} + p^- . \tag{5.59}$$

The tangential component of the balance of momentum equation also leads to an important consequence: the jump in the tangential velocity component across the shock wave is zero:

$$\llbracket v_t \rrbracket = v^+ - v^- = 0 . \tag{5.60}$$

Balance of energy

The balance of energy equation pertaining to the shock surface can be written using Eqs (4.101) or (5.49). In the present case we have

$$\Phi \equiv \frac{v^2}{2} + c_v T; \qquad j_N = p v_N .$$

Thus the discontinuous balance of energy equation is obtained as

$$\varrho c \left\llbracket \frac{v^2}{2} + c_v T \right\rrbracket = \llbracket p v_N \rrbracket . \tag{5.61}$$

This equation expresses that the jump in the sum of kinetic and internal energy is equal to the jump in the power of the surface force. It is known that the mass

flux and the tangential velocity component are continuous across the shock surface. We assume that the heat capacity c_v is constant. Thus Eq. (5.61) can be written in the following form:

$$\frac{\varrho c}{2}\,[v_N^2] + \varrho c c_v [T] + [p v_N]\,. \tag{5.62}$$

The energy equation can be also expressed in a coordinate system which moves along with the shock surface. Remembering that

$$v_N = U_N - c\,,$$

we can write

$$\frac{\varrho c}{2}\,[(U_N - c)^2] + \varrho c [c_v T] = [p(U_N - c)]\,. \tag{5.63}$$

Note that the speed of displacement does not undergo a jump, i.e.

$$[U_N] = 0\,.$$

Thus we get

$$-\varrho c U_N [c] + \varrho c \left[\frac{c^2}{2}\right] + \varrho c [c_v T] = U_N [p] - [pc]\,. \tag{5.64}$$

Applying Eqs (5.53) and (5.57) we obtain

$$\varrho c U_N [v_N] + \varrho c \left[\frac{c^2}{2} + c_v T\right] = \varrho c U_N [v_N] - \varrho c \left[\frac{pc}{\varrho c}\right]\,. \tag{5.65}$$

By means of some simple deductions we may rewrite the equation in the more elegant form:

$$\varrho c \left[\frac{c^2}{2} + c_v T + \frac{p}{\varrho}\right] = 0\,. \tag{5.66}$$

As is well known, the specific enthalpy is given by

$$i = c_v T + \frac{p}{\varrho}\,, \tag{5.67}$$

and thus the remarkably simple formula is obtained:

$$\left[\frac{c^2}{2} + i\right] = 0\,. \tag{5.68}$$

Therefore, Bernoulli's equation Eq. (4.42) holds for steady flow even when shock surfaces intervene in the motion. The specific energy content of the gas does not

change crossing a singular surface:

$$\frac{c^{+2}}{2}+i^{+}=\frac{c^{-2}}{2}+i^{-}, \tag{5.69}$$

or in another form

$$\frac{v^{+2}}{2}+i^{+}=\frac{v^{-2}}{2}+i^{-}. \tag{5.70}$$

Zemplén's theorem

By analogy with the second law of thermodynamics the following inequality may be postulated for the entropy change of a material volume:

$$\frac{\mathrm{d}}{\mathrm{d}t}\int_{V}\varrho S\,\mathrm{d}V\geqq-\int_{(A)}\frac{\hat{q}}{T}\,\mathrm{d}\vec{A}. \tag{5.71}$$

Since heat transfer processes are excluded the conductive flux of the internal energy vanishes. Substituting $\Phi\equiv S$ into the general balance equation for a singular surface we get:

$$-[\varrho c S]\geqq 0. \tag{5.72}$$

This means that the entropy of an isentropic flow of an ideal gas increases (or is equal to zero) when crossing a shock surface. Since

$$[\varrho c]=0,$$

we obtain

$$-[S]\geqq 0, \tag{5.73}$$

or, in another form

$$S^{-}-S^{+}\geqq 0. \tag{5.74}$$

This effect, i.e. that the entropy must increase across a shock surface was pointed out by G. Zemplén in 1905. At that time this idea was far from being generally accepted, and Kelvin and Rayleigh had serious doubts, concerning its validity. Since that time it has been verified in engineering practice (e.g. shock losses in turbocompressors). Thus it has been confirmed that the generation and motion of shock surfaces is an irreversible process even an adiabatic system for the flow of an ideal gas.

5.6 Changes in the variables of state across a shock surface

Zemplén's theorem states that the entropy must increase, even in an adiabatic system, if a shock surface sweeps across an ideal gas flow. In the absence of shock surfaces the flow of an ideal gas would be isentropic in an adiabatic system. Thus the thermodynamic state of the gas must undergo a change across a shock surface.

The relationship between the pressure and the density was determined by Hugoniot for this type of change in thermodynamic state. To obtain this very important relation, we start of by considering the energy equation in the form

$$\frac{\varrho c}{2}\llbracket v_N^2 \rrbracket + \varrho c \llbracket c_v T \rrbracket = \llbracket p v_N \rrbracket . \tag{5.75}$$

The temperature may be eliminated by applying the equation of state, thus

$$\frac{\varrho c}{2}\llbracket v_N^2 \rrbracket + \frac{\varrho c}{\kappa - 1}\left\llbracket \frac{p}{\varrho} \right\rrbracket = \llbracket p v_N \rrbracket . \tag{5.76}$$

The first term of this equation can be written as

$$\frac{\varrho c}{2}\llbracket v_N^2 \rrbracket = \frac{\varrho c}{2}(v_N^{+2} - v_N^{-2}) = \frac{\varrho c}{2}(v_N^+ + v_N^-)(v_N^+ - v_N^-) . \tag{5.77}$$

Using the balance of momentum equation the jump in the normal velocity can be expressed as:

$$\llbracket v_N \rrbracket = \frac{\llbracket p \rrbracket}{\varrho c} . \tag{5.78}$$

After substitution we get for the kinetic energy term:

$$\frac{\varrho c}{2}\llbracket v_N^2 \rrbracket = \frac{1}{2}(v_N^+ + v_N^-)\llbracket p \rrbracket = \frac{1}{2}(v_N^+ p^+ + v_N^- p^+ - v_N^+ p^- - v_N^- p^-) .$$

Thus the energy equation is obtained as

$$\frac{1}{2}(v_N^+ p^+ + v_N^- p^+ - v_N^+ p^- - v_N^- p^-) + \frac{\varrho c}{\kappa - 1}\left\llbracket \frac{p}{\varrho} \right\rrbracket = p^+ v_N^+ - p^- v_N^- .$$

After some simplification we obtain

$$\frac{p^+ + p^-}{2}\llbracket v_N \rrbracket = \frac{\varrho c}{\kappa - 1}\left\llbracket \frac{p}{\varrho} \right\rrbracket . \tag{5.79}$$

As it was shown

$$\llbracket v_N \rrbracket = -\llbracket c \rrbracket ,$$

thus we can get

$$\llbracket v_N \rrbracket = -\left\llbracket \varrho c \frac{1}{\varrho} \right\rrbracket = -\varrho c \left\llbracket \frac{1}{\varrho} \right\rrbracket . \tag{5.80}$$

Substituting to Eq. (5.78) the obtained expression consists of the pressure and the density as state variables:

$$\frac{p^+ + p^-}{2}\left\llbracket \frac{1}{\varrho} \right\rrbracket + \frac{1}{\kappa - 1}\left\llbracket \frac{p}{\varrho} \right\rrbracket = 0 . \tag{5.81}$$

Expanding the brackets denoting the jumps we obtain

$$\frac{p^+ + p^-}{2}\left(\frac{1}{\varrho^+} - \frac{1}{\varrho^-}\right) + \frac{1}{\kappa - 1}\left(\frac{p^+}{\varrho^+} - \frac{p^-}{\varrho^-}\right) = 0 .$$

Multiplying by $2\varrho^+/p^-$ we first have

$$\left(\frac{p^+}{p^-} + 1\right)\left(1 - \frac{\varrho^+}{\varrho^-}\right) + \frac{2}{\kappa - 1}\left(\frac{p^+}{p^-} - \frac{\varrho^+}{\varrho^-}\right) = 0 ,$$

while after some manipulation we may write the equation as

$$\frac{p^+}{p^-}\left(1 - \frac{\varrho^+}{\varrho^-} + \frac{2}{\kappa - 1}\right) + 1 - \frac{\varrho^+}{\varrho^-} - \frac{2}{\kappa - 1}\frac{\varrho^+}{\varrho^-} = 0 .$$

Finally we obtain the well-known formula

$$\frac{p^+}{p^-} = \frac{(\kappa + 1)\dfrac{\varrho^+}{\varrho^-} - (\kappa - 1)}{(\kappa + 1) - (\kappa - 1)\dfrac{\varrho^+}{\varrho^-}} . \tag{5.82}$$

It is particularly remarkable the symmetry of the p^+/p^- and the p^-/p^+ relations. For the latter it can be written

$$\frac{p^-}{p^+} = \frac{(\kappa + 1)\dfrac{\varrho^-}{\varrho^+} - (\kappa - 1)}{(\kappa + 1) - (\kappa - 1)\dfrac{\varrho^-}{\varrho^+}} . \tag{5.82a}$$

This is the equation of the so-called Hugoniot curve, which may also be written in other suitable forms:

$$\frac{p^+}{p^-} = \frac{(\kappa + 1)\varrho^+ - (\kappa - 1)\varrho^-}{(\kappa + 1)\varrho^- - (\kappa - 1)\varrho^+} , \tag{5.83}$$

or

$$\frac{p^- - p^+}{\varrho^- - \varrho^+} = \kappa \frac{p^- + p^+}{\varrho^- + \varrho^+} . \tag{5.84}$$

This latter form was given by T. Kármán.

Hugoniot's equation determines all possible end states (p^-, ϱ^-) which can be reached across a shock surface from an initial state (p^+, ϱ^+). The locus of this end state in the p, ϱ plane is shown in *Fig. 5.6*. The function p^-/p^+ has an asymptote at

$$\frac{\varrho^-}{\varrho^+} = \frac{\kappa + 1}{\kappa - 1}$$

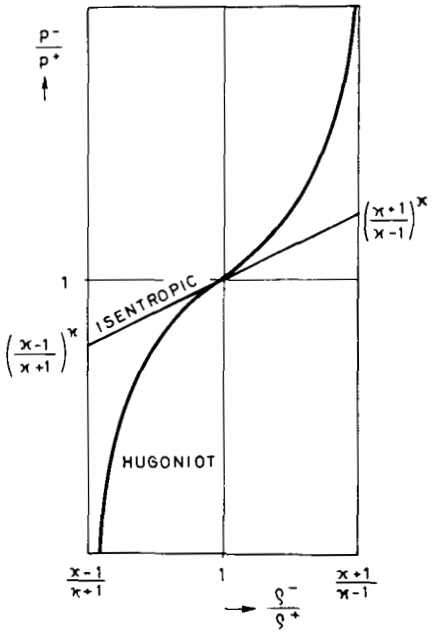

Fig. 5.6. Hugoniot adiabata and isentropic curve

and a zero value at

$$\frac{\varrho^-}{\varrho^+} = \frac{\kappa - 1}{\kappa + 1}.$$

The isentropic curve and the Hugoniot curve have a second-order contact through the point $\varrho^-/\varrho^+ = 1$.

It can be seen that only the interval

$$1 < \frac{\varrho^-}{\varrho^+} = \frac{\kappa + 1}{\kappa - 1}$$

may be realized. Since

$$S^- \gtrless S^+,$$

the equation

$$S^- - S^+ = \frac{R}{\kappa - 1} \ln\left(\frac{p^-}{p^+}\right)\left(\frac{\varrho^+}{\varrho^-}\right)^{\kappa} \gtrless 0 \tag{5.85}$$

must be positive. If $\frac{\varrho^-}{\varrho^+} < 1$, the change in entropy would be negative, which is impossible. Similarly it is impossible to have an arbitrarily great jump in density, thus the region of the Hugoniot curve where

$$\frac{\varrho^-}{\varrho^+} > \frac{\kappa + 1}{\kappa - 1}$$

is also never realized.

The entropy increase across a shock surface can be determined knowing Hugoniot's equation. From the first law of thermodynamics

$$T\,\mathrm{d}S = c_p\,\mathrm{d}T - \frac{\mathrm{d}p}{\varrho}.$$

Applying the equation of state of an ideal gas, the infinitesimal change in entropy is obtained as

$$\mathrm{d}S = c_p\frac{\mathrm{d}T}{T} - R\frac{\mathrm{d}p}{p}.$$

Since $c_p - c_v = R$, and $\kappa = c_p/c_v$ we get

$$\mathrm{d}S = \frac{\kappa}{\kappa-1}R\frac{\mathrm{d}T}{T} - R\frac{\mathrm{d}p}{p}.$$

Integrating through the shock surface

$$S^- - S^+ = \frac{\kappa R}{\kappa-1}\ln\frac{T^-}{T^+} - R\ln\frac{p^-}{p^+}.$$

Replacing the temperature by the density (from the equation of state), the change in entropy is obtained as

$$S^- - S^+ = \frac{R}{\kappa-1}\ln\left(\frac{p^-}{p^+}\right)\left(\frac{\varrho^+}{\varrho^-}\right)^{\kappa}. \tag{5.86}$$

It is obvious that the gas can flow only in that direction in which its entropy increases. Since the entropy rises not only for small but also for large pressure increments, it follows that a shock wave can occur only if the pressure increases. This always means a decrease in velocity and an increase in density. Thus only compressive shock waves can exist; shocks resulting from rarefaction are impossible.

5.7 Speed of propagation of shock surfaces

In order to determine the speed of propagation of a shock surface we begin by taking the balance of momentum equation which applies to the shock surface:

$$\llbracket \varrho c^2 + p \rrbracket = 0. \tag{5.87}$$

By means of some simple manipulations we may rewrite this equation in the following form:

$$\varrho^2 c^2\left(\frac{1}{\varrho^-} - \frac{1}{\varrho^+}\right) = \varrho^2 c^2\frac{\llbracket\varrho\rrbracket}{\varrho^+\varrho^-} = \llbracket p\rrbracket, \tag{5.88}$$

which yields the square of the speed of propagation as

$$c^2 = \frac{\varrho^+\varrho^-}{\varrho^2}\frac{\llbracket p\rrbracket}{\llbracket\varrho\rrbracket}. \tag{5.89}$$

It is well known that the speed of propagation also undergoes a jump discontinuity. The different speeds in front of and behind the shock surface are obtained by substituting the densities ϱ^+ and ϱ^- into the equation for ϱ^2. Thus we have

$$(c^+)^2 = \frac{\varrho^-}{\varrho^+} \frac{[p]}{[\varrho]}, \tag{5.90}$$

and

$$(c^-)^2 = \frac{\varrho^+}{\varrho^-} \frac{[p]}{[\varrho]}. \tag{5.91}$$

Expanding the brackets, and after some manipulation, this may be written as

$$(c^+)^2 = \frac{p^+}{\varrho^+} \frac{\varrho^-}{\varrho^+ - \varrho^-} \left(1 - \frac{p^-}{p^+}\right),$$

and

$$(c^-)^2 = \frac{p^-}{\varrho^-} \frac{\varrho^+}{\varrho^+ - \varrho^-} \left(\frac{p^+}{p^-} - 1\right),$$

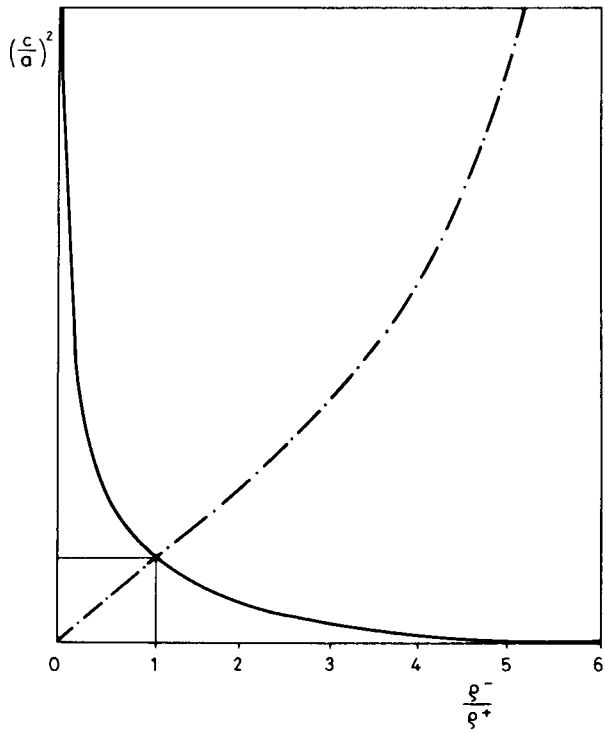

Fig. 5.7. Propagation speed of shock waves

Substituting the pressure ratio from Hugoniot's equation we have

$$(c^+)^2 = \kappa \frac{p^+}{\varrho^+} \frac{2\varrho^-}{(\kappa+1)\varrho^+ - (\kappa-1)\varrho^-}, \tag{5.92}$$

and

$$(c^-)^2 = \kappa \frac{p^-}{\varrho^-} \frac{2\varrho^+}{(\kappa+1)\varrho^- - (\kappa-1)\varrho^+}. \tag{5.93}$$

It is clear that as the jump in density decreases, the speed of propagation approaches to the limit of the speed of sound. At the same time the speed of propagation also becomes greater as the shock strength i.e. the jump in density increases. This relationship may be represented graphically by plotting the velocity ratio $(c/a)^2$ as a function of the density ratio (ϱ^-/ϱ^+) using the equations

$$\left(\frac{c^+}{a^+}\right)^2 = \frac{2\frac{\varrho^-}{\varrho^+}}{(\kappa+1)-(\kappa-1)\frac{\varrho^-}{\varrho^+}}, \tag{5.94}$$

and

$$\left(\frac{c^-}{a^-}\right)^2 = \frac{2}{(\kappa+1)\frac{\varrho^-}{\varrho^+}-(\kappa-1)}. \tag{5.95}$$

This is shown in *Fig. 5.7*. In a compressive shock the speed of propagation is greater than the speed of sound in front of the shock surface, that is $(c^+/a^+)>1$, but behind the shock front where $(c^-/a^-)<1$, the speed of propagation decreases.

5.8 The jump in the variables of state as a function of the Mach number

The most important parameter in compressible flow theory is the Mach number. It is obvious that the Mach number varies from point to point in a compressible flow, not only because of velocity changes, but also because the speed of sound, being a thermodynamic parameter, is a function of the local conditions. For practical purposes the jump in the variables of state across a shock surface may be expressed as functions of the Mach number M_1 in front of the shock. The jump in pressure is obtained from the balance of momentum equation:

$$[p] = -[\varrho c^2] = -\varrho^2 c^2 \left[\frac{1}{\varrho}\right]. \tag{5.96}$$

Expanding the brackets we get

$$p^- - p^+ = (\varrho c^2)\left(\frac{1}{\varrho^+} - \frac{1}{\varrho^-}\right). \tag{5.97}$$

In terms of a reference system which moves along with the shock surface, the normal component of the relative velocity of the gas is

$$w_N = -c\,,$$

thus we may define the Mach number by the equation

$$M_N = \frac{c}{a}. \tag{5.98}$$

Thus the jump in pressure is obtained as

$$p^- - p^+ = (\varrho^+)^2 (a^+)^2 (M_N^+)^2 \left(\frac{1}{\varrho^+} - \frac{1}{\varrho^-}\right). \tag{5.99}$$

Applying Eq. (5.38) we get:

$$p^- - p^+ = \kappa p^+ (M_N^+)^2 \left(1 - \frac{\varrho^+}{\varrho^-}\right). \tag{5.100}$$

The density change can be eliminated using the Hugoniot equation, giving

$$\frac{p^- - p^+}{p^+} = \frac{2\kappa}{\kappa+1}[(M_N^+)^2 - 1]\,, \tag{5.101}$$

where the left-hand side may be considered to be a parameter expressing the shock strength. It is evident that a finite pressure jump can occur only if the flow is supersonic in front of the shock, since $p^- - p^+ > 0$ can only be realized if $M_N^+ > 1$. Negative pressure jump is impossible even if $M_N^+ < 1$, since the entropy cannot decrease in an adiabatic flow.

The jump in density across the shock surface can be determined in a similar manner, the only difference being that in Eq. (5.100) the pressure is now eliminated. The result is:

$$\frac{\varrho^-}{\varrho^+} = \frac{(\kappa+1)(M_N^+)^2}{2+(\kappa-1)(M_N^+)^2}\,, \tag{5.102}$$

which gives the density ratio across the shock surface.

The temperature jump can also be expressed in dimensionless form:

$$\frac{T^- - T^+}{T^+} = \frac{2(\kappa-1)}{(\kappa+1)^2} \frac{[\kappa(M_N^+)^2 - 1][(M_N^+)^2 - 1]}{(M_N^+)^2}. \tag{5.103}$$

Note that for a very strong shock the calculated temperature jump is unrealistically large. For example: $M_N^+ = 50$, $T^+ = 300$ K leads to the temperature $T^- = 15\,300$ K. Such an extremely strong shock wave can occur in the chamber of a gun at the instant of firing, but if the temperature is measured it is found to be much smaller. The cause of this discrepancy is that the specific heat is not constant over such a broad interval. Shock waves can, however, cause extremely high temperatures, such as can hardly be reached by the burning of any fuel.

The jump in the speed of propagation is obatined as

$$\frac{c^- - c^+}{c^+} = \frac{1}{\kappa+1}\,\frac{1-(M_N^+)^2}{(M_N^+)^2}. \tag{5.104}$$

Naturally the jump in the relative velocities can be obtained in the same way. It can be seen that the supersonic flow becomes subsonic across the shock surface.

The same physical meaning can be recognized from the relation obtained for the Mach numbers:

$$(M_N^-)^2 = \frac{1+\dfrac{\kappa-1}{2}(M_N^+)^2}{\kappa(M_N^+)^2 - \dfrac{\kappa-1}{2}}. \tag{5.105}$$

Finally we can also derive the expression for the jump in the entropy. Substituting into Eq. (5.86) the pressure ratio from Eq. (5.101) and the density ratio from Eq. (5.102) we obtain

$$S^- - S^+ = \frac{R}{\kappa-1}\ln\left(1+\frac{2\kappa}{\kappa+1}[(M_N^+)^2-1]\right) - \frac{\kappa R}{\kappa-1}\ln\frac{(\kappa+1)(M_N^+)^2}{2+(\kappa-1)M_N^{+2}}. \tag{5.106}$$

A further interesting consequence may be found by expanding this equation into a logarithmic series. Linear and second-order terms vanish, thus we obtain

$$S^- - S^+ = \frac{2\kappa R}{(\kappa+1)^2}\,\frac{[(M_N^+)^2-1]^3}{3}. \tag{5.107}$$

Since the entropy cannot decrease, it is obvious that $M_N^+ \geqq 1$, thus the jump from supersonic to subsonic flow is possible. The jump in the entropy can be expressed in terms of the shock strength by applying Eq. (5.101):

$$S^- - S^+ = \frac{\kappa+1}{12\kappa^2}\left(\frac{p^- - p^+}{p^+}\right)^3. \tag{5.108}$$

It should be noted that the jump in the variables of state depends only on the normal component of the velocity. The tangential component does not undergo a jump and thus it is missing from these formulas.

5.9 Shock surfaces in steady supersonic planar flow

Perturbations induced by a body interacting with a supersonic flow cannot propagate in any arbitrary direction. The Mach line constitutes a demarcation boundary for the propagation of such disturbances. In the case of steady flow it is

simplest to consider the motion using a reference system in which the body is stationary while the gas flows over it. If the flow is supersonic relative to the body then the waves cannot propagate in the direction in front of the body, thus the wave pattern travels with the body. Thus in terms of the reference system used, the wave pattern is also stationary, and there is a direct correspondence between the wave pattern and the flow field. It is particularly easy to determine the shock waves which occur during steady supersonic planar flow.

From a kinematic point of view two categories of shock waves can be distinguished. The normal shock wave is a singular surface which propagates perpendicular to the streamlines, and through which the streamlines cross without change of direction. The oblique shock wave is a singular surface which does not propagate perpendicular to the streamlines, and at which the streamlines are abruptly deflected. This deflection is always towards the shock. Abrupt variations in gas density which accompany the shock wave can be observed by optical methods. Jet-aircraft pilots are reported to have seen with the naked eye, shock waves occurring at the wings of aircraft.

Normal shock waves

Since normal shock waves are stationary, the following Bernoulli equation refers to the flow in front of and behind the shock surface:

$$\frac{v^{+2}}{2}+i^{+}=\frac{v^{-2}}{2}+i^{-}. \tag{5.109}$$

The enthalpy can be expressed in terms of the pressure and the density as

$$i=c_p T=\frac{\kappa}{\kappa-1}RT=\frac{\kappa}{\kappa-1}\frac{p}{\varrho}, \tag{5.110}$$

and if the stagnation pressure and density are also substituted we obtain

$$\frac{v^{+2}}{2}+\frac{\kappa}{\kappa-1}\frac{p^{+}}{\varrho^{+}}=\frac{v^{-2}}{2}+\frac{\kappa}{\kappa-1}\frac{p^{-}}{\varrho^{-}}=\frac{\kappa}{\kappa-1}\frac{p_0}{\varrho_0}. \tag{5.111}$$

Multiplying by $\frac{\kappa-1}{\kappa v^{+}}$ and $\frac{\kappa-1}{\kappa v^{-}}$, we have

$$\frac{p^{+}}{\varrho^{+}v^{+}}=\frac{p_0}{\varrho_0 v^{+}}-\frac{\kappa-1}{2\kappa}v^{+}, \tag{5.112}$$

and

$$\frac{p^{-}}{\varrho^{-}v^{-}}=\frac{p_0}{\varrho_0 v^{-}}-\frac{\kappa-1}{2\kappa}v^{-}. \tag{5.113}$$

Substituting into Eq. (5.55) and taking into account that the velocity has a normal component only in the normal shock wave, i.e. $v_N = v$, we get

$$v^+ - v^- = \frac{p_0}{\varrho_0}\left(\frac{1}{v^-} - \frac{1}{v^+}\right)\frac{\kappa - 1}{2\kappa}(v^+ - v^-)\,. \tag{5.114}$$

After some rearranging

$$v^+ v^- = \frac{2\kappa}{\kappa + 1}\,\frac{p_0}{\varrho_0}, \tag{5.115}$$

and remembering that

$$a_0^2 = \kappa\frac{p_0}{\varrho_0},$$

and also that

$$a_0^2 = \frac{\kappa + 1}{2}a_*^2\,,$$

the so-called Prandtl—Meyer equation is obtained:

$$v^+ v^- = a_*^2\,. \tag{5.116}$$

This equation can be written as

$$M_*^- = \frac{1}{M_*^+}, \tag{5.117}$$

where M_* is the speed ratio

$$M_* = \frac{v}{a_*}. \tag{5.118}$$

This notation is an accepted and convenient parameter of transsonic flows. To avoid confusion note that M_* is not the critical Mach number (in spite of the starred notation). This latter is of course denoted by $M = 1$. The relationship between the Mach number M and the parameter M_* is readily obtained. The isentropic Bernoulli equation may be expressed in terms of the critical speed of sound as

$$\frac{v^2}{2} + \frac{a^2}{\kappa - 1} = \frac{\kappa + 1}{2}\,\frac{a_*^2}{\kappa - 1}.$$

Dividing both sides of this equation by v^2 and after some modification we obtain

$$M_*^2 = \frac{\kappa + 1}{\kappa - 1 + \dfrac{2}{M^2}}. \tag{5.119}$$

It is clear that for subsonic flow (when $M < 1$) $M_* < 1$. For supersonic flow ($M > 1$) we similarly see that $M_* > 1$. The change in thermal parameters across the shock surface can be determined using Eqs (5.101) to (5.108).

Oblique shock waves

A shock wave is said to be oblique if the upstream flow direction is not parallel to the normal of the shock surface, and the streamlines are abruptly deflected at the shock surface. This change of direction is always toward the shock surface, as shown in *Fig. 5.8*. A very simple treatment of oblique shock waves may be developed by superimposing a uniform tangential velocity v_t onto the flow field of a normal shock wave. Since

$$v_N^+ > v_N^-$$

and

$$v_t^+ = v_t^- \equiv v_t$$

the inclination of the streamlines in front of the shock surface must be different from that behind the shock surface. The angle Θ of the abrupt deflection of the streamlines is positive.

The relationship between the conditions in front of and behind the oblique shock wave can be determined using Eqs (5.101) to (5.108). The only change is that the initial Mach number

$$M^+ = \frac{v^+}{a},$$

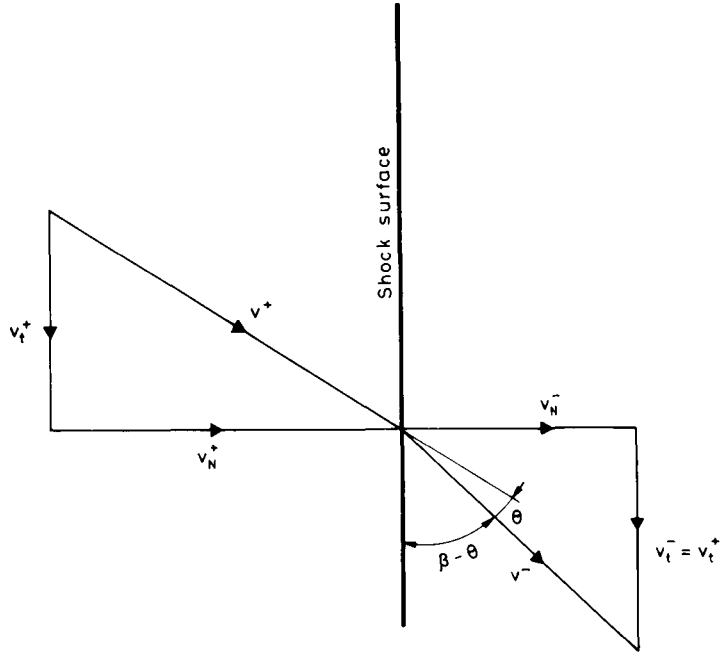

Fig. 5.8. Oblique shock wave

is chosen instead of

$$M_N = \frac{v_N^+}{a}.$$

Since

$$\frac{v_N^+}{v^+} = \frac{c^+}{v^+} = \sin\beta, \tag{5.120}$$

it is obvious that

$$M_N^+ = M^+ \sin\beta. \tag{5.121}$$

Substituting this we obtain the following equations for the change across the oblique shock surface:

$$\frac{p^- - p^+}{p^-} = \frac{(M^+)^2 \sin^2\beta - 1}{\frac{\kappa+1}{2\kappa}}, \tag{5.122}$$

$$\frac{\varrho^-}{\varrho^+} = \frac{(\kappa+1)(M^+)^2 \sin^2\beta}{(\kappa-1)(M^+)^2 \sin^2\beta + 2}, \tag{5.123}$$

$$\frac{T^- - T^+}{T^+} = 2\frac{\kappa-1}{(\kappa+1)^2} \frac{(M^+)^2 \sin^2\beta - 1}{(\kappa+1)^2 (M^+)^2 \sin^2\beta} (1 + \kappa M^{+2} \sin^2\beta), \tag{5.124}$$

$$S^- - S^+ = \frac{R}{\kappa-1} \left\{ \ln \left(1 + \frac{(M^+)^2 \sin^2\beta - 1}{\frac{\kappa+1}{2\kappa}} \right) \left(\frac{(\kappa+1)(M^+)^2 \sin^2\beta}{(\kappa-1)(M^+)^2 \sin^2\beta + 2} \right)^{-\kappa} \right\}. \tag{5.125}$$

An interesting relationship can be obtained for the angle of deflection Θ as a function of the initial Mach number M^+ and the angle β.

Consider, that

$$\tan\beta = \frac{v_N^+}{v_t}, \tag{5.126}$$

and

$$\tan(\beta - \Theta) \frac{v_N^-}{v_t}. \tag{5.127}$$

Eliminating v_t and applying the continuity equation we have

$$\frac{\tan(\beta - \Theta)}{\tan\beta} = \frac{v_N^-}{v_N^+} = \frac{\varrho^+}{\varrho^-}. \tag{5.128}$$

Substituting the density ratio from Eq. (5.123) we find

$$\frac{\tan(\beta - \Theta)}{\tan\beta} = \frac{(\kappa-1)(M^+)^2 \sin^2\beta + 2}{(\kappa+1)(M^+)^2 \sin^2\beta}, \tag{5.129}$$

which after some manipulation can be written as

$$\tan \Theta = 2 \cot \beta \frac{(M^+)^2 \sin^2 \beta - 1}{(M^+)^2(\kappa + \cos 2\beta) + 2}. \tag{5.130}$$

This expression becomes zero at $\beta = \frac{\pi}{2}$ and at $\beta = \arcsin \frac{1}{M^+}$. Within this interval Θ is positive and reaches a single maximum value. This is shown in *Fig. 5.9* for different values of the parameter M^+.

If the angle of deflection Θ is smaller than its maximum value, then for each value of Θ and M^+ there are two solutions, with different values for the angle of incidence of the wave β. The greater value of the wave angle corresponds to the stronger shock. For this stronger shock $M^- < 1$, i.e. the flow behind the shock surface becomes subsonic. The other solution, where the wave angle β has its smaller value, yields $M^- > 1$, i.e. behind this weaker shock surface the flow remains supersonic.

In perfect fluid flow any streamline may be replaced by a solid boundary surface. The above solution for an oblique shock wave is also valid for a supersonic flow

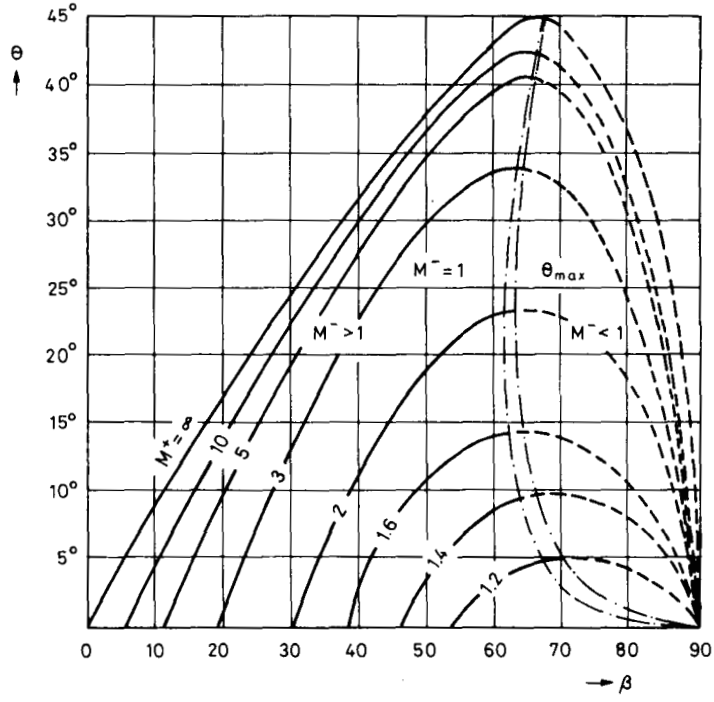

Fig. 5.9. Deflection angle for oblique shock waves

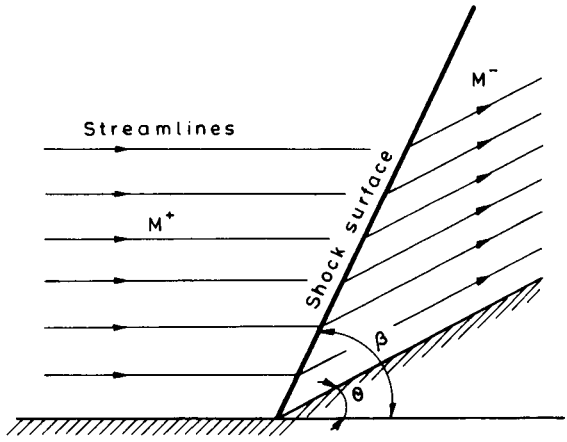

Fig. 5.10. Supersonic flow at a corner

at a corner, as shown in *Fig. 5.10*. Since the pressure and the density increase due to a shock, supersonic flow may be easily compressed by turning it at a deflecting wall.

A corner is invariably the starting point of a shock surface. The supersonic flow is parallel to the wall up to the corner. The disturbance caused by the corner can propagate only in the direction of the flow. Thus the region upstream of the corner remains unaffected.

If the turning of the supersonic flow is concave (i.e. the angle of deflection Θ is greater then 180°) an expansion wave occurs. Both the pressure and the density decrease through an expansion wave, but the velocity increases. According to Zemplén's theorem, an expansion wave cannot be a shock, it can only be a weak singular surface. The angle of deflection of an expansion wave cannot be greater than a given Θ_{max} as represented in *Fig. 5.9*. If the angle of the corner is less than the value of $\pi - \Theta_{max}$, the expansion wave cannot turn the flow sufficiently to be parallel to the wall after the corner, thus a vacuum occurs between the wall and the separated flow.

Similarly, a shock wave occurs at the nose of a wedge placed in a supersonic flow. If the symmetry axis of the wedge is parallel to the upstream flow direction, two symmetric shock waves are formed. The flow is deflected by the shock surface in the direction of the nose of the wedge. The Mach number and inclination of the flow may be obtained from the measurement of the angle of the shock wave. Owing to the change in the refractive index which accompanies the shock front, the angle β can be determined by means of a photograph. Thus a wedge may be used as a device for making velocity measurements, but this is not as accurate as a Pitot or Prandtl tube.

The case of the supersonic flow pattern around a so-called blunt-nosed body cannot be solved analytically, but it is observed experimentally that a curved shock

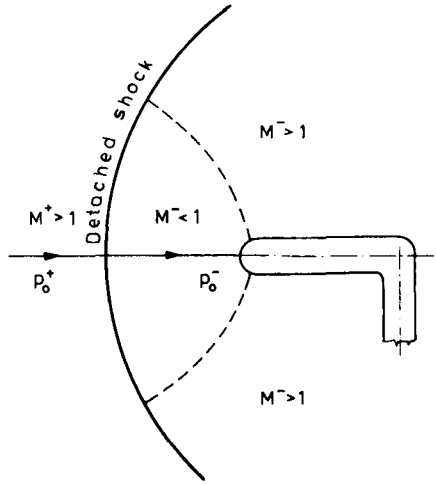

Fig. 5.11. Detached shock wave at a blunt-nose body

wave occurs at some distance ahead of the nose, as shown in *Fig. 5.11*. The shape of the shock wave and its detachment distance depends on the geometry of the body and on the Mach number of the upstream flow.

The disturbances induced by the body can propagate only in the flow direction. If the curved shock wave had not occurred the supersonic upstream flow would have been homogeneous until it reached the body surface. In this case the normal component of the velocity could not vanish at the body surface. This normal component can vanish only by passing through a strong shock and decelerating to below the speed of sound.

The strong shock front always occurs in front of the body, while between the shock front and the body a subsonic region is developed. In the subsonic region disturbances can propagate in directions opposite to that of the flow, thus the flow pattern can be modified in front of the body in such a way that only the tangential velocity component remains when the decelerated subsonic flow reaches the body surface.

Along the symmetry axis of the body a normal shock develops; the jump in the velocity and the pressure has its greatest value here. Towards both sides of the axis the shock wave is weakened, it becomes an oblique shock and the angle between the shock wave and the streamlines tends asymptotically to the Mach angle. Since the jump is weaker far away from the body, the flow passing through the shock wave here remains supersonic.

The entropy of the gas increases when passing through a shock front, thus the stagnation pressure behind such a front must be smaller than ahead of it. A Pitot tube placed within a supersonic flow can measure the decrease in the stagnation pressure behind the shock front as compared with the original stagnation pressure

of the undisturbed flow. The ratio of the two stagnation pressures is

$$\frac{p_0^-}{p_0^+} = \left[\frac{(\kappa+1)M^{+2}}{(\kappa-1)(M^+)^2+2}\right]^{\frac{\kappa}{\kappa-1}} \left[1+\frac{2\kappa}{\kappa+1}[(M^+)^2-1]\right]^{\frac{1}{1-\kappa}}. \tag{5.131}$$

Knowing the Mach number of the upstream flow, and with p_0^- measured with a Pitot tube, the original p_0^+ can be calculated.

A combined static-and-Pitot tube, the so-called Prandtl tube, is suitable to determine the Mach number of high-velocity gas flows.

For a subsonic flow without shock waves the ratio of the stagnation pressure to the static pressure is given by

$$\frac{p_0}{p} = \left(\frac{\kappa-1}{2}M^2+1\right)^{\frac{\kappa}{\kappa-1}}. \tag{5.132}$$

In a supersonic flow the Prandtl tube induces a shock wave. Ahead of the shock $p_0 = p_0^+$, while at the noise of the device the pressure is p_0^-. Dividing Eq. (5.131) by Eq. (5.132) we get

$$\frac{p_0^-}{p} = \frac{\left[\frac{\kappa+1}{\kappa}(M^+)^2\right]^{\frac{\kappa}{\kappa-1}}}{\left[1+\frac{2\kappa}{\kappa+1}[(M^+)^2-1]\right]^{\frac{1}{\kappa-1}}}. \tag{5.133}$$

Thus, by measuring the stagnation and the static pressure the Mach number can be determined.

CHAPTER 6

LAMINAR FLOW

6.1 The flow of viscous fluids

The action of material forces across a surface in a fluid is described by the stress vector $\vec{t}$. The stress vector depends on the position, the time and the unit normal vector of the surface on which it acts,

$$\vec{t} = f(\vec{r}, t, \vec{n}) .$$

As is well known, the stress vector may be expressed as a linear function of n:

$$\vec{t} = \mathbf{T}\,\vec{n} , \tag{6.1}$$

where $\mathbf{T}$ represents the stress tensor as a continuous function of the position and the time only. The state of stress for any material is determined by the stress tensor. The matrix of the coefficients $\mathbf{T}^{ij}$ forms a second-order tensor, which is symmetrical, as follows from the balance of angular momentum equation. Each component of $\mathbf{T}$ has a simple physical interpretation. $\mathbf{T}^{ij}$ is the j-component of the force on a surface element with outward unit normal vector in the i-direction.

$$\mathbf{T} = \begin{bmatrix} \sigma_x & \tau_{xy} & \tau_{xz} \\ \tau_{yx} & \sigma_y & \tau_{yz} \\ \tau_{zx} & \tau_{zy} & \sigma_z \end{bmatrix} . \tag{6.2}$$

The normal stresses σ_x, σ_y and σ_z are in the main diagonal of the matrix. For example σ_x is the normal stress acting on a face normal to x. The tangential stresses, in other words the shear stresses τ_{xy}, τ_{xz}, etc., occur outside the main diagonal. For example τ_{xy} is a shear stress acting in the y-direction on a face normal to x.

In a fluid at rest all shear stresses vanish, and all normal stresses are equal

$$\mathbf{T} = \begin{bmatrix} -p & 0 & 0 \\ 0 & -p & 0 \\ 0 & 0 & -p \end{bmatrix} . \tag{6.3}$$

This is the so-called hydrostatic state of stress, which can be written as

$$\mathbf{T} = -p\mathbf{I}. \tag{6.4}$$

It is an experimental observation that normal stresses are much greater than shear stresses, and there is a class of fluid flow problems which can be solved rather precisely by completely neglecting shear stresses. The model of a perfect fluid is obtained in this way.

Actual fluids exhibit a certain resistance to changes of shape. The viscosity of a fluid is a measure of its resistance to angular deformation. This phenomenon can be described only by taking into account the shear stresses. The first equation for the shear stresses in one-dimensional viscous flow was given by Newton,

$$\tau_{xy} = \mu \frac{\mathrm{d}v_x}{\mathrm{d}y}. \tag{6.5}$$

Thus, the shear stress is proportional to the velocity gradient. The proportionality factor μ is called the dynamic viscosity coefficient (or just dynamic viscosity). The kinematic viscosity of a fluid is the ratio of the viscosity to the density:

$$\nu = \frac{\mu}{\varrho}. \tag{6.6}$$

A fluid for which the viscosity coefficient does not change with the rate of deformation is said to be a Newtonian fluid. There are certain types of fluids, especially crude oils and drilling muds, in which the viscosity varies with the rate of deformation. In this chapter, however, only Newtonian fluids are considered.

Newton's viscosity law was generalized by Stokes in tensorial form. Stokes postulated his ideas in the following form:

1. The stress tensor $\mathbf{T}$ is a continuous function of the rate of deformation tensor $\mathbf{S}$, and is independent of all other kinematic quantities.
2. The stress tensor does not depend explicitly on the position $\vec{r}$ and the time t.
3. The fluids are isotropic, there is no preferred direction in space. Thus the viscosity coefficient is a scalar quantity.
4. When $\mathbf{S}=0$, $\mathbf{T}$ reduces to $-p\mathbf{I}$.

A medium, whose constitutive relation satisfies these postulates is called a Stokesian fluid. A Stokesian fluid is a more general hypothetical medium than a Newtonian fluid. For Newtonian fluids a further condition has to be added to Stokes's postulates, namely, that all the components of the stress tensor are linear in the components of the rate of deformation tensor:

$$\mathbf{T} = -p\mathbf{I} + \kappa \operatorname{div} \vec{v}\,\mathbf{I} + 2\mu\mathbf{S}. \tag{6.7}$$

For incompressible Newtonian fluids

$$\mathbf{T} = -p\mathbf{I} + 2\mu\mathbf{S}\,. \tag{6.8}$$

Equation (6.7) contains two viscosity coefficients κ and μ. The proportionality coefficient κ is the so-called second or bulk viscosity which induces viscous stresses only by reason of changes in the volume of the fluid element. Both viscosities μ and κ have the same dimensions [Pa s]. For an incompressible flow the term containing κ vanishes. For a compressible flow both viscosity coefficients apply, but it is difficult to perform experiments to measure κ. Kinetic gas theory shows that $\kappa = 0$ for monatomic gases. In most other cases it would appear to be rather small, so that for most compressible fluids it may be neglected. It is tacitly assumed that viscosities depend on the thermal state. The dynamic viscosity of an incompressible fluid depends on the temperature only. In the following sections, μ will be considered to be constant, thus the expressions obtained apply only to *isothermal flows.*

Observations of viscous flows show that two types of flow may occur depending on the ratio of the inertial forces to the viscous forces in the flow. Viscous forces predominate in a body or a streamtube of small size, combined with a relatively small velocity and a large kinematic viscosity. In this case the flow proceeds in well-ordered parallel layers, without any mixing. This type of flow is called laminar. Inertial forces predominate when the sizes and the velocities involved are relatively large, while kinematic viscosities are small. In most engineering applications the latter conditions are satisfied. In such cases the disordered, fluctuating flow exhibits irregular transverse movements across the adjacent layers, with intensive mixing. The most obvious property of this type of flow is that mass, momentum and energy are transferred across the flow at rates which are much greater than those of the molecular transport processes which occur in laminar flow. This type of flow is called turbulent. In the present chapter only laminar flows are considered.

6.2 The Navier—Stokes equation

The Navier—Stokes equation is the differential form of the momentum equation for Newtonian fluids. Cauchy's general equation of motion is

$$\frac{\mathrm{d}\tilde{v}}{\mathrm{d}t} = \tilde{g} + \frac{1}{\varrho}\,\mathrm{Div}\,\mathbf{T}\,. \tag{6.9}$$

The constitutive relation of a Newtonian fluid can be substituted into Cauchy's equation:

$$\frac{\mathrm{d}\tilde{v}}{\mathrm{d}t} = g + \frac{1}{\varrho}\,\mathrm{Div}\,(-p\mathbf{I} + \kappa\,\mathrm{div}\,\tilde{v}\,\mathbf{I} + 2\mu\mathbf{S})\,. \tag{6.10}$$

Each term of the divergence tensor can be obtained:

$$\operatorname{Div}(-p\mathbf{I})=\begin{bmatrix}-p & 0 & 0\\ 0 & -p & 0\\ 0 & 0 & -p\end{bmatrix}\begin{bmatrix}\frac{\partial}{\partial x}\\ \frac{\partial}{\partial y}\\ \frac{\partial}{\partial z}\end{bmatrix}=-\frac{\partial p}{\partial x}\vec{i}-\frac{\partial p}{\partial y}\vec{j}-\frac{\partial p}{\partial z}\vec{k}=-\operatorname{grad} p\,,$$

$$\operatorname{Div}(\kappa \operatorname{div}\vec{v}\,\mathbf{I})=\kappa\begin{bmatrix}\frac{\partial v_x}{\partial x} & 0 & 0\\ 0 & \frac{\partial v_y}{\partial y} & 0\\ 0 & 0 & \frac{\partial v_z}{\partial z}\end{bmatrix}\begin{bmatrix}\frac{\partial}{\partial x}\\ \frac{\partial}{\partial y}\\ \frac{\partial}{\partial z}\end{bmatrix}=\kappa \operatorname{grad}\operatorname{div}\vec{v}\,,$$

$$\operatorname{Div}(2\mu\mathbf{S})=\mu\begin{bmatrix}2\frac{\partial v_x}{\partial x} & \frac{\partial v_x}{\partial y}+\frac{\partial v_y}{\partial x} & \frac{\partial v_x}{\partial z}+\frac{\partial v_z}{\partial x}\\ \frac{\partial v_y}{\partial x}+\frac{\partial v_x}{\partial y} & 2\frac{\partial v_y}{\partial y} & \frac{\partial v_y}{\partial z}+\frac{\partial v_z}{\partial y}\\ \frac{\partial v_z}{\partial x}+\frac{\partial v_x}{\partial z} & \frac{\partial v_z}{\partial y}+\frac{\partial v_y}{\partial z} & 2\frac{\partial v_z}{\partial z}\end{bmatrix}\begin{bmatrix}\frac{\partial}{\partial x}\\ \frac{\partial}{\partial y}\\ \frac{\partial}{\partial z}\end{bmatrix}=\mu\Delta\vec{v}+\operatorname{grad}\operatorname{div}\vec{v}\,.$$

Substituting into Eq. (6.10) we get

$$\frac{\mathrm{d}\vec{v}}{\mathrm{d}t}=\vec{g}-\frac{1}{\varrho}\operatorname{grad} p+\nu\Delta\vec{v}+\left(\nu+\frac{\kappa}{\varrho}\right)\operatorname{grad}\operatorname{div}\vec{v}\,. \tag{6.11}$$

For incompressible flow we obtain

$$\frac{\mathrm{d}\vec{v}}{\mathrm{d}t}=\vec{g}-\frac{1}{\varrho}\operatorname{grad} p+\nu\Delta\vec{v}\,. \tag{6.12}$$

This differential equation states that the time rate of change of the momentum of a unit mass of fluid equals the sum of the body force, the pressure force, and the viscous force acting on it. The term $\nu\Delta\vec{v}$ is the force which resists the angular deformation, while the term $\left(\nu+\frac{\kappa}{\varrho}\right)\operatorname{grad}\operatorname{div}\vec{v}$ is the force counteracting the volume deformation.

For an incompressible flow the Navier—Stokes equation can be written in terms of a rectangular coordinate system as

$$\frac{\partial v_x}{\partial t}+v_x\frac{\partial v_x}{\partial x}+v_y\frac{\partial v_x}{\partial y}+v_z\frac{\partial v_x}{\partial z}=g_x-\frac{1}{\varrho}\frac{\partial p}{\partial x}+\nu\left(\frac{\partial^2 v_x}{\partial x^2}+\frac{\partial^2 v_x}{\partial y^2}+\frac{\partial^2 v_x}{\partial z^2}\right),$$

$$\frac{\partial v_y}{\partial t}+v_x\frac{\partial v_y}{\partial x}+v_y\frac{\partial v_y}{\partial y}+v_z\frac{\partial v_y}{\partial z}=g_y-\frac{1}{\varrho}\frac{\partial p}{\partial y}+\nu\left(\frac{\partial^2 v_y}{\partial x^2}+\frac{\partial^2 v_y}{\partial y^2}+\frac{\partial^2 v_y}{\partial z^2}\right),$$

$$\frac{\partial v_z}{\partial t}+v_x\frac{\partial v_z}{\partial x}+v_y\frac{\partial v_z}{\partial y}+v_z\frac{\partial v_z}{\partial z}=g_z-\frac{1}{\varrho}\frac{\partial p}{\partial z}+\nu\left(\frac{\partial^2 v_z}{\partial x^2}+\frac{\partial^2 v_z}{\partial y^2}+\frac{\partial^2 v_z}{\partial z^2}\right).$$

In a cylindrical coordinate system the above equations take the form

$$\frac{\partial v_r}{\partial t}+v_r\frac{\partial v_r}{\partial r}+\frac{v\varphi}{r}\frac{\partial v_r}{\partial \varphi}-\frac{v_\varphi^2}{r}+v_z\frac{\partial v_r}{\partial z}=g_r-\frac{1}{\varrho}\frac{\partial p}{\partial r}+$$

$$+\nu\left[\frac{\partial}{\partial r}\left(\frac{1}{r}\frac{\partial}{\partial r}(rv_r)\right)+\frac{1}{r^2}\frac{\partial^2 v_r}{\partial \varphi^2}-\frac{2}{r^2}\frac{\partial v_\varphi}{\partial \varphi}+\frac{\partial^2 v_r}{\partial z^2}\right],$$

$$\frac{\partial v_\varphi}{\partial t}+v_r\frac{\partial v_\varphi}{\partial r}+\frac{v_\varphi}{r}\frac{\partial v_\varphi}{\partial \varphi}+\frac{v_r v_\varphi}{r}+v_z\frac{\partial v_\varphi}{\partial z}=$$

$$=g_\varphi-\frac{1}{\varrho r}\frac{\partial p}{\partial \varphi}+\nu\left[\frac{\partial}{\partial r}\left(\frac{1}{r}\frac{\partial}{\partial r}(rv\varphi)\right)+\frac{1}{r^2}\frac{\partial^2 v_\varphi}{\partial \varphi^2}+\frac{2}{r^2}\frac{\partial v_r}{\partial \varphi}+\frac{\partial^2 v_\varphi}{\partial z^2}\right],$$

$$\frac{\partial v_z}{\partial t}+v_r\frac{\partial v_z}{\partial r}+\frac{v_\varphi}{r}\frac{\partial v_z}{\partial \varphi}+v_z\frac{\partial v_z}{\partial z}=g_z-\frac{1}{\varrho}\frac{\partial p}{\partial z}+$$

$$+\nu\left[\frac{1}{r}\frac{\partial}{\partial r}\left(r\frac{\partial v_z}{\partial r}\right)+\frac{1}{r^2}\frac{\partial^2 v_z}{\partial \varphi^2}+\frac{\partial^2 v_z}{\partial z^2}\right]. \tag{6.13}$$

To obtain solutions for the Navier—Stokes equation certain boundary condition must be satisfied. Since the equation is a second-order differential equation it is necessary to integrate twice. To determine the two constants of integration two boundary conditions need to be satisfied.

The standard boundary condition is that the fluid must adhere to the solid boundary surface, thus the relative velocity must be zero there. Direct measurement to prove this condition would be rather difficult, but it can be confirmed indirectly, for example by measuring the pressure loss at a given flow rate.

6.3 The balance of kinetic energy for laminar flow

As was shown in Chapter 4, the rate of change of the kinetic energy equals the rate of work of the body forces, plus the rate of work of surface forces, while a given part of this mechanical power also dissipates into internal energy. We shall apply the equation for the kinetic energy balance, as given by Eq. (3.57), to a fluid characterized by a linear constitutive relation. The general form of the balance of kinetic energy equation is

$$\frac{\mathrm{d}}{\mathrm{d}t}\int_V \varrho\frac{v^2}{2}\,\mathrm{d}V=\int_V \varrho\vec{g}\vec{v}\,\mathrm{d}V+\int_{(A)}\vec{v}(\mathbf{T}\,\mathrm{d}\vec{A})-\int_V \mathbf{T}:\vec{v}\circ\nabla\mathrm{d}V. \tag{6.14}$$

We substitute into this the stress tensor in the form

$$\mathbf{T}=-p\mathbf{I}+\mathbf{V}, \tag{6.15}$$

where the viscous stress tensor $\mathbf{V}$ has been separated. This leads to the equation

$$\begin{aligned}\frac{\mathrm{d}}{\mathrm{d}t}\int_V \varrho\frac{v^2}{2}\,\mathrm{d}V=&\int_V \varrho\vec{g}\vec{v}\,\mathrm{d}V-\int_{(A)}\vec{v}p\,\mathrm{d}\vec{A}+\int_{(A)}\vec{v}(\mathbf{V}\,\mathrm{d}\vec{A})+\\&+\int_V p\,\mathrm{div}\,\vec{v}\,\mathrm{d}V-\int_V \vec{v}\circ\nabla:\mathbf{V}\,\mathrm{d}V.\end{aligned} \tag{6.16}$$

Since the viscous stress tensor is symmetric its product with the antisymmetric part of $\vec{v}\circ\nabla$ must vanish. Thus we obtain

$$\vec{v}\circ\nabla:\mathbf{V}=\frac{1}{2}[(\vec{v}\circ\nabla+\nabla\circ\vec{v})+(\vec{v}\circ\nabla-\nabla\circ\vec{v})]:\mathbf{V}=\mathbf{S}:\mathbf{V}, \tag{6.17}$$

i.e. the scalar product of the viscous stress tensor and the rate of deformation tensor, so that the balance of kinetic energy equation can be written as

$$\begin{aligned}\frac{\mathrm{d}}{\mathrm{d}t}\int_V \varrho\frac{v^2}{2}\,\mathrm{d}V-\int_V p\,\mathrm{div}\,\vec{v}\,\mathrm{d}V+\int_V \mathbf{S}:\mathbf{V}\,\mathrm{d}V=\\=\int_V \varrho\vec{g}\vec{v}\,\mathrm{d}V-\int_{(A)}\vec{v}p\,\mathrm{d}\vec{A}+\int_{(A)}\vec{v}(\mathbf{V}\,\mathrm{d}\vec{A}).\end{aligned} \tag{6.18}$$

It has already been shown that

$$p\,\mathrm{div}\,\vec{v}=\varrho p\frac{\mathrm{d}}{\mathrm{d}t}\left(\frac{1}{\varrho}\right)=\varrho p\frac{\mathrm{d}\vartheta}{\mathrm{d}t},$$

i.e. this is the rate of work done by the pressure on a unit volume of the fluid; this

is the reversible part of the mechanical power which is dissipated into internal energy.

Thus the physical meaning of the equation is clear: the rate of work of the external forces (here: body forces, pressure forces and viscous forces) acting on an arbitrary finite fluid mass of volume V and bounding surface (A) equals the sum of the rates of change of the kinetic energy, the reversible part of the mechanical power which is converted into internal energy, and the irreversible part of this mechanical power. This last quantity can be expressed by the so-called dissipation function

$$\Phi = \mathbf{V} : \mathbf{S} . \tag{6.19}$$

For any material characterized by a linear constitutive relation the dissipation function can be written

$$\Phi = (2\mu \mathbf{S} + \kappa \operatorname{div} \vec{v}\, \mathbf{I}) : \mathbf{S} . \tag{6.20}$$

In terms of rectangular coordinates this can be written as

$$\begin{aligned} \Phi = (2\mu + \kappa)\left[\left(\frac{\partial v_x}{\partial x}\right)^2 + \left(\frac{\partial v_y}{\partial y}\right)^2 + \left(\frac{\partial v_z}{\partial z}\right)^2\right] + \\ + \mu\left[\left(\frac{\partial v_x}{\partial y} + \frac{\partial v_y}{\partial x}\right)^2 + \left(\frac{\partial v_x}{\partial z} + \frac{\partial v_z}{\partial x}\right)^2 + \left(\frac{\partial v_y}{\partial z} + \frac{\partial v_z}{\partial y}\right)^2\right] . \end{aligned} \tag{6.21}$$

In terms of cylindrical coordinates it becomes

$$\begin{aligned} \Phi = (2\mu + \kappa)\left[\left(\frac{\partial v_r}{\partial r}\right)^2 + \left(\frac{1}{r}\frac{\partial v_\varphi}{\partial \varphi} + \frac{v_r}{r}\right)^2 + \left(\frac{\partial v_z}{\partial z}\right)^2\right] + \mu\left[r\frac{\partial}{\partial r}\left(\frac{v_\varphi}{r}\right) + \frac{1}{r}\frac{\partial v_r}{\partial \varphi}\right]^2 + \\ + \mu\left[\frac{1}{r}\left(\frac{\partial v_z}{\partial \varphi}\right) + \frac{\partial v_\varphi}{\partial z}\right]^2 + \mu\left[\frac{\partial v_r}{\partial z} + \frac{\partial v_z}{\partial r}\right]^2 . \end{aligned} \tag{6.22}$$

Most highly viscous fluids can be considered to be incompressible. In this case the dissipation function is obtained in a simpler form

$$\Phi = 2\mu \mathbf{S} : \mathbf{S} . \tag{6.23}$$

Its scalar components are readily written by omitting all terms involving $\varkappa$ in Eqs (6.21) and (6.22).

Applying the divergence theorem to Eq. (6.18) all integrals can be written as volume integrals. This results in the differential form of the kinetic energy equation

$$\varrho \frac{\mathrm{d}}{\mathrm{d}t}\left(\frac{v^2}{2}\right) - p \operatorname{div} \vec{v} + \Phi = \varrho \vec{g} \vec{v} - \operatorname{div}(p\vec{v}) + \operatorname{div}(\mathbf{V}\vec{v}) , \tag{6.24}$$

which refers to a unit volume of the fluid. For a linearly viscous incompressible

fluid this can be written as

$$\varrho \frac{\mathrm{d}}{\mathrm{d}t}\left(\frac{v^2}{2}\right)+\Phi=\varrho \vec{g}\vec{v}-\vec{v}\ \mathrm{grad}\ p+\mathrm{div}\ (2\mu \mathbf{S}\mathbf{v})\,. \tag{6.25}$$

In this case the rate at which mechanical power is converted reversibly into internal energy is, of course, zero.

6.4 The balance of internal energy for laminar flow

In Chapter 3 the equation for the balance of internal energy was obtained in a general form as the difference between the equation expressing the conservation of energy law and the balance of kinetic energy equation:

$$\int_V \frac{\partial(\varrho\varepsilon)}{\partial t}\,\mathrm{d}V+\int_{(A)}(\varrho\varepsilon\vec{v}+\vec{q})\,\mathrm{d}\vec{A}=\int_V \mathbf{T}:\vec{v}\circ\nabla\mathrm{d}V\,. \tag{6.26}$$

In this equation ε is the specific internal energy per unit mass, $\vec{q}$ is the heat flux vector, which can be expressed by Fourier's law of thermal conduction

$$\vec{q}=-k\ \mathrm{grad}\ T\,. \tag{6.27}$$

The coefficient of thermal conductivity k is a scalar quantity for any isotropic material. The specific internal energy for incompressible fluids is

$$\varepsilon=cT,$$

where c is the heat capacity of the fluid. For an ideal gas this can be expressed in terms of the heat capacity at constant density (isochor heat capacity) as

$$\varepsilon=c_v T\,.$$

Substituting these to the balance of internal energy equation, the latter can be written as

$$\int_V \frac{\partial}{\partial t}(\varrho cT)\,\mathrm{d}V+\int_{(A)}\varrho cT\vec{v}\,\mathrm{d}\vec{A}=\int_{(A)} k\ \mathrm{grad}\ T\,\mathrm{d}\vec{A}+\int_V \mathbf{T}:\vec{v}\circ\nabla\mathrm{d}V\,. \tag{6.28}$$

In the present Chapter only linearly viscous fluids will be considered; for these the constitutive relation is

$$\mathbf{T}=-p\mathbf{I}+\mathrm{div}\ \vec{v}\,\mathbf{I}+2\mu\mathbf{S}\,.$$

Substituting this into the dissipative term of the internal energy equation, it is easy to separate the reversible and the irreversible parts of the mechanical power

converted into internal energy

$$\int_V \frac{\partial}{\partial t}(\varrho c T)\,\mathrm{d}V + \int_{(A)} \varrho c T \vec{v}\,\mathrm{d}\vec{A} + \int_V p\ \mathrm{div}\ \vec{v}\,\mathrm{d}V = \\ = \int_{(A)} k\ \mathrm{grad}\ T\,\mathrm{d}\vec{A} + \int_V \Phi\,\mathrm{d}V. \tag{6.29}$$

Using the divergence theorem all integrals can be converted into volume integrals

$$\int_V \frac{\partial}{\partial t}(\varrho c T)\,\mathrm{d}V + \int_V \mathrm{div}\ (\varrho c T \vec{v})\,\mathrm{d}V + \int_V p\ \mathrm{div}\ \vec{v}\,\mathrm{d}V = \\ = \int_V \mathrm{div}\ (k\ \mathrm{grad}\ T)\,\mathrm{d}V + \int_V \Phi\,\mathrm{d}V. \tag{6.30}$$

The differential equation form is easily obtained

$$\frac{\partial}{\partial t}(\varrho c T) + \mathrm{div}\ (\varrho c T \vec{v}) + p\ \mathrm{div}\ \vec{v} = \mathrm{div}\ (k\ \mathrm{grad}\ T) + \Phi. \tag{6.31}$$

A frequently used alternative form can be derived by writing the first and second terms as

$$\frac{\partial}{\partial t}(\varrho c T) + \mathrm{div}\ (\varrho c T \vec{v}) = \varrho \frac{\partial (cT)}{\partial t} + cT \frac{\partial \varrho}{\partial t} + cT\ \mathrm{div}\ (\varrho \vec{v}) + \varrho \vec{v}\ \mathrm{grad}\ (cT). \tag{6.32}$$

It is clear that the quantity

$$cT\left[\frac{\partial \varrho}{\partial t} + \mathrm{div}\ (\varrho \vec{v})\right] = 0, \tag{6.33}$$

thus the equation can be written as

$$\varrho \frac{\partial (cT)}{\partial t} + \varrho \vec{v}\ \mathrm{grad}\ (cT) + p\ \mathrm{div}\ \vec{v} = \mathrm{div}\ (k\ \mathrm{grad}\ T) + \Phi, \tag{6.34}$$

or in a more brief form

$$\varrho \frac{\mathrm{d}(cT)}{\mathrm{d}t} + p\ \mathrm{div}\ \vec{v} = \mathrm{div}\ (k\ \mathrm{grad}\ T) + \Phi. \tag{6.35}$$

This is the so-called Neumann equation, which expresses the first law of thermodynamics for a linearly viscous fluid, assuming cellular equilibrium. It is a rather good assumption to consider the heat capacity c and the thermal conductivity k to

be constant. Thus

$$\varrho c \frac{\mathrm{d}T}{\mathrm{d}t} + p \operatorname{div} \vec{v} = k \Delta T + \Phi , \tag{6.36}$$

where $\Delta = \nabla^2$; the Laplace operator.

The expanded form of this equation can be written in terms of rectangular coordinates:

$$\begin{aligned}
&\varrho c \left(\frac{\partial T}{\partial t} + v_x \frac{\partial T}{\partial x} + v_y \frac{\partial T}{\partial y} + v_z \frac{\partial T}{\partial z} \right) + p \left(\frac{\partial v_x}{\partial x} + \frac{\partial v_y}{\partial y} + \frac{\partial v_z}{\partial z} \right) = \\
&= k \left(\frac{\partial^2 T}{\partial x^2} + \frac{\partial^2 T}{\partial y^2} + \frac{\partial^2 T}{\partial z^2} \right) + (2\mu + \kappa) \left[\left(\frac{\partial v_x}{\partial x} \right)^2 + \left(\frac{\partial v_y}{\partial y} \right)^2 + \left(\frac{\partial v_z}{\partial z} \right)^2 \right] + \\
&+ \mu \left[\left(\frac{\partial v_x}{\partial y} + \frac{\partial v_y}{\partial x} \right)^2 + \left(\frac{\partial v_y}{\partial z} + \frac{\partial v_z}{\partial x} \right)^2 + \left(\frac{\partial v_y}{\partial z} + \frac{\partial v_z}{\partial y} \right)^2 \right].
\end{aligned} \tag{6.37}$$

In a cylindrical coordinate system we have:

$$\begin{aligned}
&\varrho c \left(\frac{\partial T}{\partial t} + v_r \frac{\partial T}{\partial r} + \frac{v_\varphi}{r} \frac{\partial T}{\partial \varphi} + v_z \frac{\partial T}{\partial z} \right) + p \left(\frac{\partial v_r}{\partial r} + \frac{v_r}{r} + \frac{1}{r} \frac{\partial v_\varphi}{\partial \varphi} + \frac{\partial v_z}{\partial z} \right) = \\
&= k \left[\frac{1}{r} \frac{\partial}{\partial r} \left(r \frac{\partial T}{\partial r} \right) + \frac{1}{r^2} \frac{\partial^2 T}{\partial \varphi^2} + \frac{\partial^2 T}{\partial z^2} \right] + \\
&+ (2\mu + \kappa) \left[\left(\frac{\partial v_r}{\partial r} \right)^2 + \left(\frac{1}{r} \frac{\partial v_\varphi}{\partial \varphi} + \frac{v_r}{r} \right)^2 + \left(\frac{\partial v_z}{\partial z} \right)^2 \right] + \\
&+ \mu \left[r \frac{\partial}{\partial r} \left(\frac{v_\varphi}{r} \right) + \frac{1}{r} \left(\frac{\partial v_r}{\partial \varphi} \right) \right]^2 + \mu \left[\frac{1}{r} \left(\frac{\partial v_z}{\partial \varphi} \right) + \frac{\partial v_\varphi}{\partial z} \right]^2 + \\
&+ \mu \left[\frac{\partial v_r}{\partial z} + \frac{\partial v_z}{\partial r} \right]^2 .
\end{aligned} \tag{6.38}$$

The internal energy equation can be expressed in terms of the enthalpy of the fluid. As well known, the specific enthalpy per unit mass is given by

$$i = \varepsilon + \frac{p}{\varrho} ,$$

or

$$\varepsilon = i - \frac{p}{\varrho} .$$

Substituting this expression for the internal energy ($c_v T$) in the Neumann equation leads to

$$\varrho \frac{\mathrm{d}i}{\mathrm{d}t} - \varrho \frac{\mathrm{d}}{\mathrm{d}t} \left(\frac{p}{\varrho} \right) + p \operatorname{div} \vec{v} = \operatorname{div} (k \operatorname{grad} T) + \Phi . \tag{6.39}$$

Carrying out the differentation of p/ϱ we obtain

$$\frac{\mathrm{d}i}{\mathrm{d}t} - \varrho\left(\frac{1}{\varrho}\frac{\mathrm{d}p}{\mathrm{d}t} - \frac{p}{\varrho^2}\frac{\mathrm{d}\varrho}{\mathrm{d}t}\right) + p \operatorname{div} \vec{v} = \operatorname{div}(k \operatorname{grad} T) + \Phi . \tag{6.40}$$

Since

$$\frac{\mathrm{d}\varrho}{\mathrm{d}t} = -\varrho \operatorname{div} \vec{v} ,$$

the Neumann equation expressed in terms of the enthalpy is obtained:

$$\varrho\frac{\mathrm{d}i}{\mathrm{d}t} - \frac{\mathrm{d}p}{\mathrm{d}t} = \operatorname{div}(k \operatorname{grad} T) + \Phi . \tag{6.41}$$

The enthalpy can be considered to be a function of the temperature and the pressure. Using the chain rule we have

$$\frac{\mathrm{d}i}{\mathrm{d}t} = \left(\frac{\partial i}{\partial T}\right)_p \frac{\mathrm{d}T}{\mathrm{d}t} + \left(\frac{\partial i}{\partial p}\right)_T \frac{\mathrm{d}p}{\mathrm{d}t} . \tag{6.42}$$

By definition

$$\left(\frac{\partial i}{\partial T}\right)_p = c_p , \tag{6.43}$$

i.e. the heat capacity at constant pressure. The other derivative can be expressed as

$$\left(\frac{\partial i}{\partial p}\right)_T = \frac{1}{\varrho}(1 - \beta T) , \tag{6.44}$$

where β is the coefficient of isobaric thermal expansion. Substituting into Eq. (6.43) the so-called thermal energy equation is obtained,

$$\varrho c_p \frac{\mathrm{d}T}{\mathrm{d}t} - \beta T \frac{\mathrm{d}p}{\mathrm{d}t} = \operatorname{div}(k \operatorname{grad} T) + \Phi . \tag{6.45}$$

It is obvious, that the physical meaning of this form of the internal energy equation remains the same. The first term on the left-hand side represents the rate of change of the enthalpy, the second is the reversible part of the mechanical power converted into internal energy (heat). This latter represents the compressive or expansive work rate, and may be either positive (compression) or negative (expansion). The fact that the sign of this term may be either positive or negative demonstrates the reversibility. The irreversible term Φ must be always positive, as will be shown later.

It is well known that the second law of thermodynamics can also be expressed by the inequality

$$\frac{\mathrm{d}}{\mathrm{d}t}\int_V \varrho S \,\mathrm{d}V \geqq -\int_{(A)} \frac{\vec{q}\,\mathrm{d}\vec{A}}{T} . \tag{6.46}$$

The rate of change of the entropy within the moving fluid volume V is greater (or equal) to the rate of the reduced heat flux through the bounding surface (A). The first law of thermodynamics can be expressed in terms of the entropy as

$$T\,\mathrm{d}S = \mathrm{d}\varepsilon + p\,\mathrm{d}\vartheta\,.$$

Dividing this expression by $\mathrm{d}t$, we have

$$T\frac{\mathrm{d}S}{\mathrm{d}t} = \frac{\mathrm{d}\varepsilon}{\mathrm{d}t} + p\frac{\mathrm{d}\vartheta}{\mathrm{d}t}\,.$$

It was shown earlier that

$$p\frac{\mathrm{d}\vartheta}{\mathrm{d}t} = p\frac{\mathrm{d}}{\mathrm{d}t}\left(\frac{1}{\varrho}\right) = -\frac{1}{\varrho^2}\frac{\mathrm{d}\varrho}{\mathrm{d}t} = \frac{1}{\varrho}\,\mathrm{div}\,\vec{v}\,,$$

so that we readily obtain

$$\varrho T\frac{\mathrm{d}S}{\mathrm{d}t} = \varrho\frac{\mathrm{d}\varepsilon}{\mathrm{d}t} + p\,\mathrm{div}\,\vec{v}\,. \tag{6.47}$$

Replacing the right-hand side by the Neumann equation, considering that $\vec{q} = -k\,\mathrm{grad}\,T$, we have

$$\varrho T\frac{\mathrm{d}S}{\mathrm{d}t} = \Phi - \mathrm{div}\,\vec{q}\,. \tag{6.48}$$

Applying the divergence theorem to the right-hand side of Eq. (6.46) we obtain

$$\frac{\mathrm{d}}{\mathrm{d}t}\int_V \varrho S\,\mathrm{d}V \geqq -\int_V \mathrm{div}\left(\frac{\vec{q}}{T}\right)\mathrm{d}V\,. \tag{6.49}$$

It can be easily recognized, that

$$\mathrm{div}\left(\frac{\vec{q}}{T}\right) = \frac{1}{T}\,\mathrm{div}\,\vec{q} - \frac{\vec{q}\,\mathrm{grad}\,T}{T^2}\,, \tag{6.50}$$

and thus we can write

$$\frac{\mathrm{d}}{\mathrm{d}t}\int_V \varrho S\,\mathrm{d}V \geqq -\int_V \left[\frac{1}{T}\mathrm{div}\,\vec{q} - \frac{\vec{q}\,\mathrm{grad}\,T}{T^2}\right]\mathrm{d}V\,. \tag{6.51}$$

On the other hand, dividing Eq. (6.48) by T and integrating over a material volume moving with the fluid leads to the expression

$$\frac{\mathrm{d}}{\mathrm{d}t}\int_V \varrho S\,\mathrm{d}V = \int_V \left[\frac{\Phi}{T} - \frac{\mathrm{div}\,\vec{q}}{T}\right]\mathrm{d}V\,. \tag{6.52}$$

In order for this equation to be consistent with the second law as expressed by Eq. (6.51) it is necessary that

$$-\frac{1}{T}\operatorname{div}\vec{q}+\frac{\vec{q}\cdot\operatorname{grad}T}{T^2}\leqq\frac{\Phi}{T}-\frac{\operatorname{div}\vec{q}}{T}. \tag{6.53}$$

Thus the inequality

$$\Phi\geqq\frac{\vec{q}\cdot\operatorname{grad}T}{T} \tag{6.54}$$

must be satisfied. This is obviously true, since

$$\vec{q}=-k\operatorname{grad}T,$$

thus

$$-k\operatorname{grad}T\cdot\operatorname{grad}T\leqq 0, \tag{6.55}$$

therefore heat never flows against the temperature gradient. The absolute temperature T is always positive thus the dissipation function must also be either positive or zero, i.e.

$$\Phi\geqq 0. \tag{6.56}$$

This inequality means that the deformation can absorb mechanical energy, converting it to heat, but never releases it. A consequence of $\Phi\geqq 0$, is that for incompressible fluids

$$\mu\geqq 0, \tag{6.57}$$

i.e. the viscosity must be positive or zero. For a compressible flow we can derive the equality

$$3\Phi=(3\kappa+2\mu)(\operatorname{div}\vec{v})^2+2\mu[(S_1-S_2)^2+(S_2-S_3)^2+(S_3-S_1)^2], \tag{6.58}$$

where S_1, S_2 and S_3 are the principal values of the deformation tensor. Since $\mu\geqq 0$, the inequality

$$3\kappa+2\mu=0$$

is always satisfied.

Finally, we shall consider the problem of heat transfer in laminar flow. The governing equations are the continuity equation, the momentum equation, the energy equation and the equation of state. There are six unknown scalar functions: three velocity components, the pressure, the temperature and the density. The solution of these equations together with the application of the appropriate boundary conditions gives the unknown variables at any point.

It should be emphasized that boundary conditions have a significant effect on the analytical results. Two frequently used thermal boundary conditions are those of a uniform temperature at the boundary surface, or a uniform rate of heat transfer across it.

The rate at which heat is transferred from a solid wall to a fluid flowing past it is proportional to the difference between the solid wall (T_w) and the fluid tem-

perature (T). The normal component of the heat flux vector can be expressed as

$$q_n = h(T_w - T) . \tag{6.59}$$

The proportionality factor h is the so-called convective heat transfer coefficient. The heat transfer coefficient may be related to the temperature gradient in the fluid at the boundary surface. Since

$$q_n = -k \frac{\partial T}{\partial n} , \tag{6.60}$$

combining the two equations we get

$$h = - \frac{k}{T_w - T} \frac{\partial T}{\partial n} . \tag{6.61}$$

This expression relates the convective heat transfer coefficient to the thermal conductivity of the fluid, the temperature gradient at the wall, and the temperature difference between the wall and the fluid. The heat transfer coefficient is a function of both the physical properties of the fluid and the character of the flow. To measure it, a variety of experimental methods are available.

6.5 Dynamical similarity

It is a well known fact that only a few exact solutions of the Navier—Stokes equations are known even now. This has been largely due to the complexity of the system of differential equations. In the absence of a general solution it is often convenient to experiment with models to obtain information on the flow phenomena e.g. the velocity distribution, flow pattern, pressure losses, etc. If accurate quantitative results are to be obtained, certain laws of similarity must be satisfied. Geometric similarity is a necessary though not a sufficient condition for the similarity of two physical processes.

Geometric similarity exists if one of the configurations can be derived from the other by a linear scaling with respect to a common center.

In order to compare two similar processes we must introduce scale relations for the coordinates and the flow variables of the type

$$\vec{r}' = \alpha_r \vec{r}, \qquad t' = \alpha_t t, \qquad \vec{v}' = \alpha_v \vec{v}, \qquad \varrho' = \alpha_\varrho \varrho, \qquad \vec{g}' = \alpha_g \vec{g},$$

$$p' = \alpha_p p, \qquad \nu' = \alpha_\nu \nu .$$

Any two points of the two processes may be called associated if their coordinates differ by a constant scale factor only. Associated points can be made to coincidence by a similar transformation as required to make the spatial boundaries to coincide. At all associated points the flow variables are related by the same scale factors. Since each scale factor has the same constant value throughout the whole system,

there is no restriction on the choice of characteristic reference values, such as for instance the diameter of a tube, the average cross-sectional velocity in a pipe, or the undisturbed velocity and pressure around a body.

Let us turn to the differential equations for the two processes. The principle of dynamical similarity requires identical solutions in both cases. The equations may therefore, differ from each other by a constant multiplier only. The continuity equation for the two processes is obtained as

$$\frac{\mathrm{d}\varrho}{\mathrm{d}t} + \varrho \nabla \vec{v} = 0 , \tag{6.62}$$

and

$$\frac{\alpha_\varrho}{\alpha_t} \frac{\mathrm{d}\varrho}{\mathrm{d}t} + \frac{\alpha_\varrho \alpha_v}{\alpha_r} \varrho \nabla \vec{v} = 0 . \tag{6.63}$$

In the second equation constant coefficients appear. If the two groups of coefficients are the same, i.e.

$$\frac{\alpha_\varrho}{\alpha_t} = \frac{\alpha_\varrho \alpha_v}{\alpha_r} , \tag{6.64}$$

the two equations are not independent. This equation leads to a dimensionless quantity, the so-called Strouhal number

$$\mathrm{St} = \frac{vt}{r} = \frac{v't'}{r'} = \mathrm{St}' . \tag{6.65}$$

This requirement applies to unsteady flow only. For a steady flow, instead of the Strouhal number, we get a simple time-scale coefficient expressed by the scale factors of the length and the velocity:

$$\alpha_t = \frac{\alpha_r}{\alpha_v} . \tag{6.66}$$

Applying this scale factor the momentum equation for two similar flows can be written

$$\frac{\mathrm{d}\vec{v}}{\mathrm{d}t} = \vec{g} - \frac{1}{\varrho} \nabla p + \nu \nabla \vec{v} , \tag{6.67}$$

and

$$\frac{\alpha_v^2}{\alpha_r} \frac{\mathrm{d}\vec{v}}{\mathrm{d}r} = \alpha_g \vec{g} - \frac{\alpha_p}{\alpha_r \alpha_\varrho} \frac{1}{\varrho} \nabla p + \frac{\alpha_\nu \alpha_v}{\alpha_r^2} \nu \Delta \vec{v} . \tag{6.68}$$

These equations correspond to two vector polygons as illustrated in *Fig. 6.1*. The non-independence of the two equations implies the geometrical similarity of the two poligons. It is obvious that the dimensionless coefficients of the second equa-

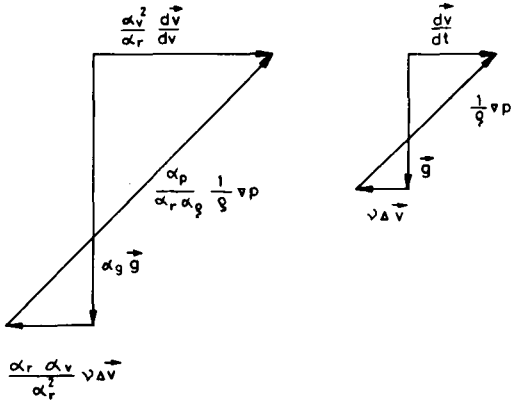

Fig. 6.1. Similar vector polygons for viscous flows

tion must be equal i.e.

$$\frac{\alpha_v^2}{\alpha_r} = \alpha_g = \frac{\alpha_p}{\alpha_r \alpha_\varrho} = \frac{\alpha_\nu \alpha_v}{\alpha_r^2}. \tag{6.69}$$

This is the condition of perfect dynamical similarity. In practice perfect dynamical similarity is technically difficult to achieve. The usual modelling procedure is to satisfy an approximate similarity which covers only the dominant forces.

For a completely enclosed flow (e.g. in pipes) or for flow round fully immersed bodies (e.g. blade rows in turbomachines) the inertial and viscous forces are the only important forces which need to be taken into account. Thus approximate dynamical similarity is attained by having

$$\frac{\alpha_v^2}{\alpha_r} = \frac{\alpha_\nu \alpha_v}{\alpha_r^2}. \tag{6.70}$$

Then the dimensionless ratio of the inertial fore to the viscous force is proportional to a dimensionless parameter, the so-called Reynolds number:

$$\mathrm{Re} = \frac{vr}{\nu}, \tag{6.71}$$

where v is some characteristic velocity, and r is some characteristic length. The approximate dynamical similarity between two flows is realized when the Reynolds numbers are the same at the corresponding points of the two flows. If the geometry of the flow is simple enough (as in pipes) it is unnecessary to compare the local Reynolds numbers at different points. In such a case it is sufficient to take only one Reynolds number defined by the average velocity c and the diameter of the pipe D:

$$\mathrm{Re} = \frac{cD}{\nu}. \tag{6.72}$$

A small Reynolds number indicates that viscous forces predominate, as in the case of oil flowing in the pores of reservoir rocks. A large Reynolds number indicates that inertial forces control the flow. The nature of any particular flow of a viscous fluid may be estimated to some extent from a knowledge of the Reynolds number. Both theory and experiment indicate that the Navier—Stokes equation is valid for flows of moderate Reynolds number. For example the critical Reynolds number of flow in a pipe is

$$\mathrm{Re}_{\mathrm{crit}} = 2300 .$$

Experimental data show, that laminar flow exists only for values of $\mathrm{Re} \leqq 2300$.

There is a great family of flows where the inertial and body forces are the predominant factors in determining the nature of the motion. Free liquid-surface flows and different kinds of multiphase flow are influenced more by inertial and gravitational forces than by viscous shear forces. Thus, for these the condition for approximate dynamical similarity is:

$$\frac{\alpha_v^2}{\alpha_r} = \alpha_g . \tag{6.73}$$

From this equation the so-called Froude number can be derived as a criterion of similarity:

$$\mathrm{Fr} = \frac{v}{\sqrt{gr}} . \tag{6.74}$$

The Froude number is useful in calculations relating to open channel flow, bubble motion and sediment transport. Experimental data pertaining to such flows is best presented expressed in terms of the Froude number.

Inertial forces and pressure forces may predominate where low-viscosity fluid flows round a slender body (e.g. an aerofoil) with a sufficiently great velocity. In this case the approximate similarity needs to meet the requirement

$$\frac{\alpha_v^2}{\alpha_r} = \frac{\alpha_p}{\alpha_\varrho \alpha_r} . \tag{6.75}$$

From this the so-called Euler number (sometimes called the pressure coefficient) is obtained as

$$\mathrm{Eu} = \frac{p}{\varrho v^2} . \tag{6.76}$$

As the characteristic pressure value of this formula may be chosen the pressure difference between a given point and the undisturbed flow, while the characteristic velocity is usually taken as the velocity of the undisturbed flow at infinity:

$$\mathrm{Eu} = \frac{p - p_\infty}{\frac{\varrho}{2} v_\infty^2} . \tag{6.77}$$

This parameter is useful to characterize the flow round aerofoils, or pump and turbine blades. The loss coefficient of pipe fittings is also analogous to the Euler number:

$$\zeta = \frac{\Delta p}{\frac{\varrho}{2} c^2}. \tag{6.78}$$

The arrangement of experimentally obtained loss coefficients as a function of the Reynolds number essentially means a relationship between two similarity invariants, thus it leads to correct correlations.

Further similarity rules can be derived from the energy equation and its boundary conditions. Let us introduce further scale relations for the heat capacities, temperatures and thermal conductivities as follows:

$$c_v' = \alpha_c c_v, \qquad T' = \alpha_T T, \qquad k' = \alpha_k k .$$

Since we have stipulated that the two energy equations may not be independent, we have

$$\varrho \frac{\mathrm{d}}{\mathrm{d}t}\left(\frac{v^2}{2}\right) + \varrho \frac{\mathrm{d}}{\mathrm{d}t}(c_v T) =$$

$$= \varrho \vec{g}\vec{v} - \operatorname{div}(p\vec{v}) + \operatorname{div}[\varrho v\vec{v}(\vec{v} \circ \nabla + \nabla \circ \vec{v})] - \operatorname{div}(k \operatorname{grad} T), \tag{6.79}$$

and

$$\frac{\alpha_\varrho \alpha_v^3}{\alpha_r} \varrho \frac{\mathrm{d}}{\mathrm{d}t}\left(\frac{v^2}{2}\right) + \frac{\alpha_\varrho \alpha_c \alpha_T \alpha_v}{\alpha_r} \varrho \frac{\mathrm{d}}{\mathrm{d}t}(c_v T) =$$

$$= \alpha_\varrho \alpha_g \alpha_v \varrho \vec{g}\vec{v} - \frac{\alpha_p \alpha_v}{\alpha_r} \operatorname{div}(p\vec{v}) + \frac{\alpha_\varrho \alpha_v \alpha_v^2}{\alpha_r^2} \operatorname{div}[\varrho v\vec{v}(\vec{v} \circ \nabla + \nabla \circ \vec{v})] -$$

$$- \frac{\alpha_k \alpha_T}{\alpha_r^2} \operatorname{div}(k \operatorname{grad} T) \tag{6.80}$$

respectively.

If there is perfect similarity, the dimensionless groups of the second equation must be equal:

$$\frac{\alpha_\varrho \alpha_v^3}{\alpha_r} = \frac{\alpha_\varrho \alpha_c \alpha_T \alpha_v}{\alpha_r} = \alpha_\varrho \alpha_g \alpha_v = \frac{\alpha_p \alpha_v}{\alpha_r} = \frac{\alpha_\varrho \alpha_v \alpha_v^2}{\alpha_r^2} = \frac{\alpha_k \alpha_T}{\alpha_r^2}. \tag{6.81}$$

The equality of the first and the second dimensionless groups leads to the expression:

$$\alpha_v^2 = \alpha_c \alpha_T .$$

From this criterion of approximate similarity we can derive the so-called Eckert number:

$$\mathrm{Ec} = \frac{v^2}{c_v T}. \tag{6.82}$$

It represents the ratio of a characteristic kinetic energy to a characteristic internal energy. Comparing the fifth and the sixth dimensionless groups we have

$$\alpha_k \alpha_T = \alpha_\varrho \alpha_v \alpha_v^2 .$$

Since the Eckert number determines the scale factor for the temperature, i.e.

$$\alpha_T = \frac{\alpha_v^2}{\alpha_c},$$

we have

$$\alpha_\varrho \alpha_c \alpha_v = \alpha_k .$$

This expression leads to the next criterion of similarity, the so-called Prandtl number:

$$\mathrm{Pr} = \frac{\nu}{\frac{k}{\varrho c_v}} . \tag{6.83}$$

The Prandtl number is the ratio of the kinematic viscosity to the thermal diffusivity. It is a characteristic parameter in all problems involving heat transfer and heat conduction processes which are bound to accompany all types of frictional processes in fluids and gases. The Prandtl number of most gases is close to unity. The number is greater for a liquid, becoming more so as the viscosity increases (e.g. the Prandtl number of water is 7.0).

Comparing the terms representing the convective and the conductive heat fluxes we get

$$\frac{\alpha_\varrho \alpha_c \alpha_T \alpha_v}{\alpha_r} = \frac{\alpha_k \alpha_T}{\alpha_r^2} .$$

The so-called Peclet number can be derived from this expression:

$$\mathrm{Pe} = \frac{vr}{\frac{k}{\varrho c_v}} . \tag{6.84}$$

The characteristic velocity and length may be chosen from the boundary conditions. For a flow in a pipe the velocity obviously is the averaged velocity over the cross section, while the length is the pipe diameter. The value of the Peclet number for a pipeline or an oil well is of the order of 10^4. For seepage flows through porous media it is close to unity.

If the fluid is at rest, there can only be conductive heat flow. In this case comparing the rate of change of the internal energy with the conductive heat flux yields the equality

$$\frac{\alpha_\varrho \alpha_c \alpha_T}{\alpha_t} = \frac{\alpha_k \alpha_T}{\alpha_r^2} . \tag{6.85}$$

Thus we get the so-called Fourier number

$$\mathrm{Fo} = \frac{k}{\varrho c}\frac{t}{r^2}. \tag{6.86}$$

Note, that the temperature does not appear in the Fourier number. It is solely a criterion of the similarity of transient heat conduction processes.

The physical similarity of two processes requires not only identical solutions of the two sets of differential equations, but the boundary conditions must also be similar. Consider the expressions for the heat flux at a solid-fluid boundary. Using the convective heat transfer coefficient h we can write

$$q_n = h(T_w - T). \tag{6.87}$$

The same heat flux may also be expressed in terms of the thermal conductivity and the temperature gradient at the boundary as

$$q_n = -k\left(\frac{\partial T}{\partial n}\right)_w. \tag{6.88}$$

Since the two heat fluxes are equal

$$h(T_w - T) = -k\left(\frac{\partial T}{\partial n}\right)_w. \tag{6.89}$$

In this case we obtain the following relation for the dimensionless scale factors

$$\alpha_h \alpha_T = \alpha_k \frac{\alpha_T}{\alpha_r}.$$

The result is the Nusselt number

$$\mathrm{Nu} = \frac{hr}{k}, \tag{6.90}$$

where h is the local heat transfer coefficient, r is a characteristic length of the system, and k is the thermal conductivity of the fluid.

Experimental heat transfer data are usually interpreted in terms of the Nusselt number and the Reynolds number.

Similarity conditions for the case of free convection will be discussed later.

6.6 Some general properties of incompressible viscous flow

In this section we shall be concerned with incompressible viscous fluids. If it is assumed that the body force can be derived from a potential we can write

$$\tilde{g} = -\mathrm{grad}\ U.$$

Thus the Navier—Stokes equation takes the form

$$\frac{\mathrm{d}\vec{v}}{\mathrm{d}t} = -\operatorname{grad}\left(U + \frac{p}{\varrho}\right) + \nu \Delta \vec{v}\,, \tag{6.91}$$

while the continuity equation is obviously

$$\operatorname{div} \vec{v} = 0\,.$$

The viscous force term can be expanded,

$$\Delta \vec{v} = \operatorname{grad} \operatorname{div} \vec{v} - \operatorname{curl} \operatorname{curl} \vec{v} = -\operatorname{curl} \operatorname{curl} \vec{v}\,. \tag{6.92}$$

The acceleration field can be broken down into the familiar form for perfect fluid flow,

$$\frac{\mathrm{d}\vec{v}}{\mathrm{d}t} = \frac{\partial \vec{v}}{\partial t} + \operatorname{curl} \vec{v} \times \vec{v} + \operatorname{grad} \frac{v^2}{2}\,. \tag{6.93}$$

Substituting these into the Navier—Stokes equation an alternative form of the latter is obtained:

$$\frac{\partial \vec{v}}{\partial t} + \operatorname{curl} \vec{v} \times \vec{v} = -\operatorname{grad}\left(\frac{v^2}{2} + U + \frac{p}{\varrho}\right) - \nu \operatorname{curl} \operatorname{curl} \vec{v}\,. \tag{6.94}$$

This equation seems to be suitable to generalize the Bernoulli equation for viscous flows. Helmholz and Rayleigh introduced the basic assumption that the vector curl curl $\vec{v}$ can be derived from a scalar potential, Ψ, i.e.

$$\operatorname{curl} \operatorname{curl} \vec{v} = \operatorname{grad} \Psi\,. \tag{6.95}$$

Substituting this into Eq. (6.94) we get

$$\frac{\partial \vec{v}}{\partial t} + \operatorname{curl} \vec{v} \times \vec{v} = -\operatorname{grad}\left(\frac{v^2}{2} + U + \frac{p}{\varrho} + \nu \Psi\right). \tag{6.96}$$

It is evident, that for a steady flow along a streamline or a vortex line the function

$$\frac{v^2}{2} + U + \frac{p}{\varrho} + \nu \Psi = \text{const}\,. \tag{6.97}$$

This viscous Bernoulli equation expresses the fact that the sum of the mechanical energy per unit mass and the potential of the viscous force is constant along streamlines and vortex lines. In this case it is obvious, that the acceleration also has a potential:

$$\vec{a} = \frac{\mathrm{d}\vec{v}}{\mathrm{d}t} = -\operatorname{grad}\left(U + \frac{p}{\varrho} + \nu \Psi\right). \tag{6.98}$$

It follows from the existence of this acceleration potential that Kelvin's circulation theorem and the Helmholz vorticity theorem remain valid. Since it was shown

in Eq. (4.87) that

$$\frac{d\Gamma}{dt} = \int_{(G)} \frac{d\vec{v}}{dt} d\vec{r} + \int_{(G)} d\left(\frac{v^2}{2}\right) = 0,$$

it is obvious that

$$\frac{d\vec{v}}{dt} d\vec{r} = -d\vec{r} \text{ grad} \left(U + \frac{p}{\varrho} + \nu\Psi\right) = -d\left(U + \frac{p}{\varrho} + \nu\Psi\right). \tag{6.99}$$

Since both integrands are total differentials, both integrals over a closed curve will vanish

$$\frac{d\Gamma}{dt} = 0. \tag{6.100}$$

If the viscous force can be derived from a scalar potential, the flow must be circulation-preserving. If the flow is not circulation-preserving there is no Bernoulli equation of the usual type.

Taking the curl of Eq. (6.96) we obtain an equation for the vorticity distribution:

$$\frac{d\vec{\Omega}}{dt} = \vec{\Omega}(\vec{v} \circ \nabla) + \nu \Delta \vec{\Omega}. \tag{6.101}$$

In spite of the last term, the vorticity distribution in a viscous fluid would satisfy the Helmholz theorem. This term shows that vorticity variations in the flow field cause the diffusion of that same vorticity. An important consequence is that vorticity cannot be generated in the interior of a viscous incompressible fluid, but must become diffused inward from the boundaries. The experimental observation, that vorticity is important only near the solid walls bounding a flowing fluid, confirms the theory.

6.7 Steady incompressible flow in a cylindrical pipe

Consider a straight cylindrical pipe of infinite length and radius R, whose axis does not coincide with any axis of a rectangular coordinate system. The fluid is incompressible, its density and viscosity are constant. The flow is laminar and steady. The fluid has no velocity components normal to the pipe axis *(Fig. 6.2)*.

Let us investigate a section of the pipe of length L, where the isothermal laminar flow is fully developed. Let 1 denote the inlet cross section, and 2 the outlet cross section of this section of pipe. The difference in the vertical level between the inlet and outlet points of the pipe axis is h.

The Navier—Stokes equation is obtained in a reduced form in the directions x, y and z in the forms

$$0 = g_x - \frac{1}{\varrho} \frac{\partial p}{\partial x}, \tag{6.102a}$$

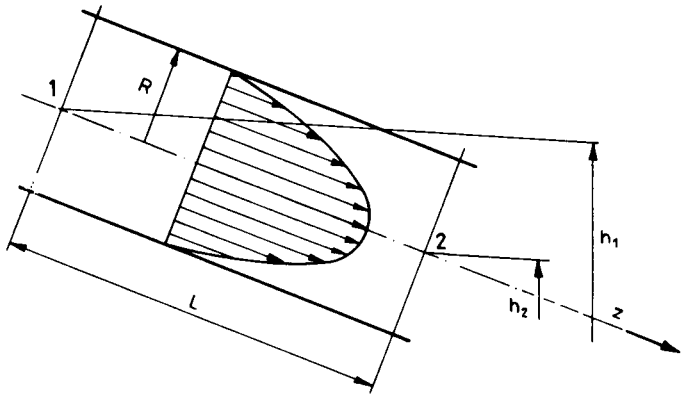

Fig. 6.2. Laminar flow in cylindrical pipe

$$0 = g_y - \frac{1}{\varrho}\frac{\partial p}{\partial y}, \tag{6.102b}$$

$$v_z \frac{\partial v_z}{\partial z} = g_z - \frac{1}{\varrho}\frac{\partial p}{\partial z} + \nu\left(\frac{\partial^2 v_z}{\partial x^2} + \frac{\partial^2 v_z}{\partial y^2} + \frac{\partial^2 v_z}{\partial z^2}\right). \tag{6.102c}$$

The continuity equation is

$$\frac{\partial v_z}{\partial z} = 0.$$

The left-hand side of the equation for the z-component vanishes on account of the continuity equation. The only velocity component $v_z = v$ is a function of the coordinates x and y. $\partial^2 v/\partial z^2$ also vanishes. Since the gravity field is conservative its components can be written as

$$g_x = -\frac{\partial U}{\partial x} = -g\frac{\partial h}{\partial x},$$

$$g_y = -\frac{\partial U}{\partial y} = -g\frac{\partial h}{\partial y},$$

$$g_z = -\frac{\partial U}{\partial z} = -g\frac{\partial h}{\partial z}.$$

Let us introduce a new variable

$$H = h + \frac{p}{\varrho g}, \tag{6.103}$$

which is the sum of the potential energy, and the potential of the pressure forces acting on a unit fluid mass. It is independent of the x and y coordinates being a

function only of the z coordinate. Thus from the expression for the z-component of the Navier—Stokes equation we obtain

$$g\frac{\mathrm{d}H}{\mathrm{d}z}=\nu\left(\frac{\partial^2 v}{\partial x^2}+\frac{\partial^2 v}{\partial y^2}\right). \tag{6.104}$$

The left-hand side of this equation is a function of z, while the right-hand side is a function of x and y. This is possible only when both sides of the equation are constant. It is clear that H is a linear function of z, thus its derivative equals the difference ratios:

$$\frac{\mathrm{d}H}{\mathrm{d}z}=\frac{h_2-h_1}{L}+\frac{p_2-p_1}{\varrho g L}.$$

The hydraulic gradient

$$J=\frac{h_1-h_2}{L}+\frac{p_1-p_2}{\varrho g L} \tag{6.105}$$

is the energy decrease per unit length. Using this notation we get from Eq. (6.104)

$$-\frac{gJ}{\nu}=\frac{\partial^2 v}{\partial x^2}+\frac{\partial^2 v}{\partial y^2}. \tag{6.106}$$

It is convenient to replace the rectangular coordinates by cylindrical ones, in which case we have

$$-\frac{gJ}{\nu}=\frac{1}{r}\frac{\mathrm{d}}{\mathrm{d}r}\left(r\frac{\mathrm{d}v}{\mathrm{d}r}\right). \tag{6.107}$$

Thus we obtain a common second-order differential equation instead of a type of partial differential equation. The first integration yields

$$r\frac{\mathrm{d}v}{\mathrm{d}r}=-\frac{gJr^2}{2\nu}+K. \tag{6.108}$$

Subdividing by r after the second integration the velocity distribution is obtained as

$$v=-\frac{gJr^2}{4\nu}+K_1\ln r+K_2. \tag{6.109}$$

The boundary conditions for determining the constants of integrates K_1 and K_2 are:

If $r=0$, $v\neq\infty$; therefore the velocity along the pipe axis cannot be infinite. Because of this $K_1=0$.

If $r=R$, $v=0$; therefore the fluid adheres to the pipe wall. From this condition we obtain

$$K_2=\frac{gJR^2}{4\nu}.$$

Substituting into Eq. (6.109) we obtain the following expression for the velocity distribution:

$$v = \frac{gJ}{4\nu}(R^2 - r^2). \tag{6.110}$$

The maximum velocity is reached at the axis of the pipe:

$$v_{\max} = \frac{gJR^2}{4\nu}. \tag{6.111}$$

The flow rate across any cross section is given by

$$Q = 2\pi \int_0^R vr \, dr = \frac{gJR^4\pi}{8\nu}. \tag{6.112}$$

The average cross-sectional velocity is

$$c = \frac{Q}{R^2\pi} = \frac{gJR^2}{8\nu} = \frac{v_{\max}}{2}. \tag{6.113}$$

The viscous Bernoulli equation between the inlet and outlet cross sections can be written in terms of the average velocities as

$$\frac{c_1^2}{2g} + h_1 + \frac{p_1}{\varrho g} = \frac{c_2^2}{2g} + h_2 + \frac{p_2}{\varrho g} + h'_{1-2}, \tag{6.114}$$

where h'_{1-2} represents the so-called head loss of the flow. Since the cross section of the pipe is uniform, the cross-sectional average velocities are the same. Thus the head loss can be expressed as

$$h'_{1-2} = JL, \tag{6.115}$$

i.e. as equal to the product of the hydraulic gradient and the length of the pipe. Substituting into Eq. (6.113) we obtain

$$h'_{1-2} = \frac{8\nu Lc}{gR^2}. \tag{6.116}$$

Thus it is clear that the head loss is a linear function of the average cross-sectional velocity. This linear relationship is the most characteristic measurable property of a laminar flow. The calculated and measured values are in excellent agreement, thus providing indirect verification of the no-slip boundary condition at the wall.

The dissipated energy may also be expressed as a pressure loss, i.e. in the form

$$p'_{1-2} = \frac{8\varrho\nu Lc}{R^2}. \tag{6.117}$$

This is the well-known Hagen—Poiseuille law. Experimental observations show that a laminar flow becomes turbulent as the Reynolds number of the flow is

increased. The transition from laminar to turbulent flow occurs at a value of the Reynolds number in the neighborhood of 2300. The equations obtained above are valid only for laminar flow, i.e. for values of the Reynolds number of less than 2300.

6.8 Steady incompressible laminar flow in annuli

In petroleum engineering flow in annuli is encountered in drilling and cementing technology. A simple annulus consists of two concentric tubes, between which the laminar flow under consideration occurs. *Figure 6.3* shows a cross-section of a simple annulus consisting of an outer pipe of inside radius R_2 and an inner pipe of outside radius R_1. The fluid is incompressible, and since the flow is isothermal its density and viscosity remain constant. The flow is laminar, steady and one-dimensional. The common axis of the tubes can have any arbitrary orientation in space. A cylindrical coordinate system is chosen in accordance with the geometry. The z-axis coincides with the pipe axis.

The differential equation for one-dimensional laminar flow through the annulus is derived from the Navier—Stokes equations. It is the same as that for a cylindrical pipe;

$$-\frac{gJ}{\nu} = \frac{1}{r}\frac{\mathrm{d}}{\mathrm{d}r}\left(r\frac{\mathrm{d}v}{\mathrm{d}r}\right). \tag{6.118}$$

The boundary conditions for the problem are the followings:

If $r = R_1$, $v = 0$;
If $r = R_2$, $v = 0$;
If $R = R_0$, $\dfrac{\mathrm{d}v}{\mathrm{d}r} = 0$; $v = v_{max}$.

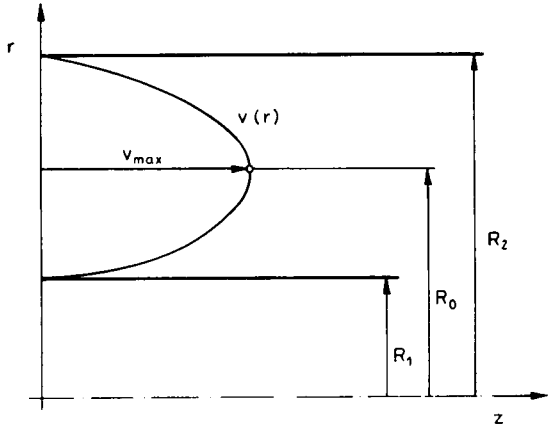

Fig. 6.3. Flow in concentric annulus

The first integration gives

$$-\frac{gJr^2}{2\nu}+K_1=r\frac{\mathrm{d}v}{\mathrm{d}r}. \tag{6.119}$$

Subdividing by r, the second integration leads to

$$v=-\frac{gJr^2}{4\nu}+K_1\ln r+K_2. \tag{6.120}$$

Taking the boundary conditions into account:

$$0=-\frac{gJR_1^2}{4\nu}+K_1\ln R_1+K_2,$$

$$0=-\frac{gJR_2^2}{4\nu}+K_1\ln R_2+K_2,$$

$$0=-\frac{gJR_0^2}{2\nu}+K_1.$$

From these equations the position of the velocity maximum can be obtained:

$$R_0=\sqrt{\frac{R_2^2-R_1^2}{2\ln\dfrac{R_2}{R_1}}}. \tag{6.121}$$

This is also the position of zero shear stress. The constants of integration are determined to be:

$$K_1=\frac{gJ}{4\nu}\frac{R_2^2-R_1^2}{\ln\dfrac{R_2}{R_1}}, \tag{6.122}$$

$$K_2=\frac{gJ}{4\nu}\left[R_2^2-\frac{R_2^2-R_1^2}{\ln\dfrac{R_2}{R_1}}\ln R_2\right]. \tag{6.123}$$

Substituting into Eq. (6.120), the radial velocity distribution is obtained as

$$v=\frac{gJ}{4\nu}\left[R_2^2-r^2+\frac{R_2^2-R_1^2}{\ln\dfrac{R_2}{R_1}}\ln\frac{r}{R^2}\right]. \tag{6.124}$$

Or, in another form,

$$v=\frac{gJ}{4\nu}\left(R_2^2-r^2+2R_0\ln\frac{r}{R_2}\right). \tag{6.125}$$

If $R_1=0$ and $R_2=R$, this expression is the same as was obtained for the velocity distribution in a circular pipe. The average cross-sectional velocity can be calculated as

$$c=\frac{2}{R_2^2-R_1^2}\int_{R_1}^{R_2} vr\,\mathrm{d}r\,. \tag{6.126}$$

Using the relation between the average velocity c and the hydraulic gradient J the head loss for an annular section of length L can be obtained.

$$h'_{1-2}=\frac{8\nu Lc}{R_2^2+R_1^2-\dfrac{R_2^2-R_1^2}{\ln\dfrac{R_2}{R_1}}}\,. \tag{6.127}$$

The Reynolds number for an annular flow can be calculated to be

$$\mathrm{Re}=\frac{c(D_2-D_1)}{\nu}\,. \tag{6.128}$$

Experimental observations show that laminar flow can exist up to $\mathrm{Re}=2200$. This value of the Reynolds number therefore, corresponds to the transition between laminar and turbulent flow in an annulus.

6.9 Elementary boundary-layer theory

It is obvious that the inclusion of frictional forces in the momentum equation causes considerable mathematical difficulties. The main source of these difficulties lies in the non-linear and second-order character of the Navier—Stokes equation. Present-day mathematical methods are unsufficient to provide a general solution of the Navier—Stokes equation. Nevertheless, in many engineering applications an approximate solution is better than no solution at all. A promising technique can be used for the case of a fluid of relatively small viscosity flowing around an immersed body. In this case the effect of internal fluid friction is significant only in a narrow region immediately adjacent to the boundaries of the fluid. Recognizing this fact, Prandtl developed his so-called boundary-layer theory. On this hypothesis the flow outside the narrow layer adjacent to the solid boundaries may be considered to be that of a perfect fluid. Within the boundary layer viscous effects predominate, but the Navier—Stokes equation may be simplified in accordance with the simpler geometry of this relatively thin layer.

The essential physical difference between the flow of a perfect fluid and that of a viscous one, demonstrates itself at the solid boundary surface of an immersed body. In a perfect fluid only a normal stress can be present at this boundary. In contrast to this, tangential stresses are present in viscous fluids causing an adhesion

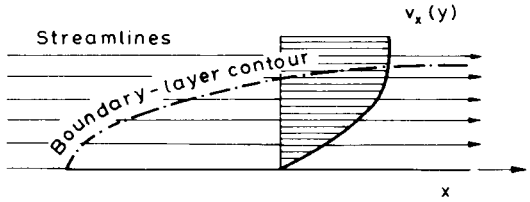

Fig. 6.4. Boundary-layer near a wall

of the fluid to the wall wetted by it. Thus, while a perfect fluid may slip on the boundary wall, in viscous fluid flow there is no relative tangential velocity at this wall. The velocity in the boundary layer approaches the velocity of the perfect fluid asymptotically. Since the fluid at the boundary has zero velocity, there is a steep velocity gradient from the boundary into the flow. Streamlines can cross the edge of the boundary layer; in general the thickness δ of the boundary layer increases in the direction of the flow, crossing more and more streamlines, as shown in *Fig. 6.4.*

Boundary-layer equations

Consider a steady, two-dimensional laminar flow of an incompressible viscous fluid. The two scalar components of the Navier—Stokes equation are

$$v_x \frac{\partial v_x}{\partial x} + v_y \frac{\partial v_x}{\partial y} = g_x - \frac{1}{\varrho} \frac{\partial p}{\partial x} + \nu \left(\frac{\partial^2 v_x}{\partial x^2} + \frac{\partial^2 v_x}{\partial y^2} \right), \tag{6.129}$$

$$v_x \frac{\partial v_y}{\partial x} + v_y \frac{\partial v_y}{\partial y} = g_y - \frac{1}{\varrho} \frac{\partial p}{\partial y} + \nu \left(\frac{\partial^2 v_y}{\partial x^2} + \frac{\partial^2 v_y}{\partial y^2} \right). \tag{6.130}$$

Since the fluid is incompressible

$$\frac{\partial v_x}{\partial x} + \frac{\partial v_y}{\partial y} = 0 . \tag{6.131}$$

Although the Navier—Stokes equation has been considerably simplified this is not yet sufficient. An order of magnitude analysis can produce a simpler form. In order to compare the boundary layer flow with the potential perfect fluid flow outside the boundary layer, a so-called anamorphosis is applied. This means that the scale of the boundary layer length is taken as being the same as the scale of the immersed body, while the scale of the boundary layer thickness is taken as a special quantity which is a function of the Reynolds number, and is obtained from the momentum equation of the boundary layer. Analogously, the same is also done for the velocities. The velocity component in the length direction of the boundary layer v_x has the same order of magnitude as the velocity of the potential flow U. We

introduce the following dimensionless variables:

$$v^* = \frac{v_x}{U}, \quad v_y^* = \frac{v_y}{V}, \quad x^* = \frac{x}{L}, \quad y^* = \frac{y}{\delta}.$$

Thus the continuity equation is

$$\frac{\partial v_x^*}{\partial x^*} + \frac{\partial v_y^*}{\partial y^*} = 0, \tag{6.132}$$

and therefore

$$\frac{L}{U}\frac{\partial v_x}{\partial x} + \frac{\delta}{V}\frac{\partial v_y}{\partial y} = 0. \tag{6.133}$$

Subdividing by L/U, we have

$$\frac{\partial v_x}{\partial x} + \frac{U}{V}\frac{\delta}{L}\frac{\partial v_y}{\partial y} = 0. \tag{6.134}$$

It is clear that

$$\frac{U}{V}\frac{\delta}{L} = 1.$$

Thus, the relationship

$$\frac{v_y}{v_x} = 0\left(\frac{\delta}{L}\right)$$

holds for the order of magnitude of the velocities, i.e. the ratio of v_y to v_x is the same as the ratio of the boundary layer thickness δ to the boundary layer length L. Since $\delta \ll L$, it is possible to simplify the system of differential equations on the basis of such an order of magnitude analysis. If therefore, we take v_x, $\partial v_x/\partial x$ and $\partial p/\partial x$ as being of a standard order of magnitude 0(1) the continuity equation shows that v_y is $0(\delta)$. The terms of the left-hand side of Eq. (6.129) are 0(1), since v_y is $0(\delta)$, while $\partial v_x/\partial y$ is $0(1/\delta)$. On the right-hand side of this equation $\partial^2 v_x/\partial x^2$ is 0(1), whilst $\partial^2 v_x/\partial y^2$ is $0(1/\delta^2)$, and much larger than $\partial^2 v_x/\partial x^2$. In addition we assume that the inertial forces, pressure forces and friction forces are balanced, all having the same order of magnitude. This manifests itself kinematically as a very strong vorticity, and dynamically as an increase in the frictional forces. Outside the boundary layer the velocity gradient normal to the flow direction is very small, thus the vorticity and viscosity may be neglected. This is in accordance with Eq. (6.101) which implies that vorticity cannot be generated within a viscous incompressible fluid flow, but must of necessity diffuse inward from its solid boundaries, with its intensity simultaneously decreasing due to the viscous dissipation.

Note, that the thickness of the boundary layer is not a geometrically and numerically determined parameter. It has only a qualitative value, i.e. that distance from the wall where the velocity is equal to the velocity of the undisturbed perfect fluid flow. A convenient definition is the distance to the point, where the actual

velocity of the fluid reaches 99% of the theoretical flow velocity. A further remark is that the edge of the boundary layer need not to coincide with any streamline.

It is obvious, that v/δ^2 must be 0(1). Thus Eq. (6.129) has the approximate form

$$v_x \frac{\partial v_x}{\partial x} + v_y \frac{\partial v_x}{\partial y} = g_x - \frac{1}{\varrho} \frac{\partial p}{\partial x} + \nu \frac{\partial^2 v_x}{\partial y^2}. \tag{6.135}$$

Taking Eq. (6.130), we see that all the terms on its left-hand side are $\sigma(\delta)$, whilst the viscous terms on the right-hand side are $\sigma(\delta)$. Therefore, it is obvious that

$$0 = g_y - \frac{1}{\varrho} \frac{\partial p}{\partial y}.$$

Since the boundary layer thickness δ is very small the body force g_y may be neglected, thus

$$\frac{\partial p}{\partial y} = 0,$$

i.e. the pressure normal to the boundary may be taken as being constant at the boundary layer, and the pressure values at the boundary and outside the boundary layer are equal. Thus a static pressure gauge at the wall can perceive the pressure of the flow outside the boundary layer. Although the velocity is zero at the wall, the pressure here is not equal to the stagnation value.

Separation of the boundary layer

Fluid particles of the boundary-layer flow do not always remain as a thin layer near the solid wall. It is possible for the boundary layer to thicken appreciably especially in the downstream direction along the immersed body contour. In this process the particles retarted in the boundary layer are carried into the external perfect fluid flow and are forced away from the body. This phenomenon is the so-called boundary layer separation. It occurs in diverging channels, at the blades of turbomachines, or around blunt bodies such as spheres or cylinders. In order to understand the phenomenon of boundary layer separation let us consider the differential equations for the boundary-layer flow. It is possible to derive some important qualitative results without integrating the equation of motion. Neglecting body forces, we obtain the set of equations:

$$v_x \frac{\partial v_x}{\partial x} + v_y \frac{\partial v_x}{\partial y} = -\frac{1}{\varrho} \frac{\partial p}{\partial x} + \nu \frac{\partial^2 v_x}{\partial y^2}, \tag{6.136}$$

$$0 = -\frac{1}{\varrho} \frac{\partial p}{\partial y}, \tag{6.137}$$

$$\frac{\partial v_x}{\partial x} + \frac{\partial v_y}{\partial y} = 0. \tag{6.138}$$

The boundary conditions are:

$$y=0, \qquad v_x=0, \qquad v_y=0,$$
$$y=\delta, \qquad v_x=U.$$

For the potential perfect fluid flow outside the boundary layer the following equation of motion can be written:

$$U\frac{\mathrm{d}U}{\mathrm{d}x}=-\frac{1}{\varrho}\frac{\mathrm{d}p}{\mathrm{d}x}.$$

Substituting into the boundary-layer equation we get

$$v_x\frac{\partial v_x}{\partial x}+v_y\frac{\partial v_x}{\partial y}=U\frac{\mathrm{d}U}{\mathrm{d}x}+\nu\frac{\partial^2 v_x}{\partial y^2}. \tag{6.139}$$

Since at the wall both v_x and v_y are zero

$$-U\frac{\mathrm{d}U}{\mathrm{d}x}=\nu\left(\frac{\partial^2 v_x}{\partial y^2}\right)_{y=0}. \tag{6.140}$$

The properties of the boundary-layer flow depend on the velocity distribution of the potential flow. The nature of the flow in the vicinity of the point where the boundary layer separates from the wall is illustrated in *Fig. 6.5.*

At point A $U>0$, the velocity of the potential flow is increasing, hence $\mathrm{d}U/\mathrm{d}x>0$. Since $\nu>0$, $\partial^2 v_x/\partial y^2<0$, thus the velocity distribution must have a maximum. The pressure gradient $\partial p/\partial x<0$.

At point B the velocity distribution of the potential flow has a maximum $\partial U/\partial x=0$. Of necessity $\frac{\partial p}{\partial x}=0$, and $\frac{\partial^2 v_x}{\partial y^2}=0$, therefore the velocity distribution of the boundary-layer flow has an inflexion point at the wall.

At point C the velocity of the potential flow decreases: $\mathrm{d}U/\mathrm{d}x<0$. Thus $\frac{\partial^2 v_x}{\partial y^2}>0$, although we still have $\frac{\partial v_x}{\partial y}>0$. The inflexion point has moved from the wall toward the inside of the boundary layer.

At point D the velocity of the potential flow has decreased further. This is a critical point at which

$$\frac{\mathrm{d}U}{\mathrm{d}x}<0, \qquad \frac{\partial^2 v_x}{\partial y^2}>0, \qquad \frac{\partial v_x}{\partial y}=0.$$

The tangent of the velocity profile at the wall is normal to the wall, i.e. the boundary-layer flow stops at the wall, the streamlines move away from the wall, a stagnation region develops, and the boundary layer separates from the body contour.

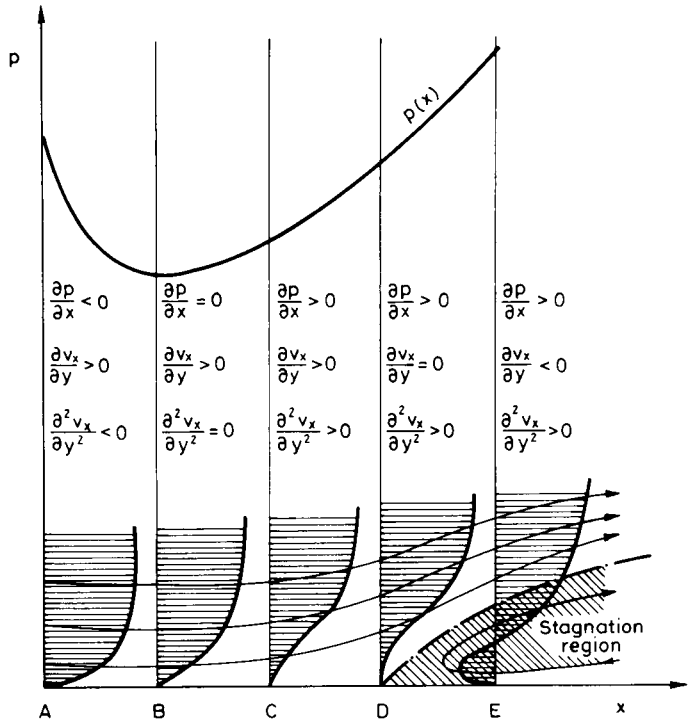

Fig. 6.5. Boundary-layer separation

At the point E the separation is complete, and behind the separation point backflow occurs adjacent to the wall:

$$\frac{dU}{dx} < 0, \qquad \frac{\partial^2 v_x}{\partial y^2} > 0, \qquad \text{moreover } \frac{\partial v_x}{\partial y} < 0 .$$

Boundary-layer separation causes the drag of immersed bodies, and is accompanied by a considerable loss of mechanical energy. If a body is placed in a perfect fluid flow, an accelerated flow occurs along its leading surface, accompanied by a negative pressure gradient. Along the trailing surface the flow decelerates and there is a positive pressure gradient. Since a perfect fluid can slip along the body surface, the kinetic energy may be sufficient to maintain the flow near the wall against the decelerated motion and the positive pressure gradient. A particle within the boundary-layer flow finds itself affected by a similar velocity distribution and pressure gradient. The velocity at the body surface is zero while near the wall it is rather small. In the deceleration section the flow has lost so much kinetic energy that the remainder is insufficient to move it against the positive pressure gradient. It comes to rest and because of the increasing pressure distribution of the external forfeit

fluid flow, a backward motion sets in. This backflow marks the beginning of the separation and is accompanied by the occurrence of large-scale vortices.

It has been found as a general rule that separation of the boundary layer always occurs in the region where the potential flow is decelerating, i.e. where there is a positive pressure gradient. This phenomenon reduces the efficiency of the transformation of energy in diffusers, or at the impellers and volute casings of pumps.

The above simplified treatment serves only as a brief qualitative account of this very important phenomenon. A detailed analysis is outside the scope of this book.

6.10 Resistance of a solid sphere in laminar flow

The transport of fluid-solid mixtures by pipeline is of considerable importance in the petroleum industry. An example of such a case is the transport of proppant with fracturing gel through the drilling pipe. In a number of design applications for drilling it is necessary to calculate the forces acting on the dispersed particles. The simplest model of this problem is that of laminar flow around a single sphere. Since the size of the particles is generally small it is convenient to consider flows of small Reynolds number.

It is known that the convective momentum flux is proportional to the square of the velocity, while the conductive momentum transfer of the laminar flow is a linear function of the velocity. Thus the convective momentum flux may be neglected at small Reynolds numbers. If the Reynolds number is smaller than unity, the term $(\vec{v}\nabla)\vec{v}$ of the Navier—Stokes equation may be omitted. In a steady flow the local component of the acceleration also vanishes. Therefore, neglecting the body forces we get the equation

$$\frac{1}{\varrho}\nabla p = \nu \Delta \vec{v} .$$

Taking into account the geometry of the body it is convenient to use spherical coordinates. It is assumed that the velocity has radial and meridional components only, and is independent of the asimuthal coordinate φ:

$$v_r = v_r(r, \vartheta), \qquad v_\vartheta = v_\vartheta(r, \vartheta), \qquad v_\varphi = 0 .$$

Thus

$$\frac{\partial v_r}{\partial \varphi} = \frac{\partial v_\vartheta}{\partial \varphi} = 0 .$$

The scalar components of the Navier—Stokes equation in the usual notation are

$$\frac{1}{\varrho}\frac{\partial p}{\partial r} = \nu\left(\frac{\partial^2 v_r}{\partial r^2} + \frac{1}{r^2}\frac{\partial^2 v_r}{\partial \vartheta^2} + \frac{2}{r}\frac{\partial v_r}{\partial r} + \frac{\cot \vartheta}{r^2}\frac{\partial v_r}{\partial \vartheta} - \right.$$
$$\left. - \frac{2}{r^2}\frac{\partial v_\vartheta}{\partial \vartheta} - \frac{2v_r}{r^2} - \frac{2\cot \vartheta}{r^2} v_\vartheta\right), \tag{6.141}$$

$$\frac{1}{r}\frac{\partial p}{\varrho\partial\vartheta}=\nu\left(\frac{\partial^2 v_\vartheta}{\partial r^2}+\frac{1}{r^2}\frac{\partial^2 v_\vartheta}{\partial\vartheta^2}+\frac{2}{r}\frac{\partial v_\vartheta}{\partial r}+\frac{\cot\vartheta}{r^2}\frac{\partial v_\vartheta}{\partial\vartheta}+\frac{2}{r^2}\frac{\partial v_r}{\partial\vartheta}-\frac{v_\vartheta}{r^2\sin^2\vartheta}\right). \tag{6.142}$$

The continuity equation is

$$\frac{\partial v_r}{\partial r}+\frac{2v_r}{r}+\frac{1}{r}\frac{\partial v_\vartheta}{\partial\vartheta}+\frac{v_\vartheta\cot\vartheta}{r}=0. \tag{6.143}$$

The boundary conditions for this set of differential equations are

$$v_r(R,\vartheta)=0, \qquad v_\vartheta(R,\vartheta)=0,$$
$$v_r(\infty,\vartheta)=c\cos\vartheta \qquad v_\vartheta(\infty,\vartheta)=-c\sin\vartheta.$$

Therefore, the velocity components v_r and v_ϑ vanish at the surface of the sphere while the velocity at infinity v_∞ is constant. We introduce the following notations:

$$v_r=e(r)\cos\vartheta, \tag{6.144}$$

$$v_\vartheta=f(r)\sin\vartheta, \tag{6.145}$$

$$p=\varrho\nu g(r)\cos\vartheta. \tag{6.146}$$

Substituting into the partial differential equations we obtain a set of common differential equations:

$$g'=e''+\frac{2}{r}e'-4\frac{e-f}{r^2}, \tag{6.147}$$

$$\frac{g}{r}=f''+\frac{2}{r}f'+2\frac{e-f}{r^2}, \tag{6.148}$$

$$e'+2\frac{e-f}{r}=0. \tag{6.149}$$

Naturally, the boundary conditions must be similarly transformed. Thus we get

$$e(R)=f(R)=0, \tag{6.150}$$

and

$$e(\infty)=f(\infty)=c. \tag{6.151}$$

From Eq. (6.149)

$$f=\frac{r}{2}e'+e. \tag{6.152}$$

Substituting into Eq. (6.148) we get

$$g=\frac{r}{2}e'''+3re''+2e'. \tag{6.153}$$

After differentiation and some further manipulation a fourth-order, linear, homogeneous differential equation is obtained:

$$r^3 e'''' + 8re''' + 8re'' - 8e' = 0 \quad . \tag{6.154}$$

The general solution of this equation comprises a series of terms of the form

$$e = r^k, \tag{6.155}$$

where the individual values of the exponent k may be determined from the equation

$$k(k-1)(k-2)(k-3) + 8k(k-1)(k-2) + 8k(k-1) - 8k = 0 \,. \tag{6.156}$$

The result is

$$k_1 = 0 \,, \qquad k_2 = 2 \,, \qquad k_3 = -1 \,, \qquad k_4 = -3 \,.$$

Thus we obtain

$$e = A + Br^2 + \frac{C}{r} + \frac{D}{r^3} \,. \tag{6.157}$$

Substituting into Eq. (6.152) we obtain

$$f = A + 2Br^2 + \frac{C}{2r} - \frac{D}{2r^3} \,. \tag{6.158}$$

Similarly, from Eq. (6.153) we get

$$g = \frac{C}{r^2} + 10Br \,. \tag{6.159}$$

The coefficients A, B, C and D are determined from the boundary conditions:

$$A = c \,, \qquad B = 0 \,, \qquad C = -\frac{3Rc}{2} \,, \qquad D = \frac{R^3 c}{2} \,.$$

Substituting into Eqs (6.144) to (6.147), the velocity components and the pressure are obtained as

$$v_r = \left[1 - \frac{3}{2}\frac{R}{r} + \frac{1}{2}\left(\frac{R}{r}\right)^3\right] c \cos \vartheta \,, \tag{6.160}$$

$$v_\vartheta = \left[1 - \frac{3}{4}\left(\frac{R}{r}\right) - \frac{1}{4}\left(\frac{R}{r}\right)^3\right] c \sin \vartheta \,, \tag{6.161}$$

$$p - p_0 = -\frac{3}{2}\varrho v \frac{Rc}{r^2} \cos \vartheta \,. \tag{6.162}$$

The force acting on the surface of the sphere originates from the dynamic pressure and the shear stress. Its component in the direction of the velocity v is the drag force

of the sphere. This may be easily determined as

$$F = \int_{(A)} p_R \cos\vartheta \, dA + \int_{(A)} \tau_R \sin\vartheta \, dA =$$

$$= \int_0^{\pi} \frac{3}{2} v\varrho \frac{c}{R} \cos\vartheta \, 2R\pi \sin\vartheta \, d\vartheta + \int_0^{\pi} 3R\pi\varrho v c \sin^3\vartheta \, d\vartheta . \tag{6.163}$$

After integration we have

$$F = 6R\pi\varrho v c . \tag{6.164}$$

This is the well-known Stokes resistance law, which at low Reynolds numbers, is in very good agreement with experimental measurements. Introducing the drag coefficient

$$C_D = \frac{F}{R^2\pi \frac{\varrho c^2}{2}}, \tag{6.165}$$

we may write it as a function of the Reynolds number,

$$C_D = \frac{24}{\mathrm{Re}} . \tag{6.166}$$

The close agreement between the results of Stokes's formula and experimental measurements is shown in *Fig. 6.6*. At higher Reynolds numbers the increasing inertial forces and the turbulence totally change the relationship between the drag coefficient C_D and the Reynolds number. In a real fluid-solid mixture additional complications arise because of the non-spherical shape and the different sizes of the

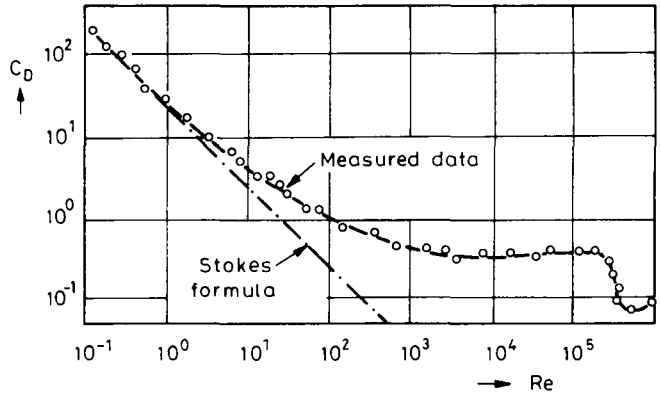

Fig. 6.6. Calculated and experimental drag coefficient for a sphere

particles and their interaction. It is impossible to arrive at an analytical solution for an assemblage of discrete particles. Instead of this, semi-empirical methods are developed.

The simplest problem is that of a dispersion of solid particles in an incompressible viscous fluid. Uniform, spherical particles of density ϱ_p and diameter D are assumed. The particles are separated from each other and do not interact. Then, at equilibrium the gravitational force and the buoyancy represent the body forces. Their resultant, which causes a particle to rise ($\varrho_p < \varrho$), or fall ($\varrho_p > \varrho$) will be

$$F_1 = \frac{D^3\pi}{6}(\varrho_p - \varrho)\, g\,. \tag{6.167}$$

The drag force acting on the falling or rising particle is

$$F_2 = C_D \frac{D^2\pi}{4}\,\frac{\varrho c^2}{2}, \tag{6.168}$$

where c is the velocity with which the particle falls or rises. After a relatively short period of acceleration the particle attains a constant velocity at which stage the gravitational, buoyancy and drag forces are balanced. This velocity is called the terminal settling velocity C_0. Thus

$$\frac{D^3\pi}{6}(\varrho_p - \varrho)\, g = C_D \frac{D^2\pi}{4}\,\frac{\varrho c_0^2}{2}\,.$$

Substituting C_D from Eq. (6.166) we get

$$C_0 = \frac{gD^2}{18\nu}\,\frac{\varrho_p - \varrho}{\varrho}\,. \tag{6.169}$$

This equation is valid for the laminar settling of non-interacting, spherical particles. Swanson devised a semi-empirical equation applicable to particles of arbitrary shape:

$$C_0 = \frac{1}{\alpha}\,\frac{\sqrt{\frac{4}{3}gD\,\frac{\varrho_p - \varrho}{\varrho}}}{1 + \dfrac{\beta\nu}{6\sqrt{gD\,\dfrac{\varrho_p - \varrho}{\varrho}}}}, \tag{6.170}$$

where α and β are boundary-layer coefficients determined from actual settling data. Swanson's equation is in good agreement with experimental data.

6.11 Free convection

The motion of a fluid which is caused solely by the density differences brought about by temperature gradients is called free, or natural convection.

A fluid body may be in mechanical equilibrium without being in thermal equilibrium. The hydrostatic equation

$$\varrho \vec{g} = \operatorname{grad} p\,,$$

may be satisfied even though the temperature distribution is not uniform. There are certain temperature gradients which allow the mechanical equilibrium to be maintained. Other temperature distributions may induce movements in the fluid.

In order to investigate the conditions of the equilibrium, consider a fluid particle of a specific volume $\vartheta(p, S)$ at a height z in the gravity field, where p and S are the pressure and the entropy at equilibrium. Assume a small upward adiabatic displacement Δz of this particle. At the new height $z+\Delta z$, the new pressure p', and entropy s' determine the local specific volume $\vartheta(p', S')$. As a result of the adiabatic displacement the specific volume of the chosen particle will become $\vartheta(p', S)$. The mechanical equilibrium is stable only if

$$\vartheta(p', S') - \vartheta(p', S) > 0\,. \tag{6.171}$$

This small difference can be expanded into a series, in which the inequality

$$\left(\frac{\partial \vartheta}{\partial S}\right)_p \frac{\mathrm{d}S}{\mathrm{d}z} > 0 \tag{6.172}$$

must be satisfied. On the other hand we also have

$$\left(\frac{\partial \vartheta}{\partial S}\right)_p = \frac{T}{c_p}\left(\frac{\partial \vartheta}{\partial T}\right)_p. \tag{6.173}$$

Since both T and c_p are positive, the two above conditions imply that

$$\left(\frac{\partial \vartheta}{\partial T}\right)_p \frac{\mathrm{d}S}{\mathrm{d}z} > 0\,. \tag{6.174}$$

It is a well-known fact, that any material expands when the temperature is increased (except water between 0 C° and 4 C°). It is obvious that

$$\left(\frac{\partial \vartheta}{\partial T}\right)_p > 0\,,$$

thus

$$\frac{\mathrm{d}S}{\mathrm{d}z} > 0\,,$$

therefore the entropy must increase with the height in the gravity field. Thus we can

write

$$\frac{\mathrm{d}S}{\mathrm{d}z} = \left(\frac{\partial S}{\partial T}\right)_p \frac{\mathrm{d}T}{\mathrm{d}z} + \left(\frac{\partial S}{\partial p}\right)_T \frac{\mathrm{d}p}{\mathrm{d}z} = \frac{c_p}{T}\frac{\mathrm{d}T}{\mathrm{d}z} - \left(\frac{\partial \vartheta}{\partial T}\right)_p \frac{\mathrm{d}p}{\mathrm{d}z} > 0 . \tag{6.175}$$

Since

$$\vartheta = \frac{1}{\varrho},$$

the pressure gradient is obtained as

$$\frac{\mathrm{d}p}{\mathrm{d}z} = -\frac{g}{\vartheta}.$$

Thus we have

$$\frac{\mathrm{d}T}{\mathrm{d}z} > -\frac{T}{c_p}\frac{g}{\vartheta}\left(\frac{\partial \vartheta}{\partial T}\right)_p . \tag{6.176}$$

Therefore, free convection can occur, if

$$\frac{\mathrm{d}T}{\mathrm{d}z} < 0 , \tag{6.177}$$

and

$$\left|\frac{\mathrm{d}T}{\mathrm{d}z}\right| > \frac{gT}{c_p \vartheta}\left(\frac{\partial \vartheta}{\partial T}\right)_p . \tag{6.178}$$

For an ideal gas

$$\frac{T}{\vartheta}\left(\frac{\partial \vartheta}{\partial T}\right)_p = 1 , \tag{6.179}$$

thus

$$\frac{\mathrm{d}T}{\mathrm{d}z} > -\frac{g}{c_p}. \tag{6.180}$$

Therefore, mechanical equilibrium can exist when the temperature gradient satisfies certain restrictions. If these conditions are not satisfied, natural convective flow develops, tending to homogenize the temperature distribution.

Balance equations for this type of motion can be written, treating the fluid as incompressible, except for the density variation caused by the inhomogeneous temperature. This simplification is permissible since the density differences are relatively small.

Initially the fluid body is in mechanical and thermal equilibrium. The temperature T_0 and density ϱ_0 referring to this state are constant. The pressure distribution is determined by the equation

$$\varrho_0 \mathfrak{g} = \operatorname{grad} p_0 ,$$

where p_0 is the equilibrium pressure, which is a linear function of z. Any finite temperature change T' can be considered to be a perturbation, which leads to

further perturbations of density, pressure and velocity:

$$T = T_0 + T', \tag{6.181}$$

$$\varrho = \varrho_0 + \varrho', \tag{6.182}$$

$$p = p_0 + p', \tag{6.183}$$

and finally

$$\vec{v} = \vec{v}'. \tag{6.184}$$

The density perturbation can be expressed as

$$\varrho' = \left(\frac{\partial \varrho_0}{\partial T}\right)_p T' = -\varrho_0 \beta T', \tag{6.185}$$

where

$$\beta = -\frac{1}{\varrho}\frac{\partial \varrho}{\partial T} \tag{6.186}$$

is the coefficient of thermal expansion. Substituting Eqs (6.182) and (6.184) into the continuity equation, the latter can be written as

$$\frac{\partial(\varrho_0 + \varrho')}{\partial t} + \operatorname{div}\left[(\varrho_0 + \varrho')\vec{v}'\right] = 0. \tag{6.187}$$

As the equilibrium value of the density is constant, it is obvious that

$$\frac{\partial \varrho_0}{\partial t} = 0.$$

Since the temperature perturbation is small, the density perturbation is much smaller than the initial, equilibrium value of density, i.e.

$$\varrho_0 \gg \varrho',$$

and thus

$$\varrho_0 \vec{v}' \gg \varrho' \vec{v}'.$$

It is obvious that, taking these order of magnitude considerations into account, the continuity equation can be written as

$$\frac{\partial \varrho'}{\partial t} + \operatorname{div}(\varrho_0 \vec{v}') = 0. \tag{6.188}$$

It is assumed, that a small temperature perturbation can induce only laminar flow in a fluid body. Substituting Eqs (6.182) to (6.184) into the Navier—Stokes equation, the latter can be written as

$$(\varrho_0 + \varrho')\left[\frac{\partial \vec{v}'}{\partial t} + (\vec{v}' V)\vec{v}'\right] = (\varrho_0 + \varrho')\vec{g} - V(p_0 + p') + \nu(\varrho_0 + \varrho')\Delta \vec{v}'. \tag{6.189}$$

Taking into consideration, that

$$\varrho_0 \vec{g} = \nabla p_0 ,$$

we obtain

$$(\varrho_0 + \varrho') \left[\frac{\partial \vec{v}'}{\partial t} + (\vec{v}' \nabla) \vec{v}' \right] = \varrho' \vec{g} - \nabla p' + (\varrho_0 + \varrho') \nu \Delta \vec{v}' . \tag{6.190}$$

Using an order of magnitude analysis we get

$$\varrho_0 \left[\frac{\partial \vec{v}'}{\partial t} + (\vec{v}' \nabla) \vec{v}' \right] = \varrho' \vec{g} - \nabla p' + \varrho_0 \nu \Delta \vec{v} . \tag{6.191}$$

Substituting Eq. (6.185) and dividing by ϱ_0, the momentum equation for free convection is obtained

$$\frac{\mathrm{d}\vec{v}'}{\mathrm{d}t} = -\beta T' \vec{g} - \frac{1}{\varrho_0} \nabla p' + \nu \Delta \vec{v}' . \tag{6.192}$$

The internal energy balance equation can be written in a similar way. Assuming a constant heat capacity and thermal conductivity we obtain

$$(\varrho_0 + \varrho') c \left[\frac{\partial (T_0 + T')}{\partial t} + \vec{v}' \nabla (T_0 + T') \right] = k \Delta (T_0 + T') . \tag{6.193}$$

Since T_0 is constant, its derivatives vanish. Taking into account that $\varrho_0 \gg \varrho'$, the internal energy equation is obtained in the simple form

$$\varrho_0 c \frac{\mathrm{d}T'}{\mathrm{d}t} = k \Delta T' . \tag{6.194}$$

The set of equations comprising Eqs (6.188), (6.192) and (6.194) can be solved numerically. In petroleum engineering practice experimental methods are more useful, with the measured data arranged in the form of similarity invariants. Similarity invariants for free convection can be determined in a manner similar to the one outlined in Section 6.5. Two free convection processes are physically similar if they are related by the expressions

$$\begin{aligned} &\varrho_* = \alpha_\varrho \varrho , \quad && \vec{v}_* = \alpha_v \vec{v} , \quad && \vec{r}_* = \alpha_r \vec{r} , \\ &t_* = \alpha_t t , && p_* = \alpha_p p , && \beta_* = \alpha_\beta \beta , \\ &T_* = \alpha_T T , && \nu_* = \alpha_\nu \nu , && \vec{g}_* = \alpha_g \vec{g} . \end{aligned} \tag{6.195}$$

The continuity equation imposes no new conditions, thus we proceed to the momentum equation. The equations

$$\frac{\mathrm{d}\vec{v}'}{\mathrm{d}t} = -\beta T' \vec{g} - \frac{1}{\varrho_0} \nabla p' + \nu \Delta \vec{v}' \tag{6.196}$$

and

$$\frac{\alpha_v^2}{\alpha_r}\frac{\mathrm{d}\tilde{v}}{\mathrm{d}t} = -\alpha_\beta\alpha_T\alpha_g\beta T'\tilde{g} - \frac{\alpha_p}{\alpha_\varrho\alpha_r}\frac{1}{\varrho_0}\nabla p' + \frac{\alpha_\nu\alpha_v}{\alpha_r^2}\nu\Delta v' \tag{6.197}$$

cannot be independent; they may differ only by a constant multiplier, thus all the dimensionless groups of scale factors must have the same constant value, i.e.

$$\frac{\alpha_v^2}{\alpha_r} = \alpha_\beta\alpha_g\alpha_T = \frac{\alpha_p}{\alpha_\varrho\alpha_r} = \frac{\alpha_\nu\alpha_v}{\alpha_r^2} = \text{const}\,. \tag{6.198}$$

It is significant that there is no characteristic velocity for free convection. The velocity at the boundaries is everywhere zero and thus it is impossible to derive a similarity invariant for the velocity. The two most important forces are the buoyancy and the viscous force which respectively induce and dampen the motion of the fluid. These two forces can be related by the equation

$$\alpha_\beta\alpha_T\alpha_g = \frac{\alpha_\nu\alpha_v}{\alpha_r^2}\,. \tag{6.199}$$

The scale factor for the velocity α_v can be eliminated, since from the equality

$$\frac{\alpha_v^2}{\alpha_r} = \frac{\alpha_\nu\alpha_v}{\alpha_r^2}\,, \tag{6.200}$$

we obtain

$$\frac{\alpha_v\alpha_r}{\alpha_\nu} = 1\,.$$

Multiplying Eq. (6.199) by α_r^3/α_v^2 we get

$$\frac{\alpha_\beta\alpha_T\alpha_g\alpha_r^3}{\alpha_v^2} = \frac{\alpha_v\alpha_r}{\alpha_\nu} = 1\,. \tag{6.201}$$

This leads to the similarity invariant called the Grashof number

$$\mathrm{Gr} = \frac{\beta T g r^3}{\nu^2} \tag{6.202}$$

which characterizes the fluid motion for free convective flows. The value of the Grashof number is large when free convection currents are intense, and it tends to zero as fluid motion decreases.

The internal energy equation leads to the expression

$$\frac{\alpha_\varrho\alpha_c\alpha_T\alpha_v}{\alpha_r} = \frac{\alpha_k\alpha_T}{\alpha_r^2}\,. \tag{6.203}$$

Dividing by α_ν, and after a little manipulation we obtain

$$\frac{\alpha_k}{\alpha_\varrho\alpha_c\alpha_\nu} = \frac{\alpha_v\alpha_r}{\alpha_\nu} = 1\,.$$

This leads to the similarity invariant called the Prandtl number, which also characterizes free convective heat transfer:

$$\mathrm{Pr} = \frac{\varrho c v}{k}.$$

The boundary condition at the solid-fluid interface obviously leads to the Nusselt number

$$\mathrm{Nu} = \frac{hr}{k}$$

as the similarity invariant for free convection.

Thus, experimental data can be arranged in terms of the relationship between Nu, Pr and Gr. One of the most important free convective heat transfer processes is the transfer which takes place from a heated horizontal pipe. This situation arises quite naturally when oil, gas and geothermal brine collecting pipes are built at the ground surface. In this case

$$\mathrm{Gr} = \frac{\beta \Delta T g D^3}{v^2}$$

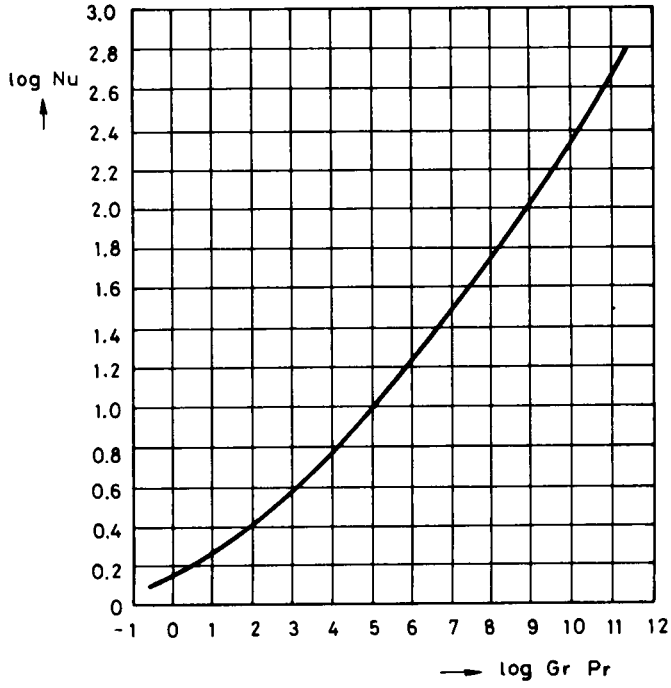

Fig. 6.7. Nusselt number for free convection flow around a horizontal pipe

in which ΔT is the temperature difference between the outer surface of the pipe wall and the undisturbed air, β is the coefficient of thermal expansion of the air, which is

$$\beta = \frac{1}{273\,^{\circ}\mathrm{C}},$$

ν is the kinematic viscosity of the air, and D is the outer diameter of the pipe. The Nusselt number for this case is

$$\mathrm{Nu} = \frac{hD}{k}.$$

Within the range

$$10^3 < \mathrm{Gr\,Pr} < 10^9$$

the experimental results plot onto a single curve as shown in *Fig. 6.7*. This curve can be adequately approximated by the equation

$$\mathrm{Nu} = 0.52\sqrt[4]{\mathrm{Gr\,Pr}}.$$

CHAPTER 7

TURBULENT FLOW

7.1 The nature of turbulent motion

When observing the flow of a viscous fluid in a pipe, a channel, or around an immersed body, we find that the flow remains stable and laminar as long as the flow velocity is less than a certain critical value. Above this critical velocity the regularity of the laminar flow disappears, and as the viscous forces can no longer dampen instabilities, small disturbances progressively increase until the laminar flow pattern disintegrates and undergoes a transition to turbulent flow. The term "turbulence" was introduced by Reynolds and denotes the irregular stochastic motion of all fluid elements. Many flow-visualization techniques have been developed to permit direct observation of turbulent flow. Such methods can involve the pouring of aluminium powder or fluorescent additives onto a free water surface, or the injection of smoke into an air flow, as tracers for visualization. These methods are simple and suitable for the simultaneous observation of the greater part of a body of flowing fluid. The results obtained from such observations reveal that the flow paths of the particles are chaotic and change rapidly; the motion of a single particle is meaningless from the point of view of the whole flow. The velocity of a single particle changes at random and it moves chaotically, flitting forwards, backwards and sideways; the magnitude and direction of movement seemingly inexpressible. None of the researchers in this field, however, has ever doubted being able to describe turbulent motion using the tools of continuum mechanics. Their solution has been to investigate turbulent flow on the basis of statistics, regardless of the laws of mechanics.

Reynolds has had a splendid idea for describing the stochastic turbulent motion using the methods of continuum mechanics. Reynolds was not satisfied repeating and refining the attractive but unprofitable visual observations. He put forward the idea that although the turbulent motion was composed of a complicated system of irregular eddies and fluctuations, the averaged parameters of a flowing fluid (e.g. the flow rate and the pressure drop), should show a deterministic conformity with the general laws of dynamics.

The most conspicuous feature of turbulent flow is that momentum, energy and heat are transferred across the flow by molecular transport processes (viscous momentum transfer, diffusion), at a rate much greater than would be the case in a laminar flow. This phenomenon is the result of additional transport by the

random motion of fluid particles across the flow and the concurrent mixing of the convectively transported momentum and energy between neighboring fluid elements. In steady flow, time-averaged mean values are determined. These mean values can be compared with turbulent fluctuations in a similar manner as the macroscopic quantities of laminar flow with the thermal motion of molecules. The particles which mix in a turbulent flow are much larger than molecules, thus turbulent transport is a much more intensive phenomenon than the molecular transport process. Thus the sudden increase in fluid friction or heat transfer is as suitable a method for detecting the occurrence of turbulent flow as direct visual observation. The engineer is fortunate in being able to measure such a sudden increase easily by using the usual equipment of petroleum engineering practice.

A further effective method of making velocity measurements in a turbulent flow is that of hot-wire anemometry. The operating principle of this instrument is simple. A platinum wire of very small diameter (0.01 mm) and length (1–2 mm) is heated by a weak direct current. This wire is placed in the turbulent flow, perpendicular to the mean direction of the flow. As the velocity increases, the wire is cooled down, and thus its electrical resistance changes. The hot wire forms one arm of a Wheatstone-bridge, thus making it possible to measure the change in resistance. The galvanometer deflection can be correlated with the velocity of the fluid by calibration, or be registered by an oscillograph. By analyzing the oscillograms, velocity fluctuations can be measured. Although the hot wire is very thin, it does have a small heat capacity, so that some retardation occurs. The results obtained

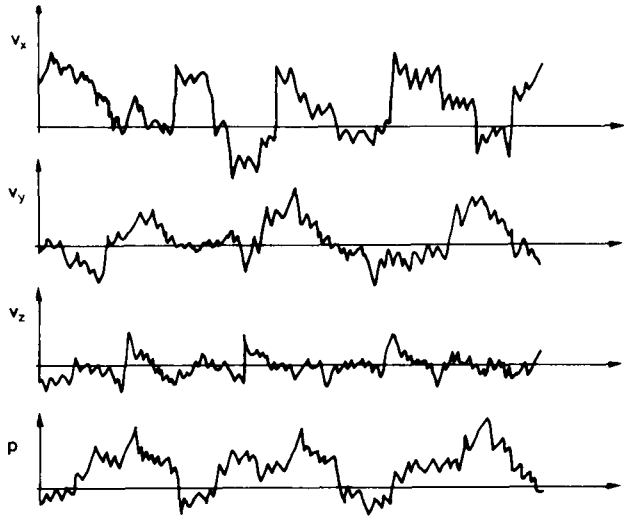

Fig. 7.1. Turbulent velocity and pressure fluctuations

by this method have, nevertheless, proved very significant. It appears, that unlike molecular motion, a turbulent flow is highly anisotropic and shows a considerable degree of ordering. Some elements of the motion are almost periodic, with close observation showing that the frequency of the fluctuations shows some degree of regularity. A few characteristic oscillograms are shown in *Fig. 7.1.*

7.2 Reynolds's equation: the balance of momentum for turbulent flow

Time-averaged mean values of stochastic quantities

The oscillograms of Eq. (7.1) suggest that the velocity of a turbulent flow should be interpreted in terms of a mean value with a superimposed high-frequency stochastic fluctuation of irregular, changing amplitude. If instead of a hot wire anemometer one uses a Prandtl tube for measuring the velocity, fluctuations cannot be perceived but only the time-averaged mean value. Thus the velocity of a turbulent flow can be considered as the resultant of the mean velocity and the fluctuations. The pressure of a turbulent flow can be similarly split up:

$$\begin{aligned} \vec{v}_t &= \vec{v} + \vec{v}' \\ p_t &= p + p' , \end{aligned} \tag{7.1}$$

where $\vec{v}_t$ and p_t are the real instantaneous velocity and pressure of the flow, $\vec{v}$ and p represent their averaged values over a sufficiently long period of time, and $\vec{v}'$ and p' are the fluctuations of the velocity and pressure about the mean. Reynolds proposed the following simple relationship for determining the mean values:

$$F(\vec{r}, t) = \overline{F_t}(\vec{r}, t) = \frac{1}{t_0} \int_t^{t+t_0} F_t(\vec{r}, t)\, \mathrm{d}t , \tag{7.2}$$

in which $F_t\ (\vec{r}, t)$ is some arbitrarily chosen scalar or vector function. The overbar represents the time-averaged value of F_t. Assume the existence a of time interval t_0 which is large relative to the time interval of a fluctuation, but relatively small compared to the time interval over which the mean velocity was determined. Averaging over this interval yields a result which is independent of t_0, and remains unchanged during further averaging processes. Thus

$$F(\vec{r}, t) = \overline{F}(\vec{r}, t) , \tag{7.3}$$

i.e. the further time average of the time average remains unchanged. This mean value is not necessary constant, all time-averaged functions can undergo slow variations, but the time-dependence of the macroscopic phenomena is of a different

order of magnitude than the period of the turbulent fluctuations. Consider for example, the velocity of a fluid discharging from a tank. The velocity obtained from the Torricelli equation is the mean velocity v. The turbulent fluctuations are superimposed onto this mean. As the water level in the tank decreases, the value of v also decreases. The duration of the discharging T is considerably greater than the time interval over which t_0 is averaged, which may be the time used to measure the outflow velocity by means of a Pitot tube.

It follows from Eq. (7.3) that the time average of the fluctuations is zero:

$$\overline{F}(\vec{r}, t) = F(\vec{r}, t) - \overline{F}_t(\vec{r}, t) = 0 . \tag{7.4}$$

A consequence of Eq. (7.2) is that the time average of a spatial derivative is equal to the spatial derivative of a time-averaged function, since the time-averaging operation is independent of the differentiation with respect to the coordinates:

$$\overline{\frac{\partial F_t}{\partial x}} = \frac{\partial \overline{F}_t}{\partial x} . \tag{7.5}$$

The same relationship is also valid for the partial derivative w.r.t. time which relates to large scale changes in time:

$$\overline{\frac{\partial F_t}{\partial t}} = \frac{\partial \overline{F}_t}{\partial t} . \tag{7.6}$$

Time-averaged form of the balance of momentum

Reynolds, using the above method of time-averaging, stated that the Navier—Stokes equation is also valid for turbulent flow provided that the instantaneous values $\vec{v}_t$ and p_t are substituted into it. It is necessary to carry out the averaging using Eq. (7.2) in order to replace the rather impractical values $\vec{v}_t$ and p_t by the readily measurable values $\vec{v}$ and p, which already are suitable for boundary conditions.

Consider the equation of motion for a viscous fluid in integral form, substituting $\vec{v}_t$ and p_t into it. Further assumptions are that the density and viscosity of the fluid are constant. Thus the momentum equation is:

$$\int_V \frac{\partial(\varrho \vec{v}_t)}{\partial t} \, \mathrm{d}V + \int_{(A)} \varrho(\vec{v}_t \circ \vec{v}_t) \, \mathrm{d}\vec{A} =$$

$$= \int_V \varrho \vec{g} \, \mathrm{d}V - \int_{(A)} p_t \, \mathrm{d}\vec{A} + \int_{(A)} \mu(\vec{v}_t \circ \nabla + \nabla \circ \vec{v}_t) \, \mathrm{d}\vec{A} . \tag{7.7}$$

Replacing $\vec{v}_i$ and p_i with the sum of their mean and fluctuations, and after averaging, we have:

$$\int_V \frac{\partial}{\partial t}(\overline{\varrho\vec{v}+\varrho\vec{v}'})\,\mathrm{d}V + \int_{(A)} \varrho[\overline{(\vec{v}+\vec{v}')\circ(\vec{v}+\vec{v}')}]\,\mathrm{d}\vec{A} =$$

$$= \int_V \varrho\vec{g}\,\mathrm{d}V - \int_{(A)} (\overline{p+p'})\,\mathrm{d}\vec{A} + \int_{(A)} \mu[\overline{(\vec{v}+\vec{v}')\circ\nabla+\nabla\circ(\vec{v}+\vec{v}')}]\,\mathrm{d}\vec{A}\,. \quad (7.8)$$

We must consider the following relationship for averaging the term representing the convective transport of momentum, since for averaging the dyadic product we have:

$$\overline{(\vec{v}+\vec{v}')\circ(\vec{v}+\vec{v}')} = \overline{\vec{v}\circ\vec{v}} = \vec{v}\circ\vec{v} + \overline{\vec{v}\circ\vec{v}'} + \overline{\vec{v}'\circ\vec{v}} + \overline{\vec{v}'\circ\vec{v}'}\,. \quad (7.9)$$

The average of the product of the mean velocities remains unchanged, the average of the product of the mean and the fluctuation is equal to zero, but the average of the product of the velocity fluctuations does not vanish. Thus

$$\overline{(\vec{v}+\vec{v}')\circ(\vec{v}+\vec{v}')} = \vec{v}\circ\vec{v} + \overline{\vec{v}'\circ\vec{v}'}\,. \quad (7.10)$$

The average of the fluctuations vanishes in all other terms. Finally, the momentum equation can be written in the following form:

$$\int_V \frac{\partial(\varrho\vec{v})}{\partial t}\,\mathrm{d}V + \int_{(A)} \varrho(\vec{v}\circ\vec{v})\,\mathrm{d}\vec{A} + \int_{(A)} \varrho\overline{(\vec{v}'\circ\vec{v}')}\,\mathrm{d}\vec{A} =$$

$$= \int_V \varrho\vec{g}\,\mathrm{d}V - \int_{(A)} p\,\mathrm{d}\vec{A} + \int_{(A)} \mu(\vec{v}\circ\nabla+\nabla\circ\vec{v})\,\mathrm{d}\vec{A}\,. \quad (7.11)$$

The rate of change of the momentum relative to the mean velocity field is not equal to the resultant of the external forces. The third integral on the left-hand side expresses the irreversible convective transport of momentum due to the turbulent velocity fluctuation. If this term is carried over to the right-hand side of the momentum equation, we can interpret it as an external force acting on the surface (A) with its work dissipating into the internal energy of the fluid in a manner similar to the viscous force. The dyadic product in this term can be interpreted as a second-order tensor of the apparent turbulent shear stresses:

$$\mathbf{T}' = -\varrho\overline{(\vec{v}'\circ\vec{v}')}\,. \quad (7.12)$$

Its product with the vectorial surface element $\mathrm{d}\vec{A}$ yields at the bounding surface the apparent external force caused by the momentum flux resulting from the turbulent fluctuations. It is called the apparent surface force since in reality this additional turbulent force acts on the intermixing layers of the fluid rather than on a surface.

The integral form of the momentum equation can be replaced by a differential equation. The integral equation expresses the balance of momentum for an arbitrary finite volume of fluid, in contrast, the differential equation refers to a unit volume of fluid. Using Gauss's theorem, the surface integrals may be expressed as volume integrals after which all integrals are taken over an infinitesimal control volume, i.e. the earlier finite volume shrinks to a point. By this method we obtain the equation

$$\frac{\partial(\varrho\vec{v})}{\partial t} + \mathrm{Div}\,(\varrho\vec{v}\circ\vec{v}) = \varrho\vec{g} - \mathrm{grad}\;p + \mu\Delta\vec{v} + \\ + (\mu+\kappa)\,\mathrm{grad}\,\mathrm{div}\,\vec{v} - \mathrm{Div}\,\overline{(\varrho\vec{v}'\circ\vec{v}')}\,. \tag{7.13}$$

If the fluid is incompressible and no diffusion occurs, we obtain the momentum equation for a unit mass after dividing by the density. The resulting equation has the dimensions of an acceleration:

$$\frac{\partial\vec{v}}{\partial t} + (\vec{v}V)\,\vec{v} = \vec{g} - \frac{1}{\varrho}Vp + \nu\Delta\vec{v} - \overline{(\vec{v}'\circ\vec{v}')}\,V. \tag{7.14}$$

This is the so-called Reynolds equation, named after its originator Osborne Reynolds. The equations for the scalar components, in rectangular coordinates, are

$$\frac{\partial v_x}{\partial t} + v_x\frac{\partial v_x}{\partial x} + v_y\frac{\partial v_x}{\partial y} + v_z\frac{\partial v_x}{\partial z} = g_x - \frac{1}{\varrho}\frac{\partial p}{\partial x} + \\ + \nu\left(\frac{\partial^2 v_x}{\partial x^2} + \frac{\partial^2 v_x}{\partial y^2} + \frac{\partial^2 v_x}{\partial z^2}\right) - \frac{\partial}{\partial x}\overline{(v_x'v_x')} - \frac{\partial}{\partial y}\overline{(v_x'v_y')} - \frac{\partial}{\partial z}\overline{(v_x'v_z')}\,;$$

$$\frac{\partial v_y}{\partial t} + v_x\frac{\partial v_y}{\partial} + v_y\frac{\partial v_y}{\partial y} + v_z\frac{\partial v_y}{\partial z} = g_y - \frac{1}{\varrho}\frac{\partial p}{\partial y} + \\ + \nu\left(\frac{\partial^2 v_y}{\partial x^2} + \frac{\partial^2 v_y}{\partial y^2} + \frac{\partial^2 v_y}{\partial z^2}\right) - \frac{\partial}{\partial x}\overline{(v_y'v_x')} - \frac{\partial}{\partial y}\overline{(v_y'v_y')} - \frac{\partial}{\partial z}\overline{(v_y'v_z')}\,;$$

$$\frac{\partial v_z}{\partial t} + v_z\frac{\partial v_z}{\partial_x} + v_y\frac{\partial v_z}{\partial y} + v_z\frac{\partial v_z}{\partial z} = g_z - \frac{1}{\varrho}\frac{\partial p}{\partial z} + \\ + \nu\left(\frac{\partial^2 v_z}{\partial x^2} + \frac{\partial^2 v_z}{\partial y^2} + \frac{\partial^2 v_z}{\partial z^2}\right) - \frac{\partial}{\partial x}\overline{(v_z'v_x')} - \frac{\partial}{\partial y}\overline{(v_z'v_y')} - \frac{\partial}{\partial z}\overline{(v_z'v_z')}\,. \tag{7.15}$$

It is clear from this equation, that the apparent turbulent stress tensor has six independent scalar components. There is no relationship between the apparent turbulent stresses and other kinematical quantities equivalent to Stokes's law for viscous stresses. A very good approximation, however, is provided by Prandtl's mixing-length theory for one-dimensional flow. This theory, within its range of validity, is in excellent agreement with experimental results.

The Kármán similarity criterion

The determination of similarity conditions for turbulent momentum transport is based on the momentum equation of turbulent flow. It is obvious, that our basic point of departure should be the Reynolds equation instead of the Navier—Stokes equation which is valid only for laminar flow. The scale equations for Eq. (7.13) which must be completed for the equation referring to the apparent turbulent stress, consist of the time averages of the dyadic product of the velocity fluctuations

$$\overline{(\vec{v}' \circ \vec{v}')}_* = \alpha_{v'v'} \overline{(\vec{v}' \circ \vec{v}')} . \tag{7.16}$$

We should note that the Reynolds equation has not three new unknown functions (v_x', v_y', v_z'), but six ($\overline{v_x' v_x'}$; $\overline{v_x' v_y'}$, etc.). It is necessary to write scale equations for the averaged products of the velocity fluctuations instead of for the fluctuation components. The condition of restricted similarity is satisfied by fulfilling the similarity for the inertial forces and the apparent turbulent forces. Thus we obtain the following relationship for the scale coefficients:

$$\frac{\alpha_v^2}{\alpha_r} = \frac{\alpha_{v' \circ v'}}{\alpha_r} . \tag{7.17}$$

After substitution, the Kármán number is obtained:

$$\mathrm{Ka} = \frac{\overline{(\vec{v}' \circ \vec{v}')_*}}{v_*^2} = \frac{\overline{(\vec{v}' \circ \vec{v}')}}{v^2} . \tag{7.18}$$

The conditions of uniqueness must be maintained. This is satisfied by taking the characteristic averaged fluctuations at the boundary of the domain, and a well-measurable mean velocity:

$$\mathrm{Ka} = \frac{\overline{(\vec{v}' \circ \vec{v}')_0}}{v_0^2} . \tag{7.19}$$

Turbulent flow is a relatively stochastic phenomenon. In spite of this it is possible to make an interpretation of the similarity between two turbulent flows. This is done by assessing the similarity of the two flows on the basis of the distribution of the averaged values of the function rather than their instantaneous values.

7.3 The balance of kinetic energy for turbulent flow

As is well known, the instantaneous velocity $\vec{v}_t$ of a turbulent flow may be considered to be the sum of the time-averaged velocity $\vec{v}$ and the superimposed velocity fluctuation $\vec{v}'$. Thus the kinetic energy of the averaged velocity field differs

from the average of the instantaneous kinetic energy, since the latter also includes the time average of the kinetic energy of the fluctuation:

$$\overline{\frac{\varrho v_t^2}{2}} = \varrho \frac{v^2}{2} + \varrho \overline{\frac{v'^2}{2}}. \tag{7.20}$$

The kinetic energy does not satisfy a conservation law, thus the balance of the kinetic energy of a turbulent flow is not an axiom of the conservation law, it can only be derived from the balance of momentum equation. From a practical point of view it is obvious that the most important equation is the one for the balance of the term $\varrho v^2/2$. However, the equations for the balance of $\overline{\varrho v_t^2/2}$ and $\overline{\varrho v'^2/2}$ also yield valuable information on the nature of a turbulent flow. To simplify the problem our attention is restricted solely to incompressible fluid flows.

The complete kinetic energy balance

In order to derive the balance equation for the total kinetic energy of a turbulent flow, the momentum equation is multiplied by the velocity $\vec{v}_t$, after which the time average is taken. In this manner we obtain

$$\begin{aligned}&\overline{(\vec{v}+\vec{v}')\frac{\partial}{\partial t}[\varrho(\vec{v}+\vec{v}')]} + \overline{(\vec{v}+\vec{v}')\varrho\{[(\vec{v}+\vec{v}')\circ(\vec{v}+\vec{v}')]\nabla\}} = \\ &= \varrho\overline{\vec{g}(\vec{v}+\vec{v}')} - \overline{(\vec{v}+\vec{v}')[\nabla(p+p')]} + \overline{\mu(\vec{v}+\vec{v}')\{[(\vec{v}+\vec{v}')\circ\nabla + \nabla\circ(\vec{v}+\vec{v}')]\nabla\}}.\end{aligned} \tag{7.21}$$

The averaging process is best understood by applying it term by term. For the first term on the left-hand side:

$$\overline{(\vec{v}+\vec{v}')\frac{\partial}{\partial t}[\varrho(\vec{v}+\vec{v}')]} = \frac{\partial}{\partial t}\left(\varrho\frac{v^2}{2}\right) + \frac{\partial}{\partial t}\overline{\left(\varrho\frac{v'^2}{2}\right)}.$$

The terms which are linear in $\vec{v}'$ disappear. This is also the case during the averaging of second term on the left-hand side (the convective term). This can first be resolved into the sum:

$$\begin{aligned}&\varrho\vec{v}[(\vec{v}\circ\vec{v})] + \varrho\overline{\vec{v}'[(\vec{v}\circ\vec{v})\nabla]} + \varrho\overline{\vec{v}[(\vec{v}'\circ\vec{v})\nabla]} + \varrho\overline{v[(v^*\circ\vec{v})\nabla]} + \\ &+ \varrho\overline{\vec{v}[(\vec{v}\circ\vec{v}')\nabla]} + \varrho\overline{\vec{v}'[(\vec{v}\circ\vec{v}')\nabla]} + \varrho\overline{\vec{v}[(\vec{v}'\circ\vec{v}')\nabla]} + \overline{\varrho\vec{v}'[(\vec{v}'\circ\vec{v}')\nabla]}.\end{aligned}$$

After a little manipulation and taking into account that

$$\operatorname{div}\vec{v}' = 0,$$

the averaging leads to the following result:

$$\varrho\vec{v}[(\vec{v}\circ\vec{v})\nabla] = \vec{v}\operatorname{grad}\left(\varrho\frac{v^2}{2}\right) = \operatorname{div}\left(\varrho\frac{v^2}{2}\vec{v}\right);$$

$$\varrho\overline{v'[(\vec{v}\circ\vec{v})\nabla]}=\vec{v}\,\mathrm{grad}\left(\varrho\frac{\overline{v'^2}}{2}\right)=\mathrm{div}\left(\varrho\frac{\overline{v'^2}}{2}\vec{v}\right);$$

$$\varrho\overline{v'[(\vec{v}\circ\vec{v}')\nabla]}=\varrho\overline{\vec{v}'[(\vec{v}'\nabla)\vec{v}]}=\varrho\overline{\vec{v}'\circ\vec{v}'}:\vec{v}\circ\nabla;$$

$$\varrho\vec{v}[\overline{(\vec{v}'\circ\vec{v}')\nabla}]=\mathrm{div}\,[\varrho\overline{(\vec{v}'\circ\vec{v}')\vec{v}}]=\varrho\overline{\vec{v}'\circ\vec{v}'}:\vec{v}\circ\nabla;$$

$$\varrho\overline{\vec{v}'[(\vec{v}'\circ\vec{v}')\nabla]}=\overline{\vec{v}'\,\mathrm{grad}\left(\varrho\frac{\overline{v'^2}}{2}\right)}=\mathrm{div}\left(\varrho\frac{\overline{v'^2}}{2}\vec{v}'\right).$$

For the first term on the right-hand side it is clear, that

$$\varrho\vec{g}(\vec{v}+\vec{v}')=\varrho\vec{g}\vec{v},$$

while for the second right-hand side term we have:

$$\overline{(\vec{v}+\vec{v}')[\nabla(p+p')]}=\vec{v}(\nabla\vec{p})+\overline{\vec{v}'(\nabla p)}+\overline{\vec{v}(\nabla p')}+$$

$$+\overline{\vec{v}'(\nabla p')}=\mathrm{div}\,(p\vec{v})+\mathrm{div}\,(\overline{p'\vec{v}'})-p\,\mathrm{div}\,\vec{v}-\overline{p'\,\mathrm{div}\,\vec{v}'}.$$

Terms linear in fluctuations disappear while the last two terms are also zero because of the incompressibility.

Finally, the averaging of the last term on the right-hand side (the viscous term) can be carried out. This can be easily modified before averaging:

$$\overline{\mu(\vec{v}+\vec{v}')[(\vec{v}\circ\nabla+\nabla\circ\vec{v}+\vec{v}'\circ\nabla+\nabla\circ v')\nabla]}=$$

$$=\mathrm{div}\,(2\mu\mathbf{S}\vec{v})-2\mu\mathbf{S}:\vec{v}\circ\nabla+\mathrm{div}\,(2\overline{\mu\mathbf{S}'\vec{v}'})-2\mu\mathbf{S}':v'\circ\nabla.$$

Since both $\mathbf{S}$ and

$$\mathbf{S}'=\frac{1}{2}(\vec{v}'\circ\nabla+\nabla\circ\vec{v}')$$

are symmetric second-order tensors, their products taken by the derivative tensors $\vec{v}\circ\nabla$ and $\vec{v}'\circ\nabla$ may be replaced by $\mathbf{S}:\mathbf{S}$ and $\mathbf{S}':\mathbf{S}'$.

Substituting all this into Eq. (7.21) we obtain the total kinetic energy equation:

$$\frac{\partial}{\partial t}\left(\varrho\frac{v^2}{2}+\varrho\frac{\overline{v'^2}}{2}\right)+\mathrm{div}\left[\varrho\frac{v^2}{2}\vec{v}+\varrho\frac{\overline{v'^2}}{2}\vec{v}+\varrho\frac{\overline{v'^2}}{2}\vec{v}'\right]=$$

$$=\varrho\vec{g}\vec{v}-\mathrm{div}\,(p\vec{v}+\overline{p'\vec{v}'})+\mathrm{div}\,[2\mu\mathbf{S}\vec{v}+2\overline{\mu\mathbf{S}'\vec{v}'}-\varrho\overline{(\vec{v}'\circ\vec{v}')\vec{v}}]-$$

$$-2\mu\mathbf{S}:\mathbf{S}-2\overline{\mu\mathbf{S}':\mathbf{S}'}. \tag{7.22}$$

The total kinetic energy equation for the turbulent flow of a fluid mass enclosed in an arbitrary, finite volume V, bounded by the closed surface (A), is obtained in

the familiar manner using Gauss's theorem:

$$\int_V \frac{\partial}{\partial t}\left(\varrho \frac{v^2}{2}\right) \mathrm{d}V + \int_{(A)} \varrho \frac{v^2}{2} \vec{v}\, \mathrm{d}\vec{A} + \int_V \frac{\partial}{\partial t}\left(\varrho \frac{\overline{v'^2}}{2}\right) \mathrm{d}V +$$

$$+ \int_{(A)} \varrho \frac{\overline{v'^2}}{2} \vec{v}\, \mathrm{d}\vec{A} + \int_{(A)} \varrho \frac{\overline{v'^2}}{2} \vec{v}'\, \mathrm{d}\vec{A} + \int_V 2\mu \mathbf{S} : \mathrm{d}V +$$

$$+ \int_V 2\overline{\mu \mathbf{S}' : \mathbf{S}'}\, \mathrm{d}V = \int_V \varrho \vec{g} \vec{v}\, \mathrm{d}V - \int_{(A)} p\vec{v}\, \mathrm{d}\vec{A} - \int_{(A)} \overline{p'\vec{v}'}\, \mathrm{d}\vec{A} +$$

$$+ \int_{(A)} 2\mu \mathbf{S} \vec{v}\, \mathrm{d}\vec{A} + \int_{(A)} 2\overline{\mu \mathbf{S}' \vec{v}'}\, \mathrm{d}\vec{A} + \int_{(A)} \overline{(-\varrho \vec{v}' \circ \vec{v}')} \vec{v}\, \mathrm{d}\vec{A}\,. \tag{7.23}$$

This equation indicates that the rate of change of the total kinetic energy consists of the following five terms: the local and the convective derivatives of the kinetic energy of the mean flow, the local derivative of the averaged kinetic of the fluctuations, and two components of the convective derivative of the latter (depending on whether some particle crossed the bounding surface as a function of the mean velocity or of the fluctuation). The dissipation function consists of two parts: one of them is the dissipation function relating to the mean flow, the other is the irreversible conversion to internal energy due to the damping of the turbulent velocity fluctuations.

The turbulent velocity fluctuations show strong, random changes from one point to another; their derivative tensor is greater than the derivative tensor of the mean velocity field, especially away from the boundary walls. Thus the viscous dissipation function Φ may generally be neglected compared to the turbulent dissipation function Φ_t:

$$\Phi_t = 2\overline{\mu \mathbf{S}' : \mathbf{S}'} \gg 2\mu \mathbf{S} : \mathbf{S} = \Phi. \tag{7.24}$$

On the right-hand side of the balance of kinetic energy equation are terms representing the rate of work done by external forces. It is clear that turbulent energy transfer increases as a result of the work done by pressure fluctuations. The other terms represent the rate of work done by viscous forces and by the turbulent mixing process. The energy resulting from the rate of work of viscous and turbulent stresses is not totally lost. The last two terms on the left-hand side represent the irreversible production of internal energy. The work done by the viscous forces and the turbulent mixing may also take the form of the transfer mechanical energy (e. g. the energy transfer in the throat and diffuser of jet pumps).

Balance of kinetic energy in terms of the mean velocity

To derive the balance of kinetic energy in terms of the mean velocity, we multiply the balance of momentum equation scalarly with the mean velocity $\vec{v}$ and then, analogous to the previous deduction, we obtain a differential equation valid for a unit volume of fluid:

$$\frac{\partial}{\partial t}\left(\varrho\frac{v^2}{2}\right)+\operatorname{div}\left[\varrho\frac{v^2}{2}\vec{v}+\overline{(\varrho\vec{v}'\circ\vec{v}')}\vec{v}+p\vec{v}-2\mu\mathbf{S}\vec{v}\right]=$$

$$=\varrho\vec{g}\vec{v}+\varrho\overline{v'\circ v'}:\vec{v}\circ\nabla-2\mu\mathbf{S}:\mathbf{S}. \tag{7.25}$$

Let us transcribe this in the usual way into an integral equation taking into consideration that

$$\mathbf{T}':\mathbf{S}=-\varrho\overline{\vec{v}'\circ\vec{v}'}:\vec{v}\circ\nabla, \tag{7.26}$$

where $\mathbf{T}'$ is the symmetrical tensor of the apparent turbulent shear stress. This yields:

$$\int_V\frac{\partial}{\partial t}\left(\varrho\frac{v^2}{2}\right)\mathrm{d}V+\int_{(A)}\varrho\frac{v^2}{2}\vec{v}\,\mathrm{d}\vec{A}+\int_V 2\mu\mathbf{S}:\mathbf{S}\,\mathrm{d}V+\int_V\mathbf{T}':\mathbf{S}\,\mathrm{d}V=$$

$$=\int_V\varrho\vec{g}\vec{v}\,\mathrm{d}V-\int_{(A)}p\vec{v}\,\mathrm{d}\vec{A}+\int_{(A)}2\mu\mathbf{S}\vec{v}\,\mathrm{d}\vec{A}+\int_{(A)}\mathbf{T}'\vec{v}\,\mathrm{d}\vec{A}. \tag{7.27}$$

This equation indicates that the power due to the external forces on the right-hand side — body force, pressure force, viscous friction, and the apparent frictional force which replaces the turbulent momentum transfer — gives, on the one hand, the change in the kinetic energy per unit time, while on the other hand, in represents a loss of kinetic energy expressed by the average velocities. The first term of this loss represents the rate of viscous dissipation which is transformed irreversibly into internal energy during the average motion. The $\mathbf{T}':\mathbf{S}$ term represents the kinetic energy loss of the average motion as a consequence of the turbulent mixing. This is not identical to the turbulent dissipation function Φ_t! In the following we demonstrate that this proportion of the work rate is the source of the kinetic energy of the fluctuations.

Kinetic energy balance of velocity fluctuations

It is for this very reason that we define the kinetic energy balance of the velocity fluctuations. We multiply the momentum balance equation scalarly with $\vec{v}'$ and after averaging, we obtain the following relationship:

$$\frac{\partial}{\partial t}\left(\varrho\frac{\overline{v'^2}}{2}\right)+\operatorname{div}\left[\varrho\frac{\overline{v'^2}}{2}\vec{v}+\varrho\frac{\overline{v'^2}}{2}\vec{v}'+\overline{p'\vec{v}'}-2\overline{\mu\mathbf{S}'\vec{v}'}\right]=$$

$$=-\varrho\overline{\vec{v}'\circ\vec{v}'}:\vec{v}\circ\nabla-2\overline{\mu\mathbf{S}':\mathbf{S}'}. \tag{7.28}$$

If we now convert this into an integral equation, we get an expression where the physical meaning of the terms is extraordinarily well described:

$$\int_V \frac{\partial}{\partial t}\left(\varrho \frac{\overline{v'^2}}{2}\right) \mathrm{d}V + \int_{(A)} \varrho \frac{\overline{v'^2}}{2} \tilde{v}\, \mathrm{d}\vec{A} + \int_{(A)} \varrho \frac{\overline{v'^2}}{2} \tilde{v}'\, \mathrm{d}\vec{A} +$$

$$+ \int_V 2\mu \overline{\mathbf{S}' : \mathbf{S}'}\, \mathrm{d}V = - \int_{(A)} \overline{p'\tilde{v}'}\, \mathrm{d}\vec{A} + \int_{(A)} 2\mu \overline{\mathbf{S}'\tilde{v}'}\, \mathrm{d}\vec{A} + \int_{(V)} \mathbf{T}' : \mathbf{S}\, \mathrm{d}V. \quad (7.29)$$

The local and convective changes in the kinetic energy of the turbulent speed fluctuations result from the work expanded by the fluctuations in the static pressure and the frictional force that act on the bounding surface, as well as from the $\mathbf{T}' : \mathbf{S}$ source within the volume. Meanwhile that part of the rate of work defined by Φ_l will be irreversibly converted into internal energy.

In the case where a turbulently flowing mass of fluid is bounded by a fluid which is in equilibrium or experiencing laminar flow, the surface integrals will necessarily reduce to zero, since no fluctuation can originate from outside the volume. In this case kinetic energy can only be supplied to the velocity fluctuations from the $\mathbf{T}' : \mathbf{S}$ source.

Then the intensity of the $\mathbf{T}' : \mathbf{S}$ source will become less and less and not only will the turbulent velocity fluctuations decay, but the rate of strain vector $\mathbf{S}$ of the average motion will also tend to zero. The liquid body then moves like a solid body, i. e. solely by translation and rotation. This is how the oil in a tank-wagon takes up the speed of the tank after departure. Neglecting this phenomenon during sudden manoeuvres with large tankers has led to serious accidents at sea.

The equation of mechanical energy, which is of major importance in practice in transportation by pipeline, will be deduced from the equation in Chapter 8.

7.4 Determination of the apparent turbulent shear stress according to the mixing length theory

On the preceding pages it has already been mentioned that when the Reynolds equation of motion is used to describe turbulent flow, the number of unknown variables is increased: even in the simplest case where the tensor of the apparent turbulent shear stress is symmetrical, it is necessary to define six new unknown variables. At the present time no system of correlation analogous to Stokes's law is known, according to which the Reynolds' stresses and the kinematic parameters characterizing the average velocity field can be related to each other.

For practical purposes it has thus been tried to find such correlations between approximations which are suitable, at least in the case of one-dimensional flows, to permit the determination of the distribution of the mean velocity and the flow

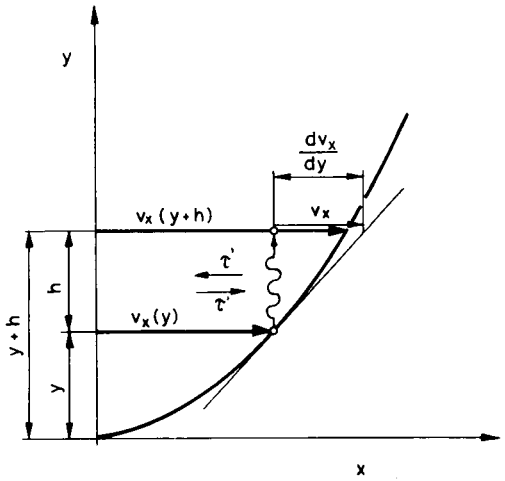

Fig. 7.2. Turbulent velocity profile showing the mixing length

resistance. The simplest of these approximation procedures was worked out by Prandtl.

Prandtl's hypothesis. Consider the mean velocity profile outlined in *Fig. 7.2.* At the wall the mean velocity is zero and it increases gradually with increasing distance away from the wall. At a distance y from the wall the mean velocity is $v_x(y)_p$ and the fluctuation components v_x' and v_y' are superimposed on it. The turbulent momentum transfer due to the fluctuations may be approximated in the following way. Consider that a fluid particle in the layer with a mean velocity v_x as moves upward as a result of the transverse fluctuation v_y' to a region at a distance $y+h$ from the wall. Here the mean velocity is greater, it is obtained by the linearization of the velocity profile as $v_x+\mathrm{d}v_x/\mathrm{d}y\,h$. In the new surrounding the mean velocity of the particle is smaller than the local average there. The difference

$$v_x(y)-v_x(y+h)$$

appears as the (negative) velocity fluctuation of the particle

$$v_x'=v_x-\left(v_x+\frac{\mathrm{d}v_x}{\mathrm{d}y}h\right)=-h\frac{\mathrm{d}v_x}{\mathrm{d}y}.$$

Conversely, the particle which arrives from above the layer with a negative v_y' gives rise to a positive v_x' in it. On the average therefore a positive v_y' is associated with a negative v_x', and a negative v_y' is associated with a positive v_x'.

Assume that v_x' and v_y' are of the same order of magnitude, thus we obtain

$$v_y'=\alpha h\frac{\mathrm{d}v_x}{\mathrm{d}y},$$

where α is a dimensionless multiplier.

Since the apparent turbulent shear stress for the one-dimensional mean flow is

$$\tau'_{xy} = -\varrho \overline{v'_x v'_y}, \tag{7.30}$$

it can be written, that

$$\tau'_{xy} = \varrho \alpha h^2 \overline{\left|\frac{dv_x}{dy}\right| \frac{dv_x}{dy}}.$$

Since α, h, and the mean velocity gradient are non-fluctuating quantities, they remain unchanged during averaging, so that we can simply write

$$\tau'_{xy} = \varrho \alpha h^2 \left|\frac{dv_x}{dy}\right| \frac{dv_x}{dy}. \tag{7.31}$$

It is obvious that there is a certain distance h between the mixing layers, at which the absolute values of the velocity fluctuations v'_x and v'_y are equal, so that $\alpha = 1$. This length is obtained to a characteristic quantity of the turbulent flow. It may be regarded as a correlation factor, and it is called the mixing length l. The mixing length can be considered as the average distance perpendicular to the mean flow covered by the mixing particles. If the turbulent momentum transfer is intense, the value of l increases. If, however, the degree of fluctuations decreases, l tends to zero. The mixing length changes with the distance from the wall. Prandtl assumed that

$$l_p = \kappa y, \tag{7.32}$$

where κ is a dimensionless constant, which is obtained indirectly from observations of the mean velocity distribution.

Kármán introduced another concept by means of the similarity theory. He assumed that mixing length had a real physical sense only, if the correlation is the same in all points of the flow region considered. This assumption seems to be valid in all cases in which mixing length is small in comparison with the dimensions of the region. Kármán's mixing length expression is

$$l_\kappa = \kappa \frac{\left|\frac{dv_x}{dy}\right|}{\left|\frac{d^2 v_x}{dy^2}\right|}, \tag{7.33}$$

where κ is the same constant as in Eq. (7.32). Thus the apparent turbulent shear stress is obtained as

$$\tau'_{xy} = \varrho \kappa^2 \left|\frac{dv_x}{dy}\right|^3 \left|\frac{d^2 v_x}{dy^2}\right|^{-2} \frac{dv_x}{dy}. \tag{7.34}$$

This relation yields velocity distributions and pipe resistance factors which are in excellent agreement with experimental results for flow in pipes or between parallel plates.

7.5 Turbulent flow through pipes

Balance of momentum for one-dimensional axisymmetric flow

Consider a steady flow through a straight cylindrical pipe of infinite length. The fluid is incompressible and the mean velocity has only one component; in the direction of the pipe axis. It is assumed that the distribution of the velocity fluctuations $u'$and $w'$are also axisymmetric. This assumption seems at first rather arbitrary, but the velocity distribution obtained from this solution is in good agreement with experimental data. The gravitational force has a potential

$$\vec{g} = -\operatorname{grad}(gh) .$$

Let us use cylindrical coordinates as shown in *Fig. 7.3.* Then the control volume of the integration is a cylinder of radius r and length L, coaxial with the pipe axis. The mean velocity field is steady, thus the local derivative of the momentum is zero. Hence:

$$\int_{(A)} \varrho \vec{v}(\vec{v}\,\mathrm{d}\vec{A}) = \int_{V} \varrho \vec{g}\,\mathrm{d}V - \int_{(A)} p\,\mathrm{d}\vec{A} + \int_{(A)} \mathbf{V}\,\mathrm{d}\vec{A} - \int_{(A)} \varrho\overline{(\vec{v}' \circ \vec{v}')}\,\mathrm{d}\vec{A} . \quad (7.35)$$

The surface integral on the left-hand side represents the convective change of momentum due to the mean velocity field. Along the *cylindrical stream surface* $\vec{v}\mathrm{d}\vec{A} = 0$. The *velocity distributions* are identical at the inlet and the outlet cross section but the unit normal vectors are in opposite directions. Thus this integral vanishes on account of the continuity condition. We now transform the surface integral of the pressure force into a volume integral, thus the first and the second terms of the right-hand side can be added up to form a volume integral of a

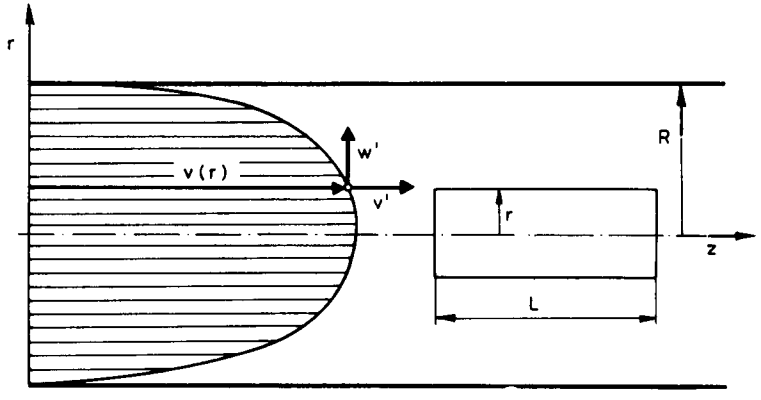

Fig. 7.3. Turbulent flow in cylindrical pipe

gradient vector. Equation (7.35) thus becomes:

$$0 = -\int_V \operatorname{grad}(\varrho g h + p)\,\mathrm{d}V + \int_{(A)} \mathbf{V}\,\mathrm{d}\vec{A} - \int_{(A)} \varrho\overline{(\vec{v}' \circ \vec{v}')}\,\mathrm{d}\vec{A}\,.$$

The viscous shear stress generated on the *cylindrical surface* is constant since the flow pattern is axisymmetric and does not change in the Z-direction.

At the inlet and the outlet cross section the flow patterns are the same but the unit normal vectors are in opposite directions, thus these two terms vanish. This is obviously also valid for the apparent turbulent shear stress. Consequently the second and third integrals should only be taken over the cylindrical surface of radius r.

The evaluation of the integrals is done in the following way. The force maintaining the motion is:

$$-\int_V \operatorname{grad}(\varrho g h + p)\,\mathrm{d}V = -\vec{k}\int_V \frac{\mathrm{d}}{\mathrm{d}z}(\varrho g h + p)\,\mathrm{d}V = Jr^2\pi L\vec{k}\,.$$

The sum $\varrho g h + p$ is a linear function of z only, thus its gradient is constant $(-J)$. Instead of integration we can multiply it simply by the volume. This does not require any special explanation. The viscous force acting on the cylindrical surface is:

$$\int_{Ap} \mathbf{V}\,\mathrm{d}\vec{A} = \int_{Ap} \varrho\frac{\mathrm{d}v}{\mathrm{d}r}\vec{k}\,\mathrm{d}A = \mu\frac{\mathrm{d}v}{\mathrm{d}r}2\pi rI\vec{k}\,.$$

Since the velocity decreases radially, the value of the derivative $\mathrm{d}v/\mathrm{d}r$ is negative and the sign of the viscous friction force is opposite to that of the force maintaining the motion. (Although this is not indicated by a negative sign.)

To determine the apparent force due to the turbulent exchange of momentum the following integral needs to be evaluated:

$$-\int_{Ap} \varrho\overline{(\vec{v}' \circ \vec{v}')}\,\mathrm{d}\vec{A}\,.$$

Let us assume an axisymmetric distribution for u' w' though of course, it also changes both with the radius and with z.

Based on Taylor's correlation theorem it is possible to replace the time average of the product of the velocity fluctuations with the mean integrated value of the same over the length L. This is acceptable since we can regard the mean integrated value of $\overline{u'w'}$ over the length L as a time average formed during the time $t_0 = L/v$ over which the averaging is carried out. Accordingly:

$$-\int_{Ap} \varrho\overline{(\vec{v}' \circ \vec{v}')}\,\mathrm{d}\vec{A} = -\int_{Ap} \varrho\overline{u'w'}\vec{k}\,\mathrm{d}A = -\varrho\overline{u'w'}2\pi rL\vec{k}\,.$$

If the evaluated integrals are now added and their sum divided by $2\pi rL$ we obtain the differential equation for turbulent flow in a pipe:

$$\frac{\varrho g J r}{2} + \mu \frac{\mathrm{d}v}{\mathrm{d}r} - \varrho \overline{u'w'} = 0 . \tag{7.36}$$

Solving this equation we can distinguish two domains in which the flow behavior is totally different.

Velocity distribution in the laminar sublayer

Experimental data show that all turbulent fluctuations vanish at the pipe wall, while they are very small in its immediate neighborhood. Thus the Reynolds stresses are zero in a very thin layer. Consequently, in every turbulent flow there exists this so-called laminar sublayer, in which the motion is laminar; thus for this laminar sublayer the third term of Eq. (7.36) may be omitted so that the differential equation for this sublayer is:

$$\frac{\varrho g J r}{2} + \mu \frac{\mathrm{d}v}{\mathrm{d}r} = 0 . \tag{7.37}$$

Integrating this the velocity profile may be obtained in this domain.

The thickness of the laminar sublayer δ is very small in comparison to the radius of the pipe, thus Prandtl introduced an additional assumption, namely that the shear stress τ is constant throughout the laminar sublayer and equal to the shear stress at the wall τ_R:

$$\tau = \tau_R = \frac{\varrho g J R}{2} .$$

Dividing the shear stress at the wall by the density, and then extracting the square root results in a parameter called the friction velocity

$$v_* = \sqrt{\frac{gJR}{2}} , \tag{7.38}$$

which has the dimension of velocity. Thus the differential equation

$$\frac{\mathrm{d}v}{\mathrm{d}r} = -\frac{v_*^2}{\nu} \tag{7.39}$$

is obtained from which, after integration, we obtain the velocity distribution in the laminar sublayer:

$$v = \frac{v_*^2}{\nu}(R - r) . \tag{7.40}$$

Velocity distribution in the turbulent region

Outside the laminar sublayer the effect of the viscous shear stress diminishes and the role of the turbulent momentum flux, the so-called Reynolds stress, increases. Under these conditions we can omit the second term, the viscous shear stress, from Eq. (7.36). In order to determine the velocity distribution of the turbulent core flow it is necessary to find an expression for the apparent turbulent shear stress which would relate it to the mean velocity. Prandtl's mixing-length theory is one of the simplest methods of estimating the Reynolds stress. As an extension of the mixing-length theory Kármán proposed the following expression

$$l_K = \frac{\left|\frac{dv}{dr}\right|}{\left|\frac{d^2v}{dr^2}\right|}, \tag{7.41}$$

which leads to the expression

$$\tau' = -\varrho\overline{u'w'} = -\varrho\kappa^2 \frac{\left(\frac{dv}{dr}\right)^4}{\left(\frac{d^2v}{dr^2}\right)^2} \tag{7.42}$$

for the turbulent momentum flux. After substitution we obtain:

$$\frac{gJr}{2} = \kappa^2 \frac{\left(\frac{dv}{dr}\right)^4}{\left(\frac{d^2v}{dr^2}\right)^2}. \tag{7.43}$$

This equation requires some manipulation, while care should also be taken with the sign of the square roots.

The derivative d^2v/dr^2 must be negative, since the velocity distribution reaches a maximum value along the centerline of the pipe. Thus, again using the friction velocity, we obtain:

$$-v_* \sqrt{\frac{r}{R}} = \kappa \frac{\left(\frac{dv}{dr}\right)^2}{\left(\frac{d^2v}{dr^2}\right)}. \tag{7.44}$$

Taking the reciprocal of both sides, we have

$$-\frac{\frac{d^2v}{dr^2}}{\left(\frac{dv}{dr}\right)^2} = \frac{\kappa}{v_*}\sqrt{\frac{R}{r}}, \tag{7.45}$$

80which can be readily integrated. After integration we obtain:

$$\frac{1}{\frac{dv}{dr}} = \frac{2\kappa}{v_*}\sqrt{Rr} + K_1 . \tag{7.46}$$

In order to determine the constant of integration K_1 we may prescribe as a boundary condition that the velocity gradient at the wall becomes infinite:

$$\left(\frac{dv}{dr}\right)_{r=R} = \infty .$$

This assumption is permitted since it is outside the validity interval of the solution.

Thus:

$$K_1 = -\frac{2\kappa R}{v_*} .$$

Substituting the constant K_1, the following expression is obtained:

$$\frac{1}{\left(\frac{dv}{dr}\right)} = -\frac{2\kappa R}{v_*}\left(1 - \sqrt{\frac{r}{R}}\right).$$

Taking the reciprocal of both sides and integrating yields

$$v = \frac{v_*}{\kappa}\left[\sqrt{\frac{r}{R}} + \ln\left(1 - \sqrt{\frac{r}{R}}\right)\right] + K_2 . \tag{7.47}$$

Now we need one more boundary condition to determine the constant of integration K_2. It is a known experimental fact, that the maximum of the velocity distribution is at the pipe axis. Therefore, at $r=0$, $v=v_{max}$, thus $K_2=v_{max}$.

Thus we obtain the following dimensionless velocity profile:

$$\frac{v_{max}-v}{v_*} = -\frac{1}{\kappa}\left[\sqrt{\frac{r}{R}} + \ln\left(1 - \sqrt{\frac{r}{R}}\right)\right]. \tag{7.48}$$

This relation offers a good description of the velocity distribution, but does contain v_{max} as an unknown arbitrary additional term. It is obvious that the velocities are equal on both sides of the surface which forms the boundary between the turbulent core flow and the laminar sublayer adjacent to the wall. Thus the turbulent velocity profile must match that of the laminar sublayer at the position $r=R-\delta$, i. e.

$$\frac{v_*\delta}{\nu} = \frac{v_{max}}{v_*} + \frac{1}{\kappa}\left[\sqrt{\frac{R-\delta}{R}} + \ln\left(1 - \sqrt{\frac{R-\delta}{R}}\right)\right]. \tag{7.49}$$

A very important observation of Prandtl is that

$$\frac{v_* \delta}{\nu} = \alpha = \text{const}.$$

Since $\delta/R \ll 1$, the following approximations based on the binominal theorem are convenient:

$$\sqrt{1-\frac{\delta}{R}} = 1$$

and

$$\ln\left(1-\sqrt{1-\frac{\delta}{R}}\right) = \ln\left[1-\left(1-\frac{\delta}{2R}\right)\right] = \ln\frac{\delta}{2R}.$$

Substituting these expressions into the velocity profile which matches that of the laminar sublayer as given by Eq. (7.40), the following result is obtained:

$$\frac{v_{\max}}{v_*} = \frac{1}{\kappa}\ln\frac{v_* 2R}{\nu} - \frac{1}{\kappa}(1+\ln\alpha)+\alpha. \tag{7.50}$$

The constants α and κ can be determined from experimental data. One possible method is to evaluate these constants from velocity profile measurements, another one, which has less uncertainty, is by measuring the pressure drop for different flow rates. These methods yield the following values:

$$\alpha = 12.087,$$

$$\kappa = \ 0.407.$$

The velocity distribution along a radius is:

$$\frac{v}{v_*} = \frac{1}{\kappa}\left[\sqrt{\frac{r}{R}}+\ln\left(1-\sqrt{\frac{r}{R}}\right)\right] + \frac{1}{\kappa}\ln\left(\frac{\mathrm{Re}\, v_*}{c}\right) - \frac{1}{\kappa}(1+\ln\alpha)+\alpha. \tag{7.51}$$

This dimensionless velocity profile satisfies the boundary conditions. From this expression, the influence of the Reynolds number (Re) on the radial velocity distribution is obvious. The cross-sectional average velocity may be obtained by equation

$$\frac{c}{v_*} = \frac{1}{R^2\pi}\int_0^R \frac{v}{v_*} 2\pi r \, \mathrm{d}r. \tag{7.52}$$

Substituting v/v_* from Eq. (7.51) into Eq. (7.52), using the values for α and κ, and integrating we have:

$$\frac{c}{v_*} = \frac{v_{\max}}{v_*} - \frac{1}{\kappa}\frac{77}{60} = \frac{v_{\max}}{v_*} - 3.153. \tag{7.53}$$

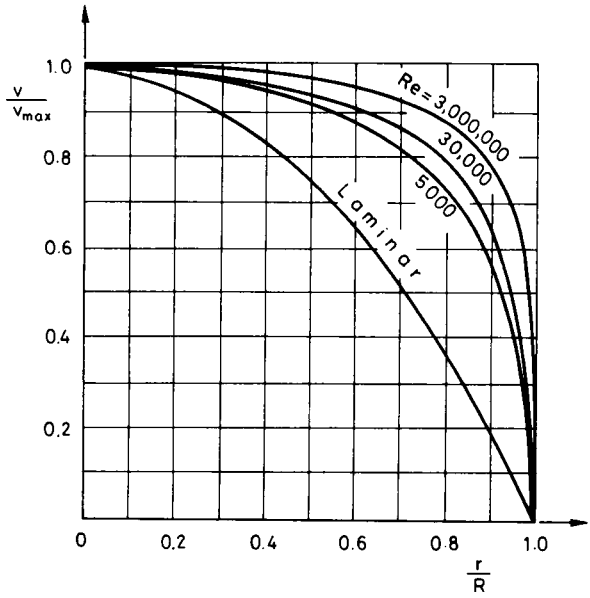

Fig. 7.4. Turbulent velocity distribution in a pipe

Finally, the averaged velocity is obtained as

$$\frac{c}{v_*} = 2.49 \cdot \ln\left(\frac{\mathrm{Re}\, v_*}{c}\right) - 2.811 .$$

Another dimensionless velocity profile is:

$$\frac{v}{v_{\max}} = 1 + \frac{\sqrt{\frac{r}{R}} + \ln\left(1 + \sqrt{\frac{r}{R}}\right)}{1.42 + \ln \mathrm{Re}\, \frac{v_*}{c}} . \tag{7.54}$$

Figure 7.4 demonstrates velocity distributions along the dimensionless pipe radius (r/R), taking the Reynolds number as parameter. This shows that the velocity distribution becomes more uniform over the cross section as the Reynolds number increases, while the averaged velocity tends to the hypothetical velocity distribution of a perfect fluid. As a consequence, during kinematic investigations, the inviscid, perfect fluid model can be used satisfactorily in the range of high Reynolds numbers. Naturally the perfect fluid model cannot be used for pressure-drop calculations because of the intensive turbulent dissipation.

7.6 Turbulent boundary-layer flow

The main feature of a turbulent flow is that the high frequency velocity fluctuations superimposed on the local time-averaged velocity tend to equalize the mean velocity distribution through a greater domain due to turbulent mixing accompanied by an intense dissipation of energy. Without other influences to disturb the flow, the mean velocity distribution of the turbulent flow will gradually become smoother and approximate closer and closer to the hypothetical velocity distribution of an inviscid perfect fluid flow. This tendency is very well reflected by the "dense" velocity profile of flows with high Reynolds numbers in pipes. For kinematic investigations it is a good approximation to assume the turbulent flow to be inviscid far away from disturbing influences e.g. solid boundaries. The surface of an immersed solid body represents a strong disturbance; it deforms the flow pattern. On the boundary surface of a solid body immersed in a turbulent flow the velocity is zero, and a laminar sublayer occurs along the body contour as well as along the pipe walls. Outside these very thin laminar sublayers, the velocity fluctuations increase rapidly, molecular transport of momentum becomes insignificant in comparison to turbulent momentum exchange, and a turbulent boundary layer is developed. The velocity gradient normal to the wall is very large across the boundary layer, outside of it the velocity gradients are small and the flow can be taken to be an inviscid potential flow. The velocity profile of the turbulent boundary layer will then gradually approximate a potential velocity distribution which is independent of the wall disturbances.

As with the laminar boundary layer, it is also difficult to determine the edge of the turbulent boundary layer. A broadly accepted convention is to define the boundary layer thickness as the distance from the wall where the velocity is smaller by 1% compared to the undisturbed velocity of the potential flow, i.e. where

$$v = 0.99\, U\,.$$

Boundary layer on a flat plate

The laminar-turbulent transition on the contour of an immersed body can be investigated in similar fashion as the flow through a pipe. Treating the undisturbed velocity U as a characteristic value and the boundary layer thickness as a characteristic length we obtain the Reynolds number for the boundary layer:

$$\mathrm{Re} = \frac{U\delta}{\nu}\,.$$

It is an interesting experimental observation that the flow is always laminar at an angle of zero incidence near the leading edge of an immersed flat plate, but that at a critical distance X_{cr} from the leading edge turbulent flow develops. The distance of the transition point depends on the intensity of turbulence in the

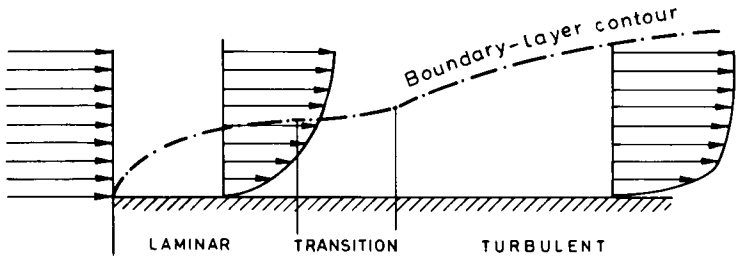

Fig. 7.5. Turbulent boundary-layer on a flat plate

undisturbed potential flow. A critical Reynolds number can be defined based on this critical length:

$$\mathrm{Re}_{cr} = \frac{UX_{cr}}{\nu}.$$

Thus, it can be seen that the numerical value of the critical Reynolds number lies within the interval

$$5 \times 10^5 \leq \mathrm{Re}_{cr} \leq 3 \times 10^6.$$

There are similar phenomena for boundary layers around spheres, cylinders and aerofoils. However, there are also significant differences concerning the detailed circumstances of these transition phenomena. For example, the intensity of turbulence in the upstream flow noticeably influences the position of the transition point. Whether the potential flow is accelerating or decelerating also has an impact on the laminar-turbulent transition: an accelerating potential flow delays the disintegration of the initial laminar boundary-layer flow, while in a decelerating potential flow the laminar-turbulent transition occurs sooner.

On the surface of a body immersed in a turbulent flow a boundary layer develops with a laminar and with a turbulent domain. The transition domain between these two is in practice found to be very narrow, thus it is an accepted approximation to regard this as the transition point *(Fig. 7.5)*.

For the flow between the leading edge and the transition point we can apply the formulas elaborated for laminar boundary layers. For the turbulent flow behind the critical point we have to generalize Prandtl's boundary-layer equations. In the same way that the Navier—Stokes equation led to the laminar boundary-layer equations, we can derive the correlations for turbulent boundary layers from the Reynolds equation. In this section only steady, two-dimensional turbulent boundary layers will be investigated. In view of the above analogy we find it unnecessary to go into the details of derivation. The equation of motion for the turbulent boundary layer is obtained in the following form:

$$v_x \frac{\partial v_x}{\partial x} + v_y \frac{\partial v_x}{\partial y} = U \frac{\mathrm{d}U}{\mathrm{d}x} + \frac{1}{\varrho} \frac{\partial \tau}{\partial y}, \tag{7.55}$$

to which clearly corresponds the continuity equation

$$\frac{\partial v_x}{\partial x} + \frac{\partial v_y}{\partial y} = 0 .$$

Here U is the velocity of the undisturbed potential flow outside of the boundary layer and τ is the sum of the viscous and the apparent turbulent shear stresses:

$$\tau = \mu \frac{\partial v_x}{\partial y} - \varrho \overline{v_x' v_y'} . \tag{7.56}$$

Using Prandtl's assumption for the apparent turbulent shear stress together with Kármán's formula for the mixing length, the apparent turbulent shear stress is obtained as:

$$\tau' = \varrho \kappa^2 \frac{\left(\frac{\mathrm{d}v_x}{\mathrm{d}y}\right)^4}{\left(\frac{\mathrm{d}^2 v_x}{\mathrm{d}y^2}\right)^2} .$$

Thus the equation of motion for the turbulent boundary layer can be written as:

$$v_x \frac{\partial v_x}{\partial x} + v_y \frac{\partial v_x}{\partial y} = U \frac{\mathrm{d}U}{\mathrm{d}x} + \nu \frac{\partial^2 v_x}{\partial y^2} + \kappa^2 \frac{\left|\frac{\mathrm{d}v_x}{\mathrm{d}y}\right|^3}{\left|\frac{\mathrm{d}^2 v_x}{\mathrm{d}y^2}\right|^2} \frac{\mathrm{d}v_x}{\mathrm{d}y} . \tag{7.57}$$

Since the velocity increases with the distance y from the wall, the derivatives are positive thus it is unnecessary to denote the absolute values. The continuity and momentum equations can thus be modified:

$$\frac{\partial}{\partial x}(v_x^2) + \frac{\partial}{\partial y}(v_x v_y) = U \frac{\mathrm{d}U}{\mathrm{d}x} + \nu \frac{\partial^2 v_x}{\partial y^2} + \kappa^2 \left(\frac{\mathrm{d}v_x}{\mathrm{d}y}\right)^4 \left(\frac{\mathrm{d}^2 v_x}{\mathrm{d}y^2}\right)^{-2} ,$$

$$\frac{\partial}{\partial x}(U v_x) + \frac{\partial}{\partial y}(U v_y) = v_x \frac{\mathrm{d}U}{\mathrm{d}x} . \tag{7.58}$$

If we subtract the first equation from the second we get the equation

$$\frac{\partial}{\partial x} v_x (U - v_x) + \frac{\partial}{\partial y} v_y (U - v_x) + (U - v_x) \frac{\mathrm{d}U}{\mathrm{d}x} =$$

$$= -\nu \frac{\partial^2 v_x}{\partial y^2} - \kappa^2 \frac{\left(\frac{\mathrm{d}v_x}{\mathrm{d}y}\right)^4}{\left(\frac{\mathrm{d}^2 v_x}{\mathrm{d}y^2}\right)^2} . \tag{7.59}$$

We should now integrate this equation with respect to y from zero to infinity or, as an approximation, from the wall to the boundary layer thickness $\delta(x)$. This approximation assumes that the velocity of the boundary layer tends asymptotically to the potential flow velocity U at an infinite distance from the wall.

If

$$y \to \infty; \qquad v_x = U(x), \quad \text{and} \quad \partial v_x/\partial y = 0 .$$

Instead of these, we use the approximations:

$$y = \delta(x); \qquad v_x = U(x), \quad \text{and} \quad \partial v_x/\partial y = 0 .$$

Thus the last two terms of Eq. (7.59) disappear at $y = \delta$. In the other hand, the apparent turbulent stress is zero at the wall:

$$y = 0; \qquad \tau' = 0; \qquad \tau_w = \mu \frac{\mathrm{d}v_x}{\mathrm{d}y} .$$

Integrating on the basis of these assumptions:

$$\int_0^\delta \frac{\partial}{\partial x}[v_x(U-v_x)]\,\mathrm{d}y + [v_y(U-v_x)]_0^\delta + \frac{\mathrm{d}U}{\mathrm{d}x}\int_0^\delta (U-v_x)\,\mathrm{d}y = -\nu\left[\frac{\partial v_x}{\partial y}\right]_0^\delta . \tag{7.60}$$

Let us also take into consideration that

$$\int_0^{\delta(x)} \frac{\partial}{\partial x}[v_x(U-v_x)]\,\mathrm{d}y = \frac{\mathrm{d}}{\mathrm{d}x}\int_0^{\delta(x)} v_x(U-v_x)\,\mathrm{d}y - [v_x(U-v_x)]_0^\delta \frac{\mathrm{d}\delta}{\mathrm{d}x} . \tag{7.61}$$

Thus we obtain the equation

$$\frac{\mathrm{d}}{\mathrm{d}x}\int_0^\delta v_x(U-v_x)\,\mathrm{d}y + \frac{\mathrm{d}U}{\mathrm{d}x}\int_0^\delta (U-v_x)\,\mathrm{d}y = \frac{\tau_w}{\varrho} . \tag{7.62}$$

Boundary-layer parameters

At this point we must digress slightly since we now have to define two important parameters of boundary-layer theory namely the so-called displacement thickness and the momentum thickness.

Let us consider an actual streamline inside the boundary layer, intersecting the edge of the boundary layer at the point B, where the boundary layer has a thickness δ. Let us furthermore examine the streamline of the inviscid potential flow, which is congruent with this actual streamline at infinity *(Fig. 7.6)*. We shall define the displacement thickness as $\delta^* = BB_{id}$ the distance between the real and the ideal streamlines. Since the same quantity of fluid must flow between these streamlines,

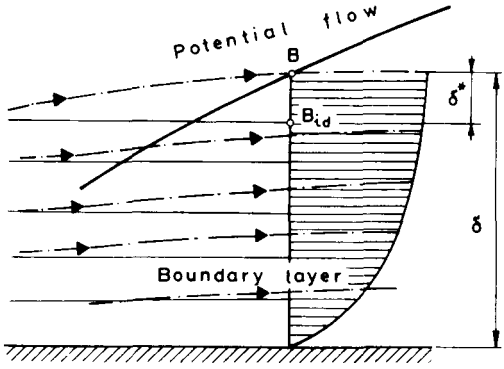

Fig. 7.6. Displacement and momentum thickness

applying the continuity equation for both the boundary-layer flow and the potential flow, we get:

$$\int_0^y v_x \, dy = U(y - \delta^*) . \tag{7.63}$$

Because of the relatively small boundary-layer thickness, the velocity of the potential flow U may be considered to remain constant. At the wall ($y=0$) there is obviously no difference between the real and the ideal streamlines, both being a zero streamline. As the distance from the wall increases, the difference between the real and the ideal streamlines will also increase, reaching a maximum at the edge of the boundary layer ($y=\delta$). The thickness of the layer δ^* by which the real streamline is deflected away from the ideal one is a function of the reduction in velocity in the boundary layer. It is equivalent to a thickening of the body contour by the thickness δ^*. The displacement of the streamline, the so-called displacement thickness, is given by the formula

$$\delta^* = \int_0^\delta \left(1 - \frac{v_x}{U}\right) dy , \tag{7.64}$$

and attains its maximum value at the edge of boundary layer.

Applying the momentum equation to the boundary layer flow, we obtain a physically meaningful parameter, the so-called momentum thickness:

$$\delta^{**} = \int_0^\delta \frac{v_x}{U}\left(1 - \frac{v_x}{U}\right) dy . \tag{7.65}$$

The momentum thickness expresses the reduction of momentum of the flow due to the frictional resistance of the wall.

Substituting these expressions into the momentum equation and integrating in the y-direction across the boundary layer we obtain

$$\frac{\mathrm{d}}{\mathrm{d}x}(U^2\delta^{**})+U\frac{\mathrm{d}U}{\mathrm{d}x}\delta^{*}=\frac{\tau_w}{\varrho}. \tag{7.66}$$

Completing the derivation we get

$$\frac{\mathrm{d}\delta^{**}}{\mathrm{d}x}+\frac{U'}{U}(2\delta^{**}+\delta^{*})=\frac{\tau_w}{\varrho U^2}. \tag{7.67}$$

Introducing the so-called form-parameter as the ratio of the displacement thickness and the momentum thickness

$$H^{*}=\frac{\delta^{*}}{\delta^{**}}, \tag{7.68}$$

we obtain a simpler expression:

$$\frac{\mathrm{d}\delta^{**}}{\mathrm{d}x}+\frac{1}{U}\frac{\mathrm{d}U}{\mathrm{d}x}\delta^{**}(2+H^{*})=\frac{\tau_w}{\varrho U^2}. \tag{7.69}$$

This kind of momentum equation has a fundamental significance for boundary layer flows. (Note, that pro forma the same equation is also obtained for laminar boundary layers.)

Investigations of turbulent boundary layers generally make use of approximate methods. Some forms of semi-empirical treatment based on δ^{*} and δ^{**} values obtained from velocity profile measurements have important practical applications. When applying such semi-empirical methods, or during the experimental verification of theoretically obtained results, we tacitly assume that the experimental values, which have already been "time averaged" by the instruments employed, are equal to the mean values in the averaged Reynolds equation. Experimental results obtained for flow in pipes and for boundary layers along flat plates are in good agreement with this assumption.

Skin-friction drag for a flat plate with a turbulent boundary layer

The simplest application of the above-mentioned method is to determine the skin-friction drag of a flat plate placed in a potential flow at zero angle of incidence.

On the plate a turbulent boundary layer is formed. Let the potential flow velocity $U_\infty = U$ be constant; its gradient in the x-direction is clearly zero. Thus the momentum equation can be written as:

$$\frac{\mathrm{d}\delta^{**}}{\mathrm{d}x}=\frac{\tau_w}{\varrho U^2}. \tag{7.70}$$

For this approximate method we assume that the velocity distribution in the boundary layer is steady, i. e. $v_x(y)$ is the same at all cross sections along the length of the plate, and the dimensionless velocity profile is identical with that inside a pipe:

$$\frac{v_x}{v_*} = 2.5 \ln\left(\frac{v_* y}{\nu}\right) + 5.5 .$$

In the transition from the case of flow in a pipe to that of flow over a plate, the maximum velocity v_{max} in the pipe corresponds to the potential flow velocity of the plate, and the radius R of the pipe corresponds to the boundary layer thickness δ. The difference between the two cases is that the shear stress on the wall τ_w is not constant along the length of the plate, thus the friction velocity

$$v_* = \sqrt{\frac{\tau_w}{\varrho}}$$

is not constant; it is a function of x.

Let us first express the momentum thickness using the relationship for the dimensionless velocity distribution. At the edge of the boundary layer $y = \delta$, thus

$$\frac{U_\infty}{v_*} = 2.5 \ln\left(\frac{v_* \delta}{\nu}\right) + 5.5 = 2.5 \ln\left(\mathrm{Re} \frac{v_*}{U}\right) + 5.5 . \tag{7.71}$$

On the other hand

$$\frac{v_x}{v_*} = 2.5 \ln\left(\frac{y}{\delta} \frac{v_*}{\nu}\right) + 5.5 = 2.5 \ln\left(\mathrm{Re} \frac{y}{\delta} \frac{v_*}{U_\infty}\right) + 5.5 . \tag{7.72}$$

Comparing the two equations this leads to the expression:

$$\frac{v_x - U_\infty}{v_*} = 2.5 \ln \frac{y}{\delta} . \tag{7.73}$$

Substituting this into the equation for the momentum thickness, we get

$$\frac{c_F}{2} = \frac{\tau_w}{\varrho U_\infty^2} = \frac{1}{(5.75 \lg \mathrm{Re}^{**} + 3.8)^2} . \tag{7.74}$$

The constants A and B can be evaluated easily:

$$A = -2.5 \int_0^1 \ln\left(\frac{y}{\delta}\right) \mathrm{d}\left(\frac{y}{\delta}\right) = 2.5$$

$$B = -6.25 \int_0^1 \ln^2\left(\frac{y}{\delta}\right) \mathrm{d}\left(\frac{y}{\delta}\right) = -12.5 .$$

Since the momentum thickness δ^{**} can be determined more accurately than the boundary layer thickness δ, it is reasonable to introduce a modified Reynolds number Re_δ as follows:

$$\frac{\mathrm{Re}^{**}}{\mathrm{Re}_\delta} = 2.5\frac{v_*}{U_\infty} - 12.5\left(\frac{v_*}{U_\infty}\right)^2. \tag{7.75}$$

Expressing Re** in terms of this equation, and after substitution into Eq. (7.71) we get:

$$\frac{U_\infty}{v_*} = 2.5\ln\frac{\mathrm{Re}^{**}}{2.5 - 12.5\dfrac{v_*}{U_\infty}} + 5.5. \tag{7.76}$$

In this way the relationship between skin-friction drag and the modified Reynolds number is obtained. It is obvious, that

$$\frac{v_*}{U_\infty} = \sqrt{\frac{\tau_w}{\varrho U_\infty^2}}. \tag{7.77}$$

Thus

$$\frac{1}{\sqrt{\dfrac{\tau_w}{\varrho U_\infty^2}}} = 5.75\lg\mathrm{Re}^{**} - 5.75\lg\left(1 - 5\sqrt{\frac{\tau_w}{\varrho U^2}}\right) + 3.22. \tag{7.78}$$

The value of $\tau_w/\varrho U_\infty^2$ can be determined from this implicit expression by iteration or another approximate method. The last two terms depend only very slightly on Re**, thus it is an acceptable approximation to take an averaged value 3.8 for the last two terms of the equation. Thus the local drag coefficient is

$$\frac{c_F}{2} = \frac{\tau_F}{\varrho U_\infty^2} = \frac{1}{(5.75\lg\mathrm{Re}^{**} + 3.8)^2}. \tag{7.79}$$

Falkner suggests the simple formula:

$$\frac{c_F}{2} = 0.00655\,(\mathrm{Re}^{**})^{-\frac{1}{6}}. \tag{7.80}$$

Using this expression, the momentum equation is readily integrated to yield

$$\frac{\mathrm{d}\delta^{**}}{\mathrm{d}x} = \frac{\mathrm{d}\,\mathrm{Re}^{**}}{\mathrm{d}\left(\dfrac{U_\infty x}{\nu}\right)}. \tag{7.81}$$

From this equation we obtain

$$(\mathrm{Re}^{**})^{\frac{7}{6}} = \frac{7}{6}\cdot 0.00655\cdot\frac{U_\infty x}{\nu} + C. \tag{7.82}$$

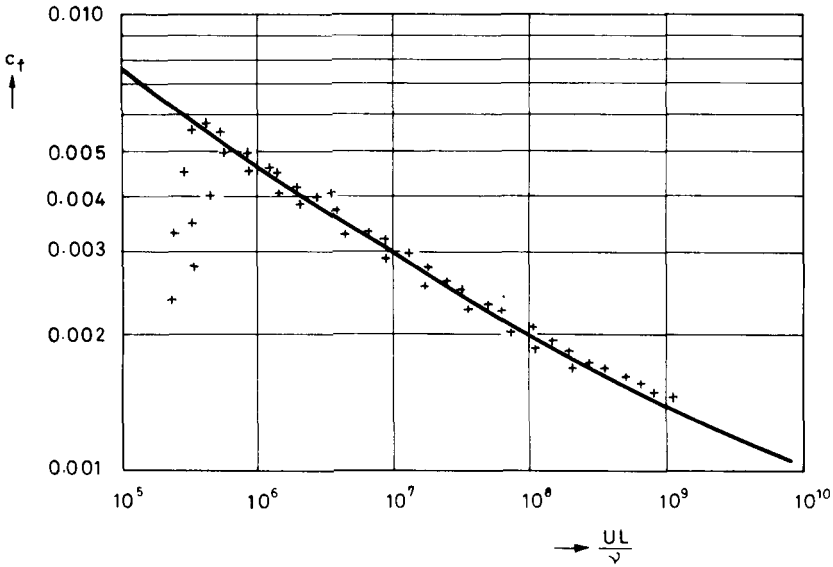

Fig. 7.7. Drag coefficient of a flat plate

Assuming, that the boundary layer at the plate is turbulent from the leading edge, i. e. neglecting the length of the laminar domain, we find that at $x=0$, $\delta^{**}=0$, and the constant of integration $C=0$. Thus the momentum thickness depends on the length as:

$$\delta^{**}=0.015\left(\frac{\nu}{U_\infty}\right)^{\frac{1}{7}} x^{\frac{6}{7}}. \tag{7.83}$$

Finally the total drag coefficient of the flat plate of length L is obtained as:

$$C_F=\int_0^1 c_F \,\mathrm{d}\left(\frac{x}{L}\right)=0.0307\,\mathrm{Re}^{-\frac{1}{7}}. \tag{7.84}$$

This agrees well with experimental measurement, especially at large Reynolds numbers, up to $\mathrm{Re}=10^9$ *(Fig. 7.7)*.

7.7 Turbulent flow in annuli

Figure 7.8 shows the cross section of a plain annulus consisting of an outer tube of inside radius R_2, and an inner tube of outside radius R_1. The position of the annulus is arbitrary, its symmetry axis coincides with the z-axis of the cylindrical coordinate system. The flow is one-dimensional, having only one velocity component $v_z=v$, while $v_r=v_\varphi=0$. The differential equation for this steady incom-

pressible flow (see Section 6.8) is

$$\varrho g J r + \mu \frac{\mathrm{d}}{\mathrm{d}r}\left(r \frac{\mathrm{d}v}{\mathrm{d}r}\right) + \frac{\mathrm{d}}{\mathrm{d}r}(r\tau'_{rz}) = 0 . \tag{7.85}$$

In the present case the apparent shear stress can be expressed in terms of the mixing length (see Section 7.3), as:

$$\tau'_{rz} = -\varrho l^2 \left|\frac{\mathrm{d}v}{\mathrm{d}r}\right| \frac{\mathrm{d}v}{\mathrm{d}r} .$$

Making use of Kármán's assumption that

$$l_\kappa = \kappa \frac{\left|\frac{\mathrm{d}v}{\mathrm{d}r}\right|}{\left|\frac{\mathrm{d}^2 v}{\mathrm{d}r^2}\right|},$$

we obtain the equation

$$g J r + \nu \frac{\mathrm{d}}{\mathrm{d}r}\left(r \frac{\mathrm{d}v}{\mathrm{d}r}\right) + \frac{\mathrm{d}}{\mathrm{d}r}\left[-r\kappa^2 \frac{\left|\frac{\mathrm{d}v}{\mathrm{d}r}\right|^3}{\left|\frac{\mathrm{d}^2 v}{\mathrm{d}r^2}\right|^2} \frac{\mathrm{d}v}{\mathrm{d}r}\right]. \tag{7.86}$$

A measured velocity profile is also shown in *Fig. 7.8*. The velocity of the fluid at the walls of the annulus is zero, while at some point between these walls the velocity

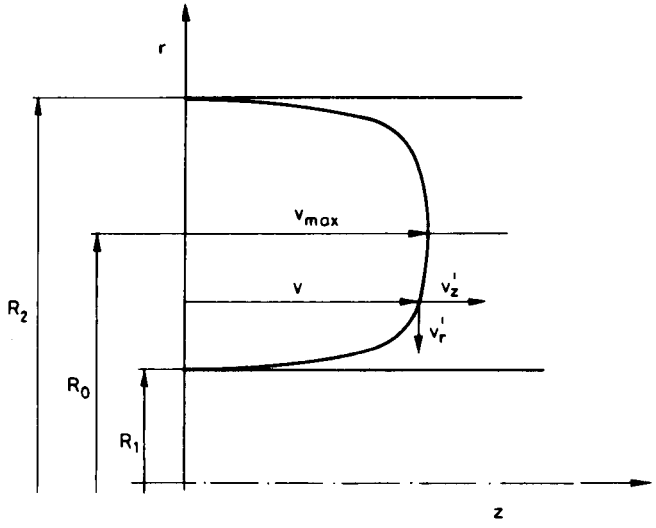

Fig. 7.8. Turbulent jet

distribution has a maximum value. These observations lead to certain consequences.

At the annulus walls laminar sublayers develop, inside which turbulence cannot occur. The turbulent region may be subdivided into two domains, depending on the sign of the turbulent shear stress. Where the velocity increases with the radius, e.g. $R_1 \leq r \leq R_0$,

$$\tau' = \varrho \kappa^2 \frac{\left(\frac{dv}{dr}\right)^4}{\left(\frac{d^2v}{dr^2}\right)^2}.$$

At the radius $r = R_0$, where the velocity distribution reaches a maximum

$$\tau' = 0.$$

Where the velocity decreases with the radius, e.g. $R_0 \leq r \leq R_2$

$$\tau' = -\varrho \kappa^2 \frac{\left(\frac{dv}{dr}\right)^4}{\left(\frac{d^2v}{dr^2}\right)^2}.$$

Thus the momentum equation has to be solved for four domains: the two laminar sublayers, and the regions of the increasing and decreasing turbulent stresses, as shown in *Fig. 7.9.*

For the laminar sublayers the linearized velocity distributions are obtained as

$$v_1 = \frac{gJ}{2\nu} \frac{R_0^2 - R_1^2}{R_1} (r - R_1), \tag{7.87}$$

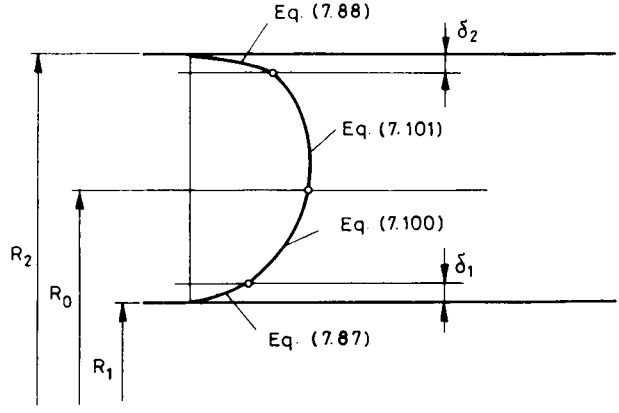

Fig. 7.9. Velocity maximums of a turbulent jet

and

$$v_2 = \frac{gJ}{2\nu}\,\frac{R_2^2 - R_0^2}{R_2}(R_2 - r)\,. \tag{7.88}$$

The friction velocities can be calculated as

$$v_{*_1}^2 = \frac{\tau_{R_1}}{\varrho} = \frac{gJ}{2}\,\frac{R_0^2 - R_1^2}{R_1}\,, \tag{7.89}$$

and

$$v_{*_2}^2 = \frac{\tau_{R_2}}{\varrho} = \frac{gJ}{2}\,\frac{R_2^2 - R_0^2}{R_2}\,. \tag{7.90}$$

In the region where $R_0 \geq r \geq R_1$ the momentum equation can be written

$$-gJr = \frac{\mathrm{d}}{\mathrm{d}r}\left[r\kappa^2\,\frac{\left(\dfrac{\mathrm{d}v}{\mathrm{d}r}\right)^4}{\left(\dfrac{\mathrm{d}^2v}{\mathrm{d}r^2}\right)^2}\right]. \tag{7.91}$$

After the first integration we have

$$-\frac{gJr}{2\kappa^2} + \frac{A}{\kappa^2 r} = \frac{\left(\dfrac{\mathrm{d}v}{\mathrm{d}r}\right)^4}{\left(\dfrac{\mathrm{d}^2v}{\mathrm{d}r^2}\right)^2}\,. \tag{7.92}$$

Since at the point where $r = R_0$ the velocity reaches a maximum, i.e. $\mathrm{d}v/\mathrm{d}r = 0$, it is obvious that the constant of integration

$$A = \frac{gJR_0^2}{2}\,. \tag{7.93}$$

Substituting into Eq. (7.92) we obtain

$$\frac{gJ}{2\kappa^2}\left(\frac{R_0^2}{r} - r\right) = \frac{\left(\dfrac{\mathrm{d}v}{\mathrm{d}r}\right)^4}{\left(\dfrac{\mathrm{d}^2v}{\mathrm{d}r^2}\right)^2}\,. \tag{7.94}$$

By substituting the friction velocity, and after taking the square root we obtain

$$\frac{\dfrac{\mathrm{d}^2v}{\mathrm{d}r^2}}{\left(\dfrac{dv}{\mathrm{d}r}\right)^2} = \frac{\kappa}{v_{*_1}}\sqrt{\frac{R_0^2 - R_1^2}{R_0^2 - r^2}\,\frac{r}{R_1}}\,. \tag{7.95}$$

This equation cannot be integrated directly, but the integrand can be approximated by an integrable function:

$$\sqrt{\frac{r}{R_0^2-r^2}} = \sqrt{\frac{R_1}{R_0+R_1}}\,\frac{1}{\sqrt{R_0-r}}.$$

Thus we get

$$\frac{1}{\dfrac{dv}{dr}} = -\frac{2\kappa}{v_{*_1}}\sqrt{(R_0-R_1)(R_0-r)}+B. \tag{7.96}$$

The boundary condition to determine the constant of integration B is

$$r=R_1; \qquad dv/dr=\infty .$$

Therefore,

$$B=\frac{2\kappa}{v_{*_1}}(R_0-R_1). \tag{7.97}$$

Substituting this constant we obtain

$$\frac{1}{\dfrac{dv}{dr}} = \frac{2\kappa(R_0-R_1)}{v_{*_1}}\left[1-\sqrt{\frac{R_0-r}{R_0-R_1}}\right]. \tag{7.98}$$

After integration the result is

$$\frac{v}{v_{*_1}} = -\frac{1}{\kappa}\left[\sqrt{\frac{R_0-r}{R_0-R_1}}+\ln\left(1-\sqrt{\frac{R_0-r}{R_0-R_1}}\right)\right]+C. \tag{7.99}$$

Since, at the point where $r=R_0$, $v=v_{\max}$, we obtain the equation

$$\frac{v-v_{\max}}{v_{*_1}} = -\frac{1}{\kappa}\left[\sqrt{\frac{R_0-r}{R_0-R_1}}+\ln\left(1-\sqrt{\frac{R_0-r}{R_0-R_1}}\right)\right]. \tag{7.100}$$

For the region $R_0 \le r \le R_2$ the solution is obtained in a similar way as:

$$\frac{v-v_{\max}}{v_{*_2}} = -\frac{1}{\kappa}\left[\sqrt{\frac{r-R_0}{R_2-R_0}}+\ln\left(1-\sqrt{\frac{r-R_0}{R_2-R_0}}\right)\right]. \tag{7.101}$$

At the laminar-turbulent interface, where

$$r=R_2-\delta_2$$

and

$$r=R_1-\delta_1,$$

we can write

$$\frac{v_{*_2}\delta_2}{\nu} = \frac{v_{*_2}}{\kappa}\left[\sqrt{1-\frac{\delta_2}{R_2-R_0}} + \ln\left(1-\sqrt{1-\frac{\delta_2}{R_2-R_0}}\right)\right],$$

and

$$\frac{v_{*_1}\delta_1}{\nu} = \frac{v_{*_1}}{\kappa}\left[\sqrt{1-\frac{\delta_1}{R_0-R_1}} + \ln\left(1-\sqrt{1-\frac{\delta_1}{R_0-R_1}}\right)\right].$$

Since $\delta_1 \ll R_0 - R_1$, and $\delta_2 \ll R_2 - R_0$, expanding into a binomial series we obtain

$$\frac{v_{*_2}\delta_2}{\nu} = \frac{v_{*_2}}{\kappa}\left[1+\ln\frac{\delta_2}{2(R_2-R_0)}\right] + v_{\max}, \tag{7.102}$$

and

$$\frac{v_{*_1}\delta_1}{\nu} = \frac{v_{*_1}}{\kappa}\left[1+\ln\frac{\delta_1}{2(R_0-R_1)}\right] + v_{\max}. \tag{7.103}$$

We may assume that Prandtl's hypothesis is valid for both laminar sublayers, thus resulting in the same value of

$$\frac{v_{*_1}\delta_1}{\nu} = \frac{v_{*_2}\delta_2}{\nu} = \alpha. \tag{7.104}$$

This leads to the expression

$$v_{*_1}\left[1+\ln\frac{\delta_1}{2(R_0-R_1)}\right] = v_{*_2}\left[1+\ln\frac{\delta_2}{2(R_2-R_0)}\right]. \tag{7.105}$$

The above equations, together with Eqs (7.89) and (7.90), form a system of equations with the unknowns v_{*_1}, v_{*_2}, $\delta_1\delta_2$, and R_0. The values of R_0 obtained by an iterative process can be approximated by the equation

$$R_0 = \frac{R_1 + R_2\left(\frac{R_1}{R_2}\right)^{\frac{7}{20}}}{1+\left(\frac{R_1}{R_2}\right)^{\frac{7}{20}}}. \tag{7.106}$$

Knowing R_0, the friction velocities v_{*_1} and v_{*_2} can be calculated, together with the laminar sublayer thicknesses δ_1 and δ_2. Thus the velocity distribution of the annular flow can be determined.

CHAPTER 8

ONE-DIMENSIONAL PIPE FLOW

8.1 One-dimensional approximation for flow in pipes

Problems of one-dimensional flow in pipes occur widely scattered throughout petroleum engineering practice. Design methods for drilling, cementing, hydraulic fracturing, production and pipeline transportation of oil and gas require the handling of such problems. The equations obtained earlier in this book are totally adequate for calculating the flow variables for the one-dimensional case. The particular importance of this type of flow requires a detailed review of the fundamental principles, limitations, and recommended design methods.

The flow of a fluid along a streamline in the form of an infinitesimal stream tube of varying cross section, is the simplest example of one-dimensional flow. Any flow through a pipe forms an analogy with a stream-tube flow. The bounding surface of a stream tube consists of streamlines, thus the velocity has no component normal to it. Since the pipe wall is obviously impermeable, it may be considered to represent a stream tube of finite cross section. An essential difference is that the flow variables are uniform over an infinitesimal cross-sectional area of the stream tube, while a pipe has a finite cross section across which the flow variables may have predetermined non-uniform distributions, though it is always possible to take at least the integral mean values as uniform variables. In engineering practice the pipe flow is assumed to be one-dimensional. This assumption is only an approximation, and certain corrections have to be applied in order to get practical results.

Difficulties arise due to the entrance section of the pipe, the curvature of the flow and changes in the cross section. The longer the section of pipe, the better does the approximation of considering the flow to be one-dimensional apply. For large curvatures or moderate changes in cross section, the deviation from the one-dimensional character of the flow may be neglected.

It was shown in Chapter 6, that any pressure change normal to the flow direction is hydrostatic. Consider now a flow in a cylindrical pipe in which all streamlines are parallel to the pipe axis. In any cross section the hydrostatic equation for two arbitrary points 1 and 2 can be written:

$$p_1 + z_1 \varrho g = p_2 + z_2 \varrho g \,.$$

From this it can be seen that although the pressure and the potential energy may vary considerably over the cross section, their sum remains constant. Thus for any

cross section of a pipe with finite size, the single value represented by this sum applies to the whole flow or to any of the individual streamlines which compose it. Thus no change has to be made as an infinitesimal stream tube is expanded to encompass a pipe of finite size; the sum of the pressure and the potential energy is uniform over any cross section, assuming, of course, that the streamlines are straight, parallel lines. It is obvious, that $p+z\varrho g$ cannot remain constant if the streamlines are sharply convergent, divergent or curved, so that the flow cannot be considered to be one-dimensional.

8.2 Basic equations for one-dimensional flow in pipes

An arbitrary flow problem can be solved, at least in principle, by the simultaneous solution of a set of balance equations. These are the equations for the conservation of mass, the balance of momentum, balance of kinetic and internal energy, and the equation of state. Tacitly, the balance of angular momentum is taken into account by the symmetry of the stress tensor. Similarly, the constitutive relation of a Newtonian fluid is incorporated into the Navier—Stokes, Reynolds, or energy equations. Boundary conditions are added to complete the mathematical model. The integral forms of these basic equations are especially suitable to obtain the simpler expressions for pipe flow. Consider first the equation for the conservation of mass. As previously shown in Chapter 3.

$$\int_V \frac{\partial \varrho}{\partial t} \mathrm{d}V + \int_{(A)} \varrho \vec{v} \, \mathrm{d}\vec{A} = 0 . \tag{8.1}$$

Let us apply the equation to the control volume shown in *Fig. 8.1.* The closed control surface (A) can be divided into three parts: the inlet surface A_1, the outlet surface A_2, and the pipe wall, treated as an impermeable stream surface A_3. As a result of this impermeability:

$$\vec{v} \, \mathrm{d}\vec{A} = 0 \qquad \text{at } A_3 .$$

The inlet and outlet cross sections are not necessarily perpendicular to the streamlines, thus the velocity vector $\vec{v}$ and the surface element vector $\mathrm{d}\vec{A}$ are not necessarily parallel. At the inlet cross section their scalar product must be negative, at the outlet cross section it is obviously positive. Let the mass of fluid contained in V be designated by M

$$M = \int_V \varrho \, \mathrm{d}V . \tag{8.2}$$

The integral mean of the velocity at any cross section is

$$c = \frac{1}{A} \int_A \vec{v} \, \mathrm{d}\vec{A} . \tag{8.3}$$

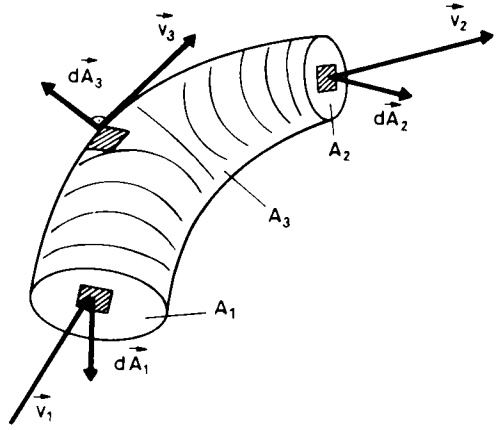

Fig. 8.1. Control volume for one-dimensional flow in a pipe

The area-averaged density is

$$\varrho = \frac{1}{A} \int_A \varrho \, \mathrm{d}A \,. \tag{8.4}$$

Thus the equation for the conservation of mass for the pipe section shown in *Fig. 8.1* can be written

$$-\frac{\partial M}{\partial t} = \varrho_2 A_2 c_2 - \varrho_1 A_1 c_1 \,. \tag{8.5}$$

For a steady flow

$$\varrho_2 A_2 c_2 = \varrho_1 A_1 c_1 = \dot{m} \tag{8.6}$$

(where $\dot{m}$ = mass/time [kg/s]),
thus the mass flow rate is the same across any cross section. For incompressible fluids

$$A_2 c_2 = A_1 c_1 = Q \,, \tag{8.7}$$

thus the flow rate Q at any cross section is constant and given by the usual expression for the cross-sectional average velocity

$$c = \frac{Q}{A} \,. \tag{8.8}$$

The momentum equation can be applied to a pipe section in the same way as the continuity equation. In its general form, we have

$$\int_V \frac{\partial(\varrho \vec{v})}{\partial t} \mathrm{d}V + \int_{(A)} \varrho \vec{v} (\vec{v} \, \mathrm{d}\vec{A}) = \int_V \varrho \vec{g} \, \mathrm{d}V + \int_{(A)} \mathbf{T} \, \mathrm{d}\vec{A} \,. \tag{8.9}$$

For steady flow this simplifies to

$$\int_{(A)} \varrho \vec{v}(\vec{v}\,\mathrm{d}\vec{A}) = \int_{V} \varrho \vec{g}\,\mathrm{d}V + \int_{(A)} \mathbf{T}\,\mathrm{d}\vec{A}\,. \tag{8.10}$$

The convective momentum flux through the pipe wall is obviously zero. Calculating the integral mean of the convective momentum flux it should be noted, that the integral mean of the product of velocities is not equal to the product of the integral means of the velocity. This can be corrected by using a multiplier α defined by the equation

$$\alpha = \frac{\int_{A} \varrho |\vec{v}|\,(\vec{v}\,\mathrm{d}\vec{A})}{Ac^2}\,. \tag{8.11}$$

The resultant of the body forces in a gravity field is obviously

$$\int_{V} \varrho \vec{g}\,\mathrm{d}V = M\vec{g}\,. \tag{8.12}$$

The stress tensor can be split into three components,

$$\mathbf{T} = -p\mathbf{I} + \mathbf{V} + \mathbf{T}', \tag{8.13}$$

where $\mathbf{V}$ is the viscous stress tensor and $\mathbf{T}'$ is the tensor of the Reynolds stresses.

For incompressible flow the shear stress distribution, as well as the Reynolds-stress distribution, is the same at any cross section. Since the surface normals at the inlet and at the outlet cross sections are opposite, the integrals of $(\mathbf{V}+\mathbf{T}')$ over A_1 and A_2 will cancel. For compressible flow this condition is only an approximation. At A_1 and A_2 the pressure will give non-zero integrals only. At the pipe wall, the normal stresses will cancel due to the symmetry, thus only the $(\mathbf{V}+\mathbf{T}')$ term produces non-zero results.

Thus, we finally obtain

$$\varrho Q(\alpha_2 \vec{c}_2 - \alpha_1 \vec{c}_1) = M\vec{g} + \vec{f}_1 + \vec{f}_2 + \vec{f}_3\,, \tag{8.14}$$

where

$$\vec{f}_1 = -\int_{A_1} p_1\,\mathrm{d}\vec{A}$$

$$\vec{f}_2 = -\int_{A_2} p_2\,\mathrm{d}\vec{A}$$

$$\vec{f}_3 = \int_{A_3} (\mathbf{V}+\mathbf{T}')\,\mathrm{d}\vec{A}\,.$$

In these expressions $\vec{f}_1$ is the resultant pressure force at the inlet, $\vec{f}_2$ is the same at the outlet, $\vec{f}_3$ is the resultant shear force acting on the system. The vector polygon which represents Eq. (8.14) geometrically is shown in *Fig. 8.2.*

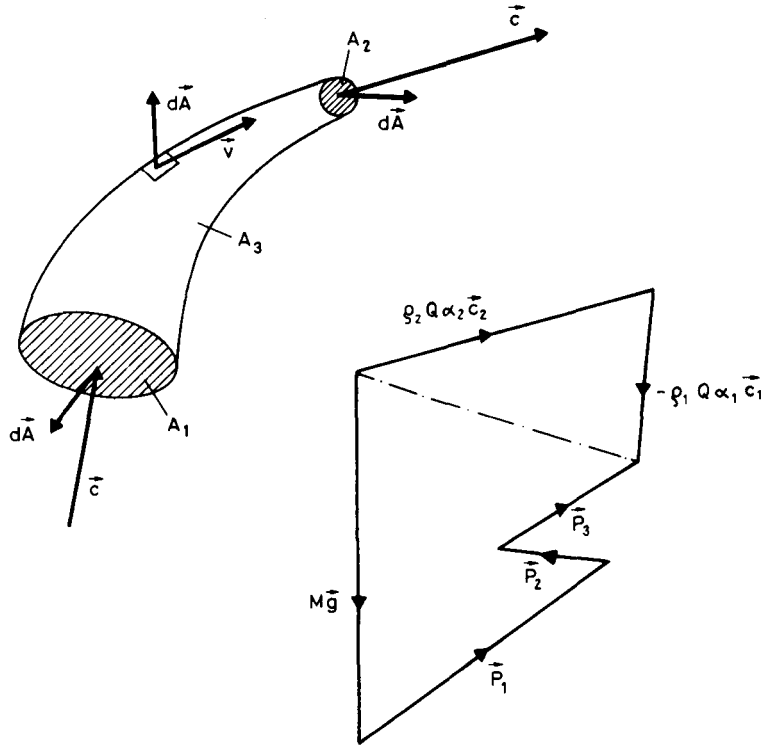

Fig. 8.2. Forces acting on a control volume of pipe flow

In the case of a one-dimensional flow in a pipe inclined at an angle φ to the horizontal, the equation simplifies to

$$p_1 A_1 - p_2 A_2 - f_3 = Mg \sin \varphi \,. \tag{8.15}$$

The mechanical energy equation for a barotropic fluid in a conservative body-force field can be written as

$$\int_V \frac{\partial}{\partial t}\left(\frac{v^2}{2} + U + \mathscr{P}\right) \varrho \, \mathrm{d}V + \int_{(A)} \varrho \left(\frac{v^2}{2} + U + \mathscr{P}\right) \vec{v} \, \mathrm{d}\vec{A} =$$

$$= \int_{(A)} \vec{v}(\mathbf{V} + \mathbf{T}') \, \mathrm{d}\vec{A} - \int_V (\mathbf{V} + \mathbf{T}') : \mathbf{S} \, \mathrm{d}V. \tag{8.16}$$

In discussing the continuity or the momentum equation, it is of no consequence whether the flow is laminar or turbulent, but for the kinetic energy equation this is of importance. For a turbulent flow it is even possible to write different formula-

tions for the balance of kinetic energy equation, based either on time-averaged velocities, or on the actual velocity fluctuations. For a one-dimensional flow in a pipe the first type of equation is most suitable. We shall confine ourselves to steady flows only. At the pipe wall $\vec{v}\,\mathrm{d}\vec{A} \equiv 0$. Note, that on the right-hand side of the equation the product $(\mathbf{V}+\mathbf{T}')\,\mathrm{d}\vec{A}$ must first be obtained, thus in this surface integral the condition $\vec{v}\,\mathrm{d}\vec{A} \equiv 0$ is not fulfilled. In spite of this the velocity at the pipe wall is zero, thus the integral over A_3 must vanish. The result is the same, but the manner in which it is obtained is different. Thus we have

$$\int_{A_2} \varrho\left(\frac{v^2}{2}+U+\mathscr{P}\right)\vec{v}\,\mathrm{d}\vec{A}+\int_{A_1}\varrho\left(\frac{v^2}{2}+U+\mathscr{P}\right)\vec{v}\,\mathrm{d}\vec{A}=$$

$$=\int_{A_2}\vec{v}(\mathbf{V}+\mathbf{T})\,\mathrm{d}\vec{A}+\int_{A_1}\vec{v}(\mathbf{V}+\mathbf{T}')\,\mathrm{d}\vec{A}-\int_V(\mathbf{V}+\mathbf{T}'):\mathbf{S}\,\mathrm{d}V. \tag{8.17}$$

Remember, that the turbulent shear stress is much greater than the viscous shear stress except within the laminar sublayer. Since the thickness of the latter is negligibly small relative to the diameter of the pipe, the viscous shear stress may be neglected. For a pipe of constant cross section the two surface integrals will cancel, since the velocity distributions are equal and the surface normals opposite. If the cross section changes, this condition is satisfied only approximately. For a long pipeline such an approximation is acceptable. For the integral mean of the convective kinetic energy flux a correction factor β is defined as

$$\beta=\frac{\int_A\left(\frac{v^2}{2}\right)\vec{v}\,\mathrm{d}\vec{A}}{\frac{c^3}{2}A}. \tag{8.18}$$

Thus we have

$$\varrho_2 A_2 c_2\left(\beta_2\frac{c_2^2}{2}+U_2+\mathscr{P}_2\right)+P_T=\varrho_1 A_1 c_1\left(\beta_1\frac{c_1^2}{2}+U_1+\mathscr{P}_1\right), \tag{8.19}$$

where P_T is the mechanical power loss due to the turbulent shear stress:

$$P_T=\int_V \mathbf{T}:\mathbf{S}\,\mathrm{d}V. \tag{8.20}$$

Since

$$\varrho_2 A_2 c_2=\varrho_1 A_1 c_1=\dot{m},$$

subdividing by the mass flow rate $\dot{m}$ we obtain

$$\beta_2\frac{c_2^2}{2}+U_2+\mathscr{P}_2+\frac{P_T}{\dot{m}}=\beta_1\frac{c_1^2}{2}+U_1+\mathscr{P}_1. \tag{8.21}$$

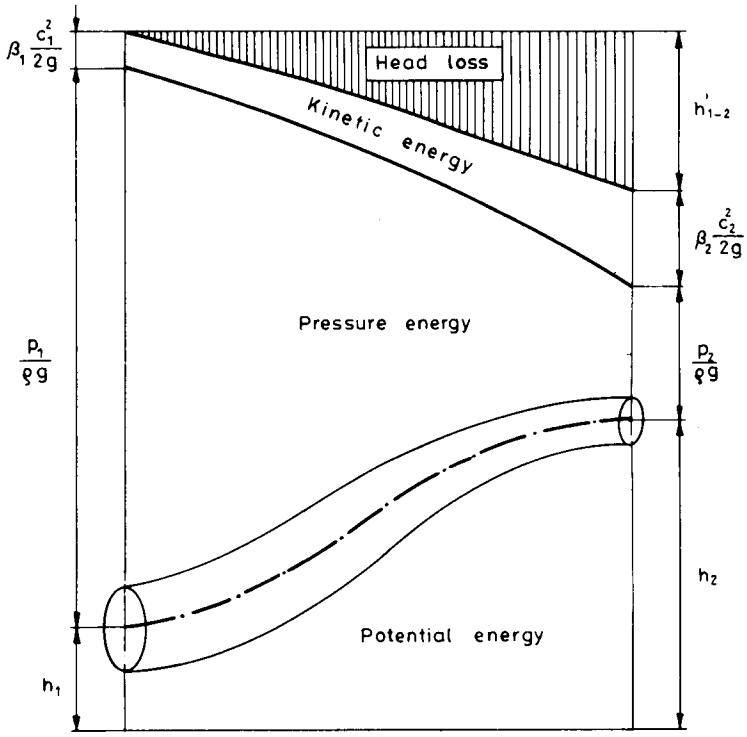

Fig. 8.3. Energy diagram for pipe flow

For the case of a gravity field and an incompressible fluid we obtain, after subdividing by $\tilde{g}$, the so-called viscous Bernoulli equation

$$\beta_2 \frac{c_2^2}{2g} + z_2 + \frac{p_2}{\varrho g} + h'_{1-2} = \beta_1 \frac{c_1^2}{2g} + z_1 + \frac{p_1}{\varrho g}, \tag{8.22}$$

in which

$$h'_{1-2} = \frac{P_T}{\dot{m} g} \tag{8.23}$$

is the so-called *head loss* it is the mechanical energy decrease per unit mass of fluid flowing between cross sections 1 and 2.

This mechanical energy equation in this Bernoulli-like form all the terms have the dimension of length. Because of this they may also be taken to represent vertical linear distances to visualize the equation as shown in *Fig. 8.3*. This visualization can be realized experimentally by using vertical piezometer tubes. In this case the slope of the *energy line* is parallel to the *hydraulic grade line*. This type of graphical representation, which is called an *energy diagram*, is widely used in the analysis of

engineering problems. The energy line and the hydraulic grade line are also known as the *total head line* and the *piezometric head line*, respectively.

For a laminar flow the head loss can be determined in a purely analytical way, since the Hagen—Poiseuille equation is valid for such a flow.

For a turbulent flow an approximate, almost analytical computation, the so-called Weisbach equation yields the head loss. This was originally determined as an empirical formula, and later confirmed by dimensional analysis. In this Chapter it will be derived by solving the momentum equation for turbulent flow.

The balance of total energy equation is applicable if the flow is steady and barotropic and the body force field is conservative. Thus the total energy is the sum of the mechanical energy and the internal energy. It can be written as

$$\int_{(A)} \left(\frac{v^2}{2} + U + \mathscr{P} + \varepsilon\right) \varrho \vec{v} \, \mathrm{d}\vec{A} = \int_{(A)} \vec{v}(\mathbf{V} + \mathbf{T}') \, \mathrm{d}\vec{A} - \int_{(A)} \vec{q} \, \mathrm{d}\vec{A}, \tag{8.24}$$

where ε is the specific internal energy and $\vec{q}$ is the heat flux vector. At the pipe wall its normal component can be expressed as

$$q_n = h(T_w - \tilde{T}), \tag{8.25}$$

where h is the convective heat transfer coefficient, T_w is the temperature of the pipe wall, and $\tilde{T}$ is the so-called bulk fluid temperature defined by the equation

$$\tilde{T} = \frac{\int_A T\vec{v} \, \mathrm{d}\vec{A}}{\int_A \vec{v} \, \mathrm{d}\vec{A}} = \frac{\int_A T\vec{v} \, \mathrm{d}\vec{A}}{Ac}. \tag{8.26}$$

The averaged value of the specific internal energy can be expressed in terms of this temperature as

$$\tilde{\varepsilon} = c_v \tilde{T}. \tag{8.27}$$

Experimental observations show that the convective flux of the internal energy across the surfaces A_1 and A_2 is much greater than the conductive heat flux across these surfaces. The Peclet number indicates that for a typical petroleum pipeline the convective flux is some 10^4 times greater than the conductive flux in the axial direction. A conductive heat flux can occur at the pipe wall only. The power of the viscous and turbulent stresses will cancel as in the preceding, see Eq. (8.17). Thus the total energy balance for a non-isothermal one-dimensional pipe flow is obtained:

$$\int_{A_2} \left(\frac{v^2}{2} + U + \mathscr{P} + c_v \tilde{T}\right) \varrho \vec{v} \, \mathrm{d}\vec{A} + \int_{A_1} \left(\frac{v^2}{2} + U + \mathscr{P} + c_v \tilde{T}\right) \varrho \vec{v} \, \mathrm{d}\vec{A} =$$

$$= \int_{A_3} h(T_w - \tilde{T}) \, \mathrm{d}A. \tag{8.28}$$

Using integral mean values this can be written as

$$\varrho_2 A_2 c_2 \left(\beta_2 \frac{c_2^2}{2} + U_2 + \mathscr{P}_2 + c_v \tilde{T}_2\right) - \varrho_1 A_1 c_1 \left(\beta_1 \frac{c_1^2}{2} + U_1 + \mathscr{P}_1 + c_v \tilde{T}_1\right) =$$

$$= \int_{A_3} h(T_w - \tilde{T})\, \mathrm{d}A\,. \tag{8.29}$$

If we assume a constant temperature at the wall, the last integral may be expressed as the log mean temperature difference for the wall surface A_3:

$$\int_{A_3} h(T_w - \tilde{T})\, \mathrm{d}A = h_{\ln} A_3 \left(\frac{T_w - \tilde{T}_2 - T_w - \tilde{T}_1}{\ln \dfrac{T_w - \tilde{T}_2}{T_w - \tilde{T}_1}} \right), \tag{8.30}$$

where we can now define the log mean temperature difference as

$$\Delta T_{\ln} = \frac{T_w - \tilde{T}_2 - T_w - \tilde{T}_1}{\ln\left(\dfrac{T_w - \tilde{T}_2}{T_w - \tilde{T}_1}\right)}. \tag{8.31}$$

The heat transfer coefficient corresponding to this case is called the log mean heat transfer coefficient.

The internal energy and the barotropic potential may be added; thus the enthalpy (i) is obtained. The total energy equation expressed in terms of the enthalpy is

$$\frac{\beta_2 c_2^2 - \beta_1 c_1^2}{2} + U_2 - U_1 + i_2 - i_1 = \frac{h_{\ln} A_3}{\dot{m}} \frac{T_w - \tilde{T}_2 - T_w - \tilde{T}_1}{\ln\left(\dfrac{T_w - \tilde{T}_2}{T_w - \tilde{T}_1}\right)}. \tag{8.32}$$

(h = convective heat transfer coefficient.)

For a perfectly insulated pipe the right-hand side of this equation becomes zero.

A comparison of the mechanical and the total energy equations shows that the head loss h'_{1-2} represents not an energy loss, but the sum of the change in internal energy and the transferred heat.

$$g h'_{1-2} = \varepsilon_2 - \varepsilon_1 - \frac{h_{\ln} A_3}{\dot{m}} \Delta T_{\ln}\,. \tag{8.33}$$

For a perfectly thermally insulated case, the head loss is equal to the increase in the internal energy of the flowing fluid.

8.3 Criteria for laminar, transitional and turbulent flow

It is well known that the flow of a viscous fluid may be laminar or turbulent. At sufficiently low velocities the fluid flows in laminae without mixing, whereas at greater velocities eddy currents develop and apparently random fluctuations occur in the flow. The criterion for the breakdown of laminar motion and the transition into turbulent flow is the critical value represented by the Reynolds number. As previously shown, the Reynolds number is a similarity criterion relating inertial forces to viscous forces. For circular pipes

$$\mathrm{Re} = \frac{cD}{\nu},$$

and its critical value is 2300. At lower Reynolds numbers the flow is always laminar, at greater Reynolds numbers it becomes turbulent. Notwithstanding this, laminar flow may still be observed at Reynolds numbers greater than 2300. Schlichting (1968) observed laminar flow at $\mathrm{Re} = 50\,000$, with a rounded pipe entrance and a vibrationless system.

In the other hand, deviations from a rigorously laminar flow may be observed at values as low as $\mathrm{Re} = 1200$. Repeating Reynolds's classical experiment the breakdown of a dye filament can be observed to proceed through certain characteristic phases.

Below the value of 1200 for the Reynolds number the dye filament is straight and stable. In the interval $1200 < \mathrm{Re} < 1250$ the filament remains threadlike but very small amplitude sinuous waves propagate along it. Above $\mathrm{Re} = 1250$ the thickness of the dye filament increases, as does the waviness. In the region $\mathrm{Re} \sim 1500$ a spiral motion develops in the core flow, and the further increase of the Reynolds number results eventually the generation of eddies. If the Reynolds number is greater than 2000 the flow is only just laminar; eddies of increasing size and frequency are generated. At the critical Reynolds number no abrupt change is observed. The completely turbulent flow develops in the interval of $2300 < \mathrm{Re} < 2800$. Random fluctuations of velocity and pressure are especially large in the interval $2300 < \mathrm{Re} < 4000$. Some characteristic flow patterns are shown in *Fig. 8.4*.

Similar behavior is observed for flow between parallel plates where the critical Reynolds number is found to be 2000. For a concentric annulus the critical Reynolds number is about 2200.

A stability analysis was made by Ryan and Johnson. It is based upon the assumption that a small perturbation is applied to the equation of motion for laminar flow. They obtained a stability parameter

$$Z = -\frac{R\varrho}{\tau_R} v \frac{\mathrm{d}v}{\mathrm{d}r}. \tag{8.34}$$

(τ_R is the stress shear at the pipe wall.)

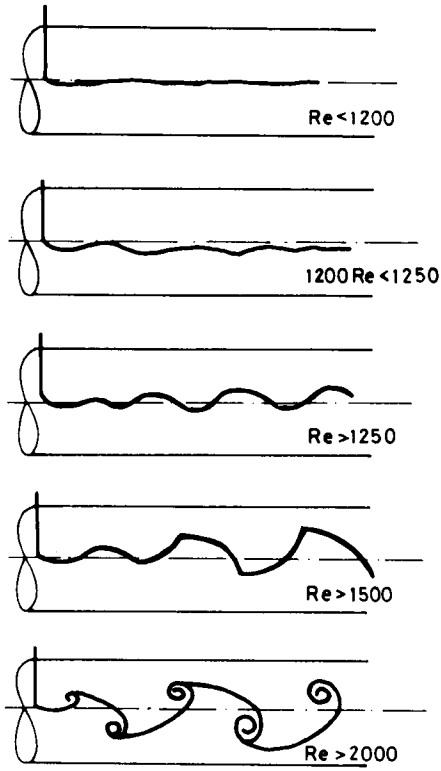

Fig. 8.4. Characteristic flow patterns during the laminar-turbulent transition in pipe flow

At the pipe wall $v=0$, thus $Z=0$. Along the pipe axis $dv/dr=0$, thus again $Z=0$. The maximum value of Z may be determined by substituting the velocity distribution of the laminar flow. Since

$$v=\frac{gJ}{4\nu}(R^2-r^2),$$

and

$$\frac{dv}{dr}=-\frac{gJr}{2\nu},$$

we obtain

$$Z=\frac{\varrho}{\tau_R}\left(\frac{gJ}{2\nu}\right)^2\frac{R^3r-Rr^3}{2}. \tag{8.35}$$

Since at the maximum value of Z

$$\frac{dZ}{dr}=\frac{\varrho}{2\tau_R}\left(\frac{gJ}{2\nu}\right)^2(R^3-3Rr^2)=0, \tag{8.36}$$

the location of the maximum is found to be at

$$r = \frac{R}{\sqrt{3}}. \tag{8.37}$$

Thus the maximum value of Z can be calculated since

$$\tau_R = \frac{\varrho g J R}{2},$$

and

$$c = \frac{g J R^2}{8\nu}.$$

Finally we obtain

$$Z_{\max} = \frac{2\mathrm{Re}}{\sqrt{27}}. \tag{8.38}$$

Since the turbulence occurs at $\mathrm{Re} = 2300$ this is equivalent with a value of $Z = 800$.

This criterion for the onset of turbulence in pipe flow is in a good agreement with experimental observations. Note, that the turbulence originates at a radius of $R/\sqrt{3}$ rather than at the axis of the pipe.

It was assumed in the derivation of the expression for the velocity distribution that the velocity did not change in the direction of the flow. This assumption is not quite valid; a certain distance is required for the development of the stabilized flow.

Consider first the case where the stabilized flow is laminar. When the fluid enters the pipe, the velocity profile is uniform. At the wall a boundary layer develops, which increases in thickness with increasing distance from the pipe entrance. The flow in the boundary layer remains entirely laminar. The final velocity profile develops when the growing boundary layer extends right up to the pipe axis *(Fig. 8.5)*.

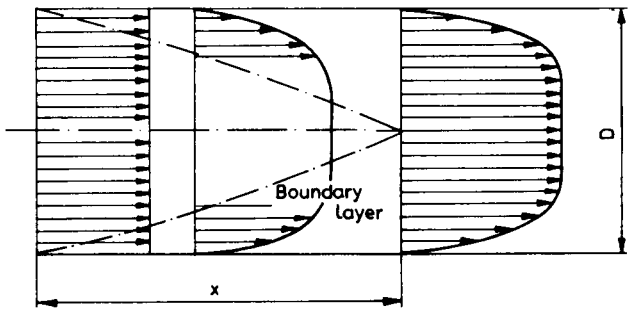

Fig. 8.5. Development of the velocity profile in the entrance section of a pipe

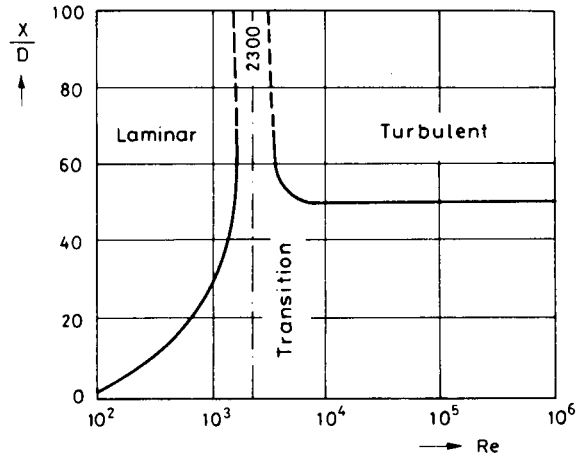

Fig. 8.6. Entry lengths of pipe flow

This phenomenon was investigated experimentally by Collins (in Schowalter) and McComas. The results obtained by them are shown in *Fig. 8.6*. At low Reynolds numbers the distance X from the entrance of the pipe to the occurrence of the fully developed laminar velocity profile depends on the Reynolds number and the diameter of the pipe and may be represented by the relation

$$\frac{X}{D} = 0.0280 \, \mathrm{Re} \, .$$

When the stabilized flow is turbulent, the distance required for stabilization is particularly sensitive to the nature of the pipe entrance. Knudsen and Katz determined experimentally, that in this case

$$\frac{X}{D} \geqq 50 \, .$$

Experimental observations indicate that very large entrance lengths are required for the development of stabilized flow in the interval of

$$2300 < \mathrm{Re} < 4000 \, .$$

This transition instability superimposing to the entrance instability leads to the uncertain length in this case.

8.4 Head loss in straight cylindrical pipes

The determination of head loss as a function of the flow rate is perhaps the most common problem of fluid mechanics. In this section we shall only consider the case of an incompressible Newtonian fluid. It is obvious, that the flow through a pipe

can be either laminar or turbulent. For a laminar flow the Hagen—Poiseuille equation gives the head loss as

$$h'_{1-2} = \frac{8\nu L c}{gR^2}. \tag{8.39}$$

For practical applications this equation has to be somewhat modified. In engineering practice the diameter of a pipe is given rather than the radius. We also wish to obtain an equation for the head loss which depends explicitly on the Reynolds number. Expressing Eq. (8.39) in terms of the diameter D and rearranging the terms, we have

$$h'_{1-2} = \frac{64}{\frac{cD}{\nu}} \frac{L}{D} \frac{c^2}{2g}, \tag{8.40}$$

which may be written as

$$h'_{1-2} = \lambda \frac{L}{D} \frac{c^2}{2g}, \tag{8.41}$$

where λ is called the friction factor. It can be calculated from the equation

$$\lambda = \frac{64}{\mathrm{Re}}. \tag{8.42}$$

This expression is valid for the range of $\mathrm{Re} < 2300$, i.e. laminar flow only. If the Reynolds number of the flow exceeds the critical value of 2300, the flow becomes turbulent, and the friction factor increases abruptly. Thus the smallest value of the friction factor is obtained for laminar flow immediately before the transition. For $\mathrm{Re} = 2300$ the friction factor is

$$\lambda = \frac{64}{2300} = 0.0278.$$

If the laminar-turbulent transition could be retarted the friction factor, and thus the head loss, would be much smaller. This is a frequently applied technique in the petroleum industry. Long-chain polymer additives can reduce the friction factor of a "solvent", thus retarding the laminar-turbulent transition. This phenomenon will be discussed in detail in the next chapter.

Turbulent flow is a more complex phenomenon compared to laminar flow. Thus the determination of the head loss for such flows is a rather difficult problem. For turbulent flow in a pipe two cases can be distinguished. If the laminar sublayer covers the surface roughness of the pipe wall the turbulent flow is not affected by the roughness, as the pipe can be considered to be absolutely smooth. This case is referred to as that of a turbulent flow in a hydraulically smooth pipe. On the other hand there are flows, where the laminar sublayer cannot cover the surface roughness of the pipe wall, or there is no laminar sublayer at the pipe wall. Such a flow is independent of the Reynolds number; all flow variables are functions of the

surface roughness only. When a pipe wall exhibits this behavior, it is called hydraulically fully rough.

Consider first the turbulent flow in a hydraulically smooth pipe. The mechanical energy equation can be written as

$$h'_{1-2} = \frac{\beta_1 c_1^2 - \beta_2 c_2^2}{2g} + h_1 - h_2 + \frac{p_1 - p_2}{\varrho g}. \tag{8.43}$$

Since the cross section of the pipe is constant and the fluid is incompressible

$$c_1 \equiv c_2; \qquad \beta_1 \equiv \beta_2 .$$

The head loss is obtained as

$$h'_{1-2} = h_1 - h_2 + \frac{p_1 - p_2}{\varrho g} = JL, \tag{8.44}$$

therefore it is the product of the hydraulic gradient J and the pipe length L. The hydraulic gradient can be expressed in terms of the friction velocity V_*, since by definition

$$J = \frac{2}{gR} v_*^2 . \tag{8.45}$$

Substituting this into the equation for h' we get

$$h'_{1-2} = \frac{2L}{gR} v_*^2 . \tag{8.46}$$

The friction velocity can be expressed in terms of the cross-sectional average velocity c:

$$\frac{c}{v_*} = \frac{1}{\kappa} \ln\left(\mathrm{Re}\frac{v_*}{c}\right) - \frac{1}{\kappa}(2.283 + \ln\alpha) + \alpha . \tag{8.47}$$

(See Chapter 7.)

It is clear that v_*/c depends on the Reynolds number only, since α and κ are temporarily unknown constants. Therefore,

$$\frac{v_*}{c} = f(\mathrm{Re}) . \tag{8.48}$$

This relationship together with Eq. (8.46) leads to the equation for the head loss

$$h'_{1-2} = 8f^2 \frac{L}{D} \frac{c^2}{2g}, \tag{8.49}$$

in which the group of coefficients $8f^2$ is designated by

$$\lambda = 8f^2(\mathrm{Re}), \tag{8.50}$$

which is the friction factor for the turbulent flow.

We can write

$$\frac{v_*}{c} = \sqrt{\frac{\lambda}{8}}. \tag{8.51}$$

This can be substituted into Eq. (8.47), thus resulting in an implicit equation for the friction factor:

$$\frac{1}{\sqrt{\frac{\lambda}{8}}} = \frac{1}{\kappa} \ln\left(\mathrm{Re}\sqrt{\frac{\lambda}{8}}\right) - \frac{1}{\kappa}(2.283 + \ln\alpha) + \alpha. \tag{8.52}$$

Assuming that α and κ are constants, we obtain the following values from friction factor measurements

$$\alpha = 12.087,$$

$$\kappa = 0.407.$$

Thus, using common logarithms, we can write

$$\frac{1}{\sqrt{\lambda}} = 2\lg(\mathrm{Re}\sqrt{\lambda}) - 0.8. \tag{8.53}$$

Experimental results confirm this equation to be valid with a fair degree of accuracy. Nikuradse conducted experiments on the turbulent flow of water in smooth pipes for Reynolds numbers ranging from 4000 to 3,240,000. The data of his investigation are shown in *Fig. 8.7*, where the friction factor is plotted versus the Reynolds number. The curve representing Eq. (8.53) is plotted as comparison.

Since the equation for the friction factor is obtained in implicit form, λ can be calculated by iteration. The convergence of the iteration is rather fast, particularly when the starting value of λ is chosen using *Fig. 8.7*. In such a case two, or at the most three, iteration steps are sufficient.

The surface of the pipe walls is usually quite rough. Glass and PVC pipes or drawn steel pipes may be considered to be smooth, but standard pipes are generally rather rough, even when new. This boundary roughness is shown schematically in *Fig. 8.8*. The average height of the roughness projections is expressed by the height k. The radius of the pipes is a fictitious length extending from the pipe axis to the average distance of the wall.

In hydraulically rough pipes there is no continuous boundary surface between the laminar sublayer and the turbulent core flow. For very large Reynolds numbers or very rough pipe walls there is no continuous laminar sublayer at all. The derived velocity distribution for the turbulent core flow is connected to the velocity of the laminar sublayer. It is obvious that this velocity profile equation cannot be valid for turbulent flow in rough pipes. Thus for rough pipes

a new equation for the velocity distribution is required in order to derive the friction factor equation.

Examining the micro-geometry of a commercial pipe wall, *(Fig. 8.8)* it is clear that this random surface profile is too complex to be characterized by a single parameter. A full characterization of the roughness would require a complete description of its geometry, including the height, length, width and shape of all protrusions or indentations, together with their distribution. This would be a hopeless task, thus for experimental purposes an artificially created roughness is used. Nikuradse (1933) applied uniform sand grains to cover the pipe wall; in his experiments the parameter k_s represents the grain size of the sand. The roughness of the wall in this case may be characterized by a single roughness parameter,

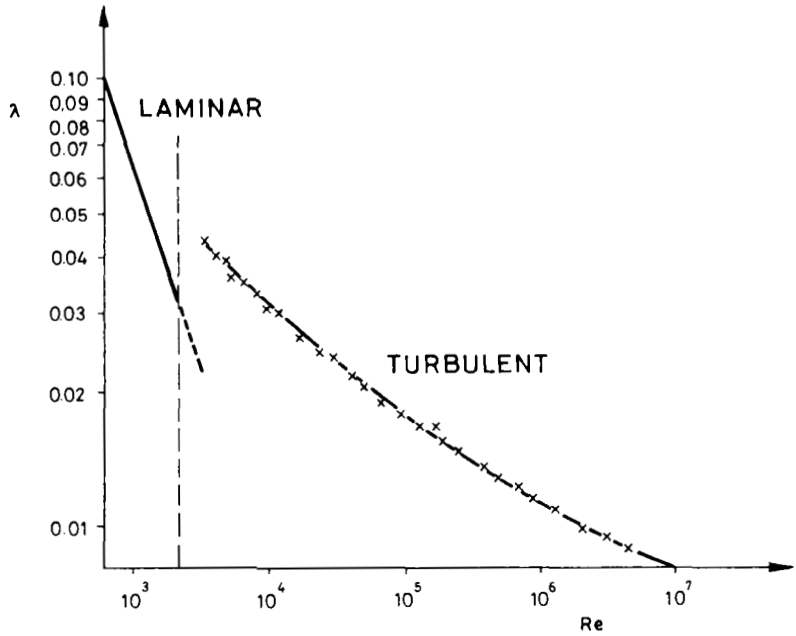

Fig. 8.7. Friction factor data of Nikuradse for smooth pipes

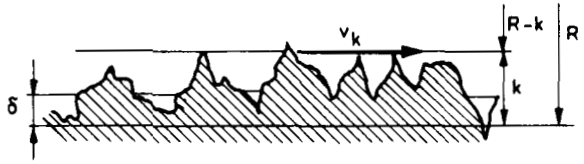

Fig. 8.8. Pipe wall roughness and laminar sublayer

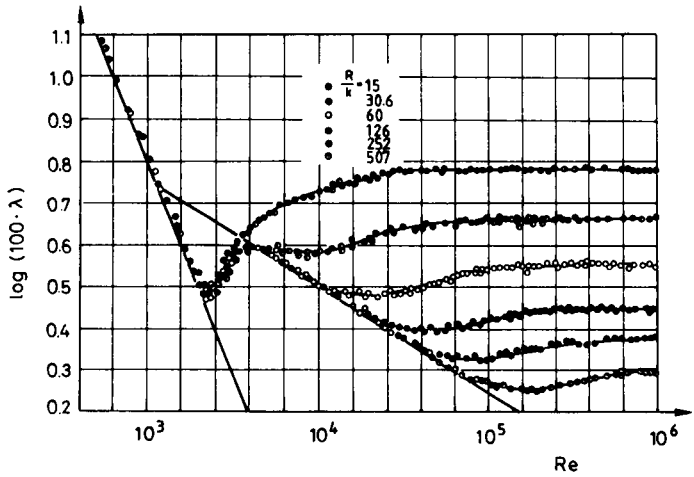

Fig. 8.9. Friction factor data of Nikuradse for artificially roughened pipes

the relative roughness k_s/R. Nikuradse's results are shown in *Fig. 8.9*, where the friction factor is plotted against the Reynolds number. It is seen that for each value of R/k_s an individual friction factor curve is obtained. In the turbulent region of the flow each friction factor curve eventually tends to be horizontal as the Reynolds number increases.

This shows that in this region the friction factor is independent of the Reynolds number and is solely a function of the relative roughness. This region, where the friction factor curves are horizontal, is called the region of fully developed turbulent flow. Nikuradse obtained experimentally a friction factor equation for fully developed turbulent flow:

$$\frac{1}{\sqrt{\lambda}} = 2 \lg \frac{R}{k_s} + 1.74 . \tag{8.54}$$

In Nikuradse's experiments the sand roughness k_s could be measured directly. The natural roughness of a commercial pipe can be determined indirectly as follows. If, for a given section of pipe, the flow rate Q and the pressure difference Δp is measured, the friction factor can be calculated as

$$\lambda = \frac{2D\Delta p}{L\varrho c^2} . \tag{8.55}$$

The value of Reynolds number can be obtained from its definition

$$\mathrm{Re} = \frac{cD}{\nu} .$$

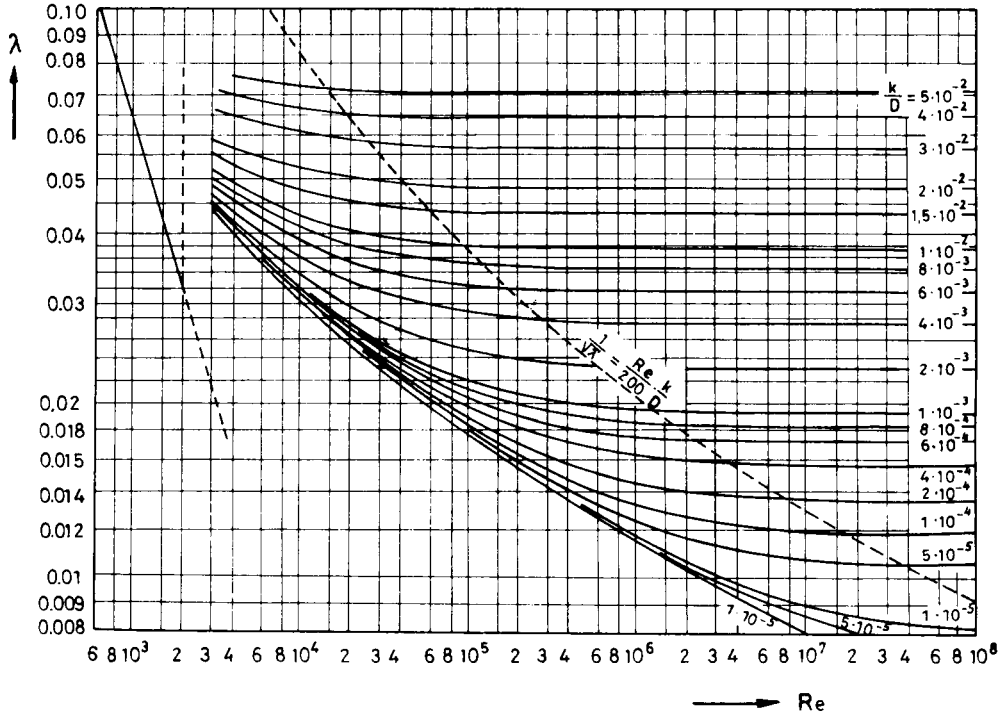

Fig. 8.10. Moody's friction factor diagram for commercial pipes

Thus the point corresponding to the measured values of λ and Re can be determined in the friction factor chart. If it is in the fully developed turbulent region, we obtain

$$k = R\,10^{-\frac{1}{2}\left(\frac{1}{\sqrt{\lambda}} - 1.74\right)}. \tag{8.56}$$

Note, that k is the equivalent sand grain roughness and that the natural roughness of the pipe is expressed in terms of the sand grain roughness which would result from the same friction factor. The only way this can be done to compare the behavior of a naturally rough pipe with an artificially roughened pipe. Moody has made these comparisons; his results are plotted in *Fig. 8.10.*

The friction factor and the relative roughness can also be related theoretically. Kármán derived such an equation for fully developed turbulent flow. Consider the rough pipe wall in *Fig. 8.8.* The thickness δ of the laminar sublayer is smaller than the average height of the roughness. Since the height k is much smaller than the radius of the pipe R, it seems to be an acceptable approximation to consider the turbulent shear stress near the wall to be constant within a layer of thickness k.

Thus it is assumed, that

$$\tau'_R = \tau'_k = f\left(\frac{v_k k}{\nu}\right) \varrho v_k^2 , \tag{8.57}$$

where v_k is the velocity at the edge of the constant shear stress layer.

Introducing the friction velocity v_*, we can write

$$\frac{v_*^2}{v_k^2} = f\left(\frac{v_k}{v_*}\frac{v_* k}{\nu}\right). \tag{8.58}$$

It is clear that the v_k/v_* ratio depends only on the so-called roughness Reynolds Re_k number, i.e.

$$\frac{v_k}{v_*} = \Phi\left(\frac{v_* k}{\nu}\right). \tag{8.59}$$

It is well known that the integration constant of the velocity profile of a turbulent flow in a pipe is an additional unknown. It can be determined using v_k/v_*. At the radius $r = R - k$ we have

$$\frac{v_k}{v_*} = \frac{v_{\max}}{v_*} + \frac{1}{\kappa}\left[\sqrt{\frac{R-k}{R}} + \ln\left(1 - \sqrt{\frac{R-k}{R}}\right)\right]. \tag{8.60}$$

(See Chapter 7.)

Since $k \ll R$, expanding the expression in binomial form we get

$$\sqrt{\frac{R-k}{R}} \cong 1 ,$$

and

$$\ln\left[1 - \sqrt{\frac{R-k}{R}}\right] \cong \ln\frac{k}{2R} .$$

Applying these formulas, we obtain

$$\Phi = \frac{v_k}{v_*} = \frac{v_{\max}}{v_*} + \frac{1}{\kappa}\left(1 + \ln\frac{k}{D}\right). \tag{8.61}$$

Alternatively, the cross-sectional average velocity c, given by

$$\frac{c}{v_*} = \frac{v_{\max}}{v_*} - \frac{1}{\kappa}\left(\frac{25}{12} - \frac{4}{5}\right), \tag{8.62}$$

can be used to eliminate $v_{\max}/v_*$. Thus we get

$$\frac{c}{v_*} = \Phi - \frac{1}{\kappa}\left(2.283 + \ln\frac{k}{D}\right). \tag{8.63}$$

From Eq. (8.51) we have

$$\frac{c}{v_*} = \sqrt{\frac{8}{\lambda}}$$

so that the friction factor is obtained as

$$\sqrt{\frac{8}{\lambda}} = \frac{1}{\kappa} \ln \frac{D}{k} - \frac{2.283}{\kappa} + \Phi . \tag{8.64}$$

The coefficient κ has the same value for both smooth and rough pipes. The relationship between Φ and the roughness Reynolds Re_k number can be determined experimentally. The result is shown in *Fig. 8.11*. In the interval $\mathrm{Re}_k < 3$ a linear relation is evident. In the region $\mathrm{Re}_k > 70$ the horizontal line shows that Φ is independent of Re_k. In this region Φ is constant, thus λ is a function of the relative roughness D/k only. In the interval $3 < \mathrm{Re}_k < 70$ the curve of Φ attains a maximum. This is the transition zone between the smooth and the fully developed turbulent behavior.

If $\mathrm{Re}_k < 3$, as long as the roughness is covered by the laminar sublayer, it has no effect on the friction factor.

It is clear from *Fig. 8.11* that the roughness makes itself felt only at values of $\mathrm{Re}_k > 3$. The measured points start to plot away from the straight line for a smooth pipe. Up to a value of $\mathrm{Re}_k = 70$, the friction factor depends on both the relative roughness and the Reynolds number.

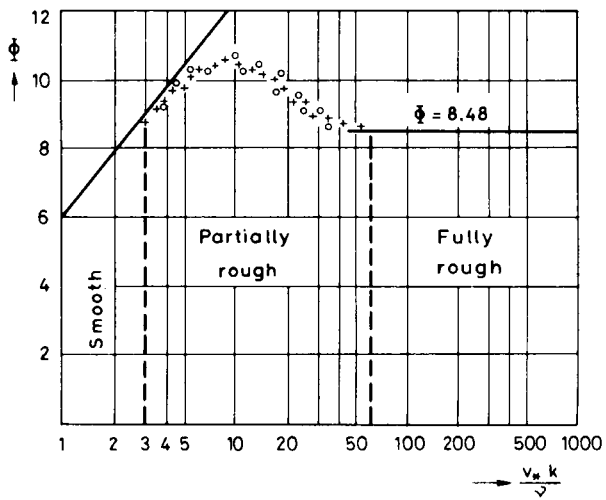

Fig. 8.11. Regions of smooth, transition and fully rough flow depending on Re_k

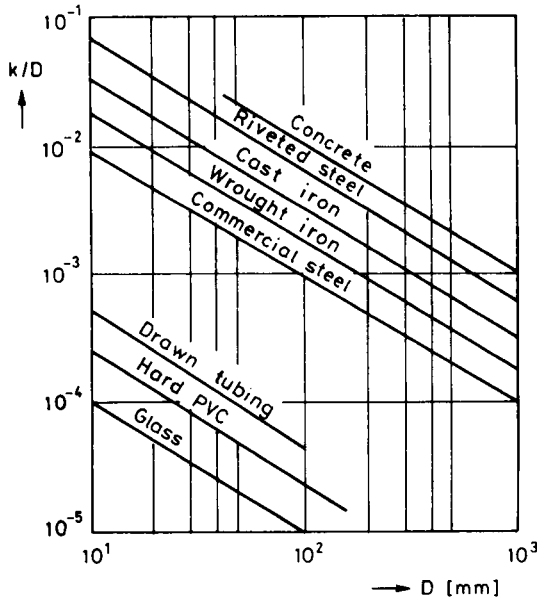

Fig. 8.12. Relative roughness of different type pipes

For values of $\mathrm{Re}_k > 70$ the laminar sublayer vanishes and the friction factor depends solely on the relative roughness. For this fully developed turbulent flow, after substitution of κ and Φ, the friction factor equation is obtained as

$$\frac{1}{\sqrt{\lambda}} = 2 \lg \frac{3.715 D}{k}. \tag{8.65}$$

For the transition region, where the friction factor is a function of both the Reynolds number and the relative roughness, Colebrook's equation is applicable:

$$\frac{1}{\sqrt{\lambda}} = -2 \lg \left(\frac{k}{3.715 D} + \frac{2.51}{\mathrm{Re} \sqrt{\lambda}} \right). \tag{8.66}$$

Colebrook's equation is an implicit expression, thus iteration is required to calculate the friction factor in the transition zone.

Finally a series of curves is presented *(Fig. 8.12)* to estimate the relative roughness of a pipe as a function of the diameter and the material of the pipe. These roughnesses are representative of the materials indicated, but cannot be expected to be sufficiently accurate for actual calculations. It is recommended that whenever possible and economic, the results of an actual flow test through a certain length of the pipe in question be used to calculate the friction factor and the actual relative roughness. These values are sufficient for further engineering calculations.

Similarity condition for turbulent flow in pipes

A very simple correlation is obtained for the similarity condition for turbulent flow in pipes. This is known as Kármán's similarity criterium and is based on Reynolds's equation. This criterium expresses the ratio between the inertial forces and the apparent forces due to turbulent momentum transfer:

$$\mathrm{Ka} = \frac{\overline{\vec{v}' \circ \vec{v}'}}{v^2}.$$

The conditions of uniqueness are satisfied if this expression consists of characteristic values of $\overline{\vec{v}' \circ \vec{v}'}$ and v. To characterize the turbulent momentum exchange for a unit mass of fluid, let us choose the value of $\overline{\vec{v}' \circ \vec{v}'}$ at the edge of the laminar sublayer. This will be approximately equal to the shear stress at the wall because of the very small thickness of the laminar sublayer, i.e.

$$(\overline{\vec{v}' \circ \vec{v}'})_{r=R-\delta} = \frac{\tau_R}{\varrho} = \frac{gJR}{2}.$$

Substituting the equation

$$h' = JL$$

as well as the Weisbach equation we obtain

$$\mathrm{Ka} = \frac{\lambda}{8}.$$

Thus the similarity condition for turbulent flows in two different pipes is the equality of the two friction factors:

$$\lambda_1 = \lambda_2.$$

This is valid for pipes with both smooth and rough walls; even for non-Newtonian fluids. This restricted similarity criterium is not valid for the entrance length of the pipe since there the wall shear stress is not constant. The longer the pipe is, the better does the deduced similarity criterium approach actual conditions.

8.5 Head losses resulting from fittings

Head losses for flows through pipes may result from features of flow other than pipe resistance: such features include abrupt changes in flow cross section or the direction of the streamlines, large accelerations or decelerations, separation of the flow from the pipe (or other boundary) walls, and different combinations of these. It is known that the turbulent shear stress increases with the increase in the

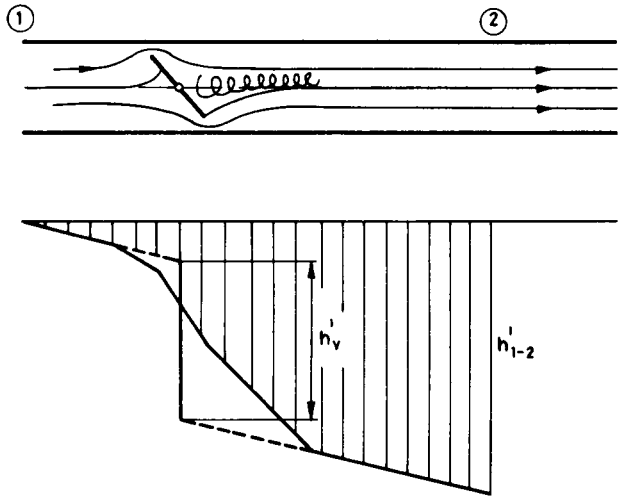

Fig. 8.13. Head losses near a butterfly valve

inhomogeneity of the velocity distribution:

$$\tau' = \varrho \kappa^2 \frac{\left(\frac{dv}{dr}\right)^4}{\left(\frac{d^2v}{dr^2}\right)^2}.$$

Any disturbance of the velocity field is equalized by turbulent momentum transfer which leads to energy dissipation. These losses can be localized at the place of the object which deforms the regular one-dimensional flow pattern. Only in a few cases can these local losses be determined by integrating the equation of motion. In spite of this, this problem may be solved adequately for petroleum engineering purposes by mainly empirical methods. The complexities of flow resulting from even a simple change in boundary geometry may be seen in *Fig. 8.13*, where the parameters relating to the head loss produced by a butterfly valve have been defined. Examining the flow pattern it can be seen that the presence of the valve disturbs the flow a rather short distance upstream, and a considerable distance downstream from the valve, the disturbances dying out in this extended region, accompanied by boundary layer growth and vortex diffusion which restores regular one-dimensional flow at and beyond section 2.

The pressure distribution in the section of pipe between cross sections 1 and 2 can be determined by simple measurements. *Figure 8.13* also shows the potential energy lines of the flow for the sections upstream and downstream of the valve, as well as the vicinity of the valve itself. The difference in their vertical distance is

defined as the head loss of the valve. This means that the height h'_{1-2} between the two zones of undisturbed one-dimensional flow is simply the sum of the flow losses measured for an undisturbed section of pipe of the same length and the losses induced by the butterfly valve. Thus the local head loss of the butterfly valve can be determined as

$$h'_v = (h'_{1-2})_{\text{measured}} - \lambda \frac{L_{12}}{D} \frac{c^2}{2g}, \tag{8.67}$$

without understanding the complex and unknown interaction between the undisturbed pipe flow and the disturbance caused by the valve. Defining local losses in this way provides an easy solution to many engineering problems.

It is convenient to define a dimensionless loss coefficient, analogous to the Euler number

$$\zeta_v = \frac{\Delta p'_v}{\frac{\varrho c^2}{2}} = \frac{h'_v}{\frac{c^2}{2g}}. \tag{8.68}$$

It is obvious, that the loss coefficient of the valve depends on the angle of attack: i.e. the angle between the valve disc and the streamlines of the undisturbed flow upstream. For a fixed angle, ζ_v depends on the Reynolds number and the relative roughness of the pipe.

In a similar way loss coefficients can be determined for different type of fittings as detailed below. As the next example a confuser, a conical contraction element, is considered. This is shown in *Fig. 8.14*. In section 1-*A* the flow accelerates, the pressure decreases faster than it decreases in the steady undisturbed flow.

In the converging section *A*–*B* the flow accelerates considerably. Since the pressure gradient is negative separation cannot occur, except in the section beyond *B*, where the "vena contracta" effect acts. Thus through a length of approximately $20 D_2$ the flow pattern is restabilized with an increasing dissipation and head loss. Thus the energy line has a steeper slope than that of the undisturbed flow.

At cross section 2 the re-established flow pattern is the same as that of a pipe of infinite length. Thus the head loss induced by the confuser occurs within the section of the pipe between points 1 and 2. For this flow the mechanical energy equation can be written:

$$\frac{\beta_1 c_1^2}{2g} + \frac{p_1}{\varrho g} + h_1 = \frac{\beta_2 c_2^2}{2g} + \frac{p_2}{\varrho g} + h_2 + h'_{1A} + h'_{B2} + h'_c. \tag{8.69}$$

In this h'_{1A} is the head loss of the section 1-*A* given by the equation for a pipe of infinite length:

$$h'_{1A} = \lambda_1 \frac{L_{1A}}{D_1} \frac{c_1^2}{2g}. \tag{8.70}$$

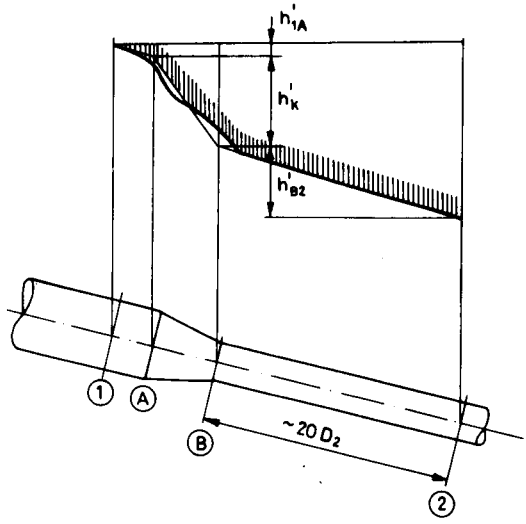

Fig. 8.14. Head losses in a confuser

Similarly

$$h'_{B2}=\lambda_2 \frac{L_{B2}}{D_2} \frac{c_2^2}{2g}. \tag{8.71}$$

Thus the head loss due to the confuser is given by

$$h'_c=\frac{p_1-p_2}{\varrho g}+h_1-h_2+\frac{\beta_1 c_1^2-\beta_2 c_2^2}{2g}-h'_{1A}-h'_{B2}. \tag{8.72}$$

The flow rate can be measured easily thus the velocities and the head losses h'_{1A} and h'_{B2} can be calculated. The difference

$$p_1-p_2+\varrho g(h_1-h_2) \tag{8.73}$$

can be measured by a differential manometer connected between points 1 and 2. The loss coefficient of the confuser can be defined as

$$\zeta_c=\frac{2gh'_c}{c_2^2}. \tag{8.74}$$

This loss coefficient depends on the shape of the confuser, the Reynolds number and the relative roughness. For a confuser of a given shape the relationship between the loss coefficient and the Reynolds number can be plotted on a graph, analogous to Moody's diagram, as shown in *Fig. 8.15.*

The loss coefficient increases with the cone angle, since a loss of acceleration is added to the loss due to friction. As the flow accelerates, the velocity profile

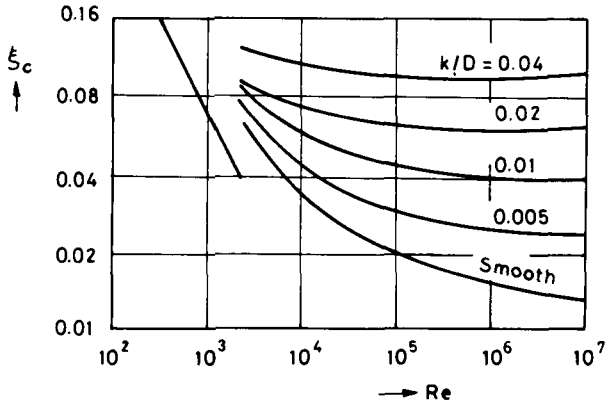

Fig. 8.15. Loss coefficient for a confuser

reshapes and the turbulent momentum transfer becomes stronger, causing an increase in the energy dissipation.

Diffusers are widely used for reducing the velocity of a flow, with a simultaneous pressure recovery, such as downstream from the throat of a Venturi meter or in the spiral casing of a centrifugal pump. As the cross-sectional area increases, the velocity decreases causing a positive pressure gradient. The boundary layer at the wall thickens and separates from the wall, thus forming a stagnation region. In the stagnation region large eddies are generated. Their kinetic energy, which originated from the mechanical energy of the flowing fluid is dissipated into heat by vortex diffusion. In addition to this, the flow outside the boundary layer becomes extremely unsteady. The undisturbed flow is re-established for beyond the diffuser. Because of separation, the head loss from a diffuser is always greater than that of a confuser of the same shape.

The friction loss of a diffuser depends on the Reynolds number and the relative roughness. The separation loss, which is more considerable, depends on the cone angle.

A diffuser efficiency can be defined by the equation

$$\eta_D = \frac{p_2 - p_1}{\frac{\varrho}{2}(c_1^2 - c_2^2)}, \tag{8.75}$$

where $p_2 - p_1$ is the actual pressure difference, which is related to the pressure difference for perfect fluid flow as calculated by the Bernoulli equation.

In *Fig. 8.16* it can be seen, that the maximum diffuser efficiency occurs at a cone angle (Θ) of 8°.

It is also clear that for a given area ratio, diffusers with very small cone angles yield high losses because of the excessive wall area in contact with the flowing fluid.

For cone angles in the range $\Theta < 8°$, the diffuser efficiency decreases considerably. In the region $\Theta > 10°$ diffuser losses again increase and the diffuser becomes inefficient. This determines the geometry to be avoided by engineers. If the velocity of the upstream flow has a peripheral component v_φ, this acts in such a way as to oppose separation. A variety of designs have been suggested for this purpose, some containing internal vanes. The loss coefficient of well-designed diffusers is no greater than

$$\zeta_D = 0.12 - 0.30 .$$

The only loss coefficient which can be determined by elementary fluid mechanical methods is that due to an abrupt axisymmetric enlargement. This situation is shown in *Fig. 8.17*. If we separate a control volume, in which the excess head loss is generated, the momentum equation can be written in the z direction as

$$\varrho A_2 v_2^2 - \varrho A_1 v_1^2 = p_1 A_2 - p_2 A_2 . \tag{8.76}$$

It is obvious that the pressure p_1 acts on the area A_2.

Since the flow is axisymmetric the component of the momentum equation in the r-direction has vanished. It has also been assumed, that $\beta_1 = \beta_2 = 1$, and that the friction at the wall may be neglected.

The mechanical energy equation is obtained as

$$\frac{p_1}{\varrho} + \frac{v_1^2}{2} = \frac{p_2}{\varrho} + \frac{v_2^2}{2} + g h'_{1-2} . \tag{8.77}$$

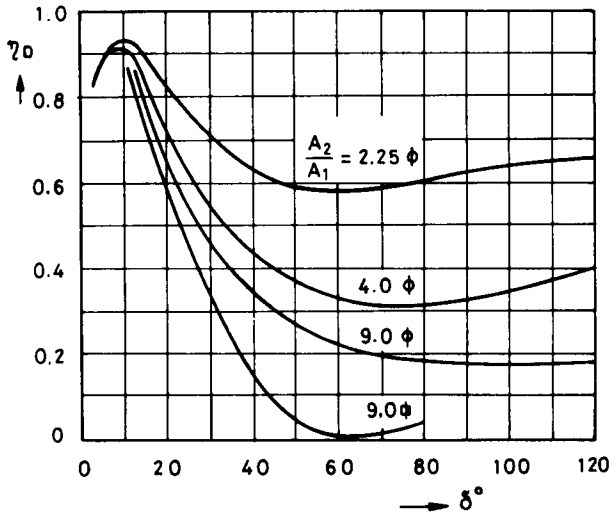

Fig. 8.16. Diffuser efficiency

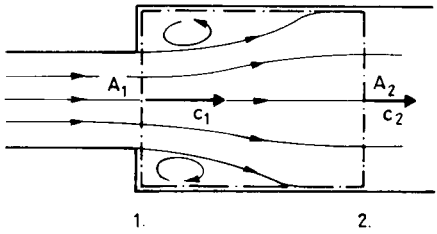

Fig. 8.17. Head loss at an abrupt enlargement

The continuity equation is

$$A_1 v_1 = A_2 v_2 .$$

Dividing the momentum equation by A_2, and taking into account the continuity equation, we get

$$p_1 - p_2 = \varrho \left(v_2^2 - \frac{A_1}{A_2} v_1^2 \right) = \varrho (v_2^2 - v_2 v_1) . \tag{8.78}$$

From the mechanical energy equation the pressure difference is obtained:

$$p_1 - p_2 = \varrho \frac{v_2^2 - v_1^2}{2} + \varrho g h'_{1-2} . \tag{8.79}$$

Eliminating the pressure difference, Eqs (8.78) and (8.79) yield

$$2 g h'_{1-2} = 2 v_2 (v_2 - v_1) - v_2^2 + v_1^2 , \tag{8.80}$$

so that finally

$$h'_{1-2} = \frac{(v_1 - v_2)^2}{2g} . \tag{8.81}$$

Experimental data agree with this simple result to within a few percent. A more accurate investigation should take into account the unsteady nature of the flow exemplified by the periodically occurring eddies downstream from the area of separation as indicated in *Fig. 8.17.*

The limiting case $A_2 \to \infty$, $v_2 \to 0$ is of practical importance. It represents the discharge of a pipe into a very large tank. In this case

$$h' = \frac{v_1^2}{2g} ,$$

i.e. the total kinetic energy content of the flow is dissipated in the tank. This is the so-called outflow loss.

The above calculation of the head loss can also be applied to the abrupt contraction depicted in *Fig. 8.18.* As is shown, a vena contracta develops, thus an acceleration section is followed by a deceleration section. The coefficient of con-

traction, defined as

$$\alpha_c = \frac{A_c}{A_2}, \tag{8.82}$$

depends on the ratio of A_2/A_1. Experimental investigation leads to the relationship plotted in *Fig. 8.19*. The head loss of the deceleration section is obtained from Eq. (8.81) as

$$h'_{c2} = \frac{(v_c - v_2)^2}{2g}. \tag{8.83}$$

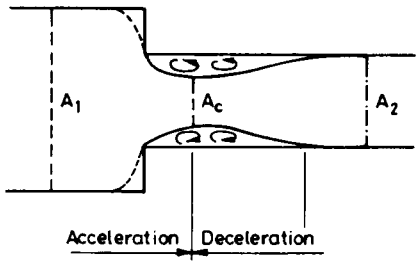

Fig. 8.18. Head loss at an abrupt contraction

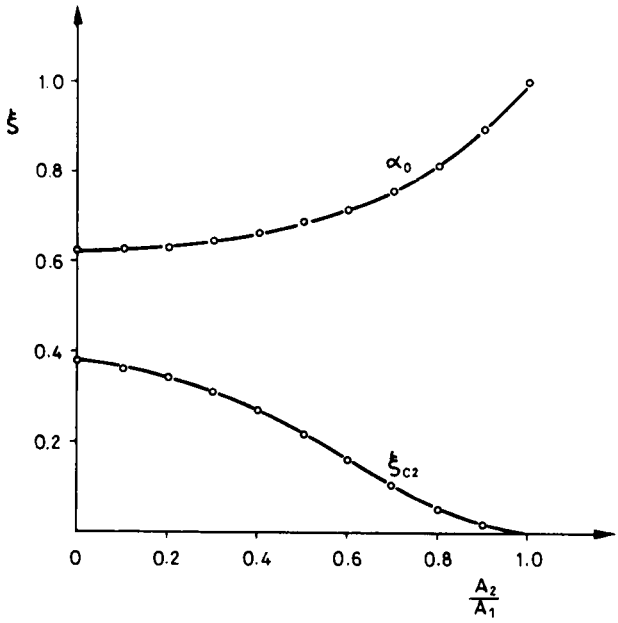

Fig. 8.19. Loss coefficient for an abrupt contraction

From the continuity equation

$$v_c = \frac{A_2}{A_c}; \qquad v_2 = \frac{v_2}{\alpha_c}.$$

Substituting into Eq. (8.83) we get

$$h'_{c2} = \frac{v_2^2}{2g}\left(\frac{1}{\alpha_c} - 1\right)^2 = \zeta_{c2}\frac{v_2^2}{2g}. \tag{8.84}$$

The total head loss can be determined experimentally. The results are shown in *Fig. 8.20,* plotted as a function of A_2/A_1. It is clear that a considerable part of the total head loss is generated in the deceleration section. The head loss of the acceleration section is obtained as

$$h'_{1c} = \zeta\frac{v_2^2}{2g} - \zeta_{c2}\frac{v_2^2}{2g} = \left[\zeta_c - \left(\frac{1}{\alpha_c} - 1\right)^2\right]\frac{v_2^2}{2g}, \tag{8.85}$$

which can be also expressed as

$$h'_{1c} = \zeta_{1c}\frac{v_c^2}{2g}. \tag{8.86}$$

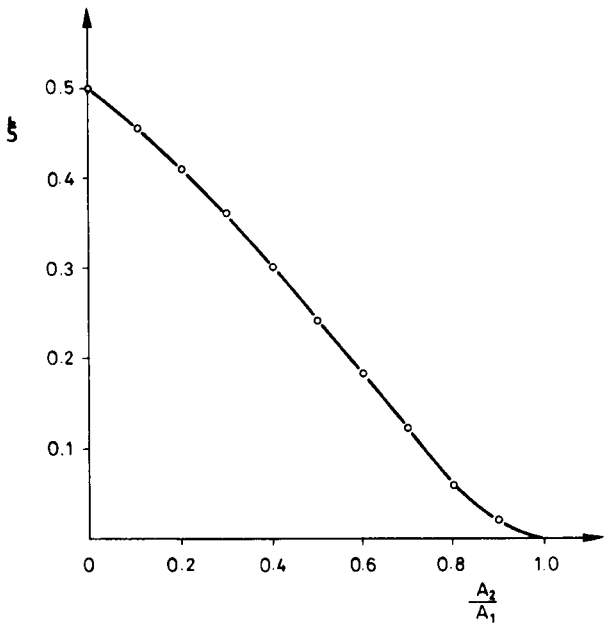

Fig. 8.20. Total head loss of an abrupt contraction

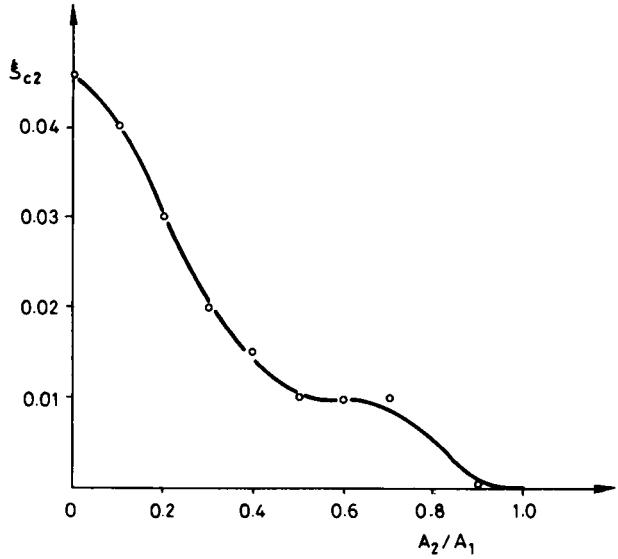

Fig. 8.21. Loss coefficient of acceleration section of a pipe

By equating these two expressions, and making use of Eq. (8.84) we obtain

$$\zeta_{1c}=\alpha_c^2\left[\zeta-\left(\frac{1}{\alpha_c}-1\right)^2\right]. \tag{8.87}$$

This expression is also plotted in *Fig. 8.21.*

Experimental observations confirm that ζ_{1c} values may be used to determine head losses for short acceleration sections at the entrance of pipes. Since $A_2/A_1 \approx$ ≈ 0 for a pipe entrance following from a large tank, the value of ζ_{1c} calculated above represents a rather good approximation for a square-edged entrance. A well-designed rounded entrance, which eliminates vena contracta, separation and deceleration, leads to a considerably smaller loss coefficient. In contrast to the value of 0.5 typical of the square edged form, a rounded entrance can reduce the loss coefficient between 0.10 and 0.12.

Another type of localized head loss occurs in flow through bends and elbows. In addition to friction and separation loss, secondary flows also generate head losses.

In these cases the characteristic source of loss is the secondary flow which develops perpendicular to the streamlines of the main flow. For a qualitative understanding of this phenomenon consider an elbow of square cross section as depicted in *Fig. 8.22.* At the entrance cross section *ABCD* the inflow velocity distribution along *EH* induces vortices with axes which lie in the entrance plane. Their directions are opposite in the upper and lower boundary layer in accordance with the sign of the velocity gradient. The flow particles along the path line *EE'* are

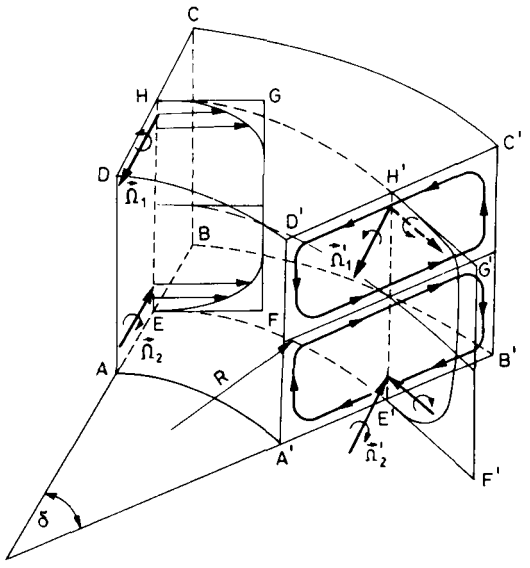

Fig. 8.22. Secondary flows in an elbow

deflected from the entrance direction by the angle δ. In spite of this the vorticity vectors $\vec{\Omega}_1$ and $\vec{\Omega}_2$ continue to exert pressure in their original direction as shown in *Fig. 8.22*. Thus vorticity components occur perpendicular to the plane $A'B'C'D'$ which induce secondary clockwise and counterclockwise flow in this plane. At the horizontal plane of symmetry these two motions are complementary; the direction of the secondary flow is centrifugally outward. Near the upper and the lower boundary surfaces vortices induce centripetal flow. The secondary flow velocities increase with the velocity of the mean flow, and the angle of the bend δ.

The kinetic energy of the secondary flow decreases the mechanical energy of the mean flow, since after the elbow it is dissipated by turbulent momentum transfer, like any other disturbance in the flow.

Loss coefficients for elbows and bends ζ_B can be determined experimentally. They depend on the shape (R/D and δ), the Reynolds number and the relative roughness. The relationship between ζ_B and R/D for different values of δ is depicted in *Fig. 8.23*. For a given R/D and δ we can obtain a diagram to illustrate the dependence of ζ_B on the Reynolds number and the relative roughness, as is shown in *Fig. 8.24*.

Note, that the equation

$$h'_B = \zeta_B \frac{c^2}{2g} \tag{8.88}$$

does not yield the total head loss caused by the bend. Rather, it gives an excess head loss which would have occurred in an established flow through a pipe of length

equal to the axis of the bend. Thus the total head loss of the bend is

$$h' = \left(\zeta_B + \lambda \frac{R\delta}{D}\right) \frac{c^2}{2g}, \tag{8.89}$$

in which the angle of the bend δ must be expressed in radians.

Valves come in a great variety of shapes while their openings may also vary considerably. The head loss of any type of value is usually determined in the wide-open position. Approximate loss coefficients for certain well-known valves

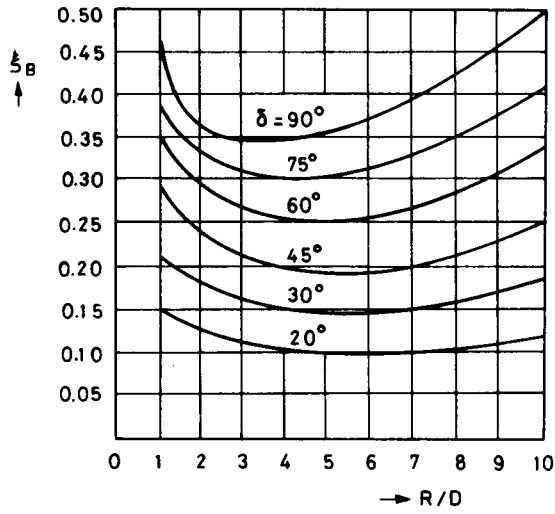

Fig. 8.23. Loss coefficient of elbows

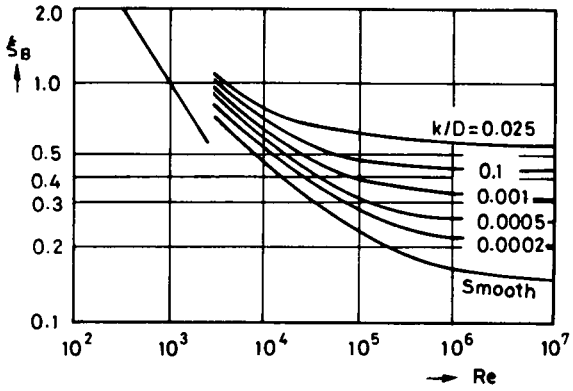

Fig. 8.24. Elbow loss coefficient depending on Reynolds number and relative roughness

are shown in *Fig. 8.25*. These "open state" loss coefficients may increase to infinity for the closed state.

It should be obvious that the head loss of a number of pipes connected in series is equal to the sum of the head losses of individual pipe sections and fittings. An additional complication may occur where fittings are close together and the disturbances induced by one do not die out before the next one is reached. Experimental observations show that the total head loss produced by closely spaced fittings is somewhat less than the sum of the individual head losses.

It is useful to reduce a given pipeline to an equivalent single pipe, for which the total head loss is the same at the same flow rate. The total head loss can be written

$$h' = \sum_{i=1}^{n} \lambda_i \frac{L_i}{D_i} \frac{c_i^2}{2g} + \sum_{j=1}^{k} \zeta_j \frac{c_j^2}{2g}, \tag{8.90}$$

where i and j is the number of the pipe sections and the fittings. The same head loss can be produced by a single pipe of "equivalent" diameter D_E, and "equivalent" friction factor λ_E:

$$h' = \lambda_E \frac{L_E}{D_E} \frac{c_E^2}{2g}. \tag{8.91}$$

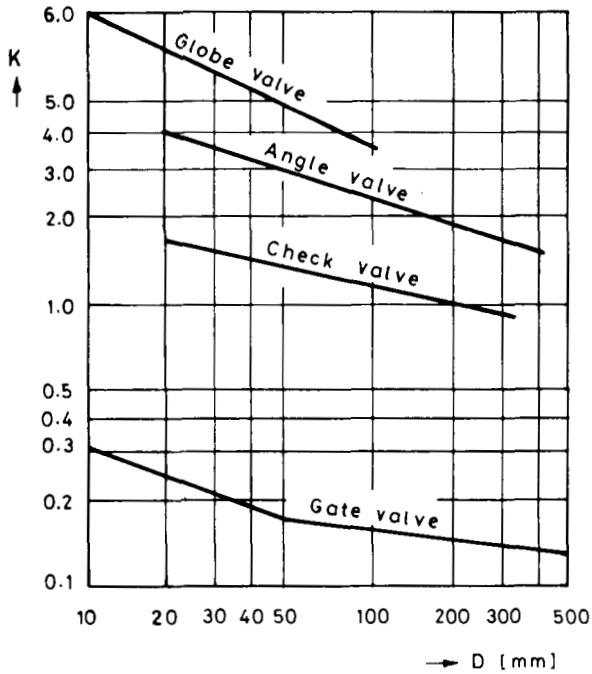

Fig. 8.25. Loss coefficients for different type valves

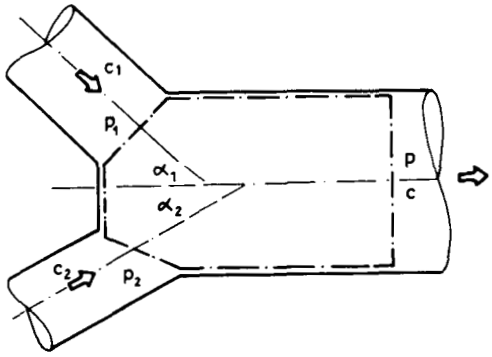

Fig. 8.26. Pipe junction with control volume

This "equivalent pipe length" L_E can be used to express the loss coefficient of various fittings. For a given fitting built into a pipe of diameter D_E, we can express as

$$\zeta = \lambda_E \frac{L_E}{D_E}. \tag{8.92}$$

At pipe junctions two flows join and flow away together with intensive turbulent mixing. This mixing induces pressure losses, which can be calculated by a simple analytical method.

Consider the pipe junction shown in *Fig. 8.26*. The arriving flows are mixed within the control volume. At the outlet cross section A the flow has been fully homogenized and a stable velocity profile developed.

For non-mixing inviscid flows the pressure at the outlet cross section A can be calculated from the Bernoulli equation. The calculated pressure p_{id} (id = ideal fluid) is different for each branch A_1A and A_2A:

$$\left(\frac{p_{id}}{\varrho}\right)_1 + \frac{c^2}{2} = \frac{p_1}{\varrho} + \frac{c_1^2}{2}, \tag{8.93a}$$

$$\left(\frac{p_{id}}{\varrho}\right)_2 + \frac{c^2}{2} = \frac{p_2}{\varrho} + \frac{c_2^2}{2}. \tag{8.93b}$$

The calculated pressure p_{id} is greater than the actual pressure p. Thus two different pressure losses can be defined for the two branches as

$$\left(\frac{\Delta p'}{\varrho}\right)_1 = \left(\frac{p_{id}}{\varrho}\right)_1 - \frac{p}{\varrho} = \zeta_1 \frac{c^2}{2}, \tag{8.94a}$$

$$\left(\frac{\Delta p'}{\varrho}\right)_2 = \left(\frac{p_{id}}{\varrho}\right)_2 - \frac{p}{\varrho} = \zeta_2 \frac{c^2}{2}, \tag{8.94b}$$

Since the flow is slow and its velocity is far from the speed of sound, we can assume that the inlet pressures are the same

$$p_1 = p_2 = p_i .$$

For the actual flow the momentum equation can be written as

$$\varrho c^2 A - \varrho c_1^2 A_1 \cos\alpha_1 - \varrho c_2^2 A_2 \cos\alpha_2 = (p_i - p)_A . \tag{8.95}$$

The actual outlet pressure can be expressed as

$$\frac{p}{\varrho} = \frac{p_i}{\varrho} - c^2 + c_1^2 \frac{A_1}{A} \cos\alpha_1 + c_2^2 \frac{A_2}{A} \cos\alpha_2 . \tag{8.96}$$

Combining Eqs (8.93) to (8.96), the pressure losses of the pipe junctions are obtained as

$$\left(\frac{\Delta p'}{\varrho}\right)_1 = \frac{c_1^2}{2} + \frac{c^2}{2} - c_1^2 \frac{A_1}{A} \cos\alpha_1 - c_2^2 \frac{A_2}{A} \cos\alpha_2 , \tag{8.97a}$$

$$\left(\frac{\Delta p'}{\varrho}\right)_2 = \frac{c_2^2}{2} + \frac{c^2}{2} - c_1^2 \frac{A_1}{A} \cos\alpha_1 - c_2^2 \frac{A_2}{A} \cos\alpha_2 . \tag{8.97b}$$

The loss coefficients defined by Eqs (8.95) to (8.96) are obtained as

$$\zeta_1 = 1 + \left[1 - 2\frac{A_1}{A}\cos\alpha_1\right]\left(\frac{c_1}{c}\right)^2 - 2\frac{A_2}{A}\left(\frac{c_2}{c}\right)^2 \cos\alpha_2 , \tag{8.98a}$$

$$\zeta_2 = 1 + \left[1 - 2\frac{A_2}{A}\cos\alpha_2\right]\left(\frac{c_2}{c}\right)^2 - 2\frac{A_1}{A}\left(\frac{c_1}{c}\right)^2 \cos\alpha_1 , \tag{8.98b}$$

Introducing the notation

$$\gamma = \frac{Q_1}{Q} = \frac{c_1 A_1}{cA} , \tag{8.99}$$

the continuity equation

$$c_1 A_1 + c_2 A_2 = cA , \tag{8.100}$$

leads to the expressions

$$\frac{c_1}{c} = \frac{A\gamma}{A_1} ; \qquad \frac{c_2}{c} = \frac{A}{A_2}(1-\gamma) . \tag{8.101}$$

Thus the loss coefficients can be expressed as

$$\zeta_1 = 1 + \left[\left(\frac{A}{A_1}\right)^2 - 2\left(\frac{A}{A_1}\right)\cos\alpha_1\right]\gamma^2 - 2\frac{A}{A_2}(1-\gamma)^2 \cos\alpha_2 , \tag{8.102a}$$

$$\zeta_2 = 1 + \left[\left(\frac{A}{A_2}\right)^2 - 2\left(\frac{A}{A_2}\right)\cos\alpha_2\right](1-\gamma)^2 - 2\frac{A}{A_1}\gamma^2 \cos\alpha_1 . \tag{8.102b}$$

In the particular case, when $\alpha_1=\alpha_2=\alpha$ and $A_1=A_2=A$, $\gamma=0.5$, thus the two loss coefficients are equal

$$\zeta=\zeta_1=\zeta_2=1+\frac{1}{4}-\cos\alpha\,. \tag{8.103}$$

The calculated loss coefficients are in good agreement with experimental data. *Figures 8.27* and *8.28* show calculated and measured loss coefficients for $A_1=A_2=A$; $\alpha_2=0$, as a function of γ for different values of α_1.

Calculated and measured results show that in certain cases the pipe junction loss coefficient ζ may be negative. This unexpected result can be explained by considering the energy transfer during the turbulent mixing of the joining flows. There are certain cases when one of the joining flows can acquire a greater amount of mechanical energy by turbulent mixing than is dissipated in the form of internal energy in this process. The work of the viscous and turbulent forces thus partly increases the mechanical energy and partly dissipates into internal energy. This can be recognized from an examination of the mechanical energy equation.

Finally a few equivalent lengths are given for selected fittings:

	L_E/D_E		L_E/D_E
Globe valve (fully open)	350	45° standard elbow	16
Gate valve (fully open)	15	Butterfly valve (fully open)	40
Angle valve (with pin-guided disc)	200	Foot valve with leather-hinged disc	75
90° standard elbow	30		

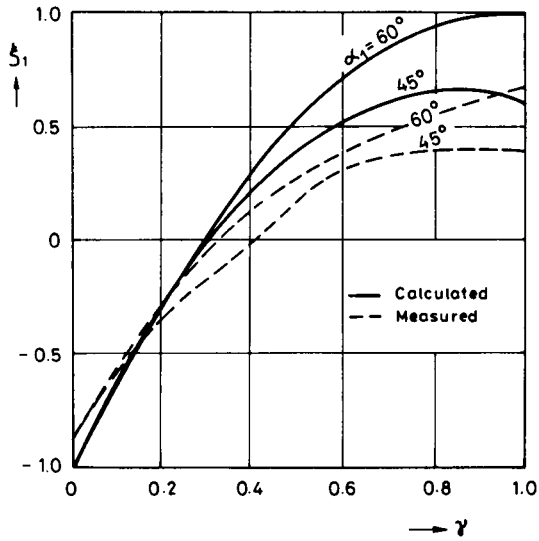

Fig. 8.27. Calculated and measured loss coefficients for pipe junctions

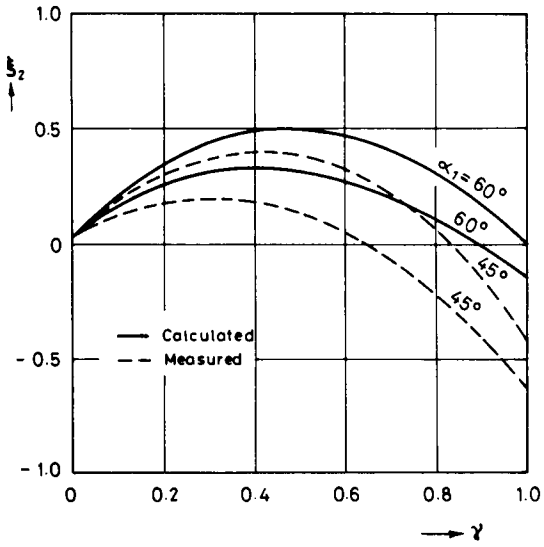

Fig. 8.28. Calculated and measured loss coefficients for pipe junctions

8.6 Pressure loss of a low velocity gas flow

It was shown in Chapter 4 that in a high velocity compressible flow the density change accompanying a pressure loss is considerable and the irreversibility of the rapid expansion causes a much greater increase in entropy than the viscous friction. The obtained loss coefficient depends on the Mach number only; it is not affected by the Reynolds number nor by the relative roughness.

For a low velocity compressible flow the pressure loss causes a slow density change, which at these low Mach numbers ($M < 0.1$) is negligible. The pressure loss depends mainly on the Reynolds number and the relative roughness, while the effect of the slow expansion is taken into consideration by means of an additional loss coefficient. As the Fanno curves in a T—S diagram show, the flow in the low Mach number region is almost isothermal. It is thus an acceptable approximation to treat a low velocity compressible flow as being isothermal.

Consider first a horizontal pipeline for which the change in potential energy is zero. Thus for an infinitesimal length of this pipe the mechanical energy equation can be written as

$$c\,\mathrm{d}c + \frac{\mathrm{d}p}{\varrho} + g\,\mathrm{d}h' = 0\,. \tag{8.104}$$

The infinitesimal change in kinetic energy caused by the expansion of the gas can be treated as being the effect of an additional friction factor $\bar{\lambda}$, i.e. we can write

$$c\,\mathrm{d}c = \bar{\lambda}\frac{\mathrm{d}L}{D}\frac{c^2}{2}\,. \tag{8.105}$$

The infinitesimal friction loss is

$$g\,\mathrm{d}h' = \lambda \frac{\mathrm{d}L}{D} \frac{c^2}{2}. \tag{8.106}$$

Using the above expressions the mechanical energy equation can be written as

$$\frac{\mathrm{d}p}{\varrho} + (\lambda + \bar{\lambda}) \frac{\mathrm{d}L}{D} \frac{c^2}{2} = 0. \tag{8.107}$$

For isothermal flow

$$\frac{p_0}{\varrho_0} = \frac{p}{\varrho}. \tag{8.108}$$

Since the cross section of the pipe is uniform the continuity equation becomes

$$\varrho_0 c_0 = \varrho c. \tag{8.109}$$

Thus the kinetic energy at any cross section can be expressed as

$$\frac{c^2}{2} = \frac{p_0 \varrho_0}{p \varrho} \frac{c_0^2}{2}. \tag{8.110}$$

Substituting this into the mechanical energy equation we have

$$\frac{p_0}{\varrho_0} \frac{\mathrm{d}p}{p} + \frac{\lambda + \bar{\lambda}}{2D} \frac{p_0 \varrho_0}{p \varrho} c_0^2 \,\mathrm{d}L = 0. \tag{8.111}$$

Multiplying this equation by $p\varrho$, and using the relation

$$\frac{\varrho}{\varrho_0} = \frac{p}{p_0}, \tag{8.112}$$

we get the differential equation

$$p\,\mathrm{d}p = -(\lambda + \bar{\lambda}) \frac{p_0 \varrho_0 c_0^2}{2D} \mathrm{d}L. \tag{8.113}$$

Before integrating this expression, consider the change in the friction factors λ and $\bar{\lambda}$ along the length of the pipe due to velocity and density changes. For a "fully developed" turbulent flow the friction factor does not depend on the Reynolds number, nor of course on the velocity. For smooth pipes λ depends on the Reynolds number only. Since

$$\mathrm{Re} = \frac{cD}{\nu} = \frac{\varrho c D}{\mu},$$

and

$$\varrho c = \mathrm{const}, \tag{8.114}$$

the Reynolds number is constant along the pipe axis, and therefore, the friction

factor is also constant:

$$\frac{\mathrm{d}\,\mathrm{Re}}{\mathrm{d}L}=0\,;\qquad \frac{\mathrm{d}\lambda}{\mathrm{d}L}=0\,. \tag{8.115}$$

The additional friction factor $\bar{\lambda}$ is not constant along the length of the pipe. From Eq. (8.105) it can be expressed as

$$\bar{\lambda}=\frac{2D}{c}\,\frac{\mathrm{d}c}{\mathrm{d}L}\,. \tag{8.116}$$

For an isothermal flow

$$\frac{p}{\varrho}=\text{const}\,;\qquad \varrho c=\text{const}\,,$$

thus

$$pc=\text{const}\,. \tag{8.117}$$

This leads to the relation

$$\frac{\mathrm{d}c}{c}=\frac{\mathrm{d}p}{p}\,, \tag{8.118}$$

thus the additional friction factor can be written as

$$\bar{\lambda}=-\frac{2D}{p}\,\frac{\mathrm{d}p}{\mathrm{d}L}\,. \tag{8.119}$$

Substituting this into Eq. (8.113) and replacing p_0, ϱ_0, c_0 by the inlet flow variables p_1, ϱ_1, c_1 the following integral is obtained:

$$\int_{p_1}^{p_2} p\,\mathrm{d}p=-\frac{p_1\varrho_1 c_1^2}{2D}\int_0^L\left(\lambda-\frac{2D\,\mathrm{d}p}{p\,\mathrm{d}L}\right)\mathrm{d}L\,. \tag{8.120}$$

This, after a little manipulation, leads to the following result

$$\left(\frac{p_2}{p_1}\right)^2-\frac{\varrho_1 c_1^2}{p_1}\ln\left(\frac{p_2}{p_1}\right)^2=1-\frac{2\varrho_1}{p_1}\lambda\frac{L}{D}\,\frac{c_1^2}{2}\,. \tag{8.121}$$

This expression is implicit for p_2 or p_2-p_1, but p_2 can be more readily determined using the Newton—Raphson method as described below.

Consider the error caused by neglecting the kinetic energy change due to expansion. The ratio of the two friction factors is

$$\frac{\bar{\lambda}}{\lambda}=\frac{\varrho c^2}{p-\varrho c^2}=\frac{c^2}{RT-c^2}\,. \tag{8.122}$$

For natural gas at 20 °C and a velocity of 50 m/s this ratio is 0.012. For superheated steam at 400 °C and 50 m/s, it is 0.0083. Therefore, for a low velocity compressible flow, e.g. natural gas pipelines, the effect of expansion may be

neglected. Thus Eq. (8.121) is obtained in a simpler form:

$$p_1^2 - p_2^2 = \lambda p_1 \varrho_1 \frac{L}{D} c_1^2 . \tag{8.123}$$

For an inclined high-pressure pipeline or in a vertical natural gas well, gravity effects must be taken into account. In the mechanical energy equation the acceleration term $c\,\mathrm{d}c$ is again neglected, so that we can write

$$\frac{p_1}{\varrho_1}\frac{\mathrm{d}p}{p} + g\,\mathrm{d}z + \frac{\mathrm{d}Lc^2}{D2} = 0 . \tag{8.124}$$

Let α be the angle between the pipe axis and the horizontal direction, thus

$$\mathrm{d}z = \mathrm{d}L \sin\alpha . \tag{8.125}$$

Substituting into the mechanical energy equation, and multiplying by $p^2\varrho_1/p_1$, and since $c^2p^2 = c_1^2p_1^2$, we obtain

$$p\,\mathrm{d}p + g\frac{\varrho_1}{p_1}p^2\,\mathrm{d}L\sin\alpha + \lambda p_1\varrho_1\frac{\mathrm{d}L}{D}\frac{c_1^2}{2} = 0 . \tag{8.126}$$

For an infinitesimal length of pipe we thus obtain the expression

$$\mathrm{d}L = -\frac{p\,\mathrm{d}p}{g\frac{\varrho_1}{p_1}p^2\sin\alpha + \lambda\frac{p_1\varrho_1}{2D}c_1^2} . \tag{8.127}$$

Integrating this expression we obtain

$$L = \frac{p_1}{2\varrho_1 g\sin\alpha}\ln\left(\frac{g\sin\alpha + \frac{\lambda c_1^2}{2D}}{\left(\frac{p_2}{p_1}\right)^2 g\sin\alpha + \frac{\lambda c_1^2}{2D}}\right) . \tag{8.128}$$

Rearranging, the pressure ratio (p_2/p_1) can be expressed as

$$\left(\frac{p_2}{p_1}\right)^2 = \left(1 - \frac{\lambda c_1^2}{2Dg\sin\alpha}\right)\exp\left(-\frac{2L\varrho_1 g\sin\alpha}{p_1}\right) - \frac{\lambda c_1^2}{2Dg\sin\alpha} . \tag{8.129}$$

A better approximation for high pressure pipelines is obtained by considering the equation of state in the form

$$\frac{p}{\varrho} = ZRT ,$$

where Z is the compressibility factor of the gas. For modest temperature variations along the length of the pipe, it is convenient to perform the calculations assuming an average temperature. If the temperature variation is considerable, the pipeline should be divided along its length into a finite number of isothermal sections, each of which is then treated individually.

8.7 Flow in pipes with mechanical energy addition

The mechanical energy equation for a one-dimensional steady flow is obtained as

$$\beta_1 \frac{c_1^2}{2} + z_1 g + \mathscr{P}_1 = \beta_2 \frac{c_2^2}{2} + z_2 g + \mathscr{P}_2 + g h'_{1-2} . \tag{8.130}$$

For an incompressible fluid in a pipe of constant diameter this can be written in a particularly simple form:

$$(z_1 - z_2) g + \frac{p_1 - p_2}{\varrho} = g h'_{1-2} . \tag{8.131}$$

It is obvious that the mechanical energy decrease maintains the flow against viscous and turbulent forces. Natural flows through channels or river beds always take place from an inlet with a high mechanical energy level to an outlet with a low mechanical energy level. This mechanical energy difference is dissipated by the irreversible process of friction. In engineering practice most flows are directed from a low energy inlet to a higher energy outlet while at the same time a considerable amount of mechanical energy is converted into heat. It is obvious that such a flow can exist only by adding mechanical energy to the flowing fluid. This energy

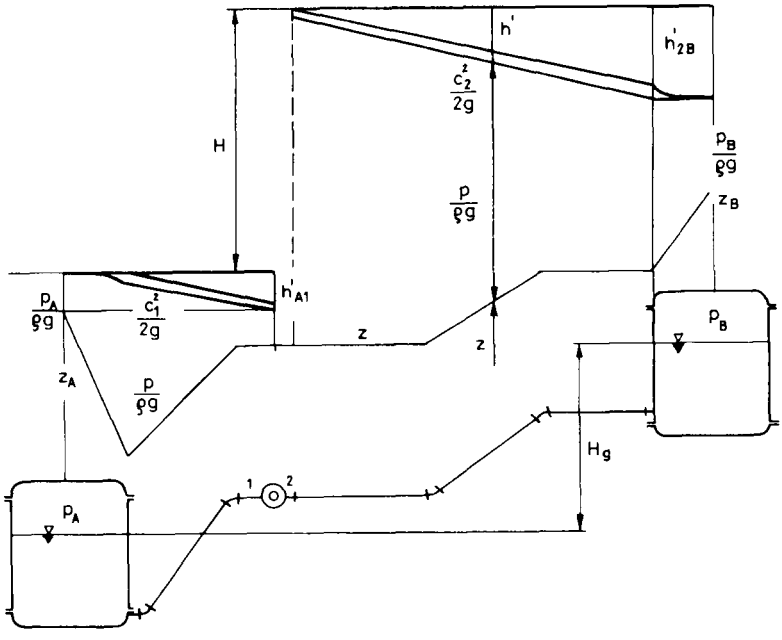

Fig. 8.29. Manometric head of a pump

addition is possible only by introducing unsteady flow resulting from the rotating blading of a pump or a compressor. The work done by a rigid body on the fluid can be determined if the velocity distribution on the blading is known, as was shown in Chapter 4.

On the other hand, it is also possible to calculate the mechanical energy required to maintain the flow against the increasing energy level and fluid friction from the variables of one-dimensional steady flow in the pipe.

Consider the flow system depicted in *Fig. 8.29*. Fluid is pumped from reservoir A to reservoir B. The flow is steady between reservoir A and the pump inlet 1, and also between the pump outlet 2 and reservoir B. For the two steady-flow sections the mechanical energy equation can be written:

$$\frac{p_A}{\varrho g} + z_A + \frac{c_A^2}{2g} = \frac{p_1}{\varrho g} + z_1 + \beta_1 \frac{c_1^2}{2g} + h'_{A-1}, \tag{8.132}$$

$$\frac{p_2}{\varrho g} + z_2 + \beta_2 \frac{c_2^2}{2g} = \frac{p_B}{\varrho g} + z_B + \frac{c_2^2}{2g} + h'_{2-B}. \tag{8.133}$$

Since the diameters of the reservoirs are much greater than the diameters of the pipes the kinetic energy terms $c_A^2/2g$ and $c_B^2/2g$ may be neglected. It can be seen from the energy diagram that the sum of the mechanical energy and the head loss is constant for both the sections $A-1$ and $2-B$ of the pipe. The discontinuity in the energy curve represents the amount of mechanical energy added to the fluid by the pump. Using the energy equation this can be expressed as:

$$H = \frac{p_2 - p_1}{\varrho g} + z_2 - z_1 + \frac{\beta_2 c_2^2 - \beta_1 c_1^2}{2g}. \tag{8.134}$$

Using Eqs (8.132) and (8.133) this energy difference can be rewritten in the form

$$H = \frac{p_B - p_A}{\varrho g} + z_B - z_A + h'_{A1} + h'_{2B}. \tag{8.135}$$

Since at the free surfaces of the reservoirs the pressure is atmospheric, it is obvious that

$$p_B = p_A = p_0.$$

The major part of the energy increase takes the form of a pressure increase. The potential energy difference between the pump outlet and inlet, as well as the kinetic energy difference there is negligibly small compared to the pressure difference. Thus the energy increase expressed by Eq. (8.135) is called the manometric head H of the pump. The potential energy difference between the levels of the fluids in the reservoirs is called the geodetic head H_g. Thus

$$H_g = z_B - z_A. \tag{8.136}$$

Using this notation the manometric head can be written

$$H = H_g + \Sigma h'_{AB} . \tag{8.137}$$

In this expression the geodetic head is independent of the flow rate but the sum of the head losses does depend on the flow rate. For a laminar flow this dependence is linear, for a fully developed turbulent flow it is parabolic. For a smooth pipe, or in the transition region between laminar and turbulent flow head losses vary approximately with the 1.8th power of the flow rate.

8.8 Flow in pipes with heat exchange

In many engineering applications a considerable amount of thermal energy crosses the pipe walls which confine the flowing fluid. Examples of such problems are the flow of warm oil through a pipeline buried in cold soil, or the upflowing warm oil in a well.

Consider a one-dimensional steady flow in a pipe of circular cross section. Using log mean values which relate to the inlet and outlet cross sections, the balance of internal energy equation can be written

$$\varepsilon_2 - \varepsilon_1 = \frac{h_{\ln} A_3 \Delta T_{\ln}}{\dot{m}} + g h'_{1-2} , \tag{8.138}$$

where ε_2 and ε_1 are the specific internal energy at the outlet and the inlet, $h_{\ln}$ is the logarithmic mean heat transfer coefficient, A_3 is the area of the pipe wall between the inlet and outlet, $\Delta T_{\ln}$ is the logarithmic mean temperature difference, $\dot{m}$ is the mass flow rate, g is the acceleration due to gravity and h'_{1-2} is the head loss of the flow. Since the determination of the head loss can be done using the mechanical energy equation, the term

$$\frac{h_{\ln} A_3 \Delta T_{\ln}}{\dot{m}}$$

form the crux of the internal energy equation.

To begin our investigation of the heat transfer coefficient we examine the steady one-dimensional flow of an incompressible fluid confined in a pipe which has a constant wall temperature. The bulk flow temperature $\tilde{T}$ is greater than the wall temperature T_w. The unit normal vector n for a solid-fluid interface is taken as being directed from the fluid into the solid, thus the heat flux normal to the wall can be written as

$$q_n = h_{\text{loc}} (\tilde{T} - T_w) , \tag{8.139}$$

where h_{loc} is the local heat transfer coefficient.

Consider now an infinitesimal length dl of the pipe. Neglecting the head loss, the

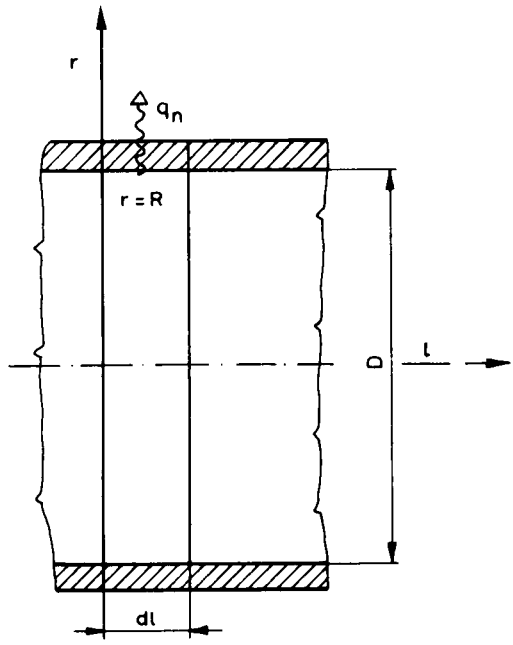

Fig. 8.30. Infinitesimal control volume for non-isothermal flow

internal energy balance for this control volume (see *Fig. 8.30*) is obtained as

$$\varrho c_v \frac{D^2\pi}{4} c(\tilde{T}-\mathrm{d}\tilde{T}) - \varrho c_v \frac{D^2\pi}{4} c\tilde{T} = h_{\mathrm{loc}} D\,\mathrm{d}l(\tilde{T}-T_w)\,. \tag{8.140}$$

This equation can be simplified to

$$-\varrho\pi c_v Dc \frac{\mathrm{d}\tilde{T}}{\mathrm{d}l} = 4h_{\mathrm{loc}}(\tilde{T}-T_w)\,. \tag{8.141}$$

Since T_w is constant, its derivative must be zero. Subtracting this derivative from the left-hand side of the equation we get

$$\varrho c_v Dc \frac{\mathrm{d}}{\mathrm{d}l}(\tilde{T}-T_w) = -4h_{\mathrm{loc}}(\tilde{T}-T_w)\,. \tag{8.142}$$

This equation may be divided by $k(\tilde{T}_1-T_w)$, where k is the coefficient of thermal conductivity of the fluid and $\tilde{T}_1$ is the bulk fluid temperature at the inlet of the pipe.

Introducing the dimensionless temperature

$$\Theta = \frac{\tilde{T}-T_w}{\tilde{T}_1-T_w} \tag{8.143}$$

and the dimensionless length l/D, the internal energy equation can be written as

$$\frac{\varrho c_v}{k} c \frac{\mathrm{d}\Theta}{\mathrm{d}\left(\frac{l}{D}\right)} = -4 \frac{h_{\mathrm{loc}} \cdot \Theta}{k}. \tag{8.144}$$

Multiplying both sides of the equation by D, and the left-hand side by v/v, we get

$$\frac{\varrho c_v v}{k} \frac{cD}{v} \frac{\mathrm{d}\Theta}{\mathrm{d}\left(\frac{l}{D}\right)} = -4 \frac{h_{\mathrm{loc}} D}{k} \cdot \Theta \tag{8.145}$$

It is clear that the equation can be expressed by three dimensionless similarity invariants: the Prandtl number, the Reynolds number and the Nusselt number. The last term, of course, only represents the local value of the latter:

$$\mathrm{Pr} = \frac{\varrho c_v v}{k},$$

$$\mathrm{Re} = \frac{cD}{v},$$

$$\mathrm{Nu}_{\mathrm{loc}} = \frac{h_{\mathrm{loc}} D}{k}.$$

Thus we get a simple differential equation

$$\frac{\mathrm{d}\Theta}{\mathrm{d}\left(\frac{l}{D}\right)} = -4\Theta \frac{\mathrm{Nu}_{\mathrm{loc}}}{\mathrm{Pr}\,\mathrm{Re}}, \tag{8.146}$$

which is readily integrated to give

$$\ln \Theta = -4 \frac{\mathrm{Nu}_{\mathrm{loc}}}{\mathrm{Re}\,\mathrm{Pr}} \frac{l}{D} + \ln C,$$

where C is a constant of integration. As a boundary condition to evaluate this constant we can make use of the fact that if $l/D = 0$, $\Theta = 1$. Thus we get

$$\ln \Theta = -\frac{4\mathrm{Nu}_{\mathrm{loc}}}{\mathrm{Re}\,\mathrm{Pr}} \frac{l}{D}. \tag{8.147}$$

From Eq. (8.143) the temperature distribution along the pipe axis is obtained as

$$\tilde{T} = T_w + (\tilde{T}_1 - T_w)\, \mathrm{e}^{-\frac{4\mathrm{Nu}_{\mathrm{loc}}}{\mathrm{Re}\,\mathrm{Pr}} \frac{l}{D}}. \tag{8.148}$$

The difference in the internal energy fluxes between the inlet and outlet can be

expressed as

$$\dot{Q}=\varrho c_v \frac{D^2\pi}{4} c(\tilde{T}_2-\tilde{T}_1). \tag{8.149}$$

This equation may be modified

$$\dot{Q}=\frac{\varrho c_v \nu}{k}\,\frac{cD}{\nu}\,\frac{D\pi k}{4}(\tilde{T}_2-\tilde{T}_1), \tag{8.150}$$

i.e.

$$\dot{Q}=\mathrm{Pr}\,\mathrm{Re}\,\frac{D\pi k}{4}(\tilde{T}_2-\tilde{T}_1).$$

At the outlet of the pipe, the temperature can be written

$$\tilde{T}_2=T_w+(\tilde{T}_1-T_w)\,\mathrm{e}^{-\frac{4\mathrm{Nu}_{\mathrm{loc}}}{\mathrm{Re}\,\mathrm{Pr}}\frac{L}{D}}. \tag{8.151}$$

Expressing from this the product Pr Re we get

$$\mathrm{Pr}\,\mathrm{Re}=-\frac{4\mathrm{Nu}_{\mathrm{loc}}L}{D\ln\dfrac{\tilde{T}_2-T_w}{\tilde{T}_1-T_w}}. \tag{8.152}$$

Substituting this into Eq. (8.150) we obtain

$$\dot{Q}=\frac{kL\pi\,\mathrm{Nu}_{\mathrm{loc}}(\tilde{T}_2-\tilde{T}_1)}{\ln\dfrac{\tilde{T}_2-T_w}{\tilde{T}_1-T_w}}. \tag{8.153}$$

After rearranging, this can be written as

$$\dot{Q}=h_{\mathrm{loc}}D\pi L\frac{(T_w-\tilde{T}_2)-(T_w-\tilde{T}_1)}{\ln\dfrac{T_w-\tilde{T}_2}{T_w-\tilde{T}_1}}. \tag{8.154}$$

Note, that this result is valid only for the case of a constant wall temperature, constant physical properties of the fluid and a constant heat transfer coefficient h_{loc}. If these conditions are satisfied, the above equation can be written in the brief form

$$\dot{Q}=h_{\mathrm{loc}}A_3\,\Delta T_{\ln}. \tag{8.155}$$

The heat transfer coefficient can be determined experimentally. Measuring the flow rate Q, the bulk temperatures $\tilde{T}_1$ and $\tilde{T}_2$, the wall temperature T_w in a pipe of diameter D and length L, the so-called logarithmic mean heat transfer coefficient is obtained as

$$h_{\ln}=\frac{Qc_v(\tilde{T}_1-\tilde{T}_2)}{D\pi L\,\Delta T_{\ln}}. \tag{8.156}$$

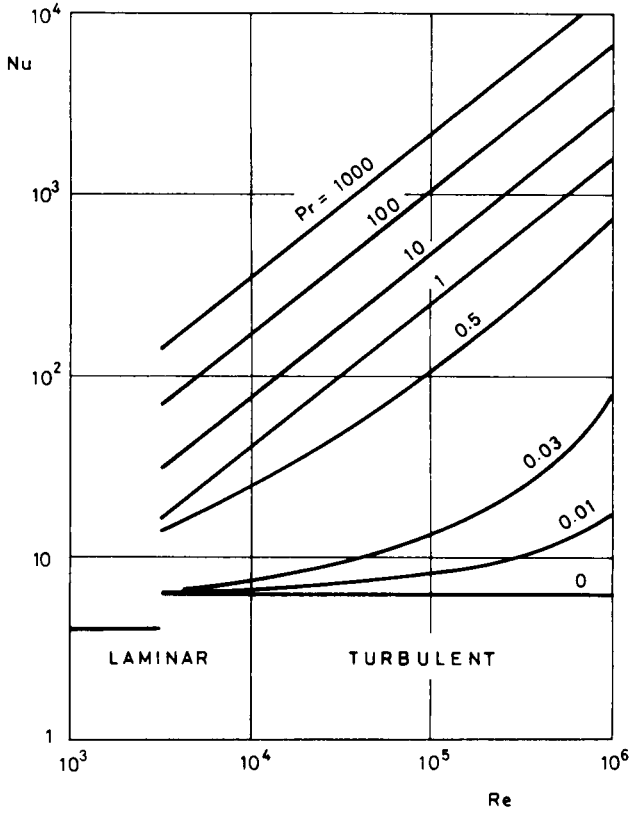

Fig. 8.31. Nusselt number for laminar and turbulent flow

The obtained experimental results can be interpreted in the form of a similarity invariant. As shown in *Fig. 8.31,* the laminar and turbulent regions can be distinguished easily. In the laminar region a satisfactory expression is obtained:

$$\mathrm{Nu_{ln}} = 1.86 \left(\frac{\mathrm{Re\,Pr}\, D}{L} \right)^{\frac{1}{3}} \left(\frac{\mu}{\mu_w} \right)^{0.14} . \tag{8.157}$$

In this equation the fluid properties (ϱ, c_v, k, ν) are evaluated at the mean bulk fluid temperature $\frac{1}{2}(\tilde{T}_1 + \tilde{T}_2)$. The viscosity μ is taken at this temperature, while μ_w is the viscosity at wall temperature.

For turbulent flow, experimental results lead to the following expression:

$$\mathrm{Nu_{ln}} = 0.015\, \mathrm{Re}^{0.83}\, \mathrm{Pr}^{0.42} \left(\frac{\mu}{\mu_w} \right)^{0.14} . \tag{8.158}$$

For ease of graphical interpretation this is rearranged in the form

$$\Psi = \frac{\mathrm{Nu}_{\ln}}{\mathrm{Pr}^{0.42}\left(\frac{\mu}{\mu_w}\right)^{0.14}} = 0.015\,\mathrm{Re}^{0.83}. \tag{8.159}$$

This quantity is plotted in *Fig. 8.32*. For laminar flow the effect of L/D is considerable and the Nusselt number decreases as the dimensionless length increases. In the turbulent region all measured points fall onto a single curve. This fact shows that Eq. (8.159) is a reasonably satisfactory empirical formula to estimate the heat transfer coefficient for turbulent flow.

For incompressible fluids it has already been noted that the pressure is not a thermodynamic variable; thus it is independent of the temperature. This fact makes possible an easy method of calculating the head loss of an incompressible non-isothermal flow. Since there is no relation between the pressure and the temperature, the mechanical energy equation and the thermal energy equation can be solved independently. The change in viscosity as a function of temperature is the only non-isothermal effect affecting the flow variables.

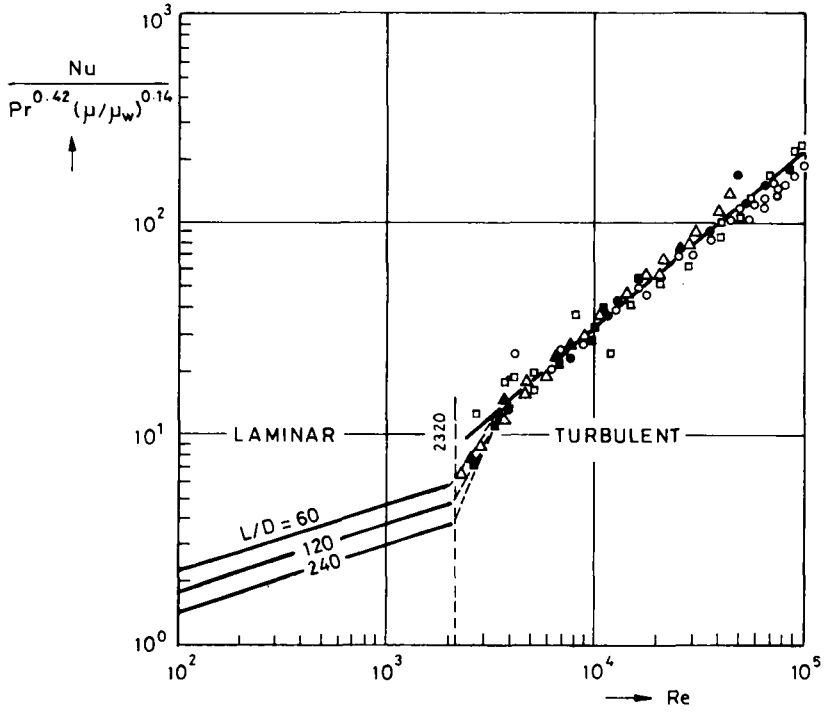

Fig. 8.32. Forced convection Nusselt numbers for pipe flow

By determining the temperature distribution along the pipe axis, the viscosity variation is obtained. For practical purposes it is convenient to divide the total pipe length into a number of finite isothermal sections, each with a constant viscosity. For each such isothermal section the head loss can be determined by the usual procedure. As the final step the head losses of these individual isothermal sections is then summed.

8.9 Pressure waves in one-dimensional pipe flow

Certain boundary conditions of a one-dimensional steady flow may suddenly change in a pipeline. The opening or closing of a valve, and the starting or stopping of a pump produce a jump in the continuous velocity and pressure distribution at a given point, which will propagate in wavelike form with the speed of sound both downstream and upstream through the pipe. The wave front is a singular surface with respect to both the velocity and the pressure field simultaneously. It is called simply a pressure wave in engineering practice since the pressure change is the most obvious indication of the phenomenon.

If the disturbance is relatively small, the flow variables themselves are continuous, but certain derivatives of these variables are discontinuous across the wave front. Such a wave is called a propagating weak singular surface. When the disturbance is strong enough, the flow variables themselves suffer a finite jump discontinuity. Such a wave is called a propagating strong singular surface or more commonly a shock wave. The increase in pressure which accompanies a shock wave can exceed the design specifications of the pipeline, leading to the rupture of the latter. Thus this phenomenon is of considerable importance, both from a theoretical and a practical point of view.

The equations governing an unsteady one-dimensional flow can be written very simply by neglecting the head losses and the force of gravity. The head loss for a relatively short section of pipe is much smaller than the other energy terms. The concept of friction joints considers an actual pipeline as being divided into a sufficiently large number of appropriately short, frictionless pipe segments, with all the head losses concentrated at the end of each segment, as shown in *Fig. 8.33*. The individual joints at which all pipe friction is assumed to be concentrated are called friction joints. By using the concept of friction joints the mathematical formulation of the problem becomes simple and easy to calculate. The force of gravity has no component in a horizontal component of the momentum equation. For the sake of simplicity pressure waves will be treated first.

Consider a uniform pipe section in which no body force or friction force is present. Let l be the coordinate along the pipe axis. For the momentum equation we obtain

$$\frac{\partial c}{\partial t} + c\frac{\partial c}{\partial l} = -\frac{1}{\varrho}\frac{\partial p}{\partial l}, \tag{8.160}$$

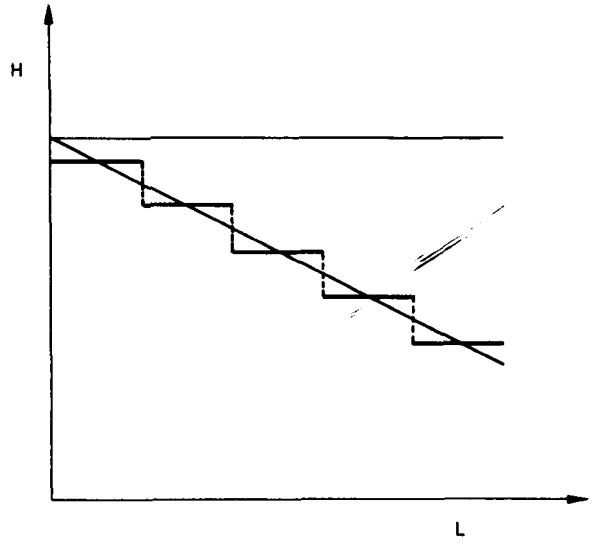

Fig. 8.33. Frictionless pipe segments for pressure wave calculations

while the continuity equation can be written as

$$\frac{\partial \varrho}{\partial t} + c\frac{\partial \varrho}{\partial l} = -\varrho\frac{\partial c}{\partial l}. \tag{8.161}$$

The relationship between the pressure and the density can be expressed by the equation for the speed of sound

$$a = \sqrt{\frac{\mathrm{d}p}{\mathrm{d}\varrho}}.$$

In gases the speed of sound is a variable of the thermal state. For isentropic flow it is given by

$$a = \sqrt{\kappa\frac{p}{\varrho}}. \tag{8.162}$$

The velocity of the flowing gas may even exceed the speed of sound, and thus it cannot be neglected. Since the speed of sound depends on the pressure and density, it changes with both the length l and time.

For liquids the speed of sound varies with the bulk modulus of elasticity B as

$$a = \sqrt{\frac{B}{\varrho}}. \tag{8.163}$$

Since the density variations of liquids are negligibly small, the speed of sound in a given liquid is always nearly constant, even for wide variations of pressure. The speed of sound in liquids is much greater than the usual flow velocities, and thus the latter may be neglected.

The above results are based upon the assumption of a planar wave propagating in an unbounded mass of fluid. However, the pressure wave problems considered here involve flows confined within a pipe. A major difference is that the velocity of propagation of a wave in a pipe is distinctly different from the speed of sound in an unbounded fluid. As the fluid pressure increases, the fluid is not only compressed (with a concomitant density increase), but the pipe walls also expand elastically. Thus the density increase is less than it would be if confined in a rigid pipe. Thus, the elasticity of the pipe reduced the velocity of propagation of the pressure waves through it. For a thin-walled pipe of circular cross section the resulting bulk modulus of elasticity B^* is obtained from the formula

$$\frac{1}{B^*} = \frac{1}{B} + \frac{D}{\delta}\frac{1}{E}, \tag{8.164}$$

where δ is the wall thickness, E is the modulus of elasticity of the pipe material. Thus the wave velocity in a fluid confined within a thin walled pipe is

$$a_w = \sqrt{\frac{B^*}{\varrho}} = \sqrt{\frac{B/\varrho}{1+\frac{D}{\delta}\frac{B}{E}}}. \tag{8.165}$$

Since this can also be written as

$$a_w = \frac{a}{\sqrt{1+\frac{D}{\delta}\frac{B}{E}}}, \tag{8.166}$$

it is clear that a_w must be smaller than the speed of sound. Some typical values of a_w are collected in the *Table*.

Liquid	B[N/m^2]	ϱ[kg/m^3]	Pipe material	E[N/m^2]	$\frac{D}{\delta}$	a_w[m/s]
Water (20 °C, 1...25 bar)	2.105×10^9	998	steel	2×10^{11}	100	1012
			cast iron	1.1×10^{11}	20	1215
			lead	1.9×10^{10}	5	1175
Crude oil	1.594×10^9	805	steel	2×10^{11}	100	1054
Gasoline	1.092×10^9	690	steel	2×10^{11}	100	1041

It is obvious, that the velocity of propagation of a pressure wave in an elastic pipe is

$$a_w^2 = \frac{\mathrm{d}p}{\mathrm{d}\varrho}. \tag{8.167}$$

By using this expression the continuity equation can be modified. Applying the chain rule we get

$$\frac{\mathrm{d}\varrho}{\mathrm{d}t} = \frac{\mathrm{d}\varrho}{\mathrm{d}p}\frac{\mathrm{d}p}{\mathrm{d}t} = \frac{1}{a_w^2}\frac{\mathrm{d}p}{\mathrm{d}t}. \tag{8.168}$$

Doing the same for $\frac{\mathrm{d}\varrho}{\mathrm{d}l}$, and after substitution into the continuity equation, we obtain

$$\frac{1}{a_w^2}\left(\frac{\partial p}{\partial t} + c\frac{\partial p}{\partial l}\right) = -\varrho\frac{\partial c}{\partial l}. \tag{8.169}$$

Multiplying by a_w, this equation can be added to the momentum equation. The result is

$$\varrho\left[\frac{\partial c}{\partial t} + (c+a_w)\frac{\partial c}{\partial l}\right] + \frac{1}{a_w}\left[\frac{\partial p}{\partial t} + (c+a_w)\frac{\partial p}{\partial l}\right] = 0. \tag{8.170}$$

Certain material derivatives are easily recognized within the square brackets. These derivatives represent the rate of change of the velocity and the pressure at a point moving downstream with a velocity $c+a_w$. Thus we can write Eq. (8.170) in the form

$$\varrho\left.\frac{\mathrm{d}c}{\mathrm{d}t}\right|_{c+a_w} = -\left.\frac{1}{a_w}\frac{\mathrm{d}p}{\mathrm{d}t}\right|_{c+a_w}. \tag{8.171}$$

If, instead of adding, we subtract the continuity equation from the momentum equation, we obtain

$$\varrho\left[\frac{\partial c}{\partial t} + (c-a_w)\frac{\partial c}{\partial l}\right] - \frac{1}{a_w}\left[\frac{\partial p}{\partial t} + (c-a_w)\frac{\partial p}{\partial l}\right] = 0. \tag{8.172}$$

This leads obviously to the material derivatives

$$\varrho\left.\frac{\mathrm{d}c}{\mathrm{d}t}\right|_{c-a_w} = \left.\frac{1}{a_w}\frac{\mathrm{d}p}{\mathrm{d}t}\right|_{c-a_w}. \tag{8.173}$$

The above results can be interpreted in terms of characteristic variables. In the t, l plane the differential equations

$$\frac{\mathrm{d}l_1}{\mathrm{d}t} = \tan\alpha_1 = c + a_w, \tag{8.174}$$

and

$$\frac{\mathrm{d}l_2}{\mathrm{d}t} = \tan\alpha_2 = c - a_w, \tag{8.175}$$

define two families of curves which are called the characteristic curves of these equations, while $\tan \alpha_1$ and $\tan \alpha_2$ are called the characteristic directions. Along the first family of characteristic curves

$$\frac{dp}{dc} = -\varrho a_w \tag{8.176}$$

while along the second family of curves

$$\frac{dp}{dc} = \varrho a_w . \tag{8.177}$$

In the plane of the variables c and p two other families of characteristic lines are similarly obtained. Along the first characteristics

$$p + \varrho a_w c = \text{const} , \tag{8.178}$$

while along the second characteristics

$$p - \varrho a_w c = \text{const} . \tag{8.179}$$

Any point in the t, l plane can be mapped onto the c, p plane. This makes a simple graphical representation possible.

By using these characteristic curves a conjugate pair of differential equations satisfying the initial conditions can be solved in a simple numerical way. We need to know the values of the pressure, velocity and density at the time $t = 0$. These can be given either as their distribution functions along the pipe axis, or as discrete values at given points. Further, at one point along the length of the pipe (for practical purposes this is chosen at the end), the time-dependency of the perturbation must be known, i.e. the variation of p, c, and ϱ as a function of time. Thus, p, c and ϱ are known along two orthogonal lines of the t, l plane. By determining the families of characteristic lines a network is obtained as shown in *Fig. 8.34*. If

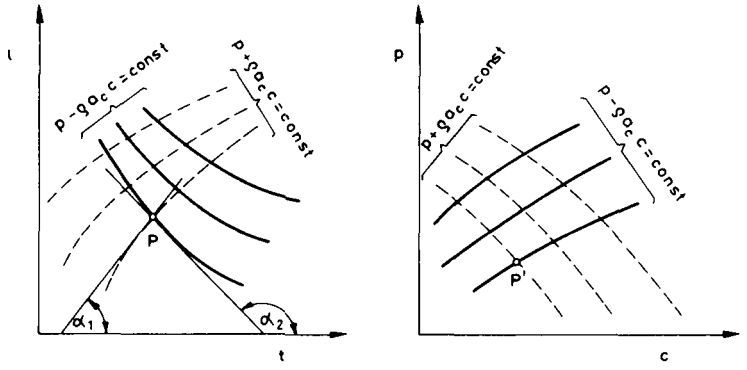

Fig. 8.34. Characteristic lines

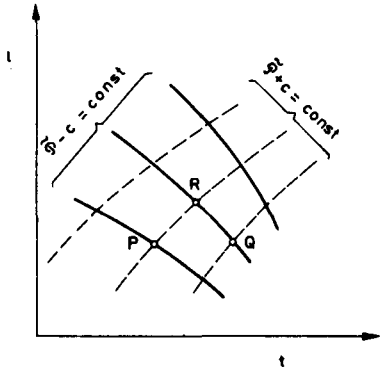

Fig. 8.35. Characteristic lines for gas pipeline

the network of the intersecting characteristics is sufficiently dense, the curvilinear rectangles may be replaced by perfect squares. The pressure, velocity and density values are known at the intersections of the characteristics and at the $t=0$, $l=0$ lines. Along the characteristics further intersections may be obtained step by step, at which the pressure, velocity and density can be determined. Knowing the values of the pressure and the density, the local speed of sound can be calculated. This determines the slope of the characteristic towards the next intersection. By this step-by-step method the flow variables can be determined at any point in the t, l plane.

Consider the points P and Q (for which both the flow variables and the variables of state are known), in the t, l plane as shown in *Fig. 8.35*. The intersection of a first characteristic through P, and a second characteristic through Q, defines the point R in the t, l plane, which represents a position l_R in the pipe at the corresponding instant t_R. The derivatives of Eqs (8.174) and (8.175) can be replaced by the finite differences

$$\frac{l_R - l_P}{t_R - t_P} = \frac{1}{2}[(c - a_w)_R + (c - a_w)_P] \tag{8.180}$$

$$\frac{l_R - l_Q}{t_R - t_Q} = \frac{1}{2}[(c - a_w)_R + (c - a_w)_Q]\,. \tag{8.181}$$

By introducing the modified barotropic potential

$$\tilde{\mathcal{P}} = \int_{p_0}^{p} \frac{\mathrm{d}p}{a_w \varrho}, \tag{8.182}$$

we can write

$$(\tilde{\mathcal{P}} + c)_R = (\tilde{\mathcal{P}} + c)_P \tag{8.183}$$

$$(\tilde{\mathcal{P}} - c)_R = (\tilde{\mathcal{P}} - c)_Q\,. \tag{8.184}$$

If the nature of the change of the thermal state is known the barotropic potential can be determined. For the isentropic case

$$\tilde{\mathscr{P}} = \frac{\kappa}{\kappa - 1} \frac{p}{a_w \varrho}. \tag{8.185}$$

The speed of sound at point R is obtained as

$$a_{wR} = a_{0w} + \frac{\kappa - 1}{2} \mathscr{P}_R, \tag{8.186}$$

where a_{0w} is the stagnation or reservoir value of the acoustic velocity:

$$a_{0w} = \frac{a_0}{\sqrt{1 + \frac{D}{\delta} \frac{B}{E}}}. \tag{8.187}$$

Thus the five unknowns (l_R, t_R, $\tilde{\mathscr{P}}_R$, c_R, a_{wR}) can be determined using five equations. In this way the flow variables of a one-dimensional unsteady gas flow can be calculated step by step at the intersections of the characteristics.

In the case of the flow of a liquid, in particular, the calculations are much simplified. The velocity of propagation of the waves is independent of the pressure, and much greater than the flow velocity (about 1000 m/s, vs. 1–2 m/s). Thus the wave velocity can be considered to be constant. For a pipe of constant diameter the characteristics are straight lines. Knowing the initial and boundary conditions, the flow parameters at any point can be determined directly, without a narrow grid of characteristics being required.

Consider *Fig. 8.36*. The flow parameters for the arbitrary point R are unknown. The velocity and pressure distribution along the pipe is known for the instant $t = 0$. Similarly, the change in the pressure and the velocity with time at the inlet, where $l = 0$, is also known. The first and second characteristic can be drawn through the

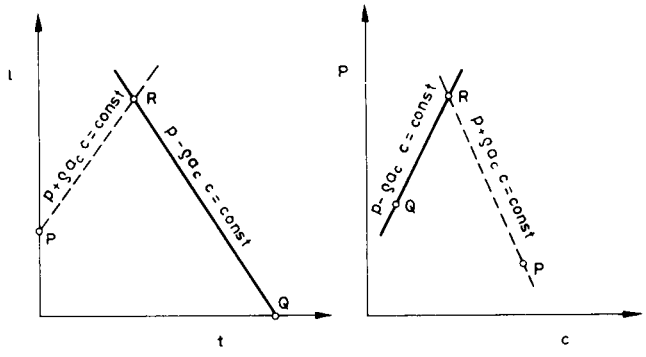

Fig. 8.36. Determination of flow variables by characteristics

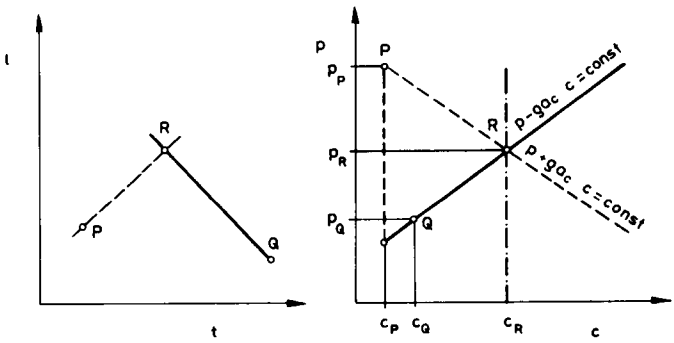

Fig. 8.37. Determination of pressure by characteristics

point R as shown in *Fig. 8.36*. The characteristics intersect the coordinate axes at the points P and Q. The flow variables c and p are known at these points. Since the characteristics are straight lines we obtain the relations

$$\frac{l_R - l_p}{t_R - t_p} = a_w , \tag{8.188}$$

$$\frac{l_R - l_Q}{t_R - t_Q} = -a_w , \tag{8.189}$$

$$\frac{p_R - p_P}{c_R - c_p} = -\varrho a_w , \tag{8.190}$$

$$\frac{p_R - p_Q}{c_R - c_Q} = \varrho a_w . \tag{8.191}$$

These equations are totally adequate for calculating the pressure and the velocity at any arbitrary point R.

The initial and boundary conditions for a transient pipe flow may vary widely. A common situation is the one where the velocity or the pressure is known at the point R. In this case it is sufficient to know the flow variables at only one other point P. Consider *Fig. 8.37*, where the velocity and the pressure are known for point P, as is the velocity at point R. The pressure at point R is obtained as

$$p_R = p_P - \varrho a_w (c_R - c_P) . \tag{8.192}$$

Knowing the flow variables at the point Q, the equation for the second characteristic can be written as

$$p_R = p_Q + \varrho a_w (c_R - c_Q) . \tag{8.193}$$

Now consider *Fig. 8.38* where the pressure at point R is known. Along a first characteristic which passes through the point P, where both the velocity and the

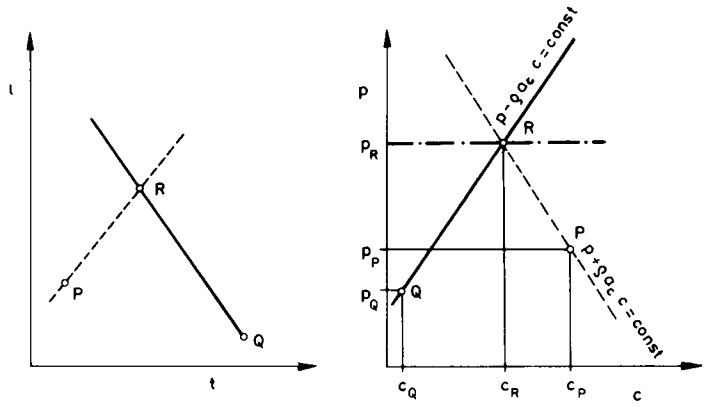

Fig. 8.38. Determination of velocity by characteristics

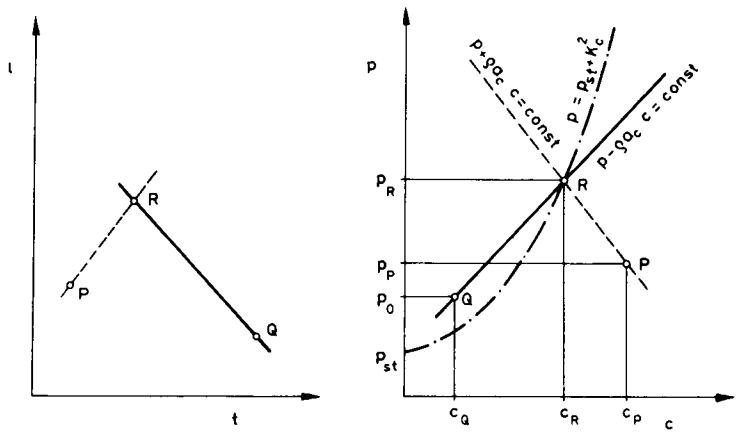

Fig. 8.39. Determination of pressure and velocity by characteristics

pressure are known, the velocity c_R is given by

$$c_R = c_P - \frac{p_R - p_P}{\varrho a_w}. \tag{8.194}$$

By using a second characteristic passing through point Q, we get

$$c_R = c_Q + \frac{p_R - p_Q}{\varrho a_w}. \tag{8.195}$$

Knowing that the pressure loss-velocity relation for a pipe can be written as

$$p = p_{st} + Kc^2, \tag{8.196}$$

while the flow variables at the point P have been calculated using a first characteristic, the pressure and the velocity at the point R can be calculated as

$$p_R = p_{st} + Kc_R^2, \tag{8.197}$$

$$\frac{p_R - p_P}{c_R - c_P} = -\varrho a_w. \tag{8.198}$$

(The static pressure p_{st} is independent of the velocity c.)

The graphical interpretation of this solution is shown in *Fig. 8.39.*

In the method discussed above, the fluid friction is considered as having been taken into account in the boundary conditions. The direct consideration of the viscous effects leads to more complicated basic equations. For a pipeline of arbitrary inclination let

$$U = \frac{p}{\varrho} + gh \tag{8.199}$$

be the sum of the barotropic and the gravitational potential. We can now write the continuity and momentum equations as

$$\frac{\partial c}{\partial t} + c\frac{\partial c}{\partial l} + \frac{\partial U}{\partial l} = -\frac{\lambda}{2D}|c|c, \tag{8.200}$$

$$\frac{\partial U}{\partial t} + c\frac{\partial U}{\partial l} + a_w^2\frac{\partial c}{\partial l} = -gc\sin\alpha. \tag{8.201}$$

The equations of the characteristics in the t, l plane are

$$\frac{dl_1}{dt} = c + a_w,$$

$$\frac{dl_2}{dt} = c - a_w.$$

In the same manner as used earlier, the material derivatives of the velocity c and the energy U along the characteristics are obtained as

$$\left(\frac{dc}{dt}\right)_{c+a_w} + \frac{1}{a_w}\left(\frac{dU}{dt}\right)_{c+a_w} = -\frac{c}{a_w}g\sin\alpha - \frac{\lambda}{2D}|c|c, \tag{8.202}$$

and

$$\left(\frac{dc}{dt}\right)_{c-a_w} - \frac{1}{a_w}\left(\frac{dU}{dt}\right)_{c-a_w} = \frac{c}{a_w}g\sin\alpha - \frac{\lambda}{2D}|c|c. \tag{8.203}$$

These differential equations can be expressed in terms of finite differences, and a numerical solution obtained.

CHAPTER 9

NON-NEWTONIAN FLUID FLOW

9.1 Specific types of flow behavior

The formulation of any flow problem is based on the general principles of mechanics. These principles are expressed in the form of balance equations. The continuity, momentum or energy equation is valid for any material system. In spite of this generality the fact that the number of these equations is less than the number of unknown flow variables is a serious problem. On the other hand, the response of a fluid to a mechanical action is determined not only by general laws, but also by the specific properties of the fluid. Such properties manifest themselves in the relationship between the imposed stress **T**, and the resulting strain **S**. Everyday experience shows that these variables are related differently for different fluids. The relationship

$$\mathbf{T} = \mathbf{T}(\mathbf{S})$$

which is characteristic of a given fluid is called the constitutive or rheological relation. A useful classification of fluids is possible on the basis of their constitutive relations. Although considerable effort has been expanded in the search for exact relationships between the variables which characterize the rheological behavior of fluids, only a few individual equations, of an approximative character are known.

A particular constitutive relation is rigorously valid only for a hypothetical model-fluid. Thus the construction of a constitutive relation is equivalent to the definition of a hypothetical fluid model; i.e. one which describes the rheological behavior of a certain type of fluid in an approximate manner.

The simplest case is the model of a perfect fluid in which the shear stresses are neglected. Its constitutive relation is

$$\mathbf{T} = -p\mathbf{I} \,. \tag{9.1}$$

So-called Newtonian fluids are characterized by a linear relationship between the stress and the rate of deformation:

$$\mathbf{T} = -p\mathbf{I} + \mu(\vec{v} \circ \nabla + \nabla \circ \vec{v}) \,. \tag{9.2}$$

Here the viscosity μ is a single constant at a given temperature. Gases and low molecular weight liquids are almost always Newtonian under conventional shear

rates (below 10^5 s^{-1}). In this case the viscosity is independent of the type of motion.

Fluids, that do not follow a Newtonian behavior are particularly important to petroleum engineers. Many crude oils, drilling muds, fracturing gels, and cement pastes exhibit non-Newtonian behavior. The major division amongst non-Newtonian fluids is between those that can be described as purely viscous, and those that exhibit both viscous and elastic behavior.

Purely viscous fluids may be completely characterized by their shear stress-shear rate relationship under conditions of one-dimensional laminar flow. Thus the shear stress-shear rate function can be determined by measuring only one component of the stress tensor and the deformation rate tensor. In view of the wide range over which measurements need to be made for these variables, it is convenient to plot the shear rate-shear stress relationship. The curve thus obtained, the so-called flow curve, is suitable to characterize the rheological behavior of the fluid and forms an important aid in the classification of the different types of non-Newtonian fluids.

The flow curve of a Newtonian fluid is a straight line. Flow curves of Newtonian fluids of different viscosities pass through the origin; the slope of the lines representing viscosity of the fluid. Logarithmically plotted flow curves are parallel straight lines with slopes equal to unity. They have intercepts at $dv/dr = 1$ equal to their viscosities. Both types of flow curve are shown in *Figs 9.1* and *9.2*.

The terms pseudoplastic and dilatant refer to fluids for which the logarithmically plotted flow curves have slopes of less than unity and greater than unity respectively. The apparent viscosity

$$\mu_a = \frac{\tau}{\frac{dv}{dr}} \tag{9.3}$$

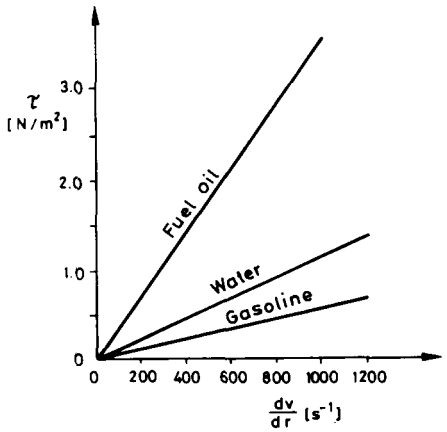

Fig. 9.1. Flow curves of Newtonian fluids with arithmetic coordinates

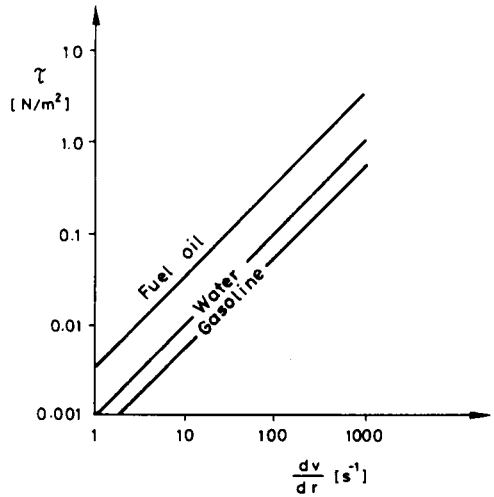

Fig. 9.2. Flow curves of Newtonian fluids with logarithmic coordinates

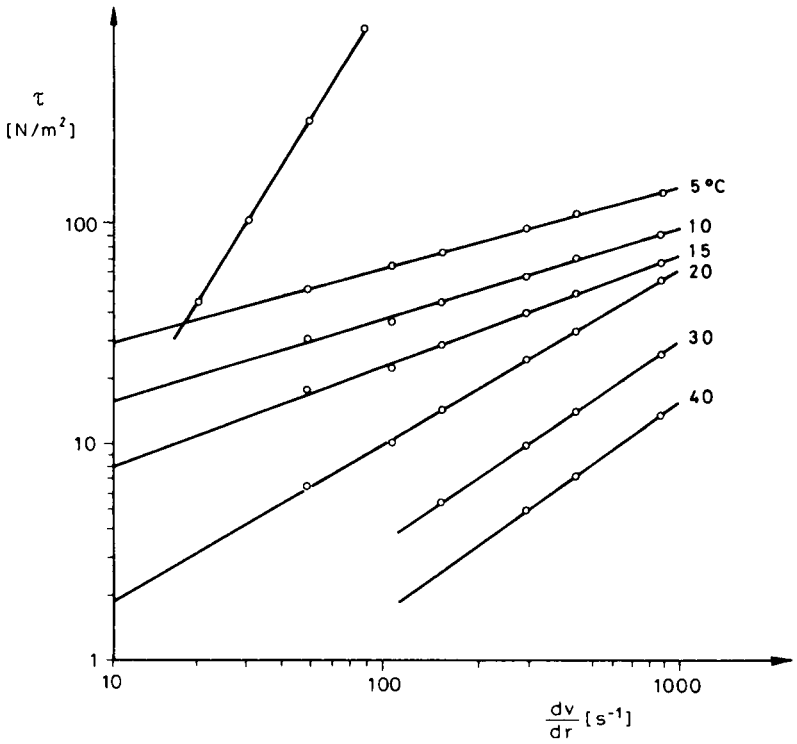

Fig. 9.3. Pseudoplastic and dilatant flow curves

decreases with increasing shear rate for pseudoplastic fluids, while it increases as the shear rate increases for dilatant material, as shown in *Fig. 9.3*. These flow curves also show that pseudoplastic and dilatant behavior may exist only over a limited range of the shear rate.

There is no single simple form of the constitutive relation that adequately expresses the rheological behavior of pseudoplastic materials. Widely used in petroleum engineering is the so-called power law equation, which is valid over a limited range of the shear rate, where the logarithmic flow curve is a straight line. This law is obtained empirically as

$$|\tau| = K\left|\frac{dv}{dr}\right|^n. \tag{9.4}$$

In this equation K is the so-called consistency index, and n is the behavior index. Both K and n depend on the temperature of the fluid. *Figure 9.3* shows the flow curves of a Hungarian crude oil (from Algyő) at different temperatures. The variation of the consistency index and the behavior index as a function of temperature is shown in *Fig. 9.4*.

A more precise expression for the power law can be written using cylindrical coordinates as

$$\tau_{rz} = K\left|\frac{dv}{dr}\right|^{n-1}\frac{dv}{dr}. \tag{9.5}$$

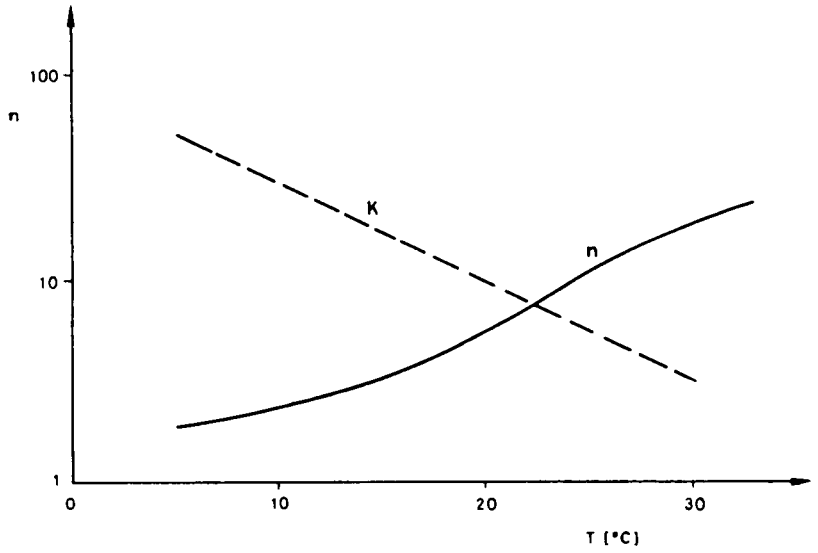

Fig. 9.4. Flow curves of an Algyő crude oil at different temperatures; consistency index and behavior index varying with temperature

It is obvious that the apparent viscosity

$$\mu_a = K\left|\frac{\mathrm{d}v}{\mathrm{d}r}\right|^{n-1} > 0\,.$$

The constitutive relation of a purely viscous fluid must per definitionem be the same in the tensorial form as when obtained for a single component only. Thus we can write

$$\mathbf{T} = -p\mathbf{I} + K(\mathbf{S}:\mathbf{S})^{\frac{n-1}{2}}\mathbf{S}\,. \tag{9.6}$$

Within its validity range, the power law equation is in excellent agreement with experimental data. The accuracy of the power law equation decreases at very low and very high shear rates. For pseudoplastic fluids the behavior index is always less than unity. Most crude oils, fine clay suspensions, certain types of drilling muds, and washing fluids exhibit pseudoplastic behavior.

The power law equation may also be applied to dilatant fluids with appropriately different values of the consistency index and the behavior index. The behavior index of dilatant fluids is always greater than unity. Dilatancy can be observed in

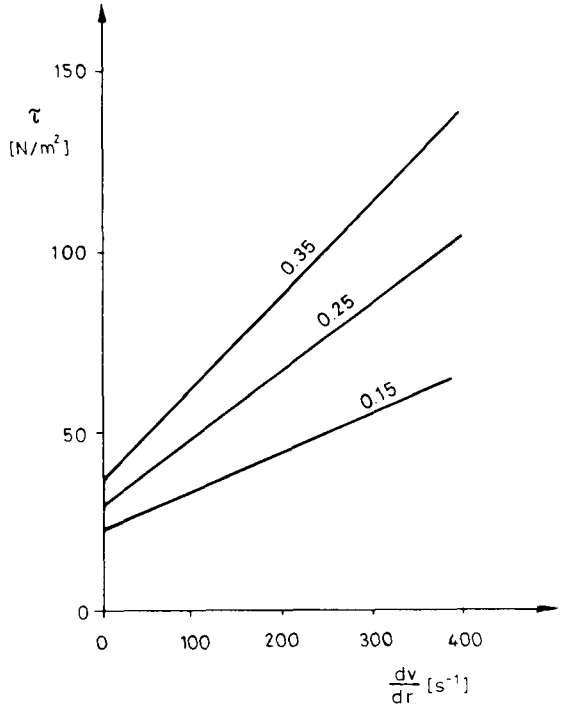

Fig. 9.5. Flow curve of a Bingham plastic fluid: a drilling mud at different concentrations

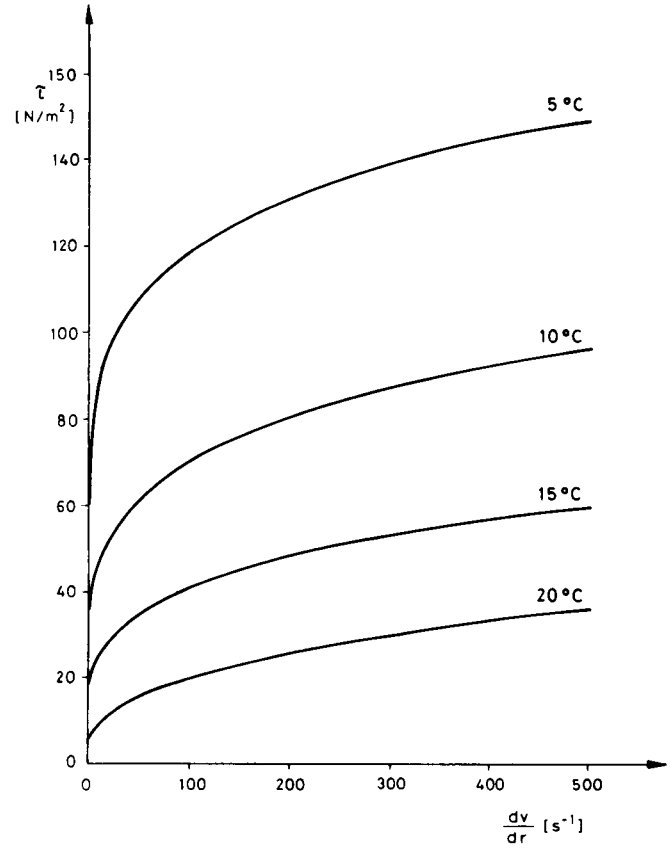

Fig. 9.6. Flow curves of a yield-pseudoplastic crude oil from Mezősas, Hungary

dense suspensions of irregularly shaped solids in liquids. The dilatancy can vary rapidly with the concentration. The same suspension at lower a concentration may be pseudoplastic, while at a higher concentration the behavior is dilatant.

The so-called Bingham plastic materials are fluids for which a finite shearing stress is required to initiate motion, and for which there is a linear relationship between the shear rate and the shear stress once the initiating stress has been exceeded. This behavior characterizes asphalt, bitumen, certain drilling muds, fly ash suspensions, sewage sludge, etc.

The constitutive relation of a Bingham fluid is of the form

$$|\tau| = \tau_y + \mu \left| \frac{dv}{dr} \right|, \tag{9.7}$$

where τ_y is the yield stress. *Figure 9.5* shows the flow curves of a Bingham drilling mud at different concentrations.

Certain materials exhibit a yield stress like a Bingham fluid, but the relationship between the shear rate and the shear stress after the yield stress has been exceeded is not linear. This category comprises mainly drilling muds, but there are some crude oils which also display this yield pseudoplastic character. *Figure 9.6* shows the flow curve of a crude oil from Mezősas (Hungary) which exhibits such behavior. The constitutive relation for these fluids can be written as

$$\tau = \tau_y + K\left|\frac{\mathrm{d}v}{\mathrm{d}r}\right|^{n-1}\frac{\mathrm{d}v}{\mathrm{d}r}. \tag{9.8}$$

Newtonian, pseudoplastic and dilatant fluids respond instantaneously to a change in the shear stress. Their rheological behavior is influenced by structural changes in the system. Their equilibrium structure depends on the shear rate, and follows any change in the shear rate without the slightest delay. This structural change can be considered as instantaneous and reversible.

In contrast to this, certain other fluids exhibit slow structural changes, which follow changes in the shear rate with a considerable delay. The reconstruction of the changed structure may be so extremely slow that the process can be considered irreversible. This time-dependent rheological behavior is rather common. Certain drilling fluids and crude oils exhibit time-dependent rheological properties. *Figure 9.7* shows the decrease in the shear stress at a constant shear rate as a function of the duration of shear, as measured for a Kiskunhalas (Hungary) crude oil.

If the shear stress at a constant shear rate decreases with the duration of shear, the fluid is called thixotropic. As *Fig. 9.7* shows, the shear stress decreases asymptotically to a stabilized value τ_s. The duration of shear necessary to reach the stabilized value decreases as the shear rate increases. The value of the stabilized shear stress depends on the shear rate as

$$\tau_s = K_s\left(\frac{\mathrm{d}v}{\mathrm{d}r}\right)^m. \tag{9.9}$$

This power law equation has a behavior index m of less than unity, thus the relationship is of a pseudoplastic type. It characterizes an ultimate structural state which is independent of time, i.e. stable. Equation (9.9) can be used as an adequate constitutive relation for a flow of crude oil after the first few kilometers of a pipeline.

The thixotropic character of a crude oil may be important for relatively short pipelines, especially for the collecting system of an oilfield.

A great number of constitutive relations have been proposed for thixotropic fluids, which of necessity are more complex than the power law equation. A relative simple constitutive relation was developed by Bobok and Navratil (1982) for thixotropic crude oils on the basis of a wide range of experimental results. In this model the thixotropic oil is considered to be a pseudoplastic fluid with changing rheological properties.

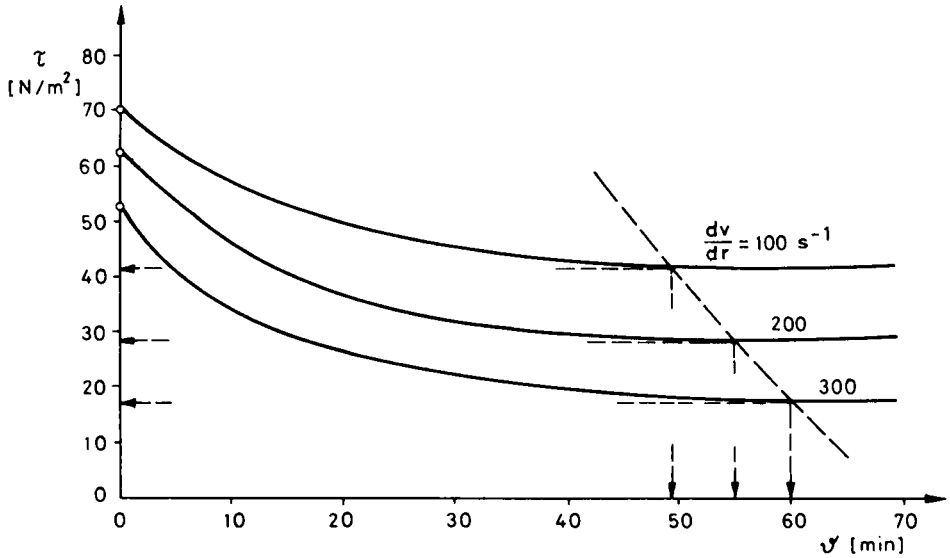

Fig. 9.7. Thixotropic shear stress decrease of a crude oil from Kiskunhalas, Hungary

The shear stress in this model depends on two variables: the shear rate and a dimensionless structural parameter δ:

$$\tau = \left(\frac{dv}{dr}, \delta\right). \tag{9.10}$$

It is assumed, that the structure of a thixotropic fluid can be completely characterized by the structural parameter which depends on the shear rate and the duration of shear. The function, given by Eq. (9.10) can be represented by a surface in the coordinate system dv/dr, δ, τ as shown in *Fig. 9.8*. Any changes in the shear condition occur along a curve on this surface of the shear state. The path on this surface between two arbitrary points can be broken down along the orthogonal parameter coordinates $\left(\frac{dv}{dr} \text{ and } \delta\right)$, into a constant shear rate, and a constant δ section. The processes of constant shear rate, and of constant structural parameter are having merely different nature.

The constant-shear-rate process is considered as irreversible. It can proceed along a $dv/dr = \text{const}$ curve in one direction only, namely that in which the structural parameter decreases i.e. the thixotropic structure is broken down. Since the breakdown of the structure is much faster than its regeneration (less than an hour as opposed to a few days) and regeneration may already have started at rest, the irreversibility of this process seems to be acceptable. Another important feature of the constant-shear-rate process is, that its ultimate state is on the stabilized flow curve. At any constant shear rate both δ and τ decrease as the duration of shear

increases, until the stabilized values δ_s and τ_s are reached. Values of δ and τ smaller than δ_s and τ_s cannot be achieved by the further increase in the duration of shear only. The stabilized-flow curve cannot be crossed along a constant-shear-rate line.

Along the constant structural-parameter curves the consistency index and the flow-behavior index are constant, thus the parameter curves $\delta = \text{const}$ are real pseudoplastic flow curves, i.e.

$$\tau = K\left(\frac{dv}{dr}\right)^n. \tag{9.11}$$

Experimental observations show, that the consistency index changes with δ, but that the behavior index may be considered constant. Along the parameter lines $\delta = \text{const}$, the stabilized flow curve can be crossed in both directions. The shear rate of the crossing point C is an important quantity in evaluating the consistency index K of an arbitrary flow curve of constant δ.

As is shown in *Fig. 9.9* at the point C the stabilized flow curve and an arbitrary flow curve of constant δ intersect each other. It is obvious, that

$$\tau_{sc} = K_s\left(\frac{dv}{dr}\right)_c^m = K\left(\frac{dv}{dr}\right)_c^n = \tau_c, \tag{9.12}$$

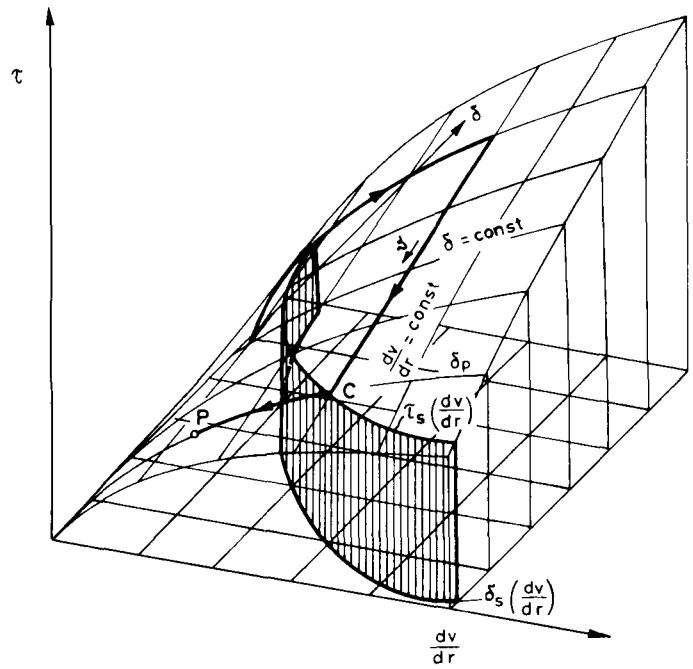

Fig. 9.8. Shear state surface of thixotropic fluids

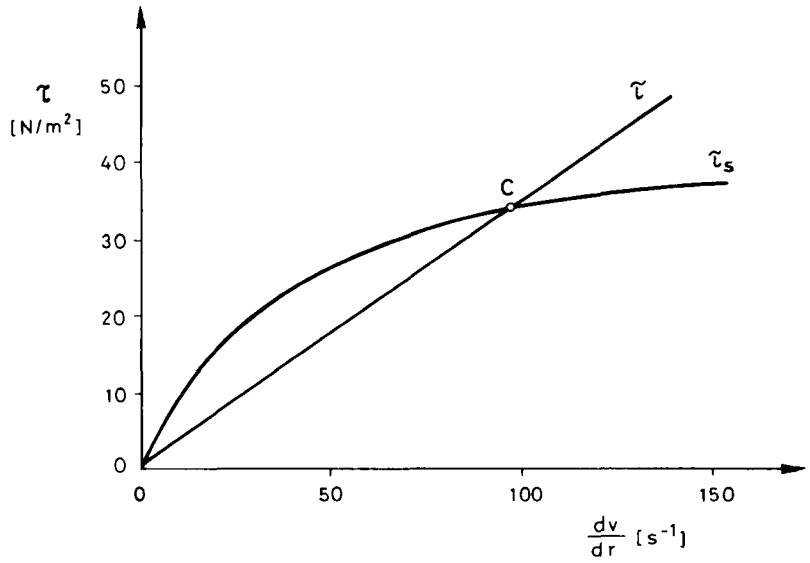

Fig. 9.9. Flow curves of thixotropic fluid

thus K can be expressed as

$$K = K_s \left(\frac{dv}{dr}\right)_c^{m-n}. \tag{9.13}$$

Substituting this into Eq. (9.11) we get

$$\tau = K_s \left(\frac{dv}{dr}\right)_c^{m-n} \left(\frac{dv}{dr}\right)^n. \tag{9.14}$$

In the interval where

$$\frac{dv}{dr} < \frac{dv}{dr_c}$$

it is possible, at a given dv/dr, to achieve smaller shear stresses than the stabilized shear stress at this dv/dr.

The flow curve in the interval

$$0 \leqq \frac{dv}{dr} \leqq \frac{dv}{dr_c}$$

is reversible, changing the shear rate whenever the measured shear stress falls to the curve $0C$. Increasing the shear rate to a greater value $\frac{dv}{dr_p}$, the immediately obtained shear stress τ_p will be on the same flow curve of constant δ, since the thixotropic structure remains the same. But from this instant the breakdown of the

structure begins, and the state of shear will reach the stabilized flow curve, along a constant-shear-rate line at point C'. The shear stress for this constant-shear-rate breakdown process can be expressed as

$$\tau = K_s \left(\frac{dv}{dr}\right)^m \left\{ 1 + \left[\frac{\left(\frac{dv}{dr}\right)^{n-m}}{\left(\frac{dv}{dr}\right)_c^{n-m}} - 1 \right] e^{-\left(\alpha \frac{dv}{dr} + \beta\right)\vartheta} \right\} \tag{9.15}$$

in which $\frac{dv}{dr}$ is the actual shear rate,

$\left(\frac{dv}{dr}\right)_c$ is the earlier shear rate for the stabilized state of shear,

α and β are material constants,

ϑ is the duration of shear at the present shear rate.

The equation contains five material constants (K_s, m, n, α, β) which can be determined using a rotational viscosimeter. Thus we have piecewise, valid constitutive relations for certain restricted changes of the shear state of a thixotropic fluid.

For the entrance region of a one-dimensional steady thixotropic flow in a pipe, Eq. (9.15) can be used. Naturally, the "entrance region" is thought of in a thixotropic sense. After the necessary duration of shear the stabilized shear state will be attained for which Eq. (9.9) is valid. For an abrupt change in the shear rate (change in pipe diameter or flow rate) the new shear stress can be determined using Eq. (9.14). For a decreased shear rate (increase in pipe diameter or decrease in flow rate) the developed shear stress is stable, and smaller than the stabilized shear stress τ_s. For an increased shear rate (decrease in pipe diameter or increase in flow rate) the obtained shear stress represents the initial value of a beginning structure breakdown process, which can be determined using Eq. (9.15).

An important consequence of Eq. (9.14) is that a considerable shear stress decrease can be achieved by applying an initially large shear rate. The flow through a centrifugal pump is not sufficient for this purpose because of the very short duration of shear. An entrance pipe section of smaller diameter may be satisfactory provided it is of a suitable length to produce the necessary duration of shear.

If the shear stress at a constant shear rate increases with the duration of shear, the fluid is called rheopectic. The best known example of this type of behavior is that of egg-white. Rheopectic behavior is less commonly encountered than thixotropy, although a rheopectic material would be useful as a fracturing fluid.

Viscoelastic fluids are materials for which the shear stress depends both on the shear rate and the extent of the deformation. In a certain sense all liquids exhibit viscoelastic properties, particularly at very high shear rates. Considerable viscoelastic effects may occur during sudden flow rate changes, in oscillatory flows and

in flows at high shear rates. In a normal steady flow, or in a slowly transient flow most fluids behave as purely viscous materials. The only exception to this is in the turbulent flow in pipes, where important viscoelastic effects occur in pressure gradients and in the laminar-turbulent transition.

Viscoelastic effects manifest themselves through the development of normal stresses perpendicular to the direction of flow, which are of a different magnitude than the normal stress parallel to the flow. A further important phenomenon is the stress relaxation which occurs during rapid deformation.

The simplest constitutive relation for a viscoelastic fluid was proposed by Maxwell. The shear rate of a Maxwell fluid is the sum of a viscous and an elastic shear rate. The viscous part is

$$\left(\frac{\mathrm{d}v}{\mathrm{d}r}\right)_v = \frac{\tau}{\mu} \tag{9.16}$$

while the elastic component of the shear rate is:

$$\left(\frac{\mathrm{d}v}{\mathrm{d}r}\right)_e = \frac{1}{E}\frac{\mathrm{d}\tau}{\mathrm{d}t}, \tag{9.17}$$

where E is the modulus of elasticity.

Their sum represents the constitutive equation of a Maxwell fluid:

$$\frac{\mathrm{d}v}{\mathrm{d}r} = \frac{\tau}{\mu} + \frac{1}{E}\frac{\mathrm{d}\tau}{\mathrm{d}t}. \tag{9.18}$$

By introducing the notation

$$\Theta_r = \frac{\mu}{E}, \tag{9.19}$$

the constitutive equation can be written

$$\tau + \Theta_r \frac{\mathrm{d}\tau}{\mathrm{d}t} = \mu \frac{\mathrm{d}v}{\mathrm{d}r}. \tag{9.20}$$

The velocity gradient $\mathrm{d}v/\mathrm{d}r$ can be an arbitrary function of time, thus the solution of Eq. (9.20) yields the shear stress as a function of time. The simplest solution is obtained when the velocity gradient suddenly decreases from an initial constant value to zero. In this case

$$\tau + \Theta_r \frac{\mathrm{d}\tau}{\mathrm{d}t} = 0, \tag{9.21}$$

while the initial condition is $t=0$, $\tau=\tau_0$. Separating the variables and integrating we have

$$\tau = \tau_0 \, \mathrm{e}^{-\frac{t}{\Theta_r}}. \tag{9.22}$$

This is shown in *Fig. 9.10*. Since

$$\left(\frac{d\tau}{dt}\right)_{t=0} = -\frac{\tau_0}{\Theta_r} \tag{9.23}$$

it is clear that Θ_r is the relaxation time of the Maxwell fluid.

A Maxwell fluid can reproduce certain properties of a viscoelastic fluid. Nevertheless this constitutive relation is not capable of quantitatively describing the behavior of real viscoelastic materials over the range of flow conditions of engineering interest.

Perhaps the most practical constitutive relation is the one proposed by White and Metzner (1963). This can be written in tensorial form as

$$\mathbf{V} = -2\mu_a \mathbf{S} + \Theta_r \frac{\delta \mathbf{V}}{\delta t} \tag{9.24}$$

in which μ_a is the apparent viscosity, Θ_r is the relaxation time, and $\frac{\delta}{\delta t}$ is Oldroyd's convected derivative, the time rate of change of a quantity relative to a coordinate system which is moving and deforming with the fluid. It is clear that in the case $\Theta_r = 0$ the equation is simply that of a purely viscous fluid. The normal stresses, together with the relaxation phenomenon, arise from the second term which contains the relaxation time and Oldroyd's derivative. Only one scalar quantity is necessary to take into consideration the effect of elasticity in the flow.

For a one-dimensional steady laminar flow the White—Metzner equation implies that

$$\tau_{rz} = \mu_a \frac{dv}{dr}, \tag{9.25}$$

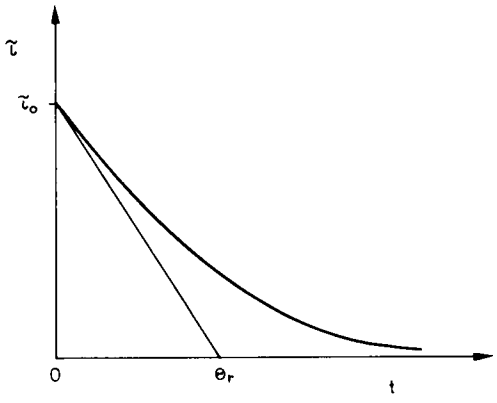

Fig. 9.10. Viscoelastic relaxation

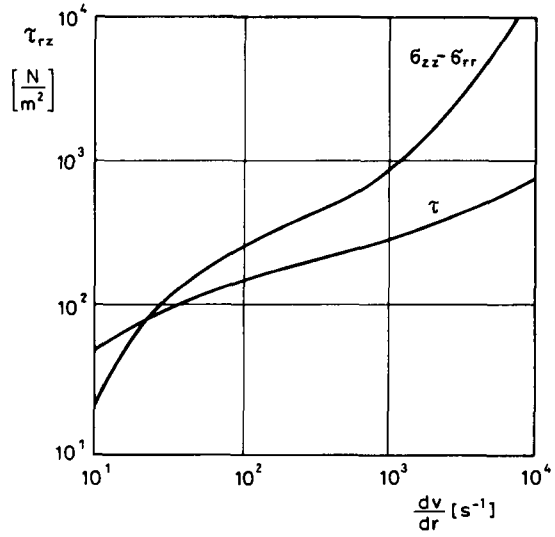

Fig. 9.11. Difference of normal stresses plotted against shear rate

$$\sigma_{zz}-\sigma_{rr}=2\Theta_r\tau_{rz}\frac{dv}{dr}, \tag{9.26}$$

$$\sigma_{rr}-\sigma_{\varphi\varphi}=0. \tag{9.27}$$

The White—Metzner equation is easily tested experimentally. The normal stress difference can be written as

$$\sigma_{zz}-\sigma_{rr}=2\Theta_r\frac{\tau_{rz}^2}{\mu_a}. \tag{9.28}$$

Rheogoniometric measurements and jet expansion results confirm the above equations. In *Fig. 9.11* the normal stress difference and the shear stress are plotted as functions of the shear rate. It is significant, that the normal stress difference is comparable to the shear stress at low shear rates, while at high shear rates the normal stress difference is greater by an order of magnitude than the shear stress.

9.2 Laminar flow of pseudoplastic fluids in pipes

Consider a straight cylindrical pipe of constant cross section. The orientation of the pipe is arbitrary w.r.t. the gravity field. A steady, one-dimensional flow of an incompressible pseudoplastic fluid is investigated. It is convenient to choose a cylindrical coordinate system with the notation as shown in *Fig. 9.12*. The momen-

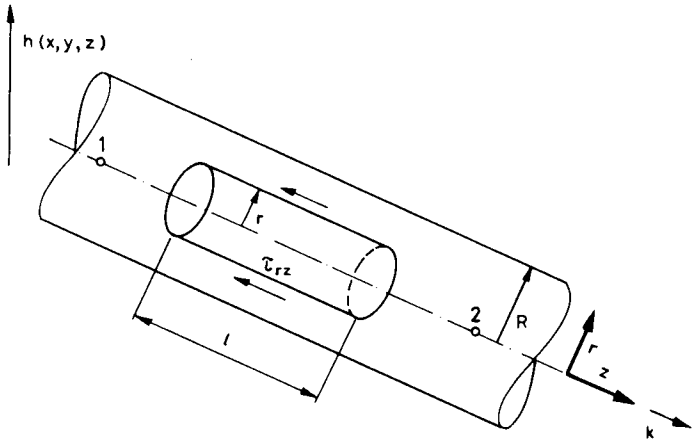

Fig. 9.12. Cylindrical coordinate system and control volume for pseudoplastic pipe flow

tum equation for the depicted control volume can be written as

$$0 = -\int_V \text{grad}\,(\varrho g h + p)\,\mathrm{d}V + \int_{(A)} \mathbf{V}\,\mathrm{d}\vec{A}\,. \tag{9.29}$$

It was shown in Chapter 6, that the quantity $(\varrho g h + p)$ is a linear function of the coordinate z. Thus we can write

$$-\text{grad}\,(\varrho g h + p) = -\frac{\mathrm{d}}{\mathrm{d}z}(\varrho g h + p) = -\varrho g(-J)\,, \tag{9.30}$$

where

$$J = \frac{p_1 - p_2}{\varrho g l} + \frac{h_1 - h_2}{l}\,, \tag{9.31}$$

is the well-known hydraulic gradient. Since it is constant, the volume integral is readily calculated:

$$-\int_V \text{grad}\,(\varrho g h + p)\,\mathrm{d}V = \varrho g J r^2 \pi l \vec{k}\,. \tag{9.32}$$

Since the flow is axisymmetric, the viscous stress tensor has only one non-zero component:

$$\tau_{rz} = K\left|\frac{\mathrm{d}v}{\mathrm{d}r}\right|^{n-1}\frac{\mathrm{d}v}{\mathrm{d}r}\,. \tag{9.33}$$

It is obvious, that since $K > 0$, and $\mathrm{d}v/\mathrm{d}r < 0$, we must have $\tau_{rz} < 0$, i.e. the shear stress acts against the flow direction. The velocity distribution of an incompressible flow is the same at any cross section, thus the shear-stress distribution must also be the same at the inlet- and outlet cross sections of the control volume.

Since the surface unit normal vectors are opposite at the two surfaces the sum of the integrals over them vanish. The integration yields a non-vanishing result for the cylindrical surface A_3 only. Here the shear stress is constant since $r=\text{const.}$ Thus we have

$$\int_V \mathbf{V}\,\mathrm{d}\vec{A} = -\vec{k}\,|\tau_{rz}| \int_{A_3} \mathrm{d}A = -K\left|\frac{\mathrm{d}v}{\mathrm{d}r}\right|^n 2\pi r l\vec{k}\,. \tag{9.34}$$

Substituting expressions (9.32) and (9.34) back into Eq. (9.29) the momentum equation can now be written as

$$\frac{\varrho g J r}{2} - K\left|\frac{\mathrm{d}v}{\mathrm{d}r}\right|^n = 0\,. \tag{9.35}$$

Rearranging, the velocity gradient can be expressed as

$$-\frac{\mathrm{d}v}{\mathrm{d}r} = \left(\frac{\varrho g J r}{2K}\right)^{\frac{1}{n}}. \tag{9.36}$$

Integrating this equation yields

$$v = -\left(\frac{\varrho g J}{2K}\right)^{\frac{1}{n}} \frac{n}{n+1} r^{\frac{n+1}{n}} + k\,, \tag{9.37}$$

where k is a constant of integration, which can be obtained from the usual boundary conditions

$$r=R\,; \qquad v=0\,.$$

Substituting these values into Eq. (9.37) we get

$$k = \frac{n}{n+1}\left(\frac{\varrho g J}{2K}\right)^{\frac{1}{n}} R^{\frac{n+1}{n}},$$

which leads to the final form of the velocity distribution along the pipe radius

$$v = \frac{n}{n+1}\left(\frac{\varrho g J r}{2K}\right)^{\frac{1}{n}} R\left[1-\left(\frac{r}{R}\right)^{\frac{n+1}{n}}\right]. \tag{9.38}$$

The flow rate is obtained as

$$Q = 2\pi \int_0^R rv\,\mathrm{d}r = \frac{n}{3n+1}\left(\frac{\varrho g J r}{2K}\right)^{\frac{1}{n}} R^3\pi\,. \tag{9.39}$$

Consequently the cross-sectional average velocity is

$$c = \frac{Q}{R^2\pi} = \frac{n}{3n+1}\left(\frac{\varrho g J R}{2K}\right)^{\frac{1}{n}} R\,. \tag{9.40}$$

It is convenient to express the velocity distribution in terms of the averaged velocity:

$$v = \frac{3n+1}{n+1} c \left[1 - \left(\frac{r}{R} \right)^{\frac{n+1}{n}} \right]. \tag{9.41}$$

The velocity maximum is obtained at the pipe axis:

$$v_{\max} = \frac{3n+1}{n+1} c \,. \tag{9.42}$$

The maximum shear rate occurs at the pipe wall:

$$\left(\frac{\mathrm{d}v}{\mathrm{d}r} \right)_R = - \left(\frac{\varrho g J R}{2K} \right)^{\frac{1}{n}} = - \frac{c}{R} \frac{1+3n}{n} \,. \tag{9.43}$$

The shear stress at the wall is

$$\tau_R = - \frac{\varrho g J R}{2} \,. \tag{9.44}$$

The shear-stress distribution along the radius is obviously linear:

$$\tau = \frac{\varrho g J R}{2} = \frac{\tau_R}{R} r \,. \tag{9.45}$$

The relation between the wall-shear stress and the wall-shear rate is obtained by combining Eqs (9.43) and (9.44)

$$\tau_R = K \left(\frac{\mathrm{d}v}{\mathrm{d}r} \right)_R^n \,. \tag{9.46}$$

The dimensionless velocity distributions are plotted in *Fig. 9.13* for pseudoplastic fluids of different behavior indexes, as

$$\frac{v}{c} = \frac{3n+1}{n+1} \left[1 - \left(\frac{r}{R} \right)^{\frac{n+1}{n}} \right]. \tag{9.47}$$

This figure illustrates the effect of the behavior index on the velocity profile. In the special case of a Newtonian fluid $n = 1$, and the usual parabola is obtained. It can be seen that as n approaches zero the velocity profiles flattens (resembling a plug flow), whereas as n increases in the dilatant region the profile steepens, tending towards an inclined straight line.

The head loss of a pipe section of length L and diameter D can be also determined. The mechanical energy equation in its general form can be written as

$$\frac{c_1^2}{2g} + \frac{p_1}{g} + h_1 = \frac{c_2^2}{2g} + \frac{p_2}{g} + h_2 + h'_{1-2} \,. \tag{9.48}$$

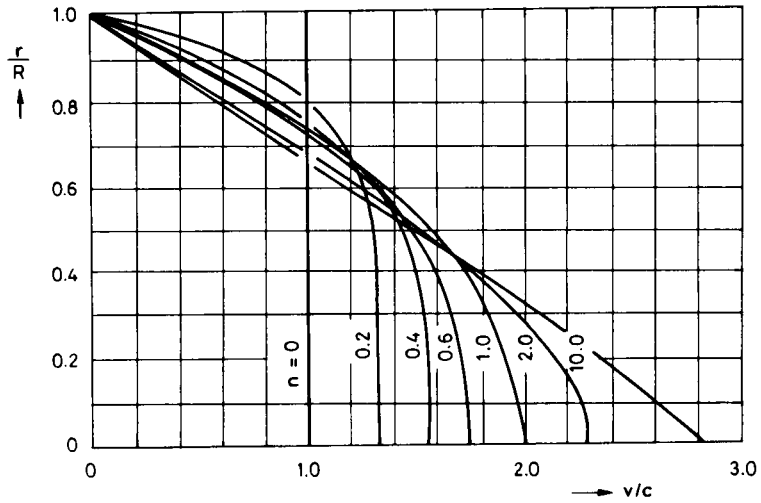

Fig. 9.13. Dimensionless velocity distribution of pseudoplastic fluid flows

Since the cross section of the pipe is constant,

$$c_1 = c_2 ,$$

thus we get

$$h'_{1-2} = \frac{p_1 - p_2}{\varrho g} + h_1 - h_2 = JL . \tag{9.49}$$

Using Eq. (9.40) to express the hydraulic gradient J, and after substitution into Eq. (9.49) the head loss is obtained as

$$h'_{1-2} = \frac{2K}{\varrho g}\left(\frac{3n+1}{n}\right)^n \frac{L}{R^{n+1}} c^n . \tag{9.50}$$

It is conspicuous that the head loss is not a linear function of the cross-sectional average velocity, not even for laminar flow. The head loss for pseudoplastic flow increases with the averaged velocity to a lesser degree than in the Newtonian case. The head loss is linearly proportional to the length of the pipe. For pseudoplastic flow a decrease in the diameter causes a smaller increase in the head loss than for a Newtonian fluid. Naturally, for $n = 1$ Eq. (9.50) reduces to the special case of the Hagen—Poiseuille equation.

Metzner and Reed (1955) proposed extending the Weisbach equation

$$h'_{1-2} = \lambda \frac{L}{D} \frac{c^2}{2g} , \tag{9.51}$$

to pseudoplastic fluid flow, as well.

Comparing Eqs (9.50) and (9.51) the friction factor is obtained as

$$\lambda = \frac{8K}{\varrho}\left(\frac{6n+2}{n}\right)^n \frac{c^{n-2}}{D^n}. \tag{9.52}$$

In the manner usual for Newtonian fluids we shall express the friction factor in terms of the Reynolds number. By comparing Eq. (9.52) and the final term of the expression

$$\varrho \frac{\mathrm{d}\vec{v}}{\mathrm{d}t} = \ldots + \mathrm{Div}\left[K(\mathbf{S}:\mathbf{S})^{\frac{n-1}{2}}\mathbf{S}\right]. \tag{9.53}$$

A modified, pseudoplastic Reynolds number can be defined:

$$\mathrm{Re}_p = \frac{c^{n-2}D^n\varrho}{K}. \tag{9.54}$$

Combining Eqs (9.52) and (9.54) the following relationship between the friction factor and the pseudoplastic Reynolds number is obtained:

$$\lambda = \frac{64}{\mathrm{Re}_p}\left(\frac{6n+2}{n}\right)^n \frac{1}{8}. \tag{9.55}$$

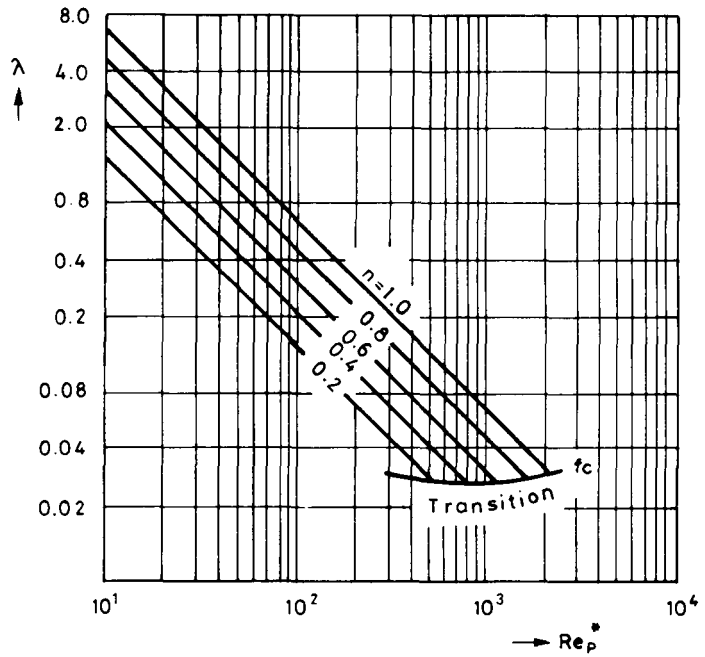

Fig. 9.14. Friction factor versus Reynolds number Re_p^* for pseudoplastic fluids

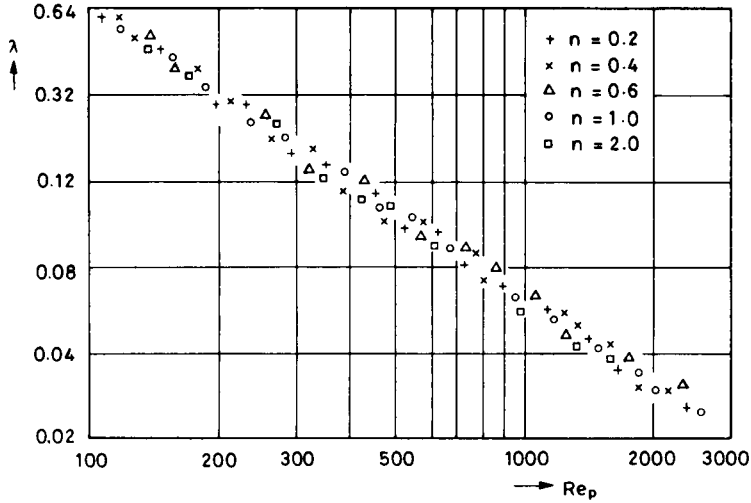

Fig. 9.15. Friction factor versus Reynolds number Re_p for pseudoplastic fluids

There is an alternate form of the pseudoplastic Reynolds number, defined by the equation

$$\lambda = \frac{64}{\mathrm{Re}_p^*}. \tag{9.56}$$

Using this, we obtain the expression

$$\mathrm{Re}_p^* = \frac{c^{n-2} D^n \varrho}{\frac{K}{8}\left(\frac{6n+2}{n}\right)^n}. \tag{9.57}$$

If the friction factor is plotted against Re_p^* all points fall along the same curve, irrespective of the value of n, as shown in *Fig. 9.14.*

If plotted against Re_p the relationship is not independent of n. This can be seen in *Fig. 9.15*, where a family of parallel lines representing different values of n are obtained. Experimental data show that the transition from laminar to turbulent flow occurs at progressively smaller Reynolds numbers as the behavior index decreases.

It has already been noted that the power law equation is not applicable at very low shear rates. Near to the pipe axis the shear rate approaches zero, thus in this region the accuracy of the power law approximation decreases. Fortunately, the shear stress similarly tends to zero in this inner region so that the contribution of this zone to the energy dissipation is negligible. Thus friction factor- and head loss calculations based on the power law equation are sufficiently accurate for practical purposes.

9.3 Bingham fluid flow in pipes

It has previously been shown that for any type of fluid, its steady, laminar flow through a pipe can be described by the momentum equation

$$\frac{\varrho g J r}{2} + \tau_{rz} = 0 . \tag{9.58}$$

The constitutive relation of a Bingham fluid is

$$|\tau_{rz}| = \tau_y + \mu \left| \frac{\mathrm{d}v}{\mathrm{d}r} \right| . \tag{9.59}$$

Substituting Eq. (9.59) into (9.58) the momentum equation for the steady laminar flow of a Bingham fluid is obtained

$$\frac{\varrho g J r}{2} - \tau_y + \mu \frac{\mathrm{d}v}{\mathrm{d}r} = 0 . \tag{9.60}$$

From this it is clear that the yield stress τ_y must be overcome before the material will sustain a nonzero rate of deformation. If

$$\frac{\varrho g J r}{2} - \tau_y > 0 ,$$

a steady axisymmetric laminar flow develops, whereas if

$$\frac{\varrho g J r}{2} - \tau_y \leqq 0 ,$$

the material moves as a plug, pushed along by the laminar flow around it. The radius of the plug can be calculated as

$$R_p = \frac{2\tau_y}{\varrho g J} . \tag{9.61}$$

In the region between the pipe wall and the plug, i.e. where

$$R \geqq r \geqq R_p ,$$

the equation of motion can be integrated. The result is

$$v = -\frac{\varrho g J r^2}{4\mu} + \frac{\tau_y}{\mu} r + k .$$

The constant of integration can be determined by satisfying the boundary condition: $r = R$; $v = 0$. The velocity distribution is then obtained as

$$v = \frac{\varrho g J}{4\mu} (R^2 - r^2) - \frac{\tau_y}{\mu} (R - r) . \tag{9.62}$$

A few calculated velocity distributions along the radius are shown in dimensionless form in *Fig. 9.16*. The velocity maximum of the Newtonian fluid is $v_{0\,\max}$.

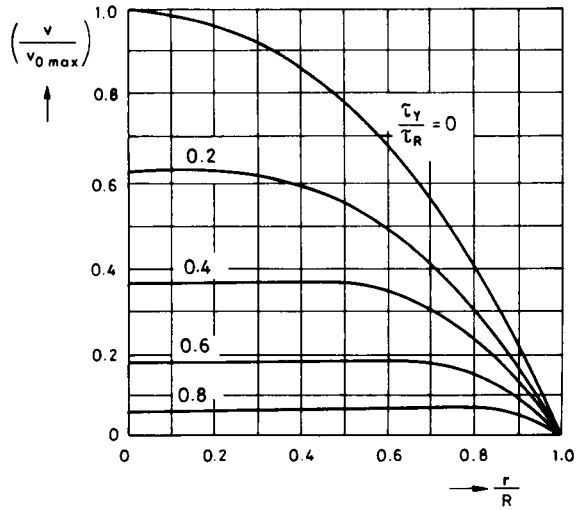

Fig. 9.16. Velocity distribution of a Bingham fluid

The hydraulic gradient is the same for each curves, while the parameter is the yield stress-wall shear-stress ratio. As τ_y/τ_R increases, the plug diameter increases, the plug velocity decreases with a flattening velocity profile.

A few calculated curves are shown in *Fig. 9.16.*

The velocity of the plug is obtained as

$$v_p = \frac{\varrho g J}{4\mu}(R^2 - R_p^2) - \frac{\tau_y}{\mu}(R - R_p). \tag{9.63}$$

The flow rate is the sum of the annular flow rate and the flow rate of the plug:

$$Q = 2\pi \int_{R_p}^{R} vr\,\mathrm{d}r + R_p^2 \pi v_p. \tag{9.64}$$

Knowing the flow rate the cross-sectional average velocity is obtained:

$$c_B = \frac{\varrho g J R^2}{8\mu}\left[1 - \left(\frac{R_p}{R}\right)^4\right] - \frac{R\tau_y}{3\mu}\left[1 - \left(\frac{R_p}{R}\right)^3\right]. \tag{9.65}$$

The averaged shear rate is obviously

$$\frac{c_B}{R} = \frac{\varrho g J R}{8\mu}\left[1 - \left(\frac{R_p}{R}\right)^4\right] - \frac{\tau_y}{3\mu}\left[1 - \left(\frac{R_p}{R}\right)^3\right]. \tag{9.66}$$

Taking into account that

$$\frac{R_p}{R} = \frac{2\tau_y}{\varrho g J R} \tag{9.67}$$

and the pressure loss

$$\Delta p' = \varrho g J L, \tag{9.68}$$

and substituting these into Eq. (9.65), we obtain the so-called Buckingham equation

$$\frac{c_B}{R} = \frac{\varrho g}{4\mu} \frac{D\Delta p'}{4L} \left[1 - \frac{4\tau_y}{3}\left(\frac{4L}{D\Delta p'}\right) + \frac{\tau_y^4}{3}\left(\frac{4L}{D\Delta p'}\right)^4\right]. \tag{9.69}$$

The pressure loss for a Bingham fluid flow can be calculated from this equation. The friction factor can be expressed as

$$\lambda = \frac{64\mu}{c_B D \varrho} \frac{1}{1 - \frac{4}{3}\frac{\tau_y}{\tau_R} + \frac{1}{3}\left(\frac{\tau_y}{\tau_R}\right)^4}, \tag{9.70}$$

where τ_R is the shear stress at the pipe wall. By dimensional analysis Hedström (1952) showed that the friction factor for Bingham plastic flows is a function of two dimensionless groups

$$\lambda = \lambda\left(\frac{c_B D \varrho}{\mu}; \frac{D^2 \tau_y \varrho}{\mu^2}\right).$$

The first of these is the modified Reynolds number for a Bingham fluid. Note that c_B is the averaged velocity over the full cross section of the pipe, even though flow can develop only in the annulus between the pipe wall and the plug. To distinguish it from the real Reynolds number it is designated as

$$\mathrm{Re}_B = \frac{c_B D \varrho}{\mu}. \tag{9.71}$$

The second group forms the so-called Hedström number

$$\mathrm{He} = \frac{D^2 \tau_y \varrho}{\mu^2}. \tag{9.72}$$

In *Fig. 9.17* the friction factor is plotted against the Bingham—Reynolds number Re_B, with the Hedström number taken as a parameter. An important observation is that at large Hedström numbers the transition from laminar to turbulent flow occurs at substantially greater Reynolds numbers than is the case for Newtonian fluids.

To calculate the laminar pressure loss for a Bingham fluid flow, the Buckingham equation seems to be the most suitable. It is advisable to treat $\Delta p'$ as an independent variable and calculate c/R knowing τ_y and μ. From the sequences of values of c/R and $\Delta p'$ thus obtained the actual values can be determined by interpolation. Another possibility is to obtain $\Delta p'$ as the solution of the biquadratic equation by the Newton—Raphson method.

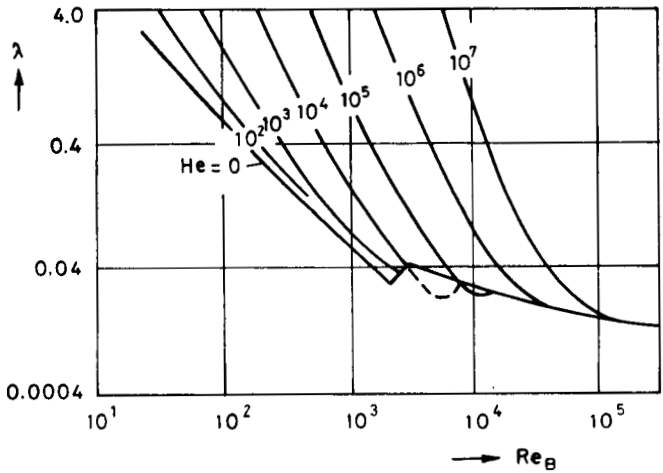

Fig. 9.17. Friction factor versus Bingham—Reynolds number

The flow of a yield-pseudoplastic fluid can be described in a similar way. Here the constitutive relation is

$$|\tau - \tau_y| = K\left|\frac{dv}{dr}\right|^n. \tag{9.73}$$

Substituting into the momentum equation for pipe flow we obtain

$$-\frac{dv}{dr} = \left(\frac{\varrho g J r}{2K} - \frac{\tau_y}{K}\right)^{\frac{1}{n}}. \tag{9.74}$$

The velocity distribution (using the boundary condition $v=0$ when $r=R$) is

$$v = \frac{n}{n+1}\frac{2K}{\varrho g J}\left[\left(\frac{\varrho g J R}{2K} - \frac{\tau_y}{K}\right)^{\frac{n+1}{n}} - \left(\frac{\varrho g J r}{2K} - \frac{\tau_y}{K}\right)^{\frac{n+1}{n}}\right]. \tag{9.75}$$

The averaged shear rate can be obtained analogously to the Buckingham equation:

$$\frac{c}{R} = \frac{\left(\frac{D\Delta p'}{4L} - \tau_y\right)^{\frac{n+1}{n}}}{\left(\frac{D\Delta p'}{4L}\right)^3 K^{\frac{1}{n}}}\left[\frac{\left(\frac{D\Delta p'}{4L} - \tau_y\right)^2}{\frac{3n+1}{n}} + \frac{2\tau_y\left(\frac{D\Delta p'}{4L} - \tau_y\right)}{\frac{2n+1}{n}} + \frac{\tau_{y^2}}{\frac{n+1}{n}}\right]. \tag{9.76}$$

This equation reduces to the Buckingham equation if $n=1$. The equation can be solved in a similar manner as discussed for the case of Bingham fluid flow. The

pressure loss thus obtained is always less than that for a Bingham fluid. Thus the problem may be simplified by replacing the yield-pseudoplastic model by a Bingham fluid at the sacrifice of a slight overestimation of the pressure loss.

9.4 Unsteady viscoelastic fluid flow in a cylindrical pipe

For the steady laminar flow of a viscoelastic fluid in a cylindrical pipe of constant diameter the elastic forces do not enter into the balance of momentum equation. Experimental data confirm that in such a steady laminar flow the pressure loss is not affected by the elastic properties of the fluid. Since the flow depends only on the viscous properties of the fluid, the steady laminar pipe flow of a viscoelastic fluid may be treated as that of a purely viscous fluid; either a Newtonian or a pseudoplastic one. Viscoelastic effects may be especially important in rapidly oscillating flows. In order to illustrate the consideration of viscoelastic properties let it be supposed that we wish to find the relation between the flow rate and the pressure loss for a Maxwell fluid. For laminar flow and sufficiently small velocities the constitutive relation for a Maxwell fluid is

$$\tau + \Theta_r \frac{\mathrm{d}\tau}{\mathrm{d}t} = \mu \frac{\mathrm{d}v}{\mathrm{d}r}.$$

It is convenient to choose a cylindrical coordinate system. It is assumed that the velocity has only an axial component i.e.

$$v_z = v; \qquad v_r = 0; \qquad v_\varphi = 0.$$

The continuity equation can then be written as

$$\frac{1}{r}\frac{\partial}{\partial r}(rv_r) + \frac{1}{r}\frac{\partial v_\varphi}{\partial \varphi} + \frac{\partial v_z}{\partial z} = 0 \tag{9.77}$$

since the fluid is incompressible. In consequence of $v_r = v_\varphi = 0$, the third term also vanishes even though the axial velocity is nonzero.

The momentum equation (neglecting the body forces) can be expressed in terms of the stress components as

$$\varrho\left(\frac{\partial v_z}{\partial t} + v_r\frac{\partial v_z}{\partial r} + \frac{v_\varphi}{r}\frac{\partial v_z}{\partial \varphi} + v_z\frac{\partial v_z}{\partial z}\right) = -\frac{\partial p}{\partial z} + \frac{1}{r}\frac{\partial (r\tau_{rz})}{\partial r} + \frac{1}{r}\frac{\partial \tau_{\varphi z}}{\partial \varphi} + \frac{\partial \sigma_z}{\partial z}. \tag{9.78}$$

The convective terms must vanish in a one-dimensional incompressible flow. Since the fluid is incompressible, σ_z must be zero. Because of the rotational symmetry, $\partial\tau_{\varphi z}/\partial\varphi$ also vanishes. Thus the only stress component that remains is $\tau_{rz} = \tau$.

Thus the momentum equation becomes

$$\varrho \frac{\partial v}{\partial t} = -\frac{\partial p}{\partial z} + \frac{1}{r}\frac{\partial}{\partial r}(r\tau). \tag{9.79}$$

The assumption of periodicity can be expressed by the equations

$$\tau = \tau_0 e^{i\omega t}, \tag{9.80}$$

$$v = v_0 e^{i\omega t}, \tag{9.81}$$

$$-\frac{\partial p}{\partial z} = p_0 e^{i\omega t}. \tag{9.82}$$

In addition we can write

$$\frac{d\tau}{dt} = i\omega\tau. \tag{9.83}$$

Thus the constitutive relation of the Maxwell fluid can be written as

$$\tau(1 + i\omega\Theta_r) = \mu\frac{dv}{dr}. \tag{9.84}$$

By substituting into the momentum equation we obtain

$$\frac{1}{r}\frac{d}{dr}\left(r\frac{dv_0}{dr}\right) + i\omega(1 + i\omega\Theta_r)\frac{\varrho v_0}{\mu} = \frac{1 + i\omega\Theta_r}{\mu}p_0. \tag{9.85}$$

This equation can be solved for the velocity by integrating twice, with the boundary conditions

$$r = 0. \qquad v_0 \neq 0,$$

and

$$r = R; \qquad v_0 = 0.$$

The final result is obtained as

$$v_0 = \frac{p_0}{i\varrho\omega}\left[1 - \frac{J_0(\alpha r)}{J_0(\alpha R)}\right], \tag{9.86}$$

where J_0 is the zero-order Bessel function. Integrating over the pipe cross-section the flow rate is obtained as

$$Q_0 = 2\pi\int_0^R v_0 r\,dr.$$

After integration we have

$$Q_0 = \frac{p_0 R^2\pi}{i\varrho\omega}\left[1 - \frac{2J_1(\alpha R)}{\alpha R J_0(\alpha R)}\right], \tag{9.87}$$

where J_1 is the first-order Bessel function, and α represents the consecutive roots of the Bessel equation derived from the boundary conditions.

The Bessel functions can be expanded into McLaurin series, since $\omega\Theta_r \ll 1$. Thus, the flow rate is obtained as

$$Q = \frac{R^4 \pi p_0}{8\mu}\left[\cos \omega t - \omega\Theta_r\left(1 - \frac{\varrho R^2}{6\mu\Theta_r}\right)\sin \omega t\right]. \tag{9.88}$$

The out-of-phase components are $\omega\Theta_r \sin \omega t$ and $\frac{\omega\varrho R^2}{6\mu} \sin t$; the first representing the elastic term, the latter the inertial term.

9.5 The Rabinowitsch equation

There are certain fluids, or certain intervals of their flow curves, for which the power law equation is not applicable. Such a flow curve, when plotted in a logarithmic coordinate system, has a changing slope. Mathematical formulations for these flow curves may be obtained even if the resulting equations are rather ponderous. A useful general equation for a steady, laminar, purely viscous fluid flow in circular pipes can be developed from a generalized constitutive relation. An entirely general constitutive relation is

$$\tau = F\left(\frac{\mathrm{d}v}{\mathrm{d}r}\right). \tag{9.89}$$

Its inverse function is

$$\frac{\mathrm{d}v}{\mathrm{d}r} = f(\tau), \tag{9.90}$$

where $f(\tau)$ is a temporarily unknown function of the shear stress. Using Eq. (9.90), an infinitesimal velocity change can be expressed as

$$\mathrm{d}v = f(\tau)\,\mathrm{d}r.$$

The flow rate is obtained as

$$Q = 2\pi \int_0^R v r \,\mathrm{d}r,$$

which can be integrated as a product to give

$$Q = 2\pi \frac{r^2}{2} v - \left[\frac{r^2}{2}\mathrm{d}v\right]_0^R.$$

Since $v = 0$, when $r = R$, we have

$$Q = \pi \int_0^R r^2 f(\tau)\,\mathrm{d}r. \tag{9.91}$$

Since the shear-stress distribution along the radius is linear this can be written as

$$dr = \frac{R}{\tau_R} d\tau .$$

Substituting this expression into Eq. (9.91) we have

$$Q = \pi \int_0^R \frac{R^3}{\tau_R^3} \tau^2 f(\tau) d\tau . \tag{9.92}$$

After a simple rearrangement the averaged shear rate is obtained:

$$\frac{c}{R} = \frac{Q}{R^3 \pi} = \frac{1}{\tau_R^3} \int_0^{\tau_R} \tau^2 f(\tau) d\tau . \tag{9.93}$$

It is evident that the averaged shear rate depends only on the wall shear stress τ_R:

$$\frac{c}{R} = \psi(\tau_R) , \tag{9.94}$$

where ψ is some function of τ_R.

Thus we obtain the expression

$$\tau_R^3 \psi = \int_0^{\tau_R} \tau^2 f(\tau) d\tau . \tag{9.95}$$

Differentiating this w.r.t. τ_R we obtain

$$\frac{d}{d\tau_R}(\tau_R^3 \psi) = \tau_R^2 f(\tau_R) . \tag{9.96}$$

Completing the differentiation of the product, and after dividing by τ_R^2 we have

$$f(\tau_R) = 3\psi + \tau_R \frac{d\psi}{d\tau_R} . \tag{9.97}$$

Considering Eq. (9.94) we obtain

$$\frac{8c}{D} = 4\psi . \tag{9.98}$$

An obvious identity is that

$$\tau_R \frac{d(\ln \tau_R)}{d\tau_R} = 4\psi \frac{d(\ln 4\psi)}{d(4\psi)} .$$

Let n' be the slope of the $\ln 4\psi - \ln \tau_R$ curve, thus

$$n' = \frac{d(\ln \tau_R)}{d(\ln 4\psi)} = \frac{4\psi}{\tau_R} \frac{d\tau_R}{d(4\psi)} . \tag{9.99}$$

From Eq. (9.99) we obtain that

$$\frac{\mathrm{d}\psi}{\mathrm{d}\tau_R} = \frac{1}{n'}\frac{\psi}{\tau_R}. \tag{9.100}$$

It is obvious, that Eq. (9.90) is also valid at the pipe wall

$$\left(\frac{\mathrm{d}v}{\mathrm{d}r}\right)_R = f(\tau_R),$$

which can be substituted into Eq. (9.97) as well as into Eq. (9.98) and Eq. (9.100). Thus we have

$$\left(\frac{\mathrm{d}v}{\mathrm{d}r}\right)_R = \frac{3n'+1}{4n'}\frac{8c}{D}. \tag{9.101}$$

This is the Rabinowitsch equation, which can be used to design a pipeline for the steady laminar flow of a purely viscous non-Newtonian fluid. It is also applicable to determine rheological parameters of non-Newtonian fluids in capillary tube viscometers.

It is recommended that the first step of the design procedure should be the determination of the flow curve of the fluid. Using a capillary viscosimeter the flow rate and the pressure difference can be measured. From the flow rate the quantity $8c/D$ is easily calculated. The pressure difference Δp can be used to obtain the wall shear stress from the equation

$$\tau_R = \frac{D\Delta p}{4L}, \tag{9.102}$$

where D and L are the diameter and the length of the capillary tube. Plotting corresponding values we obtain a diagram such as shown in *Fig. 9.18*. These points define the flow curve. The slope of the curve at a given point provides the value of n':

$$n' = \frac{\mathrm{d}\left[\lg\dfrac{D\Delta p}{4L}\right]}{\mathrm{d}\left(\lg\dfrac{8c}{D}\right)}. \tag{9.103}$$

The ordinate of this point gives the shear stress at the pipe wall, its abscissa and n' yield the shear rate at the wall by means of Eq. (9.101). The measured points fall onto a single curve even though the diameter of the pipe may vary. Thus a single flow curve measured by a capillary tube of a given diameter is sufficient to design a pipe of any arbitrary diameter. The consistency index is obtained as

$$K = K'\left(\frac{n}{3n+1}\right)^n,$$

where K' is the vertical intersection at $8c/D = 1$. If the slope of the flow curve is

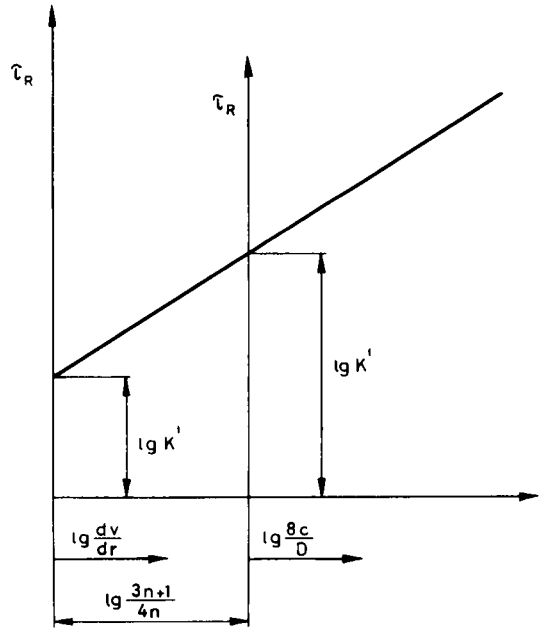

Fig. 9.18. Measured flow curve

constant, $n=n'$. Knowing K and n, the friction factor can be calculated from Eq. (9.52).

For a flow curve with a changing slope the power law equation is not applicable. In this case the wall-shear stress can be expressed by Eq. (9.102). Substituting this into Eq. (9.93) we obtain the expression

$$\frac{8Q}{D^3\pi} = \frac{c}{R} \frac{1}{\left(\frac{D\Delta p}{4L}\right)^3} \int_0^{\frac{D\Delta p}{4L}} \tau^2 f(\tau)\,\mathrm{d}\tau\,. \tag{9.104}$$

The integral can be determined numerically. Thus we obtain a direct relationship between the flow rate and the pressure loss.

9.6 Laminar flow of thixotropic fluids in pipes

The essential feature of thixotropic fluid flow in pipes is that the structural breakdown of the fluid in the entrance section of the pipeline, or during an initial period of the flow, results in a decrease of the head loss at a constant flow rate. In

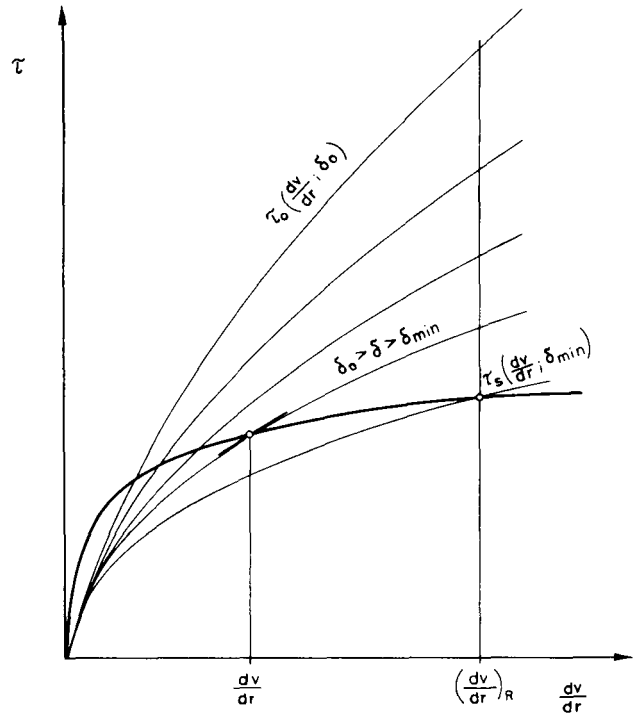

Fig. 9.19. Flow curves for a thixotropic fluid

the meantime the thixotropic structure degrades and the fluid eventually achieves purely viscous behavior. The complexity and restricted applicability of the thixotropic constitutive relations do not allow these to be used directly for solving the equation of motion to obtain the head loss of the flow. It is nevertheless, necessary to consider the constitutive relation in order to get at least a qualitative description of the flow.

We must remember that the rheological behavior of thixotropic fluids depends on their previous shear history, or rather on the thixotropic structure developed under the influence of the previous shear event. Assuming that the flow curves

$$\tau=\tau\left(\frac{dv}{dr},\delta\right)$$

are available certain specific shear processes of practical importance can be understood on the basis of the thixotropic-pseudoplastic model.

An important case is that where the fluid has an entirely intact thixotropic structure characterized by the structural parameter δ_0. In *Fig. 9.19* the uppermost flow curve represents this structural state. This may occur when the fluid has

passed a sufficiently long time at rest in a large tank, or in a shut down transport pipe so that its thixotropic structure has been perfectly reformed.

Entering from a large tank, the fluid with this intact structure undergoes a structural degradation within the entrance section of the pipe where the shear stress and the pressure gradient gradually decrease and tend to approach the stabilized pseudoplastic values. In the other case, if the flow in a thixotropic fluid transporting pipeline is stopped and the fluid in it remains at rest for a sufficiently long time, then after re-starting, the shear stress and the pressure gradient decrease with time along the whole length of the pipeline until the stabilized shear state is achieved.

Such a constant flow-rate process may be considered as equivalent to a constant shear-rate process. Although the shear rate has a maximum value at the pipe wall, which decreases to zero at the pipe axis, at a cylindrical surface of constant radius the shear rate is constant. Thus the duration of shear necessary to achieve the stabilized shear stress varies as a function of the radius. In an idealized situation the fluid at the pipe axis remains unsheared. Because of the variations of both duration of shear and shear rate the properties of the fluid in the pipe vary with the radius and the distance from the entrance.

In accordance with the constitutive relation

$$\tau = K_s\left(\frac{\mathrm{d}v}{\mathrm{d}r}\right)^m \left\{1+\left[\frac{\left(\frac{\mathrm{d}v}{\mathrm{d}r}\right)^{n-m}}{\left(\frac{\mathrm{d}v}{\mathrm{d}r}\right)_c^{n-m}}-1\right]\mathrm{e}^{-\left(\alpha\frac{\mathrm{d}v}{\mathrm{d}r}+\beta\right)\vartheta}\right\},$$

the degradation of the thixotropic structure is most effective at the wall. As can be seen from *Fig. 9.19*, the lowest structural parameter and consistency index is obtained at the wall shear rate. At smaller shear rates the consistency index of the stabilized flow curve is greater. Thus, far from the entrance the stabilized laminar flow has rheological properties which are no longer uniform in the radial direction. As a result, the initial velocity profile of the flow will be changed. The fluid particles near the wall will accelerate, while those of the inner core will decelerate.

Therefore, the flow is strictly speaking no longer one-dimensional.

In spite of these complications, petroleum engineering practice requires a directly applicable method to calculate the head loss for the entrance section of a laminar flow of a thixotropic fluid entering from a large tank.

In solving this problem it is obviously assumed, that a complete set of flow curves is available, including the uppermost flow curve of the original "intact" shear state as well the shear stress decay curves at different shear rates.

For a given flow rate the cross-sectional average velocity c, and the quantity $8c/D$ can be calculated. The shear rate at the wall is obtained as

$$\left(\frac{\mathrm{d}v}{\mathrm{d}r}\right)_R = -\frac{8c}{D}\left(\frac{3n+1}{n}\right). \tag{9.105}$$

The shear stress at the wall in the "intact" shear state is

$$\tau_{R0} = K_0 \left(\frac{\mathrm{d}v}{\mathrm{d}r} \right)_R^n . \tag{9.106}$$

The stabilized shear stress at the wall is

$$\tau_{Rs} = K_s \left(\frac{\mathrm{d}v}{\mathrm{d}r} \right)_R^m . \tag{9.107}$$

The shear stress decay can then be expressed as

$$\tau_R = K_s \left(\frac{\mathrm{d}v}{\mathrm{d}r} \right)_R^m + \left[K_0 \left(\frac{\mathrm{d}v}{\mathrm{d}r} \right)_R^n - K_s \left(\frac{\mathrm{d}v}{\mathrm{d}r} \right)_R^m \right] \mathrm{e}^{-\left(\alpha \frac{\mathrm{d}v}{\mathrm{d}r_R} + \beta \right) \vartheta} . \tag{9.108}$$

An averaged travel length for a fluid particle can be calculated as

$$l = c\vartheta . \tag{9.109}$$

Thus for any shear duration ϑ the corresponding l and τ_R can be determined from Eqs (9.109) and (9.108). Since the hydraulic gradient is given by

$$J = \frac{2\tau_R}{\varrho g R} \tag{9.110}$$

the distribution of J along the length of the pipe is obtained. Taking into account that J is not constant in this case, the head loss of a pipe section of length L can be calculated from the integral

$$h' = \int_0^L J(l)\,\mathrm{d}l . \tag{9.111}$$

The intersection of the unsheared flow curve and the stabilized flow curve yields a very inaccurate value of $(\mathrm{d}v/\mathrm{d}r)_c$. The power law equation is not sufficiently accurate in this interval. For this reason it is recommended that the equivalent Eq. (9.108) be used instead of Eq. (9.104). The consistency index K_0 of the unsheared flow curve can be determined more accurately than the parameter $(\mathrm{d}v/\mathrm{d}r)_c$.

In the case where the "intact" thixotropic structure is reformed after standing in a pipe the calculations are rather similar. The only difference is that the decay of the wall shear stress now takes place along the whole length of the pipeline. The hydraulic gradient will be constant through the pipe thus, instead of integrating Eq. (9.111), the head loss is obtained as

$$h' = JL . \tag{9.112}$$

This head loss value will decrease until the stabilized shear stress, and the corresponding stabilized head loss, have been achieved.

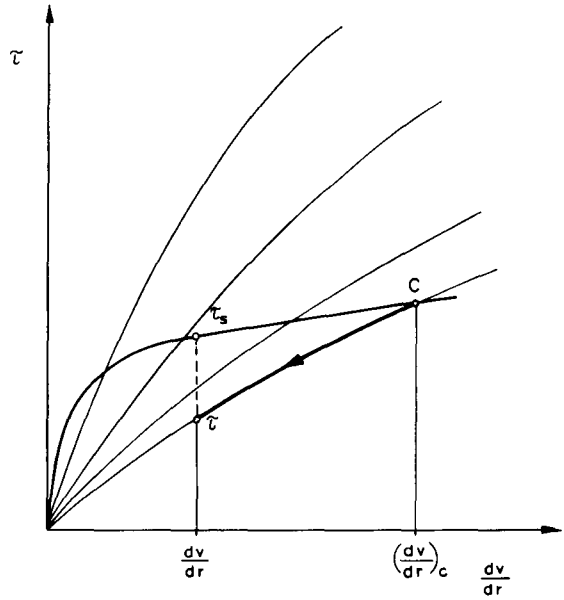

Fig. 9.20. Shear stress under the stabilized flow curve

Another situation is where a pre-sheared fluid enters a pipe. We assume that the pre-sheared thixotropic structure can be characterized by a given value of the structural parameter δ. This flow curve intersects the stabilized flow curve at a point *C (Fig. 9.20)* of which the shear rate $(dv/dr)_c$ is an important parameter. If the shear rate at the wall is smaller than $(dv/dr)_c$ an immediate thixotropic shear stress decrease occurs in accordance with the constitutive relation:

$$\tau = K_s \left(\frac{dv}{dr}\right)_c^{m-n} \left(\frac{dv}{dr}\right)^n . \tag{9.113}$$

The shear stress thus obtained is smaller than the stabilized shear stress at the same shear rate, as is clear from *Fig. 9.20.*

The momentum equation for a laminar flow in a pipe is

$$\frac{\varrho g J r}{2} + \tau_{rz} = 0 . \tag{9.114}$$

Substituting Eq. (9.113) into Eq. (9.114) we obtain

$$\frac{\varrho g J r}{2} + K_s \left(\frac{dv}{dr}\right)_c^{m-n} \left(\frac{dv}{dr}\right)^n = 0 . \tag{9.115}$$

The shear rate of the flow can be expressed as

$$-\frac{dv}{dr}=\left(\frac{\varrho g J}{2K_s}\right)^{\frac{1}{n}}\left(\frac{dv}{dr}\right)_c^{\frac{n-m}{n}} r^{\frac{1}{n}}. \tag{9.116}$$

After integration, and using the boundary condition $r=R$; $v=0$, the velocity distribution is obtained as

$$v=\frac{n}{n+1}\left(\frac{\varrho g J}{2K_s}\right)^{\frac{1}{n}}\left(\frac{dv}{dr}\right)_c^{\frac{n-m}{n}}\left(R^{\frac{n+1}{n}}-r^{\frac{n+1}{n}}\right). \tag{9.117}$$

The flow rate can be expressed as

$$Q=\frac{n}{3n+1}\left(\frac{\varrho g J R}{2K_s}\right)^{\frac{1}{n}}\left(\frac{dv}{dr}\right)_c^{\frac{n-m}{n}} R^3\pi. \tag{9.118}$$

The cross-sectional average velocity is easily obtained:

$$c=\frac{n}{3n+1}\left(\frac{\varrho g J R}{2K_s}\right)^{\frac{1}{n}}\left(\frac{dv}{dr}\right)_c^{\frac{n-m}{n}} R. \tag{9.119}$$

The hydraulic gradient can be expressed as

$$J=\left(\frac{3n+1}{n}\right)^n\left(\frac{dv}{dr}\right)_c^{m-n}\frac{2K_s c^n}{\varrho g R^{\frac{n+1}{n}}}. \tag{9.120}$$

Finally the head loss for a pipe section of length L is obtained as

$$h'=\left(\frac{3n+1}{n}\right)^n\left(\frac{dv}{dr}\right)_c^{m-n}\frac{2K_s}{\varrho g}\frac{L}{R^{\frac{n+1}{n}}}c^n. \tag{9.121}$$

The head loss obtained for the reduced shear stress is smaller than would be obtained for the stabilized parameters. The ratio of these head losses is given by

$$\frac{h'}{h'_s}=\left(\frac{3n+1}{n}\right)^n\left(\frac{m}{3m+1}\right)\left(\frac{dv}{dr}\right)_c^{m-n} c^{n-m}. \tag{9.122}$$

Since $n>m$, and $\left(\frac{dv}{dr}\right)_c$ is usually greater than unity, the reduction in the head loss may be considerable. By applying a previous shear, e.g. mixing in the tank, it is possible to achieve a considerable, and economically important reduction of the head loss, the necessary pump head and the pumping power when transporting a thixotropic oil.

A more complex situation results when the shear rate at the wall is greater than $(dv/dr)_c$. As shown in *Fig. 9.21* two different regions will develop in the pipe. In

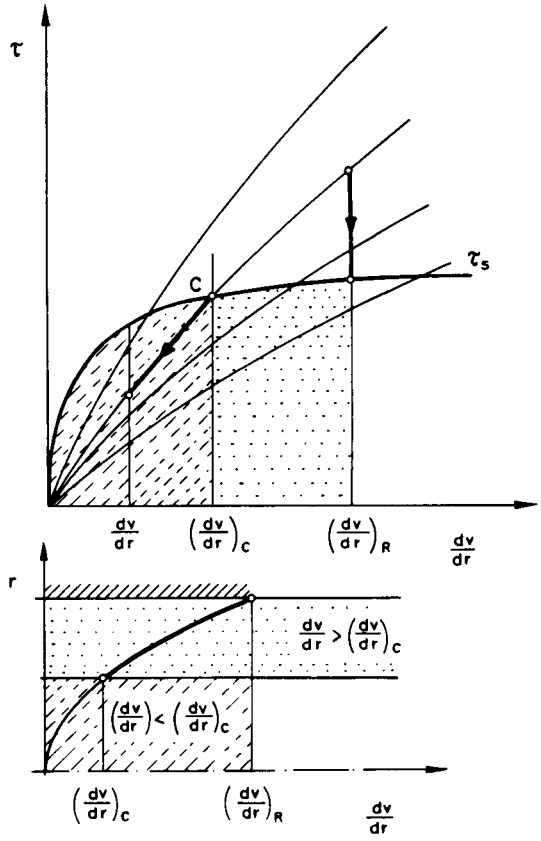

Fig. 9.21. Shear stress over the stabilized flow curve

the region near the wall where

$$\frac{dv}{dr} > \left(\frac{dv}{dr}\right)_c$$

the flowing fluid will suffer a time-dependent structure degradation with a gradually decreasing shear stress. In the inner region, where

$$\frac{dv}{dr} < \left(\frac{dv}{dr}\right)_c$$

an immediate decrease in the shear stress occurs in accordance with Eq. (9.113).

The flow of the annulus with the gradually decreasing shear stresses plays the dominant role in determining the head losses. Not only are both the shear stresses and the shear rates considerably higher here, than in the inner core flow, but the

consistency index is also higher in this annulus so that the dissipation which occurs in the core flow may be neglected. Metzner has shown for pseudoplastics that, even if the velocity profile were truncated and the flow taken as plug-like in the region $r=0$ to $r=0.5R$, the error in the flow rate calculated from the profile would be only 6 percent for n close the unity, and 3 percent for $n=0.5$. Accordingly, the simplification of neglecting the dissipation of inner core flow is quite permissible when calculating the head loss for petroleum engineering purposes.

For a given flow rate the shear rate at the wall is

$$\left(\frac{dv}{dr}\right)_R = -\frac{8c}{D}\left(\frac{3n+1}{n}\right).$$

The shear rate which characterized the pre-shear process is $(dv/dr)_c$. The wall-shear stress when the fluid enters the pipe, according to Eq. (9.113) is

$$\tau_R = K_s\left(\frac{dv}{dr}\right)_c^{m-n}\left(\frac{dv}{dr}\right)_R^{n}.$$

The stabilized wall-shear stress is

$$\tau_{RS} = K_s\left(\frac{dv}{dr}\right)_R^{m}.$$

During this process of structural decay the wall-shear stress is given by the equation

$$\tau_R = K_s\left(\frac{dv}{dr}\right)_R^{m}\left\{1+\left[\left(\frac{dv}{dr}\right)_c^{m-n}\left(\frac{dv}{dr}\right)_R^{n-m}-1\right]e^{-\left(\alpha\frac{dv}{dr_R}+\beta\right)\vartheta}\right\}.$$

The average travel length is

$$l = c\vartheta,$$

and thus the corresponding ϑ, l, τ_R and J values can be determined. The head loss is obtained as the integral

$$h' = \int_0^L J(l)\,dl.$$

This calculation is imposed with certain simplifications. In spite of this it is rather simple and easy to do for normal engineering design applications.

A final note: the decreasing temperature in a collecting pipe system causes an increase in the shear stresses along the length of the pipe, while the thixotropy of the oil decreases at the same time. Thus the non-isothermal nature of the flow and the thixotropy, acting in opposite directions, decrease the error due to the approximations.

9.7 Pseudoplastic fluid flow in annuli

Flow in annuli is encountered in drilling and well-completion technology, in which drilling mud or cement paste flows between the borehole wall and the drilling pipe or between two concentric pipes of casing. Since most drilling fluids are pseudoplastic, or thixotropic-pseudoplastic the importance of this problem is obvious.

We consider a steady laminar flow of an incompressible pseudoplastic fluid in a straight, infinitely long, concentric annulus. The position of the symmetry axis is arbitrary w.r.t. the gravity field. A cylindrical coordinate system is chosen; its z-axis directed parallel with the flow. The velocity field is axisymmetric, having only one nonzero component

$$v_z = v; \qquad v_r = 0; \qquad v_\varphi = 0 .$$

The momentum equation for this case can be written as

$$\varrho g J r = -\frac{\mathrm{d}}{\mathrm{d}r}\left(r\frac{\mathrm{d}\tau_{rz}}{\mathrm{d}r}\right). \tag{9.123}$$

Considering *Fig. 9.22* it is seen that at a radial position $r = R_0$ both $\mathrm{d}v/\mathrm{d}r$ and τ_{rz} change sign. As is well known, the power law constitutive relation is

$$\tau_{rz} = K\left|\frac{\mathrm{d}v}{\mathrm{d}r}\right|^{n-1}\frac{\mathrm{d}v}{\mathrm{d}r}.$$

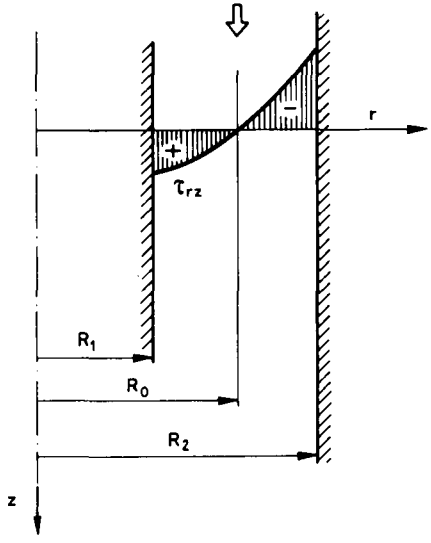

Fig. 9.22. Pseudoplastic fluid flow through an annulus

The sign of shear stress is determined by the sign of the velocity gradient. Where

$$r<R_0; \qquad \frac{dv}{dr}>0, \qquad \text{and thus} \qquad \tau_{rz}>0.$$

In the region

$$r>R_0; \qquad \frac{dv}{dr}<0, \qquad \text{and} \qquad \tau_{rz}<0.$$

The differential equation for this problem is

$$-\varrho g J r=\frac{d}{dr}\left[rK\left|\frac{dv}{dr}\right|^{n-1}\frac{dv}{dr}\right]. \tag{9.124}$$

Its first integral is readily obtained

$$rK\left|\frac{dv}{dr}\right|^{n-1}\frac{dv}{dr}=A-\frac{\varrho g J r^2}{2}. \tag{9.125}$$

Using the fact that at

$$r=R_0 \qquad \frac{dv}{dr}=0$$

we obtain the constant of integration as

$$A=\frac{\varrho g J R_0^2}{2}. \tag{9.126}$$

Substituting into Eq. (9.125) we obtain

$$\left|\frac{dv}{dr}\right|^{n-1}\frac{dv}{dr}=\frac{\varrho g J}{2K}\left(\frac{R_0^2}{r}-r\right). \tag{9.127}$$

It is clear that the differential equation (9.127) has two domains of solution which interconnect at $r=R_0$.

When $r<R_0$, the right-hand side of the equation has a positive sign since $\frac{R_0^2}{r}>r$, accordingly we have the condition $dv/dr>0$.

On the other hand, when $r>R_0$, the right-hand side of the equation has a negative sign since $\frac{R_0^2}{r}<r$, so that we now have the condition $\frac{dv}{dr}<0$.

We will first solve the differential equation in the domain $r<R_0$. The sign of the nth root is of course positive:

$$\frac{dv}{dr}=\left(\frac{\varrho g J}{2K}\,\frac{R_0^2-r^2}{r}\right)^{\frac{1}{n}}. \tag{9.128}$$

The function

$$\frac{R_0^2-r^2}{r}$$

cannot be integrated in quadratic form, since it does not satisfy Tschebischew's conditions. Since the function is monotonic in the region of $R_1 \leqq r \leqq R_0$, it can be replaced by a linear function of interpolation.

$$f_1 = a_1 r + b_1$$

fitted to the points R_1 and R_0:

$$\left(\frac{R_0^2-R_1^2}{R_1}\right)^{\frac{1}{n}} = a_1 R_1 + b_1 ,$$

$$\left(\frac{R_0^2-R_0^2}{R_0}\right)^{\frac{1}{n}} = a_1 R_0 + b_1 = 0 .$$

From these the coefficients a_1 and b_1 are obtained as

$$a_1 = \frac{\left(\frac{R_0^2-R_1^2}{R_1}\right)^{\frac{1}{n}}}{R_1-R_0} ,$$

$$b_1 = \frac{\left(\frac{R_0^2-R_1^2}{R_1}\right)^{\frac{1}{n}}}{R_0-R_1} R_0 .$$

After substitution and integration we obtain

$$v = \left(\frac{\varrho g J}{2K}\right)^{\frac{1}{n}} \left[\frac{\left(\frac{R_0^2-R_1^2}{R_1}\right)^{\frac{1}{n}}}{R_1-R_0} \left(\frac{r^2}{2} - R_0 r\right) \right] + C_1 .$$

Since the velocity must be zero at $r = R_1$ the constant of integration can be obtained. Thus the velocity distribution in the interval $R_1 < r < R_0$ is given by

$$v = \left(\frac{\varrho g J}{2K}\right)^{\frac{1}{n}} \frac{\left(\frac{R_0^2-R_1^2}{R_1}\right)^{\frac{1}{n}}}{R_1-R_0} \left(\frac{r^2}{2} - R_0 r + R_0 R_1 - \frac{R_1^2}{2}\right). \tag{9.129}$$

This equation contains the temporarily unknown parameter R_0. This can be eliminated by relating the two velocity distributions obtained from the two solutions. To do this it is necessary to make use of the maximum velocity. Substituting

the condition $r=R_0$; $v=v_{\max}$ we get

$$v_{\max}=\left(\frac{\varrho g J}{2K}\right)^{\frac{1}{n}} \frac{\left(\frac{R_0^2-R_1^2}{R_1}\right)^{\frac{1}{n}}}{R_1-R_0}\left[\frac{R_0^2-R_1^2}{2}-R_0(R_0-R_1)\right]. \tag{9.130}$$

After simplification the maximum velocity is obtained as

$$v_{\max}=\left(\frac{\varrho g J}{2K}\,\frac{R_0^2-R_1^2}{R_1}\right)^{\frac{1}{n}} \frac{R_0-R_1}{2}. \tag{9.131}$$

The second part of the solution is that for the region of $R_0 \leqq r \leqq R_2$, where

$$r>R_0, \qquad \frac{\mathrm{d}v}{\mathrm{d}r}<0, \qquad \text{and} \qquad \left(\frac{R_0^2}{r}-r\right)<0.$$

The shear stress is also negative in this region. To take into account the signs, Eq. (9.127) may be written as

$$\left|\frac{\mathrm{d}v}{\mathrm{d}r}\right|^n \operatorname{sign}\left(\frac{\mathrm{d}v}{\mathrm{d}r}\right)=-\frac{\varrho g J}{2K}\left(\frac{R_0^2}{r}-r\right). \tag{9.132}$$

For the velocity gradient we get

$$\frac{\mathrm{d}v}{\mathrm{d}r}=\left[\frac{\varrho g J}{2K}\left(\frac{R_0^2}{r}-r\right)\right]^{\frac{1}{n}} \operatorname{sign}\left(\frac{R_0^2}{r}-r\right). \tag{9.133}$$

Since

$$\left(\frac{R_0^2}{r}-r\right)<0, \quad \text{we have} \quad \left|\frac{R_0^2}{r}-r\right|=r-\frac{R_0^2}{r},$$

and thus $\operatorname{sign}\left(\frac{R_0^2}{r}-r\right)=-1$.

Thus the differential equation which we have to solve is

$$\frac{\mathrm{d}v}{\mathrm{d}r}=-\left[\frac{\varrho g J}{2K}\,\frac{r^2-R_0^2}{r}\right]^{\frac{1}{n}}. \tag{9.134}$$

The integral of this expression cannot be obtained in quadratic form, we must again interpolate using the linear function

$$f_2=a_2 r+b_2.$$

The function is fitted to the points R_0 and R_2. The coefficients are found to be

$$a_2=\frac{\left(\frac{R_2^2-R_0^2}{R_2}\right)^{\frac{1}{n}}}{R_2-R_0},$$

$$b_2 = \frac{\left(\frac{R_2^2 - R_0^2}{R_2 - R_0}\right)^{\frac{1}{n}}}{R_2 - R_0} R_0 .$$

After substitution and integration we obtain

$$v = -\left(\frac{\varrho g J}{2K}\right)^{\frac{1}{n}} \frac{\left(\frac{R_2^2 - R_0^2}{R_2}\right)^{\frac{1}{n}}}{R_2 - R_0} \left(\frac{r^2}{2} - R_0 r\right) + C_2 . \tag{9.135}$$

Since at $r = R_2$, $v = 0$, expressing and substituting the constant of integration C_2, we obtain

$$v = \left(\frac{\varrho g J}{2K}\right)^{\frac{1}{n}} \frac{\left(\frac{R_2^2 - R_0^2}{R_2}\right)^{\frac{1}{n}}}{R_2 - R_0} \left[\frac{R_2^2 - r^2}{2} - R_0 (R_2 - r)\right]. \tag{9.136}$$

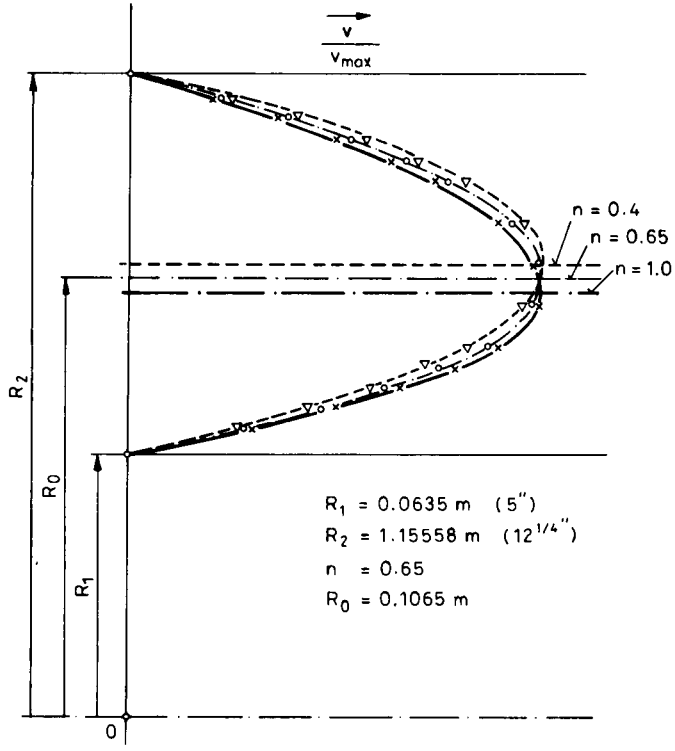

Fig. 9.23. Velocity distribution of the annular flow

The maximum velocity at $r = R_0$ is obtained as

$$v_{max} = \left[\frac{\varrho g J}{2K}\,\frac{R_2^2 - R_0^2}{R_2}\right]^{\frac{1}{n}} \frac{R_2 - R_0}{2}. \tag{9.137}$$

(See *Fig. 9.23.*)

Since the v_{max} obtained by Eqs (9.131) and (9.137) has to have the same value, we can equate Eqs (9.131) and (9.137) and obtain the following equation for R_0

$$\left(\frac{R_2}{R_1}\,\frac{R_0^2 - R_1^2}{R_2^2 - R_1^2}\right)^{\frac{1}{n}} = \frac{R_2 - R_0}{R_0 - R_1}. \tag{9.138}$$

This implicit equation can be solved by iteration if R_1, R_2 and n are known. The results can be tabulated, as for example for a borehole with a diameter of $D_2 = 12\ 1/4$ inches and a drill-pipe diameter of $D_1 = 5$ inches.

Knowing the two parts of the velocity distribution the flow rate can be determined. After determination of the integrals

$$Q = 2\pi\left(\int_{R_1}^{R_0} vr\,\mathrm{d}r + \int_{R_0}^{R_2} vr\,\mathrm{d}r\right),$$

the flow rate is obtained as

$$Q = 2\pi\left(\frac{\varrho g J}{2K}\right)^{\frac{1}{n}}\left\{\frac{\left(\frac{R_0^2 - R_1^2}{R_1}\right)^{\frac{1}{n}}}{R_1 - R_0}\left[\frac{R_0^4 - R_1^4}{8} - \frac{R_0(R_0^3 - R_1^3)}{3} + \frac{R_0 R_1(R_0^2 - R_1^2)}{2} - \right.\right.$$

$$\left. - \frac{R_1^2(R_0^2 - R_1^2)}{4}\right] + \frac{\left(\frac{R_2^2 - R_0^2}{R_2}\right)^{\frac{1}{n}}}{R_2 - R_0}\left[-\frac{R_2^4 - R_0^4}{8} + \frac{R_0(R_2^3 - R_0^3)}{3} - \right.$$

$$\left.\left. - \frac{R_0 R_2(R_2^2 - R_0^2)}{2} + \frac{R_2^2(R_2^2 - R_0^2)}{4}\right]\right\}. \tag{9.139}$$

If we designate the quantity in the curl bracket by A, then

$$Q = 2\pi A\left(\frac{\varrho g J}{2K}\right)^{\frac{1}{n}}. \tag{9.140}$$

Representative values of A together with values of R_0 are listed in *Table 9.1.* The cross-sectional average velocity is

$$c = \frac{2A}{R_2^2 - R_1^2}\left(\frac{\varrho g J}{2K}\right)^{\frac{1}{n}}. \tag{9.141}$$

Table 9.1. Borehole diameter 12 1/4"
Outer diameter drilling pipe 5"

n	R_0[m]	Φ
0.30	0.1116	1.422274
0.35	0.1108	1.617641
0.40	0.1099	1.827188
0.45	0.1091	2.049351
0.50	0.1084	2.283278
0.55	0.1078	2.534876
0.60	0.1071	2.803840
0.65	0.1065	3.092167
0.70	0.1060	3.401992
0.75	0.1054	3.735550
0.80	0.1049	4.092524
0.85		
0.90	0.1040	4.903305
0.95	0.1036	5.357264
1.00	0.1032	5.847680

Using this equation the hydraulic gradient is found to be:

$$J = \frac{2K}{\varrho g}\left(\frac{R_2^2 - R_1^2}{2A}\right)^n c^n. \tag{9.142}$$

The head loss of an annulus of length L can thus be expressed as

$$h' = \frac{2KL}{\varrho g}\left(\frac{R_2^2 - R_1^2}{2A}\right)^n c^n.$$

A so-called annulus shape parameter can be defined by the equation

$$\Phi = (R_2 - R_1)^{n+1}\left(\frac{R_2^2 - R_1^2}{2A}\right)^n. \tag{9.143}$$

Applying this notation the head loss is obtained as

$$h' = \frac{2K}{\varrho g}\,\frac{\Phi L}{(R_2 - R_1)^{n+1}}\,c^n. \tag{9.144}$$

The Weisbach equation for non-circular channels can be written as

$$h' = \lambda \frac{L}{4R_H}\,\frac{c^2}{2g}, \tag{9.145}$$

where R_H is the hydraulic radius. By comparing of Eqs (9.144) and (9.145) we

obtain the friction factor for the annulus:

$$\lambda_a = \frac{8K\Phi}{\varrho} \frac{c^{n-2}}{(R_2 - R_1)^n}. \tag{9.146}$$

A modified "annulus" Reynolds number can be defined in terms of the equation

$$\lambda_a = \frac{64}{\mathrm{Re}_a}. \tag{9.147}$$

From Eqs (9.146) and (9.147) the annulus Reynolds number can be expressed as

$$\mathrm{Re}_a = \frac{8\varrho c^{2-n}(R_2 - R_1)^n}{K\Phi}. \tag{9.148}$$

Thus the recommended steps of calculation to determine the head loss for a laminar annular flow of a pseudoplastic fluid are the following:

1. Determination of the radial position R_0 of the maximum velocity by iteration from Eq. (9.138).
2. Knowing R_0, the constant A, and the annulus form parameter Φ can be calculated from Eqs (9.139) and (9.143).
3. Determination of the modified annulus Reynolds number from Eq. (9.148).
4. Calculation of the friction factor using Eq. (9.147).
5. Finally we can determine the head loss for the annulus by applying Eq. (9.145) or, more directly, by omitting Steps 3 and 4 and using Eq. (9.144).

9.8 Turbulent flow of non-Newtonian fluids in pipes

For any kind of non-Newtonian fluid laminar flow gives way to turbulent flow once a critical value of the Reynolds number is exceeded. Experimental data show that the value of the critical Reynolds number differs slightly from fluid to fluid. For the most common pseudoplastic fluids the following relationship is found to hold:

$$(\mathrm{Re}_p^*)_{\mathrm{cr}} = \frac{6464n(n+2)^{\frac{n+2}{n+1}}}{(3n+1)^2}. \tag{9.149}$$

The friction factor values corresponding to the critical Reynolds number are shown in *Fig. 9.24*. The laminar-turbulent transition is strongly influenced by the elastic properties of the fluid. Methods of retarding this transition will be discussed later in connection with turbulent drag reduction.

In the following, our analysis will be restricted solely to pseudoplastic turbulent flow. The analogous equations for other types of flow are obtained in a similar way.

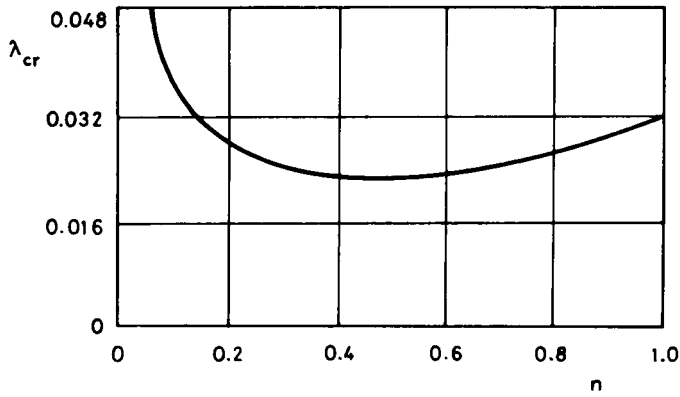

Fig. 9.24. Critical friction factor values for different pseudoplastic fluids

We consider the case of a steady, one-dimensional axisymmetric turbulent flow in a circular, infinitely long pipe. A cylindrical coordinate system is chosen. The momentum equation for this case is

$$\frac{\varrho g J r}{2} + K\left|\frac{dv}{dr}\right|^{n-1}\left(\frac{dv}{dr}\right) - \varrho\overline{u'w'} = 0, \tag{9.150}$$

where $-\varrho\widetilde{u'w'}$ is the τ'_{rz} component of the turbulent stress tensor.

The solution of this differential equation can be resolved into two parts in accordance with the nature of the flow. The flow near the wall is laminar within a very thin laminar sublayer. Turbulent momentum transfer cannot be developed here. Since the thickness of the laminar sublayer δ is very small relative to the radius R of the pipe, the velocity distribution within the laminar sublayer may be taken as linear. This is equivalent to there existing a uniform shear stress in the sublayer equal to the wall-shear stress τ_R. Thus, we can write

$$\frac{\varrho g J R}{2} - K\left|\frac{dv}{dr}\right|^{n} = 0. \tag{9.151}$$

The definition of the friction velocity

$$v_* = \sqrt{\frac{gJR}{2}} \tag{9.152}$$

can be used again, so that we obtain

$$-\frac{dv}{dr} = \left(\frac{v_*^2 \varrho}{K}\right)^{\frac{1}{n}}. \tag{9.153}$$

The linearized velocity profile within the laminar sublayer can be expressed in dimensionless form:

$$\frac{v}{v_*} = v_*^{\frac{2-n}{n}} \left(\frac{\varrho}{K}\right)^{\frac{1}{n}} (R-r). \tag{9.154}$$

Outside the laminar sublayer, the viscous shear stresses are negligibly small compared to the turbulent stresses. Applying Kármán's equation for the mixing length the momentum equation is obtained as

$$\frac{\varrho g J r}{2} = \varrho \kappa^2 \frac{\left(\frac{\mathrm{d}v}{\mathrm{d}r}\right)^4}{\left(\frac{\mathrm{d}^2 v}{\mathrm{d}r^2}\right)^2}. \tag{9.155}$$

The integration of this differential equation is the same as for the Newtonian case. Thus the dimensionless velocity distribution for the turbulent core flow is obtained as

$$\frac{v}{v_*} = \frac{1}{\kappa}\left[\sqrt{\frac{r}{R}} + \ln\left(1 - \sqrt{\frac{r}{R}}\right)\right] + \frac{v_{\max}}{v_*}. \tag{9.156}$$

The velocity distribution of the laminar sublayer and that of the turbulent core flow have to yield the same value for the velocity at the boundary of the two regions, i.e. where $r = R - \delta$. Thus, equating the two expressions for the velocity distributions, we obtain

$$\frac{v_{\max}}{v_*} + \frac{1}{\kappa}\left[\sqrt{1-\frac{\delta}{R}} + \ln\left(1 - \sqrt{1-\frac{\delta}{R}}\right)\right] = \frac{v_*^{\frac{2-n}{2}}\,\delta}{\left(\frac{K}{\varrho}\right)^{\frac{1}{n}}}. \tag{9.157}$$

Since $\frac{\delta}{R} \ll 1$, the quantity $\ln\left(1 - \sqrt{1-\frac{\delta}{R}}\right)$ can be expanded into a binomial series. Neglecting the higher-order terms we get

$$\sqrt{1-\frac{\delta}{R}} \cong 1 - \frac{\delta}{2R} = 1,$$

$$\ln\left(1 - \sqrt{1-\frac{\delta}{R}}\right) \cong \ln\left[1 - \left(1 - \frac{\delta}{2R}\right)\right] = \ln\frac{\delta}{2R}.$$

After substitution the maximum velocity is obtained as

$$\frac{v_{\max}}{v_*} = \left(\frac{v_*^{2-n}\varrho}{K}\right)^{\frac{1}{n}} \delta - \frac{1}{\kappa}\left(1+\ln\frac{\delta}{D}\right). \tag{9.158}$$

To calculate the maximum velocity it is necessary that δ be known. Prandtl assumed that for a Newtonian fluid

$$\mathrm{Re}_\delta = \frac{v_*\delta}{\nu} = \text{const}.$$

Analogously, we assume that for a pseudoplastic fluid

$$\mathrm{Re}_{p\delta} = \frac{v_*^{2-n}\delta^n\varrho}{\frac{K}{8}\left(\frac{6n+2}{n}\right)^n} \text{const}. \tag{9.159}$$

Using Eqs (9.159) and (9.57) the thickness of the laminar sublayer can be expressed as

$$\delta = \left(\frac{\mathrm{Re}_{p\delta}}{\mathrm{Re}_p}\right)^{\frac{1}{n}} \left(\frac{c}{v_*}\right)^{\frac{2-n}{n}} D. \tag{9.160}$$

Substituting this into Eq. (9.158) we get

$$\frac{v_{\max}}{v_*} = \frac{1}{n\kappa}\ln\left[\mathrm{Re}_p\left(\frac{v_*}{c}\right)^{2-n}\right] - \frac{1}{\kappa}\left(1+\frac{\ln \mathrm{Re}_{p\delta}}{n}\right) + \frac{6n+2}{n}\left(\frac{\mathrm{Re}_{p\delta}}{8}\right)^{\frac{1}{n}}. \tag{9.161}$$

This expression contains two temporarily unknown constants $\mathrm{Re}_{p\delta}$ and κ. The velocity distribution is obtained as

$$\frac{v}{v_*} = \frac{1}{\kappa}\left[\sqrt{\frac{r}{R}} + \ln\left(1-\sqrt{\frac{r}{R}}\right)\right] + \frac{1}{n\kappa}\ln\left[\mathrm{Re}_p\left(\frac{v_*}{c}\right)^{2-n}\right] -$$

$$- \frac{1}{\kappa}\left(1+\frac{\ln \mathrm{Re}_{p\delta}}{n}\right) + \frac{6n+2}{n}\left(\frac{\mathrm{Re}_{p\delta}}{8}\right)^{\frac{1}{n}}. \tag{9.162}$$

The cross-sectional average velocity can be calculated in the usual way, and is found to be

$$\frac{c}{v_*} = \frac{v_{\max}}{v_*} - \frac{1}{\kappa}\left(\frac{25}{12} - \frac{4}{5}\right), \tag{9.163}$$

thus

$$\frac{c}{v_*} = \frac{1}{n\kappa}\ln\left[\mathrm{Re}_p\left(\frac{v_*}{c}\right)^{2-n}\right] - \frac{1}{\kappa}\left(\frac{137}{60} + \frac{\ln(\mathrm{Re}_{p\delta})}{n}\right) + \\ + \frac{6n+2}{n}\left(\frac{\mathrm{Re}_{p\delta}}{8}\right)^{\frac{1}{n}}. \tag{9.164}$$

The friction factor can be calculated in the same manner as for the Newtonian case:

$$\frac{1}{\sqrt{\lambda}} = \frac{0.8141}{n\kappa}\lg\left(\mathrm{Re}_p\lambda^{\left(1-\frac{n}{2}\right)}\right) + 0.7532\frac{n-2}{2n} + \\ + 0.3535\left[\frac{6n+2}{n}\left(\frac{\mathrm{Re}_{p\delta}}{8}\right)^{\frac{1}{n}}\right] - \frac{1}{\kappa}\left(2.283 + \frac{\ln \mathrm{Re}_{p\delta}}{n}\right). \tag{9.165}$$

Laboratory and *in situ* measurements by Navratil (1978) both provided similar values of

$$\mathrm{Re}_{p\delta} = 12.087,$$
$$\kappa = 0.407.$$

These values are the same as those obtained for the Newtonian case. Thus, finally we can write

$$\frac{1}{\sqrt{\lambda}} = \frac{2}{n}\lg\left(\mathrm{Re}_p\lambda^{\left(1-\frac{n}{2}\right)}\right) + 1.511^{\frac{1}{n}}\left(\frac{0.707}{n} + 2.121\right) - \frac{4.015}{n} - 1.057, \tag{9.166}$$

or in a simpler form

$$\frac{1}{\sqrt{\lambda}} = \frac{2}{n}\lg\left(\mathrm{Re}_p\lambda^{\left(1-\frac{n}{2}\right)}\right) + \beta. \tag{9.167}$$

For a fully rough pipe the friction factor is invariably

$$\frac{1}{\sqrt{\lambda}} = 2\lg\left(3.715\frac{D}{K}\right). \tag{9.168}$$

In the transition region between the friction factor curve for a smooth pipe and that for a wholly rough region, an interpolation formula can be obtained analogous to the Colebrook equation

$$\frac{1}{\sqrt{\lambda}} = -2\lg\left[\frac{10^{-\frac{\beta}{2}}}{\mathrm{Re}_p^{\frac{1}{n}}\lambda^{\frac{2-n}{2n}}} + \frac{k}{3.715D}\right]. \tag{9.169}$$

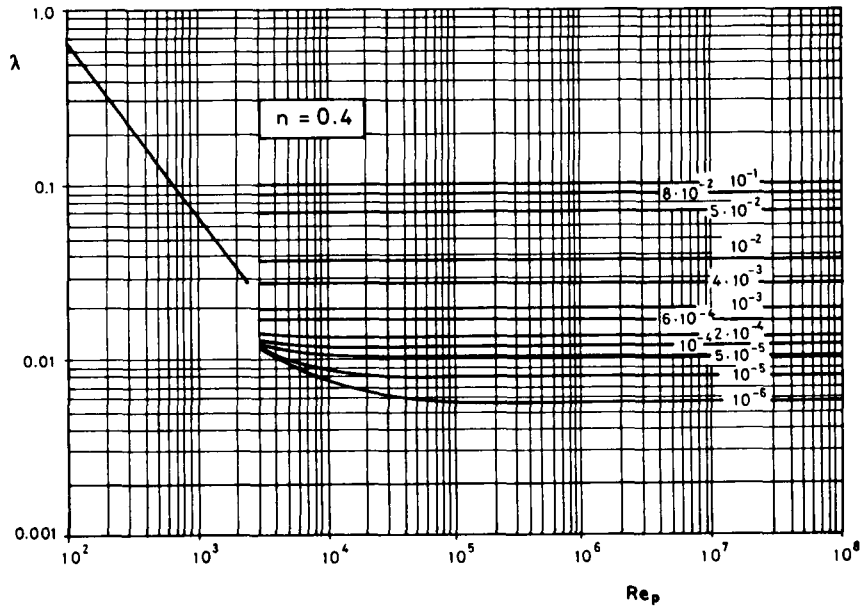

Fig. 9.25. Friction factor chart for turbulent flow of a pseudoplastic fluid $n=0.4$

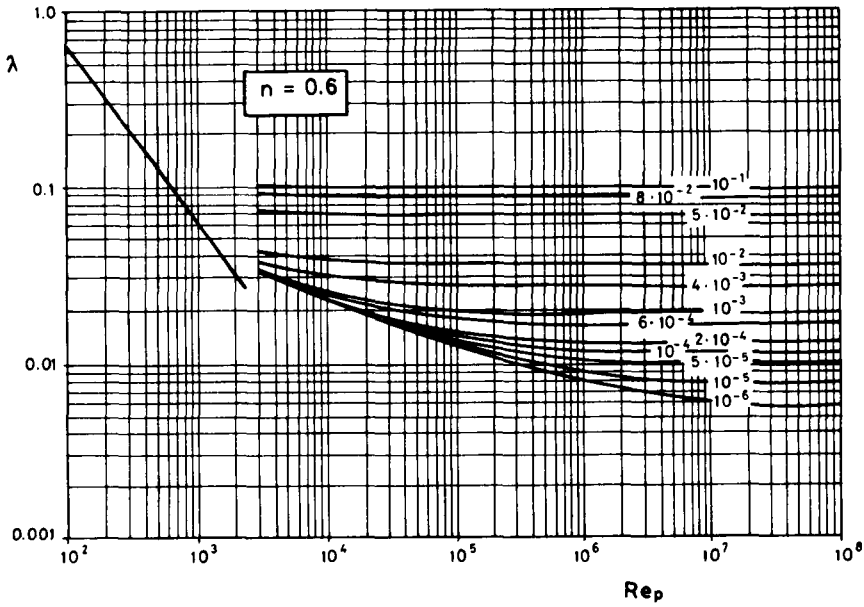

Fig. 9.26. Friction factor chart for turbulent flow of a pseudoplastic fluid $n=0.6$

This equation was further elaborated by Szilas, Bobok and Navratil (1981). Friction factor charts based on the BNS equation are shown in *Figs 9.25* and *9.26*. The slope of friction factor curves for smooth pipes decreases as the behavior index decreases. The eventual laminar-turbulent transition is the other remarkable feature of the curves for a certain range of n. Experimental data obtained for crude oil pipelines with diameters ranging from 100 mm to 600 mm are in good agreement with the BNS equation.

CHAPTER 10

FLOW OF MULTIPHASE MIXTURES

10.1 Properties of multiphase mixtures

The term "multiphase mixture" is used in this chapter to refer to all multiphase material systems which can flow as fluids while their flow variables undergo finite jumps at macroscopically observable interfaces. The category "multiphase mixture flow" encompasses a wide variety of different kinds of flows. The main types of multiphase mixture flow are liquid-gas, liquid-liquid, liquid-solid and gas-solid flows. All of these are encountered in the petroleum industry. Liquid-gas flows exist in oil and gas wells, in field gathering systems, in condensate transporting pipelines, in geothermal wells and pipelines. Liquid-liquid flow is most commonly found in oil wells and gathering systems as flows of oil-water mixtures. Liquid-solid flows are frequently encountered during drilling and well-completion as flows of drilling mud with cuttings, different types of cement flow, or the flow of fracturing gel carrying proppant material. Gas-solid flows can be found in compressed-air drilling systems.

Any material system can be considered as multicomponent, if the flow properties of its immiscible constituents are different. A chemically multicomponent system such as crude oil, natural gas, geothermal brine or a fine clayey suspension in water, is homogeneous in the mechanical sense. On the other hand the different particle size fractions in a coarse sandy slurry lead to a more complex behavior than would be expected for a chemical two-component system.

In addition to knowing the properties of the separate homogeneous fluids it is also important to know the behavior of the mixture at the hydrostatic state under consideration: one phase of it may be rising, or settling, in the other. This phenomenon can be characterized by the so-called terminal settling velocity, which depends on the properties of both the particles and the continuous phase.

The simplest case is that of spherical, solid particles dispersed in a Newtonian fluid at rest. Depending on the density of the particles ϱ_p and that of the continuous fluid phase ϱ, the force of gravity can cause a particle to either rise ($\varrho_p < \varrho$), or settle ($\varrho_p > \varrho$). The body force acting on a particle of diameter d is

$$f_g = \frac{\pi d^3}{6}(\varrho_p - \varrho)g \,. \tag{10.1}$$

In the most general case the phases are not in thermal equilibrium and the

concentrations of the components vary along the flow path. In this case heat and mass transfer occur across the phase interfaces, and must be taken into account in the balance equations.

The separate phases move with different velocities. Thus separate velocity fields have to be considered simultaneously for each phase in the flow field of the mixture.

Because of the difference in density particles will tend to settle or rise, so that phase separation occurs in most multiphase mixtures. This phenomenon is most clearly seen in the hydrostatic state, and can be characterized by the terminal settling velocity.

The simplest case refers to spherical solid particles dispersed on a Newtonian fluid at rest. Depending on the density of the particles ϱ_p and of the continuous fluid phase ϱ, the force of gravity can cause a particle to settle ($\varrho_p > \varrho$), or to rise ($\varrho_p < \varrho$). For non-interacting particles, the laminar settling velocity is

$$U = \frac{gd^2}{18\nu} \frac{\varrho_p - \varrho}{\varrho}. \tag{10.1a}$$

This equation is valid when the Reynolds number of the particle

$$\mathrm{Re}_p = \frac{U\delta}{\nu} < 1. \tag{10.2}$$

In the transition region between laminar and turbulent settling, when

$$1 < \mathrm{Re}_p < 1000,$$

the terminal settling velocity is found to be

$$U = 0.2 \left(g \frac{\varrho_p - \varrho}{\varrho} \right)^{0.72} \frac{d^{1.18}}{\nu^{0.45}}. \tag{10.3}$$

For turbulent motion, when $\mathrm{Re}_p > 1000$,

$$U = 1.74 \sqrt{gd \frac{\varrho_p - \varrho}{\varrho}}. \tag{10.4}$$

Small fluid droplets and gas bubbles are usually spherical on account of capillary forces. Since there is internal fluid motion within such droplets, the terminal settling velocity is not the same as for solid particles. For laminar motion it is found that

$$U = \frac{gd^2}{18\nu} \frac{\varrho_p - \varrho}{\varrho} \frac{3\mu + 3\mu_p}{2\mu + 3\mu_p}, \tag{10.5}$$

where μ_p is the viscosity of the dispersed phase, and μ is the viscosity of the continuous phase. For gas bubbles rising in a liquid, when $\mu_p \ll \mu$, Eq. (10.5) can be reduced to

$$U = \frac{gd^2}{12\nu} \frac{\varrho_p - \varrho}{\varrho}. \tag{10.6}$$

The drag coefficient of irregularly shaped particles is higher than that of spheres of the same volume. The most simple method of taking the non-spherical shape into consideration is to use a shape factor ψ, defined by the quotient of the surface of a sphere of volume equal to that of the particle and the surface of the particle. For regularly shaped non-spherical particles, ψ can be calculated directly. For irregularly shaped particles, for which screen analysis results are known, we find

$$\psi = \frac{d_{av}}{nd}, \tag{10.7}$$

where d_{av} is the average screen size of the particle, d is the diameter of a sphere of volume equal to that of the particle, n is the ratio of the surface area per unit mass of the spherical particles with diameter d_{av}. The effect of particle shape on the settling velocity is shown in *Fig. 10.1*, where the ratio of U_ψ/U is plotted against the particle Reynolds number, while ψ is taken as parameter.

The interaction between the dispersed particles increases with increasing concentration. The effect of an increased concentration reduces the terminal settling velocity, as shown in *Fig. 10.2*.

In order to generalize the balance equations for multiphase mixtures it is necessary to introduce a notation for the concentrations in the flow system.

Let the mass of the ith component in a unit volume be designated by α_i. This is obviously a point function, forming a scalar field i.e.

$$\alpha_i(\vec{r}, t) = \frac{\mathrm{d}m_i}{\mathrm{d}V}. \tag{10.8}$$

It is clear, that the sum of mass concentrations is equal to the density of the n-component mixture

$$\sum_{i=1}^{n} \alpha_i = \varrho. \tag{10.9}$$

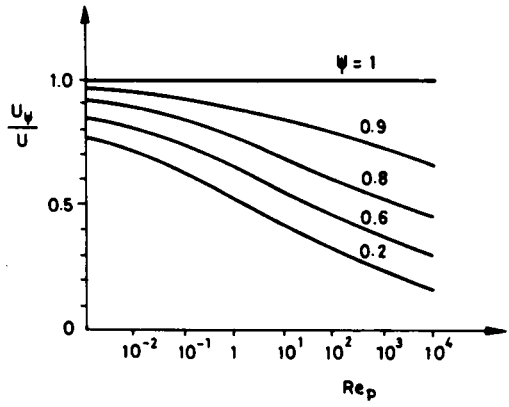

Fig. 10.1. The effect of particle shape on the settling velocity

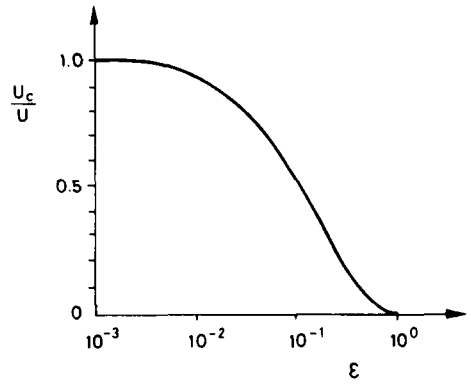

Fig. 10.2. The effect of concentration on the settling velocity

The mass fraction of the ith phase can be expressed by the equation

$$\beta_i = \frac{\alpha_i}{\varrho}. \tag{10.10}$$

It is obvious, that

$$\sum_{i=1}^{n} \beta_i = 1. \tag{10.11}$$

The volume fraction of the ith phase is defined by the expression

$$\varepsilon_i = \frac{\mathrm{d}V_i}{\mathrm{d}V}, \tag{10.12}$$

where $\mathrm{d}V_i$ is the volume of the ith phase within the infinitesimal volume $\mathrm{d}V$.

The sum of the volume fractions is equal to unity

$$\sum_{i=1}^{n} \varepsilon_i = 1. \tag{10.13}$$

The density of the ith phase can be expressed as

$$\varrho_i = \frac{\alpha_i}{\varepsilon_i}. \tag{10.14}$$

In the flow system there are as many simultaneous velocity fields as there are phases present in the flowing mixture, i.e.

$$\vec{v}_i = \vec{v}_i(\vec{r}, t) \qquad i = 1, 2, \ldots n. \tag{10.15}$$

The mass-averaged velocity of the mixture is obtained as

$$\vec{v} = \sum_{i=1}^{n} \beta_i \vec{v}_i. \tag{10.16}$$

The mass-averaged velocity $\tilde{v}$ is the velocity which would be measured by a Pitot tube. It also forms a vector field, since it is an average only within the volume element $\mathrm{d}V$; in the flow system as a whole it can be considered to be a continuously varying point function:

$$\tilde{v}=\tilde{v}(\vec{r}, t)\,. \tag{10.17}$$

The existence of simultaneous velocity fields leads to a consequence in the expressions of the material derivatives relating to the variables of a phase. As is well known, the material derivative expresses the rate of change of some quantity in a coordinate system moving together with the flowing fluid:

$$\frac{\mathrm{d}\,..}{\mathrm{d}t}=\frac{\partial\,..}{\partial t}+(\tilde{v}V)\ldots$$

The convective term depends on the velocity.
If simultaneous velocity fields exist, each velocity field determines a material derivative of its own. Thus each phase has its own material derivative

$$\frac{\mathrm{d}\,..}{\mathrm{d}t_i}=\frac{\partial\,..}{\partial t}+(\tilde{v}_i V)\ldots \tag{10.18}$$

These definitions added to the familiar idea of a continuum constitute a common framework within which multiphase mixture flows may be described and interrelated.

10.2 The continuity equation for multiphase mixtures

In order to express the conservation of mass consider a finite volume V of a multiphase mixture bounded by the closed surface (A). In this region continuous functions of concentration, density and velocity belong to each phase of the mixture expressing the values of these variables at any point and time. The mass of the ith phase in the infinitesimal volume $\mathrm{d}V$ can be expressed as

$$\varepsilon_i \varrho_i \,\mathrm{d}V=\alpha_i \,\mathrm{d}V. \tag{10.19}$$

The volume V contains the mass

$$\int_V \varepsilon_i \varrho_i \,\mathrm{d}V=\int_V \alpha_i \,\mathrm{d}V \tag{10.20}$$

of the ith phase. The total mass in the material volume V is obviously

$$\int_V \sum_{i=1}^{n} \varepsilon_i \varrho_i \,\mathrm{d}V=\int_V \varrho \,\mathrm{d}V. \tag{10.21}$$

The conservation of the total mass of the mixture can be expressed by the equation

$$\frac{\mathrm{d}}{\mathrm{d}t}\int_V \varrho \,\mathrm{d}V = 0\,, \tag{10.22}$$

where ϱ is the density of the mixture, and $\mathrm{d}\,../\mathrm{d}t$ is the material derivative with respect to the mass-averaged velocity of the mixture. The bounding surface (A) of the moving material volume is considered to be such that each point of (A) moves with the mass-averaged velocity $\vec{v}$. In this form the continuity equation is formally the same as for a homogeneous fluid. Separating the local from the convective rate of change of mass we obtain

$$\int_V \frac{\partial \varrho}{\partial t}\,\mathrm{d}V + \int_{(A)} \varrho \vec{v}\,\mathrm{d}\vec{A} = 0\,. \tag{10.23}$$

As is well-known, the surface integral may be transformed into a volume integral by means of the divergence theorem. Since both integrals are taken over the same volume V, and this volume is arbitrary, the integral signs may be removed to give

$$\frac{\partial \varrho}{\partial t} + \operatorname{div}(\varrho \vec{v}) = 0\,. \tag{10.24}$$

The continuity equation for one of the phases of the mixture will change. In general the mass of a certain phase is not a preserving quantity since mass transfer may occur at the phase boundary surfaces. This can be considered as equivalent to the individual phases having sources or sinks within the volume V. Thus the integral form of the mass balance equation for the ith phase can be expressed as

$$\int_V \frac{\partial(\varepsilon_i \varrho_i)}{\partial t}\,\mathrm{d}V + \int_{(A)} \varepsilon_i \varrho_i \vec{v}_i\,\mathrm{d}\vec{A} = \int \xi_i\,\mathrm{d}V, \tag{10.25}$$

where ξ_i is the rate at which mass of the ith phase is produced or vanished within V. In differential form this can be written as

$$\frac{\partial(\varepsilon_i \varrho_i)}{\partial t} + \operatorname{div}(\varepsilon_i \varrho_i \vec{v}_i) = \xi_i\,. \tag{10.26}$$

In the case of an n-phase system, ξ_i is the sum of the mass sources and sinks (with minus sign) referring to other phases

$$\xi_i = \sum_{j=1}^{n-1} \xi_{ij}\,. \tag{10.27}$$

It is obvious, that

$$\sum_{i=1}^{n} \xi_i = 0\,, \tag{10.27a}$$

therefore the sum of the mass sources and sinks for the whole system is zero.

The interphase mass transfer can be characterized by the velocity difference

$$\vec{v}_i^* = \vec{v}_i - \vec{v} \tag{10.28}$$

which is called the diffusion velocity.

The continuity equation for the ith phase can be expressed as

$$\frac{\partial(\varepsilon_i \varrho_i)}{\partial t} + \operatorname{div}\left[\varepsilon_i \varrho_i (\vec{v} + \vec{v}_i^*)\right] = \xi_i , \tag{10.29}$$

or in an alternate form

$$\frac{\partial(\beta_i \varrho)}{\partial t} + \operatorname{div}\left[\alpha_i (\vec{v} + \vec{v}_i^*)\right] = \xi_i . \tag{10.30}$$

Similarly, the continuity equation can be written in terms of the mass fraction of the ith phase and the density of the mixture

$$\frac{\partial(\beta_i \varrho)}{\partial t} + \operatorname{div}(\beta_i \varrho \vec{v}_i^*) + \operatorname{div}(\beta_i \varrho \vec{v}) = \xi_i . \tag{10.31}$$

After a little manipulation we get

$$\beta_i \left[\frac{\partial \varrho}{\partial t} + \operatorname{div}(\varrho \vec{v})\right] + \varrho \left[\frac{\partial \beta_i}{\partial t} + \vec{v} \operatorname{grad} \beta_i\right] = \xi_i - \operatorname{div}(\beta_i \varrho \vec{v}_i^*) . \tag{10.32}$$

It is clear that the quantity in the first square bracket is equal to zero, thus we obtain

$$\varrho \frac{\partial \beta_i}{\partial t} + \varrho \vec{v} \operatorname{grad} \beta_i = \xi_i - \operatorname{div}(\beta_i \varrho \vec{v}_i^*) , \tag{10.33}$$

therefore, the local and convective rates of change of the mass fraction are caused by the mass source and the diffusion.

For everyday petroleum engineering purposes it is adequate to consider only one-dimensional two-phase flow, expressing the balance equations in terms of the cross-sectional average values of the flow variables.

Consider a straight circular pipe with an arbitrary orientation, as shown in *Fig. 10.3*. The control volume V is bounded by the closed surface (A), which consists

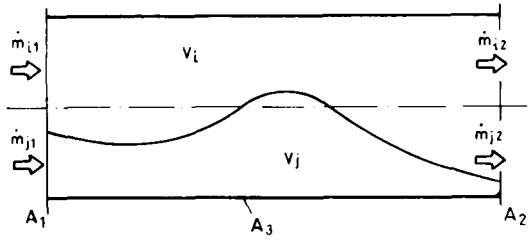

Fig. 10.3. Cylindrical control volume for continuity equation

of the inlet and outlet cross sections A_1 and A_2, and the impermeable pipe wall A_3. Let i and j refer respectively to the less and the more dense phase. The volumes occupied by the two phases are denoted by V_i and V_j. The rate of accumulation of mass within the control volume must equal the difference between the inflow and the outflow at A_1 and A_2:

$$\int_V \left(\frac{\partial \alpha_i}{\partial t} + \frac{\partial \alpha_j}{\partial t}\right) \mathrm{d}V + \int_{A_1} (\alpha_i \vec{v}_i + \alpha_j \vec{v}_j)\, \mathrm{d}\vec{A} + \int_{A_2} (\alpha_i \vec{v}_i + \alpha_j \vec{v}_j)\, \mathrm{d}\vec{A} = 0 . \quad (10.34)$$

Let the mass of the whole system be

$$M = \int_V (\alpha_i + \alpha_j)\, \mathrm{d}V , \quad (10.35)$$

and the mass fluxes of phases i and j

$$\dot{m}_i = \int_A \alpha_i \vec{v}_i\, \mathrm{d}\vec{A} , \quad (10.36)$$

$$\dot{m}_j = \int_A \alpha_j v_j\, \mathrm{d}\vec{A} . \quad (10.37)$$

In this case the continuity equation can be expressed as

$$\frac{\partial M}{\partial t} = \dot{m}_{i1} + \dot{m}_{j1} - \dot{m}_{i2} - \dot{m}_{j2} , \quad (10.38)$$

where M is the mass of whole system.

The mass fluxes of phases i and j can be expressed in terms of the cross-sectional average velocities and densities as

$$\dot{m}_i = \int_A \varepsilon_i \varrho_i \vec{v}_i\, \mathrm{d}\vec{A} = E_i \varrho_i c_i A , \quad (10.39)$$

$$\dot{m}_j = \int_A \varepsilon_j \varrho_j \vec{v}_j\, \mathrm{d}\vec{A} = E_j \varrho_j c_j A , \quad (10.40)$$

where E_i and E_j are the average volume fractions of phases i and j over an infinitesimal length of the pipe:

$$E_i = \frac{1}{A} \int_{(A)} \varepsilon_i\, \mathrm{d}A ; \qquad E_j = \frac{1}{A} \int_{(A)} \varepsilon_j\, \mathrm{d}A . \quad (10.41)$$

They may also be expressed as

$$E_i = \frac{A_i}{A}, \qquad E_j = \frac{A_j}{A}, \tag{10.42}$$

i.e. as the fractional cross-sectional areas occupied by the phases i and j. It is obvious that

$$E_i + E_j = 1 . \tag{10.43}$$

Applying these expressions the equation for the conservation of mass is obtained as

$$\frac{\partial M}{\partial t} = A_1(E_i \varrho_i c_i + E_j \varrho_j c_j)_1 - A_2(E_i \varrho_i c_i + E_j \varrho_j c_j)_2 . \tag{10.44}$$

Since the diameter of the pipe is uniform the above equation can be written in the form

$$\frac{1}{A}\frac{\partial M}{\partial t} = E_{i1}\varrho_{i1}c_{i1} + E_{j1}\varrho_{j1}c_{j1} - E_{i2}\varrho_{i2}c_{i2} - E_{j2}\varrho_{j2}c_{j2} . \tag{10.45}$$

In the special case where the inflows $\dot{m}_{i1}$ and $\dot{m}_{j1}$ are constant and the flow is stabilized in the pipe, the flow will be steady, in which case

$$E_{i1}\varrho_{i1}c_{i1} + E_{j1}\varrho_{j1}c_{j1} = E_{i2}\varrho_{i2}c_{i2} + E_{j2}\varrho_{j2}c_{j2} . \tag{10.46}$$

The in situ volume fractions usually change along the flow path. The more viscous phase tends to flow at a lower average velocity than the other phase. The result is the salient feature of multiphase flows called holdup. In most cases the relation pertaining to the holdup phenomenon can be determined experimentally. This will be more fully discussed later.

10.3 The momentum equation for multiphase mixtures

Newton's second law obviously also applies to flows of multiphase mixtures. In order to obtain an expression for the momentum equation for this case, consider an arbitrary material volume V, bounded by the closed surface (A), within which a mixture of n components is present. The variations in density, concentration, velocity, and stress, are given by the appropriate scalar, vector and tensor fields. The momentum of the ith phase within the infinitesimal volume $\mathrm{d}V$ can be written as

$$\varepsilon_i \varrho_i \vec{v}_i \, \mathrm{d}V = \alpha_i \vec{v}_i \, \mathrm{d}V . \tag{10.47}$$

Integrating over the volume V the momentum of the ith phase within V is obtained as

$$\int_V \varepsilon_i \varrho_i \vec{v}_i \, \mathrm{d}V = \int_V \alpha_i v_i \, \mathrm{d}V . \tag{10.48}$$

The total momentum of the mixture is obviously the sum of the momentums of each phase. It is evident that the extensive variables can also be summed. Thus

$$\sum_{i=1}^{n} \int_V \varepsilon_i \varrho_i \vec{v}_i \, \mathrm{d}V = \int_V \sum_{i=1}^{n} \varepsilon_i \varrho_i \vec{v}_i \, \mathrm{d}V = \int_V \varrho \vec{v} \, \mathrm{d}V, \tag{10.49}$$

where ϱ is the density of the mixture, and $\vec{v}$ is the mass-averaged velocity.

The rate of change of the momentum can be expressed by the material derivative of this integral:

$$\frac{\mathrm{d}}{\mathrm{d}t} \int_V \sum_{i=1}^{n} \varepsilon_i \varrho_i \vec{v}_i \, \mathrm{d}V = \frac{\mathrm{d}}{\mathrm{d}t} \int_V \sum_{i=1}^{n} \alpha_i \vec{v}_i \, \mathrm{d}V = \frac{\mathrm{d}}{\mathrm{d}t} \int_V \varrho \vec{v} \, \mathrm{d}V. \tag{10.50}$$

The material derivative $\mathrm{d}../\mathrm{d}t$ refers to the mass-averaged velocity field. Material derivatives relating to individual phase velocities are different. Thus the expression for the rate of change of the momentum of the mixture needs to be discussed in detail. Since differentiation and summation are independent operations it is allowed to interchange them. Thus

$$\frac{\mathrm{d}}{\mathrm{d}t}\left(\sum_{i=1}^{n} \alpha_i \vec{v}_i\right) + \left(\sum_{i=1}^{n} \alpha_i \vec{v}_i\right) \operatorname{div} \vec{v} = \sum_{i=1}^{n} \left[\frac{\mathrm{d}}{\mathrm{d}t} (\alpha_i \vec{v}_i + \alpha_i \vec{v}_i \operatorname{div} \vec{v}\right]. \tag{10.51}$$

We can write

$$\frac{\mathrm{d}}{\mathrm{d}t}(\alpha_i \vec{v}_i) = \frac{\partial}{\partial t}(\alpha_i \vec{v}_i) + (\vec{v}\nabla)(\alpha_i \vec{v}_i), \tag{10.52}$$

and

$$\frac{\mathrm{d}}{\mathrm{d}t_i}(\alpha_i \vec{v}_i) = \frac{\partial}{\partial t}(\alpha_i \vec{v}_i) + (\vec{v}_i \nabla)(\alpha_i \vec{v}_i). \tag{10.53}$$

Eliminating the local derivatives we get

$$\frac{\mathrm{d}}{\mathrm{d}t}(\alpha_i \vec{v}_i) = \frac{\mathrm{d}}{\mathrm{d}t_i}(\alpha_i \vec{v}_i) - (\vec{v}_i \nabla)(\alpha_i \vec{v}_i) + (\vec{v}\nabla)(\alpha_i \vec{v}_i), \tag{10.54}$$

or in alternative form

$$\frac{\mathrm{d}}{\mathrm{d}t}(\alpha_i \vec{v}_i) = \frac{\mathrm{d}}{\mathrm{d}t_i}(\alpha_i \vec{v}_i) + [(\vec{v} - \vec{v}_i)\nabla]\alpha_i \vec{v}_i. \tag{10.55}$$

This can be expressed in terms of the diffusion velocity $\vec{v}_i^*$:

$$\frac{\mathrm{d}}{\mathrm{d}t}(\alpha_i \vec{v}_i) = \frac{\mathrm{d}}{\mathrm{d}t_i}(\alpha_i \vec{v}_i) - (\vec{v}^* \nabla)(\alpha_i \vec{v}_i) = \alpha_i \frac{\mathrm{d}\vec{v}_i}{\mathrm{d}t_i} + \vec{v}_i \frac{\mathrm{d}\alpha_i}{\mathrm{d}t_i} - (\vec{v}^* \nabla)(\alpha_i \vec{v}_i). \tag{10.56}$$

By using the continuity equation for the ith phase we obtain the equation

$$\frac{\mathrm{d}}{\mathrm{d}t}(\alpha_i \vec{v}_i) = \alpha_i \frac{\mathrm{d}\vec{v}_i}{\mathrm{d}t_i} - \alpha_i \vec{v}_i \operatorname{div} \vec{v}_i + \xi_i \vec{v}_i - \operatorname{Div}(\alpha_i \vec{v}_i^* \circ \vec{v}_i^*) + \alpha_i \vec{v}_i \operatorname{div} \vec{v}_i^*. \tag{10.57}$$

In order to express the rate of change of momentum in terms of the density of the mixture and the mass-averaged velocity Eq. (10.57) must be summed over all n components of the mixture

$$\varrho \frac{\mathrm{d}\vec{v}}{\mathrm{d}t} = \sum_{i=1}^{n} \left[\alpha_i \frac{\mathrm{d}\vec{v}_i}{\mathrm{d}t_i} - \alpha_i \vec{v}_i \operatorname{div} \vec{v}_i + \xi_i \vec{v}_i^* - \operatorname{Div} (\alpha_i \vec{v}_i^* \circ \vec{v}_i^*) + \xi_i \vec{v} - \operatorname{Div} (\alpha_i \vec{v}_i^* \circ \vec{v}) + \right.$$
$$\left. + \alpha_i \vec{v}_i \operatorname{div} \vec{v}_i - \alpha_i \vec{v}_i \operatorname{div} \vec{v} + \alpha_i \vec{v}_i \operatorname{div} \vec{v} \right]. \tag{10.58}$$

This rather difficult expression may be simplified by taking into account that

$$\sum_{i=1}^{n} \xi_i \vec{v} = \vec{v} \sum_{i=1}^{n} \xi_i = 0\,, \tag{10.59}$$

and

$$\sum_{i=1}^{n} \operatorname{Div} (\alpha_i \vec{v}_i^* \circ \vec{v}) = \operatorname{Div} \left(\sum_{i=1}^{n} \alpha_i \vec{v}_i^* \circ \vec{v} \right) = \left[\left(\sum_{i=1}^{n} \alpha_i \vec{v}_i^* - \vec{v} \sum_{i=1}^{n} \alpha_i \right) \vec{v} \right] V = 0\,, \tag{10.60}$$

since the expression in the square bracket is $\varrho\vec{v} - \vec{v}\varrho = 0$. After some further simplification we finally get

$$\varrho \frac{\mathrm{d}\vec{v}}{\mathrm{d}t} = \sum_{i=1}^{n} \left[\alpha_i \frac{\mathrm{d}\vec{v}_i}{\mathrm{d}t_i} + \xi_i \vec{v}_i^* - \operatorname{Div} (\alpha_i \vec{v}_i^* \circ \vec{v}_i^*) \right]. \tag{10.61}$$

The rate of change of the total momentum of the mixture is obtained as

$$\frac{\mathrm{d}}{\mathrm{d}t} \int_V \varrho \vec{v} \, \mathrm{d}V = \int_V \sum_{i=1}^{n} \left[\alpha_i \frac{\mathrm{d}\vec{v}_i}{\mathrm{d}t_i} + \xi_i \vec{v}_i^* - \operatorname{Div} (\alpha_i \vec{v}_i^* \circ \vec{v}_i^*) \right] \mathrm{d}V\,. \tag{10.62}$$

This should be equal to the resultant external force acting on the material volume.

The resultant body force can be expressed as

$$\varrho \vec{g} = \sum_{i=1}^{n} \alpha_i \vec{g}_i\,. \tag{10.63}$$

In addition to the usual gravity, centrifugal or Coriolis forces, interphase body forces occur, such as the lifting force or the drag acting on a bubble or a dispersed solid particle. Terms representing these forces may occur in the momentum equations of individual phases, but they vanish when the momentum equations for the total system are summed, since

$$\vec{g}_{ij} = -\vec{g}_{ji} \tag{10.64}$$

in accordance with Newton's third law.

The stress tensor of the whole system is the sum of the individual stress tensors relating to each phase. Since momentum is an external variable, its conductive flux

is obviously additive. Therefore

$$\mathbf{T} = \sum_{i=1}^{n} \mathbf{T}_i \,. \tag{10.65}$$

The stress tensor $\mathbf{T}_i$ can be decomposed to two parts: one, $\mathbf{T}_{0i}$ relates to the pure ith phase, the other, $\mathbf{T}_{ji}$ expresses the interphase effects at the boundary surface between the ith and jth phase

$$\mathbf{T}_i = \alpha_i \mathbf{T}_{0i} - \alpha_j \mathbf{T}_{ji} \,. \tag{10.66}$$

The interphase transfer of mass provides an additional force. The mass transfer from the ith to the jth phase is characterized by the mass source (or sink) ξ_{ji}. Let the velocity at which mass is transferred be $\vec{v}_{ji}$, then the resulting force can be expressed as

$$\vec{f}_{mij} = \xi_{ji}(\vec{v}_{ji} - \vec{v}_i) \,. \tag{10.67}$$

The total resulting force between the ith phase and the other $n-1$ phases is given by

$$f_{mi} = \sum_{j=1}^{n-1} \xi_{ji}(\vec{v}_{ji} - \vec{v}_i) \,. \tag{10.68}$$

Taking all this into account the momentum equation for the ith phase can be written as

$$\alpha_i \frac{\mathrm{d}\vec{v}_i}{\mathrm{d}t_i} = \alpha_i \vec{g}_i + \operatorname{Div} \mathbf{T}_i + \sum_{j=1}^{n-1} \left[\vec{g}_{ji} + \xi_{ji}(\vec{v}_{ji} - \vec{v}_i)\right] . \tag{10.69}$$

The momentum equation for the whole system is obtained by summing the momentum equations for the individual phases, while taking into account that

$$\sum_{i,j} \vec{g}_{ij} = 0 \,, \tag{10.70}$$

and

$$\sum_{i,j} \xi_{ji}(\vec{v}_{ji} - \vec{v}_i) = 0 \,. \tag{10.71}$$

This is obvious, since $\vec{g}_{ji} = -\vec{g}_{ij}$, and $\vec{v}_{ij} = -\vec{v}_{ji}$. Thus we can obtain the following sum:

$$\sum_{i=1}^{n} \alpha_i \frac{\mathrm{d}\vec{v}_i}{\mathrm{d}t_i} = \sum_{i=1}^{n} \alpha_i \vec{g}_i + \sum_{i=1}^{n} \operatorname{Div} \mathbf{T}_i - \sum_{i,j} \xi_{ji}(\vec{v}_i^* - \vec{v}_i) \,. \tag{10.72}$$

Substituting the previously calculated terms we can write

$$\varrho \frac{\mathrm{d}\vec{v}}{\mathrm{d}t} = \varrho \vec{g} + \operatorname{Div} \mathbf{T} - \sum_{i=1}^{n} \operatorname{Div} (\alpha_i \vec{v}_i^* \circ \vec{v}_i^*) + \sum_{i,j} \xi_{ji}(\vec{v}_i^* - \vec{v}_i) \,. \tag{10.73}$$

The last term must vanish, since

$$\sum_{i,j} \xi_{ji}(\vec{v}_i^* - \vec{v}_i) = -\vec{v} \sum_{i,j} \xi_{ji} = 0 . \tag{10.74}$$

Thus, we finally obtain the equation

$$\varrho \frac{\mathrm{d}\vec{v}}{\mathrm{d}t} = \varrho\vec{g} + \operatorname{Div} \mathbf{T} - \sum_{i=1}^{n} \operatorname{Div} (\alpha_i \vec{v}_i^* \circ \vec{v}_i^*) . \tag{10.75}$$

The analogy with Reynolds's equation is evident. The equation of motion written in terms of mass-averaged quantities shows, that the rate of change of momentum equals the sum of the resultant body forces, the surface forces and an additional force resulting from the mixing of the phases. This last force is expressed by the divergence of a symmetric second-order tensor. The dyadic product of the diffusion velocities is analogous to the dyadic product of the velocity fluctuations. Although the tensor is apparent, the force obtained by it is real, a force occurring in a volume is localized to the bounding surface of this volume. Since

$$-\sum_{i=1}^{n} \operatorname{Div} (\alpha_i \vec{v}_i^* \circ \vec{v}_i^*) = \operatorname{Div} \sum_{i=1}^{n} (-\alpha_i \vec{v}_i^* \circ \vec{v}_i^*) \tag{10.76}$$

an imaginary stress tensor may be defined by the equation

$$\mathbf{T}^* = \sum_{i=1}^{n} (-\alpha_i \vec{v}_i^* \circ \vec{v}_i^*) . \tag{10.77}$$

Thus the equation of motion is obtained in the elegant form

$$\varrho \frac{\mathrm{d}\vec{v}}{\mathrm{d}t} = \varrho\vec{g} + \operatorname{Div} (\mathbf{T} + \mathbf{T}^*) . \tag{10.78}$$

The stress tensor $\mathbf{T}$ can be broken down into three components as

$$\mathbf{T} = -p\mathbf{I} + \mathbf{V} + \mathbf{T}' .$$

Substituting this into Eq. (10.78) we obtain

$$\varrho \frac{\mathrm{d}\vec{v}}{\mathrm{d}t} = \varrho\vec{g} - \operatorname{grad} p + \operatorname{Div} (\mathbf{V} + \mathbf{T}' + \mathbf{T}^*) . \tag{10.79}$$

For an arbitrary volume V bounded by the closed surface (A) the integral form of the momentum equation can be written:

$$\begin{aligned} \int_V \frac{\partial(\varrho\vec{v})}{\partial t} + \int_{(A)} \varrho\vec{v}(\vec{v}\,\mathrm{d}\vec{A}) = \int_V \varrho\vec{g}\,\mathrm{d}V - \int_{(A)} p\,\mathrm{d}\vec{A} + \\ + \int_{(A)} \mathbf{V}\,\mathrm{d}\vec{\mathrm{A}} + \int_{(A)} (\mathbf{T}' + \mathbf{T}^*)\,\mathrm{d}\vec{A} . \end{aligned} \tag{10.80}$$

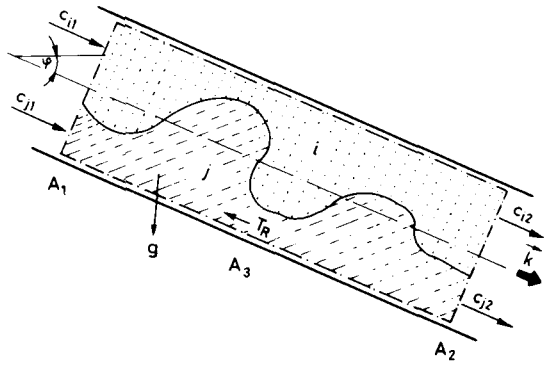

Fig. 10.4. Cylindrical control volume for momentum equation

At a solid boundary surface both $\mathbf{T}'$ and $\mathbf{T}^*$ are zero because of the no-slip boundary condition, therefore $\vec{v}=0$ at the solid boundary. The one-dimensional form of the momentum equation for a two-phase pipe flow can be expressed in terms of the cross-sectional average values of the flow variables. Consider a straight circular pipe with an arbitrary orientation. *Figure 10.4* shows the cylindrical control volume V, bounded by the inlet and outlet cross sections A_1 and A_2, as well as the pipe wall A_3. Let i and j refer respectively to the less and the more dense phase of the mixture, $\vec{k}$ is the unit vector in the flow direction, which is parallel to the pipe axis. The momentum of the flowing mixture within V is

$$\vec{I}=\int_V (\alpha_i\vec{v}_i+\alpha_j\vec{v}_j)\,\mathrm{d}V\,. \tag{10.81}$$

Its axial component is

$$I=\vec{k}\int_V (\alpha_i\vec{v}_i+\alpha_j\vec{v}_j)\,\mathrm{d}V=\int_V (\alpha_i v_i+\alpha_j v_j)\,\mathrm{d}V\,. \tag{10.82}$$

The convective fluxes of momentum can be readily expressed in terms of cross-sectional average values

$$\int_{A_1}\alpha_i\vec{v}_i\,(\vec{v}_i\,\mathrm{d}\vec{A})=-\dot{m}_{i1}\vec{c}_{i1}=-\dot{m}_{i1}c_{i1}\vec{k}\,, \tag{10.83}$$

$$\int_{A_1}\alpha_j\vec{v}_j\,(\vec{v}_j\,\mathrm{d}\vec{A})=-\dot{m}_{j1}\vec{c}_{j1}=-\dot{m}_{j1}c_{j1}\vec{k}\,, \tag{10.84}$$

$$\int_{A_2}\alpha_i\vec{v}_i\,(\vec{v}_i\,\mathrm{d}\vec{A})=-\dot{m}_{i2}\vec{c}_{i2}=\dot{m}_{i2}c_{i2}\vec{k}\,, \tag{10.85}$$

$$\int_{A_2} \alpha_j \vec{v}_j (\vec{v}_j \, \mathrm{d}\vec{A}) = \dot{m}_{j2} \vec{c}_{j2} = \dot{m}_{j2} c_{j2} \vec{k} , \tag{10.86}$$

and finally

$$\int_{A_3} \alpha_i \vec{v}_i (\vec{v}_i \, \mathrm{d}\vec{A}) = 0 , \quad \int_{A_3} \alpha_j \vec{v}_j (\vec{v}_j \, \mathrm{d}\vec{A}) = 0 . \tag{10.87}$$

For the body force term

$$\int_V (\alpha_i \vec{g}_i + \alpha_j \vec{g}_j) \, \mathrm{d}V = \int_V (\alpha_i + \alpha_j) \, \vec{g} \, \mathrm{d}V . \tag{10.88}$$

Let φ be the angle of inclination of the pipe axis, thus in the axial direction

$$\vec{k} \int_V (\alpha_i + \alpha_j) \, \vec{g} \, \mathrm{d}V = Mg \sin \varphi , \tag{10.89}$$

where M is the mass of the mixture in the volume V. It is assumed, that the pressure is constant over a cross section. Thus the integral of the pressure over the closed surface can be calculated:

$$- \int_{(A)} p \, \mathrm{d}\vec{A} = A_1 p_1 \vec{k} - A_2 p_2 \vec{k} = A (p_1 - p_2) \vec{k} . \tag{10.90}$$

The integral of the pressure over A_3 must vanish because of the rotational symmetry.

As is well known, at the pipe wall a laminar sublayer develops, in which the wall shear stress is uniform along the perimeter. The shear stresses at the inlet and outlet are not the same, but their contribution in the momentum equation may be neglected relative to that of the pressure. Thus we obtain

$$\int_{(A)} \mathbf{V} \, \mathrm{d}\vec{A} = - \int_{A_3} \tau_R \, \mathrm{d}A \, \vec{k} . \tag{10.91}$$

The contribution of the turbulent and phase-mixing stresses over the inlet and outlet cross sections is relatively small compared to the pressure, and may also be neglected. At the same time at the pipe wall both $\mathbf{T}'$ and $\mathbf{T}^*$ are zero. Thus the last integral of the momentum equation will vanish i. e.

$$\int_{(A)} (\mathbf{T}' + \mathbf{T}^*) \, \mathrm{d}\vec{A} = 0 . \tag{10.92}$$

Substituting all these individual results into the momentum equation, we obtain

the following expression:

$$\frac{\partial I}{\partial t} = \dot{m}_{i1} c_{i1} + \dot{m}_{j1} c_{j1} - \dot{m}_{i2} c_{i2} - \dot{m}_{j2} c_{j2} + A (p_1 - p_2) + Mg \sin \varphi - \tau_R A_3 . \tag{10.93}$$

The wall-shear stress τ_R cannot be evaluated in the general case, since the hydraulic gradient J may be a very complex function of the developed flow pattern. We will deal with this subject later.

10.4 The mechanical energy equation for multiphase flow

The balance of kinetic energy may be extended to flows of multiphase mixtures in the same way as the momentum equation was extended. For a homogeneous fluid we had

$$\varrho \frac{\mathrm{d}}{\mathrm{d}t}\left(\frac{v^2}{2}\right) = \varrho \vec{g} \vec{v} - \operatorname{div}(p\vec{v}) + \operatorname{div}(\mathbf{V}\vec{v}) + p \operatorname{div} \vec{v} - \mathbf{V} : \vec{v} \circ \nabla . \tag{10.94}$$

For the ith phase within a unit volume of a flowing mixture this can be written as

$$\alpha_i \frac{\mathrm{d}}{\mathrm{d}t_i}\left(\frac{v_i^2}{2}\right) = \alpha_i \vec{g}_i \vec{v}_i - \operatorname{div}(p_i \vec{v}_i) + \operatorname{div}(\mathbf{V}_i \vec{v}_i) + p_i \operatorname{div} \vec{v}_i - \mathbf{V}_i : \vec{v}_i \circ \nabla . \tag{10.95}$$

The summation over all n component is easily done, using the equality

$$\vec{v}_i = \vec{v} + \vec{v}^* .$$

Thus the sums of the individual terms of Eq. (10.95) are obtained as follows:

$$\sum_{i=1}^{n} \alpha_i \vec{g}_i \vec{v}_i = \varrho \vec{g} \vec{v} + \sum_{i=1}^{n} \alpha_i \vec{g}_i \vec{v}_i^* , \tag{10.96}$$

$$\sum_{i=1}^{n} \operatorname{div}(p_i \vec{v}_i) = \operatorname{div}(p\vec{v}) + \operatorname{div} \sum_{i=1}^{n} p_i \vec{v}_i^* , \tag{10.97}$$

$$\sum_{i=1}^{n} \operatorname{div}(\mathbf{V}_i \vec{v}_i) = \operatorname{div}(\mathbf{V}\vec{v}) + \operatorname{div} \sum_{i=1}^{n} \mathbf{V}_i \vec{v}_i^* , \tag{10.98}$$

$$\sum_{i=1}^{n} p_i \operatorname{div} \vec{v}_i = p \operatorname{div} \vec{v} + \sum_{i=1}^{n} p_i \operatorname{div} \vec{v}_i^* , \tag{10.99}$$

$$\sum_{i=1}^{n} \mathbf{V}_i : \vec{v}_i \circ \nabla = \mathbf{V} : \vec{v}_i \circ \nabla + \sum_{i=1}^{n} \mathbf{V}_i : \vec{v}_i^* \circ \nabla . \tag{10.100}$$

It should also be remembered that

$$\varrho \frac{\mathrm{d}}{\mathrm{d}t}\left(\frac{v^2}{2}\right) = \sum_{i=1}^{n} \left[\alpha_i \frac{\mathrm{d}}{\mathrm{d}t_i}\left(\frac{v_i^2}{2}\right) + \xi_i \frac{v_i^2}{2} - \operatorname{div}\left(\alpha_i \vec{v}_i^* \frac{v_i^2}{2}\right) \right]. \tag{10.101}$$

By summing expressions (10.96) to (10.101) the kinetic energy equation is obtained in terms of mass-averaged quantities and the diffusion velocities of each phase:

$$\varrho \frac{\mathrm{d}}{\mathrm{d}t}\left(\frac{v^2}{2}\right)=\varrho \vec{g}\vec{v}-\operatorname{div}(p\vec{v})+\operatorname{div}(\mathbf{V}\vec{v})+p\operatorname{div}\vec{v}-$$

$$-\mathbf{V}:\vec{v}\circ\nabla+\sum_{i=1}^{n}\alpha_i\vec{g}_i\vec{v}_i^{*}-\operatorname{div}\sum_{i=1}^{n}(p_i\vec{v}_i^{*})+\operatorname{div}\sum_{i=1}^{n}\mathbf{V}_i\vec{v}_i^{*}+ \tag{10.102}$$

$$+\sum_{i=1}^{n}p_i\operatorname{div}\vec{v}_i^{*}-\sum_{i=1}^{n}\mathbf{V}_i:\vec{v}_i^{*}\circ\nabla-\sum_{i=1}^{n}\operatorname{div}\left(\alpha_i\vec{v}_i^{*}\frac{v_i^2}{2}\right).$$

The comparison of Eq. (10.102) and the kinetic energy equation for a homogeneous fluid (10.94) shows the difference between them. The diffusion velocity $\vec{v}^{*}$ tends to be zero for finely dispersed mixtures. In this case all terms will vanish in which $\vec{v}^{*}$ is present. The above kinetic energy equation will then reduce to Eq. (10.94) and thus a finely dispersed system may be considered as being homogeneous. Such pseudo-homogeneous multiphase systems generally show non-Newtonian behavior, as is the case for drilling muds and cement pastes. For flows of coarsely dispersed mixtures $\vec{v}^{*}$ is obviously greater, and the behavior of the system is substantially different as is evident from a comparison of Eqs (10.94) and (10.102).

Using certain common assumptions the kinetic energy equation can be transformed into mechanical energy equation. Assuming that the body force field has a potential such that

$$\vec{g}=-\operatorname{grad}U,$$

and that the field is steady, i. e.

$$\frac{\partial U}{\partial t}=0,$$

we can write

$$\varrho\vec{g}\vec{v}=-\varrho\vec{v}\operatorname{grad}U=-\varrho\frac{\mathrm{d}U}{\mathrm{d}t}.$$

On the other hand

$$p\operatorname{div}\vec{v}-\operatorname{div}(p\vec{v})=-\vec{v}\operatorname{grad}p.$$

Assuming barotropic flow we obtain

$$\varrho\vec{v}\frac{1}{\varrho}\operatorname{grad}p=\varrho\vec{v}\operatorname{grad}\mathscr{P}=\varrho\left(\frac{\mathrm{d}\mathscr{P}}{\mathrm{d}t}-\frac{\partial\mathscr{P}}{\partial t}\right),$$

where $\mathscr{P}$ is the barometric potential given by

$$\mathscr{P} = \int_{p_0}^{p} \frac{\mathrm{d}p}{\varrho}.$$

After substitution we obtain the following equation for the mechanical energy balance:

$$\varrho \frac{\mathrm{d}}{\mathrm{d}t}\left(\frac{v^2}{2} + U + \mathscr{P}\right) = \varrho \frac{\partial \mathscr{P}}{\partial t} + \operatorname{div}(\mathbf{V}\vec{v}) - \mathbf{V} : \vec{v} \circ \nabla +$$

$$+ \sum_{i=1}^{n} \left[\alpha_i \vec{g}_i \vec{v}_i^* - \operatorname{div}(p_i \vec{v}_i^*) + \operatorname{div}(\mathbf{V}_i \vec{v}_i^*) + p_i \operatorname{div} \vec{v}_i^* - \right. \tag{10.103}$$

$$\left. - \mathbf{V}_i : \vec{v}_i^* \circ \nabla - \operatorname{div}\left(\alpha_i \vec{v}_i^* \frac{v^2}{2}\right)\right].$$

This can also be expressed in integral form:

$$\int_V \frac{\partial}{\partial t}\left(\frac{v^2}{2} + U + \mathscr{P}\right) \varrho \,\mathrm{d}V + \int_{(A)} \left(\frac{v^2}{2} + U + \mathscr{P}\right) \varrho \vec{v} \,\mathrm{d}\vec{A} = \int_V \varrho \frac{\partial \mathscr{P}}{\partial t} \mathrm{d}V +$$

$$+ \int_{(A)} \vec{v}(\mathbf{V}\,\mathrm{d}\vec{A}) - \int_V \mathbf{V} : \vec{v} \circ \nabla \mathrm{d}V + \sum_{i=1}^{n} \left\{ \int_V (\alpha_i \vec{g}_i \vec{v}_i^* + p_i \operatorname{div} \vec{v}_i^* - \mathbf{V}_i : \vec{v}_i^* \circ \nabla) \mathrm{d}V + \right.$$

$$\left. + \int_{(A)} \left(p_i \vec{v}_i^* + \mathbf{V}_i \vec{v}_i^* - \alpha_i \vec{v}_i^* \frac{v^2}{2}\right) \mathrm{d}\vec{A} \right\}. \tag{10.104}$$

For a two-phase flow in a pipe the one-dimensional form of this equation, expressed in terms of cross-sectional average quantities, is easily obtained. Consider a cylindrical control volume V bounded by the inlet and outlet cross sections A_1 and A_2 as well as the pipe wall A_3. Indices i and j refer respectively to the less and the more dense phase. All mass-averaged velocities are parallel to the pipe axis. Since the velocity is zero at the pipe wall, all surface integrals over this surface vanish.

The mechanical energy content of the mixture within the control volume V is

$$E = \int_V \left[\alpha_i \left(\frac{v_i^2}{2} + U_i + \mathscr{P}_i\right) + \alpha_j \left(\frac{v_j^2}{2} + U_j + \mathscr{P}_j\right)\right] \mathrm{d}V. \tag{10.105}$$

The convective fluxes of mechanical energy are obtained as

$$\int_{A_1} \alpha_i \left(\frac{v_i^2}{2} + U_i + \mathscr{P}_i\right) \vec{v}_i \,\mathrm{d}\vec{A} = -\dot{m}_{i1} \left(\beta_{i1} \frac{c_{i1}^2}{2} + U_{i1} + \mathscr{P}_{i1}\right), \tag{10.106}$$

$$\int_{A_1} \alpha_j \left(\frac{v_j^2}{2} + U_j + \mathscr{P}_j\right) \vec{v}_j \, \mathrm{d}\vec{A} = -\dot{m}_{j1} \left(\beta_{j1} \frac{c_{j1}^2}{2} + U_{j1} + \mathscr{P}_{j1}\right), \tag{10.107}$$

$$\int_{A_2} \alpha_i \left(\frac{v_i^2}{2} + U_i + \mathscr{P}_i\right) \vec{v}_i \, \mathrm{d}\vec{A} = \dot{m}_{i2} \left(\beta_{i2} \frac{c_{i2}^2}{2} + U_{i2} + \mathscr{P}_{i2}\right), \tag{10.108}$$

$$\int_{A_2} \alpha_j \left(\frac{v_j^2}{2} + U_j + \mathscr{P}_j\right) \vec{v}_j \, \mathrm{d}\vec{A} = \dot{m}_{j2} \left(\beta_{j2} \frac{c_{j2}^2}{2} + U_{j2} + \mathscr{P}_{j2}\right), \tag{10.109}$$

where

$$\beta = \frac{\int_A \frac{v^2}{2} \vec{v} \, \mathrm{d}\vec{A}}{\frac{A c^3}{2}}.$$

The contribution of the shear stresses over the inlet and outlet cross sections may be neglected. The diffusion velocity $\vec{v}^*$ vanishes at the pipe wall, thus the last surface integral of Eq. (10.104) becomes zero. Finally the mechanical energy balance may be written as

$$\frac{\partial E}{\partial t} + \dot{m}_{i2} \left(\beta_{i2} \frac{c_{i2}^2}{2} + U_{i2} + \mathscr{P}_{i2}\right) + \dot{m}_{j2} \left(\beta_{j2} \frac{c_{j2}^2}{2} + U_{j2} + \mathscr{P}_{j2}\right) - \dot{m}_{i1} \left(\beta_{i1} \frac{c_{i1}^2}{2} + U_{i1} + \mathscr{P}_{i1}\right) -$$

$$- \dot{m}_{j1} \left(\beta_{j1} \frac{c_{j1}^2}{2} + U_{j1} + \mathscr{P}_{j1}\right) + P_{\Phi i} + P_{\Phi j} = \int_V \left(\frac{\partial \mathscr{P}_i}{\partial t} + \frac{\partial \mathscr{P}_j}{\partial t}\right) \mathrm{d}V, \tag{10.110}$$

where $P_{\Phi i}$ and $P_{\Phi j}$ are terms representing all power dissipated by each of the phases. For a steady flow this equation can be substantially simplified

$$\dot{m}_{i2} \left(\beta_{i2} \frac{c_{i2}^2}{2} + U_{i2} + \mathscr{P}_{i2}\right) + \dot{m}_{j2} \left(\beta_{j2} \frac{c_{j2}^2}{2} + U_{j2} + \mathscr{P}_{j2}\right) + P_{\Phi i} + P_{\Phi j} =$$

$$= \dot{m}_{i1} \left(\beta_{i1} \frac{c_{i1}^2}{2} + U_{i1} + \mathscr{P}_{i1}\right) + \dot{m}_{j1} \left(\beta_{j1} \frac{c_{j1}^2}{2} + U_{j1} + \mathscr{P}_{j1}\right). \tag{10.111}$$

The physical meaning of this equation is clear. Since mechanical energy addition is possible, only in an unsteady flow, the energy level of the steady flow continuously decreases due to dissipative processes. The total energy loss is equal to the sum of the losses of each of the two phases. Relating this equation to a unit fluid mass a Bernoulli-like equation would be expected. Because of the holdup-phenomenon the rate of mass flow is not always constant in two-phase flow. Thus the steady-flow one-dimensional mechanical energy equation may be related to the inlet mass flow rate. A simplifying assumption is that the potential energy at a given

cross-section is the same for both phases, i.e.

$$U_{i1} = U_{j1}; \qquad U_{i2} = U_{j2}.$$

Using these assumptions we can write

$$\frac{\varrho_{i2} c_{i2}}{\varrho_1 c_1} E_{i2} \beta_{i2} \frac{c_{i2}^2}{2} + \frac{\varrho_{j2} c_{j2}}{\varrho_1 c_1} E_{j2} \beta_{j2} \frac{c_{j2}^2}{2} - \frac{\varrho_{i1} c_{i1}}{\varrho_1 c_1} E_{i1} \beta_{i1} \frac{c_{i1}^2}{2} -$$
$$- \frac{\varrho_{j1} c_{j1}}{\varrho_1 c_1} E_{j1} \beta_{j1} \frac{c_{j1}^2}{2} + \frac{\varrho_{i2} c_{i2}}{\varrho_1 c_1} E_{i2} \mathscr{P}_{i2} + \frac{\varrho_{j2} c_{j2}}{\varrho_1 c_1} E_{j2} \mathscr{P}_{j2} - \tag{10.112}$$
$$- \frac{\varrho_{i1} c_{i1}}{\varrho_1 c_1} E_{i1} \mathscr{P}_{i1} - \frac{\varrho_{j1} c_{j1}}{\varrho_1 c_1} E_{j1} \mathscr{P}_{j1} + \frac{\varrho_2 c_2}{\varrho_1 c_1} U_2 - U_1 + \frac{P_{\Phi i}}{A \varrho_1 c_1} + \frac{P_{\Phi j}}{A \varrho_1 c_1} = 0.$$

For most pipelines encountered in petroleum engineering practice the change in potential and pressure energy as well as the energy losses are greater by an order of magnitude than the kinetic energy change. Thus another simplification is permitted, resulting in the equation

$$\frac{\varrho_{i2} c_{i2}}{\varrho_1 c_1} E_{i2} \mathscr{P}_{i2} + \frac{\varrho_{j2} c_{j2}}{\varrho_1 c_1} E_{j1} \mathscr{P}_{j2} - \frac{\varrho_{i1} c_{i1}}{\varrho_1 c_1} E_{i1} \mathscr{P}_{i1} -$$
$$- \frac{\varrho_{j1} c_{j1}}{\varrho_1 c_1} E_{j1} \mathscr{P}_{j1} + \frac{\varrho_2 c_2}{\varrho_1 c_1} U_2 - U_1 + \frac{P_{\Phi i}}{A \varrho_1 c_1} + \frac{P_{\Phi j}}{A \varrho_1 c_1} = 0. \tag{10.113}$$

If this equation is multiplied by ϱ_1 all terms will have the dimensions of pressure. Thus the last two terms represent pressure losses, which may be denoted Δ'_{pi} and Δ'_{pj}.

$$\Delta p'_i = \frac{P_{\Phi i}}{c_1 A_1}; \qquad \Delta p'_j = \frac{P_{\Phi j}}{c_1 A_1}. \tag{10.114}$$

For incompressible fluids

$$\varrho_{i1} = \varrho_{i2}; \qquad \varrho_{j1} = \varrho_{j2},$$

while the barotropic potential is

$$\mathscr{P} = \frac{p}{\varrho}.$$

It is an acceptable assumption to consider the pressure to be constant at a given cross-section, i.e.

$$p_i = p_j.$$

Thus the balance of mechanical energy equation can be written in the form

$$p_2 \left(\frac{c_{i2}}{c_1} E_{i2} + \frac{c_{j2}}{c_1} E_{j2} \right) - p_1 \left(\frac{c_{i1}}{c_1} E_{i1} + \frac{c_{j1}}{c_1} E_{j1} \right) + \frac{\varrho_2 c_2}{c_1} U_2 - \varrho_1 U_1 + \Delta p'_i + \Delta p'_j = 0. \tag{10.115}$$

The flow rates of the phases i and j are

$$Q_i = A E_i c_i; \qquad Q_j = A E_j c_j,$$

while their sum is the flow rate of the mixture

$$Q = Q_i + Q_j.$$

The pressure loss of the mixture is obtained as

$$\Delta p' = \Delta p'_i + \Delta p'_j = p_1 - \frac{c_2}{c_1} p_2 + \varrho_1 U_1 - \frac{\varrho_2 c_2}{c_1} U_2. \tag{10.116}$$

In a flow of a finely suspended mixture holdup cannot occur, i.e. $c_1 = c_2$ therefore,

$$\Delta p' = p_1 - p_2 + \varrho(U_1 - U_2). \tag{10.117}$$

Therefore, the pressure loss can be measured in the familiar way, though this is possible in this particular case only. Generally Eq. (10.116) is recommended because of changes in mixture velocity and density in the flow direction.

10.5 The total energy equation for multiphase flow

The law of conservation of energy can be easily generalized to apply to multicomponent mixtures. For a homogeneous fluid we had obtained (Eq. 3.73)

$$\varrho \frac{\mathrm{d}}{\mathrm{d}t}\left(\frac{v^2}{2} + \varepsilon\right) = \varrho \vec{g}\vec{v} + \operatorname{div}(\mathbf{T}\vec{v}) - \operatorname{div}\vec{q}, \tag{10.118}$$

i.e. the rate of change of the kinetic and internal energy ε of a unit fluid volume equals the rate at which work is done by body forces and surface forces and the rate at which heat is transferred to the body. For the ith phase of an n-phase system this can be written in the form

$$\alpha_i \frac{\mathrm{d}}{\mathrm{d}t}\left(\frac{v_i^2}{2} + \varepsilon_i\right) = \varrho_i \vec{g}_i \vec{v}_i + \operatorname{div}(\mathbf{T}_i \vec{v}_i) - \operatorname{div}\vec{q}_i. \tag{10.119}$$

Summing over all n phases leads to the following equation

$$\frac{\mathrm{d}}{\mathrm{d}t}\left(\frac{v^2}{2} + \varepsilon\right) = \varrho \vec{g}\vec{v} + \operatorname{div}(\mathbf{T}\vec{v}) - \operatorname{div}\vec{q} + \sum_{i=1}^{n}\left\{\alpha_i \vec{g}_i \vec{v}_i^* + \right.$$

$$\left. + \operatorname{div}(\mathbf{T}_i \vec{v}_i^*) - \operatorname{div}\left[\alpha_i \vec{v}_i^*\left(\frac{v^2}{2} + \varepsilon\right)\right]\right\} \tag{10.120}$$

where ϱ, $\vec{v}$, $\vec{g}$, ε, $\mathbf{T}$, $\vec{q}$ are mass-averaged values; the others depend on the diffusion

velocity. This can be expressed in integral form as

$$\int_V \frac{\partial}{\partial t}\left(\frac{v^2}{2}+\varepsilon\right)\varrho\,\mathrm{d}V+\int_{(A)}\left(\frac{v^2}{2}+\varepsilon\right)\varrho\,\vec{v}\,\mathrm{d}\vec{A}=\int_V \varrho\,\vec{g}\vec{v}\,\mathrm{d}V+$$

$$+\int_{(A)}\vec{v}\mathbf{T}\,\mathrm{d}\vec{A}-\int_{(A)}\vec{q}\,\mathrm{d}\vec{A}+\sum_{i=1}^{n}\left\{\int_V \alpha_i\vec{g}_i\vec{v}_i^{\bullet}\,\mathrm{d}V+\int_{(A)}\left[\mathbf{T}_i\vec{v}_i^{\bullet}-\right.\right. \tag{10.121}$$

$$\left.\left.-\alpha_i\vec{v}_i^{\bullet}\left(\frac{v^2}{2}+\varepsilon\right)\right]\mathrm{d}\vec{A}\right\}.$$

It is also possible to write a one-dimensional form of this equation for a two-phase flow in a circular pipe expressed in terms of cross-sectional average quantities.

The total energy content of the mixture within V can be expressed as

$$E=\int_V\left[\alpha_i\left(\frac{v_i^2}{2}+\varepsilon_i\right)+\alpha_j\left(\frac{v_j^2}{2}+\varepsilon_j\right)\right]\mathrm{d}V. \tag{10.122}$$

The convective fluxes are obtained as:

$$\int_{A_1}\alpha_i\left(\frac{v_i^2}{2}+\varepsilon_i\right)\vec{v}_i\,\mathrm{d}\vec{A}=-\dot{m}_{i1}\left(\beta_{i1}\frac{c_{i1}^2}{2}+\varepsilon_{i1}\right), \tag{10.123}$$

$$\int_{A_1}\alpha_j\left(\frac{v_j^2}{2}+\varepsilon_j\right)\vec{v}_j\,\mathrm{d}\vec{A}=-\dot{m}_{j1}\left(\beta_{j1}\frac{c_{j1}^2}{2}+\varepsilon_{j1}\right), \tag{10.124}$$

$$\int_{A_2}\alpha_i\left(\frac{v_i^2}{2}+\varepsilon_i\right)\vec{v}_i\,\mathrm{d}\vec{A}=\dot{m}_{i2}\left(\beta_{i2}\frac{c_{i2}^2}{2}+\varepsilon_{i2}\right), \tag{10.125}$$

$$\int_{A_2}\alpha_j\left(\frac{v_j^2}{2}+\varepsilon_j\right)\vec{v}_j\,\mathrm{d}\vec{A}=\dot{m}_{j2}\left(\beta_{j2}\frac{c_{j2}^2}{2}+\varepsilon_{j2}\right). \tag{10.126}$$

As in the case of the mechanical energy equation, the shear stresses, heat fluxes and diffusion at the inlet and outlet cross-sections are neglected.

If the body forces are conservative and the flow is barotropic, we can write

$$\frac{\partial E}{\partial t}=\dot{m}_{i1}\left(\beta_{i1}\frac{c_{i1}^2}{2}+U_{i1}+\mathscr{P}_{i1}+\varepsilon_{i1}\right)+\dot{m}_{j1}\left(\beta_{j1}\frac{c_{j1}^2}{2}+U_{j1}+\mathscr{P}_{j1}+\varepsilon_{j1}\right)-$$

$$-\dot{m}_{i2}\left(\beta_{i2}\frac{c_{i2}^2}{2}+U_{i2}+\mathscr{P}_{i2}+\varepsilon_{i2}\right)-\dot{m}_{j2}\left(\beta_{j2}\frac{c_{j2}^2}{2}+\right. \tag{10.127}$$

$$\left.+U_{j2}+\mathscr{P}_{j2}+\varepsilon_{j2}\right)-\int_{A_3}\vec{q}_i\,\mathrm{d}\vec{A}-\int_{A_3}\vec{q}_j\,\mathrm{d}\vec{A}+W_{ij},$$

where W_{ij} is the work done by the system on the phase boundary surfaces. The internal energy ε and the barotropic potential $\mathscr{P}$ can be replaced by the enthalpy

$$i=\varepsilon+\frac{p}{\varrho}=\varepsilon+\mathscr{P}.$$

Thus we have

$$\frac{\partial E}{\partial t}=\dot{m}_{i1}\left(\beta_{i1}\frac{c_{i1}^2}{2}+U_{i1}+i_{i1}\right)+\dot{m}_{j1}\left(\beta_{j1}\frac{c_{j1}^2}{2}+U_{j1}+i_{j1}\right)-$$
$$-\dot{m}_{i2}\left(\beta_{i2}\frac{c_{i2}^2}{2}+U_{i2}+i_{i2}\right)-\dot{m}_{j2}\left(\beta_{j2}\frac{c_{j2}^2}{2}+U_{j2}+i_{j2}\right)-\dot{Q}+W_{ij}. \tag{10.128}$$

In order to apply this equation, the enthalpy of the phases must be evaluated at the inlet and outlet conditions. The kinetic energy terms are mostly negligible relative to the enthalpies and the heat flux across the pipe wall.

Fortunately, with the exception the case of horizontally stratified flow, the pipe wall is generally wetted by one of the phases. Thus, the determination of the proportions of the wall area wetted by the phases i and j is not necessary. Therefore the same film thermal conductivity coefficient can be applied as for homogeneous fluid flow. The work done by the system may be also neglected. Finally we get the equation

$$\frac{\partial E}{\partial t}=\dot{m}_{i1}i_{i1}+\dot{m}_{j1}i_{j1}-\dot{m}_{i2}i_{i2}-\dot{m}_{j2}i_{j2}+ \tag{10.129}$$
$$\varrho_1 c_1 A U_1-\varrho_2 c_2 A U_2+\dot{Q}.$$

(A = cross-sectional area of the uniform pipe.)

If the flow variables are already known, this equation relates the absorbed heat to changes in enthalpy and, consequently to changes in temperature. It is particularly applicable to two-phase flows in oil- or geothermal wells.

The basic equations for multiphase flows presented in this Chapter are valid for any particular form of flow system. Further details of the flow e. g. the pressure loss or the holdup relations may be determined with specific validity for certain characteristic flow patterns.

10.6 Characteristic flow patterns

A salient feature of two-phase flow is the occurrence of certain characteristic flow patterns which show how the two phases are distributed in the pipe. A homogeneous fluid flow can be characterized merely as laminar or turbulant flow. The two-phase pipe flow can be characterized approximately by certain relative quantities and the distribution of the phases. In petroleum engineering practice four types of two-phase flow are of particular importance: liquid-gas, liquid-liquid,

liquid-solid, and gas-solid flows. Because of the differences in phase densities, the flow pattern in horizontal or inclined pipes is not symmetrical w. r. t. the pipe axis. Gas-liquid flows are generally the most complex since the deformable phase boundaries and the compressibility of the gas lead to a great variety of possible flow patterns.

The determination of flow patterns is mostly carried out by direct visual observation, occasionally complemented with high-speed photography. These methods are rather subjective; nevertheless sufficiently consistent flow pattern ordination becomes possible. The most common interpretation of flow patterns is a diagram plotted in terms of the superficial velocities of each phase, i. e. the flow rate of that phase divided by the total cross section of the pipe. The thus obtained diagram is called a *flow pattern map*, in which certain regions correspond to characteristic flow patterns. A great number of flow pattern data are known from the literature, but unfortunately most relate to water-air flows, which is the most suitable fluid-pair for visual observation. The flow of a dark opaque crude oil-natural gas mixture cannot be investigated by visual methods. In this case measurements of pressure fluctuations, or *X*-radiography may be used. The transition between two flow patterns is not as sharp as the laminar-turbulent transition of homogeneous fluid flow. A wide variety of flow patterns can be observed and defined.

In the following, various types of two-phase flow will be considered and the flow patterns which occur in them discussed. Consider first a liquid-gas mixture flowing upward in a vertical transparent section of pipe. When a homogeneous liquid flows by itself, direct visual observation cannot provide any information about the flow.

Introducing gas into the liquid at progressively increasing flow rates, a series of consecutive, changing flow patterns can be distinguished. At the lowest gas flow rates the liquid phase is continuous and small, spherical gas bubbles move upward near the pipe axis, faster than the liquid. A short time exposure photograph generally shows a *bubble flow pattern*, as depicted in *Fig. 10.5 a*. As the gas flow rate is increased the number of bubbles increases, and owing to coalescence, the average bubble size increases. These larger, lens-shaped bubbles are pushed along in the liquid, with their largest cross section normal to the flow, in periodically occurring groups. This is the *bubble group flow pattern* (see *Fig. 10.5 b*). A further increase in the gas flow rate causes an increase in the volume fraction of the bubbles, up to 30 percent, while bubble coalescence leads to the occurrence of large, mushroom-shaped bubbles which nearly span the entire cross-section of the pipe (see *Fig. 10.5 c*). These large mushroom-shaped bubbles are followed by regions containing dispersions of smaller bubbles, and periodical bubble-free liquid plugs. This marks the beginning of the *slug flow pattern*. With a further increase in the gas flow rate, the large bubbles become longer having a bullet shape. These bullet-shaped bubbles are called Taylor bubbles. The slug flow pattern is characterized by periodically alternating Taylor bubbles and liquid regions containing a number of smaller spherical bubbles (see *Fig. 10.5 d*). The liquid phase flows *down* the outside of the Taylor bubbles as a falling film although the resultant flow of both liquid and gas

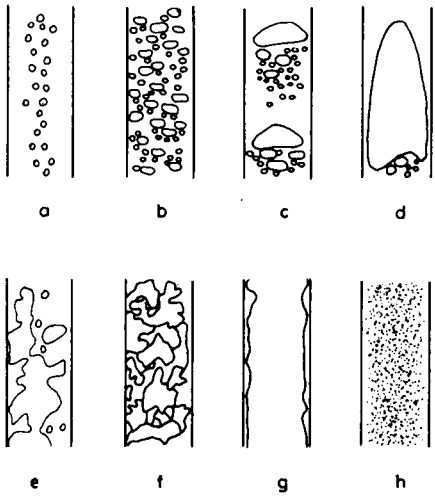

Fig. 10.5. Flow patterns of vertical fluid-gas mixture flow

is upward. In these flow patterns liquid phase is always continuous, the gas phase is dispersed.

The slug flow pattern with long Taylor bubbles corresponds to an increase in the pressure loss. The increasing pressure gradient now tends to collapse the Taylor bubbles. Surface tension acts against this tendency, but large gas bubbles become unstable and finally collapse. At this point the interfaces between the phases become highly distorted, both phases become dispersed, and the *froth flow pattern* develops (see *Fig. 10.5 e*). Froth flow is highly unstable; an oscillatory upward-downward motion occurs in the liquid phase, particularly in pipes of large diameter. This is known by the name *churn flow* (see *Fig. 10.5 f*). In small-diameter pipes the breakdown of the Taylor bubbles is not so abrupt, the transition is more gradual without the occurrence of churn.

As the gas flow rate is increased still further an upward moving wavy annular liquid layer develops at the pipe wall, and the gas flows with a substantially greater velocity in the center of the pipe. This is known as annular flow. The gas core flow may carry small fluid droplets ripped from the annular liquid layer, as is shown in *Fig. 10.5 g*. With a further increase of the gas flow rate the liquid film becomes progressively thinner while the number of the droplets in the core flow increases. Finally, the film will be removed from the wall and a pure *mist flow* occurs (see *Fig. 10.5 h*). The observed flow patterns are interpreted in *Fig. 10.6*. Repeating the previous experiment at a higher flow rate of the liquid, the number of flow patterns developed decreases. First the froth flow is omitted, later with further increasing liquid flow rates, bubble flow changes directly into annular or mist flow, without the intermediate stage of slug flow. All this is evident from *Fig. 10.6*.

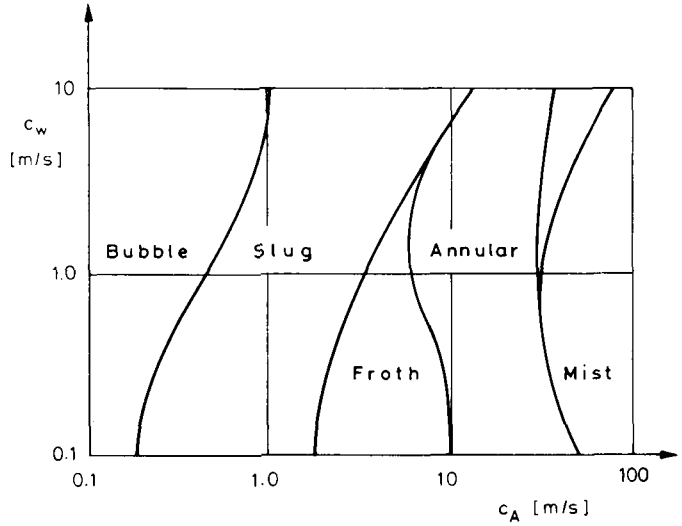

Fig. 10.6. Flow pattern map for vertical fluid-gas mixture flow

Note, that such a flow-pattern map is valid only for a given fluid pair, pipe diameter, pressure level and temperature. In spite of continuing efforts, generalized flow-pattern maps are not available. Although particular flow-pattern maps show the same sequences of flow regimes, there are no such flow variables by which congruent flow-pattern maps would be obtained.

A remarkable diagram is obtained by plotting the pressure-loss gradient against the gas flow rate, while liquid flow rate is taken as a parameter. This is shown in *Fig. 10.7.* It is seen that the pressure-loss-gradient curve goes through a local minimum, a maximum and a second minimum as the gas flow rate increases. The occurrence of these minimums and maximums corresponds to flow pattern transitions. As the liquid flow rate increases these minimums and maximums become less distinct, though the slope of the curve still shows changes. The first minimum corresponds to the transition between the bubble-group- and slug-flow patterns. The maximum marks the collapse of the Taylor bubbles and the development of froth flow. The second minimum corresponds to the transition between the froth- and annular flow patterns. This phenomenon may be used to indicate changes in the flow pattern where other experimental facilities are not available. Flow-pattern observations similar to those described above, were also found for liquid-liquid systems. Since the density differences here are considerably smaller and the viscosity differences are substantially greater, certain differences do occur in the flow pattern sequences. The most characteristic difference is the absence of the annular flow pattern. An oil-water flow-pattern map is shown in *Fig. 10.8,* where froth flow converts directly into misty flow and in which the water droplets are fewer and larger than in a liquid-gas mixture mist flow.

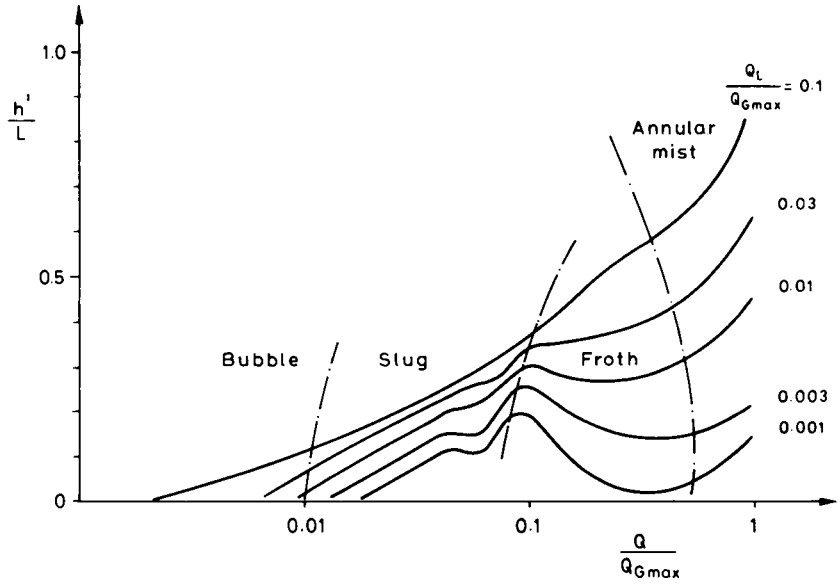

Fig. 10.7. Pressure-loss gradient depending on gas flow rate

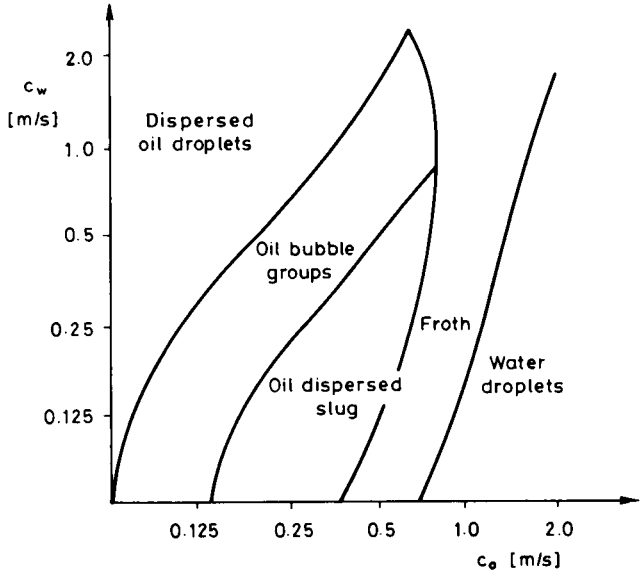

Fig. 10.8. Flow-pattern map for vertical oil-water mixture flow

Liquid-liquid and gas-liquid mixtures flowing in horizontal pipes tend to be somewhat more complex than vertical flows. If the density difference between the phases is pronounced, the flow is asymmetric: the more dense phase tends to accumulate at the bottom of the pipe.

Consider a horizontal transparent pipe with a constant liquid flow rate, into which gas is introduced. If the superficial liquid velocity is sufficiently high, say 2–3 m/s, the introduced gas is present as small spherical bubbles, as shown in *Fig. 10.9 a*. The finely dispersed bubbles have no symmetrical concentration profile; the maximum concentration occurs in the upper part of the pipe cross section. Increasing the gas flow rate leads to the formation of larger bubbles, and the occurrence of bubble groups. The larger bubbles occupy the uppermost part of the pipe, while the smaller bubbles are dispersed asymmetrically, as shown in *Fig. 10.9 b*. As the gas flow rate is increased further, still larger bubbles occur at the upper pipe wall. Here elongated bubbles are followed by smaller spherical bubbles, and they frequently coalesce (see *Fig. 10.9 c*). With the further increase in the gas flow rate, very large elongated bubbles slide along the upper pipe wall and suffer distortion resulting in unstable shapes (see *Fig. 10.9 d*). Each deformed elongated bubble is followed by a liquid plug which may contain trains of gas bubbles. A further increase in the gas flow rate leads to a separated stratified flow pattern. The horizontal phase interface may be smooth, wavy or become ripply as the gas flow rate increases (see *Fig. 10.9 e*). As the gas flow rate is increased further, the waves on this interface become so large that the thinned liquid layer can no longer

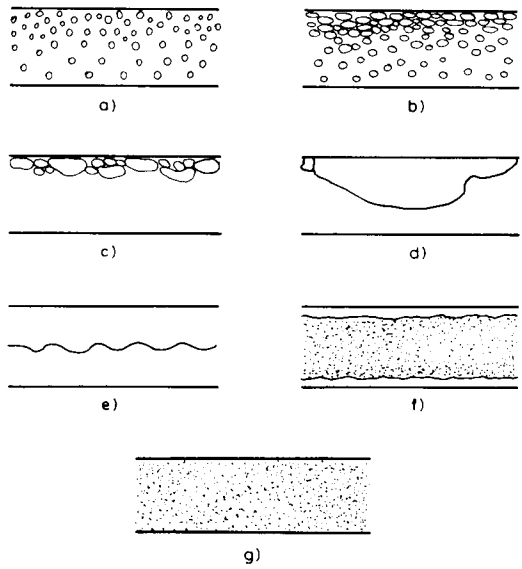

Fig. 10.9. Flow patterns of horizontal fluid-gas mixture flow

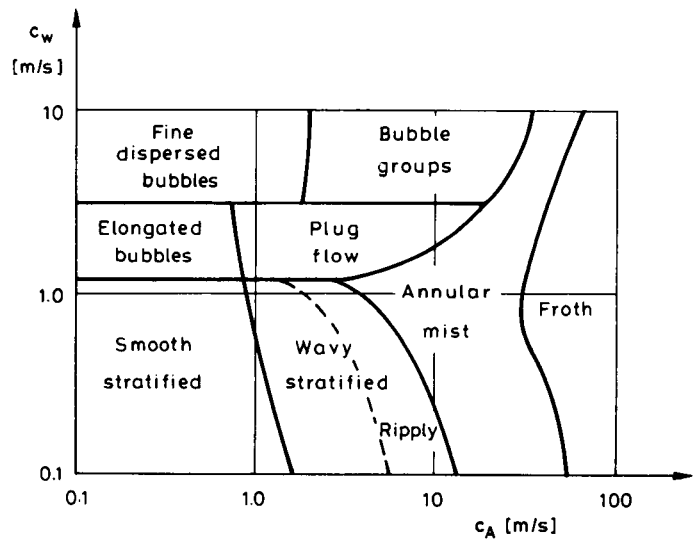

Fig. 10.10. Flow-pattern map of horizontal water-air mixture flow

support them, the liquid spreads along the walls of the pipe, forming an annular film, with some liquid droplets dispersed in the gas core flow (see *Fig. 10.9 f*). Finally, a mist flow pattern develops with the further increase in the gas flow rate, as shown in *Fig. 10.9 g*. A flow-pattern map for the flow of a water-air mixture is shown in *Fig. 10.10*.

Liquid-liquid systems show flow-pattern sequences rather similar to those described above. In water-oil mixtures the oil bubbles are greater than the gas bubbles at the same flow rate. With increasing oil flow rates, these bubbles can agglomerate, forming cylindrical elongated bubbles of a diameter nearly equal to that of the pipe. Finally a continuous core of oil moves inside a film of water. The pressure drop associated with this flow pattern is almost independent of the viscosity of the oil, it may be smaller than that of pure water. This phenomenon was observed in the Ásotthalom—Algyő pipeline, for a rather dense (970 kg/m^3) crude oil-water mixture flow. A flow-pattern map for oil-water mixtures is shown in *Fig. 10.11*.

In spite of their technical importance only a few flow-pattern maps are available for inclined pipes. *Figures 10.12 a* and *10.12 b* show the effect of a 10° downward and a 10° upward inclination on liquid-gas flow. The most significant feature of the flow-pattern maps for inclined pipes is the sensitivity of the locus of the stratified slug flow transition to the angle of inclination. In a downward inclined pipe a stratified flow pattern prevails, while in an upward inclined pipe the slug flow pattern is dominant.

Fluid-solid systems can be investigated in a similar way. In a vertical pipe without a sufficiently strong upward fluid flow the solid particles form a stationary

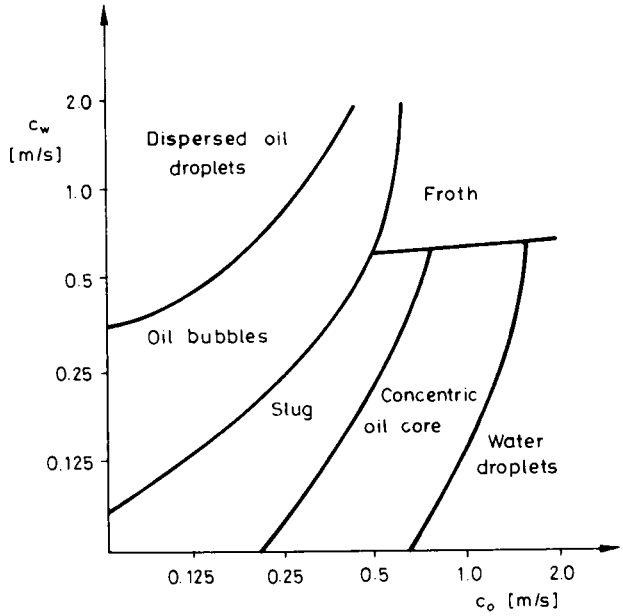

Fig. 10.11. Flow-pattern map of horizontal oil-water mixture flow

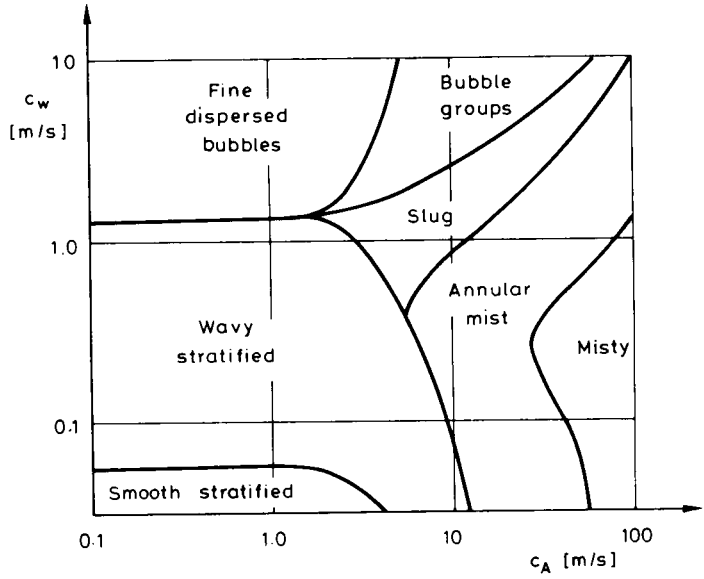

Fig. 10.12/a. Flow-pattern map for fluid-gas mixture in a 10° upward inclined pipe

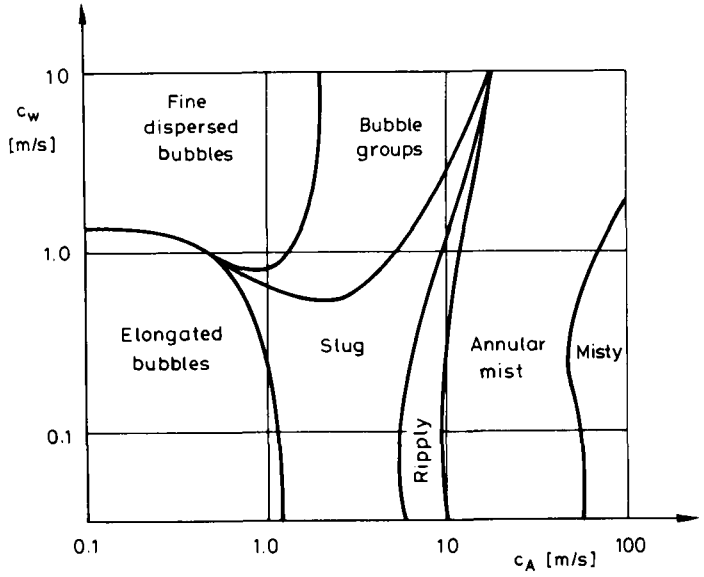

Fig. 10.12/b. Flow-pattern map for fluid-gas mixture flow in a 10° downward inclined pipe

bed. At the lowest flow rates the motion of the fluid is that of seepage flow through the pore system of the bed. As the flow rate increases, buoyancy and hydrodynamic lifting forces disrupt the stationary bed. The particles no longer form a solid bed but become suspended, though they do not as yet have an upward motion. This flow pattern is that of the so-called fluidized bed. As the flow rate is increased further, the suspended solid particles eventually begin to move upward with the flow. The solid components lay behind the fluid flow, and significant holdup phenomena develop.

When the fluid velocity is considerably greater than the terminal settling velocity of the particles the developed velocity and concentration profiles are axisymmetric, while the holdup is negligible. The behavior of the mixture tends to be pseudo-homogeneous.

Characteristic sequences of flow patterns can be observed in horizontal pipes in which fluid-solid mixtures flow. Consider a horizontal pipe section, in which a highly turbulent flow carries fine and medium-sized particles as a fully suspended mixture. If the settling velocity of the particles is sufficiently low, and the fluid velocity is at least 1–1.5 m/s a symmetric concentration profile develops. This *axisymmetric suspension* flow pattern ceases when buoyancy and turbulent lifting forces are smaller than the weight of particles. This happens below a certain transition velocity c_{H1}.

As the velocity of the mixture decreases below a transition value, the lifting forces weaken and the concentration profile suffers a distortion. A greater propor-

tion of the solids, and particularly the larger particles, move in the lower part of the pipe. This *asymmetric suspension* flow pattern ceases when the largest particles remain on the bottom of the pipe at a certain transition velocity c_{H2}.

As the velocity decreases further, the particles accumulate on the bottom of the pipe forming a continuous moving bed. The bed moves along the pipe with a velocity which is lower than that fluid until the velocity reaches a transition value c_{H3}.

As the velocity of the mixture is further reduced the lowermost particles of the bed become stationary, the thickness of the bed increases, and the cross-section of the flow is reduced. The smallest particles are suspended in the fluid above the bed. Finally, when the weakened flow ceases, the whole cross section of pipe will be blocked. Through the blocked pipe the fluid now flows with seepage motion.

In *Fig. 10.13* these flow patterns are plotted against the apparent velocity of the mixture and the average particle diameter.

The pressure-loss gradient plotted against the superficial mixture velocity, can be related to the visually observable flow patterns, as is clear from *Fig. 10.14*. The concentration is taken as a parameter. The symmetric suspension flow pattern can exist in the velocity range $c > c_{H1}$. As the concentration increases, the transition velocity c_{H1} becomes greater. The asymmetric suspension flow pattern occurs in

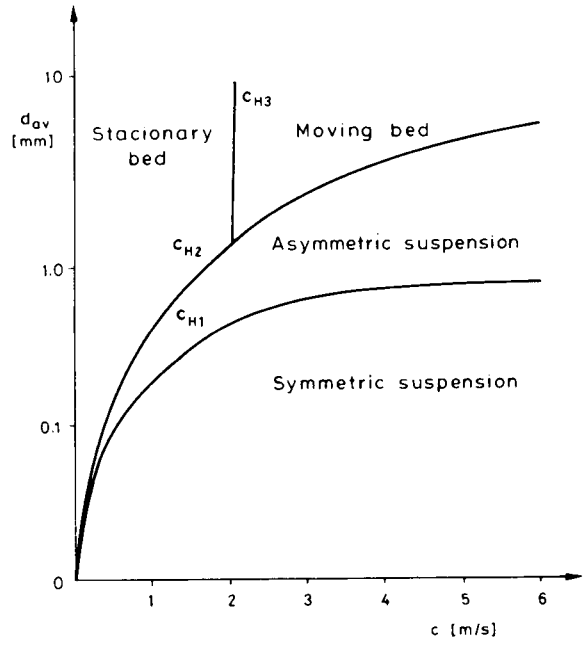

Fig. 10.13. Flow patterns depending on the superficial mixture velocity and the average particle diameter

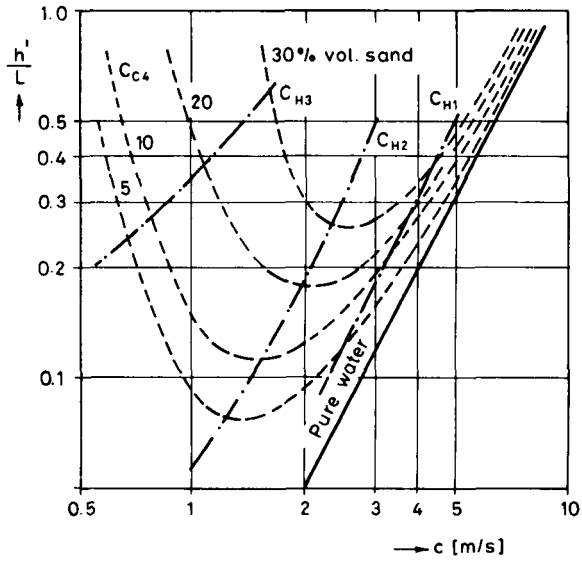

Fig. 10.14. Pressure-loss gradient and flow patterns for horizontal fluid-solid mixture flow

the interval $c_{H1} > c > c_{H2}$. The locus of the transition velocity c_{H2} coincides with that at which the minimum of the pressure loss gradient curve occurs. The interval $c_{H2} > c > c_{H3}$ is associated with the moving bed flow pattern. The stationary bed flow pattern exists when $c < c_{H4}$.

The transition velocity c_{H3} cannot be clearly recognized from the pressure-loss gradient curve, and c_{H4} is outside of the range of actual measurements.

The optimum velocity for transporting a fluid-solid mixture corresponding to the pressure loss minimum, is approximately equal to c_{H2}. On the other hand, at this velocity some of the particles strike the bottom of the pipe causing abrasion and decreasing the durability of the pipe. The recommended compromise is to choose a velocity above c_{H2}, at which the pressure loss is greater by 10 percent than the minimum value. The importance of knowing c_{H1} and c_{H2} is obvious. The best way is to determine c_{H1} and c_{H2} experimentally under the same conditions as those under which the hydraulic transport is designed to operate. As an approximate empirical guide the Tarján–Debreczeni equations can be used

$$c_{H1}^4 = \frac{140\,UD}{\sqrt{d}}, \tag{10.130}$$

$$c_{H2}^2 = gDf(E_s), \tag{10.131}$$

where U is the terminal settling velocity, D is the diameter of the pipe, d is the average particle diameter, $f(E_s)$ is some function of the volume fraction of solids.

10.7 Holdup relations for two-phase flow

It was previously mentioned that when the phases differ in density and viscosity one of them, usually the more dense phase, flows with a lower in situ average velocity than the other. This velocity difference results in a change in the concentration of the phases along the length of the pipe. In the entrance section of the pipe the less mobile phase concentrates; this concentration gradually decreases in the direction of flow. This phenomenon is called holdup. For a quantitative description of holdup a number of convenient parameters can be defined.

The local in situ volume fraction of phase i ε_i and its cross-sectional average value E_i are convenient measures of the holdup.

The average slip velocity is defined as the difference between the cross-sectional average velocities of the two phases

$$c_s = c_i - c_j \,. \tag{10.132}$$

Sometimes it is convenient to use the apparent phase velocity. This can be defined as the volumetric rate of flow of the phase divided by the total cross-sectional area of the pipe:

$$c_{oi} = \frac{Q_i}{A}, \qquad c_{oj} = \frac{Q_j}{A}. \tag{10.133}$$

It is clear that the cross-sectional average velocity of the mixture can be written as

$$c = \frac{Q}{A} = \frac{Q_i + Q_j}{A} = c_{oi} + c_{oj} \,. \tag{10.134}$$

The average slip velocity can be expressed in terms of the apparent phase velocities as

$$c_s = \frac{c_{oi}}{E_i} - \frac{c_{oj}}{E_j} \,. \tag{10.135}$$

A further convenient parameter is the flow-rate ratio

$$\xi_i = \frac{Q_i}{Q}; \qquad \xi_j = \frac{Q_j}{Q} \,. \tag{10.136}$$

By combining equations (10.134), (10.135) and (10.136) the averaged in situ volume fractions can be expressed in terms of the average velocity of the mixture and the average slip velocity

$$E_i = \frac{c + c_s}{2c_s} - \sqrt{\left(\frac{c + c_s}{2c_s}\right)^2 - \xi_i \frac{c}{c_s}} \,, \tag{10.137}$$

$$E_j = \frac{c_s - c}{2c_s} + \sqrt{\left(\frac{c_s - c}{2c_s}\right)^2 + \xi_j \frac{c}{c_s}} \,. \tag{10.138}$$

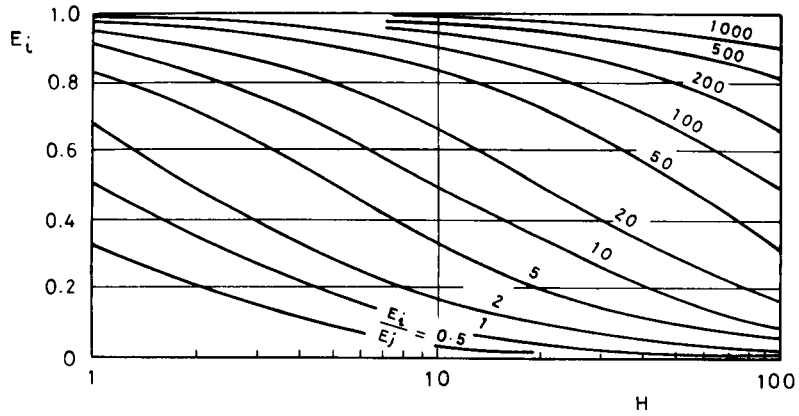

Fig. 10.15. In situ volume fraction and holdup ratio

Another measure of holdup is the ratio of the cross-sectional average in situ velocities at a given cross section, the so-called holdup ratio

$$H = \frac{c_i}{c_j}. \tag{10.139}$$

It is obvious that

$$H = \frac{c_i}{c_j} = \frac{c_{oi} E_j}{c_{oj} E_i} = \frac{\xi_i E_j}{\xi_j E_i}, \tag{10.140}$$

from which the average in situ volume fractions are obtained as

$$E_i = \frac{c_{oi}}{c_{oi} + H c_{oj}} = \frac{\xi_j}{\xi_i + H \xi_j} \tag{10.141}$$

and

$$E_j = \frac{H c_{oj}}{c_{oi} + H c_{oj}} = \frac{H \xi_j}{\xi_i + H \xi_j}. \tag{10.142}$$

The relationships of the in situ volume fraction of the less dense phase and the holdup ratio to the input volume ratio of the phases is shown in *Fig. 10.15.*

The relationship between the average slip velocity and the holdup ratio is obtained as

$$c_s = \frac{H-1}{H}(c_{oi} + H c_{oj}). \tag{10.143}$$

These relationships have general validity for any two-phase flow. The perfectly suspended two-phase flow pattern with axisymmetric velocity and concentration profiles, without holdup can be characterized by $H = 1$.

The holdup relations of various particular two-phase flows may be represented by a variety of diagrams.

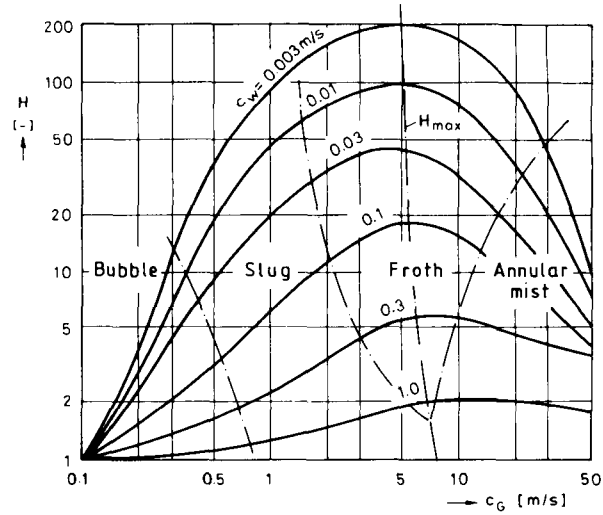

Fig. 10.16. Holdup ratio of water-air mixture flow in vertical pipe

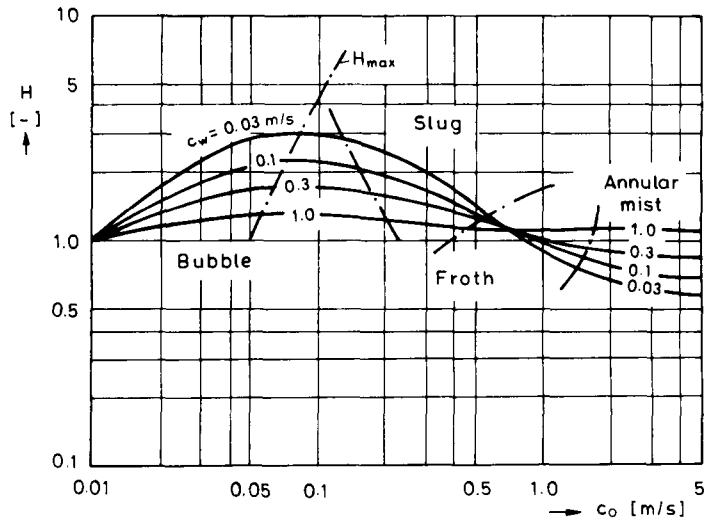

Fig. 10.17. Holdup ratio of vertical water-oil mixture flow

In *Fig. 10.16* the holdup ratio for a vertical flow of a water-air mixture is plotted against the superficial air velocity, while the superficial water velocity is taken as a parameter. In the bubble flow region the holdup ratio increases with the air velocity. An increase in the water velocity decreases the holdup ratio. The holdup ratio increases in the slug flow region, and reaches a maximum in the froth flow

domain. As the air flow rate is increased further, the holdup ratio decreases with the occurrence of annular-mist flow.

Figure 10.17 relates to a liquid system flowing upward in an inclined pipe. In this case the maximum holdup ratio occurs in the slug-flow region. In the froth-flow domain, the holdup phenomenon almost ceases, while in the annular-mist flow regime the hold-up ratio decreases to below unity.

Figure 10.18 shows the holdup ratio for a liquid-gas mixture flow in a horizontal pipe. It is noticeable, that each of the curves has a local maximum and a minimum.

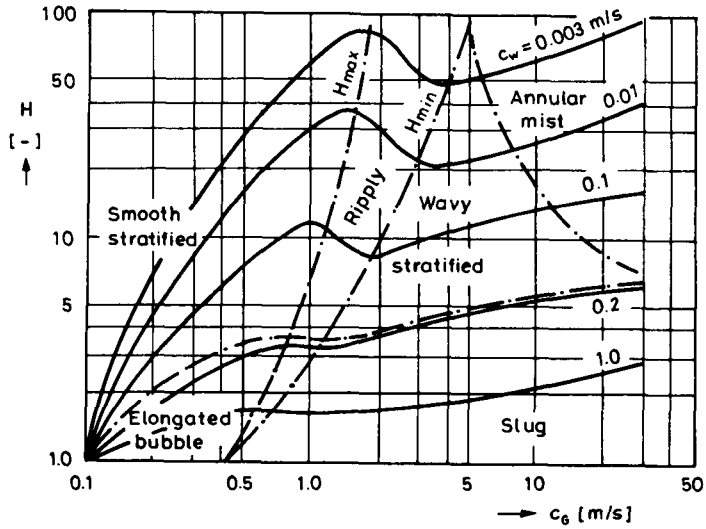

Fig. 10.18. Holdup ratio for liquid-gas mixture flow in horizontal pipe

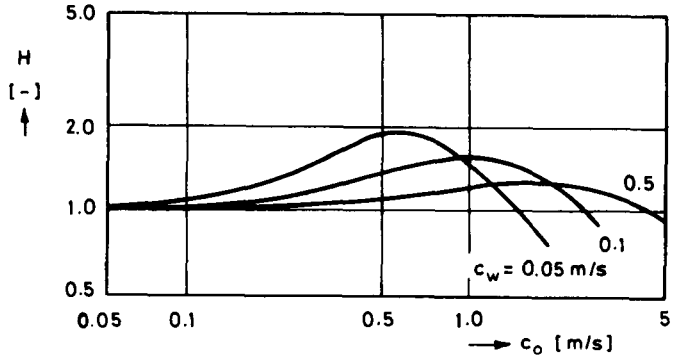

Fig. 10.19. Holdup ratio for oil-water mixture flow in horizontal pipe

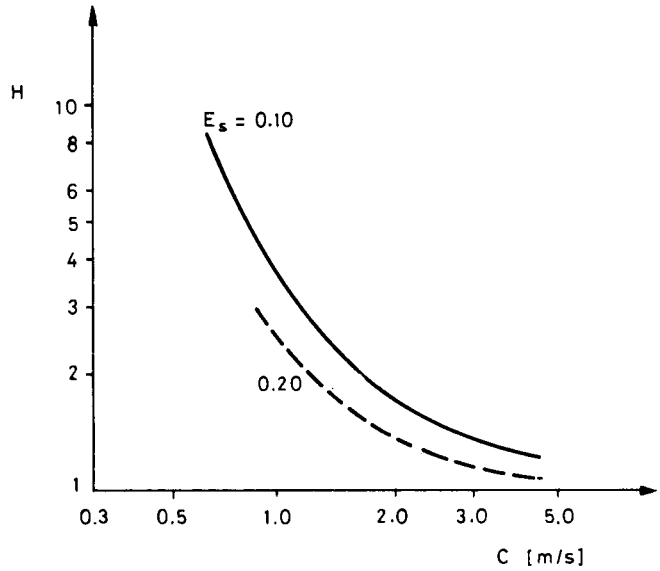

Fig. 10.20. Holdup ratio for water-sand and air-sand mixture flows

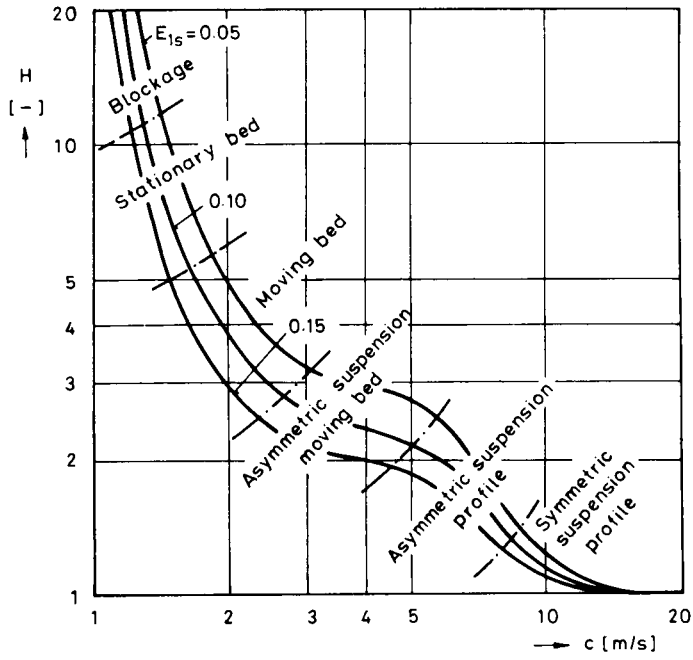

Fig. 10.21. Holdup ratio plotted against mixture velocity

The maximum corresponds to the ripply stratified flow, the minimum coincides with the occurrence of capillary waves.

That the holdup phenomenon is less significant for horizontal oil-water flows is illustrated by *Fig. 10.19*, which pertains to such a flow.

For fluid-solid mixtures flowing in vertical pipes it may be assumed that the average slip velocity would equal the terminal settling velocity, i. e.

$$c_s = \frac{H-1}{H}(c_{of} - Hc_{os}) = U_0\,, \tag{10.144}$$

where U_0 is the terminal settling velocity and c_{of} and c_{os} are the apparent velocities of the fluid and the solid respectively. *Figure 10.20* shows the holdup ratio for water-sand and air-sand mixtures as a function of the cross-sectional average velocity of the mixture.

Holdup relations can be related to visually observed flow patterns for flows of fluid-solid mixtures in horizontal pipes. The holdup ratio is plotted against the mixture velocity in *Fig. 10.21*. The holdup ratio increases as the mixture velocity decreases. When a symmetric suspension profile has been reached, it is found that if the mixture velocity is increased further, the holdup phenomenon ceases and the holdup ratio tends to unity.

10.8 Determination of pressure losses for two-phase flow in pipes

The mechanical energy equation for a two-phase flow in pipes obviously contains the dissipation terms for each of the phases. In the following form of the equation the dissipation terms are represented as pressure losses Δ'_{pi} and Δ'_{pj}:

$$p_1 - p_2 = \frac{\varrho_2 c_2}{c_1} U_2 - \varrho_1 U_1 + \left(\frac{c_2}{c_1} - 1\right) p_2 + \Delta p'_i + \Delta p'_j\,. \tag{10.145}$$

It can be recognized that holdup influences the changes of both the potential and the pressure energy. The pressure losses $\Delta p'_i$ and $\Delta p'_j$ may be combined into a two-phase pressure loss $\Delta p'$. Because of the holdup this does not equal the pressure drop, even for horizontal pipes.

The pressure loss can be determined by purely analytical methods for a homogeneous Newtonian fluid flow only. For a homogeneous fluid flow the friction factor is a function of a single similarity invariant, the Reynolds number. In contrast, for a two-phase flow, the pressure loss which can be calculated with a friction factor depends on at least six variables: Reynolds number, Froude number, Weber number, density ratio, viscosity ratio and the flow rate ratio. It is obvious that the variety of flow types and flow patterns cannot be encompassed within a single formula. It is necessary to develop semi-empirical methods of specific validity,

applicable to certain types of flow. In order to obtain pressure-loss equations suitable for direct application in petroleum engineering practice, the various types, of two-phase flows should be considered separately.

For vertical two-phase liquid-gas mixture flow Ros (1961) developed a method to determine the pressure loss. There are two separate expressions for the pressure loss. If the liquid phase is continuous, i. e. for bubble, slug and froth flow, the pressure loss is given by

$$\Delta p' = \frac{2\lambda_R \varrho_L c_{0L}^2}{gD}\left(1 + \frac{c_{0G}}{c_{0L}}\right)\Delta z\,, \tag{10.146}$$

in which λ_R is the so-called Ros friction factor, c_{0L} and c_{0G} are the superficial velocities of the liquid and the gas, Δz is a finite, short length of the vertical pipe and ϱ_L is the density of the liquid. If the gas phase is continuous, i. e. for annular-mist and mist flows, the pressure loss can be calculated as

$$\Delta p' = \frac{2\lambda_R \varrho_G c_{0G}^2}{gD}\left(1 + \frac{c_{0L}}{c_{0G}}\right)\Delta z\,, \tag{10.147}$$

where ϱ_G now represents the density of the gas.

The Ros friction factor is defined as

$$\lambda_R = \frac{\lambda_1 \lambda_2}{\lambda_3}\,, \tag{10.148}$$

where λ_1, λ_2, λ_3 are friction factors discussed below.

For continuous liquid phase flows λ_1 is a conventional Fanning friction factor which is a function of the Reynolds number, defined as

$$\mathrm{Re}_{0L} = \frac{c_{0L} D}{\nu_L} \tag{10.149}$$

and the relative roughness of the pipe wall. The familiar friction factor relations are

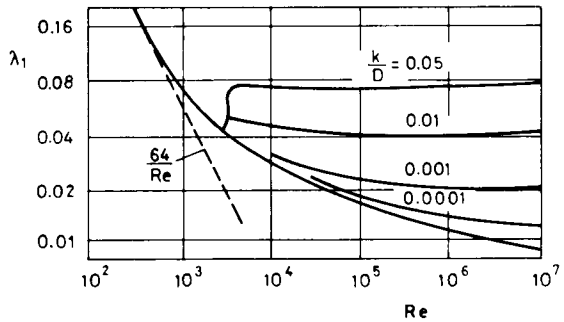

Fig. 10.22. Ros friction factor λ_1

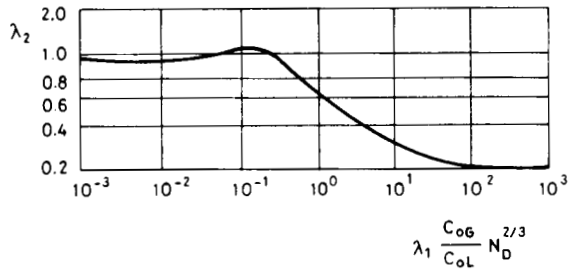

Fig. 10.23. Ros friction factor λ_2

modified by Ros in the interval

$$700 < \mathrm{Re}_{0L} < 3000 .$$

The modified friction factor interval is shown in *Fig. 10.22*. Outside of this region, for laminar flow

$$\lambda_1 = \frac{64}{\mathrm{Re}_{0L}}, \tag{10.150}$$

and for turbulent flow

$$\frac{1}{\sqrt{\lambda_1}} = -2 \lg \left(\frac{k}{3.715\, D} + \frac{2.51}{\mathrm{Re}_{0L} \sqrt{\lambda_1}} \right). \tag{10.151}$$

In this modified region the friction factor can be approximated as

$$\lambda_1 = \frac{0.5999}{\mathrm{Re}_{0L}^{0.506}}. \tag{10.152}$$

The coefficient λ_2 can be obtained from diagram in *Fig. 10.23*, where it is plotted against the parameter

$$X = \lambda_1 \frac{c_{0G}}{c_{0L}} D^{\frac{2}{3}} \left(\frac{\varrho_L g}{\sigma} \right)^{\frac{1}{3}}, \tag{10.153}$$

in which σ is the surface tension.

The correction coefficient λ_3 must be taken into account for highly viscous liquids. It can be calculated as

$$\lambda_3 = 1 + \lambda_1 \sqrt{\frac{c_{0G}}{50\, c_{0L}}}. \tag{10.154}$$

This formula applies, when

$$c_{0G} \left(\frac{\varrho_L}{g\sigma} \right)^{0.25} \leqq 50 + c_{0L} \left(\frac{\varrho_L}{g\sigma} \right)^{0.25}. \tag{10.155}$$

In the annular, and mist flow regions the gas phase is continuous. In this case

$$c_{0G}\left(\frac{\varrho_L}{g\sigma}\right)^{0.25} \geqq 75+84\, c_{oL}^{0.75}\left(\frac{\varrho_L}{g\sigma}\right)^{0.1875}, \tag{10.156}$$

while both correction coefficients λ_2 and λ_3 are equal to unity, thus $\lambda_R=\lambda_1$.

The relative roughness in this case is not calculated as the wall roughness k, but it is obtained as the "film roughness" k^*. The film roughness k^* is obtained from a curve such as the one shown in *Fig. 10.24.*

The calculated $\lambda_1=\lambda_R$, after substitution into Eq. (10.147) leads to the pressure loss for annular flow in a short pipe of length Δz. For a deep well it should be used in the form of a series of step calculations.

For a flow of a liquid-gas mixture in a horizontal pipe the pressure loss may be determined using the semi-empirical method of Lockhart and Martinelli (1949). The method is based upon the assumption that the pressure loss of the liquid phase is equal to the pressure loss of the gas phase regardless of the actual flow pattern:

$$\Delta p'_L=\Delta p'_G. \tag{10.157}$$

The gas phase is assumed to be incompressible. Thus the pressure losses are obtained as

$$\Delta p'_L=\lambda_L\frac{L}{4R_{HL}}\varrho_L\frac{c_L^2}{2} \tag{10.158}$$

and

$$\Delta p'_G=\lambda_G\frac{L}{4R_{HG}}\varrho_G\frac{c_G^2}{2}, \tag{10.159}$$

where R_{HL} and R_{HG} are the hydraulic radii of the region of the pipe in which the liquid or the gas phase flows. The cross-sectional average velocities of the liquid and the gas are

$$c_L=\frac{Q_L}{\xi_L R_{HL}^2\pi} \tag{10.160}$$

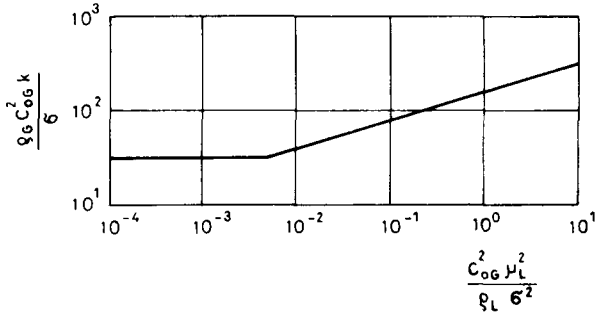

Fig. 10.24. Film roughness correlation for annular mist flow

and

$$c_G = \frac{Q_G}{\xi_G R_{HG}^2 \pi}, \tag{10.161}$$

where ξ_L and ξ_G are hydraulic radius correction factors.

The friction factors of the liquid and gas λ_L and λ_G are expressed as functions of the Reynolds number in the form of an approximate equation:

$$\lambda_L = \frac{B_L}{\left(\frac{Q_L}{\xi_L R_{HL} \pi \nu_L}\right)^m} \tag{10.162}$$

and

$$\lambda_G = \frac{B_G}{\left(\frac{Q_G}{\xi_G R_{HG} \pi \nu_G}\right)^n}. \tag{10.163}$$

B_L and B_G can be evaluated experimentally.

Let us define two fictitious pressure losses for both the liquid and the gas, using the apparent velocities

$$c_{0L} = \frac{Q_L}{R^2 \pi}; \quad c_{0G} = \frac{Q_G}{R^2 \pi}.$$

We can then write

$$\Delta p'_{0L} = \lambda_{0L} \frac{L}{2R} \varrho_L \frac{c_{0L}^2}{2} \tag{10.164}$$

and

$$\Delta p'_{0G} = \lambda_{0G} \frac{L}{2R} \varrho_G \frac{c_{0G}^2}{2}. \tag{10.165}$$

It is obvious, that

$$\lambda_{0L} = \frac{B_L}{\left(\frac{Q_L}{R\pi \nu_L}\right)^m} \tag{10.166}$$

and

$$\lambda_{0G} = \frac{B_G}{\left(\frac{Q_G}{R\pi \nu_G}\right)^n}. \tag{10.167}$$

Using these expressions the relationships between the actual and the fictitious pressure losses are obtained as

$$\Delta p'_L = \Delta p'_{0L} \xi_L^{m-2} \left(\frac{R}{R_{HL}}\right)^{5-m} \tag{10.168}$$

and

$$\Delta p'_G = \Delta p'_{0G} \xi_G^{n-2} \left(\frac{R}{R_{HG}} \right)^{5-n} . \tag{10.169}$$

The ratio of the actual to the fictitious pressure loss is designated by

$$\Phi_L^2 = \xi_L^{m-2} \left(\frac{R}{R_{HL}} \right)^{5-m} \tag{10.170}$$

and

$$\Phi_G^2 = \xi_G^{n-2} \left(\frac{R}{R_{HG}} \right)^{5-n} . \tag{10.171}$$

Lockhart and Martinelli experimentally determined the functions Φ_L and Φ_G. The results are plotted as a function of the dimensionless parameter

$$X = \sqrt{\frac{\Delta p'_{0L}}{\Delta p'_{0G}}} . \tag{10.172}$$

Lockhart and Martinelli grouped their data into four separate groups as follows.

1. Both components flow laminarly. In this case the Reynolds numbers obtained from the superficial velocities must be smaller than 1000.

$$\mathrm{Re}_{0L} = \frac{c_{0L} D}{L} < 1000; \qquad \mathrm{Re}_{0G} = \frac{c_{0G} D}{G} < 1000 .$$

2. The liquid flow is laminar, the gas flow is turbulent. In this case

$$\mathrm{Re}_{0L} = \frac{c_{0L} D}{L} < 1000; \qquad \mathrm{Re}_{0G} = \frac{c_{0G} D}{G} > 2000 .$$

3. The liquid flow is turbulent, the gas flow is laminar

$$\mathrm{Re}_{0L} = \frac{c_{0L} D}{L} > 2000; \qquad \mathrm{Re}_{0G} = \frac{c_{0G} D}{G} < 1000 .$$

4. Both phases flow turbulently, thus

$$\mathrm{Re}_{0L} = \frac{c_{0L} D}{L} > 2000; \qquad \mathrm{Re}_{0G} = \frac{c_{0G} D}{G} > 2000 .$$

These four flow regions are indicated by the subscripts 1, 2, 3, 4 in *Fig. 10.25.*

The critical value of $\mathrm{Re}_0 = 1000$ is chosen since the actual velocity is always greater than the apparent velocity, thus the actual Reynolds number is greater than Re_0.

For large, commercial size pipes the error of the Lockhart—Martinelli method may be as much as 50 percent, particularly for stratified flow. This is because the basic assumption is not valid and the pressure loss depends on the actual flow

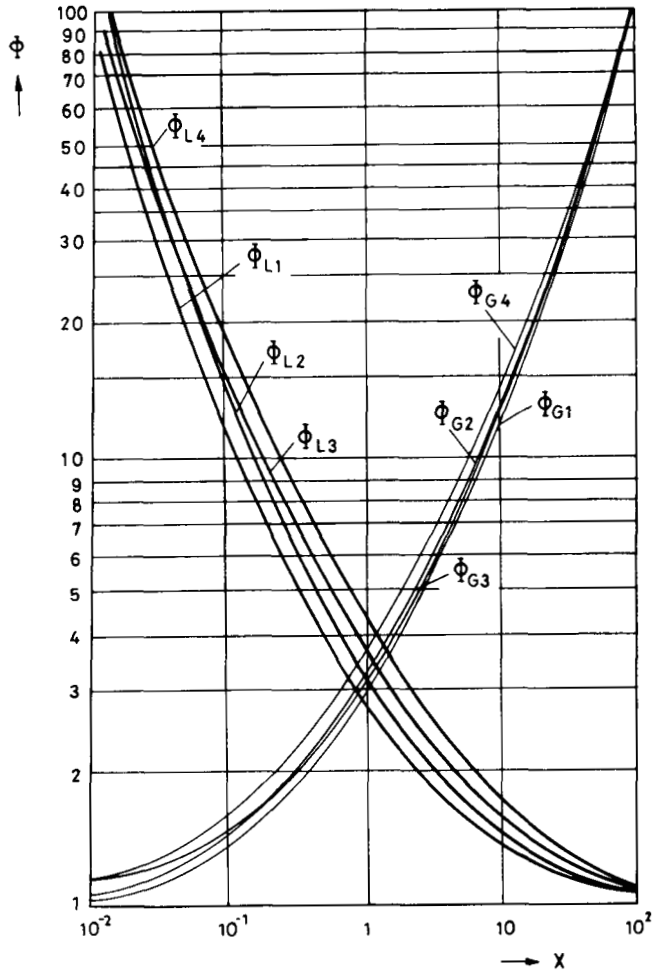

Fig. 10.25. The Lockhart—Martinelli functions

pattern. Thus modified empirical relationships can be obtained for large pipes with diameters of up to 300 mm. The source of experimental data is a flow of gasoline-natural gas mixture in a 300 mm diameter pipeline.

A comparison of the pressure losses calculated by the Lockhart—Martinelli method, with experimental data indicates that actual pressure drop is generally smaller than the calculated values. The difference varies with the flow pattern: it is least for dispersed bubble flow, and greatest for stratified flow. If both phases of a stratified flow are in turbulent motion, separate equations can be derived to modify the original Lockhart—Martinelli relationships for each flow pattern.

These approximate equations, which are recommended for design purposes, are listed below.

For a dispersed bubble flow pattern

$$\Phi_G = 4 - 12 \lg X + 28 (\lg X)^2 . \tag{10.173}$$

For elongated bubble flow

$$\Phi_G = 4 - 15 \lg X + 26 (\lg X)^2 . \tag{10.174}$$

For a smooth surface stratified flow

$$\Phi_G = 2 + 4.5 \lg X + 3.6 (\lg X)^2 . \tag{10.175}$$

For a stratified-wavy flow

$$\Phi_G = 3 + 1.65 \lg X + 0.45 (\lg X)^2 . \tag{10.176}$$

For slug flow

$$\Phi_G = 2.2 + 6.5 \lg X . \tag{10.177}$$

Finally for annular-mist flow the following equation is recommended:

$$\Phi_G = 4 + 2.5 \lg X + 0.5 (\lg X)^2 . \tag{10.178}$$

The Lockhart—Martinelli method is not very suitable for oil-water mixtures. In certain cases, particularly for very viscous and dense crude oil and water mixtures,

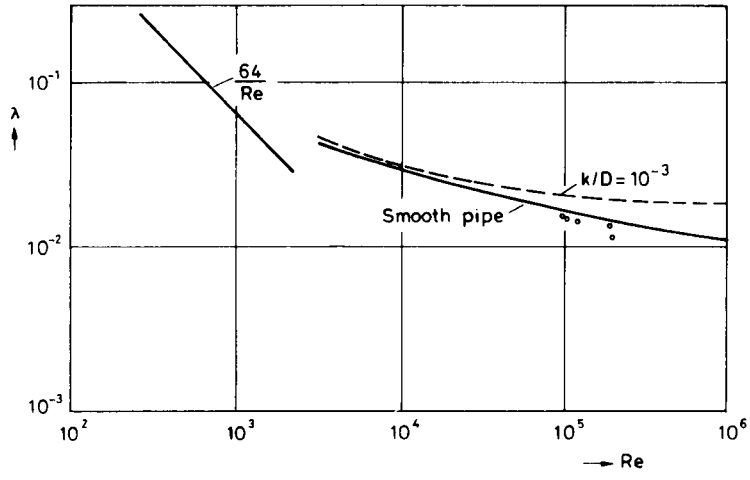

Fig. 10.26. Anomalous small friction factor of oil-water mixture flow

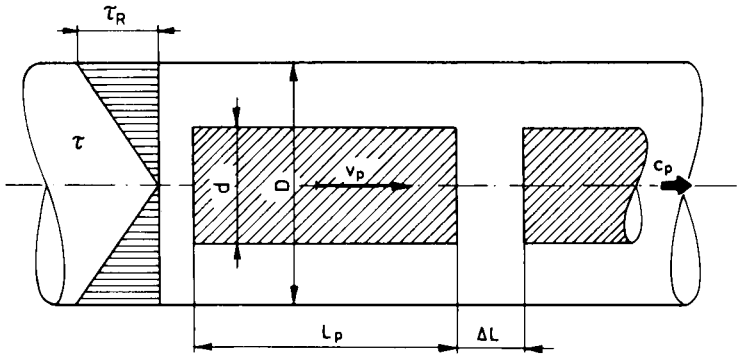

Fig. 10.27. Oil plug flowing with water in horizontal pipe

semi-rigid oil plugs develop coaxially with the pipe. The annular water flow pushes these plugs along the pipe. Applying the Lockhart—Martinelli method to such a flow pattern, the pressure loss of the oil phase is obtained as being almost independent of the oil viscosity and it is found to be remarkably small in spite of the adverse rheological properties. This is shown in *Fig. 10.26*, where the measured λ values fall below the curve of the smooth pipe.

This unusual phenomenon seems to suggest that the viscous energy dissipation cannot develop in the oil phase if it moves like a semi-rigid coaxial plug along the pipe. This is in accordance with the principle of least resistance. The oil core does not flow, it is pushed along by the annular water flow; its deformation is negligible. Thus turbulence cannot develop within the portion of the flow occupied by the oil. In addition the turbulence is also suppressed in the water flow, at least to the extent of the formation of a laminar sublayer at the oil-water interface.

In order to obtain quantitative relationships for this type of flow it is useful to consider some fundamental definitions. *Figure 10.27* illustrates a schematic flow pattern of uniform oil plug moving at a velocity v_p. The fictitious apparent velocities of the water and the oil are

$$c_{0w} = \frac{4Q_w}{D^2\pi}; \qquad c_{0o} = \frac{4Q_o}{D^2\pi}. \tag{10.179}$$

The average velocity of the mixture is

$$c_M = \frac{4(Q_w + Q_o)}{D^2\pi} = c_{0w} + c_{0o}. \tag{10.180}$$

The volume of the oil plug is

$$V_p = \frac{d^2\pi}{4} L_p. \tag{10.181}$$

The volume of water within the length $L_p + \Delta L$ is

$$V_w = \frac{\pi}{4}(D^2 - d^2)L_p + D^2 \Delta L . \tag{10.182}$$

In accordance with the continuity equation the oil plug velocity is

$$v_p = \frac{4Q_o}{d^2 \pi} \frac{L_p + \Delta L}{L_p} . \tag{10.183}$$

The cross-sectional average velocity of the water in the annulus is obtained as

$$c_w = \frac{Q_w(L_p + \Delta L)}{\frac{\pi}{4}[(D^2 - d^2)L_p + D^2 \Delta L]} . \tag{10.184}$$

Let us denote the ratio of the diameters by

$$\delta = \frac{d}{D},$$

thus we get

$$c_M = v_p \delta^2 \frac{L_p}{L_p + \Delta L} + c_w \left(1 - \delta^2 \frac{L_p}{L_p + \Delta L}\right). \tag{10.185}$$

We can approximate the velocity profile of the water in the annulus by the Blasius equation

$$v = v_{\max} \left(1 - \frac{r}{R}\right)^{\frac{1}{7}} . \tag{10.186}$$

This can be expressed in terms of the oil plug velocity v_p as

$$v = v_p \left(\frac{1 - \frac{r}{R}}{1 - \delta}\right)^{\frac{1}{7}} . \tag{10.187}$$

The cross-sectional average velocity of the mixture can be obtained as the integral of the above expression

$$c_M = v_p \left[\frac{7}{4}\delta(1 - \delta) + \frac{49}{60}(1 - \delta)^2 + \delta^2\right]. \tag{10.188}$$

The Blasius equation does not take into account the laminar sublayer at the water-oil interface. This may be corrected for by adding a velocity term v_{p*}

$$v_{p*} = 12 \sqrt{\frac{\tau_p}{\varrho_w}} , \tag{10.189}$$

where τ_p is the shear stress on the plug surface. Using these relationships we can derive an equation for the pressure loss of the flow which is pushing the oil plug along

$$\Delta p' = \Delta p'_w \left\{ \frac{0.82\left(1-\delta^2 \frac{v_{p*}}{c_M}\right)}{\left[\frac{7}{4}(1-\delta)\delta + \frac{49}{60}(1-\delta)^2 + \delta^2\right](1-\delta)^{\frac{1}{7}}} \right\}. \qquad (10.190)$$

There is some uncertainty in this equation since the diameter ratio is, for the moment, still unknown. According to the principle of least resistance we may assume that the diameter of the oil plug can be developed within the possible range which corresponds to the minimum value of the pressure loss. Thus the pressure loss ratio $\Delta p'/\Delta p'_w$ is plotted as a function of the diameter ratio k for a given mixture velocity c_M. The minimum value of the function occurs at $\delta = 0.85$, as shown in *Fig. 10.28*. The slope of the curve is particularly steep in the interval $0.95 < \delta < 1.00$.

It is immediately clear that the pressure gradient of this plug flow is smaller than the pressure gradient of pure water at the same flow rate. On the other hand under conditions where the annulus is very narrow, the oil plug slips forward on a thin film of water. In this case the pressure loss is, naturally, greater than that for pure water.

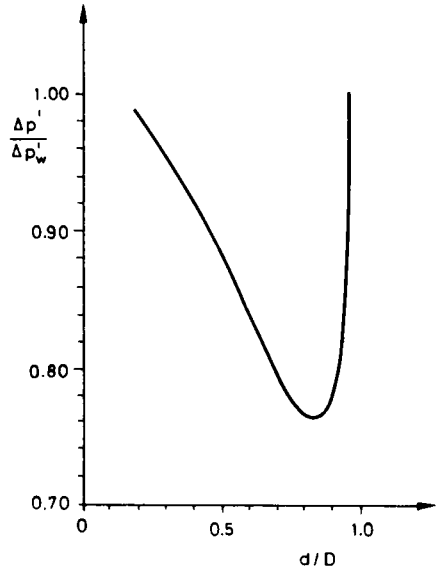

Fig. 10.28. Pressure-loss ratio for plug flow of a water-oil mixture

There are no general pressure gradient correlations applicable to any of the flow patterns of either liquid-solid or gas-solid systems. The semi-empirical approach of Gaessler (1967) seems to be the most applicable one for water-solid mixtures in horizontal pipes. The overall pressure loss is considered to be the sum of the pressure loss of the pure liquid phase and an additional pressure loss induced by the presence of the solid particles:

$$\Delta p' = \Delta p_f + \Delta p_s' . \tag{10.191}$$

The pressure loss of the fluid phase can be calculated in the usual way

$$\Delta p_f' = \lambda \frac{L}{D} \varrho_f \frac{c_f^2}{2} . \tag{10.192}$$

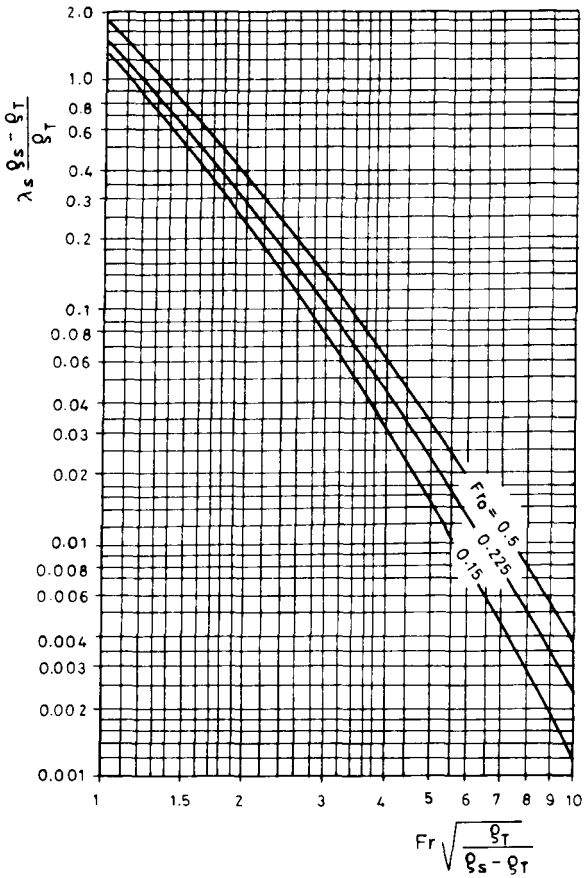

Fig. 10.29. Gaessler's diagram for solid concentration 0.1

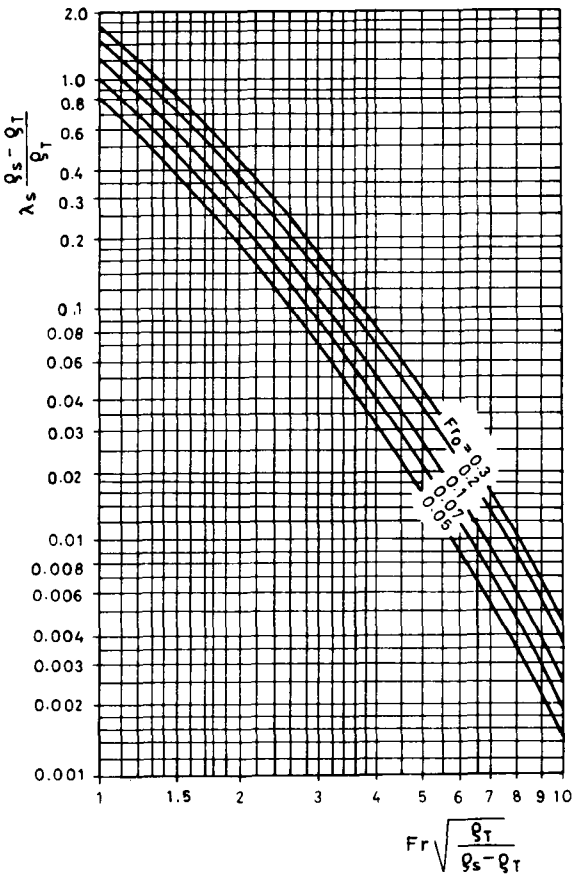

Fig. 10.30. Gaessler's diagram for solid concentration 0.2

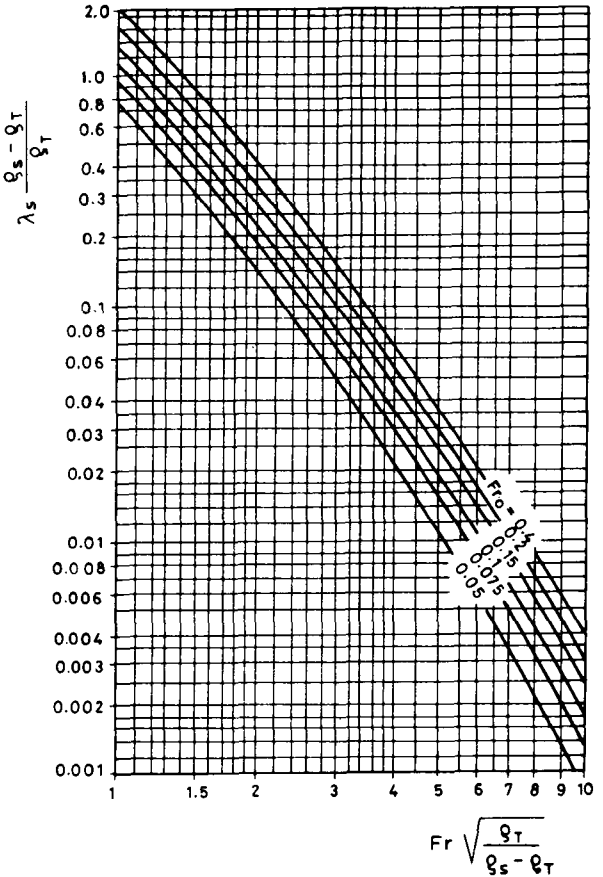

Fig. 10.31. Gaessler's diagram for solid concentration 0.4

The excess pressure loss caused by the solid particles is

$$\Delta p_s' = \lambda_s \frac{L}{D} (\varrho_s - \varrho_f) \frac{c^2}{2}, \tag{10.193}$$

where c is the cross-sectional average velocity of the mixture. The excess friction factor λ_s can be determined experimentally. Finally we obtain

$$\Delta p = \Delta p_f \left\{ 1 + E_s \frac{\lambda_s}{\lambda_f} \left(\frac{\varrho_s}{\varrho_f} - 1 \right) \right\}. \tag{10.194}$$

The excess friction factor λ_s may be determined from Gaessler's diagrams shown in *Figs 10.29–10.31*. In these diagrams the quantity

$$\lambda_s \frac{\varrho_s - \varrho_T}{\varrho_T}$$

is plotted against

$$\mathrm{Fr} \sqrt{\frac{\varrho_T}{\varrho_s - \varrho_T}},$$

where

$$\varrho_T = E_s (\varrho_s - \varrho_f) + \varrho_f. \tag{10.195}$$

(Fr is the Froude number.)

The three diagrams refer to different E_s values. For intermediate values of E_s linear interpolation is used.

LITERATURE

Abramowitsch, G. N.: *Angewandte Gasdynamik*. Berlin, VEB Verlag Technik, 1958.

Albertson, M. L.—Barton, J. R.—Simons, D. B.: *Fluid Mechanics for Engineers*. New York, Prentice-Hall, 1960.

Albring, W.: *Angewandte Strömungslehre*. Dresden—Leipzig, Steinkopff, 1962.

Allievi, L.: *Theorie du coup de bélier*. Paris, 1921.

Angus, R. W.: Waterhammer pressures in compound and branched pipes. *Trans. ASCE* **104,** 340—401, 1959.

Argyris, J. H.—Mareczek, G.—Scharpf, D. W.: Two- and three-dimensional flow using finite elements. *Aero. J. Roy, Aero. Soc.* **73,** 961—964, 1969.

Asszonyi, Cs.: Mechanical theory of continua. *Acta Geod. Geoph. et Mont.* **8 (3—4),** 1974.

Asszonyi, Cs.—Richter, R.: *The Continuum Theory of Rock Mechanics*. Trans. Techn. Publications, New York, 1979.

Aziz, K.—Gregory, G. A.: Prediction of flow pattern holdup and pressure drop in multiphase pipelines. Amsterdam, *Proc. of Symp. on Submarine Gas Pipeline Developments*, 1976.

Aziz, K.—Govier, G. W.—Fogarasi, M.: Pressure drop in wells producing oil and gas. *J. Can. Petr. Techn.* 38—48, 1972.

Bagnold, R. A.: An approach to the sediment transport problem from general physics. *U.S. Geol. Survey Paper* 422—1, 1966.

Baker, O.: Multiphase flow in pipelines. *Oil and Gas Journal* **10,** 156, 1958.

Batchelor, G. K.: *Homogeneous Turbulence*. Cambridge University Press, 1953.

Batchelor, G. K.: *An Introduction to Fluid Dynamics*. Cambridge University Press, 1967.

Batchelor, G. K.: The stress system in a suspension of force-free particles. *J. Fluid Mech.* **41,** 545—570, 1970.

Batchelor, G. K.—Binnie, A. M.—Phillips, O. M.: The mean velocity of discrete particles in turbulent flow in a pipe. *Proc. Phys. Soc. B*; **68,** 1095—1104, 1955.

Baxendell, P. B.: Pipeline flow of oil and gas mixtures. *4th WPC Section II/E4*, 1955.

Baxendell, P. B.—Thomas, R.: Calculation of pressure gradient in high rate oil wells. *JPT* **10,** 1961.

Beggs, H. D.—Brill, J. P.: A study of two-phase flow in inclined pipes. *Trans. AIME* **607,** 1973.

Beran, M. J.: *Statistical Continuum Theories*. New York, Interscience, 1968.

Berker, R.: Intégration des équations du movement d'un fluide visqueux incompressible. *Enc. of Physics*, Vol VIII/2. Berlin, Springer, 1963.

Bergeron, N.: *Du coup de bélier en hydraulique au coup de foudre en électricité. Méthode graphique générale*. Paris, Dunod, 1956.

Bertuzzi, A. F.—Tek, M. R.—Poettmann, F. H.: Simultaneous flow of liquid and gas through horizontal pipe. *Petr. Trans. AIME* **207,** 17—24, 1956.

Bewersdorff, H. W.—Berman, N. S.: The influence of flow-induced non-Newtonian fluid properties on turbulent drag reduction. *Rheologica Acta* **27,** 130—136, 1988.

Bird, R. B.—Stewart, W. E.—Lightfoot, E. N.: *Transport Phenomena*. New York, Wiley, 1960.

Birkhoff, G.: *Hydrodynamics.* Princepton University Press, 1960.
Bizzell, G. D.—Slattery, J. C.: Non-Newtonian boundary layer flow. *Chemical Eng. Science* **17,** 1962.
Blasius, H.: Grenzschichten in Flüssigkeiten mit kleiner Reibung. *Z. Math. u. Phys.* **56,** 1908.
Bobok, E.: Capillary-gravity waves of a non-Newtonian film flow on a flat plate. *Periodica Polytechnica* **13,** No. 3, 1973.
Bobok, E.: New concept to describe flow through porous media. Granada, *SIMAOS,* 1978.
Bobok, E.: The circulation-preserving nature of plane flow in homogeneous isotropic porous media. *Acta Geod. Geoph. et Mont.* **15 (2—4),** 341—348, 1980.
Bobok, E.—Navratil, L.: Investigation of turbulent velocity profiles of steady flow in pipes. *Bulletins for Applied Mathematics* **64/80,** 137—151, 1980.
Bobok, E.—Navratil, L.: Constitutive equation for thixotropic, pseudoplastic crude oils. (In Hungarian.) *Kőolaj és Földgáz* **15/115,** 6, 161—167, 1982.
Bobok, E.—Mating, B.—Navratil, L.: Flow of oil-water mixture in pipeline. *6th International Conference on Hydromechanization,* 245—251. Miskolc, 1989.
Bogárdi, J.—Szücs, E.: Balance equations of suspended sediment transportation. *Acta Technica* **69,** 1—2, 1970.
Bouge, D. C.—Metzner, A. B.: Velocity profiles in turbulent pipe flow, Newtonian and non-Newtonian fluids. *IEC Fundamentals* Vol. 2, 1963.
Bradshaw, P.: *An Introduction to Turbulence and Its Measurement.* Oxford, Pergamon, 1971.
Brenner, H.: Dissipation of energy due to solid particles suspended in a viscous liquid. *Phys. Fluids* **1,** 338—346, 1958.
Brown, K. E.: *The Technology of Artificial Lift Methods* 1—2/*a*—2/*b*. Tulsa, Petroleum Publishing Co., 1980.
Brown, K. E.: *Gas Lift Theory and Practice.* Tulsa, Petroleum Publ. Co., 1973.
Brown, S. N.—Stewartson, K.: Laminar separation. *Ann. Rev. Fluid Mech.,* 1969.
Buckley, S. E.—Leverett, M. C.: Mechanism of fluid displacement in sands. *Trans. AIME,* 1941.
Carrier, G. F.: Shock waves in a dusty gas. *J. Fluid Mech.* **4,** 376—382, 1958.
Carstoiu, I.: Vorticity and deformation in fluid mechanics. *J. Rat. Mech. Anal.* **3,** 691—712, 1954.
Castro, W.—Squire, W.: The effect of polymer additives on transition in pipe flow. *Appl. Sci. Res.* **18,** 81, 1967.
Cebeci, T.—Smith, A. M.: *Analysis of Turbulent Boundary Layers.* New York, Academic Press, 1974.
Chandrasekhar, S.: Theory of turbulence. London, *Proc. Roy. Soc.* A. **229,** 1955.
Chapman, G. T.: *Radiatively Driven Acoustic Waves in a Gas.* Ph. D. Dissertation, Stanford University, 1970.
Chong, T. H.—Sirovich, L.: On the structure of three-dimensional linearized supersonic and hypersonic flows. *Phys. Fluids* **13,** 1990 (1970).
Churchill, R. V.: *Introduction to Complex Variables and Applications.* New York, McGraw Hill, 1948.
Clauser, F. H.: *The Turbulent Boundary Layer.* New York, Academic Press, 1956.
Cole, J. D.: *Perturbation Methods in Applied Mathematics.* Waltham, Mass., 1968.
Colebrook, C. F.: Turbulent flow in pipes, with particular reference to the transition region between the smooth and rough pipe laws. London, *I. Inst. Civ. Eng.* Vol. 11, 1938/39.
Coles, D.: Computation of turbulent boundary layers. *IFP Stanford Conference,* 1968.
Collins, R. E.: *Flow of Fluids through Porous Materials.* New York, Reinhold, 1961.
Corcoran, W. H.—Lacey, W. N.: *Chemical Engineering Problems.* New York, McGraw Hill, 1960.
Courant, R.—Friedrichs, K. O.: *Supersonic Flow and Shock Waves.* New York, Interscience, 1948.
Csanády T.: *Theory of Turbomachines.* New York, McGraw Hill, 1965.
Czibere, T.: *Hydrodynamics.* (In Hungarian.) Budapest, Tankönyvkiadó, 1978.
Darwin, C. G.: Note on hydrodynamics. *Proc. Camb. Phil. Soc.* **49,** 342, 1953.
Davies, G. A.—Ponter, A. S.: Turbulent flow properties of dilute polymer solutions. *Nature* **216,** 66, 1966.
De Groot, S.: Hydrodynamics and thermodynamics. *Proc. Symp. Appl. Math.* **4,** 87—99, 1953.

Deissler, R. G.: The problem of steady-state shear flow turbulence. *Phys. Fluids* **8,** 391, 1965.
Desai, C. S.—Abel, J. F.: *Introduction to the Finite Element Method.* New York, Van Nostrand, 1972.
Dodge, D. W.—Metzner, A. B.: Turbulent flow of non-Newtonian systems. *AIChE Journal* **5,** 2, 1959.
Drouot, R.—Maugin, G. A.: Phenomenological theory for polymer diffusion in non-homogeneous velocity-gradient flow. *Rheologica Acta* **22,** 336—347, 1983.
Duhem, P.: Sur la propagation des ondes de choc an sein des fluides. *Z. Phys. Chem.* **69,** 169—186, 1909.
Dukler, A. E.: Gas-liquid flows in pipelines. *Ass. Am. Petr. Inst. Research Results* Vol. I, 1969.
Duns, H.—Ros, N. C. J.: Vertical flow of gas and liquid mixtures in wells. Frankfurt, *6th World Petr. Congr.*, 1963.
Dzung, I. S.: *Flow Research on Blading.* Elsevier, Amsterdam etc., 1970.
Eck, B.: *Technische Strömungslehre.* (6th ed.) Berlin, Springer, 1961.
Einstein, H. A.—Chien, N.: Effects of heavy sediment concentration near the bed on velocity and sediment distribution. *U.S. Army Missouri R. Corps Engrs. Omaha NRD. Series,* 1955.
Eirich: *Rheology.* New York, Academic Press, 1961.
Elata, C.—Poreh, M.: Momentum transfer in turbulent shear flow of an elasto-viscous fluid. *Rheologica Acta* **5,** 148, 1966.
Ellison, T. H.: *Mécanique de la turbulence.* Paris, CNRS, 1962.
Ericksen, D.—Rivlin, M.: Stress-deformation relations for isotropic materials. *J. Rat. Mech. Anal.* **4,** 323, 1955.
Eringen, C.: *Nonlinear Theory of Continuous Media.* New York, McGraw Hill, 1962.
Ertel, H.: *Ein neues Wirbel-Theorem der Hydrodynamik.* Berlin, Sitzsber. Akad. Wiss, 1954.
Everdingen, A. F.—Van Hurst, W.: The application of the Laplace transformations to flow problems in reservoirs. *J. Petr. Techn.* **168,** 1949.
Fabula, A. G.: The toms phenomenon in the turbulent flow of very dilute polymer solutions. *Proc. 4th Int. Congr. on Rheology,* Interscience, 1965.
Fabula, A. G.: Fire-fighting benefits of polymeric friction reduction. *Trans. ASME* **D. 93,** 453, 1971.
Fincham, A. E.: *A Review of Computer Programs for Network Analysis.* Gas Council Research Communication G. C. 189, 1971.
Furumoto, A.—Hotth, C.: *Geophysical fluid dynamics.* Woods Hole Oceonagraphic Inst. Rep., 1961.
Gadd, G. E.: Effects of drag-reducing additives on vortex stretching. *Nature* **217,** 1040, 1968.
Gaessler, H.: *Experimentelle und theoretische Untersuchungen über die Strömungsvorgange beim Transport von Feststoffen in Flüssigkeiten durch horizontale Rohrleitungen.* Karlsruhe, Diss. Techn. Hochschule, 1967.
Gallagher, R. H.—Oden, J. T.—Taylor, C.—Zienkiewicz, O. C.: *Finite Elements in Fluids.* New York, Wiley, 1975.
Goldstein, S.: *Modern Developments of Fluid Dynamics.* Oxford University Press, 1938.
Görtler, W.: Recent mathematical treatments of laminar flow transition problems. *Phys. Fluids* **10,** 1966.
Govier, G. W.—Aziz, K.: *The Flow of Complex Mixtures in Pipes.* New York, Van Nostrand Reinhold, 1972.
Griffith, P.—Wallis, G.: Two-phase slug flow. *ASME J. of Heat Transfer,* 1965.
Gruber, J.—Blahó, M.: *Fluid Mechanics.* (In Hungarian.), Budapest, Tankönyvkiadó, 1970.
Haber, S.—Mauri, R.: Boundary conditions for Darcy's flow through porous media. *Journal of Multiphase Flow* **9,** 5, 561—574, 1983.
Hadamard, J.: *Leçon sur la propagation des ondes et les équations de l'hydrodynamique.* Paris, 1903.
Hagedorn, A. R.—Brown, K. E.: The effect of liquid viscosity in vertical two-phase flow. *J. Petr. Techn.*, 1964.
Hamam, Y. M.—Brameller, A.: Hybrid methods for the solution of piping networks. *Proc. I.I.E.* **118,** 1607—1612, 1971.
Hansen, A. G.: *Similarity Analysis of Boundary Value Problems in Engineering.* New Jersey, Prentice-Hall, 1965.

Hansen, A. G.—Na, T. Y.: Similarity solutions of laminar incompressible boundary layer equations of non-Newtonian fluids. *Trans. ASME* **D. 90,** 71—74, 1968.

Happel, J.—Brenner, H.: *Low Reynolds Number Hydrodynamics.* Englewood Cliffs, Prentice-Hall, 1965.

Hatsopoulos, G. N.—Keenan, J. H.: *Principles of General Thermodynamics.* New York, Wiley, 1965.

Hayashi, N.: Similarity of the two-dimensional and axisymmetric boundary layer flows for purely viscous non-Newtonian fluids. *Journal of Fluid Mechanics* **23,** 293—303, 1965.

Hayes, W. D.: *The Basic Theory of Gasdynamic Discontinuities.* Princeton University Press, 1958.

Heath, M. J.—Blunt, J. C.: Dynamic simulation. Applied to the design and control of pipeline network. *I.G.E. Journal S* 261/279, 1969.

Hedström, B. O. A.: Flow of plastic materials in pipes. *Ind. Eng. Chem.* **44,** 651, 1952.

Helmholtz, H.: Über Integrale der hydrodynamischen Gleichungen, welche den Wirbelbewegungen entsprechen. *J. reine angew. Math.* **55,** 25—55, 1858.

Herning, F.: *Stoffströme in Rohrleitungen.* (3rd ed.) Düsseldorf, VDI, 1961.

Hino, M.: Turbulent characteristics of solid-liquid two-phase flow. *Proc. 13th Japan Congr. Appl. Mech.*, 1963.

Hinze, J. O.: *Turbulence.* New York, McGraw Hill, 1959.

Howarth, L.: Laminar boundary Layers. *Enc. of Physics*, Vol. VIII/1, Berlin, Springer, 1962.

Hoyt, J. W.: The effect of additives of fluid friction. *Trans. ASME* **D. 94,** 258—285, 1972.

Hugmark, G. A.: Holdup and pressure drop with gas-liquid flow in a vertical pipe. *Chem. Eng. Progress* **58,** 62, 1962.

Hugmark, G. A.—Pressburg, B. S.: Holdup and pressure drop with gas-liquid flow in a vertical pipe. *AIChE Journal* **7,** 677, 1961.

Illingworth, C. R.: *Modern Developments in Fluid Dynamics.* Oxford, University Press, 1953.

Ippen, A. T.: *Estuary and Coastline Hydrodynamics.* New York, McGraw Hill, 1966.

Jeffrey, D. J.—Acrivos, A.: The rheological properties of suspensions of rigid particles. *AIChE Journal* **22,** 417—432, 1976.

Jeppson, R. W.: *Techniques for solving free-streamline cavity, jet and seepage problems by finite differences.* Dept. Civ. Eng. Techn. Rep. Stanford University, 1966.

Jones, R. T.: Blood flow. *Ann. Rev. Fluid Mech.* **1,** 223—224, 1969.

Jones, W. M.—Marshall, D. E.: Relaxation effects in Couette flow between rotating cylinders. *British Journal of Applied Physics* **2,** 809, 1969.

Jotaki, T.—Tomita, Y.: Turbulent friction drag of a dusty gas. *Bull. J.S.M.E.* **16,** 93—99, 1973.

Kantorowicz, A. R.: The formation and stability of normal shock waves in channel flow. *NACA Tech.* Note no. 1225, 1947.

Kapur, J. N.—Gupta, R. C.: Two-dimensional flow of power law fluids. *ZAMM* **43,** 135—141, 1963.

Kapur, J. N.—Srivstava, R. C.: Similar solutions of the boundary layer equations for power law fluids. *ZAMP* **14,** 383, 1963.

Kármán, T.: Über laminare und turbulente Reibung. *ZAMM* **1,** 233—242, 1921.

Kármán, T.: Mechanische Ahnlichkeit und Turbulenz. Göttingen, *Math. Phys.*, 1930.

Kármán, T.: The analogy between fluid friction and heat transfer. *Trans. ASME* **61,** 1939.

Kármán, T.: Progress in the statistical theory of turbulence. *J. Mar. Res.* **7,** 252, 1948.

Kármán, T.—Biot, M. A.: *Mathematical Methods in Engineering.* New York, 1940.

Kármán, T.: *Aerodynamik.* Genf, Interavia, 1956.

Kármán, T.—Lin, C. C.: On the concept of similarity in the theory of isotropic turbulence. *Adv. Appl. Math.* **2,** 1, 1951.

Kármán, T.: Compressibility effects in aerodynamics. *J. Aeromant. Sci.* **8,** 337—356, 1941.

Kennedy, J. F.: The mechanics of dunes and antidunes in erodible beds. *J. Fluid Mech.* **16,** 521—544, 1963.

Kim, S.—Tagori, T.: Drag measurements on flat plates with uniform injection of polymer solutions and their direct application to the wall. *Proc. Ann. Meet. JSME*, 1969.

Kilian, F. P: Über die Verminderung des Reibungswertes von Grenzschichtströmungen viskoelastischer Flüssigkeiten, Berlin, *Mitt. Ver. Wasserbau u. Schiffbau*, H. 51, 52, 1970.

Kline, S. H.: *Fluid Mechanics of Internal Flow*. Amsterdam, Elsevier Publ. 1967.

Kline, S. J.—Shapiro, A. H.: *On the Normal Shock Wave in any Single-phase Fluid Substance*. Stanford University Press, 1953.

Klinkenberg, L. J.: The permeability of porous media to liquids and gases. *DPP* **200**, 1941.

Knudsen, J. G.—Katz, D. L.: *Fluid Dynamics and Heat Transfer*. New York, McGraw Hill, 1958.

Komornoki, L.—Navratil L.: Crude oil tests conducted in Hungary find optimum flow properties. *Oil and Gas Journal*, 159—160, 1978.

Kotschin, N. E.—Kibel, I. A.—Rose, N. V.: *Theoretische Hydromechanik I., II.* Berlin, Akademie Verlag, 1955.

Kovásznay, L. S. G.: Hot wire methods. *High Speed Aerodyn. and Jet Propulsion*. Princeton University Press, **9**, 219—241, 1953.

Kovásznay, L. S. G.: Turbulence measurements. *Appl. Mech. Rev.* **12**, 375, 1959.

Kovásznay, L. S. G.: Structure of the turbulent boundary layer. *Phys. Fluids*, 1967.

Kowalski, T.: Reduction of frictional drag by non-Newtonian additives. *Naval Engineers Journal*, **293**, 1966.

Landau, L. D.—Lifsic, E. M.: *Hydrodynamics*. (In Hungarian.) Budapest, Tankönyvkiadó, 1980.

Lee, S. Y.—Ames, W. F.: Similarity solutions for non-Newtonian fluids. *AIChE Journal* **12**, 700—708, 1966.

Leva, M.: *Fluidization*. New York, McGraw Hill, 1959.

Liakopoulos, A. C.: Darcy's coefficient of permeability as symmetric tensor of second rank. *AIHS* **3**, 41, 1965.

Lighthill, M. J.: *Turbulence*. Manchester, University Press, 1970.

Lin, C. C.: *The Theory of Hydrodynamic Stability*. Cambridge, University Press, 1955.

Litvai, E.: *Mechanics of Non-Newtonian Fluids*. (In Hungarian.) Budapest, Tankönyvkiadó, 1965.

Litvai, E.: Investigation of the boundary layers on radial impellers. Budapest, *Sci. Section of Techn. Univ.* **1**, 179—193, 1967.

Litvai, E.: Prediction of velocity profiles for turbulent boundary layers on the blading of radial impellers. Budapest, *Proc. of the 4th Conf. on Fluid Mech.* 771—782, 1972.

Lockhart, R. W.—Martinelli, R. C.: Proposed correlation of data for isothermal, two-phase, two-component flow in pipes. *Chem. Eng. Progress* **45**, 39, 1949.

Longwell, P. A.: *Mechanics of Fluid Flow*. New York, McGraw Hill, 1966.

Lumley, J. L.: *Stochastic Tools in Turbulence*. New York, Academic Press, 1970.

Luque, R. F.: Conditions for erosion of a sand bed by turbulent flow. Cambridge, *Symp. on Flow of Solid-Fluid Mixtures*, 1969.

Mandhane, J. M.—Gregory, G. A.—Aziz, K.: A flow pattern map for gas-liquid flow in horizontal pipes. *Int. J. Multiphase Flow*, **1**, 537—553, 1974.

Masuda, H.: A new proof of Langrange's theorem in hydrodynamics. *J. Phys. Soc. Japan* **8**, 390—393, 1953.

Maxwell, J. C.: On the displacement in a case of fluid motion. *Proc. Lond. Math. Soc.* **3**, 82—87, 1870.

Mazzarrella, F.: Determinazione della componenti di secondo ordine della deformazione riferite ad un generico sistema di coordinate curvilinee. Napoli, *Rend. Acad.* **4**, 21, 107—144, 1954.

McComas, S. T.: Hydrodynamic entrance lengths for ducts of arbitrary cross section. *J. Basic Eng. Trans. ASME* **89**, 847, 1967.

Metzner, A. B.—Metzner, A. P.: Stress levels in rapid extensional flows of polymeric fluids. *Rheologica Acta*, Vol. 9, 174, 1970.

Metzner, A. B.—Reed, J. C.: Flow of non-Newtonian fluids-correlation of the laminar, transition and turbulent flow regions. *AIChE Journal* **1**, 434, 1955.

Metzner, A. B.—Park, M. G.: Turbulent flow characteristics of viscoelastic fluids. *Journal of Fluid Mechanics* **20**, 291, 1964.

Metzner, A. B.—Dodge, D. W.: Turbulent flow of non-Newtonian systems. *AIChE Journal* **5,** 181, 1959.

Meyer, R. E.: *Introduction to Mathematical Fluid Dynamics.* Chichester, etc. Wiley-Interscience, 1971.

Mieses, R.—Friedrichs, K. O.: *Fluid Dynamics.* Berlin, Springer Verlag, 1971.

Miller, D. S.: *Internal Flow: a Guide to Losses in Pipe and Duct Systems.* BHR, 1971.

Milne-Thomson, L. M.: *Theoretical Hydrodynamics.* New York, St. Martin's, 1949.

Miloh, T.: *Boundary Layer on a Disc Rotating in Dilute Polymer Solution.* MSc. Thesis, Izrael Inst. of Technology, 1969.

Monin, A. S.—Yalgom, A. M.: *Statistical Fluid Mechanics: The Mechanics of Turbulence.* M.I.T. Press, 1971.

Moore, J.: Effects of Coriolis on turbulent flow in rotating channels. *MIT Gas Turb. Lab. Rep.* **89,** 1967.

Mori, Y.—Hijikata, K.—Komine, A.: Propagation of a pressure wave in two-phase flow. *J. Multiphase Flow* **2,** 139—152, 1975.

Müller, W. E.: *Druckrohrleitungen neuzeiteicher Wasserkraftwerke.* Berlin, Springer Verlag, 1968.

Navratil, L.: The influence of stabilization gasoline blending and inhibitor addition on the flow behavior and pressure loss of non-Newtonian crudes. *Proc. Univ. Heavy Industry, Ser. A. Mining* **34,** 219—232, 1978.

Navratil, L.: Velocity distribution of non-Newtonian turbulent flow in pipes. *Proc. Univ. Heavy Industry, Mining,* 650—664, 1986.

Németh, E.: *Hydrodynamics.* (In Hungarian.), Budapest, Tankönyvkiadó, 1963.

Neumann, E. R.: Über eine neue Reduktion bei hydrodynamischer Problemen. *J. reine angew. Math.* **132,** 189—215, 1907.

Neumann, O.: Über die Bewegung der Wärme in compressiblen oder auch incompressiblen Flüssigkeiten. *Ber. Verh. Ges. Wiss. Leipzig* **46,** 1—24, 1894.

Nicodemo, L.—Astarita, G.: Velocity distributions and normal stresses in viscoelastic pipe flow. *AIChE Journal* **12,** 478. 1967.

Nikuradse, J.: Strömungsgesetze in rauhen Rohren. *VDI Forschungsheft* **361,** 1933.

Noordziy, L.: *Shock waves in mixtures of liquids and air bubbles.* Ph.D.Thesis, Twente Inst. Techn., 1973.

Oden, J. T.: *Finite Elements of Nonlinear Continua.* New York, McGraw Hill, 1964.

Onsager, L.—Fuoss, R. M.: Irreversible properties in electrolytes. *J. Phys. Chem.* **36,** 2689—2978, 1932.

Onsager, L.: Reciprocal relations in irreversible processes I., II. *Phys. Rev.* **37,** 405; **38,** 2265, 1931.

Orkiszewski, J.: Predicting two-phase pressure drops in vertical pipes. *J. Petr. Techn.* 1967.

Országh, S. A.: Indeterminancy of the moment problem for intermittent turbulence. *Phys. Fluids* **13,** 2211, 1970.

Ortega, J. M.—Rheinboldt, W. C.: *Iterative Solution of Nonlinear Equations of Several Variables.* New York, Academic Press, 1970.

Osborn, H.: The existence of conservation laws. *Ann. of Math.* **69,** 105—118, 1959.

Oseen, C. W.: *Neuere Methoden und Ergebnisse in der Hydrodynamik.* Leipzig, 1927.

Ostergaard, K.: *Fluidization.* New York, Academic Press, 1971.

Oswatitch, K.: *Gasdynamik.* Wien, Springer Verlag, 1952.

Pápai, L.: Examination of the starting section in pneumatic grain conveying. *Acta Technica* **XIV** (1—2), 1956.

Pápai, L.: Geschwindigkeits- und Druckverhaltnisse bei lotrechter pneumatischer Förderung. *Acta Technica* **69,** 1—2, 1970.

Parmakian, J.: *Waterhammer Analysis.* New York, Prentice-Hall, 1955.

Phillips, O. M.: Shear flow turbulence. *Ann. Rev. Fluid. Mech.* **1,** 245—263, 1969.

Poettmann, F. H.—Carpenter, P. G.: The multiphase flow of gas, oil and water through vertical flow strings with application to the design of gas lift installations. *Drilling and Production Practice,* 1952.

Poreh, M.: Flow of dilute polymer solutions in rough pipes. *Journal of Hydronautics* **4,** 151, 1970.

Prandtl, L.: Über Flüssigkeitsbewegung bei sehr kleiner Reibung. *Verh. III. Int. Math. Kongr.,* Heidelberg, 1904.

Prandtl, L.: *Führer durch die Strömungslehre.* Braunschweig, 1956.
Reynolds, O.: *On the dynamical theory of incompressible viscous fluids and the determination of the criterion.* Phil. Trans. of Roy. Soc., 1895.
Richter, H.: *Rohrhydraulik.* (4th ed.) Berlin, Springer, 1961.
Richter, R.—Bobok, E.: Complex continuum model for description of the simultaneous solid-fluid movements. Granada, *SIAMOS*, 1978.
Roache, P. J.: *Computational Fluid Dynamics.* Albuquerque, Hermosa, 1972.
Ros, N. C. J.: Simultaneous flow of gas and liquid as encountered in well tubing. *J. Petr. Techn.* **13,** 1037, 1961.
Rosenhead, L.: *Laminar Boundary Layers.* Oxford, Clarendon Press, 1963.
Rouse, H.: *Advanced Mechanics of Fluids.* New York, Wiley, 1959.
Ryan, N. W.—Johnson, M. M.: Transition from laminar to turbulent flow in pipes. *AIChE Journal* **5,** 4, 433—435, 1959.
Savins, J. G.: Some comments on pumping requirements for non-Newtonian fluids. *J. Inst. Petr.* **47,** 329, 1961.
Savins, J. G.: Drag reduction characteristics of solutions of macromolecules in turbulent pipe flow. *Soc. Petr. Eng. J.* **4,** 203, 1964.
Savins, J. G.: A stress-controlled drag reduction phenomenon. *Rheologica Acta* **6,** 323, 1967.
Savins, J. G.: *Contrasts in the Solution Drag Characteristics of Polymeric Solutions and Micellar Systems.* New York, Plenum Press, 1969.
Schlichting, H.: *Boundary Layer Theory.* New York, McGraw Hill, 1968.
Schmidt, G.—Weimann, A.: Instationäre Gasnetzberechnung mit dem Programmsystem GANESI. *GWF-GAS/Erdgas* **118,** 57—63, 1977.
Schowalter, W. R.: *Mechanics of Non-Newtonian Fluids.* Oxford, Pergamon Press, 1978.
Schwaigerer, S.: *Rohrleitungen.* Berlin, Springer Verlag, 1967.
Serrin, J.: Mathematical principles of classical fluid mechanics. *Encyclopedia of Physics*, Vol. 8, Berlin, Springer Verlag, 1961.
Skelland, A. H. P.: *Non-Newtonian Flow and Heat Transfer.* New York, Wiley, 1972.
Soo, S. L.: *Fluid Dynamics of Multiphase Systems.* Waltham, Blaisdell, 1967.
Streeter, V. L.: *Fluid Mechanics.* New York, McGraw Hill, 1962.
Streeter, V. L.: *Handbook of Fluid Dynamics.* New York, McGraw Hill, 1963.
Szabó, I.: *Höhere technische Mechanik.* (5th ed.) Berlin, Springer Verlag, 1972.
Szebehely, V. G.: A measure of unsteadiness of time-dependent flows. *Proc. 3rd Midwest Conf. on Fluid Mech.* Univ. Minnesota, 221—231, 1953.
Szilas, A. P.: *Production and Transport of Oil and Gas.* Amsterdam—Oxford—New York, Elsevier, 1975.
Szilas, A. P.: *Production of Water and Steam Wells.* I.I.R.G. Pisa, 1976.
Szilas, A. P.: Startdrückänderung eines in einer Erdölfernleitung abkühlenden strukturviskosen Öles. *Erdoel-Erdgas Zeitschrift* **9,** 1968.
Szilas, A. P.—Bobok, E.—Navratil, L.: Determination of turbulent pressure loss of non-Newtonian oil flow in rough pipes. *Rheologica Acta*, **20,** 487—496, 1981.
Takács, G.: Evaluation of ten methods used for prediction of pressure drop in oil wells. *Erdoel-Erdgas Zeitschrift* **94,** 146—149, 1978.
Takács, G.: Computer study on the application of natural gas Z-factor calculation methods. *Publ. TUHI, Ser. A.* Vol. 34, 209—217, 1978.
Takács, G.: Evaluation of ten methods used for prediction of pressure drop in oil wells. *Oil Gas European Magazine* **44—46,** 51, 1983.
Takács, G.: Comparing methods for calculating Z-factor. *Oil and Gas Journal* **43—45,** 1989.
Tarján, I.—Debreczeni, E.: Theoretical and experimental investigation on the wear of pipeline caused by hydraulic transport. *2th Int. Conf. on Hydraulic Transport Coventry*, 1972.
Tarján, I.—Debreczeni, E.: Determination of hydraulic transport velocity for pumps with various characteristics. *Hydrotransport* **4,** 1976.

Taylor, G. I.: The transport of vorticity and heat through fluids in turbulent motion. *Proc. Roy. Soc.*, 1932.

Taylor, G. I.: *Problems of Hydrodynamics and Continuum Mechanics.* SIAM Publ., 1969.

Taylor, G. I.: The conditions necessary for discontinuous motion in gases. *Proc. Roy. Soc.***A. 84,** 371—377, 1910.

Terzidis, G.: Computational schemes for the Boussinesq equation. *J. Irrigation and Drainage Div. ASCE* **94,** 1968.

Thompson, P. A.: A fundamental derivative in gasdynamics. *Phys. Fluids* **14,** 1843—1849, 1971.

Thompson, P. A.: *Compressible Fluid Dynamics.* New York, McGraw Hill, 1972.

Tietjens, O.: *Strömungslehre.* Berlin, Springer Verlag, 1960.

Tihanyi, L.—Csete, J.: The role of flow rate regulation in gas transmission systems. *Oil Gas European Magazine* **1—82,** 30—36, 1982.

Tomita, Y.: A study of viscoelastic fluid flow. *Bulletin of JSME* **9,** 730, 1966.

Toms, B. A.: Some observations on the flow of linear polymer solutions through straight tubes at large Reynolds numbers. *Proc. Int. Congr. on Rheology* Vol. II, 135.

Townsend, A. A.: *The Structure of Turbulent Shear Flow.* Cambridge, University Press, 1956.

Townsend, A. A.: Entrainment and the structure of turbulent flow. *J. Fluid Mech.* **41,** 13, 1970.

Truesdell, C.—Toupin, R. A.: The classical field theories. *Encyclopedia of Physics* III/1, Berlin, Springer Verlag, 1960.

Truesdell, C.: Two measures of vorticity. *J. Rat. Mech. Anal.* **2,** 173—217, 1953.

Ward-Smith, A. J.: *Pressure Losses in Ducted Flows.* Sevenoaks, Kent, Butterworth, 1971.

Varga, J.: *Handbook of Hydraulic and Pneumatic Machines.* (In Hungarian.) Budapest, Műszaki Könyvkiadó, 1974.

Varga, R. S.: Functional analysis and approximation theory in numerical analysis. *Soc. for Ind. and Appl. Math.*, 1971.

Vavra, H. M.: *Aero-Thermodynamics and Flow in Turbomachines.* New York, Wiley, 1960.

Virk, P. S.: Drag reduction in rough pipes. *Journal of Fluid Mechanics* **45,** 225, 1971.

Volker, R. E.: Nonlinear flow in porous media by finite elements *J. Hyd. Div. ASCE* **93,** 25—33, 1969.

Wallis, G. B.: *One-Dimensional Two-Phase Flow.* New York, McGraw Hill, 1969.

Walton, W. C.: *Ground Water Resource Evaluation.* New York, McGraw Hill, 1970.

Weimann, A.—Lappus, G.: Instationäre Gasrohnetzberechnung. Möglichkeiten und Chancen. *GWF-GAS Erdgas,* **119,** 81, 1978.

Wood, D. J.—Kao, D. T. Y.: Unsteady flow of solid-liquid suspensions. *Journal ASCE,* **92,** 117—134, 1966.

Young, D.: *The Numerical Solution of Elliptic and Parabolic Partial-Differential Equations.* New York, McGraw Hill, 1962.

Zemplén, Gy.: Sur l'impossibilité des ondes de choc négatives dans les gaz. *C.R. Acad. Sci. Paris* **141,** 710—712, 1905.

Zemplén, Gy.: Besondere Ausführungen über unstetige Bewegungen in Flüssigkeiten. *Enz. math. Wiss. IV. art.* **19,** 172—205, 1905.

Zenz, F. A.—Othmer, D. F.: *Fluidization and Fluid-Particle Systems.* New York, Reinhold, 1960.

Zienkiewicz, O. C.: *Finite Element Studies of Solid and Porous Media.* Huntsville, UAH Press, 1973.

Zienkiewicz, O. C.: *The Finite Element Method in Engineering Science.* New York, McGraw Hill, 1971.

SUBJECT INDEX